Durham E-Theses

Seismic Stratigraphy and Geomorphology of Palaeocene Volcanic Rocks, Faroe-Shetland Basin

WRIGHT, KIRSTIE, ANNE-MARIE

Seismic Stratigraphy and Geomorphology of Palaeocene Volcanic Rocks, Faroe-Shetland Basin

Kirstie Anne-Marie Wright

A thesis submitted to Durham University in fulfilment of the requirements for the degree of Doctor of Philosophy

Department of Earth Sciences, Durham University

TABLE OF CONTENT

LIST OF FIGURES

CHAPTER 3: DATA AND METHODOLOGY

CHAPTER 4: APPLICATION OF SEISMIC STRATIGRAPHIC CONCEPTS TO A LAVA-FED DELTA SYSTEM IN THE FAROE-SHETLAND BASIN, UK AND FAROES

11 with shallow, semi-continuous internal reflections with an arcuate, concave upward upper bounding reflection. See Fig. 4.5 for location.

CHAPTER 5: 3D SEISMIC GEOMORPHOLOGY OF THE GROWTH AND COLLAPSE OF A LAVA-FED DELTA SYSTEM, FAROE-SHETLAND BASIN

with a 5 millisecond window of the top of the seismic reflection unit 11. The seismic amplitude map images the arcuate, concave upwards features that disrupt the delta front. The dip map reveals a rapid increase in dip that corresponds to the position of the arcuate features. The edge detection map shows a marked increase in discontinuities that corresponds to the position of the arcuate features. For location see Fig. 5.7.

with a 5 millisecond window of the top of reflection C. The seismic amplitude map images the high amplitude, bulbous lobes that are contain within reflection C. The dip map reveals the lobes have low dips and are relatively continuous and smooth compared to the surrounding reflection background. The edge detection map shows the lobes are continuous, with few discontinuities. For location see Fig. 5.13.

CHAPTER 6: AN EVALUATION OF THE VOLCANIC STRATIGRAPHY OF THE ROSEBANK FIELD, FAROE-SHETLAND BASIN

field trip to the Columbia River Flood Basalt Province, September 2012.

CHAPTER 7: DISCUSSION AND CONCLUSIONS

APPENDIX I: SUPPORT MATERIAL FOR CHAPTER 4

exhibited by inclined hyaloclastite foresets. For location of 3D survey see Chapter 5.

hyaloclastite foresets. For location of 3D survey see Chapter 5.

APPENDIX III: SUPPORT MATERIAL FOR CHAPTER 6

LIST OF TABLES

LIST OF EQUATIONS

DECLARATION

No part of this thesis has previously been submitted for a degree at this or any other university. The work described in this thesis is entirely that of the author, except where a specific reference is made to previously published or unpublished work.

Kirstie Anne-Marie Wright
Durham University
Department of Earth Sciences
December 2012

ACKNOWLEDGEMENTS

DEDICATION

This doctoral thesis is dedicated to my parents, Helen and Michael Wright. Without their unwavering strength, support and encouragement, I would not have made it.

And yes Dad, you can finally say *"what's up Doc..."*

ABSTRACT

2D and 3D seismic reflection data in the Faroe-Shetland Basin have been used to remotely study buried, large-scale Palaeocene volcanic structures emplaced during continental flood basalt volcanism in the Faroe-Shetland Basin. The flood basalts were emplaced as thick and extensive pāhoehoe lava flows from multiple sources, including fissure systems close to the Faroese shelf and from volcanic centres within the basin. This thesis has investigated the distribution and internal structure of the flood basalts based on the hypothesis that volcanic eruptions produce volcanic depositional successions that record the temporal and spatial variations of the basin into which they are emplaced. Multiple eruptions will produce cycles of volcanic deposition that are delineated by hiatal surfaces. These successions can be recognised in seismic reflection data by applying seismic stratigraphic concepts in order to gain insights into the evolution of volcanic basin-fill.

The Faroe-Shetland Basin contains a variety of depositional environments, including a deepening marine basin where continental flood basalts reached a palaeo-shoreline and constructed an extensive lava-fed delta system >1000 m thick. The delta is composed of 13 seismic reflection units whose stacking architecture primarily records variations in lava supply and accommodation. Modification of the delta front was by erosion and debris avalanches. The second environment is subaerial to shallow marine where the continental flood basalts emplaced multiple lava flows 10 – 60 m thick which coalesced to form extensive and overlapping lava flow fields. Four seismic reflection units have been recognised and record variations in source and supply of the lava flows. During reoccurring periods of volcanic quiescence, fluvial channels 350 – 500 m wide incised across the lava flow fields, constrained by flow field topography.

The volcanic depositional successions used to reconstruct the volcanic basin-fill history of the Faroe-Shetland Basin indicate that eruptive styles and volcanic structures varying significantly over relatively small areas (tens of km^2). Many of the seismic observations have been compared to outcrop analogues, are scale-independent and are indicative of emplacement environment. Analysis has also led to the development of a volcanic seismic stratigraphic model as depositional patterns produced during volcanic activity are primarily driven by volcanic supply. The results presented in this thesis have many important implications for stratigraphy, hydrocarbon exploration and basin modelling in the Faroe-Shetland Basin and therefore can be applied beyond the fields of volcanology or seismic interpretation.

CHAPTER 1: INTRODUCTION

1.1 Research Rationale

Volcanic rocks are one of the most dominant lithologies on Earth and can be a volumetrically important component of sedimentary basins (Blatt & Jones, 1975; Fisher, 1984; Fisher & Schmincke, 1994). Throughout the Earth's history, significant volumes of volcanic rock have been emplaced at or within the Earth's surface through the construction of Large Igneous Provinces (Coffin & Eldholm, 1994; Bryan & Ernst, 2008). Large Igneous Provinces are characterised by numerous, long-lived eruptions (weeks to tens of years) that are capable of producing large volumes of continental flood basalt lava (>1 km^3) which are active for a few (1-5) million years (Coffin & Eldholm, 1994; Eldholm & Grue, 1994; Bryan *et al.*, 2010). They are often associated with rifted margins and continental breakup, and as such, many of these provinces are now located in bathymetrically deep, offshore basins (White & McKenzie, 1989; Coffin & Eldholm, 1992; Courtillot *et al.*, 1999; Courtillot & Renne, 2003; Geoffroy, 2005).

A number of these offshore basins are now the target of extensive petroleum exploration, due to an increasing demand for hydrocarbons and a decrease in production from existing fields. These hydrocarbon-rich basins are located across the world and include the Northeast Atlantic Margin, Western Australia, Brazil and China (Fig. 1.1; Filho *et al.*, 2008; Cukur, *et al.*, 2010; Davison *et al.*, 2010; Holford *et al.*, 2012). The emplacement of large volumes of volcanic rock at the Earth's surface can strongly impact the structural and geodynamic development of a basin (White & McKenzie, 1989; Coffin & Eldholm, 1994). Therefore, in the quest to find new hydrocarbon reserves, the identification and interpretation of volcanic rocks is crucial for understanding the development of the sedimentary basin and the potential effects on the petroleum systems (Davies *et al.*, 2004; Archer *et al.*, 2005; Rohrman, 2007).

This study has focused on one of the offshore basins that are now at the frontier of petroleum exploration. The Faroe-Shetland Basin is located on the Northeast Atlantic Margin, which is a volcanically rifted margin that developed through multiple phases of extension throughout the Mesozoic to Early Cenozoic (Stoker *et al.*, 1993; Boldreel & Andersen, 1994; England *et al.*, 2005). The Faroe-Shetland Basin was greatly influenced by the emplacement of significant volumes of extrusive and intrusive volcanic rocks during Early Palaeocene continental breakup (Eldholm & Grue, 1994). The basin is currently the

subject of intense petroleum exploration which has revealed the presence of substantial hydrocarbon accumulations located below and within complex interbedded volcanic and non-volcanic deposits (Knott *et al.*, 1993; Dore *et al.*, 1997; Lamers & Carmichael 1999; Spencer *et al.*, 1999; Larsen *et al.*, 2010). Despite such focused exploration, there is limited information about the internal architecture, spatial distribution and geomorphology of the volcanic rocks of the Faroe-Shetland Basin.
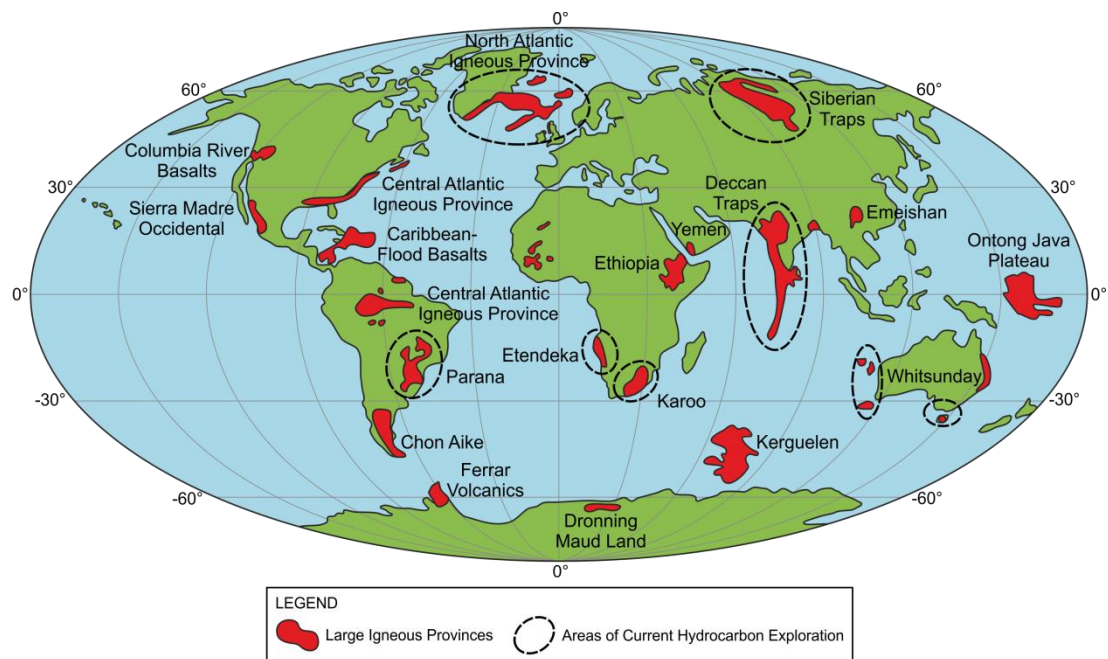
Fig. 1.1. Global distribution of large igneous province and prospective hydrocarbon exploration basins, modified from Coffin & Eldholm (1992, 1994), Courtillot *et al*. (1999), Sheth (1999), Bryan *et al*. (2002), Jerram & Widdowson (2005), Ross *et al*. (2005), Rohrman (2007) and Bryan & Ernst (2008).

Volcanic rocks are often not of any direct commercial interest, but their emplacement can greatly affect the subsequent development of hydrocarbon systems. They can hinder a hydrocarbon system by acting as barriers and baffles to migration, causing compartmentalizing of the reservoir through the emplacement of intrusions, or by decreasing the porosity and permeability of the reservoir through the inclusion of volcaniclastic material (Schutter, 2003; Rohrman, 2007; Holford *et al*., 2012). Alternatively, volcanic rocks can benefit a hydrocarbon system by acting as maturation mechanisms, creating traps or migration pathways through the emplacement of intrusions or volcanic centres, and by acting as both reservoirs if lava flows are highly vesicular or fractured, or as seals if laterally extensive (Schutter, 2003; Rohrman, 2007; Cukur *et al*., 2010; Schofield *et al.*, 2012).

In addition, volcanic rocks can affect seismic reflection imaging, one of the primary methods used in petroleum exploration (Planke *et al.*, 1999; Maresh & White, 2005; Roberts *et al.*, 2005). The complex internal structure and lithological heterogeneity of volcanic rocks causes a loss of seismic energy via the scattering and attenuation of the seismic wave, with relatively little energy returning from within and beneath the volcanic succession (Maresh *et al.*, 2006; Nelson *et al.*, 2008; Shaw *et al.*, 2008). The acquisition of extensive seismic reflection datasets in the pursuit of hydrocarbon reserves, coupled with improvements in seismic imaging techniques, has led to an unique opportunity to increase understanding of the distribution of volcanic rocks and the effect they have on basin development.

Previous seismic reflection studies of volcanic rocks in the Faroe-Shetland Basin have largely been concerned with imaging and interpretation of the transition from continental flood basalt eruptions to sea floor spreading, the intrusive sill complexes or the basin structure below the continental flood basalts (e.g. Planke *et al.*, 1999; Hansen *et al.*, 2004; White *et al.*, 2005). More recently, the internal architecture of the continental flood basalts has been considered, with the identification of lateral variations in volcanic rocks that relate to emplacement environment (Kiørboe, 1999; Thomson, 2005; Davison *et al.*, 2010; Ellefsen *et al.*, 2010). The research in this thesis contributes to the understanding of continental flood basalts by investigating the emplacement environment, distribution and geomorphology of lava flows using extensive and geographically overlapping seismic reflection data. This study demonstrates the validity of undertaking detailed seismic mapping of volcanic rocks and presents the record of basin evolution they can preserve. Such observations may not be gained by studying outcrop examples due to limitations in scale or 3D exposure (Cartwright & Huuse, 2005; Davies & Posamentier, 2005; Posamentier *et al.*, 2007). Furthering the understanding of the volcanic rocks of the North Atlantic Igneous Province has many important implications for stratigraphy, hydrocarbon exploration and basin modelling, and therefore is of general interest beyond the fields of volcanology or seismic interpretation.

1.2 Research Aims and Objectives

Volcanic rocks are often a common, but poorly defined, basin-fill. The main hypothesis of this thesis is that the emplacement of volcanic rocks will produce depositional successions that record temporal and spatial variations of the basin into which they are emplaced.

Multiple eruptions, which are common in the evolution of Large Igneous Provinces, will produce successions of volcanic rocks that are delineated by surfaces which record periods of volcanic quiescence and/or sedimentary deposition (Jolley, 1997; Widdowson, 1997; Widdowson *et al.*, 1997; Jerram *et al.*, 2005; Jolley, 2009; Jolley *et al.*, 2009). These volcanic depositional successions should therefore be recognisable in seismic reflection data through the application of seismic stratigraphic concepts, similar to those used in the seismic interpretation of sedimentary depositional successions (Planke & Alvestad, 1999; Planke *et al.*, 2000). This thesis aims to test, where possible, that seismic stratigraphy is a suitable methodology to interpret volcanic rocks in seismic reflection data in order to gain insights into the temporal and spatial evolution of volcanic basin-fill.

The seismic stratigraphic interpretation of volcanic rocks is known as "seismic volcanostratigraphy" and is still in its infancy (e.g. Planke & Alvestad, 1999; Planke *et al.*, 2000; Berndt *et al.*, 2001), unlike the seismic stratigraphic interpretation of siliciclastic or carbonate rocks, which is well established (e.g. Payton, 1977; Wilgus *et al.*, 1988). Seismic volcanostratigraphy uses the concepts of traditional seismic stratigraphy to study volcanic rocks by interpreting seismic reflection terminations and geometries (e.g. Mitchum *et al.*, 1977a; Vail *et al.*, 1977c; Posamentier & Vail, 1988). In applying seismic stratigraphy to volcanic rocks, this thesis has hypothesized that the emplacement of volcanic rocks in a submarine environment will result in depositional successions bounded by seismic reflection surfaces, similar to those recognised in siliciclastic seismic stratigraphy. These surfaces may have time-stratigraphic significance and the volcanic depositional successions could record variations in relative sea level, accommodation and sediment supply.

Seismic stratigraphic models are based on the response of depositional successions to changes in sediment supply, accommodation and relative sea level, which create varying depositional geometries and key surfaces (see Payton, 1977; Wilgus *et al.*, 1988). Deviations from traditional seismic stratigraphic models may occur due to the high supply rates that occur in continental flood basalt eruptions. Definitive conclusions on the exact nature of the volcanic depositional successions and their equivalent position in the standard seismic stratigraphy hierarchy can only be achieved with high resolution wireline data and biostratigraphic calibration from associated sedimentary rocks, which are not available in this study. Eventually volcanic rocks may require their own seismic stratigraphic model, similar to the modifications required for carbonate rocks due to the differences in sedimentation rates and the effect of physio-chemical processes (Sarg, 1988; Schlarger, 1991; Catuneanu *et al.*, 2009).

The Faroe-Shetland Basin provides an excellent case study because the basin geological history has been relatively well defined. In a bid to better constrain the structure and associated hydrocarbon accumulations of the Faroe-Shetland Basin, extensive 2D and 3D seismic surveys have been acquired. These datasets offers a unique opportunity to study volcanic rocks that would otherwise not be accessible at the surface due to limited 3D exposure or outcrop erosion (Cartwright & Huuse, 2005; Davies & Posamentier, 2005; Posamentier *et al.*, 2007). The thick continental flood basalts of the Faroe-Shetland Basin have largely been characterised on a regional scale (e.g. Planke *et al.*, 2000; Berndt *et al.*, 2001; Davison *et al.*, 2010). Fewer studies have investigated the construction and distribution of volcanic rocks on a finer scale (e.g. Kiørboe, 1999; Ellefsen *et al.*, 2010). Analysis of volcanic rocks in outcrop suggests that flood basalts can exhibit much lateral variation across relatively small distances (1-10 km) and can prove difficult to correlate (Soule *et al.*, 2005; Thomson, 2005). In order to gain information about emplacement environment and basin development, more detailed seismic studies are required. This thesis aims to examine how volcanic rocks present themselves in seismic reflection data and improve our understanding of the emplacement processes of continental flood basalts in a range of environments, using specific examples from the Faroe-Shetland Basin.

In order to achieve the aims of this thesis, the fundamental objectives are;

– To calibrate the response of seismic reflection data to volcanic lithologies and explore the validity of using seismic stratigraphy to interpret the emplacement and distribution of the volcanic rocks

– To recognise cycles of volcanic activity, in particular how the emplacement of volcanic rocks may record variations in accommodation, supply and relative sea level.

– To identify unique volcanic morphological features and relate them to volcanic processes, such as lava-water interaction, erosion and remobilisation.

– To suggest suitable outcrop analogues that exhibit similarities to the stratigraphic geometries and geomorphological features identified in seismic data.

In addition, the objectives relating to this case study are;

- To define and map key volcanic successions within the Faroe-Shetland Basin using seismic reflection data to interpret gross distribution, variations in source and supply and pre-existing basin topography.

- To reconstruct the depositional environment of the Faroe-Shetland Basin during the eruption of the continental flood basalts.

- To correlate, where possible, the key volcanic successions identified offshore with the known onshore stratigraphy of the Faroe Island Basalt Group.

1.3 Thesis Outline

Chapters 2-7 are described individually below. The main scientific sections of this thesis, Chapters 4-6, have been written as standalone manuscripts that have either been published, submitted for review or will be published once permission is received from the relevant companies. Therefore each of these chapters contains a specific introduction, geological setting, discussion and conclusions. The thesis only contains manuscripts for which I am the 1st author and I have been responsible for more than 90% of the primary data collection, interpretation and writing.

Chapter 2 introduces the tectonic history of the Northeast Atlantic Margin and specifically that of the Faroe-Shetland Basin. The North Atlantic Igneous Province is described, including both the known onshore volcanic stratigraphy and the typical seismic reflection configurations of the offshore volcanic stratigraphy. A brief history of hydrocarbon exploration to date is presented to put the research undertaken in this thesis in to context.

Chapter 3 provides a description of the datasets and the interpretation methodologies used in this thesis. The fundamental concepts of seismic reflection data are described, including details of the various 2D and 3D seismic data, interpretation software and mapping techniques used. The different wireline logging tools are described, the physical aspects of the rocks they measure and the methodology used to identify different lithologies. The location and suitability of the outcrop analogues are presented, as are the potential problems comparing seismic data to outcrop analogues.

Chapter 4 investigates the emplacement of subaerial lava flows into a marine environment which resulted in the construction of a lava-fed delta system. This chapter applies seismic stratigraphic concepts to identify distinct seismic reflection units and bounding surfaces, recognise facies associations and evaluate how the delta system affected basin development. The research undertaken in this chapter is based on multiple 2D seismic reflection surveys and one distant exploration well from the Faroe-Shetland Basin (Fig. 1.2). The data were interpreted at Durham University. This chapter has previously been published as Wright, K.A., Davies, R.J., Jerram, D.A., Morris, J. and Fletcher, R. (2012). Application of Seismic and Sequence Stratigraphic Concepts to a Lava-fed Delta System in the Faroe-Shetland Basin, UK and Faroes. *Basin Research*, 24 (1), 91–106 (DOI: 10.1111/j.1365-2117.2011.00513.x). A copy of this publication can be found in Appendix IV.

Chapter 5 examines in detail the structure and volcanic geomorphology of the lava-fed delta system identified in Chapter 4. This chapter attempts to gain insight into the internal architecture and emplacement process of the lava-fed delta to reconstruct the depositional environment. The research undertaken in this chapter builds on the 2D interpretations presented in Chapter 4 and is based on a single 3D seismic reflection survey and one distant exploration well from the Faroe-Shetland Basin (Fig. 1.2). Access to the 3D seismic reflection data were acquired from Statoil UK midway through the PhD, and was initially interpreted during in-house visits to the Statoil UK offices in London, and later at Durham University. This chapter will shortly be submitted for review for publication.

Chapter 6 analyses the distribution of lava flows in a subaerial to shallow marine environment setting south of the lava-fed delta described in Chapters 4 and 5. This chapter continues to analysis the volcanic rocks of the Faroe-Shetland Basin to understand the interaction between volcanic emplacement and siliciclastic deposition, and to identify variations in source and supply of the lava flows. The research undertaken in this chapter is based on a cropped 3D seismic survey and five exploration wells across the Rosebank field (Fig. 1.2). Initial access to the data was acquired towards the latter stage of the PhD through an internship with DONG Energy UK and with the permission of Statoil UK. Access continued with in-house visits after the completion of the internship and in collaboration with both companies. This chapter will be considered for publication at the discretion of the Rosebank partners.

Chapter 7 discusses the main observations made in this thesis, including differences in emplacement mechanisms of continental flood basalts in subaerial to submarine

environments and the resultant products, how the volcanic rocks record the evolution of the Faroe-Shetland Basin and the interaction between volcanic-siliciclastic systems. The implications for future hydrocarbon exploration and the use of field analogues are also considered. The chapter also provides a synopsis of this study, including the validity of interpreting volcanic rocks using seismic reflection data, discussion of the potential difference between volcanic and siliciclastic seismic stratigraphy and the overall conclusions gained from the individual chapters.
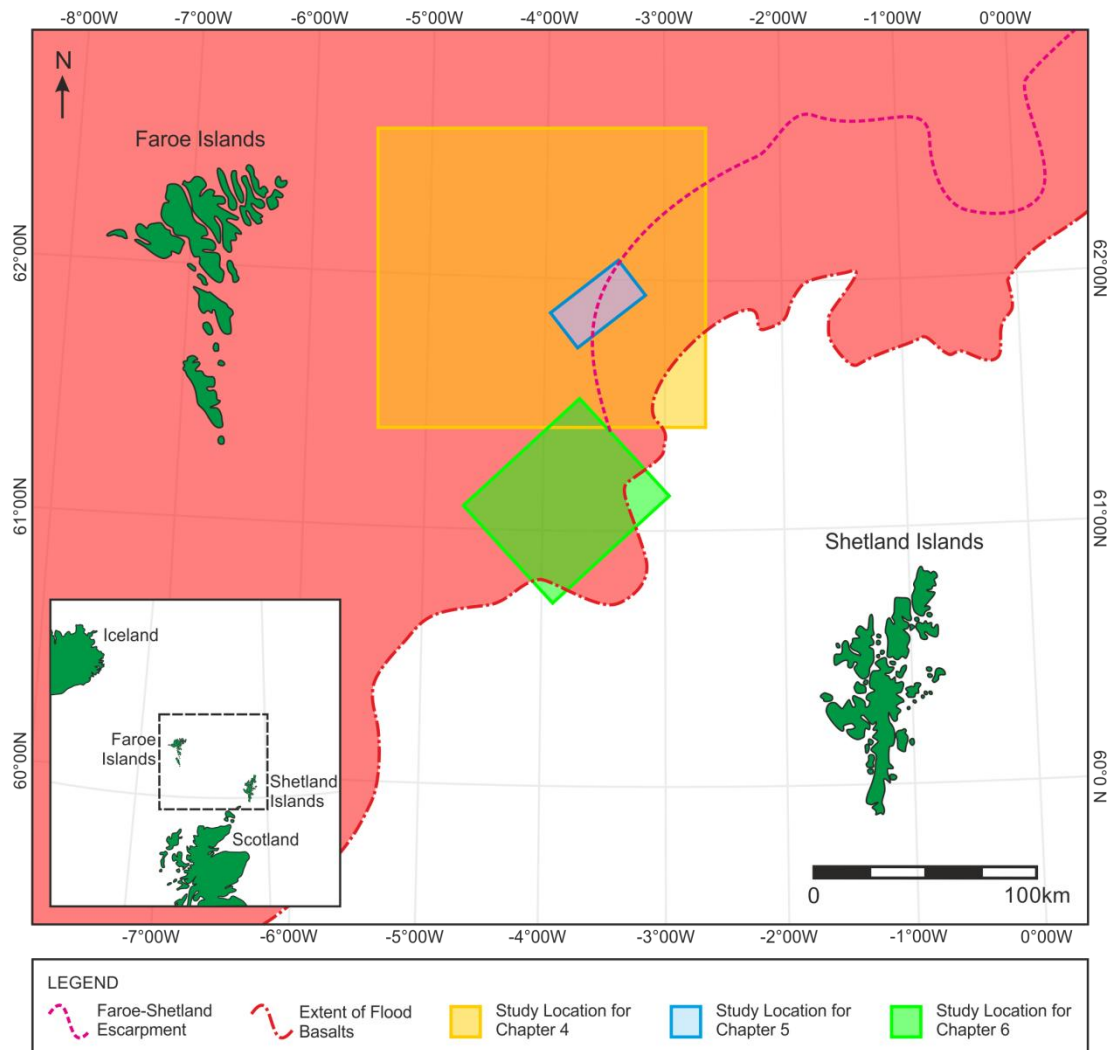
Fig. 1.2. Map of the Faroe-Shetland Basin showing the location of study areas of Chapters 4, 5 and 6. Extent of flood basalts and Faroe-Shetland Escarpment modified from Ritchie *et al.* (1996, 1999), Ellis *et al.* (2002) and Sørensen (2003).

CHAPTER 2: GEOLOGICAL SETTING

2.1 Introduction

The work presented in this thesis focuses on the North Atlantic Igneous Province and specific aspects of the Faroe-Shetland Basin. It is therefore appropriate to introduce the geological history of the Faroe-Shetland Basin, the regional tectonic setting of the Northeast Atlantic Margin and the volcanic products of the North Atlantic Igneous Province. The stratigraphy and structure of both the onshore and offshore continental flood basalts are described, and a brief overview of hydrocarbon exploration in the region is provided to place the research undertaken in this thesis in context.

2.2 The Northeast Atlantic Margin

The northeast Atlantic Margin is a volcanically rifted margin ~2600 km long and 200-800 km wide that encompasses Norwegian, Faroese, UK and Irish sectors (Ceramicola *et al*., 2005; Praeg *et al*., 2005). The margin formed as a result of multiple phases of extension between Greenland and Eurasia from the Mesozoic to the Early Cenozoic (Doré *et al*., 1999; Skogseid *et al*., 2000). Extensional movements are interpreted to have been initiated after the Caledonian orogeny, with post-orogenic collapse and formation of Carboniferous sedimentary basins (Doré *et al*., 1999; Sørensen, 2003). However little is known about these events because they are poorly resolved in seismic reflection data and have been overprinted by younger events (Doré *et al*., 1999). Extension occurred in the Permo-Triassic as a result of continental breakup of the supercontinent Pangea (Doré *et al*., 1999; Naylor *et al*., 1999). In the pre-northeast Atlantic Margin, the formation of Permo-Triassic sedimentary basins followed the regional trend created by the Caledonian fold belt. Deposition was controlled by northwest dipping faults which formed asymmetrical half-graben basins and was characterised by thick successions of continental sediments (Dean *et al*., 1999; Doré *et al*., 1999; Sørensen, 2003).

Extension continued into the Jurassic, with sea floor spreading in the Tethys to the southwest and the Central Atlantic to the northwest, with marine incursions flooding the Permo-Triassic basins in the Early to Middle Jurassic (Stoker *et al.* 1993; Doré *et al*., 1999; Sørensen, 2003). The majority of the Early to Middle Jurassic was removed by erosion that created a regional unconformity caused by a restricted seaway coupled with a decrease in

extensional tectonics and thermal subsidence on the northwest European Atlantic margin (Stoker *et al.* 1993; Doré *et al.*, 1999). Renewed rifting in the Late Jurassic formed sedimentary basins with an east to west regional trend and deposition characterised by anoxic marine conditions (Stoker *et al.* 1993; Lundin & Doré, 1997; Doré *et al.*, 1999). This led to the deposition of the organic rich Kimmeridgian mudstones which form the key source rock for hydrocarbon generation on the northeast Atlantic Margin (Lundin & Doré, 1997; Doré *et al.*, 1999; Sørensen, 2003). Rifting continued throughout the Cretaceous, with extension predominantly northeast to southwest as sea floor spreading ceased in the Tethys (Lundin & Doré, 1997; Dean *et al.*, 1999; Doré *et al.*, 1999). Deposition returned to oxic conditions during considerable syn-rift expansion and formed thick successions of coarse siliciclastic sediment. Middle Cretaceous uplift led to the shallowing of the basins, erosion and reworking of Late Cretaceous sands and increased siliciclastic input from the basin margins (Doré *et al.*, 1999; Naylor *et al.*, 1999).

By the Early Palaeocene, extension had culminated in continental breakup which was accompanied by widespread uplift and extensive volcanism that formed the North Atlantic Igneous Province (Eldholm & Grue 1994; Doré *et al.*, 1999; Hitz *et al.*, 1999; Skogseid *et al.*, 2000). Volcanism ceased when sea floor spreading became established in the Palaeocene, after which the margin was dominated by thermal subsidence (Skogseid *et al.*, 2000; Ceramicola *et al.*, 2005; Praeg *et al.*, 2005). Changes in the sea floor spreading geometry in the northeast Atlantic during the Late Palaeocene to Miocene caused a compressional phase of tectonic activity. This compression locally reactivated Mesozoic extensional faults and folded the overlying Late Palaeocene to Middle Miocene post-rift sediments into a series of northeast to southwest striking anticlinal domes (Boldreel & Anderson, 1993; Dean *et al.*, 1999; Ritchie *et al.*, 2003; 2008). The prolonged nature of extension along the northeast Atlantic Margin was due to the lateral migration of successive rift axes to the north through time (Fig. 2.1; Lundin & Doré, 1997; Doré *et al.*, 1999). This spatial evolution was controlled by the overall structural grain of the margin, which was inherited from the underlying crystalline basement and has been attributed to the Lewisian foreland of the Caledonian thrust belt (Dean *et al.*, 1999; Doré *et al.*, 1999; Skogseid *et al.*, 2000). The changes in the stress direction created by migration of rift axes over time and the influence of older, underlying basement structures produced a margin with a complex arrangement of rift basins and highs (Lundin & Doré, 1997; Doré *et al.*, 1999; Sørensen, 2003).
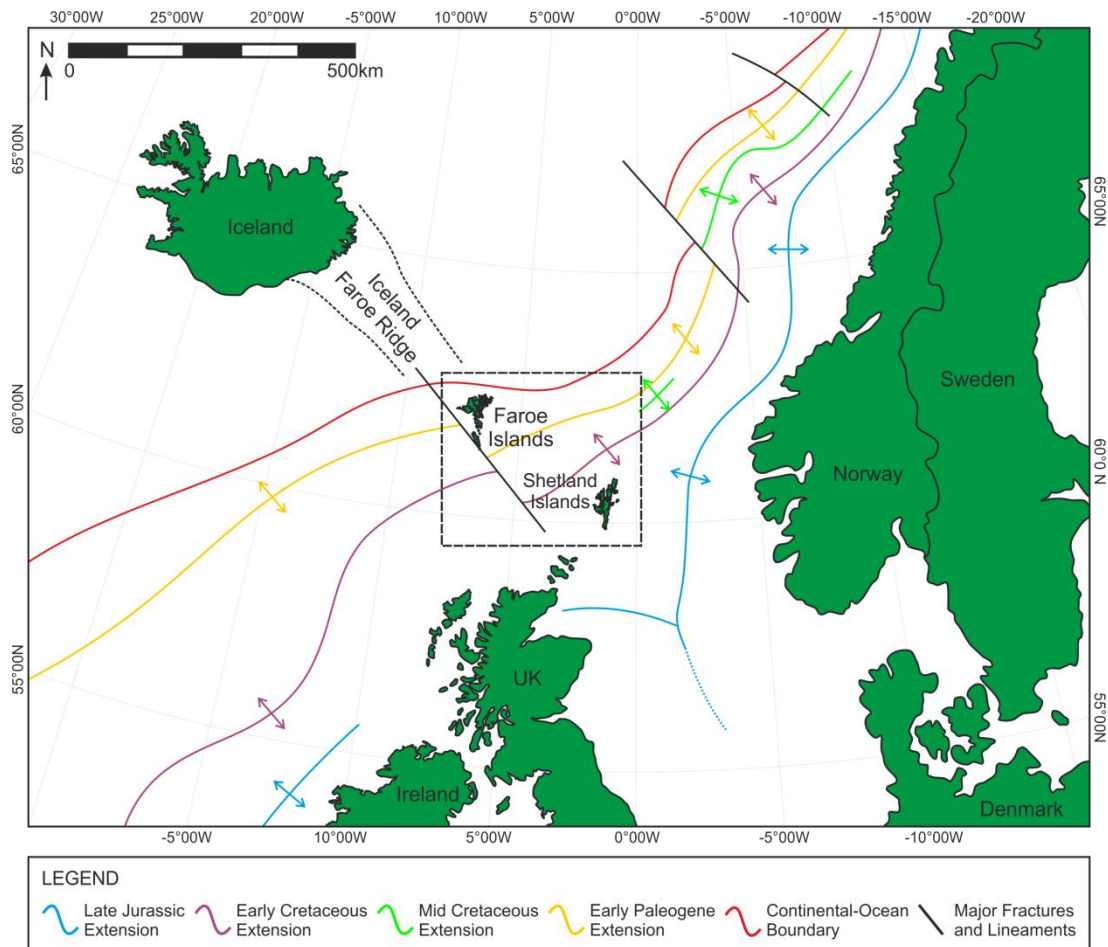
Fig. 2.1. Location of Northeast Atlantic Margin and the migration of successive rift axes though time. Modified from Lundin & Doré (1997) and Doré *et al*. (1999). Box indicates the location of the Faroe-Shetland Basin and Fig. 2.2.

2.3 The North Atlantic Igneous Province

Volcanic rifted margins are often associated with spatially constrained thermal anomalies in the upper mantle, which in the early stages are capable of producing extremely high melt production rates (White & McKenzie, 1989; Sheth, 1999; Jerram *et al*., 2005). The exact origin and form of these thermal anomalies is a matter of debate, with researchers ascribing it to either a plume (e.g. Campbell & Griffiths, 1990; Courtillot *et al*., 1999; Saunder *et al*., 2007) or a non-plume hypothesis (e.g. Anderson, 1994; King & Anderson, 1995; Sheth, 1999). The rifting of the northeast Atlantic Margin has generally been associated with the impingement of the proto-Icelandic plume at the base of the lithosphere (Nadin *et al*., 1997; Smallwood & White, 2002; Storey *et al*., 2007). However recent work that restored the North Atlantic Igneous Province to its original eruption

location has suggested that it was generated by plumes that rose from the D'' layer at the edges of fixed, low-velocity provinces and that the Icelandic plume was a much later event (Burke & Torsvik, 2004; Torsvik *et al.*, 2006; Ganerød *et al.*, 2010).

Despite uncertainty in the exact cause of rifting, the products of the North Atlantic Igneous Province are relatively well known. The minimum areal extent of the North Atlantic Igneous Province is estimated to be 1.3×10^6 km^2, with an eruptive volume of 1.8×10^6 km^3 and a total crustal volume (including erupted material and additions to the deeper crust) of 6.6×10^6 km^3 (Coffin & Eldholm, 1994; Eldholm & Grue, 1994). The province is characterised by predominantly basaltic subaerial lava flows, intrusive complexes and individual volcanic centres (White & McKenzie, 1989; Eldholm & Grue, 1994; Skogseid *et al.*, 2000). The volcanic eruptions occurred via spatially constrained fissures and vents, with the distribution of eruption sites and emplacement of volcanic rocks controlled by the arrangement of pre-existing topography, the presence of water bodies and local sedimentary systems (Coffin & Eldholm, 1992; Jerram & Widdowson, 2005; Ross *et al.*, 2005). As the province matured, localised volcanic centres began to develop and the volumes of material erupted decreased. These later stage eruptions are also associated with more silicic magmas, which are more explosive and less extensive and likely occurred due to the partial melting of either continental crust or sediments (Jerram & Widdowson, 2005; Ross *et al.*, 2005; Bryan & Ernst, 2008). Silicic volcanic rocks are often not recognised due to poor preservation following uplift and erosion (Bryan *et al.*, 2002; Bryan, 2007). However they have been identified along the margins of the North Atlantic Igneous Province, such as along the southeast Greenland margin, in northern Scotland and the Vøring Plateau (Sinton *et al.*, 1998 and references therein).

2.4 The Faroe-Shetland Basin

The Faroe-Shetland Basin is one of the many interconnected, northeast to southwest striking rift basins located along the northeast Atlantic Margin (Sørensen, 2003). It was greatly affected by the voluminous eruptions of the North Atlantic Igneous Province during the Palaeocene which emplaced extensive extrusive and intrusive volcanic rocks (Ritchie *et al.*, 1996; Naylor *et al.*, 1999; Ritchie *et al.*, 1999). During this time, sediment was sourced from the Scotland-Shetland platform to the east and deposited in a number of northeast to southwest striking sub-basins separated by structural highs (Fig. 2.2; Ritchie *et al.*, 1996;

1999; Andersen *et al*., 2000; Sørensen, 2003). These sub-basins have been affected by northwest to southeast trending rift-oblique lineaments, which are associated with abrupt changes in crustal structure. These lineaments are interpreted to have segmented the basins, controlling sediment transport and deposition (Jolley & Morton 2007; Ellis *et al*., 2009; Moy & Imber, 2009).
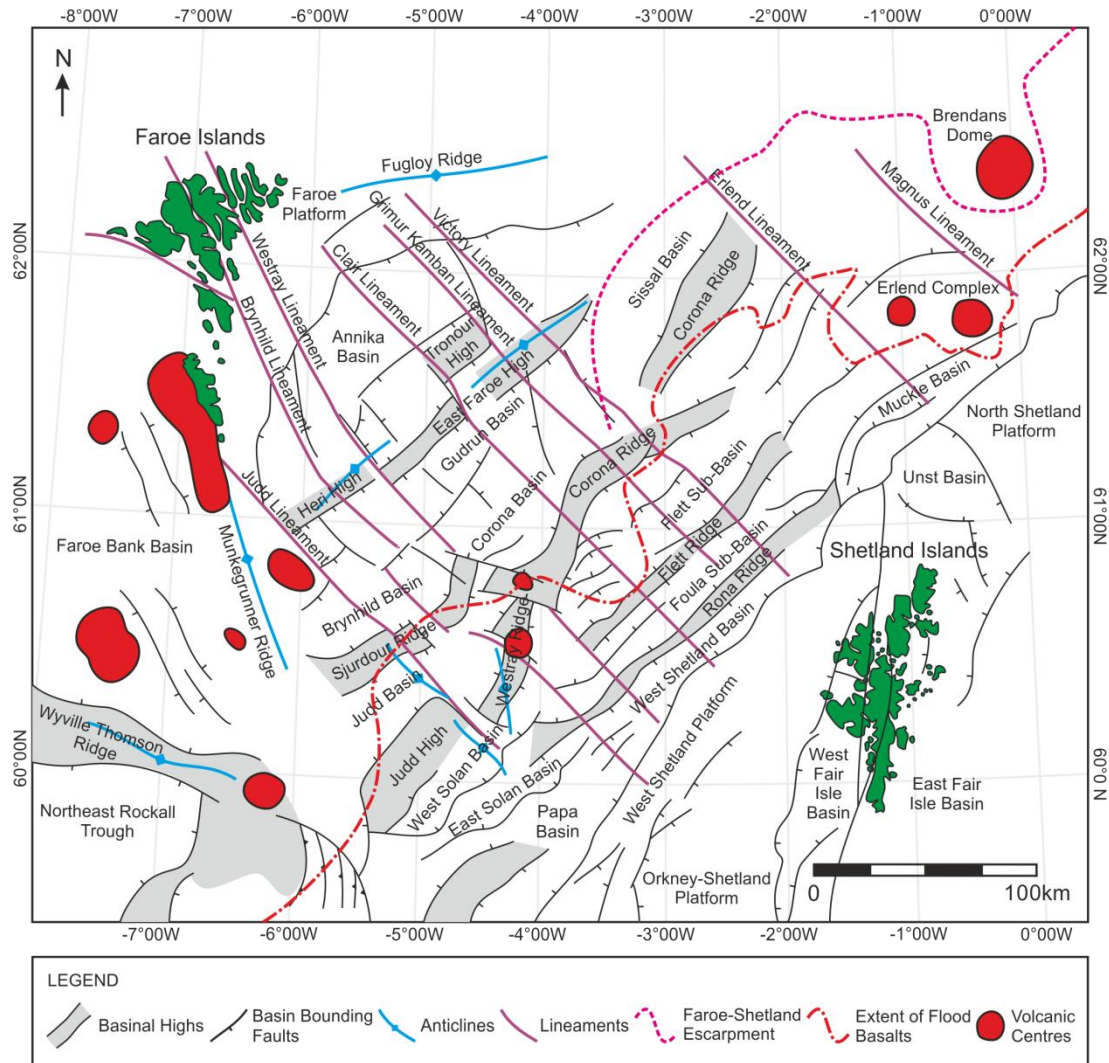
Fig. 2.2. Location and tectonic structure of the Faroe-Shetland Basin, with distribution of volcanic centres, extent of the continental flood basalts and the Faroe-Shetland Escarpment. Modified from Stoker *et al*. (1993), Ritchie *et al*. (1996, 1999), Sørensen (2003), Ellis *et al*. (2009) and Moy & Imber (2009).

2.5 Volcanic Rocks in the Faroe-Shetland Basin

2.5.1 Onshore Volcanic Stratigraphy

The volcanic products of the North Atlantic Igneous Province are found onshore in east Greenland, the east coast of Ireland, the west coast of Scotland and on the Faroe Islands (Larsen *et al*., 1999; Naylor *et al*., 1999; Hansen *et al*., 2009). On the Faroe Islands, the volcanic rocks have a thickness of ~6.6 km and have been subdivided on the basis of lithology, geochemistry and flow structure (Fig. 1.4; Ellis *et al*., 2002; Passey & Bell, 2007; Passey & Jolley, 2009). The onshore volcanic succession is penetrated by three wells, the Glyvursnes-1 borehole, which reached a depth of 700 m, Vestmanna-1 borehole, which reached a depth of 660 m and the Lopra 1/1A which reached a depth of >3500 m (Ellis *et al.*, 2002; Japsen *et al*., 2004; Passey & Bell, 2007)

The initiation of continental flood basalt volcanism is often recorded by thick basal deposits of volcaniclastic and hyaloclastic rocks which underlie the subaerial lava flows (Usktins Peate *et al*., 2003; Ross *et al*., 2005; Jerram *et al*., 2009). The Lopra Formation is composed of the oldest volcanic rocks penetrated by boreholes and is not exposed at the surface. The formation is composed of thick, subaqueous hyaloclastic breccias and subaerial lava flows and it is interpreted as the result of an initial phase of volcanism on the Faroe Islands (Fig. 2.3; Ellis *et al*., 2002; Passey & Bell, 2007; Passey & Jolley, 2009). The Beinisvørð Formation overlies the Lopra Formation and is composed of thick, subaerial lava flows that record the onset of extensive, voluminous flood basalt volcanism (Fig. 2.3). The formation was emplaced as multiple, pāhoehoe lava flow lobes which coalesced to form lava flow fields. The flows were fed by a continuous supply of lava from extensive fissure systems which allowed the flows to cover extensive areas (Self *et al.*, 1996; 1998; Jerram & Widdowson, 2005; Passey & Bell, 2007).

The Beinisvørð Formation was followed by a period of volcanic quiescence that led to the deposition of Prestfjall and Hvannhagi Formations which are composed of various siliciclastic and volcaniclastic rocks (Fig. 2.3; Passey & Bell, 2007; Passey & Jolley, 2009). Volcanism resumed with the emplacement of the Malinstindur Formation, which is composed of thin, subaerial lava flows which were emplaced as multiple, anastomosing and meandering, overlapping lava flows (Fig. 2.3). These lava flows were most likely erupted from localised igneous centres and record a change in the eruption style of the flood basalt province (Ellis *et al*., 2002; Passey & Bell, 2007; Passey & Jolley, 2009). After

emplacement of the Malinstindur Formation, a period of volcanic quiescence was recorded by the deposition of Sneis Formation which is composed of siliciclastic and volcaniclastic rocks (Fig. 2.3; Passey & Bell, 2007; Passey & Jolley, 2009). Volcanism resumed with the eruption of the Enni Formation, which is composed of a mixture of thick subaerial lava flows and multiple thin lava flows (Fig. 2.3). The presence of two types of lava suggests that the eruptions were switching between fissure systems and more localised igneous centres (Passey & Jolley, 2009).
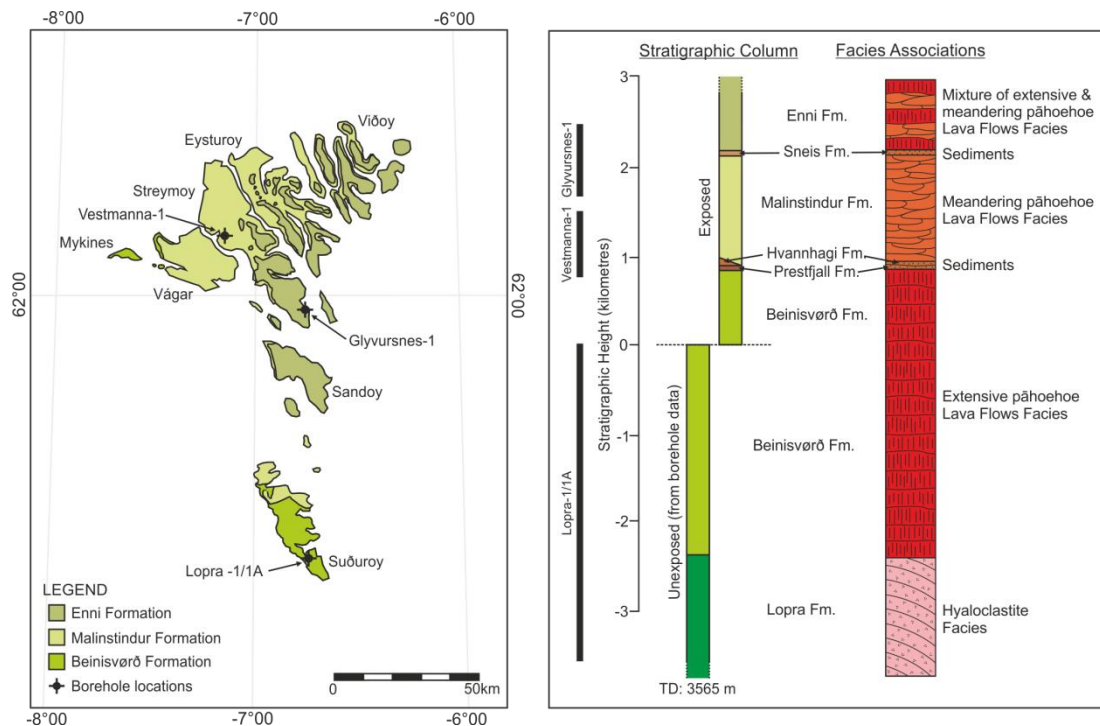
Fig. 2.3. Distribution of the Faroe Island Basalt Group on the Faroe Islands and stratigraphy compiled from both onshore and borehole data. Modified from Ellis *et al*. (2002), Passey & Bell (2007) and Passey & Jolley (2009).

2.5.2 Offshore Volcanic Stratigraphy

Offshore in the Faroe-Shetland Basin, the volcanic products of the North Atlantic Igneous Province have been mapped using seismic data, gravity and magnetic surveys (e.g. Gatliff *et al*., 1984; Boldreel & Andersen, 1994; Planke *et al*., 2000; Kimbell *et al*., 2004). Correlation between the offshore and onshore stratigraphy is difficult due to the difference in resolution between outcrop and seismic data. The offshore volcanic products in seismic reflection data can only be correlated chronostratigraphically (i.e. correlated in time). For example, two different lava flows can be erupted synchronously from different sources in the basin yet be at the same stratigraphic horizon, and so may be correlated as the same

lava flow. The correlation between the onshore and offshore volcanic products can be achieved by mapping the reflections to the onshore terminus where the outcrop formations are known. Greater resolution can be achieved if there are geochemical data available as lava flows erupted from different sources will have different geochemical signatures, while biostratigraphical data from associated sedimentary successions can also date and correlate erupted products and environments (e.g. Waagstein, 1988; Bell & Jolley, 1997; Larsen *et al.*, 1999; Jolley, 2009).

The offshore volcanic products exhibit distinctive seismic reflection geometries that are indicative of lithology and emplacement process. Much of the volcanism in the basin was extrusive, with the eruption of extensive subaerial lava flows which exhibit sub-horizontal, continuous and parallel seismic reflections (Fig. 2.4; Andersen, 1988; Planke *et al.*, 1999; 2000). These parallel bedded reflections have been mapped across the Faroe-Shetland Basin and onto the Faroese shelf where the onshore volcanic rocks outcrop. The parallel bedded reflections of the subaerial lava flows are also often interbedded with subparallel, chaotic and disrupted reflections that are interpreted to be volcaniclastic rocks (Fig. 2.5; Planke *et al.*, 1999; 2000). This indicates fluctuations in the depositional environment, as hyaloclastic breccias are indicative of a subaqueous environment, while the lava flows are indicative of a subaerial environment.
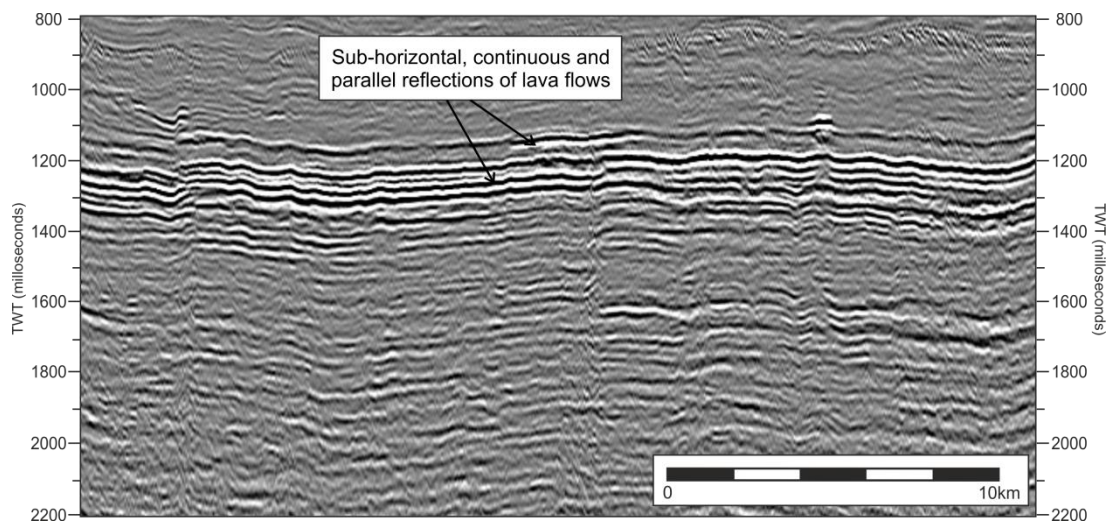
Fig. 2.4. Seismic reflection configurations of subaerial erupted lava flows which extend across much of the Faroe-Shetland Basin. Seismic data from this study.
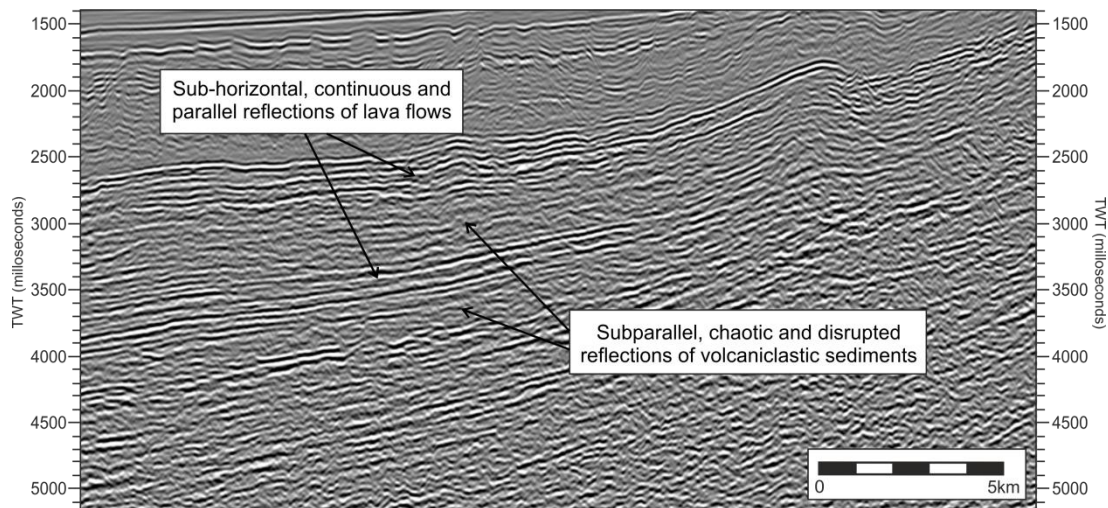
Fig. 2.5. Seismic reflection configurations of interbedded subaerial erupted lava flows and submarine emplaced hyaloclastic breccias and pillow basalts. Seismic data from this study.

More structured deposits of hyaloclastic breccias are found close to the centre of the Faroe-Shetland Basin where the sub-horizontal, continuous and parallel seismic reflections of the subaerial lava flows change to semi-continuous, inclined and prograding reflections (Fig. 2.6). These reflections created a prominent, gently curved structure across the basin known as the Faroe-Shetland Escarpment (Smythe, 1983; Smythe *et al.*, 1983; Ritchie & Hitchen, 1996). The escarpment is interpreted to be a lava-fed delta system which formed when the subaerial lava flows reached the palaeo-shoreline and produced steep, prograding foresets of hyaloclastic breccias (Smythe *et al.*, 1983; Kiørboe, 1999; Planke *et al.*, 1999; 2000; Spitzer *et al.*, 2008). Progradation of the delta system is thought to have been a function of large volumes of lava reaching the palaeo-shoreline and overwhelming the basin (Boldreel & Andersen, 1994).
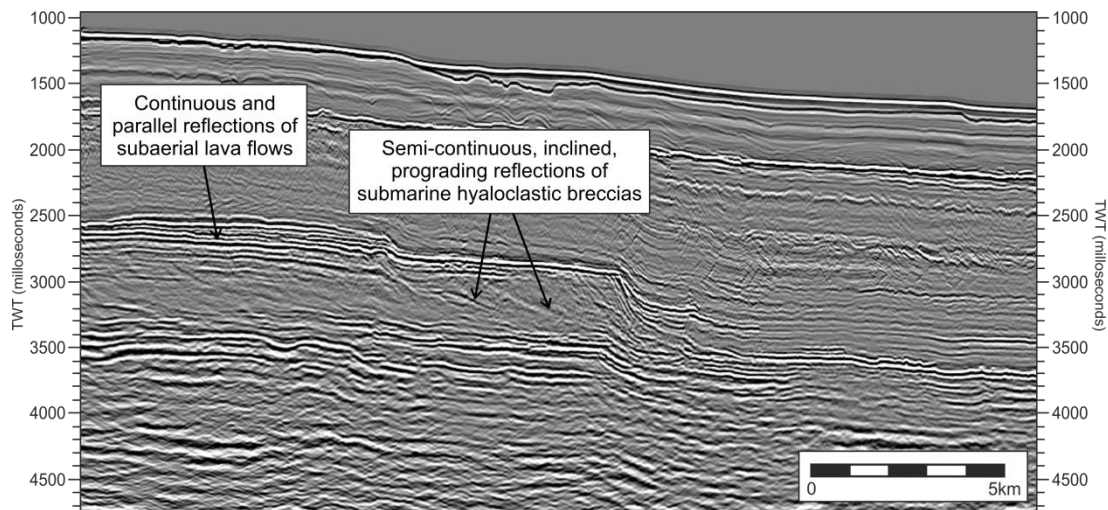
Fig. 2.6. Seismic reflection configurations of a lava-fed delta in the Faroe-Shetland Basin, with reflection geometries identifying the transition from subaerial lava flows to submarine hyaloclastic breccias. Seismic data from this study.

North of the Faroe Islands, the continental-ocean transition is characterised by seaward-dipping seismic reflections which exhibit inclined, smooth to hummocky geometries (Fig. 2.7). These reflections represent subaerial lava flows that were erupted during the early stages of sea floor spreading and are interbedded with thin volcaniclastic and fine siliciclastic rocks (Planke *et al.*, 1999). The subaerial lavas were erupted close to the axes of spreading, subsiding with age to form a wedge that thins away from the continental-ocean transition (Andersen, 1988; Hinz *et al.*, 1999; Planke *et al.*, 1999; 2000; Spitzer *et al.*, 2008). Seaward-dipping reflections represent the interplay of tectonism and magmatism where crustal growth occurred by the addition of volcanic rocks. After eruption they were affected by post-rift subsidence, with the greatest inclination seen in the oldest lava flows (Andersen, 1988; Planke *et al.*, 2000; Parkin *et al.*, 2007).
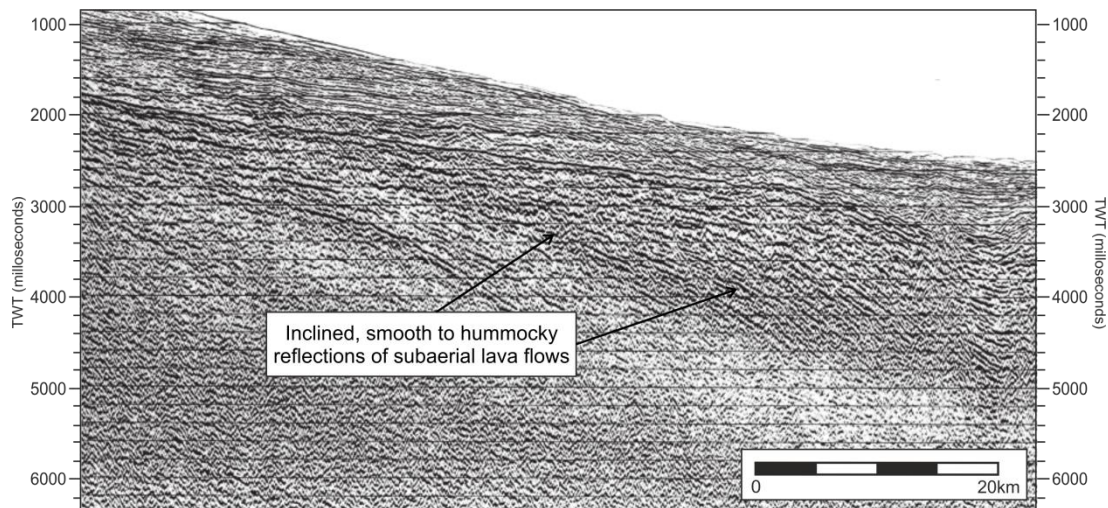
Fig. 2.7. Seismic reflection configurations of the seaward dipping reflections which were erupted as subaerial lava flows. Seismic data from Planke & Alvestad (1999).

Intrusive volcanic systems are common across the Faroe-Shetland Basin and along the Northeast Atlantic Margin, with the majority being related to the North Atlantic Igneous Province (Naylor *et al*., 1999; Ritchie *et al*., 1999; Sørensen, 2003). Individual volcanic centres have been identified using seismic reflection data, gravity surveys and magnetic surveys (e.g. the Erlend Complex and Brendans Dome; Chalmers & Western, 1979; Gatliff *et al*., 1984; Jolley & Bell, 2002). They are recognised by chaotic internal reflections that are truncated by high amplitude, parallel reflections and are interpreted to be eroded volcanic edifices with a nearly flat erosional upper surface (Fig. 2.8; Gatliff *et al*., 1984; Jolley & Bell, 2002). These structures are often circular and are surrounded by high amplitude, radial outward-dipping reflections which are interpreted as localised, subaerial lava flows sourced from the flanks of the volcanic edifice (Chalmers & Western, 1979; Gatliff *et al*., 1984; Ritchie & Hitchen, 1996; Jolley & Bell, 2002).
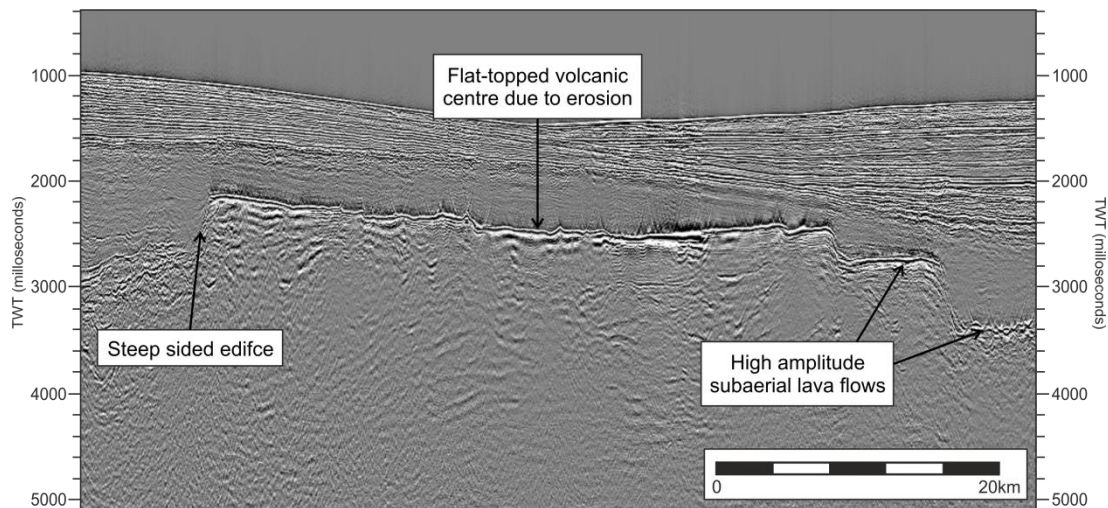
Fig. 2.8. Seismic reflection configurations of an eroded volcanic centre of the Erlend Complex with associated subaerial lava flows. Seismic data from this study.

Extensive intrusive systems including widespread sill and dyke complexes underlie most of the Faroe-Shetland Basin. The dykes are poorly imaged because vertical structures are largely invisible on seismic reflection data, but the sills are clearly visible and exhibit a range of geometries from coherent, concave-up saucer shapes to discordant sheets (Fig. 2.9; Trude, 2004; Hansen & Cartwright, 2006a; Thomson & Schofield, 2008; Hansen *et al.*, 2011). Where sills were shallowly emplaced, they formed ridged and rugose surface morphologies which are thought to be have formed as a direct result of the sill propagation mechanism. The emplacement of the sills is interpreted to have been strongly influenced by the viscosity of the magma and the interaction with the host sediment, which was most likely water-saturated. This resulted in a peperitic top surface and produced morphologies similar to those seen in subaerial lava flows (Trude, 2004). Shallowly emplaced sills have also been linked to the formation of submarine, hyaloclastite-dominated vents on the contemporaneous basin floor (Bell & Butcher, 2002; Davies *et al.*, 2002). Alternatively, shallowly emplaced sills can "jack up" the overlying sea floor, creating forced folds with sedimentary deposition onlapping the structure above the location of the sill (Trude *et al.*, 2003; Hansen & Cartwright, 2006b; Moy *et al.*, 2009). Where sills were emplaced at a deeper level, hydrothermal vent complexes formed above the crests and over edges of the sills. They are fed by sub-vertical chimneys formed by fracturing, transport and eruption of hydrothermal fluids and sediments (Bell & Butcher, 2002; Planke *et al.*, 2005; Hansen, 2006).
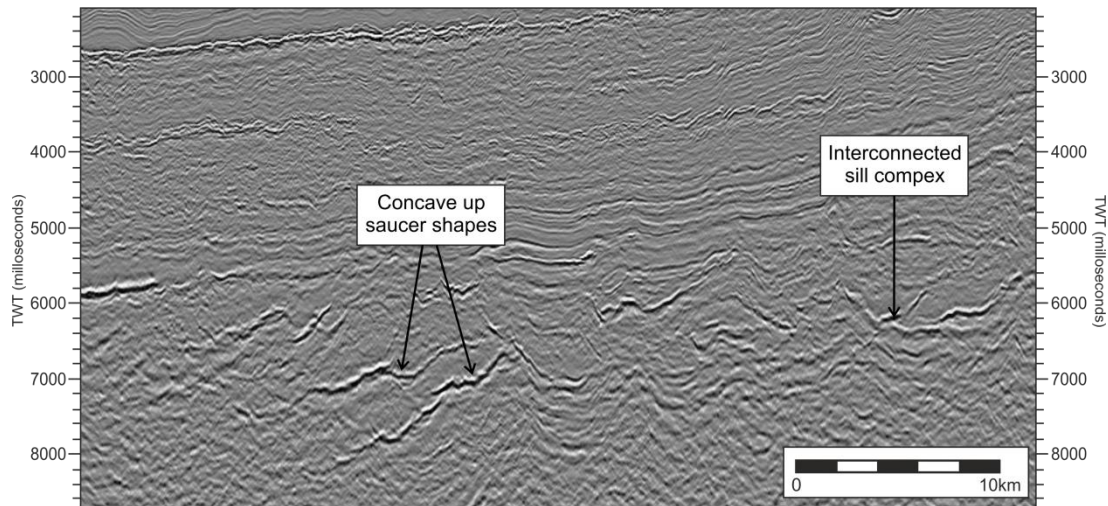
Fig. 2.9. Seismic reflection configurations of intrusive, saucer-shaped sills. Seismic data from this study.

2.6 Hydrocarbon Exploration

Hydrocarbon exploration in the Faroe-Shetland Basin began with geophysical surveys in the 1960's, and exploration wells in the 1970's (Larsen *et al*., 2010). To date, more than 160 wells have been drilled, predominantly in shallow water at the basin margins and beyond the extent of the lava flows (Fig. 2.10; Davies *et al*., 2004). The dominant source rocks are from the Upper Jurassic Kimmeridge Clay Formation, with a minor contribution from Middle Jurassic shales (Doré *et al*., 1997; Parnell *et al*., 1998; Lamers & Carmichael, 1999). The progressive burial in the Faroe-Shetland Basin through the Late Mesozoic meant that Jurassic source rocks became increasingly mature (Parnell *et al*., 1998; Spencer *et al*., 1999). Early exploration primarily targeted the Palaeozoic and Mesozoic pre- and syn-rift siliciclastic successions associated with tilted fault blocks at the basin margins (Lamers & Carmichael, 1999; Larsen *et al*., 2010). This led to the 1977 discovery of hydrocarbons in the fractured basement and Devonian-Carboniferous sandstones of the Clair field (Fig. 2.10; Lamers & Carmichael, 1999; Larsen *et al*., 2010; Witt *et al*., 2010).

Exploration waned in the 1980's due to a lack of success but was revived in the early 1990's with the discovery of hydrocarbons in the Triassic sandstones of the Strathmore field and the Jurassic sandstones of the Solan field (Fig. 2.10; Herries *et al*., 1999; Larsen *et al*., 2010). Discoveries of hydrocarbons were also made in the Early Cretaceous sandstones of the Victory field and the Palaeocene sandstones of the Laggan, Laxford and Torridon fields (Fig.

2.10; Goodchild *et al.*, 1999; Lamers & Carmichael, 1999; Gordon *et al.*, 2010; Larsen *et al.*, 2010). Recent exploration has targeted combined structural and stratigraphic traps in the Palaeogene (Davies *et al.*, 2004; Smallwood *et al.*, 2004; Loizou *et al.*, 2006), with discoveries of hydrocarbons in the Palaeocene sandstones of the Foiaven, Schiehallion and Loyal fields (Fig. 2.10; Cooper et al., 1999; Lamers & Carmichael, 1999; Leach *et al.*, 1999; Davies *et al.*, 2004). Sub- and intra-basalt siliciclastic reservoirs have also been identified, with significant hydrocarbons discoveries in thick interbedded sandstones between Palaeocene lava flows in Tobermory, Cambo, Rosebank, Laggan-Tormore and Glenlivet fields (Fig. 2.10; Larsen *et al.*, 2010; Gordon *et al.*, 2010).

Hydrocarbon exploration is currently targeting both the deeper water areas of the basin and the thicker and more complete Palaeocene successions, with exploration wells being drilled into and through the flood basalts (Jowitt *et al.*, 1999; Lamers & Carmichael, 1999; Sullivan *et al.*, 1999). Interpretation of the petroleum accumulations is challenging, as many of the prospects involve siliciclastic reservoirs above, below or interbedded the Palaeocene lava flows (Rohrman, 2007; Davison *et al.*, 2010). This is because the primary exploration tool is seismic reflection data and seismic imagining and interpretation of volcanic rocks is fraught with difficulties (Roberts *et al.*, 2005; Gallagher & Dromgoole, 2008; Nelson *et al.*, 2009a). Volcanic rocks have complex internal structures and lithological heterogeneities which causes a loss of seismic energy by attenuation and absorption of the seismic wave. This means there is relatively little energy returning from within and below the volcanic succession (Nelson *et al.*, 2008; Planke *et al.*, 2000; White *et al.*, 2003; Spitzer *et al.*, 2005).

Without constraints on the thickness, distribution and variation of volcanic products of the continental flood basalts across the Faroe-Shetland Basin, there remains much uncertainty about the thickness and lateral distribution of siliciclastic reservoirs, the reservoir quality and the hydrocarbon migration and trapping mechanisms (Verstralen & Hurst, 1994; Rohrman, 2007). The need to better understand the distribution and variations of the volcanic rocks across the Faroe-Shetland Basin is the driving force behind this study. By understanding the emplacement mechanism and the variations of volcanic rocks of the North Atlantic Igneous Province, we can better assess how the volcanic rocks impacted basin development, identify potential areas of interest and decrease the risk of drilling dry exploration wells.
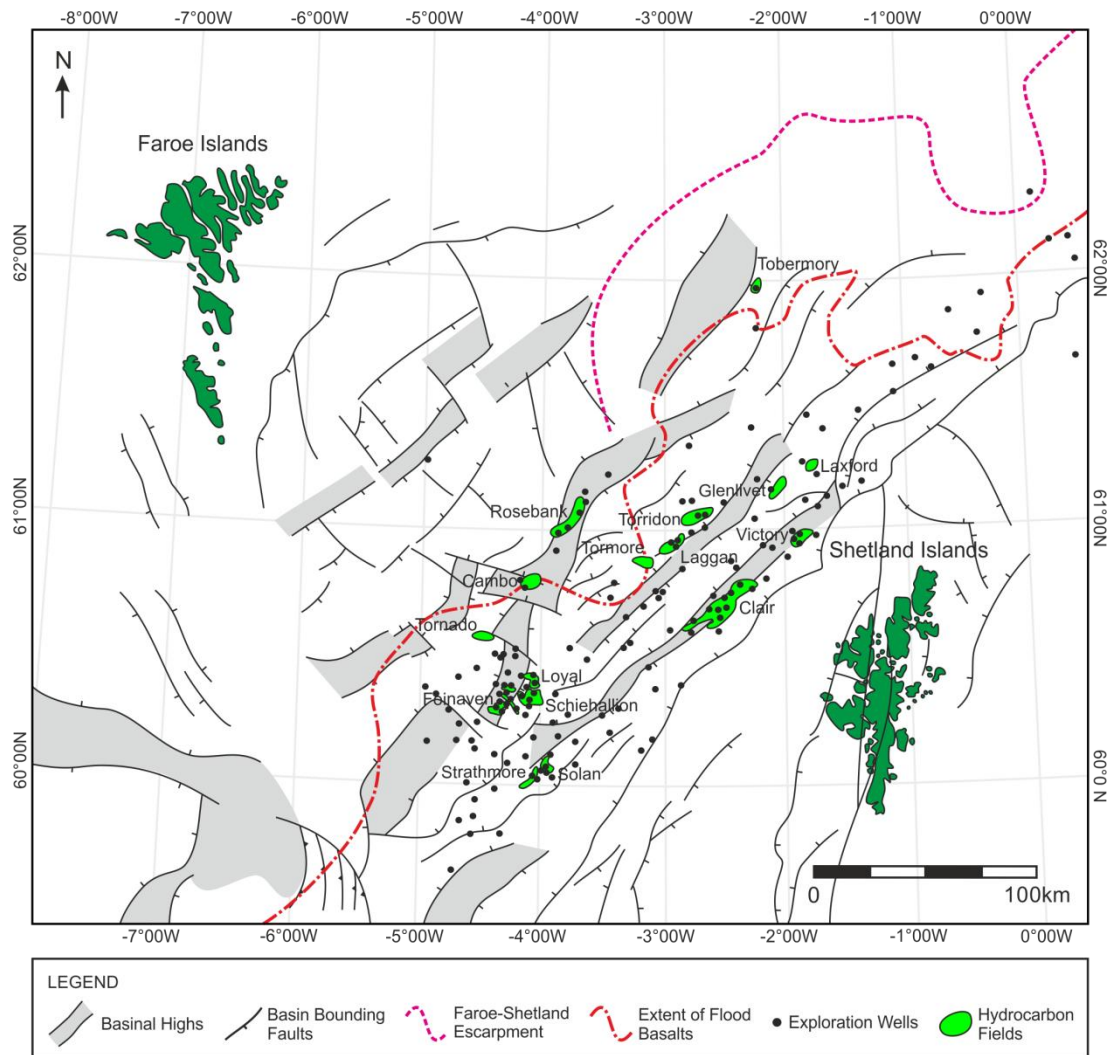
Fig. 2.10. Hydrocarbon exploration within the Faroe-Shetland Basin to date. Modified from Lamers & Carmichael (1999), Goodchild *et al*. (1999), Davies *et al*. (2004), Smallwood *et al*. (2004; 2005), Gordon *et al*. (2010) and Witt *et al*. (2010).

CHAPTER 3: DATA AND METHODOLOGY

3.1. Introduction

Seismic reflection data are primarily used by the petroleum industry to image and interpret the subsurface in order to reduce the risk of failure during hydrocarbon exploration (e.g. Nestvold, 1996; Hart, 1999; Stewart & Holt, 2004; Rohrman, 2007). A number of offshore basins that have been the target of seismic imaging have been found to contain significant amounts of volcanic rocks. This has provided a unique opportunity to study the buried, large-scale morphologies and structure of volcanic provinces that may not be accessible, or are no longer preserved at the Earth's surface (Cartwright & Huuse, 2005; Davies & Posamentier, 2005; Posamentier *et al*., 2007). This thesis is one such study and this chapter outlines the data, methodology and software used to understand the distribution, stratigraphy and morphology of the continental flood basalts of the Faroe-Shetland Basin.

3.2. The Fundamental Concepts of Seismic Reflection Data

The seismic reflection method is a geophysical technique used to image the subsurface using compressional acoustic waves. These acoustic waves are typically generated from a controlled high energy source (such as an explosion or air gun) at the Earth's surface or a few metres below the sea surface (Kearey *et al*., 2002; Bacon *et al*., 2007). The acoustic waves propagate through the subsurface, with a proportion returning to the Earth's surface, having been reflected or refracted at different geological interfaces (Fig. 3.1; Kearey *et al*., 2002; Bacon *et al*., 2007). The returning acoustic waves are collected by receivers located away from the source which measure the travel time of the wave from the source, through the subsurface to the receiver (Kearey *et al*., 2002; Bacon *et al*., 2007). Seismic reflection surveys can be conducted both onshore and offshore, with the surveys used in this study undertaken to understand offshore regions.
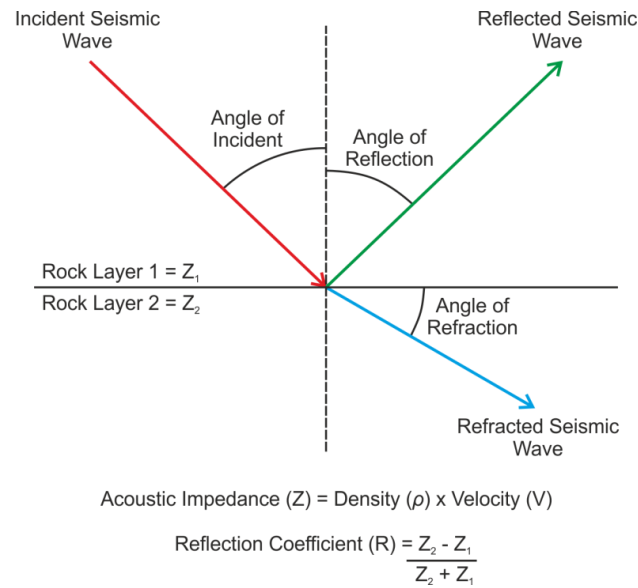
Fig. 3.1. Schematic diagram showing the reflection and refraction angles of the acoustic wave at a geological interface. Based on Snell's Law of Reflection which is a mathematical description of reflection, as the seismic wave travels from one medium to another and states that the incident and reflected angles will be identical, after Sheriff & Geldart (1995), Kearey *et al*. (2002) and Ashcroft (2011).

Seismic reflection data primarily record changes in the acoustic impedance of the subsurface as acoustic waves propagate through, and interact with, different geological interfaces (Fig. 3.1). Seismic velocities and densities depend upon the composition, texture, porosity and pore fluids of the rock, all of which can vary in three dimensions (Kearey *et al*., 2002). Therefore the velocity of the seismic wave changes depending on the rock layer it is propagating through. At the boundary between the different rock layers the seismic wave is converted into reflected and refracted waves (Fig. 3.1). The change in the velocity of the seismic wave produces an acoustic impedance contrast, while the reflection coefficient is a measure of the physical change in the direction of a wave and its velocity as it travels from one rock layer to another (Fig. 3.1; Kearey *et al*., 2002; Ashcroft, 2011). Both are important in identification of the structure of the subsurface and in calculating the velocities and densities of the rock layers. Seismic reflection data fall into three categories based on their survey geometries and end products;

2-dimensional (2D) Seismic Reflection Data were first developed in the 1920's, advancing slowly until the 1950's and through to the present day (Sheriff & Geldart, 1995). They are usually acquired as parallel and orthogonal seismic lines, often kilometres apart and effectively produces cross sections through the subsurface (Kearey *et al*., 2002; Davies *et*

al., 2004; Cartwright & Huuse, 2005). Correlation of 2D seismic lines enables a basic framework of the subsurface to be produced; however the distance between the seismic lines limits the scale of the resolvable structures (Fig. 3.2; Cartwright & Huuse, 2005).

3-dimensional (3D) Seismic Reflection Data were developed in the 1970's and are acquired from multiple, closely spaced lines, commonly 12.5 – 25 m apart that provide regular, grid-like, data point spacing (Nestvold, 1996; Davies *et al.*, 2004; Davies & Posamentier, 2005). This produces an almost continuous 3D cube of the subsurface that can be viewed from any angle or position (Bacon *et al.*, 2007). 3D seismic reflection surveys allow large geographical areas, often thousands of square kilometres, to be quickly imaged and mapped, while more subtle, smaller scale features can be identified and analysed in great detail (Fig. 3.2; Davies *et al.*, 2004; Cartwright & Huuse, 2005; Bacon *et al.*, 2007).

4-dimensional (4D) Seismic Reflection Data, otherwise known as Time-Lapse Seismic Reflection Data, are a recent advancement in seismic reflection technology and were developed in the 1990's (Brown, 2005). Multiple 3D seismic reflection surveys are acquired at different times over the same location to assess changes in the subsurface, such as extraction from a producing hydrocarbon reservoir (Kearey *et al.*, 2002; Bacon *et al.*, 2007; Brown, 2005). 4D seismic reflection data have not been used in this study and will not be discussed further.
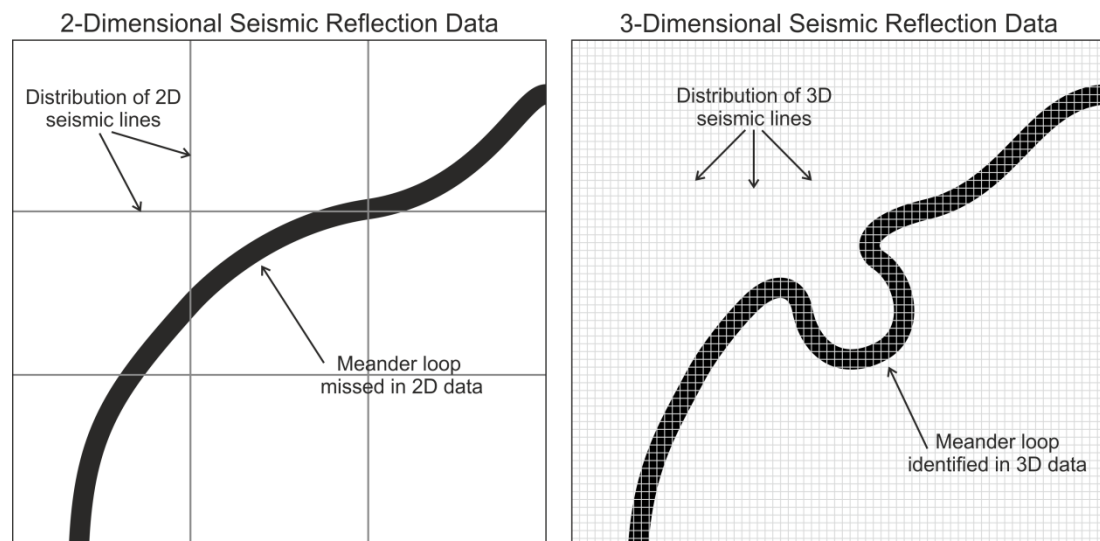
Fig. 3.2. Schematic diagram illustrating the differences between 2D and 3D seismic data and the advantages of interpreting geological features, such as a channel system, using 3D data. The geographical spread of the 2D data misses the meander loop of the channel which is captured by the 3D data, after Brown (2005) and Cartwright & Huuse (2005).

3.2.1 Acquisition of Seismic Reflection Data

All seismic reflection surveys are based on the principle of that acoustic waves generated at the Earth's surface are reflected and refracted by the subsurface. In general, 2D seismic reflection data are acquired by towing a single energy source and receiver array behind a survey ship (Fig. 3.3; Sheriff & Geldart, 1995; Bacon *et al*., 2007; Ashcroft, 2011). In contrast, 3D seismic reflection data are acquired by multi-cable surveys where up to 12 receiver arrays, each 4-8 km long are deployed at once. Multiple sources are also used and are fired at different intervals (Fig. 3.4; Sheriff & Geldart, 1995; Bacon *et al*., 2007; Ashcroft, 2011). Paravanes are hydrofoils which are towed behind the survey ship to control the head of the receiver cable because it is important that the position of the receivers to the source is known at all times, especially when towing multiple, kilometre long cables (Bacon *et al*., 2007).
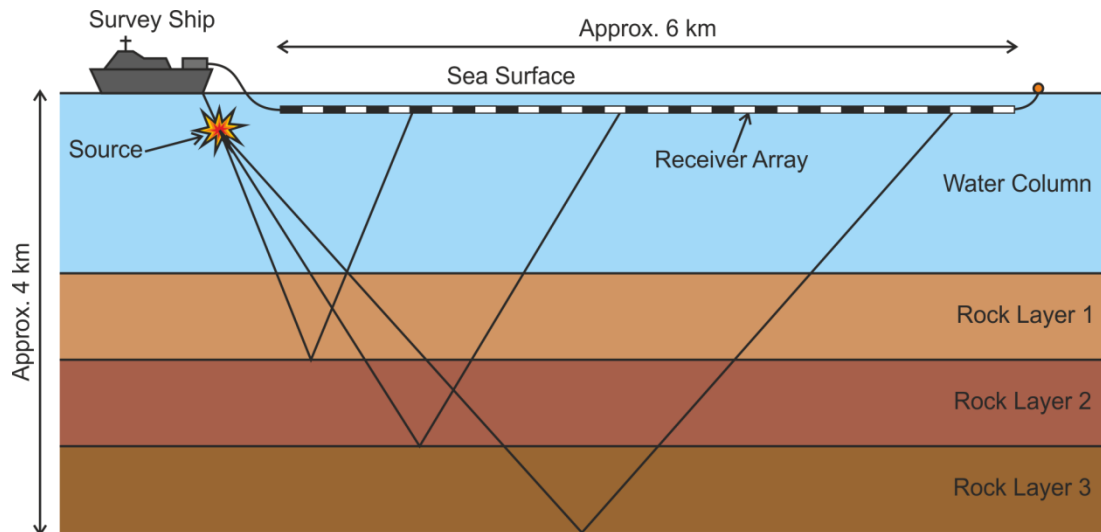
Fig. 3.3. Schematic diagram of marine acquisition of seismic reflection data, and is the typical methodology to collect 2D data. An acoustic wave is emitted from a sound source towed by the survey ship, propagates through the water column and the subsurface where the wave is reflected back and recorded by the receivers, after Bacon *et al*. (2007). Not to scale.
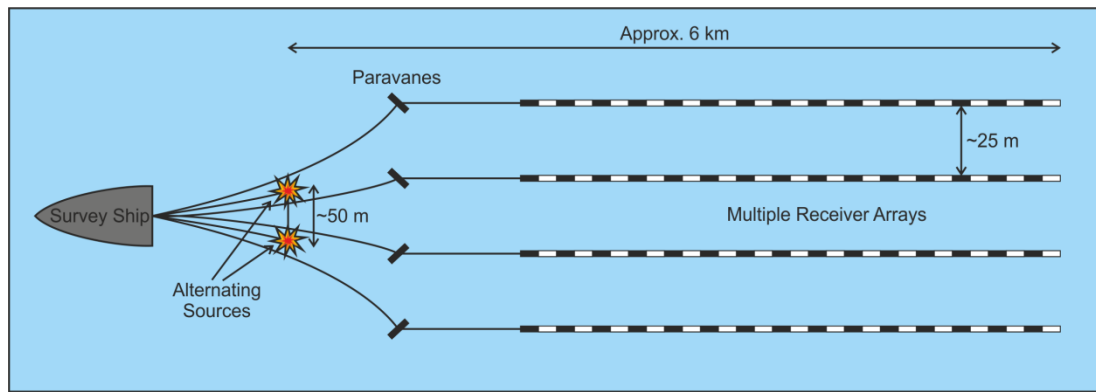
Fig. 3.4. Schematic diagram depicting the typical methodology for the acquisition of 3D seismic reflection data, where acoustic waves are emitted from multiple sound sources and are recorded by multiple receivers, after Bacon *et al.* (2007) and Ashcroft (2011). Not to scale.

Once the seismic reflection data have been collected, they must be processed. The objective of processing is to refine the data and make the resulting seismic reflections more apparent by enhancing the seismic signal, reducing noise and correcting for any physical processes that may have affected the data (Sheriff & Geldart, 1995; Kearey *et al.*, 2002). Seismic noise results from any physical process that interferes with the seismic data and is typically due to scattering of the seismic wave from near surface irregularities, heterogeneous lithologies and extraneous acoustic sources such as waves, earthquakes and vehicles (Sheriff & Geldart, 1995). The data will often go through several phases of processing and the result is highly dependent on the processer and the choice of parameters defined by the contractor (Bacon *et al.*, 2007). Therefore only the typical processing steps for both 2D and 3D seismic reflection data are briefly described;

Static Correction shifts the seismic trace to compensate for any near-surface effects such as irregular topography, differences in the elevation between the sources and receivers and delays in the time between firing the source and the start of recording seismic waves (Yilmaz & Doherty, 1987; Sheriff & Geldart, 1995; Kearey *et al.*, 2002).

Deconvolution removes distortion from the data, such as the source wavelet and multiples, to improve the signal-to-noise ratio and increase resolution (Yilmaz & Doherty, 1987; Sheriff & Geldart, 1995; Kearey *et al.*, 2002).

Frequency Filtering uses algorithms with defined parameters to eliminate unwanted parts of the data based on frequency or amplitude to enhance the signal-to-noise ratio (Yilmaz & Doherty, 1987; Sheriff & Geldart, 1995; Kearey *et al.*, 2002).

Normal Moveout compensates for the effect of separation in travel time between the seismic sources and the receivers for horizontal reflections (Yilmaz & Doherty, 1987; Sheriff & Geldart, 1995; Kearey *et al.*, 2002).

Dip Moveout compensates for the effects of separation in travel time between the seismic sources and the receivers for dipping reflections (Yilmaz & Doherty, 1987; Sheriff & Geldart, 1995; Kearey *et al.*, 2002).

Stacking corrects for the different arrival times of the seismic wave from their various offsets produced by the time-distance relationship between the seismic sources and the receivers, as determined by normal moveout (Yilmaz & Doherty, 1987; Sheriff & Geldart, 1995; Kearey *et al.*, 2002).

Migration repositions the seismic reflection events to their correct temporal and spatial location at the Earth's surface rather than the recorded location, which is offset due to the propagation of the seismic wave (Yilmaz & Doherty, 1987; Sheriff & Geldart, 1995; Kearey *et al.*, 2002).

Interpretation of the seismic reflection data is partly dependant on the methodology used to process the data, and advancements in the acquisition and processing technology of seismic reflection data have led to the reprocessing of vintage datasets. Alternatively reprocessing can be undertaken to better understand features that may have been removed during processing (such as very high or very low frequencies) or when multiple seismic reflection surveys are being merged together (Bacon *et al.*, 2007).

3.2.2 Resolution of Seismic Reflection Data

The resolution of seismic reflection data limits the size of geological structures that can be recognised in the data, and is affected by attenuation, the signal-to-noise ratio and formation thickness (Sheriff & Geldart, 1995; Bacon *et al.*, 2007). The typically recorded seismic frequency range is 5 to 150 hertz, with highest frequencies producing higher resolution as the seismic wave is reflected back from the shallow subsurface (Sheriff & Geldart, 1995; Bacon *et al.*, 2007). The dominant frequency of the seismic wave decreases with depth due to absorption and attenuation, which coupled with increasing velocity as

the sediment becomes compacted, results in poor resolution in the deeper parts of the subsurface (Sheriff & Geldart, 1995; Kearey *et al.*, 2002). The key parameters in calculating the resolution of the data are the wavelength (λ) of the dominant frequency (*f*) propagating through the subsurface and the velocity (V) of the wave;

$$\frac{V}{f} = \lambda$$ **Eq. 3.1**

Horizontal Resolution (R_H) is the resolution of the seismic reflection data on the horizontal axis (x, y) and relates to how far apart two structures on a single interface must to be in order, to be recognised as two individual structures rather than one (Sheriff & Geldart, 1995; Kearey *et al.*, 2002; Bacon *et al.*, 2007). It is calculated by;

$$R_H = \frac{\lambda}{2}$$ **Eq. 3.2**

Vertical Resolution (R_V) is the resolution of the seismic reflection data on the vertical axis (z) and relates to how far apart, in either time or space, two interfaces have to be to be recognised as two different reflections rather than one (Sheriff & Geldart, 1995; Kearey *et al.*, 2002; Bacon *et al.*, 2007). It is calculated by;

$$R_V = \frac{\lambda}{4}$$ **Eq. 3.3**

Resolution is also dependant on the quality of the data and can often be improved by careful processing. Horizontal resolution can be improved by migration, but there is a risk that even minor errors will severely degrade the result (Sheriff & Geldart, 1995; Bacon *et al.*, 2007). Vertical resolution can be improved by deconvolution which removes the lower frequencies, but there is a risk that data from the deeper structures will be lost (Kearey *et al.*, 2002; Bacon *et al.*, 2007). Recognition of structures below the resolution limit is possible if they are large enough in only one dimension, such as either the horizontal or vertical resolution limit (Sheriff & Geldart, 1995). It is also possible to identify features that, although not recognisable in the data themselves, still produce subtle effects or patterns, such as changes in the amplitude of the reflected wave (Sheriff & Geldart, 1995).

3.2.3 Polarity of Seismic Reflection Data

The polarity of the seismic reflection data relates to the change in acoustic impedance and is characterised by the position of the negative and positive portions of the seismic wave (Sheriff & Geldart, 1995). All seismic data in this thesis are displayed using the Society of Exploration Geophysists normal convention, which is otherwise known as positive standard polarity. In the seismic reflection data, a negative polarity is caused by a decrease in the

acoustic impedance as the seismic wave travels from a high velocity and density material to a low velocity and density material (Fig. 3.5). Conversely, a positive polarity is caused by an increase in the acoustic impedance as the seismic wave travels from a low velocity and density material to a high velocity and density material (Fig. 3.5).
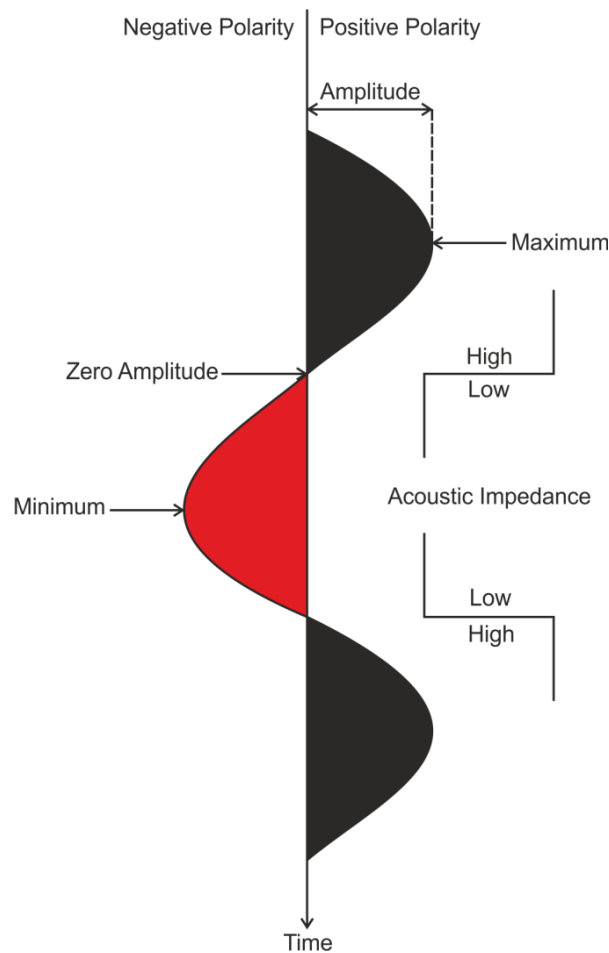
Fig. 3.5. Schematic diagram depicting the polarity of the seismic wave and its relationship to changes in acoustic impedance, after Sheriff & Geldart (1995) and Brown (2005). The polarity displayed in the diagram is the Society of Exploration Geophysists normal convention polarity, where a positive polarity is caused by a change in the acoustic impedance as the seismic wave travels from a low acoustic impedance material to a high acoustic impedance material.

3.2.4 Volcanic Rocks in Seismic Reflection Data

Seismic reflection data provide good images of the subsurface when it consists of layered sedimentary formations. However the presence of volcanic rocks in the subsurface can have a significant impact on seismic reflection data and consequently imaging through and below volcanic rocks can be difficult (Roberts *et al*., 2005; Gallagher & Dromgoole, 2008;

Nelson *et al*., 2009a). Where the volcanic rocks are relatively thin, such as at the distal extents of lava flows or in intrusive sills, the seismic reflection data may undergo a degree of distortion, but clear seismic reflections can still be identified below (Richardson *et al*., 1999; White *et al*., 2003). Where the volcanic rocks are much thicker, the impact is more dramatic, and they greatly distort the seismic reflection data and mask many of the underlying reflections (White *et al*., 2003; Spitzer *et al*., 2005).

Volcanic rocks have high velocities and densities while the overlying sedimentary rocks have lower velocities and densities. This produces a significant impedance contrast and causes a loss of seismic energy by scattering, attenuation and absorption of higher frequencies (Ogilvie *et al*., 2001; Shaw *et al*. 2008; Nelson *et al*., 2009a). Further scattering attenuation and absorption of the wavelength is caused by the internal heterogeneity of interbedded lava flows and sediments, which produce a large number of internal reflections (Maresh & White, 2005; Maresh *et al*. 2006; Shaw *et al*. 2008). Imaging is also complicated by the production of seismic multiples, which are excess reflections that appear as separate events and distort the data. They are caused by "seismic ringing" or a repetition of the seismic wave as it reverberates between the top of the volcanic rocks and the sea surface and within the volcanic rocks themselves (Fliedner & White, 2001; Nelson *et al*., 2009a). Multiples can be identified as they often cross cut reflections and typically have lower amplitudes than primary reflection, as the seismic wave loses energy each time it interacts with a geological interface (Sheriff & Geldart, 1995; Kearey *et al*., 2002).

Seismic profiles are often displayed in two-way time from the surface. The velocity contrast between the volcanic rocks and sediments can distort the geometries of the resulting seismic reflections, and therefore affect the two-way time section. Seismic pull-up can occur when a formation or structure with a low seismic velocity is overlain or surrounded by a formation with a high seismic velocity (Fig. 3.6). The travel time of the seismic wave through the high velocity formation is faster and reaches the receivers on the surface more quickly than the seismic waves returning from the surrounding material, making it appear as if the structure is closer to the surface than it really is (Sheriff & Geldart, 1995). Conversely, seismic push-down can occur when a formation or structure with a high seismic velocity is overlain or surrounded by a formation with a low seismic velocity (Fig. 3.6). The travel time of the seismic wave through the low velocity formation is slower and reaches the receivers on the surface more slowly than the seismic waves returning from the surrounding material, making it appear as if the structure is further away from the surface

than it really is (Sheriff & Geldart, 1995). These phenomena largely occur in the time domain and are reduced when converted to depth.
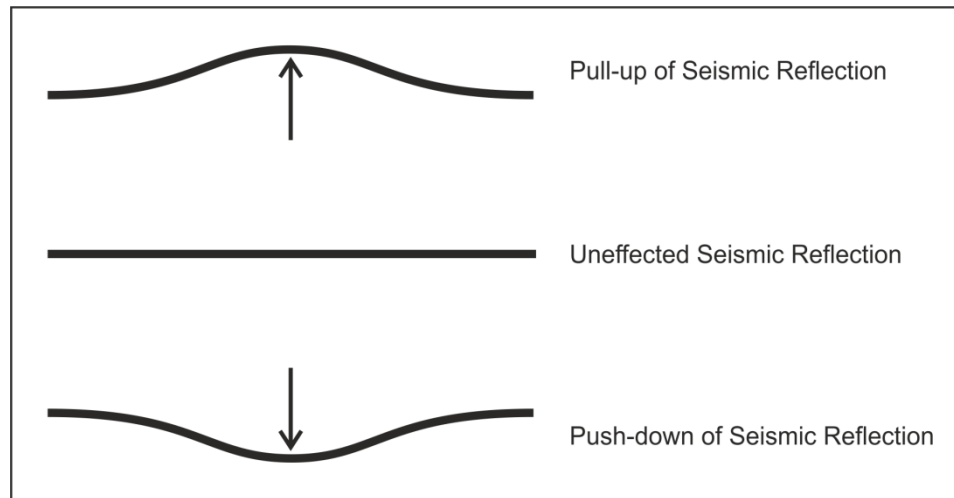
Fig. 3.6. Schematic diagram depicting the effect of sharp velocity contrasts on the geometry of a seismic reflection in a time section. Pull up of seismic reflections is caused by the seismic wave propagating from a formation with a high seismic velocity into a formation with a low seismic velocity. Push down of seismic reflections is caused by the seismic wave propagating from a formation with a low seismic velocity into a formation with a high seismic velocity.

In order to image the internal structure of the volcanic rocks and penetrate below them, seismic reflection surveys have concentrated on using very long offsets, which increases the horizontal distance between the source and receiver through the use of two survey ships with long receiver arrays. Such large reflection and refraction angles provide improved velocity control and are able to penetrate below the volcanic rocks and the underlying basement (Richardson *et al*., 1999; White *et al*., 1999; 2003; Roberts *et al*., 2005). The improved velocity control has led to better migrations of the reflection data, particularly when the deep reflectors are weak (White *et al*., 1999). In addition, very large airguns can be used to produce low frequency waves (20-30 hertz) which are able to penetrate the volcanic rocks and help mitigate the loss of energy through attenuation (Ziolkowski *et al*., 2003; Roberts *et al*., 2005: White *et al*., 2005).

3.3 Interpreting Seismic Reflection Data

Seismic reflection data provide an approximation of a cross section of the subsurface. They are typically displayed with the horizontal axis (x, y) in metres (m), while the vertical axis (z) is displayed in two-way travel time (TWT) or in depth (m). It is important to remember that while seismic reflection data can closely resemble geological cross sections, they are only a visual representation of variations in the relative velocity and density through the subsurface, with the majority of seismic reflection events being composites of the reflections produced from a number of individual interfaces (Vail *et al*., 1977c; Sheriff & Geldart, 1995). Therefore the interpretation of seismic reflection data may only provide low-resolution proxies for individual geological interfaces.

3.3.1 Interpretation Software

Seismic reflection data often consist of extremely large digital datasets and can be tens to hundreds of gigabytes in size, requiring high powered computing hardware and specialist geoscience software to interpret them (Sheriff & Geldart, 1995; Bacon *et al.,* 2007). These allow for the direct interpretation of the seismic reflection data and the integration of other geophysical information, such as wireline data and overlapping seismic surveys. The software is constantly being updated to incorporate new technological advances or suggestions from the petroleum industry, who are the primary user of this type of software. A total of four different seismic interpretation software packages were used in this thesis, with the software used dependent on when and where the interpretation of the data took place;

Landmark SeisWorks® is a seismic interpretation software package that was developed by Halliburton. It is Unix-based and is the front to the Landmark OpenWorks® project database. It provides tools to interpret 2D and 3D seismic reflection data and wireline logs. 3D seismic reflection data were restricted to being viewed in either vertical seismic sections or in the horizontal (x, y) plane. This software was available at both Durham University and the London offices of Statoil UK, and was used to interpret the seismic reflection data used in Chapter 4 and 5.

Geoprobe® is a 3D seismic volume interpretation software that was developed by Halliburton to work with SeisWorks® and the OpenWorks® project database. It allows the seismic data to be visualised and rotated 360°, with the ability to interpret data in any view and to visualise interpreted surfaces in 3D. This software was available at both Durham

University and the London offices of Statoil UK, and was used to initially interpret the seismic reflection data used in Chapter 5.

Landmark Decision Space Desktop® was developed by Halliburton to replace the Landmark SeisWorks® software package. It is still Unix-based and continues to use the Landmark OpenWorks® project database. It provides tools to interpret 2D and 3D seismic reflection data and wireline logs. 3D seismic data can be visualised and rotated 360°, interpreted in any view and to integrate 2D lines with 3D surfaces. This software was available at Durham University and replaced Landmark SeisWorks mid-way through this study. It was used to continue the interpretation of seismic reflection data used in Chapter 5.

Petrel® is a seismic interpretation software package that was developed by Schlumberger. It is Microsoft Windows® based and provides tools to interpret 2D and 3D seismic reflection data and wireline logs, with many add-on applications such as structural analysis, geological modelling and reservoir engineering. 3D seismic volumes can be visualised and rotated 360° and seismic reflections interpreted on either 2D or 3D cross sections. This software was available at the London offices of DONG Energy UK, and was used to interpret the seismic reflection data used in Chapter 6.

3.3.2 Seismic Stratigraphy

Seismic reflections are generated by contrasts in the acoustic impedance and are produced by physical interfaces of the subsurface, such as stratal surfaces and unconformities (Vail *et al.*, 1977c). The concept of interpreting seismic reflections was first known as "seismic stratigraphy" and was described by Payton (1977) and then as "sequence stratigraphy" by Wilgus *et al.* (1988) where there is the inclusion of high resolution well and outcrop data. The seismic reflections resulting from impedance contrasts are relict depositional surfaces that may be time-stratigraphic and provide a chronostratigraphic framework for the identification, correlation and prediction of sedimentary facies (Mitchum *et al.*, 1977a; Vail *et al.*, 1977c; Tipper, 1993). Therefore it is possible to make stratigraphic interpretations based on seismic reflection geometries, including the identification of distinct depositional successions bounded by reflection surfaces (Mitchum *et al.*, 1977a; 1977b). By understanding the significance of the seismic reflection surfaces and interpreting them as depositional events, it is possible to reconstruct the evolution of the basin (Emery & Myers, 1996). Seismic stratigraphy can be applied to both siliciclastic and carbonate rocks, with slight difference in methodology due to differences in environment and depositional bias

(Schlager, 1991; Catuneanu *et al.*, 2009). This section focuses on the seismic stratigraphy of siliciclastic rocks, which assumes deposition is cyclic and will produce predictable stratal geometries that record variations in sediment supply, relative sea level and accommodation (e.g. Mitchum *et al.*, 1977a; 1977b; Posamentier & Vail, 1988);

Sediment Supply is the rate at which sediment is transported from the hinterland into the basin. It is controlled by the size of the drainage area, tectonics and climate, while the amount of sediment a basin receives is dependent upon the proximity of the basin to the sediment source and the number of sedimentary entry points into the basin (Emery & Myers, 1996; Catuneanu *et al.*, 2011).

Relative Sea Level is the apparent rise or fall of sea level with respect to a local datum, such as the basement or a surface within the accumulated sediment pile (Fig. 3.7; Vail *et al.*, 1977a; Catuneanu, 2002). It differs from eustatic sea level, which is the global change in sea level with respect to a fixed datum, such as the centre of the Earth (Fig. 3.7; Vail *et al.*, 1977b; Catuneanu, 2002). Changes in relative sea level are driven by tectonic subsidence or uplift, sediment compaction and eustatic changes in sea level (Catuneanu, 2002).

Accommodation is the available space that can be filled by sedimentary deposition with respect to the sea floor or the top of the sedimentary pile (Fig. 3.7; Jervey, 1988; Muto & Steel, 2000; Catuneanu *et al.*, 2011). Changes in accommodation are driven by changes in relative sea level, tectonics and sediment accumulation (Jervey, 1988; Catuneanu, 2002).
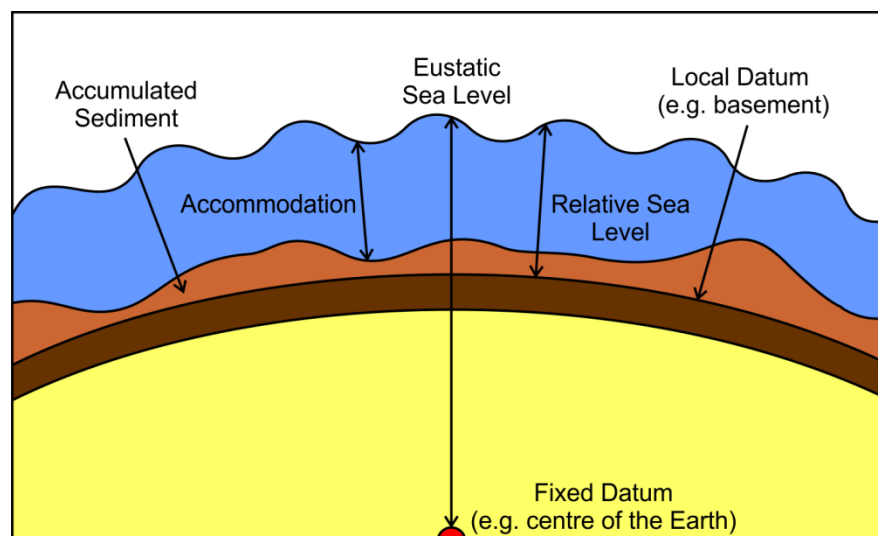
Fig. 3.7. The difference between relative and eustatic sea level, and the definition of accommodation, modified from Jervey (1988), Emery & Myers (1996) and Catuneanu (2002).

Seismic stratigraphic analysis typically begins with the division of the primary reflection successions into depositional sequences (Mitchum & Vail, 1977). Depositional sequences are the principle unit in the seismic stratigraphic hierarchy and their identification is dependent on the resolution of the data being interpreted (Neal & Abreu, 2009). They are composed of a relatively conformable succession of genetically related strata which is bounded at its top and base by an unconformity or its correlative conformity, and are known as sequence boundaries (Sloss *et al*., 1949; Mitchum *et al*., 1977a; Vail *et al*., 1977c; Posamentier & Vail, 1988; Van Wagoner *et al*., 1988). Depositional sequences form during a full cycle of relative sea level change, which involves both an increase and decrease in the available accommodation for sediments to deposit (Vail *et al*., 1977a; Catuneanu *et al*., 2011). This produces distinct stacking patterns that can be interpreted in framework of sediment supply, accommodation and relative sea level (Mitchum *et al*., 1977a; 1977b; Vail *et al*., 1977a; Emery & Myers, 1996). The geometries of the stacking pattern can be used to reconstruct the depositional environment and predict lithology (Mitchum *et al*., 1977a; 1977b; Emery & Myers, 1996). There are three distinct stacking patterns that relate directly to the sediment supply, accommodation and relative sea level;

Progradation is the deposition of sequences progressively into the basin as sediment supply exceeds the available accommodation, which is a function of relative sea level and basin subsidence. The position of the shoreline gradually migrates away from the sediment source towards the centre of the basin (Fig. 3.8; Vail *et al*., 1977a; Emery & Myers, 1996).

Aggradation is the upward deposition of sequences in a fixed position as sediment supply and accommodation are balanced, with no change in relative sea level and basin subsidence. There is little to no change in the position of the shoreline (Fig. 3.8; Vail *et al*., 1977a; Emery & Myers, 1996).

Retrogradation is the deposition of sequences towards the hinterland as sediment supply is limited and unable to fill the available accommodation within the basin, which is a function of relative sea level and basin subsidence. The position of the shoreline gradually migrates towards the sediment source and away from the centre of the basin (Fig. 3.8; Vail *et al*., 1977a; Emery & Myers, 1996).
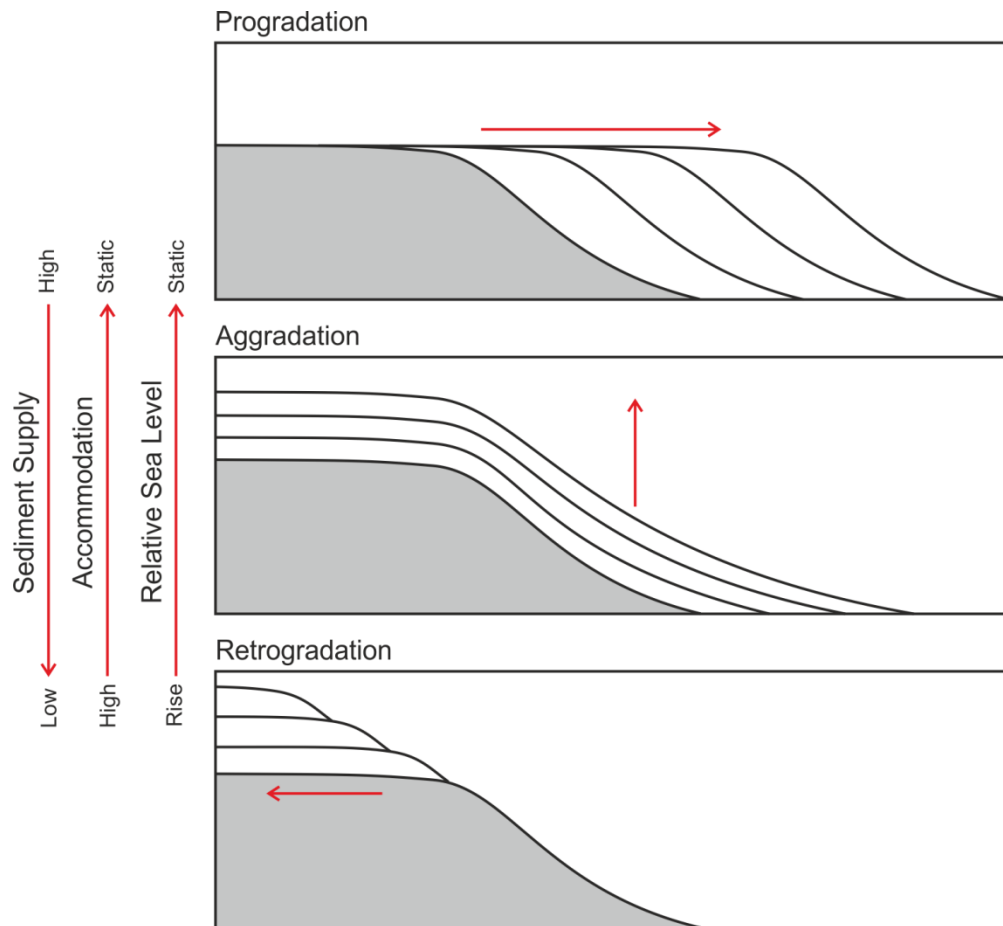
Fig. 3.8. Typical architecture of depositional sequences as seen in seismic reflection data and based of variations in sediment supply, relative sea level and accommodation, modified from Vail *et al.* (1977a), Van Wagoner *et al.* (1990) and Emery & Myers (1996).

Because depositional sequences record cycles of relative sea level change, they have a predictable internal structure. This means it is possible to divide a depositional sequence in to stratigraphic units that were deposited during specific phases of the relative sea level cycle (Posamentier *et al.*, 1988; Van Wagoner *et al.*, 1988; Catuneanu *et al.*, 2011). These units are known as system tracts and represent three-dimensional facies assemblages that are defined on the basis of bounding surfaces, stacking patterns and relative position within the depositional sequence (Posamentier & Vail, 1988; Van Wagoner *et al.*, 1988). The identification of the different system tracts can be used to reconstruct relative sea level and predict lithological patterns and facies associations of contemporaneous depositional systems. There are typically four main system tracts that are recognised;

Falling Stage System Tract is when the fall in eustatic sea level exceeds tectonic subsidence, leading to a fall in relative sea level (Fig. 3.9). This causes a forced regression as the

coastline is forced to build out into the basin and is characterised by erosion and fluvial incision (Posamentier & Vail, 1988; Van Wagoner *et al.*, 1988; Van Wagoner *et al.*, 1990).

Low Stand System Tract is when the fall in eustatic sea level slows, equals and then is exceeded by tectonic subsidence, leading to a slow rise in relative sea level (Fig. 3.9). Progradation occurs and incised fluvial systems start to flood. The base of the low stand system tract is known as the *Sequence Boundary* and marks where sea level is lowest and the greatest extent of subaerial exposure and erosion occurs (Fig. 3.9; Posamentier & Vail, 1988; Van Wagoner *et al.*, 1988; Van Wagoner *et al.*, 1990).

Transgressive System Tract is when eustatic sea level begins to rise and outpaces sediment supply, leading to an increasing rate of relative sea level rise (Fig. 3.9). This causes retrogradation towards the hinterland as sediment is trapped in the flooded incised fluvial systems. The first major flooding surface known as the *Transgressive Surface* and separates the underlying low stand system tract from the overlying transgressive system tract (Fig. 3.9; Posamentier & Vail, 1988; Van Wagoner *et al.*, 1988; Van Wagoner *et al.*, 1990).

High Stand System Tract is when eustatic sea level slows and is outpaced by sediment supply, leading to a slowing of relative sea level rise (Fig. 3.9). This causes progradation and deltas begin to build out from the flood incised fluvial systems. The switch from retrogradation during the transgressive system tract to progradation during the high stand system tract is known as the *Maximum Flooding Surface* and corresponds to the deepest water depths (Fig. 3.9; Posamentier & Vail, 1988; Van Wagoner *et al.*, 1988; Van Wagoner *et al.*, 1990).
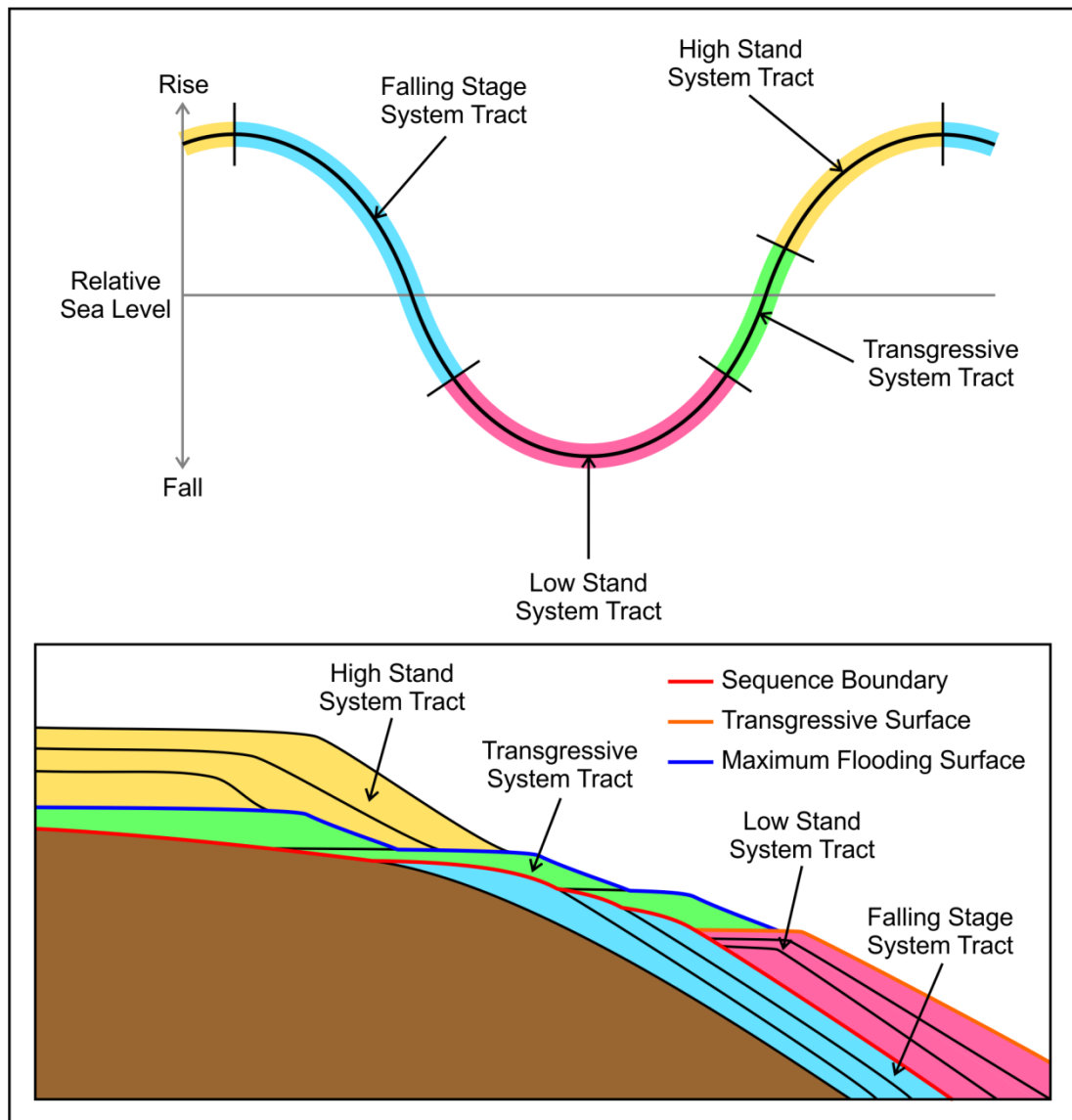
Fig. 3.9. One complete cycle of relative sea level change and corresponding system tracts and bounding surfaces, modified from Posamentier & Vail (1988), Van Wagoner *et al*. (1988) and Van Wagoner *et al*. (1990).

There are three major seismic stratigraphic models that currently exist, each with their own merits and limitations, and are not applicable to all depositional environments (Catuneanu, 2002; Catuneanu *et al*., 2010). Although the models share many similarities, the primary difference is the division of the depositional successions and the nature of the bounding seismic reflection surface (Catuneanu, 2002; Catuneanu *et al*., 2011). The depositional seismic models of Vail *et al*. (1977c), Posamentier & Vail (1988) and Van Wagoner *et al*. (1990) propose that the bounding surfaces of the depositional successions are unconformities or their correlative conformities. The genetic seismic model of Galloway (1989a; 1989b) proposes the bounding surfaces of the depositional successions are

flooding surfaces. Finally, the transgressive-regressive seismic model of Embry (1995) and Emery & Myers (1996) suggest the bounding surfaces of the depositional successions are composite surfaces that include subaerial unconformities and their correlative maximum regressive surfaces. The decision of which model to use is dependent on the tectonic setting, depositional setting, sediment types and preservation. In this study, the volcanic rocks exhibit both extensive subaerial and submarine depositional successions, leading to the use of the depositional seismic model of Vail *et al*. (1977c), Posamentier & Vail (1988) and Van Wagoner *et al*. (1990) and the interpretation of bounding reflection surfaces as unconformities or their correlative conformities.

3.3.3 Mapping Seismic Reflections

The aim of mapping seismic data is to establish the relationship between the seismic reflections and the stratigraphy (Sheriff & Geldart, 1995). Choosing which reflections to map is highly dependent on the interpretation objectives, the stage of exploration and the data available. If wireline data are available, the major geological interfaces can be identified and correlated with the seismic reflection data, providing a robust control on the interpreted stratigraphy (Sheriff & Geldart, 1995; Ashcroft, 2001). If no wireline data are available, interpretation is typically undertaken by the identification of prominent seismic reflections on the basis of amplitude, polarity and character (Mitchum & Vail, 1977; Sheriff & Geldart, 1995; Ashcroft, 2001).

Seismic interpretation should at first be undertaken on a regional scale; gradually become more focused as understanding of the data increases. Identification of the prominent seismic reflections often leads to the division of the seismic data into discrete seismic reflection packages which can be characterised on the basis of velocity, continuity, external geometry and internal reflection configurations (Mitchum & Vail, 1977; Ashcroft, 2001). The extent and external geometry of seismic reflection packages can be identified by the different seismic reflection terminations. This is the geometric relationship displayed between the seismic reflection being mapped and the seismic reflection against which it terminates, and can be indicative of original depositional limits (Fig. 3.10; Mitchum *et al*., 1977a). The internal reflection configurations of seismic reflection packages can display a range of patterns which are identified on the basis of reflection geometry, continuity and amplitude and can be indicative of lithology and depositional processes (Fig. 3.11; Mitchum *et al*., 1977a; 1977b; Posamentier & Vail, 1988).
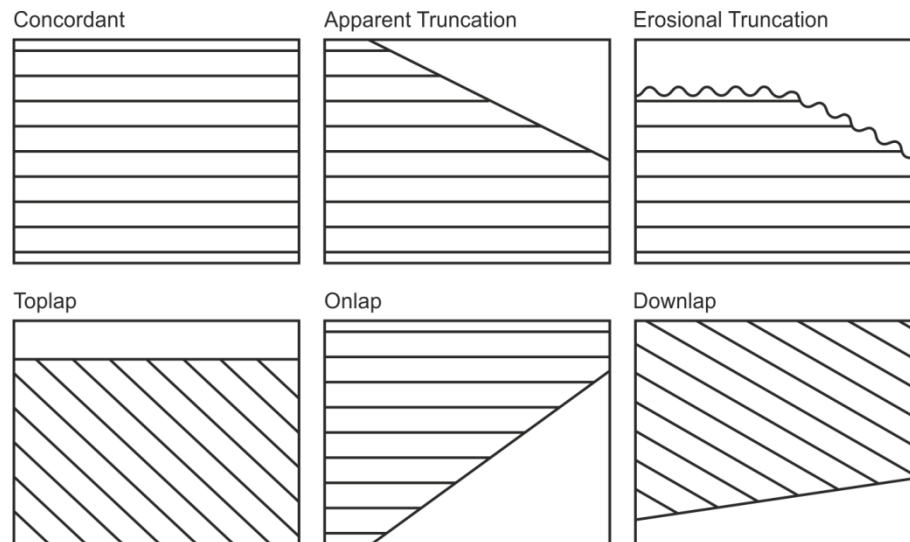
Fig. 3.10. Common seismic reflection terminations seen in seismic reflection data, modified from Mitchum *et al*. (1977a), Emery & Myers (1996) and Planke *et al*. (1999, 2000).
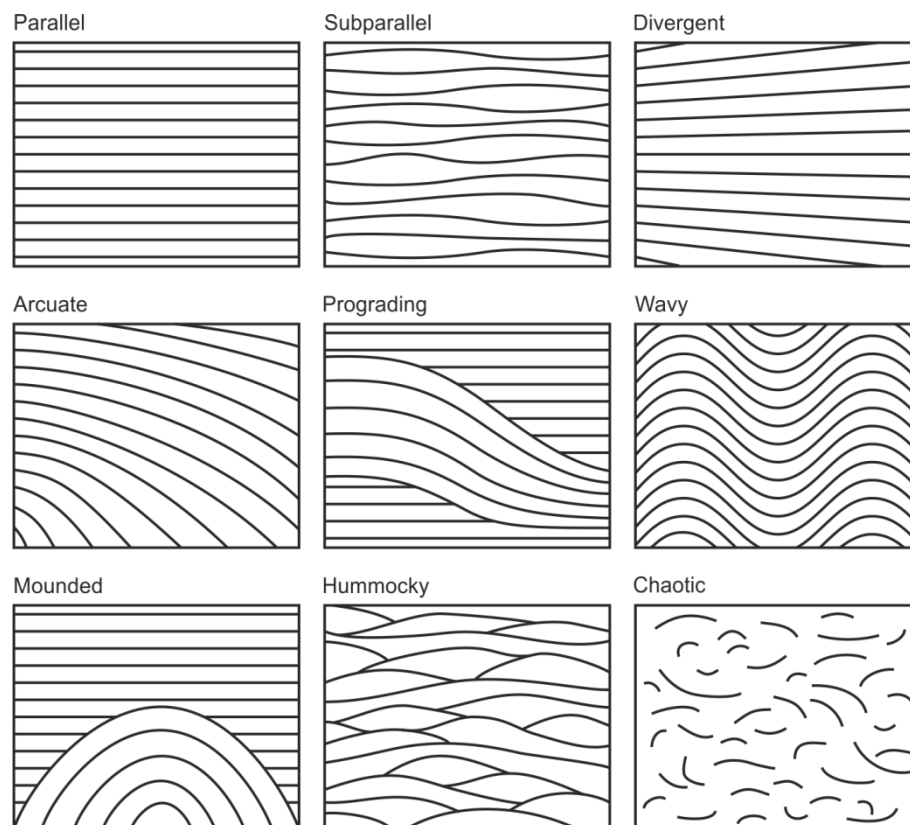
Fig. 3.11. Common internal seismic reflection configurations seen in seismic reflection data, modified from Mitchum *et al*. (1977a; 1977b), Emery & Myers (1996) and Planke *et al*. (1999, 2000).

Interpretation can also aided by a number of basic techniques which manipulate the colour, scale and geometry of seismic sections and can assist in the identification and

mapping of reflections. In the past seismic reflection data were displayed using a greyscale colour scheme (see Fig. 3.12), but with modern interpretation software there are now an infinite number of potential colour schemes to use in the interpretation of seismic reflections. Choosing the right colour scheme is dependent upon the type and quality of the seismic data, as well as the interpreter's personal preference. Simple colour schemes, such as a greyscale can identify the main reflections and major discontinuities, such as faults and edges (Fig. 3.12; Brown, 2005; Bacon *et al*., 2007). Graduations between two or three colours can delineate more subtle seismic reflections (Fig. 3.12; Brown, 2005; Bacon *et al.*, 2007). More complicated colour schemes, such as a spectrum of colour, can highlight amplitude variations and are often used to correspond to seismic velocity (Fig. 3.12; Brown, 2005; Bacon *et al.*, 2007).

Alteration of the scale and geometry of seismic sections can be achieved by changing the vertical and horizontal dimensions of the seismic data (Brown, 2005; Bacon *et al*., 2007; Ashcroft, 2001). This can be useful to squeeze or stretch seismic reflections to better understand and judge if they are real or artefacts. It is also possible to flatten the seismic data using a reference horizon. This process can be undertaken on a vertical section from either a 2D or 3D seismic data. Flattening can help reproduce original depositional geometries, and restore faulted segments and folded structures to their pre-tectonic position (Fig. 3.13; Brown, 2005). By removing the effects of overburden or post-depositional processes, it is possible to interpret complicated stratigraphy, gauge variations in lateral thickness and minimise potential reflection mis-ties. While 2D and 3D seismic data allow vertical sections through the subsurface, only 3D data allow the additional use of horizontal sections through the subsurface. These horizontal sections are known as timeslices and can provide a plan view of the seismic data across a specific depth or time on the z axis (Brown, 2005; Bacon *et al*., 2007). By taking progressively deeper or shallower timeslices through the 3D survey, it is possible to see the distribution of seismic reflections and the evolution of distinct features (Fig. 3.14).
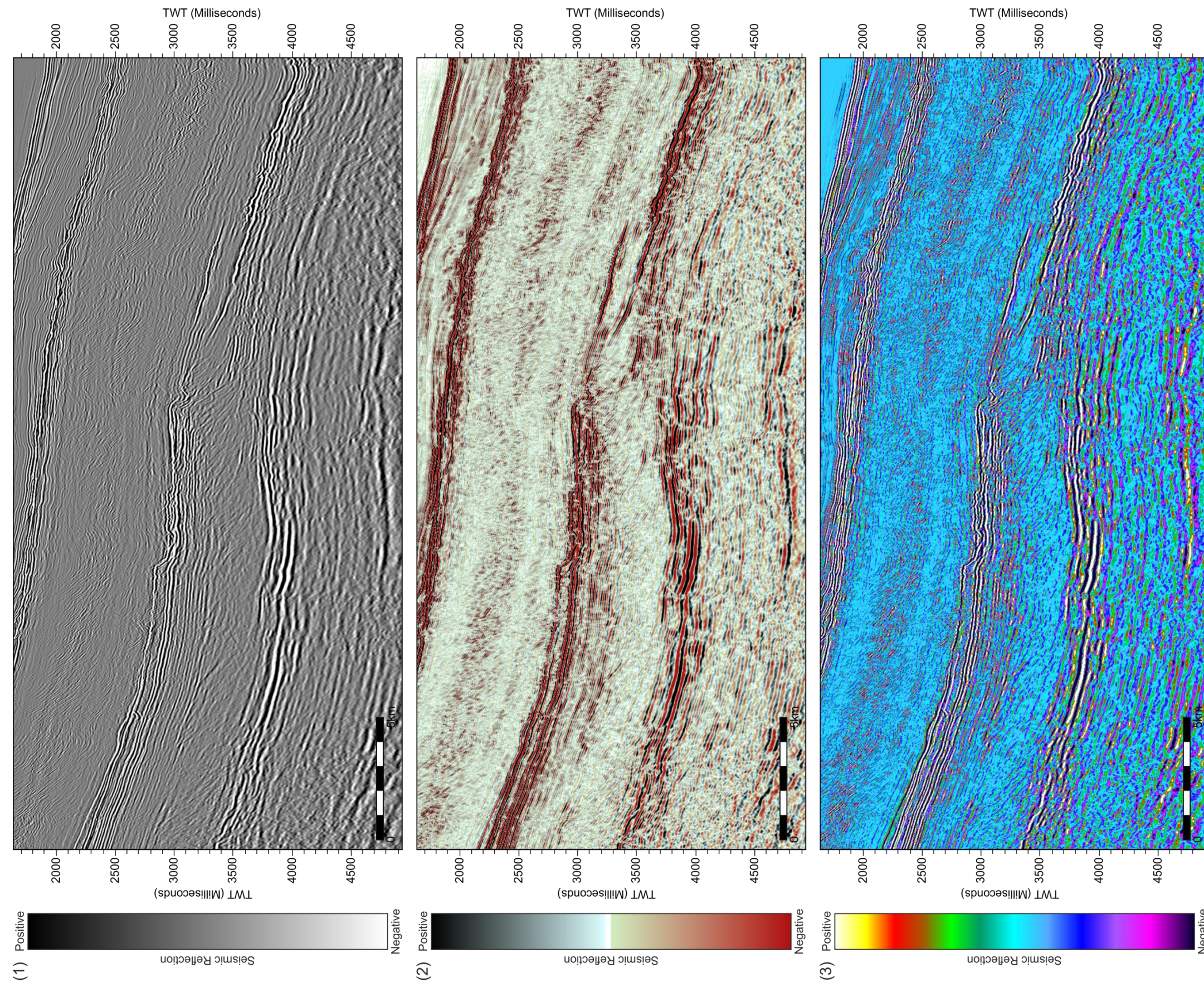
Fig. 3.12. A single seismic section displayed using different colour schemes. (1) The colour scheme used is a greyscale and highlights the main reflections and major discontinuities. (2) The colour scheme used is a graduation from red to white to black, and identifies more subtle seismic reflections. (3) The colour scheme used is a colour spectrum and reveals amplitude variations.
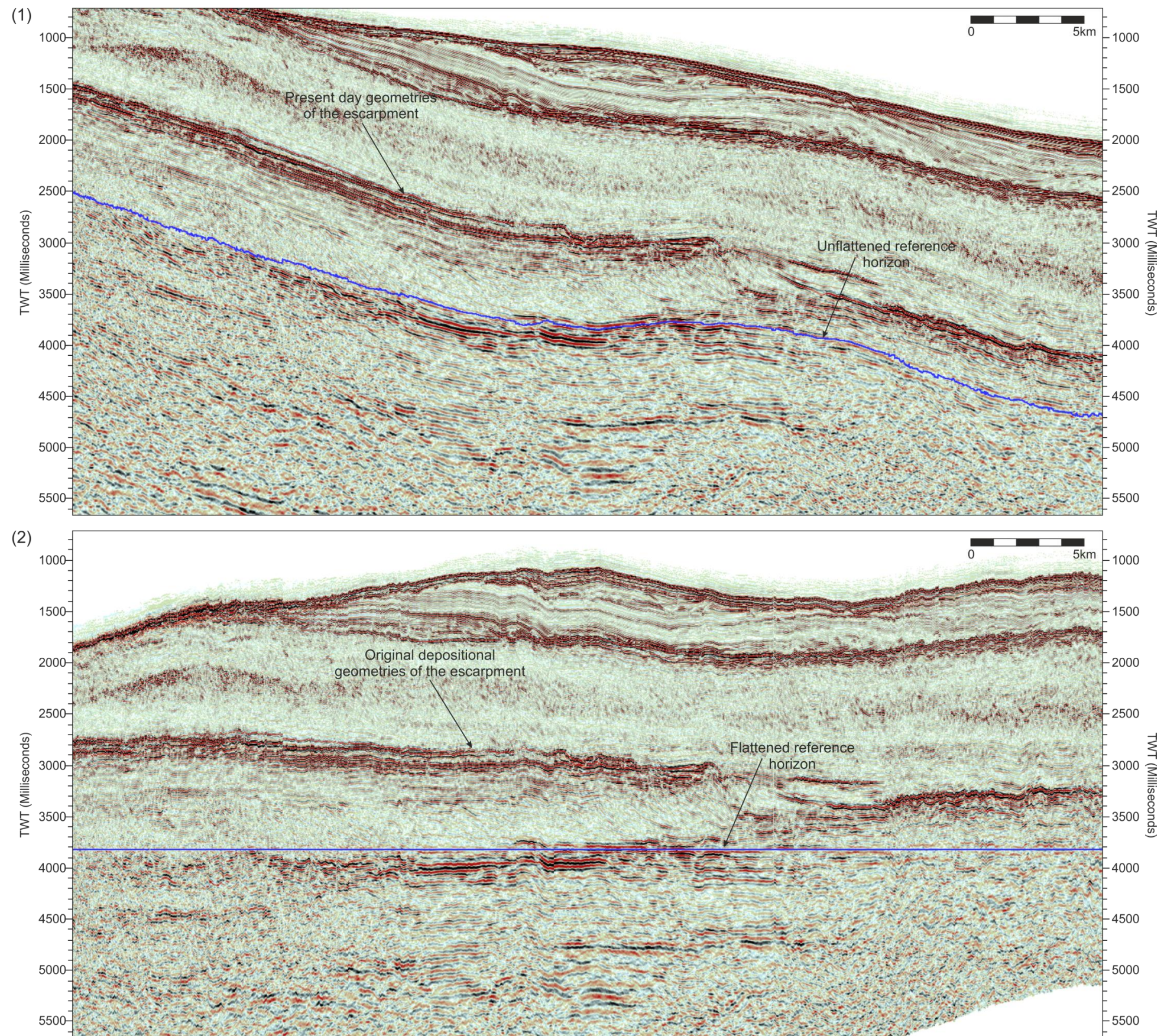
Fig. 3.13. The difference between a unflattened and a flattened seismic section using a reference horizon. (1) The unflattened section reveals the present day seismic reflection geometries of the escarpment identified and the undulating reference horizon. (2) The flattened section attempts to reproduce the original depositional geometries of the escarpment identified by making the reference horizon flat.
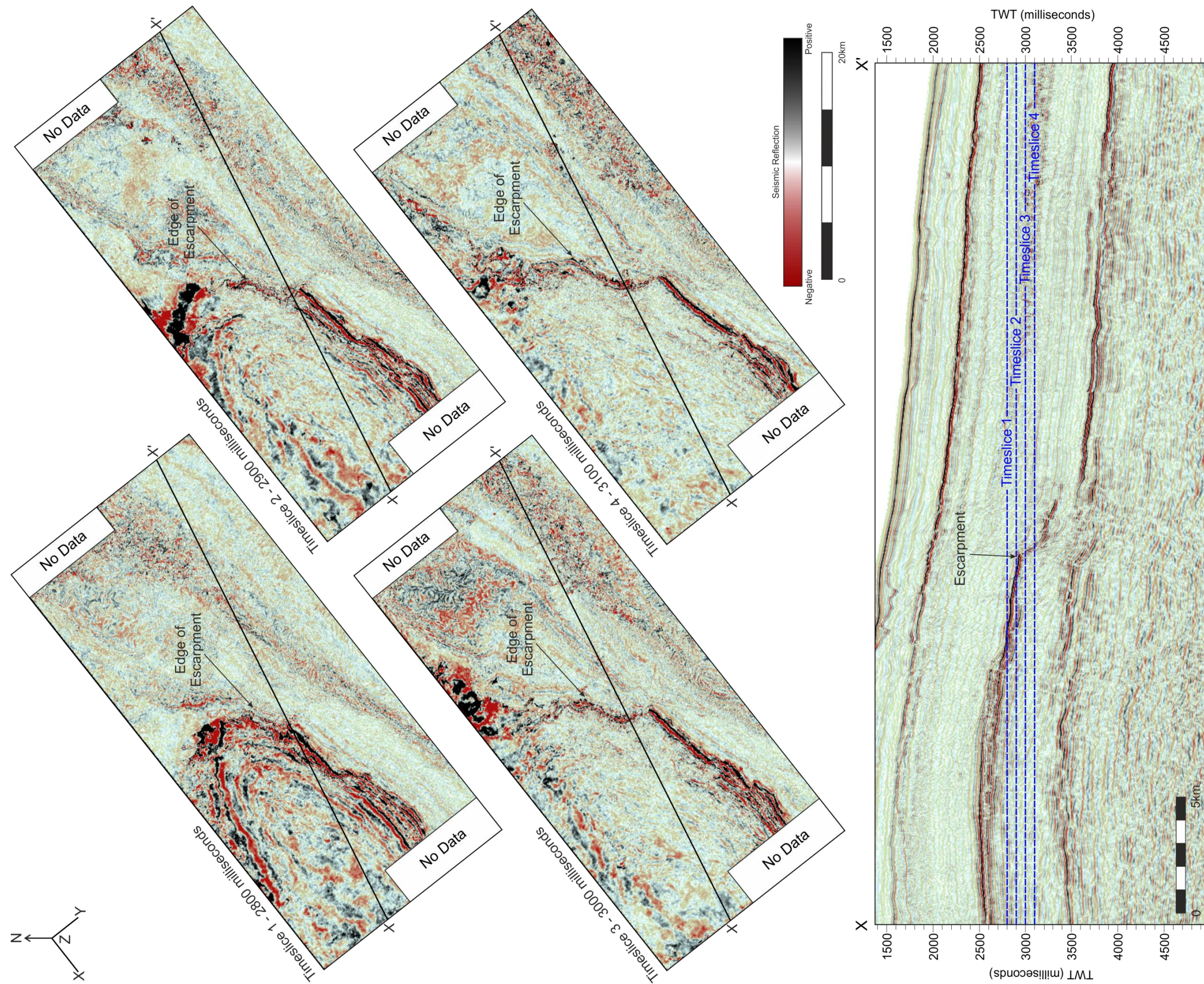
Fig. 3.14. The use of timeslices which get progressively deeper through the 3D seismic data set at 100 millisecond intervals and reveals variations in the escarpment feature identified in cross section X-X'.

When mapping seismic reflections across extensive or stratigraphically complicated data, there is an increased possibility of mis-ties and therefore a risk of mis-interpretation. It is essential that interpretations should be checked for consistency. This is through the use of cross-cutting, often perpendicular, seismic cross sections across the survey (Sheriff & Geldart, 1995; Ashcroft, 2001). In 2D seismic data, interpretation is limited by the extent of the survey lines, with the correlation of reflections via seismic cross sections that share a common intersection point and are often perpendicular (Fig. 3.15; Ashcroft, 2001; Bacon *et al*., 2007). In contrast, 3D seismic data are much more versatile because the data can be viewed in any orientation and interpretations can be made on any cross section through the 3D cube. Mapping and correlation of seismic reflections is typically undertaken by creating a grid of cross sections known as inlines and crosslines with set distances between the sections (Fig. 3.16; Ashcroft, 2001; Brown, 2005; Bacon *et al*., 2007). Once the reflection has been mapped to the extent required, it can be turned into a 3D reflection surface using the autotrack function in the interpretation software that is designed to interpolate the horizon between the gridded lines (Fig. 3.16).

Using cross-cutting sections to correlate seismic reflection interpretation across the survey can be vital when seismic data have poor resolution, rapid lateral variability or are complicated by amplitude anomalies that cross-cut stratigraphy, such as seismic multiples, methane hydrates or diagenetic zones (e.g. Bernt *et al*., 2004; Ireland *et al*., 2011). In this study, seismic reflection interpretations were complicated by the large variation in volcanic products and multiple phases of volcanic emplacement overlying one another. At times, especially at edges or escarpments, volcanic rocks were deposited adjacent to volcanic rocks, making it difficult to identify where reflections terminate and where they continue (Fig, 3.17; see Chapter 5).
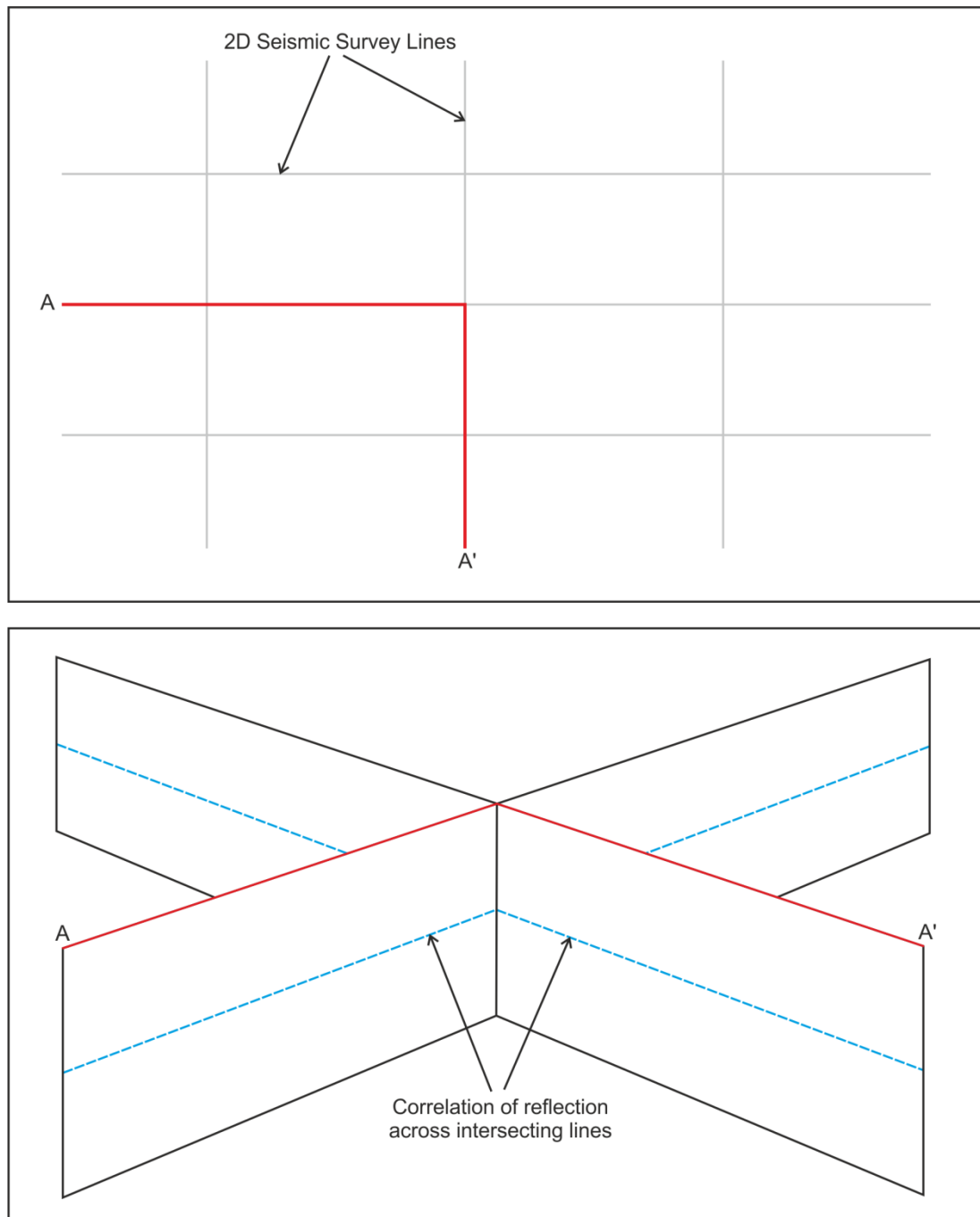
Fig. 3.15. Schematic diagram depicting the principles of interpreting 2D seismic reflection data, where the interpretation of seismic reflections is limited to the extent of the survey lines and the correlation of reflection is by perpendicular seismic cross sections that share a common intersection point.
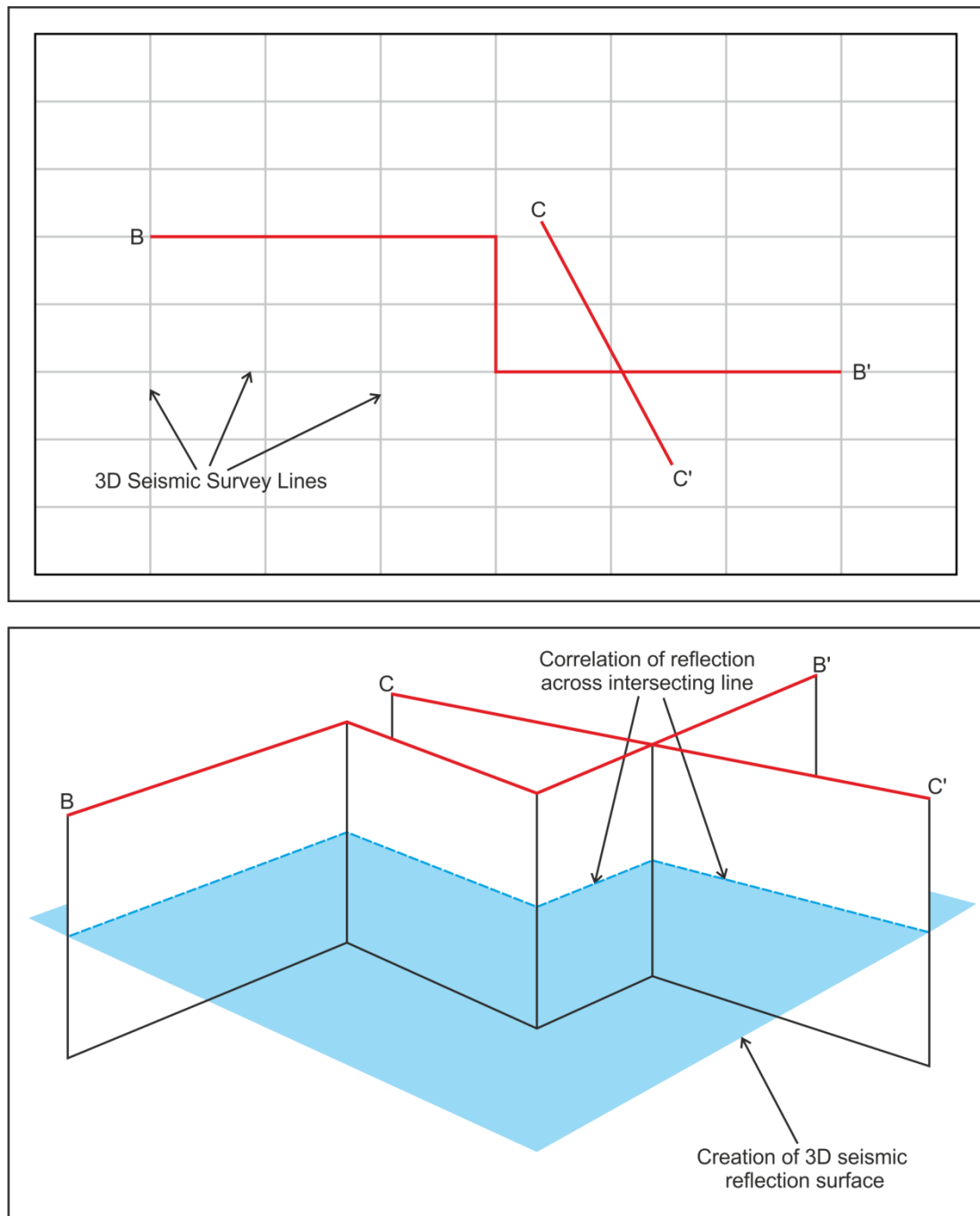
Fig. 3.16. Schematic diagram depicting the principles of interpreting 3D seismic reflection data, where the interpretation of seismic reflections is by creating a grid with set distances between the interpreted cross sections, with the creation of a 3D reflection surface using an algorithm that interpolates between the sections.
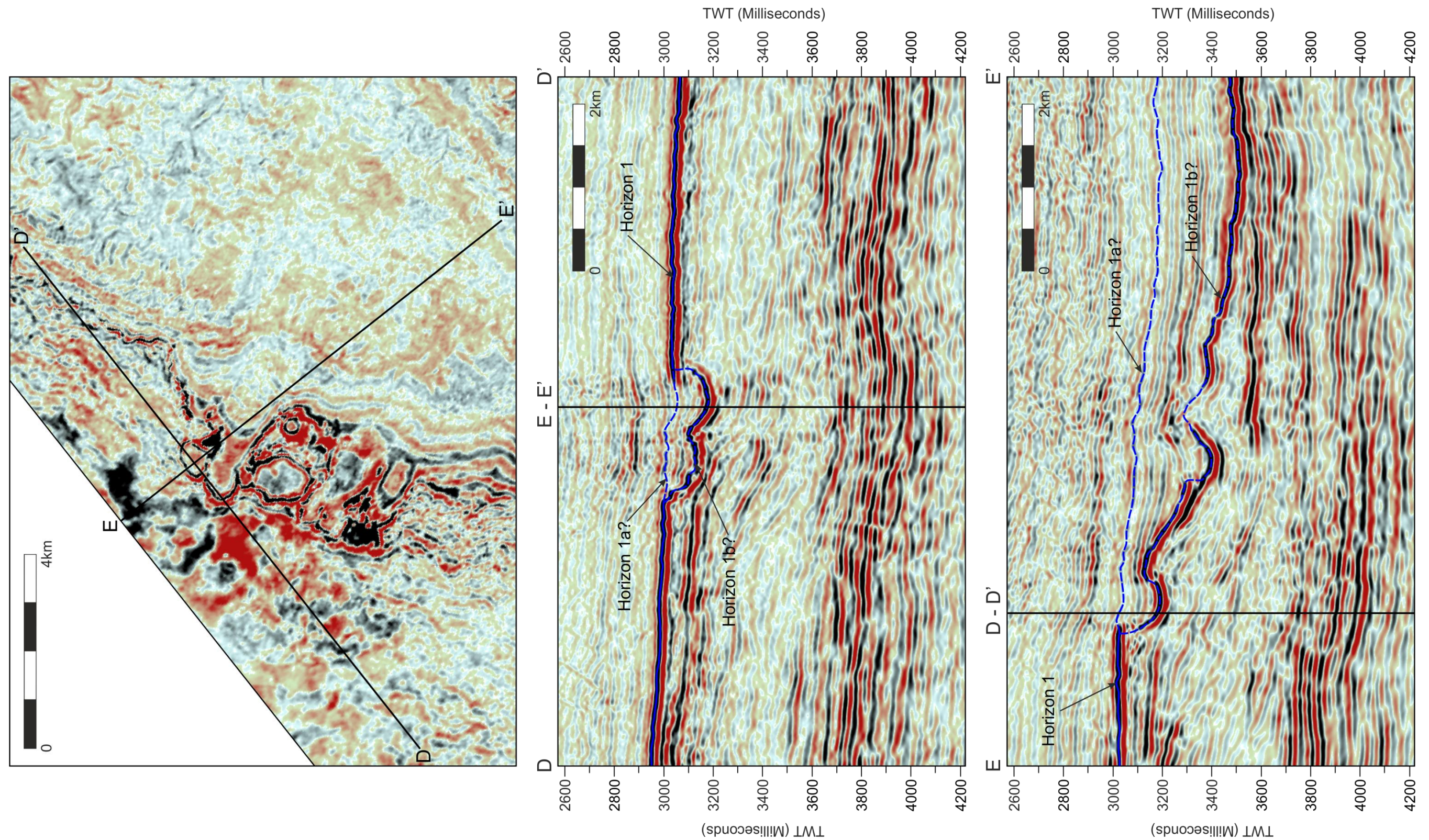
Fig. 3.17. The use of cross cutting sections D-D' and E-E' to correlate a seismic reflection across the survey. In this example, horizon 1 has 2 potential continuations; horizon 1a which appears to be at the same stratigraphic level as horizon 1, or horizon 1b which consists of a number of amplitude anomalies and is not at the same stratigraphic level as horizon 1. Using cross-cutting seismic sections and a timeslice, it was found that mapping seismic amplitude anomalies of horizon 1b could defined the edge of a feature, while mapping horizon 1 produced a false surface and actually cross-cut the true stratigraphy.

3.3.4 3D Visualisation and Seismic Attributes

The advantage of 3D seismic reflection data is the ability to map and create a reflection surface that has a fixed position in time and space within the survey volume (Bacon *et al.,* 2007). This surface is a representation of a change in velocity and density, and is therefore an approximation of a geological interface and can be coloured with any number of chosen seismic attributes (Brown, 2005). Seismic attributes are quantitative measurements extracted from the seismic data to aid in the identification of features or areas of interest that are not obvious on seismic sections (Brown, 2005; Bacon *et al.,* 2007). They are typically calculated on 3D seismic data and are best viewed in the horizontal plane. There are multiple attributes that can be customised with different parameters and algorithms to increase detection. In this thesis, three different seismic attributes have been used;

Amplitude Extraction calculates the amplitude values from a specific horizon or a constrained window over the horizon. There are many algorithms to extract amplitude values, but the most commonly used is the root mean square (RMS) algorithm which calculates the average amplitude of any given point on the horizon or specified window, and is very useful at identifying subtle changes in amplitude that relate to changes in velocity and density and therefore may relate to changes in lithology, porosity or pore fluid.

Dip is the magnitude of the gradient in two-way time and is calculated by comparing a sample point of a horizon with the two adjacent points in orthogonal directions on a plane. The magnitude of dip is measured in milliseconds per unit distance multiplied by 1000. If the seismic data are in depth or a velocity model is supplied, it is possible for the dip to be converted into depth. The individual dips are not particularly useful, but the relative difference in dip across the horizon can identify structures such as faults or escarpments. (Bacon *et al.,* 2007)

Edge Detection is an image processing tool that highlights areas of discontinuity across the horizon by exaggerating sharp changes in dip. It is calculated by comparing a single sample point to those either side of it in a 3 x 3 grid. It is useful to indicate rapid changes in dip or reflection continuity.

3.4 Interpreting Wireline Data

Exploration wells are commonly drilled after the acquisition of seismic reflection data, and their design is based on seismic interpretation and identification of areas of interest, such as potential hydrocarbon accumulations. They can provide a high resolution control on seismic reflection data, identifying lithology, age, structure and types of hydrocarbon accumulations, while assisting in the correlation of subsurface horizons, determining facies relationships and managing reservoir production. Such detailed information can then be fed back into the basin model to assist in further petroleum exploration.

3.4.1 Wireline Logging Tools

The deployment of logging tools down exploration wells provides a continuous record of the subsurface and translates the physical characteristics of rock formations into geophysical parameters which relate directly to lithology, mineralogy, porosity, permeability and water saturation (Serra, 1984; Rider, 1991; Asquith *et al.*, 2004). Interpretation is based on the evaluation of a suite of individual log responses, as analysis of an individual log response in isolation would only show variations of a single characteristic. By analysing the different logs together it is possible to reconstruct the subsurface and begin to identify distinct rock formations (Serra, 1986; Rider, 1991; Asquith *et al.*, 2004). There are many types of wireline logging tools available, from basic to more niche tools which are patented by exploration drilling companies (Rider, 1991). In this thesis I have described the wireline logging tools which are part of the standard tools deployed and which have been used within this study;

Bulk Density Logs measure the density of the whole rock formation, including the solid matrix and the enclosed pore fluid. They are inferred from the intensity of back-scattered radiation from the logging tool which is a function of the density of the minerals, porosity and pore fluid (if any) within the rock formation (Asquith *et al.*, 2004). Density logs are recorded in g/cm^3 and are sensitive to high density minerals and the roughness of the well wall (Serra, 1984; Rider, 1991).

Natural Gamma-Ray Logs measure the total natural radioactivity of a rock formation via the decay of the radioactivity isotopes of ^{40}K, ^{238}U and ^{232}Th (Serra, 1984; Asquith *et al.*, 2004). Gamma-ray logs are recorded in API units, which are based on known radiation levels of artificial formations in test wells at the University of Houston (Rider, 1991; Asquith *et al.*, 2004). The logs are sensitive to organic material (such as hydrocarbons), potassium

feldspars, micas and clay minerals which inherently have high concentrations of radioactive elements (Serra, 1984; Asquith *et al.*, 2004).

Neutron Porosity Logs measure the porosity of a rock formation via the slowing down of neutrons (which are emitted from the logging tool) as they interact with the amount of hydrogen within a formation (Serra, 1984; Rider, 1991; Asquith *et al.*, 2004). Neutron porosity logs are recorded as a fraction of the volume of pores over the total volume in either pu or m^3/m^3 and can be influenced by the presence of gas, mica or clay alteration products which give lower neutron porosity log values (Rider, 1991; Asquith *et al.*, 2004).

Resistivity Logs measure the electrical conductivity of a rock formation, with more mechanically strong rocks resisting the flow of an electrical current (Asquith *et al.*, 2004). They are recorded in ohms per metre and are divided into shallow, medium and deep resistivity logs depending on the penetration depth of the electric field into the formation (Rider, 1991; Asquith *et al.*, 2004). Resistivity logs are sensitive to porosity, clays and other conductive minerals. The fluid within the pores also affects the resistivity logs values, with hydrocarbons being more resistive than water (Serra, 1984; Asquith *et al.*, 2004).

Velocity Logs measure the travel time of an acoustic pulse through a rock formation via a sound wave emitted from the tool into the formation and back to a receiver (Rider, 1991; Asquith *et al.*, 2004). Velocity logs are recorded in either μs/ft or μs/m and are sensitive to the mechanical strength of the rocks, fractures and porosity (Rider, 1991; Asquith *et al.*, 2004). The fluid within the pores also affects the velocity logs (Serra, 1984; Asquith *et al.*, 2004).

3.4.2 Synthetic Seismograms

The resolution of wireline data is generally much higher than that of seismic data, with multiple formations identified in wireline logs, often forming one seismic reflection (Rider, 1991). However, it is still possible to use wireline data to provide information to inform the interpretation of seismic reflection data (Sheriff & Geldart, 1995). This can be achieved by creation of a synthetic seismogram, which is a one dimensional model of the acoustic energy travelling through the subsurface. A model of acoustic impedance can be generated by combining velocity and density logs, which is then convolved with a wavelet of similar frequency to, and derived from, the seismic data to create a synthetic seismogram (Sheriff & Geldart, 1995; Ashcroft, 2011). The predicted seismic reflectivity can then be compared to the real seismic reflectivity, allowing the correlation of marker beds identified on

wireline data with the seismic data and identifying the geological origin of the seismic reflections (Fig. 3.18; Sheriff & Geldart, 1995; Brown, 2005; Ashcroft, 2011). It should be noted that the wireline logs used to generate a synthetic seismogram only sample the localised area within the well borehole, while seismic reflection data samples the whole subsurface, which can lead to mis-ties between the predicted and the real seismic reflectivity (Sheriff & Geldart, 1995; Bacon *et al.*, 2007). Mis-ties between synthetic seismograms and seismic reflection data can also be caused by poor quality log data, the difference in resolution between wireline logs and seismic reflection data, and incompatible wavelets derived from the seismic reflection data (Sheriff & Geldart, 1995; Bacon *et al.*, 2007).
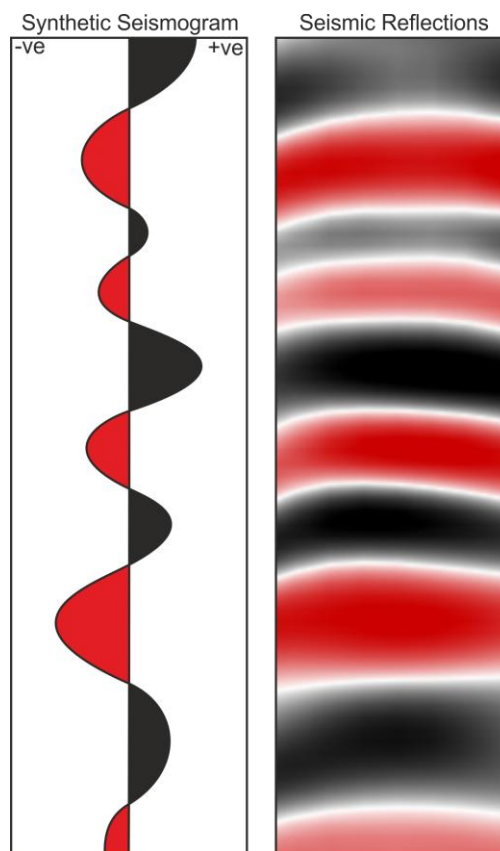
Fig. 3.18. Idealised synthetic seismogram and its correlation with the real seismic reflection data. The polarity displayed in the diagram is the Society of Exploration Geophysists normal convention polarity (see section 3.2.3).

3.4.3 Volcanic Rocks in Wireline Data

The lithological interpretation of subsurface formations using wireline logs was originally developed for sedimentary rocks, but has been successfully applied to igneous rocks (e.g. Helm-Clark *et al.*, 2004; Nelson *et al.*, 2009b). Initially the wireline data are given an overall

examination to identify the gross lithology and main formations as a precursor to detailed analysis, with a few key logs used in the identifications of lithologies. For siliciclastic rocks, the resistivity log is used to identify formations because sandstone exhibits higher log values while shale exhibits lower log values (Asquith *et al.*, 2004). For carbonate rocks, the porosity and neutron density logs are used to identify formations because resistivity is greatly affected by lithological changes in carbonate rocks (Asquith *et al.*, 2004). For volcanic rocks, the resistivity and velocity logs are used to identify formations, because the crystalline nature of the volcanic rocks produces very high resistivity and velocity log values (Schutter, 2003; Helm-Clark *et al.*, 2004). Gamma-ray logs can also prove useful in the identification of volcanic rocks as the lack of organic material produces very low gamma-ray log values, although it should be noted that high concentrations of feldspar can produce a spike in the gamma-ray response similar to organic material (Helm-Clark *et al.*, 2004).

Pāhoehoe lava flows commonly display a three-part internal structure, consisting of a thin, lower flow base, a thick, dense flow core and a thick, vesicular and fractured upper flow crust (e.g. Self *et al.*, 1997; 1998). This produces an asymmetrical, cyclic pattern which is observed across the log signatures and relates directly to the vertical variations in vesicle and fracture distribution (Fig. 3.19; Planke, 1994; Planke *et al.*, 1998; Boldreel, 2006; Nelson *et al.*, 2009b). Typically, the flow base can be identified by low neutron porosity and gamma-ray log values, with moderate bulk density, resistivity and velocity log values as lower flow crust is crystalline with few vesicles (Fig. 3.20; Helm-Clark *et al.*, 2004; Nelson *et al.*, 2009b). At the transition to the lava flow core, bulk density, resistivity and velocity log values rapidly increase due to the massive, crystalline nature of the flow core and its low degree of fracturing and low vesicularity (Fig. 3.20; Planke 1994; Helm-Clark *et al.*, 2004; Boldreel 2006; Nelson *et al.*, 2009b). Gamma-ray log values remain low due to a lack of organic material, with the exception being anomalously potassium-rich lava (Schutter, 2003; Helm-Clark *et al.*, 2004). Porosity log values are commonly low but can be seen to gradually increase as the flow core becomes more vesicular towards the lava flow crust (Fig. 3.20).
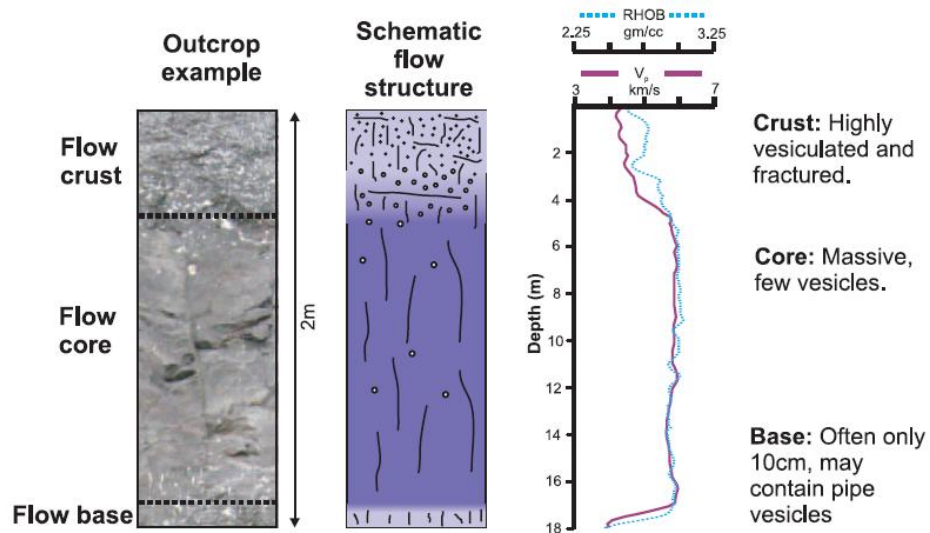
Fig. 3.19. Three-part internal structure of a typical pāhoehoe lava flow and the effect on velocity (V_s) and density (RHOB). The photo of the lava flow is at a different scale to the log data but the three-part division is independent of scale. Image from Nelson *et al*. (2009b), with log data from the Lopra-1/1A borehole, Faroe Islands and schematic flow structure from Self *et al*. (1997).

The transition into the upper flow crust is identified by a sharp decrease in bulk density, resistivity and velocity log values as the upper flow crust is high fractured and vesicular (Fig. 3.20; Helm-Clark *et al*., 2004; Nelson *et al*., 2009b). Porosity and gamma-ray logs show the inverse, with a sharp increase in log values due to the vesicularity and great degree of alteration due weathering and reworking incorporating organic material (Planke 1994; Boldreel 2006; Nelson *et al*., 2009b). Volcaniclastic rocks exhibit similar log values to lava flow crusts as they are composed of fractured, fragmented volcanic material. Primary volcaniclastic material such as hyaloclastic breccias have higher resistivity, velocity and density log values, while volcaniclastic material resulting from erosion will have higher gamma-ray and porosity log values due to having undergone a higher degree of reworking and incorporation of organic material (Mathisen & McPherson, 1991; Nelson *et al*., 2009b).

Volcanic intrusions such as sills, dykes and laccoliths exhibit similar log values to lava flow cores because they are composed of massive, crystalline rocks. However the cores of sills will have high bulk density, resistivity and velocity logs values and low porosity log values due to a low degree of fracturing and low vesicularity within the sill core (Fig. 3.20; Bell & Butcher, 2002; Smallwood & Maresh, 2002). At the sill aureoles there may be a slight decrease in the bulk density, resistivity and velocity logs values and an increase in the

porosity log values due to the presence of vesicles and small scale fractures (Fig. 3.20; Bell & Butcher, 2002; Smallwood & Maresh, 2002). Gamma-ray log values will be low throughout the sill due to a lack of organic material although any fluctuations could indicate anomalously potassium-rich magma (Bell & Butcher, 2002; Smallwood & Maresh, 2002; Schutter, 2003; Helm-Clark *et al.*, 2004).

Sedimentary rocks are common between lava flows and can be useful as marker beds, allowing correlation between well locations. Sedimentary rocks are typically identified by low to moderate density and velocity log values, and high porosity log values (Fig. 3.20; Nielsen *et al.*, 1984; Planke 1994). Sedimentary interbeds can have high gamma-ray log values as they contain more clay and other phyllosilicate minerals than basalts, which have higher radioisotope contents. Clay minerals are also more conductive, producing lower resistivity log values (Nielsen *et al.*, 1984; Planke 1994; Helm-Clark *et al.*, 2004).
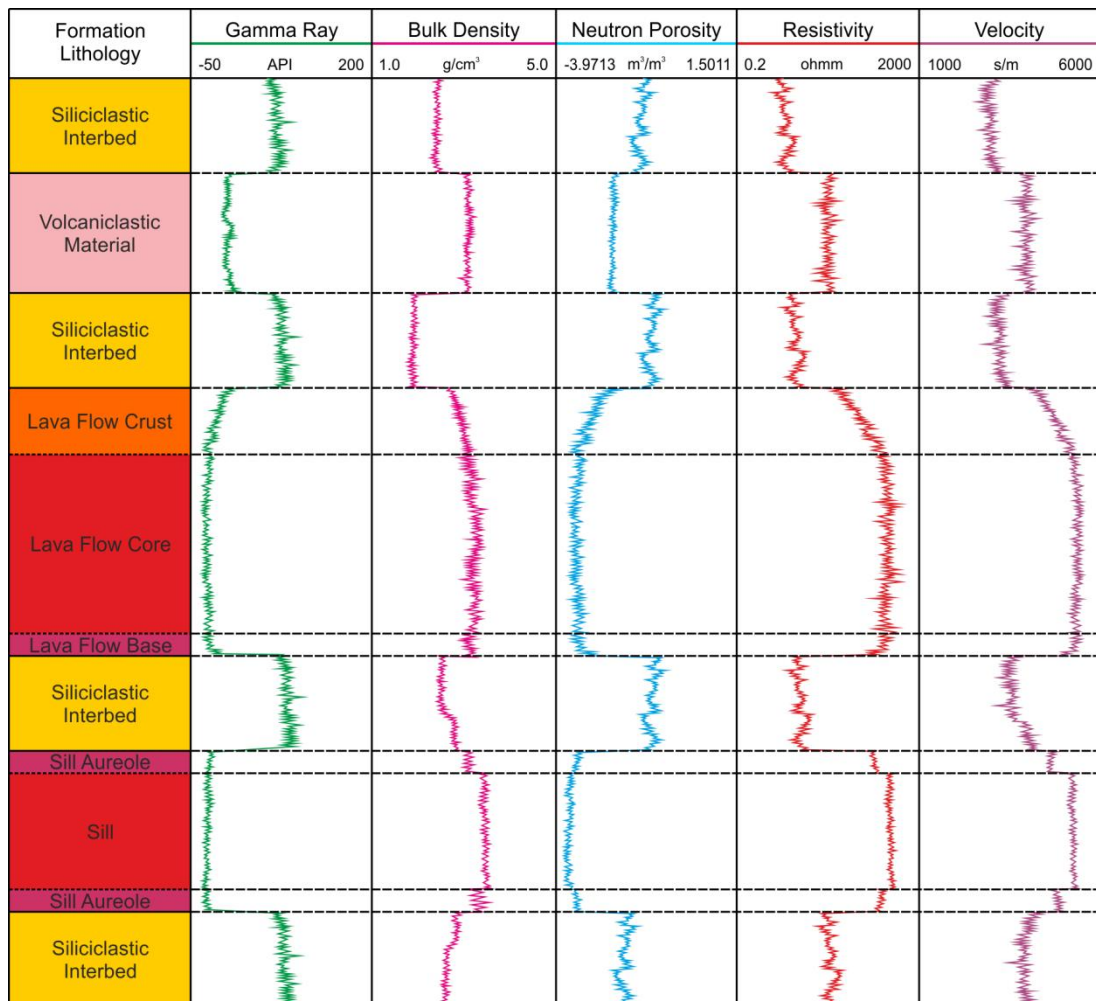
Fig. 3.20. Schematic diagram representing the typical wireline log responses to volcanic rocks, after Planke (1994), Planke *et al.* (2000), Bell & Butcher (2002), Smallwood & Maresh

(2002), Helm-Clark *et al*. (2004), Boldreel (2006), Nelson *et al*. (2009b) and observations from this study. No scale is implied, but wireline resolution can be ~2 m.

3.5 Datasets

All the seismic reflection data used in this thesis were supplied processed and ready to interpret, with only limited information supplied about the processing methods used. As previously mentioned all of the seismic reflection data were displayed using the Society of Exploration Geophysists normal convention, where an increase in the acoustic impedance is displayed as a positive polarity reflection and a decrease in the acoustic impedance is displayed as a negative polarity reflection. The seismic reflection data were also displayed in time although where appropriate time has been converted to depth using average velocities gained from the seismic data or specific velocities gained from wireline data. Where possible, the resolution limits of the data have been given, but it should be noted that this often does not take into account the loss of higher frequencies within the volcanic rocks and the subsequent decrease in resolution.

3.5.1 2D Seismic Reflection Data

This study has used a variety of 2D surveys from the Faroe-Shetland Basin which were provided by Statoil UK Ltd under licence of the respective seismic contractors for use by Durham University (Table 3.1). The dataset consists of a total of 18 2D seismic reflection surveys which were collected separately. All of the data were processed using a standard sequence of steps including deconvolution, stacking and migration. The surveys have significant geographical overlap, with 578 survey lines and a total length of ~35414 km (see Fig. 3.21). The surveys image the underlying rift structure, the continental flood basalts and post rift sedimentary basin fill, with the location of the study area chosen by the high density of data that imaged the underlying Faroe-Shetland Escarpment. Many of the 2D surveys were surplus to requirement, with this study using 8 surveys with a vertical resolution of 20 - 30 m and a horizontal resolution of 30 - 50 m (Table 3.1; Fig. 3.21).

2D Survey Name	Number of Survey Lines	Total Survey Length (km)	Licensing Company
CV05	26	1645	Chevron
IS-FST	15	2224	Inseis Terra AS/CGGVeritas/ SpectrumASA
NWZ96RE06	28	2384	Fugro Multi Client Services
OF94	41	4412	WesternGeco
OF95	22	2090	WesternGeco
ST0510	29	1546	Statoil
ST0513	19	1081	Statoil
ST0514	21	1241	Statoil

Table 3.1. Summary of 2D seismic reflections surveys used in this thesis, including number of survey lines, total survey length and ownership of data. For location of data see Fig. 3.21.
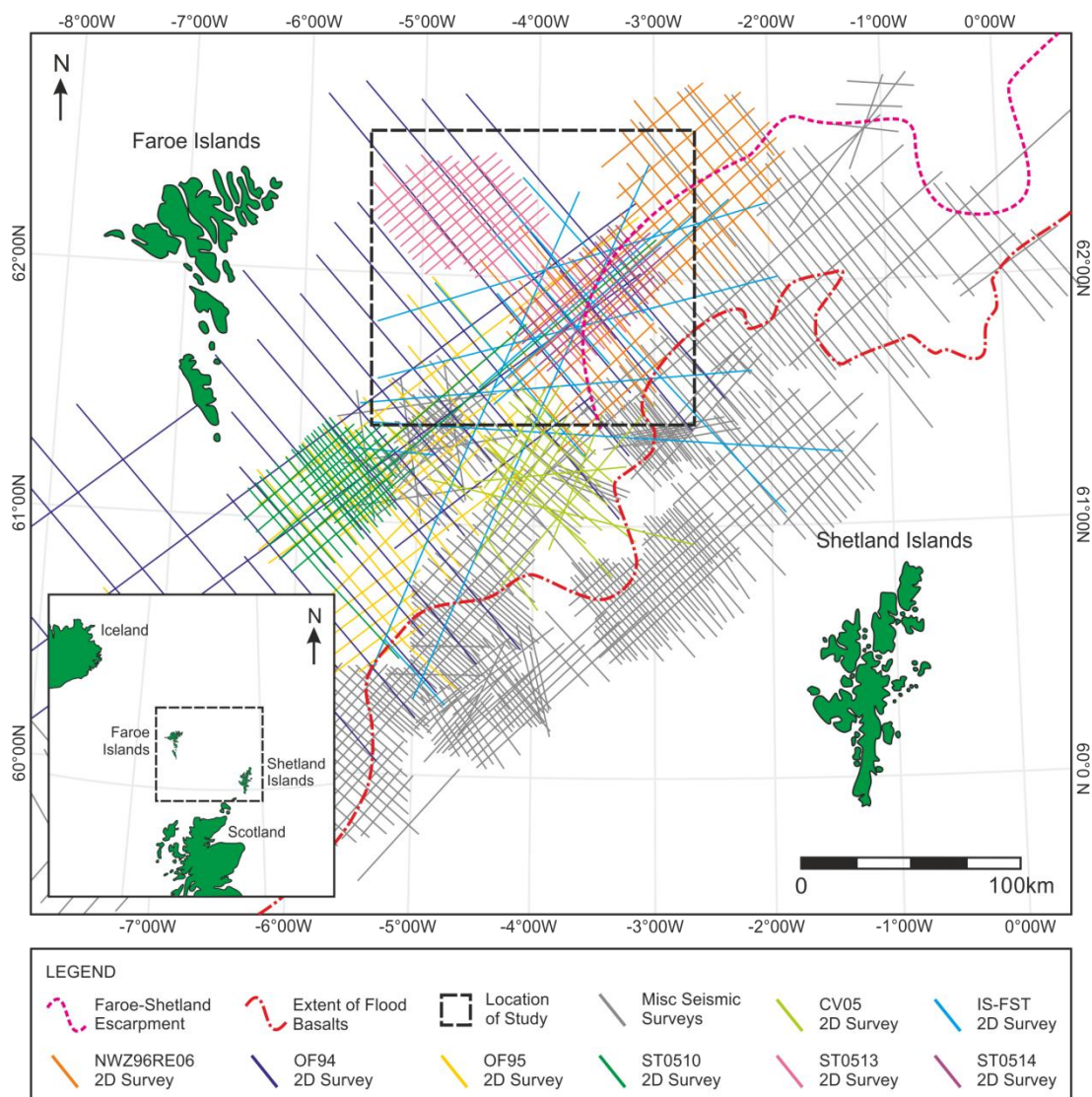
Fig. 3.21. Map of the Faroe-Shetland Basin showing the distribution of 2D seismic reflection surveys and the location of the study area (see Table 3.1). Extent of flood basalts and

Faroe-Shetland Escarpment modified from Ritchie *et al.* (1996, 1999), Ellis *et al.* (2002) and Sørensen (2003).

3.5.2 3D Seismic Reflection Data

This study also used two 3D seismic reflection surveys that cover different areas of the Faroe-Shetland Basin (Fig. 3.22). The ST0821 3D seismic reflection survey was provided under license from Statoil UK Ltd initially for use during in-house visits to the Statoil UK offices in London, and later at Durham University. The data are located in the centre of the Faroe-Shetland Basin and image the Faroe-Shetland Escarpment and post rift sedimentary basin fill (Fig. 3.22). The survey is 20 x 40 km and covers an area of 800 km^2 with a vertical resolution of ~25 m and a horizontal resolution of ~50 m (Table 3.2). The PGS MegaSurvey was provided by DONG Energy UK under licence from Petroleum Geo-Services (PGS) for use during a 3 month long internship and later in-house visits at the DONG Energy UK offices in London. The survey has a regional extent over the central and southern part of the Faroe-Shetland Basin and images the underlying rift structure, the feather edge of the continental flood basalts and post rift sedimentary basin fill (Fig. 3.22). It comprises of over 30 individual 3D seismic surveys which have been merged, providing a total coverage of >22600 km^2. The merged survey was cropped to the area of interest and was 50 x 60 km, covering 3000 km^2 of the distal flood basalts with a vertical resolution of ~30 m and a horizontal resolution of 40 - 60 m (Table 3.2).

3D Survey Name	Number of Surveys	Total Survey Area (km^2)	Licensing Company
ST0821	1	800	Statoil
Cropped PGS MegaSurvey	1	3000	Petroleum Geo-Services

Table 3.2. Summary of 3D seismic reflections surveys used in this thesis, including total survey area and ownership of data. For location of data see Fig. 3.22.
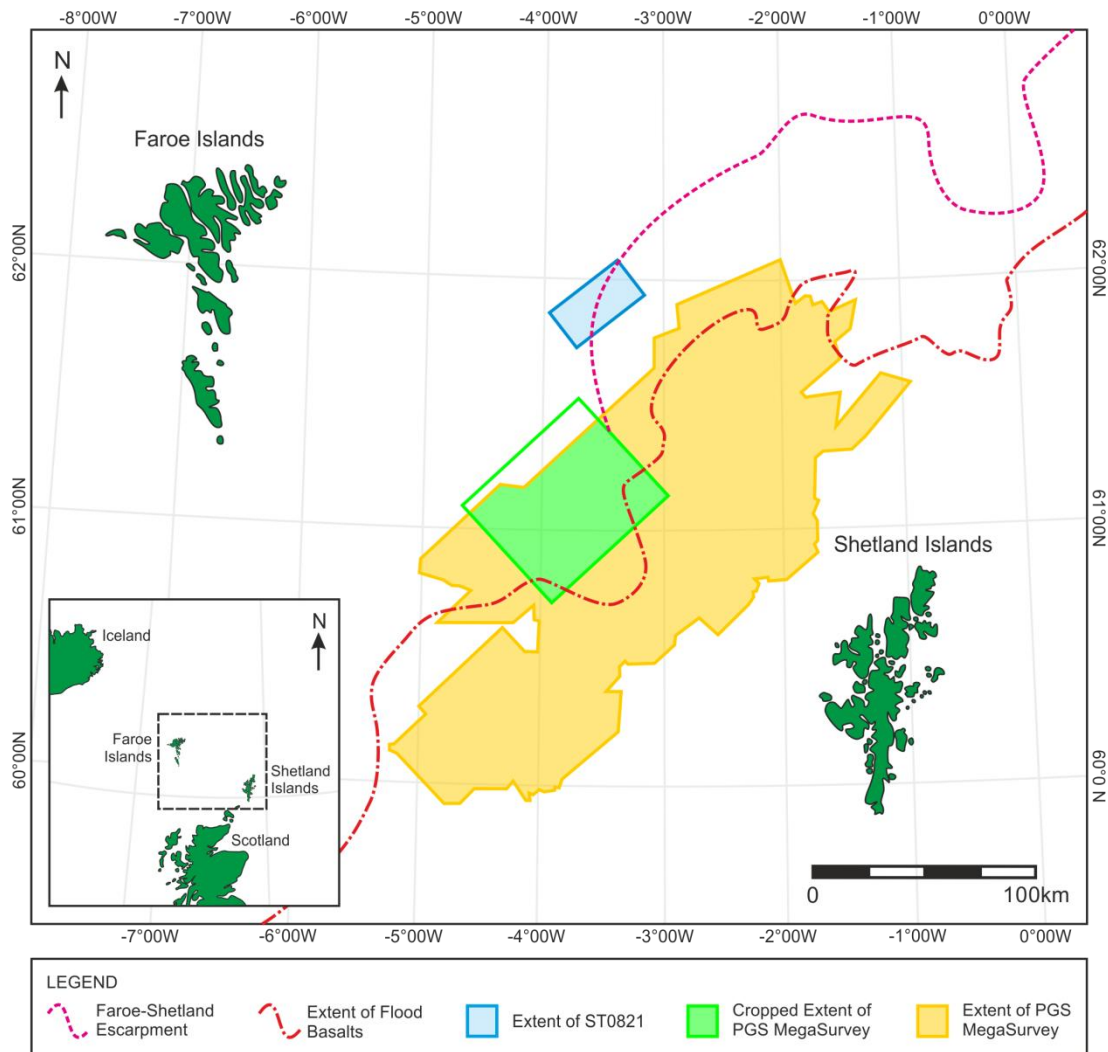
Fig. 3.22. Map of the Faroe-Shetland Basin showing the distribution of 3D seismic reflection surveys (see Table 3.2). Extent of flood basalts and Faroe-Shetland Escarpment modified from Ritchie *et al.* (1996, 1999), Ellis *et al.* (2002) and Sørensen (2003).

3.5.3 Exploration Wells

The exploration wells in the Faroe-Shetland Basin are limited to either the proximal or distal extents of the continental flood basalts (Fig. 3.23). The proximal flood basalts are penetrated by three boreholes on the Faroe Islands, the Glyvursnes-1, the Vestmanna-1 and the Lopra 1/1A boreholes (Fig. 3.23). The boreholes were drilled by Jarðfeingi, the Faroese Geological Survey and encountered thick formations of pāhoehoe lava flows and interbedded volcaniclastic rocks with a stratigraphic thickness of at least 6.6 km. Borehole data are in the public domain and were gained from the published literature (e.g. Boldreel, 2006; Chalmers & Waagstein, 2006; Passey & Bell, 2007).

The well data used in Chapter 4 and 5 have been released into the public domain and have been described in published literature (e.g. Davies *et al*., 2004; Davison *et al*., 2010). This includes well 214/4-1 which was drilled by ExxonMobil (Fig. 3.23). The digital geophysical well logs of 214/4-1 were provided by Statoil U.K. Ltd and were imported into the Landmark SeisWorks® software. The well encountered inter-bedded successions of hyaloclastite, lava and siliciclastic sedimentary rocks of varying thickness and was used to calibrate the seismic response to the volcanic lithologies with the IS-FST 2D seismic reflection survey (Table 3.3).

In Chapter 5 the distal flood basalts were penetrated by five wells over the Rosebank discovery; 205/01-1, 213/23-1, 213/26-1, 213/27-1 and 213/27-2 which were drilled in partnership between Chevron, Statoil UK Ltd, OMV and DONG Energy UK with the aim of investigating a four-way inversion structure beneath the basalts (Fig. 3.23). The wells encountered hydrocarbon accumulations in inter-bedded volcanic and siliciclastic successions as well as the sub-basalt structure (Table 3.3). The well data for all the logs in Chapter 5 were supplied as digital geophysical well logs by DONG Energy UK and imported into Petrel® for use during a 3 month long internship and later in-house visits at the DONG Energy UK offices in London.

Well Name	Location	Measured Depth (m)	Licensing Company
Glyvursnes-1	Onshore	700	Jarðfeingi
Vestmanna-1	Onshore	660	Jarðfeingi
Lopra 1/1A	Onshore	3500	Jarðfeingi
214/4-1	Offshore	4110	ExxonMobil
205/01-1	Offshore	3140	Chevron/Statoil/OMV/DONG Energy
213/23-1	Offshore	3577	Chevron/Statoil/OMV/DONG Energy
213/26-1	Offshore	3065	Chevron/Statoil/OMV/DONG Energy
213/27-1	Offshore	3676	Chevron/Statoil/OMV/DONG Energy
213/27-2	Offshore	3434	Chevron/Statoil/OMV/DONG Energy

Table 3.3. Summary of borehole and exploration well data used in this thesis, including location, measured depth and ownership of data. For location of data see Fig. 3.23.
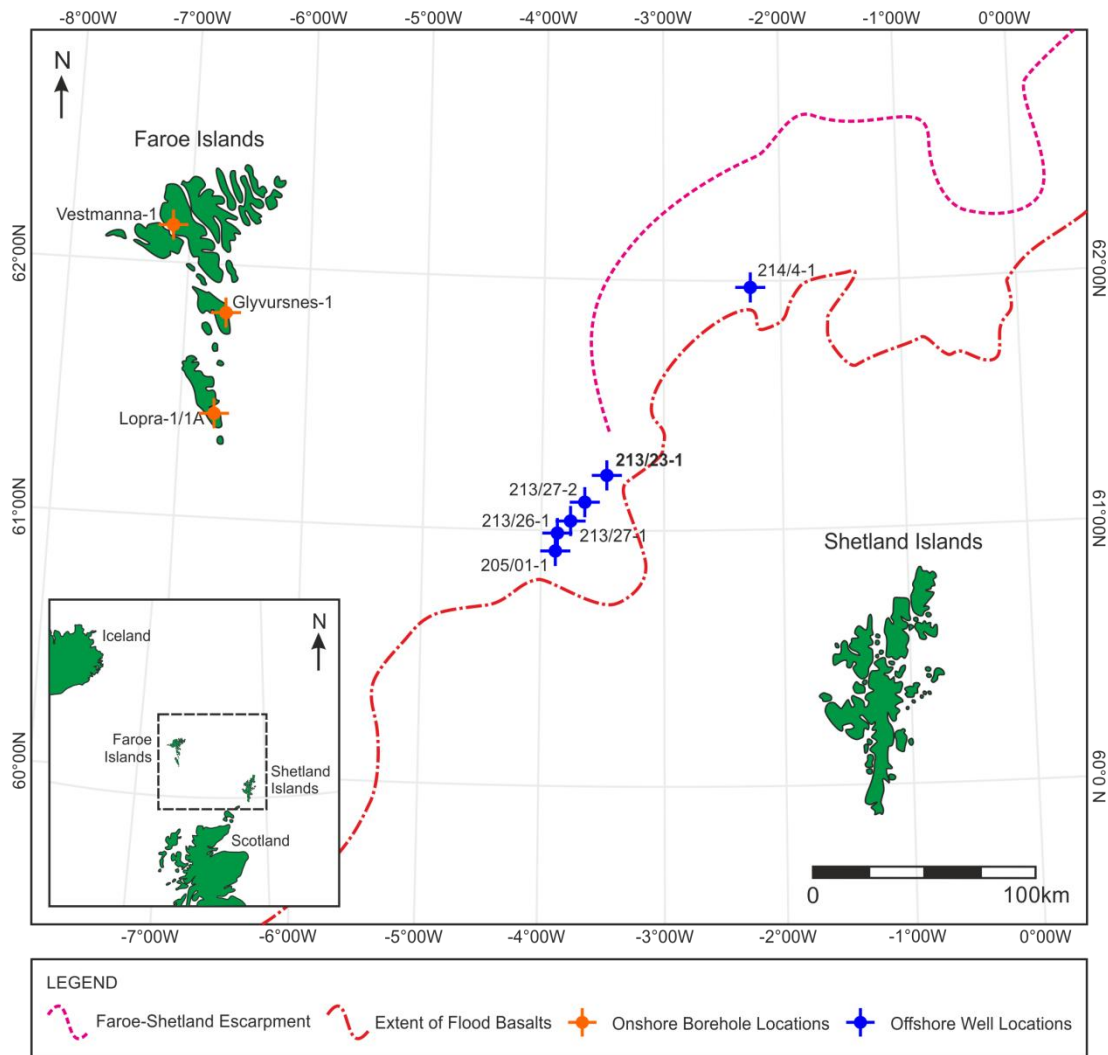
Fig. 3.23. Map of the Faroe-Shetland Basin showing the distribution of onshore boreholes and offshore exploration wells (see Table 3.3). Extent of flood basalts and Faroe-Shetland Escarpment modified from Ritchie *et al.* (1996, 1999), Ellis *et al.* (2002) and Sørensen (2003).

3.6 Outcrop Analogues for the Subsurface

Although seismic reflection data are primarily used for hydrocarbon exploration, they provide a unique opportunity to study buried, large-scale volcanic morphologies and structures that may not be accessible or are no longer preserved at the Earth's surface (Cartwright & Huuse, 2005; Davies & Posamentier, 2005; Posamentier *et al.*, 2007). Despite this, it is important to compare, where possible, seismic observations with outcrop analogues, as structures that are recognised in seismic reflection data are typically an order of magnitude larger than those seen in outcrop (Fig. 3.24; Kearey *et al.*, 2002; Nelson *et al.*,

2009a). Therefore comparison with outcrop analogue can identify features independent of scale, features which are likely to be present but are below seismic resolution and which features are unique and have not been described before.
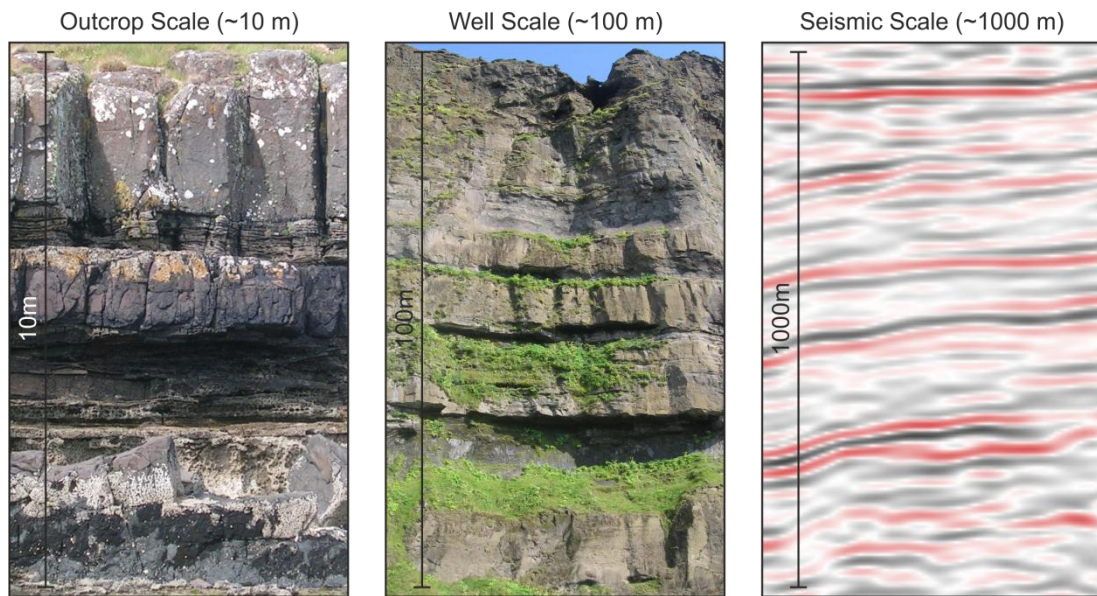
Fig. 3.24. Diagram depicting the differences in vertical resolution between outcrop (~10 m), well (~100 m) and seismic data (~1000 m).

There are currently no active continental flood basalt eruptions and so comparisons must be found with ancient flood basalts or smaller, modern day eruptions where lava flow emplacement can be observed. In this thesis many comparisons have been briefly made between the seismic observations and outcrop analogues, and are based on either field data or the published literature. This has allowed informed interpretations to be made about the seismic data, including which features are comparable and those which appear to be newly described. A total of four outcrop analogues have been used in this thesis and are briefly described below;

3.6.1 Antarctica Peninsula

Volcanism in the Antarctica Peninsula region has occurred over the last 6 Ma as relatively short lived basaltic eruptions due to waning subduction and later back-arc extensional tectonics (Saunders & Tarney, 1982; Skilling, 2002; Smellie *et al.*, 2008). The region provides suitable outcrop analogues for this thesis as the volcanic eruptions are predominantly preserved as well exposed lava-fed deltas and tuff cones (Porębski & Gradzinski, 1990; Skilling, 2002; Smellie *et al.*, 2006; 2008). Much of the volcanic material erupted was deposited in englacial lacustrine and submarine environment with multiple stacked lava-

fed deltas and interactions with contemporaneous sedimentary successions (Skilling, 2002; Smellie *et al.*, 2006; 2008). Comparisons between the volcanic rocks of the Antarctica peninsula and the seismic observations of this thesis are discussed in Chapter 4 and are based solely on the published literature.

3.6.2 Columbia River Flood Basalt Province

The Columbia River Basalt Group is a Large Igneous Province located in the Western USA and was caused by migration of the Yellowstone hot spot between 17-6 Ma (Thompson & Gibson, 1991; Camp, 1995). It provides suitable outcrop analogues for this thesis as thick successions of the eruptive products are exposed and are often large enough to be considered seismic scale. Of particular interest are the thick pāhoehoe lava flows which coalesced to form extensive sheet flows and were emplaced from a series of fissures and vents (Swanson *et al.*, 1975; *et al.*, 1992; Self *et al.*, 1996; 1997). Sedimentary interbeds reveal the effect that successive phases of flood basalt volcanism had on the pre-existing drainage system, with the damming of river systems and formation of pillow basalt delta systems in the resulting lakes (Tolan & Beeson, 1984; Lyle, 2000; Ely *et al.*, 2012). Comparisons between the volcanic rocks of the Columbia River Flood Basalt Province and the seismic observations of this thesis are discussed in Chapter 6 and are based on field observations from an excursion in September 2012 and from the published literature.

3.6.3 Greenland

The volcanic rocks exposed along the west and east coasts of Greenland were erupted at ~65 Ma during the rifting and subsequent continental break up that created the NE Atlantic Margin (Larsen *et al.*, 1992). They provide suitable outcrop analogues for this thesis as they are contemporaneous with the volcanic rocks in the Faroe-Shetland Basin and are sourced from the same mantle anomaly that caused the North Atlantic Igneous Province (Dam *et al.*, 1998; Larsen *et al.*, 1999). The volcanic successions are composed of extensive pāhoehoe lava flows with thick lava-fed delta systems and hyaloclastic deposits where indigenous drainage systems became dammed, creating lakes which were infilled by the erupting lava flows (Pedersen *et al.*, 1998; Mueller *et al.*, 2000; Dam, 2002). The pre-, syn- and post-rift sedimentary successions are currently of interest as they may contain hydrocarbon accumulations similar to those identified along the rest of the Northeast Atlantic Margin (Dam *et al.*, 1998; Bojesen-Koefoed *et al.*, 1999). Comparisons between the

volcanic rocks of Greenland and the seismic observations of this thesis are discussed in Chapter 4 and are based solely on the published literature.

3.6.4 Hawaii

The Island of Hawaii is the youngest of a chain of volcanic islands that delineates the migration of the Pacific plate over a fixed hot spot (Moore & Clague, 1992; Zhong & Watts, 2002). The island has been constructed by multiple, almost continuous subaerial volcanic eruptions for the last 300 kyrs (Moore & Clague, 1992). The volcanic rocks on the Island of Hawaii provide suitable outcrop analogues for this thesis as the Hawaiian lava flows are predominantly emplaced as extensive pāhoehoe flows from a number of discrete vents and fissures, and which are closely similar in emplacement style to continental flood basalts (Hon *et al*., 1994; Self *et al.*, 1997; Kauahikaua *et al.*, 1998). Of particular interest are the multiple lava flows which enter the ocean and construct lava-fed deltas and extensive hyaloclastite deposits in an offshore apron along the eastern coast of the island (Moore *et al.*, 1973; Mattox *et al.*, 1993; Heliker *et al.*, 1998). The Island also records subaerial erosion and subaqueous mass wasting between and occasionally during the eruptive phases on Hawaii (Mattox *et al.*, 1993; Heliker *et al.*, 1998). Comparisons between the volcanic rocks of Hawaii and the seismic observations of this thesis are discussed in Chapter 4 and are based solely on the published literature.

3.6.5 Iceland

Iceland is a volcanic island that straddles the Mid-Atlantic Ridge and was formed by crustal accretion through numerous basaltic eruptions over the last ~20 Ma (Allen *et al*., 2002). Its formation is thought to be the continuation of the mantle anomaly that caused the North Atlantic Igneous Province coupled with the sea floor spreading that created the Northeast Atlantic Margin (Vink, 1984; Larsen *et al*., 1992; Allen *et al*., 2002). The volcanic rocks on Iceland provide suitable outcrop analogues for this thesis as the thick inflated pāhoehoe lava flows were emplaced from a number of discrete vents and fissures (Self *et al*., 1996; 1997). Of particular interest are the lava-fed delta systems and hyaloclastite deposits that developed when lava flows entered glacial melt water lakes or the surrounding ocean (Furnes & Fridleifsson, 1974; Bergh & Sigvaldason, 1991; Schopka *et al*., 2006). Comparisons between the volcanic rocks of Iceland and the seismic observations of this thesis are discussed in Chapter 5 and are based on field observations from an excursion in August 2009 and from the published literature.

CHAPTER 4: APPLICATION OF SEISMIC STRATIGRAPHIC CONCEPTS TO A LAVA-FED DELTA SYSTEM IN THE FAROE-SHETLAND BASIN

4.1 Introduction

Seismic reflection imagery of sedimentary basins has resulted in the recognition of specific reflection configurations and reflection terminations that have informed the reconstruction of relative sea level changes and an understanding of basin-fill histories (e.g. Payton, 1977; Wilgus *et al.*, 1988). The seismic reflection method was initially applied to siliciclastic (e.g. Vail *et al.*, 1977c; Posamentier & Vail, 1988) and then carbonate successions (e.g. Bubb & Hatlelid, 1977; Sarg, 1988), and more recently to volcanic rifted margins (e.g. Spitzer *et al.*, 2008; Jerram *et al.*, 2009; Ellefsen *et al.*, 2010). Growing interest in exploration and production of hydrocarbons from offshore successions with a volcanic component has resulted in seismic data being acquired over such areas, including the Møre and Vøring Basins (onshore Norway) and the Faroe-Shetland Basin (UK and Faroes).

Significant volumes of flood basalts were erupted in subaerial to submarine settings in the Northeast Atlantic Region during the Late Palaeocene (e.g. White, 1989; Ellis *et al.*, 2002; Jerram *et al.*, 2009). The volcanic succession displays a variety of reflection configurations that are indicative of the style of volcanic emplacement, depositional environment and subsequent mass transport. Parallel bedded reflections are interpreted to be subaerially erupted plateau lava flows (Boldreel & Andersen, 1994). Seaward dipping reflections exhibit inclined, smooth to hummocky geometries and are interpreted to be subaerial to shallow submarine lava flows erupted during the early stages of sea floor spreading. They erupted close to, or on the axis of spreading and were later affected by post-rift subsidence, with the greatest inclination seen in the oldest lava flows (Andersen, 1988; Planke *et al.*, 2000; Parkin *et al.*, 2007). Prograding reflections with a steeper inclination (>20°) are interpreted to be subaerially erupted lava flows entering the sea, forming steep delta escarpments of hyaloclastic breccias (Smythe, 1983; Smythe *et al*., 1983; Kiørboe, 1999; Spitzer *et al.*, 2008).

Lava-fed deltas preserve the transition from subaerial to submarine strata, and are a record of the palaeo-shoreline. They often display similarities to siliciclastic delta systems, by filling the available accommodation, reacting to changes in relative sea level and variations in the

supply of material (Fig. 4.1; Jones & Nelson, 1970; Moore *et al.*, 1973; Jerram *et al.*, 2009). This has led to comparisons of lava-fed deltas with Gilbert-type siliciclastic deltas and the identification of comparable facies components (Fuller, 1931; Jones & Nelson, 1970; Porębski & Gradzinski, 1990; Naylor *et al.*, 1999). However, lava-fed delta systems, particularly those formed during flood basalt eruptions, record variations in the supply of volcanic material, which can be much greater than in siliciclastic systems. Huge volumes of lava erupt over geologically short timescales, resulting in the very efficient filling of accommodation and rapid progradation of the shoreline.

Modern examples of lava flowing into the sea (such as seen on Hawaii), undergo quenching and fragmentation into hyaloclastic breccias which are then rapidly deposited down slope under gravitational processes to form inclined foresets (Kokelarr, 1986; Fisher & Schmincke, 1994). The growth of the delta is through emplacement of new lava flows and hyaloclastic breccias, with successive phases of volcanism producing a stacking pattern that is directly related to the interaction of relative sea level, lava supply and available accommodation. The geometry of the stacking pattern depends on the dominant factor at the time of emplacement, making it possible to reconstruct the emplacement environment and interpret the lava-fed delta within a seismic stratigraphic framework (Jones & Nelson, 1970; Gatliff *et al.*, 1984; Kiørboe, 1999).
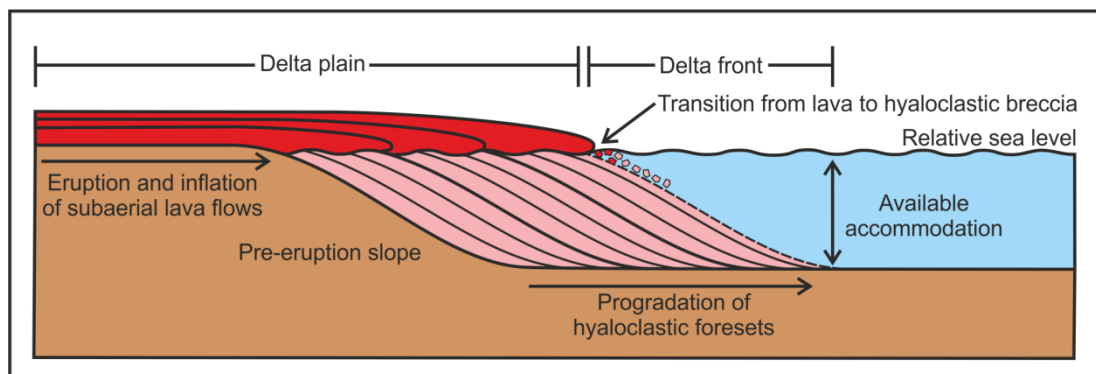
Fig. 4.1. Schematic cross section through a developing lava-fed delta. Based on this study, Fuller (1931) and Jones & Nelson (1970).

This study investigates in detail the reflection geometries of the Faroe-Shetland Escarpment and applies seismic stratigraphic concepts to define a series of volcanic units that are interpreted in terms of relative sea level, lava supply and available accommodation. Understanding how continental flood basalts develop from subaerial to submarine environments and the identification of key horizons within the volcanic

succession can be used to investigate the onset, development and closing stages of flood basalt volcanism (e.g. Jerram & Widdowson, 2005). It can constrain the spatial and temporal distribution of key volcanic facies (Nelson *et al*., 2009b) and be a valuable resource for exploration in volcanic rifted settings. This has allowed the detailed reconstruction of the development and evolution of Faroe-Shetland Escarpment and how the palaeo-shoreline evolved due to flood volcanism during the break-up of Europe from North America.

4.2 Geological Setting

The Faroe-Shetland Basin is a product of rifting between Greenland and Eurasia during the Mesozoic to Early Cenozoic (England *et al.*, 2005; Passey & Bell, 2007). Continental break-up and the onset of sea floor spreading occurred to the north and west of the Faroe-Shetland Basin and was accompanied by extensive continental flood basalt volcanism. Volcanic activity occurred throughout the Palaeocene, between 62-54 Ma (e.g. Ritchie & Hitchen, 1996; Hansen *et al.*, 2009; Søager & Holm, 2009) and is characterised by the extrusion of subaerial basaltic lavas (e.g. Passey & Bell, 2007), the intrusion of sills (e.g. Thomson & Schofield, 2008; Hansen *et al.*, 2011) and the formation of individual volcanic centres, such as the Erlend Complex and Brendans Dome (e.g. Gatliff *et al.*, 1984; Ritchie & Hitchen, 1996; Jolley & Bell, 2002).

To the east of the Faroe Islands, the Faroe-Shetland Escarpment has been identified as the subaerial extension of the flood basalts, which flowed to the southeast in-filling pre-existing topography before reaching the palaeo-shoreline (Smythe, 1983; Smythe *et al*., 1983; Kiørboe, 1999; Ritchie *et al.*, 1999). At the shoreline, flood basalt flows entered the water and formed a prograding body of hyaloclastic breccias which pushed the shoreline basinward. Initial work has shown that the distribution of these systems or deltas can be extensive, recording a significant syn-volcanic migration of the palaeo-shoreline in this region (e.g. Kiørboe, 1999; Spitzer *et al.*, 2008; Jerram *et al.*, 2009). Volcanism within the basin ceased when sea floor spreading became established to the north of the basin, with post-rift subsidence and late Cenozoic compression creating the tilted and folded structures identified today (Ritchie *et al.*, 2003; Sørensen, 2003; Davies *et al.*, 2004; Praeg *et al.*, 2005).

4.3 Data and Methodology

This study has used a variety of 2D seismic reflection surveys gathered within the Faroe-Shetland Basin between 1983 and 2005, with large areas of geographical overlap (Fig. 4.2). The study focused on the Faroe-Shetland Escarpment where the flood basalt succession and contemporaneous deep water strata are imaged at an average vertical resolution of 20 – 30 m and an average horizontal resolution of 30 – 50 m, with an average velocity between 3000 – 4000 ms^{-1}. Analysis included the detailed mapping of ~60 lines that have an average line spacing of 1 – 3 km. The top surface of the flood basalts throughout the basin is identified by a positive, high amplitude and strongly continuous reflection. This reflection event marks an abrupt change in the seismic response, with the strong reflectivity of the top surface and the internal heterogeneity within the volcanic succession often presenting a challenge for imaging, particularly near the base of the succession (e.g. White *et al.*, 2003; Roberts *et al.*, 2005).

Despite these challenges, variations in seismic amplitude and reflection geometries have been clearly imaged, and with the application of seismic stratigraphy, it is possible to define the gross stratigraphic architecture within the volcanic succession. Initial examination of the data was through seismic facies analysis, which characterised the seismic reflection configurations of the Faroe-Shetland Escarpment in terms of amplitude, continuity and configuration to interpret the depositional processes, lithologies and environmental conditions (Mitchum *et al.*, 1977b; Sangree & Widmier, 1977; Cross & Lessenger, 1988). Analysis continued with the recognition of seismic reflection units composed of relatively conformable reflections and bounded by unconformities through the identification of systematic discordances or reflection terminations against the bounding reflection (Fig. 4.3; Mitchum *et al.*, 1977a; Van Wagoner *et al*., 1988). It should be noted that the term "unit" has be used rather than "sequence" to avoid confusion with the traditional seismic stratigraphic definition (e.g. Mitchum *et al.*, 1977a) and not to imply a set scale or order.
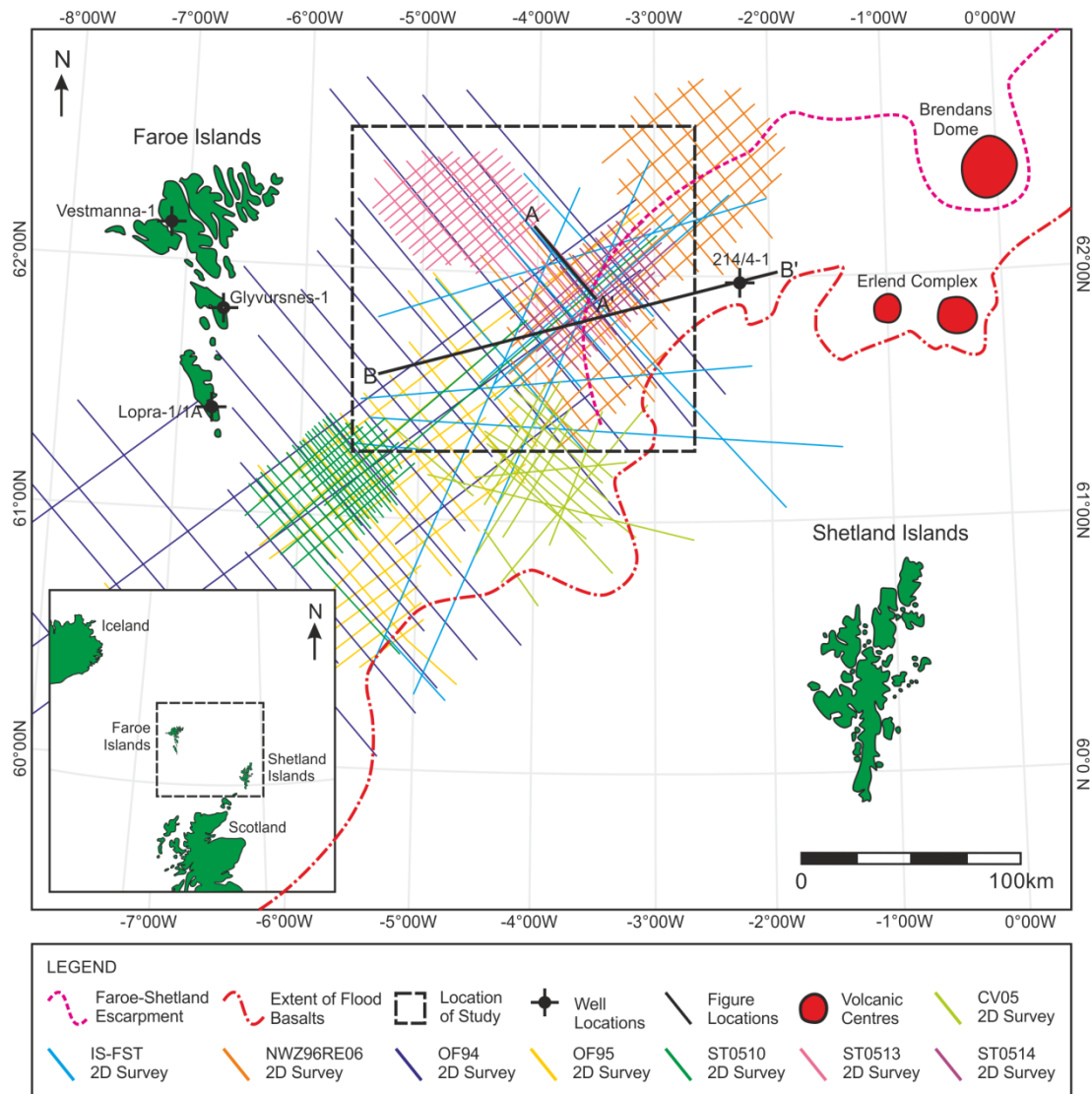
Fig. 4.2. Map of the Faroe-Shetland Basin showing the study area and location of seismic cross sections used in Fig. 4.3 and Fig. 4.5. Extent of flood basalts and Faroe-Shetland Escarpment modified from Ritchie *et al.* (1996, 1999), Ellis *et al.* (2002) and Sørensen (2003).
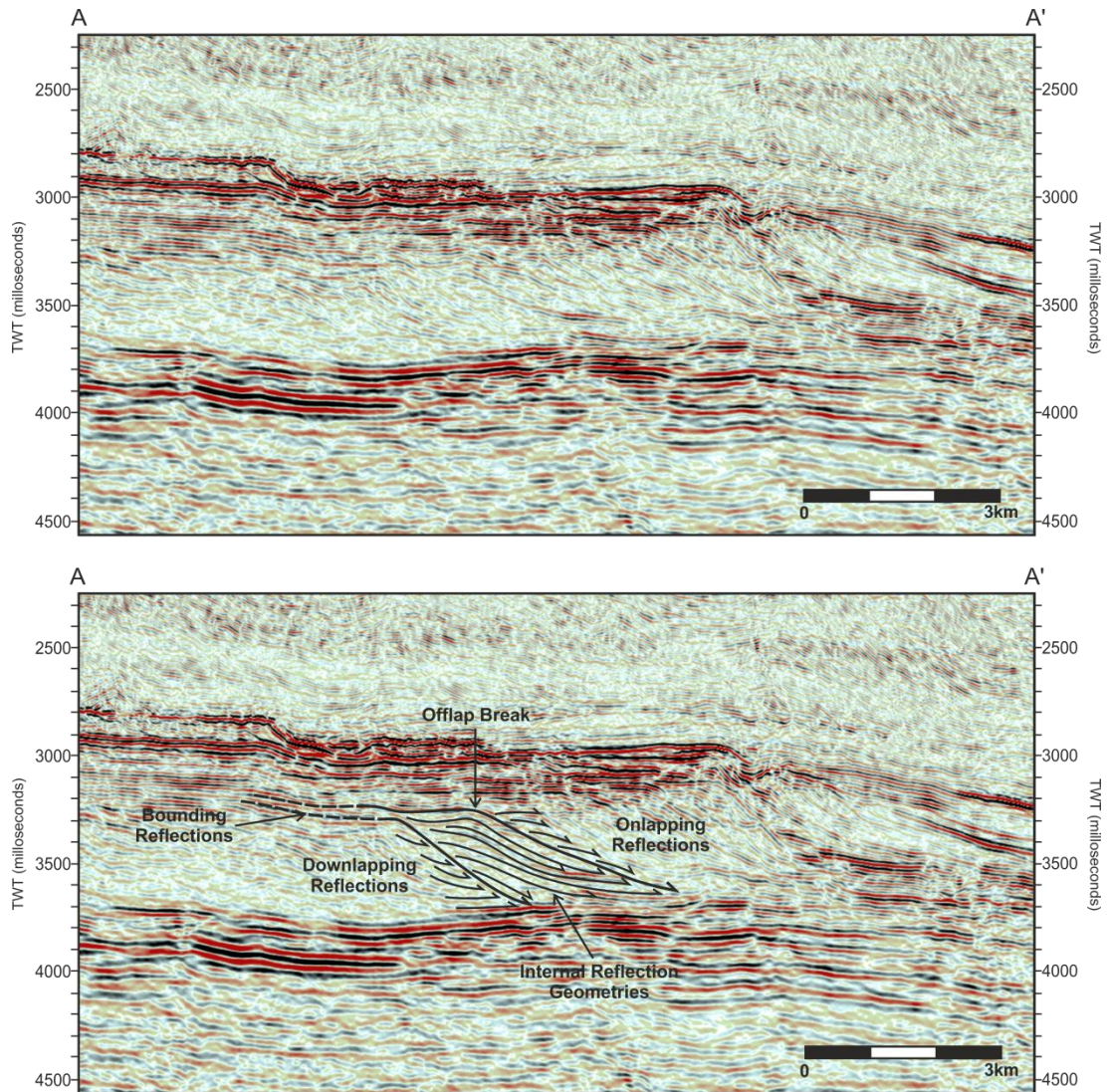
Fig. 4.3. Seismic stratigraphic methodology used to identify seismic reflection units after Vail *et al.* (1977b), Posamentier & Vail (1988) and Kiørboe (1999). See Fig. 4.2 for location.

Well control of the continental flood basalts in the Faroe-Shetland Basin is limited to either the proximal or distal extents. The proximal deposits outcrop on the Faroe Islands and are encountered by three boreholes, where the flood basalts have a stratigraphic thickness of at least ~6.6 km and have been subdivided on the basis of lithology, geochemistry and flow structure (see Chapter 2, Fig. 2.3; Ellis et al., 2002; Passey & Bell, 2007; Passey & Jolley, 2009; Jerram *et al.*, 2009). The volcanic succession penetrated in the boreholes exhibits a variety of velocities which are indicative of the volcanic facies. The thick pāhoehoe lava flows, as identified in the Beinisvørð Formation have high velocities, varying from 4000 – 7000 ms^{-1} with an average of 5500 ms^{-1}. The thinner, less extensive pāhoehoe lava flows, as identified in the Malinstindur Formation have low velocities, varying from 3000 – 6000 ms^{-1} with an average of 4500 ms^{-1}. Hyaloclastite breccias as identified in the Lopra Formation

have the lowest velocities, varying between 3000 – 5000 ms^{-1} with an average of 3500 ms^{-1} (Planke, 1994; Boldreel, 2006; Nelson *et al.*, 2009b). The distal extent of the flood basalts has been penetrated by a number of exploration wells in search of hydrocarbons which encountered inter-bedded successions of hyaloclastites, lavas and siliciclastic successions of varying thickness (Larsen *et al.*, 1999; Jolley & Morton, 2007). These include well 214/4-1, which encountered approximately ~100 m of basalt overlying ~300 m of hyaloclastite. This well was used to calibrate the seismic response to the volcanic lithologies (Fig. 4.4; Davies *et al.*, 2002; 2004; Sørensen, 2003).
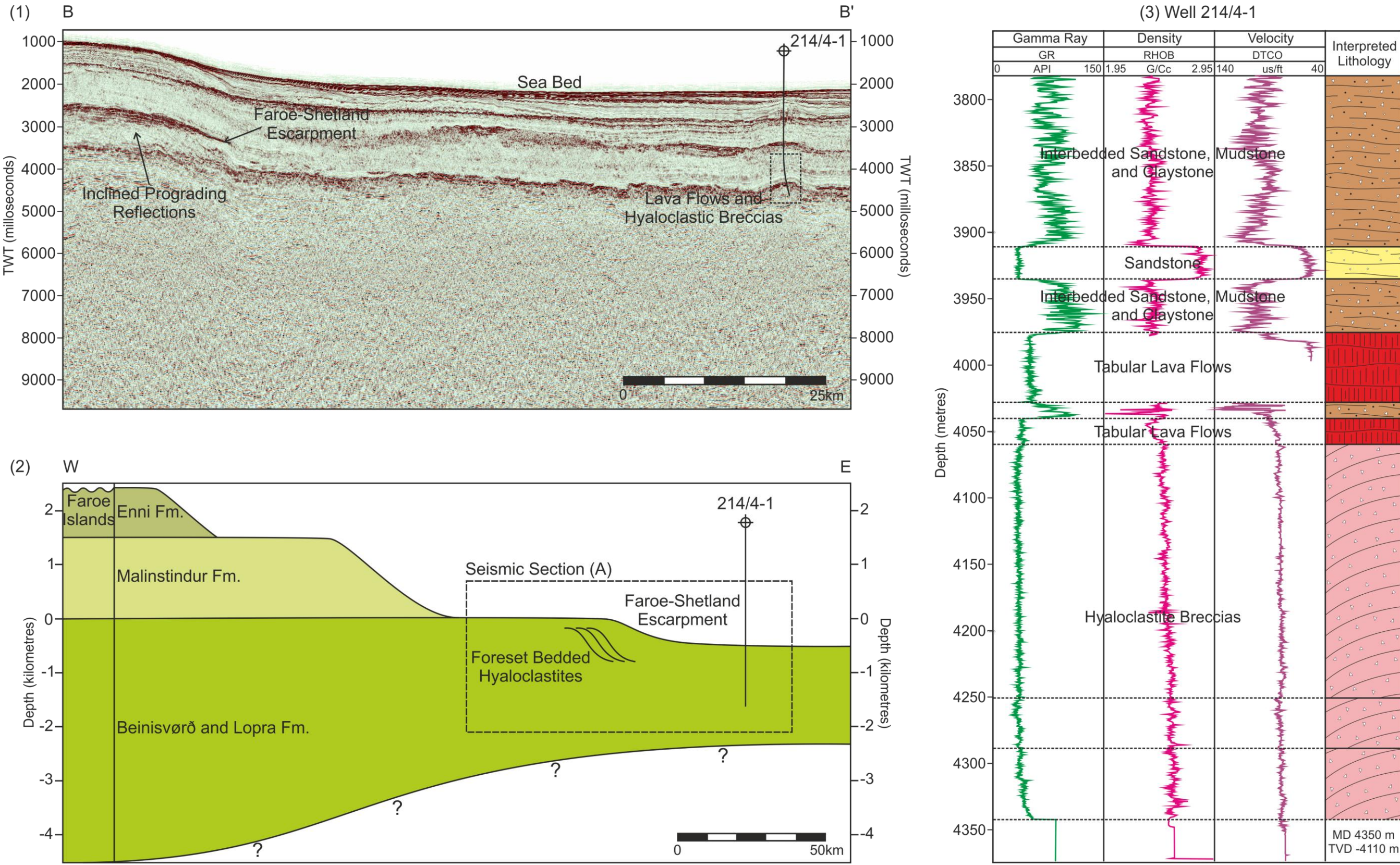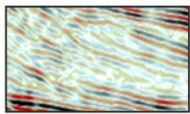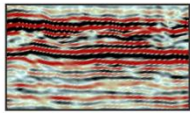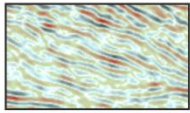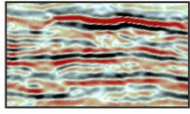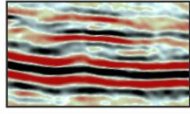
Fig. 4.4. (1) Regional correlation of seismic reflection configurations and interpreted lithologies identified in well 214/4-1. (2) Schematic correlation of onshore and offshore stratigraphy, modified from Smythe *et al.* (1983) and Ritchie *et al.* (1999). (3) Wireline log responses and interpreted lithologies for the volcanic succession in 214/4-1 (MD – measured depth and TVD – total vertical depth). See Fig. 4.2. For location.

4.4 Observations

4.4.1 Seismic Facies Analysis

Initial seismic interpretation began with the detailed analysis of seismic reflection configurations. A total of five seismic facies were identified using key observational criteria such as reflection amplitude, continuity and geometry (Table 4.1). Each facies has been named according to their distinctive reflection characteristics, as suggested by West *et al.* (2002). The identified facies have distinct distributions and spatial relationships, often with indistinct facies boundaries. The first and uppermost facies identified is composed of high amplitude, continuous reflections (HAC facies) that extend from the Faroes shelf into the basin. The second facies is composed of moderate amplitude, continuous reflections (MAC facies) that are located basinward of the offlap break. The reflections are inclined and prograde in a south-easterly direction. The third seismic facies is composed of low amplitude, semi-continuous reflections (LASC facies) that are located further basinward of the MAC facies. The fourth facies is composed of moderate amplitude, semi-continuous reflections (MASC facies) that extend from the east and appear to terminated halfway beneath the body of the MAC facies. The final and deepest facies identified is composed of high amplitude, semi-continuous reflections (HASC facies) that are located beneath all of the previously described facies, extending across the basin and towards the Faroe Islands.

Seismic Facies	Seismic Reflections	Geometry	Top Reflections	Internal Reflections	Base Reflections
Low Amplitude Semi-Continuous (LASC)		Wedge	Moderate amplitude inclined and subparallel reflections.	Low amplitude, inclined, subparallel, varies between semi-continous and disrupted reflections.	Low amplitude, subhorizontal, subparallel reflections.
High Amplitude Continuous (HAC)		Sheet-like	High amplitude, horizontal to subhorizontal. Parallel largely continuous with a irregular or undulating reflections.	High to moderate amplitude, horizontal to subhorizontal Parallel to subparallel, continuous reflections.	Moderate amplitude, subhorizontal, parallell. Varies from continuous to disrupted reflections.
Moderate Amplitude Continuous (MAC)		Wedge	Moderate amplitude, subhorizontal, parallel to subparallel reflections.	Moderate to low amplitude, inclined, parallel to subparallel, continuous to semi-continuous reflections.	Low amplitude,parallel to subparallel, semi-continuous reflections.
Moderate Amplitude Semi-Continuous (MASC)		Sheet-like to wedge	High amplitude, horizontal to subhorizontal. Parallel to subparallel, occasionally rugose reflections.	High to moderate amplitude, horizontal to subhorizontal. Parallel to subparallel, semi-continuous, hummocky reflections.	Moderate to low amplitude, subhorizontal, parallel. Varies from semi-continuous to disrupted reflections.
High Amplitude Semi-Continuous (HASC)		Sheet-like	High amplitude, horizontal to subhorizontal, largely continuous reflections.	High to moderate amplitude, parallel to subparallel, varying continuity with strong layered reflections.	Moderate to low amplitude, parallel to subparallel, semi-continuous reflections, difficult to identify.

Table 4.1. Description of seismic facies, including observational criteria, external geometry and typical reflection configurations, after West *et al.* (2002).

4.4.2 Reflection Configuration Analysis

In the seismic reflection data, the top of the flood basalts in the Faroe-Shetland Basin is identified by a prominent, high amplitude and strongly continuous reflection that defines the upper limit of a succession of high amplitude, subhorizontal and continuous reflections that decrease in amplitude and continuity with depth. This top basalt character extends from the Faroes shelf towards the Faroe-Shetland Basin, where the continuous, high amplitude reflections rapidly change to inclined, moderate amplitude reflections. This transition is marked by a clear offlap break, which is the point at which the reflection pattern changes from one of shallow marine deposition to deeper marine deposition (Mitchum, 1977). Basinward of the offlap break, the seismic reflection configurations define seismic reflection units composed of moderate to low amplitude, continuous reflections with prograding, sigmoidal geometries (see Fig. 4.3). Each unit was recognised by the bounding reflections, which were identified by reflection terminations. The base of each seismic reflection unit is identified by downlap on to deeper reflections (see Fig. 4.3).

The Faroe-Shetland Escarpment has been extensively mapped (Fig. 4.5) and at least 13 seismic reflection units composed of high amplitude topsets and moderate amplitude foresets have been identified. These have been numbered in stratigraphic order, with 1 being the oldest and 13 being the youngest. Seismic reflection units 1 – 11 have a sheet to wedge-like morphology, with heights of 700 to 1050 m and foresets inclinations of 20°, increasing up to 40°. The stacking pattern of the units 1 – 11 is largely progradational with an aggradational component that becomes increasingly apparent in units 6 – 11 (Fig. 4.6). Seismic reflection units 12 and 13 have a similar wedge-shaped morphology which mimics the reflection geometries of larger seismic reflection units 1 – 11, with foreset heights varying from 175 to 200 m. These units are directly above units 1 – 11 and display a retrogradational stacking pattern, with the extent of each unit located progressively westward, towards the Faroe Islands (Fig. 4.6).
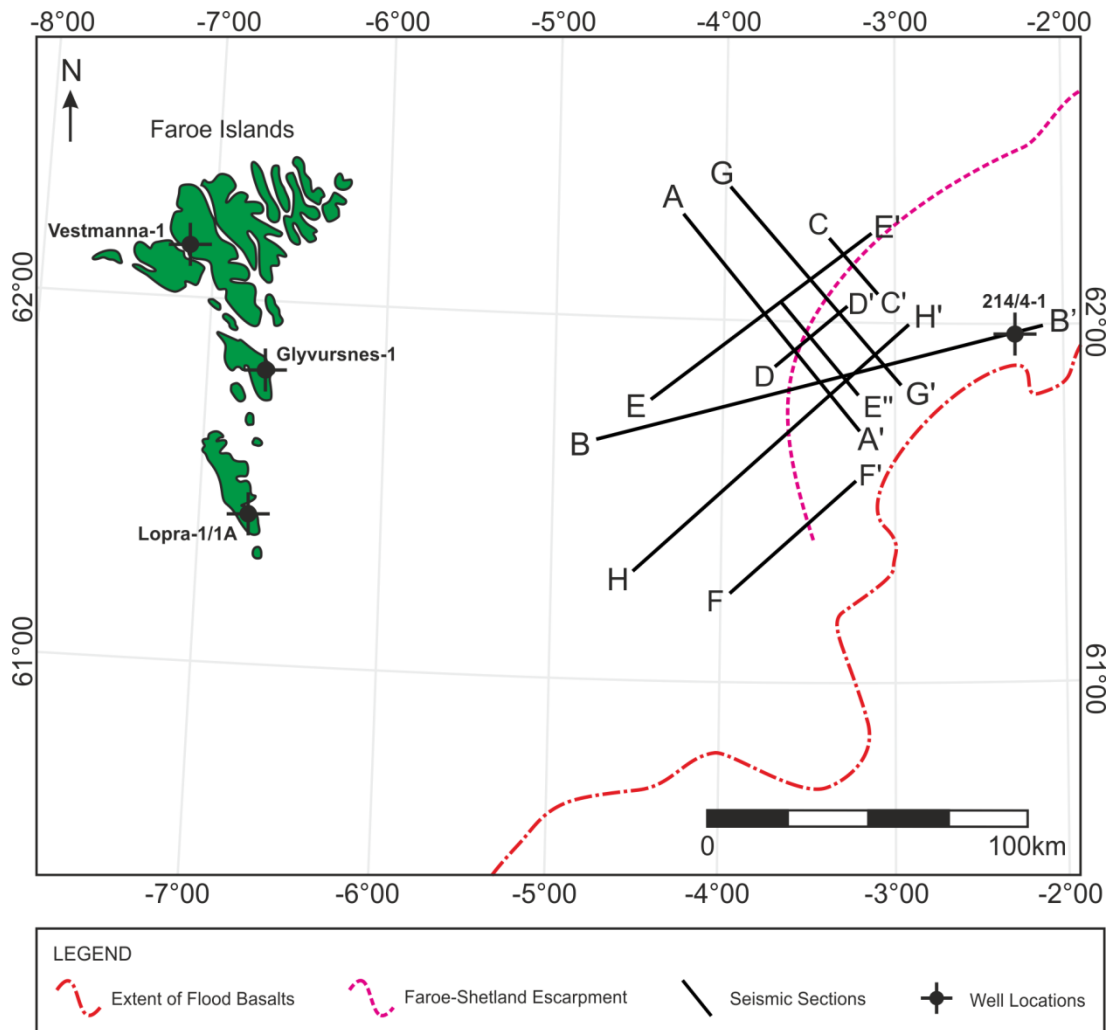
Fig. 4.5. Map of the study area with the location of seismic cross sections. Extent of flood basalts and Faroe-Shetland Escarpment modified from Ritchie *et al.* (1996, 1999), Ellis *et al.* (2002) and Sørensen (2003).

The extent of the seismic reflection units were mapped through the correlation of the bounding reflections across the different seismic reflection surveys. This became increasingly difficult the deeper the seismic reflection unit was within the escarpment. This is due to heterogeneity of the volcanic rocks causing scattering and absorption of the seismic energy (see Chapter 3). The decrease in amplitude and reflection continuity within the escarpment, potentially masks any deeper seismic reflection units. This can be seen in the deepest part of the succession, with a wedge of low to moderate amplitude indistinct reflections that thins towards the Faroese shelf. Although recognition of coherent reflections below the units can be difficult, a succession of high to moderate amplitude reflections were encountered in 214/4-1 (see Fig. 4.4) and have been identified extending beneath units 6 – 11 (Fig. 4.7).
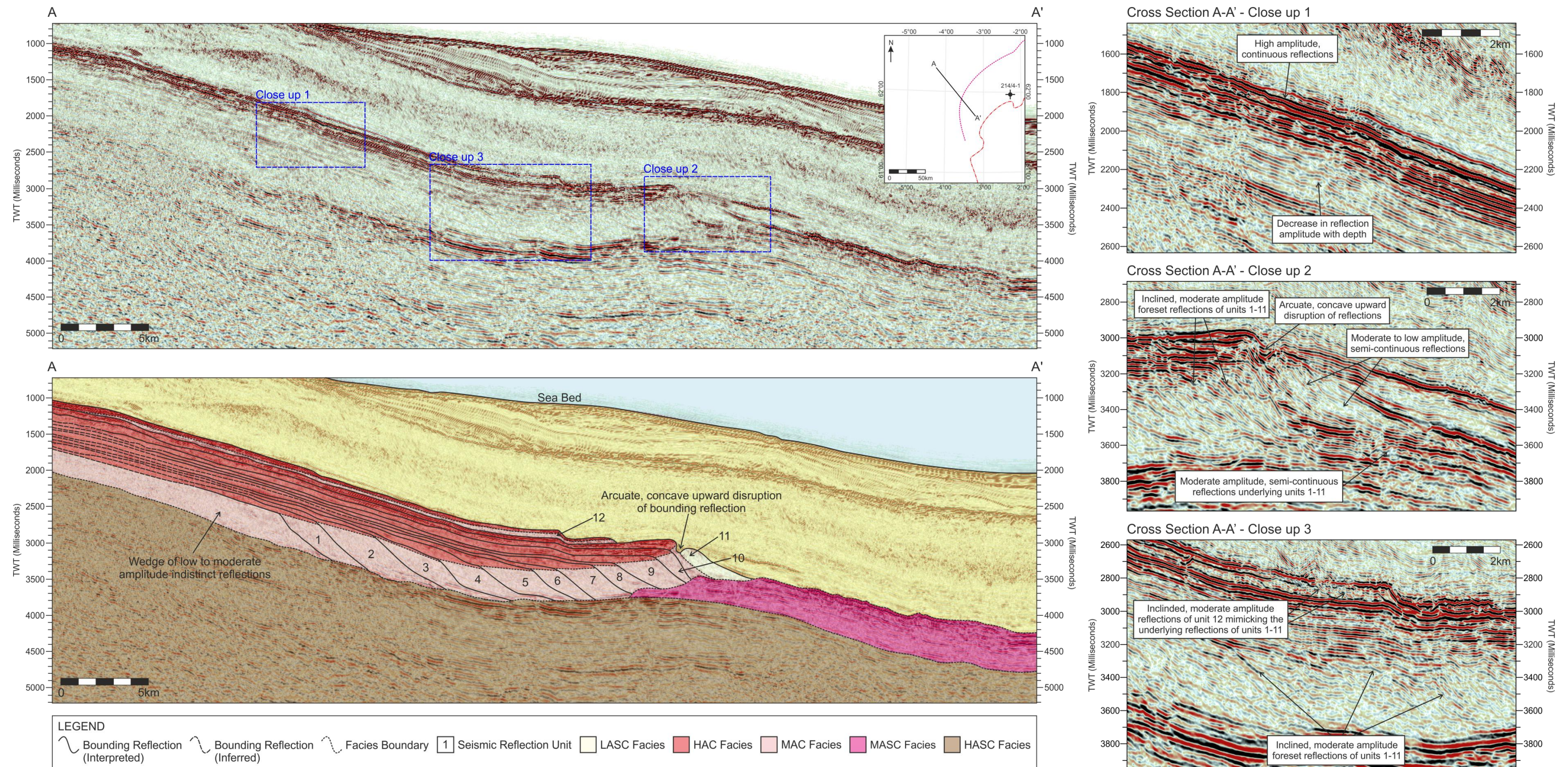
Fig. 4.6. Seismic section A-A' images the Faroe-Shetland Escarpment perpendicular to the curved escarpment edge, with close-up sections identifying the main features. Close-up 1 is of the continuous, high amplitude topsets that define the top of the flood basalts. Close-up 2 is of the most basinward extent of seismic reflection unit 11 and the arcuate, concave upward features that disrupt the unit. Close-up 3 is of the basinward extent of seismic reflection unit 12 and shows the internal structure of small prograding clinoforms that mimic the larger clinoforms exhibited by the underlying seismic reflections units. The interpreted section includes the seismic reflection units and bounding reflections, distribution of seismic facies and disruption of seismic reflection unit 11 with shallow, semi-continuous internal reflections with an arcuate, concave upward upper bounding reflection. See Fig. 4.5 for location.
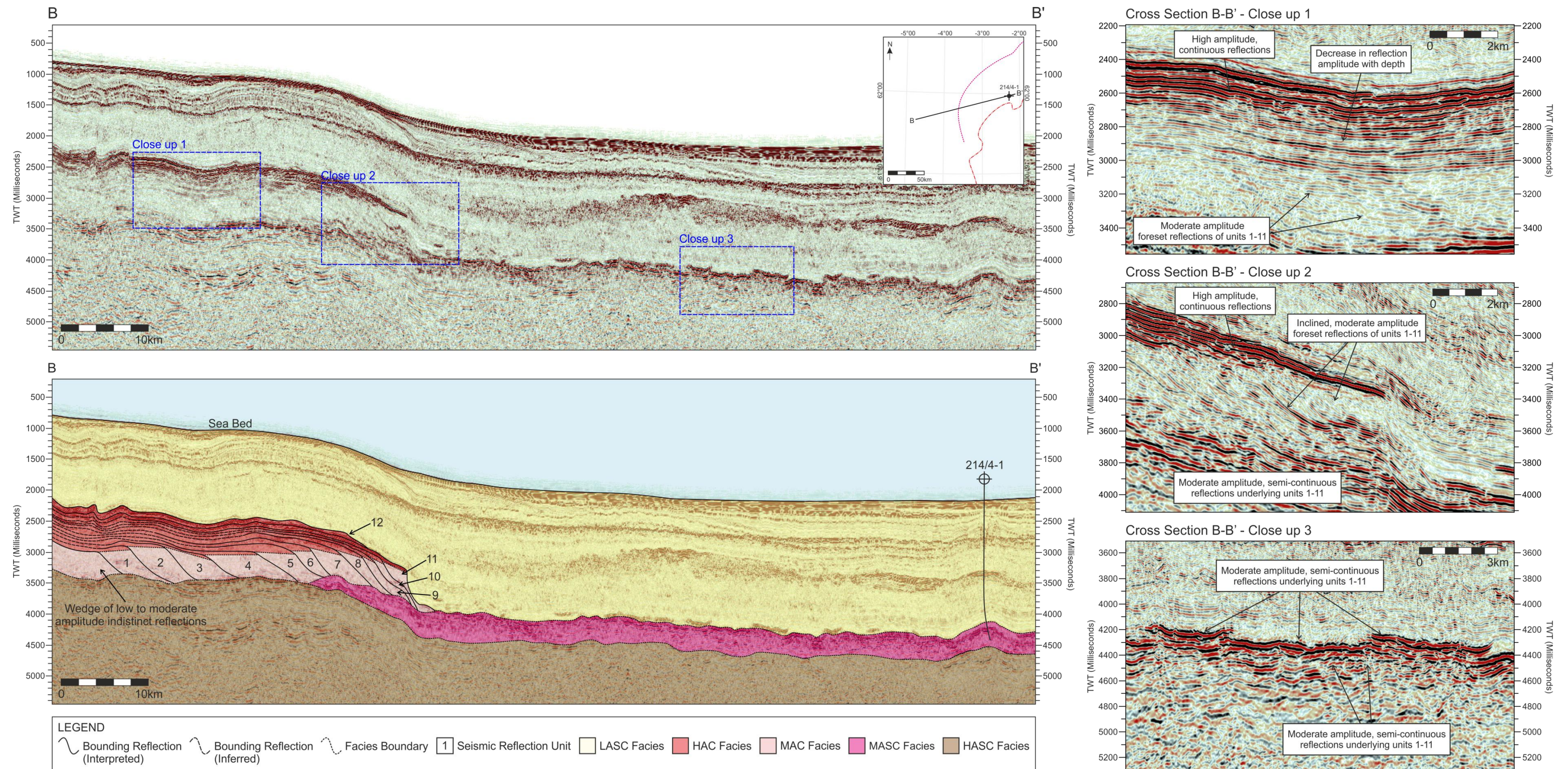
Fig. 4.7. Seismic section B-B' images the Faroe-Shetland Escarpment perpendicular to the curved escarpment edge, the location of exploration well 214/4-1 and close-up sections identifying the main features. Close up-1 is of the continuous, high amplitude topsets that define the top of the flood basalts. Close-up 2 is of the most basinward extent of seismic reflection unit 11. Close-up 3 is of the succession of high to moderate amplitude reflections were encountered in 214/4-1. The interpreted section includes the seismic reflection units and bounding reflections, distribution of seismic facies and the path of intersecting well 214/4-1. See Fig. 4.5 for location.

Seismic reflection unit 11 is the most distal progradational unit and displays foreset geometries that often become shallower and discontinuous and are affected by arcuate, concave upward amplitude anomalies (see Fig. 4.6). Mapping of the amplitude anomalies across numerous intersecting seismic lines revealed that the bounding reflection displayed a variety of arcuate, concave upward upper bounding reflection geometries (see Chapter 3, Fig. 3.17). The disrupted bounding reflection truncates and disturbs the underlying moderate amplitude foresets reflections, which form a low angle wedge composed of shallow, lower amplitudes and that has a limited lateral extent (see Fig. 4.8 and 4.9).
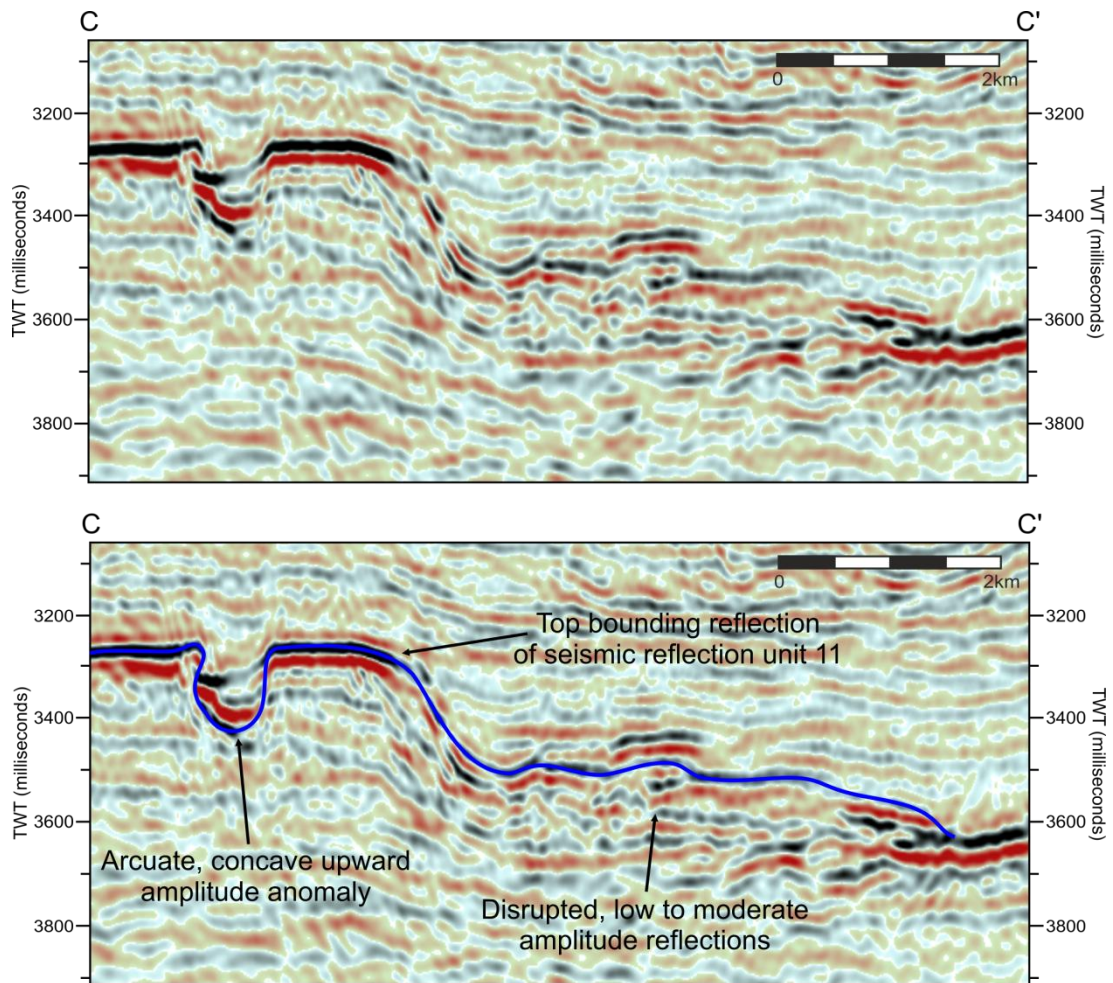
Fig. 4.8. Seismic section C-C′ is a crossline through localised areas of disruption at the distal extent of seismic reflection unit 11 and images a high amplitude, isolated arcuate, concave upward feature that disrupts the underlying moderate to low amplitude reflections. See Fig. 4.5 for locations.
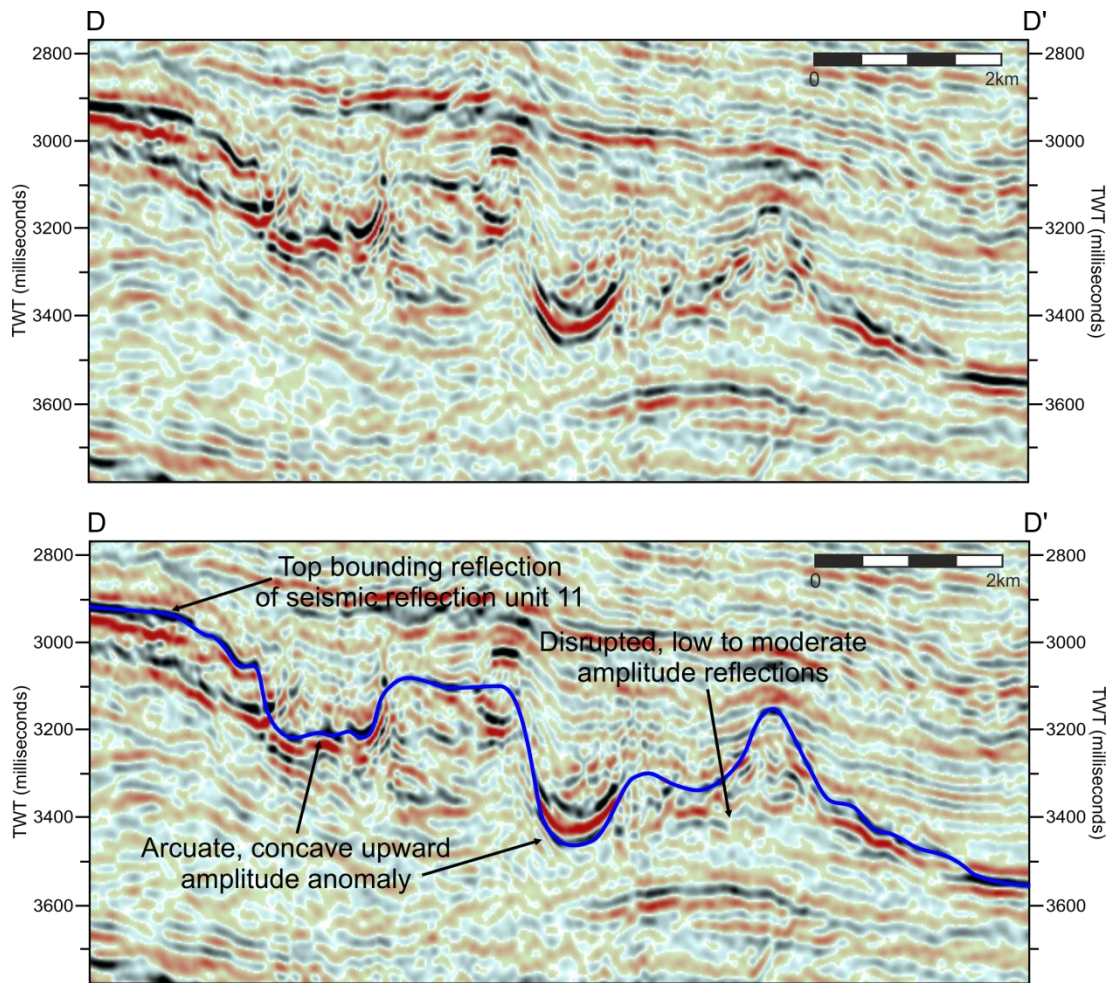
Fig. 4.9. Seismic section D-D' is a inline through localised areas of disruption at the distal extent of seismic reflection unit 11 and images multiple high amplitude, isolated arcuate, concave upward features that disrupt the underlying moderate to low amplitude reflections. See Fig. 4.5 for locations.

When the seismic reflection units are imaged perpendicular to the offlap break, they display a variety of wedge-shaped morphologies and inclined, moderate amplitude internal reflection geometries. In contrast, when imaged parallel to the offlap break, the seismic reflection units display wedge to ellipsoid-shaped, inclined to subparallel, moderate amplitude internal reflection geometries (Fig. 4.10). Within the ellipsoid-shaped reflection geometries, elongated lobate features have been identified by discontinuous moderate reflections surrounded by continuous reflections (Fig. 4.11). By taking an intersecting perpendicular line it is possible to see that the subparallel, discontinuous reflections form inclined foreset reflections (Fig. 4.12).
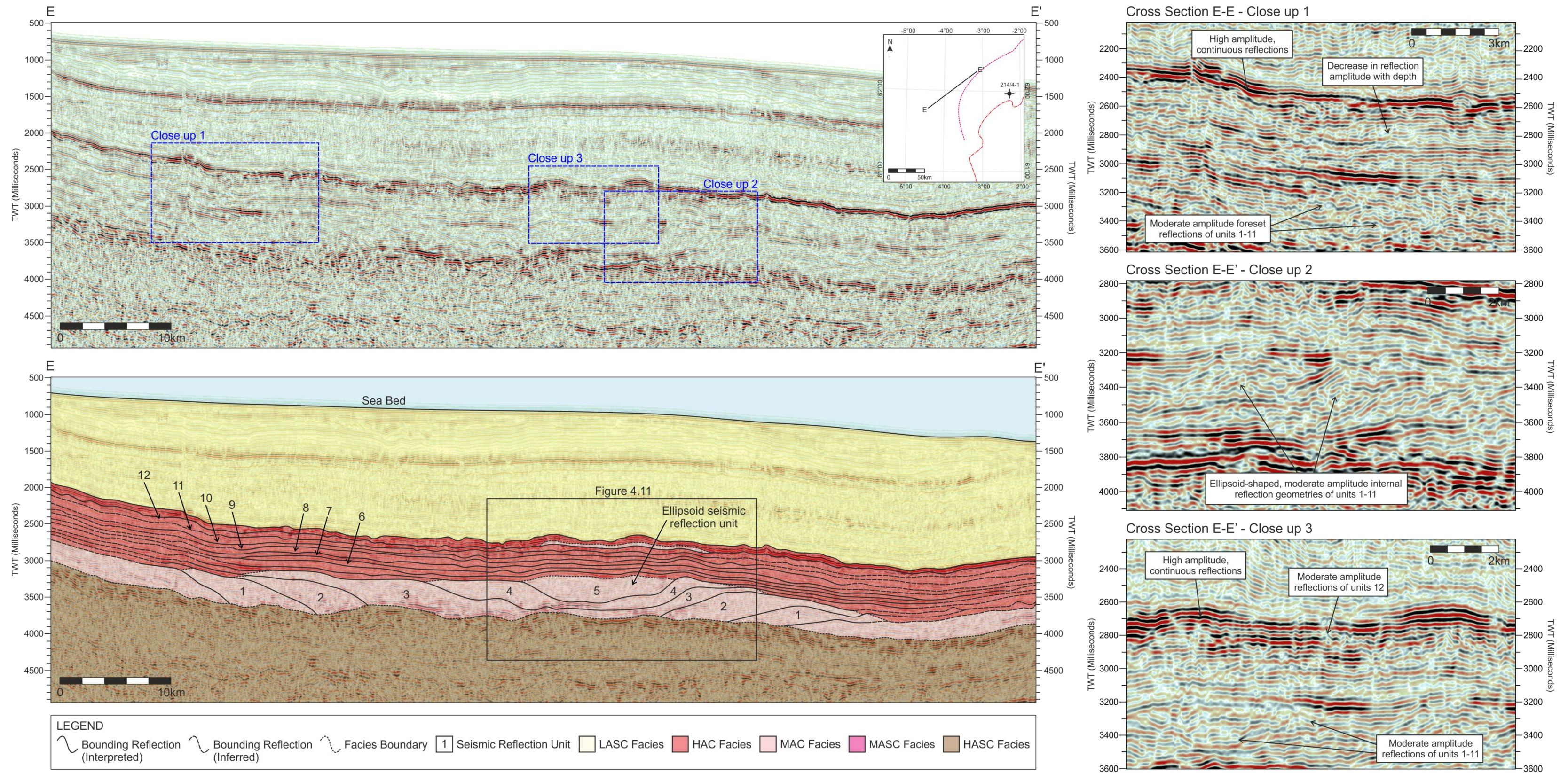
Fig. 4.10 Seismic section E-E' images the Faroe-Shetland Escarpment parallel to curved escarpment edge, with close-up sections identifying the main features. Close-up 1 is of continuous, high amplitude topsets that define the top of the flood basalts. Close-up 2 is of the inclined to subparallel, moderate amplitude internal reflection geometries within seismic reflection units 1 – 11. Close-up 3 is a transect through seismic reflection unit 12. The interpreted section includes the seismic reflection units and bounding reflections, distribution of seismic facies and ellipsoid seismic reflection unit which is shown in greater detail in Figure 4.11. See Fig. 4.5 for location.
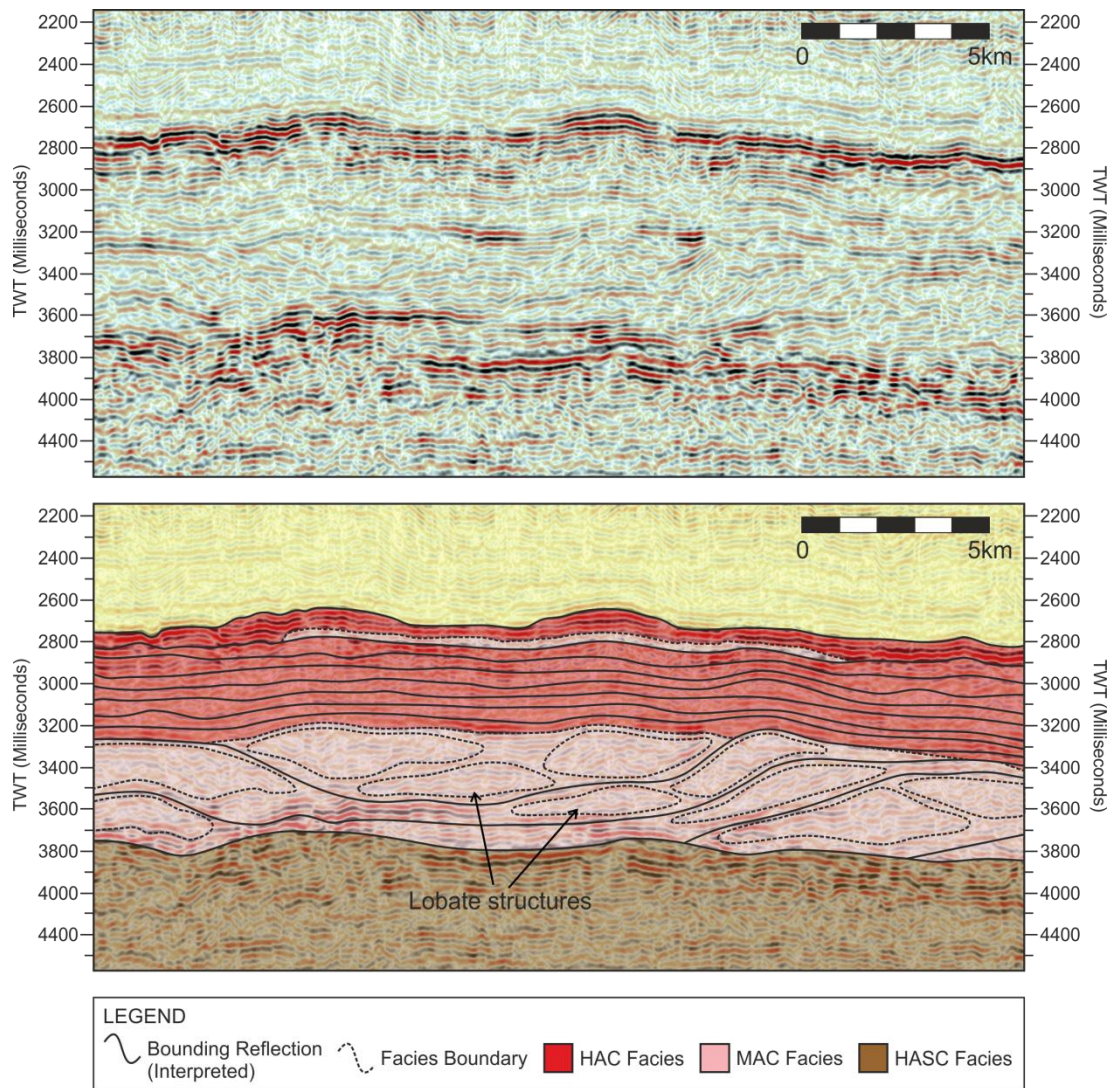
Fig. 4.11. Internal reflection geometry of the elliptical seismic reflection unit shown in Figure 4.10. Interpreted section includes lobate features consisting of discontinuous moderate reflections surrounded by continuous reflections and the distribution of seismic facies.
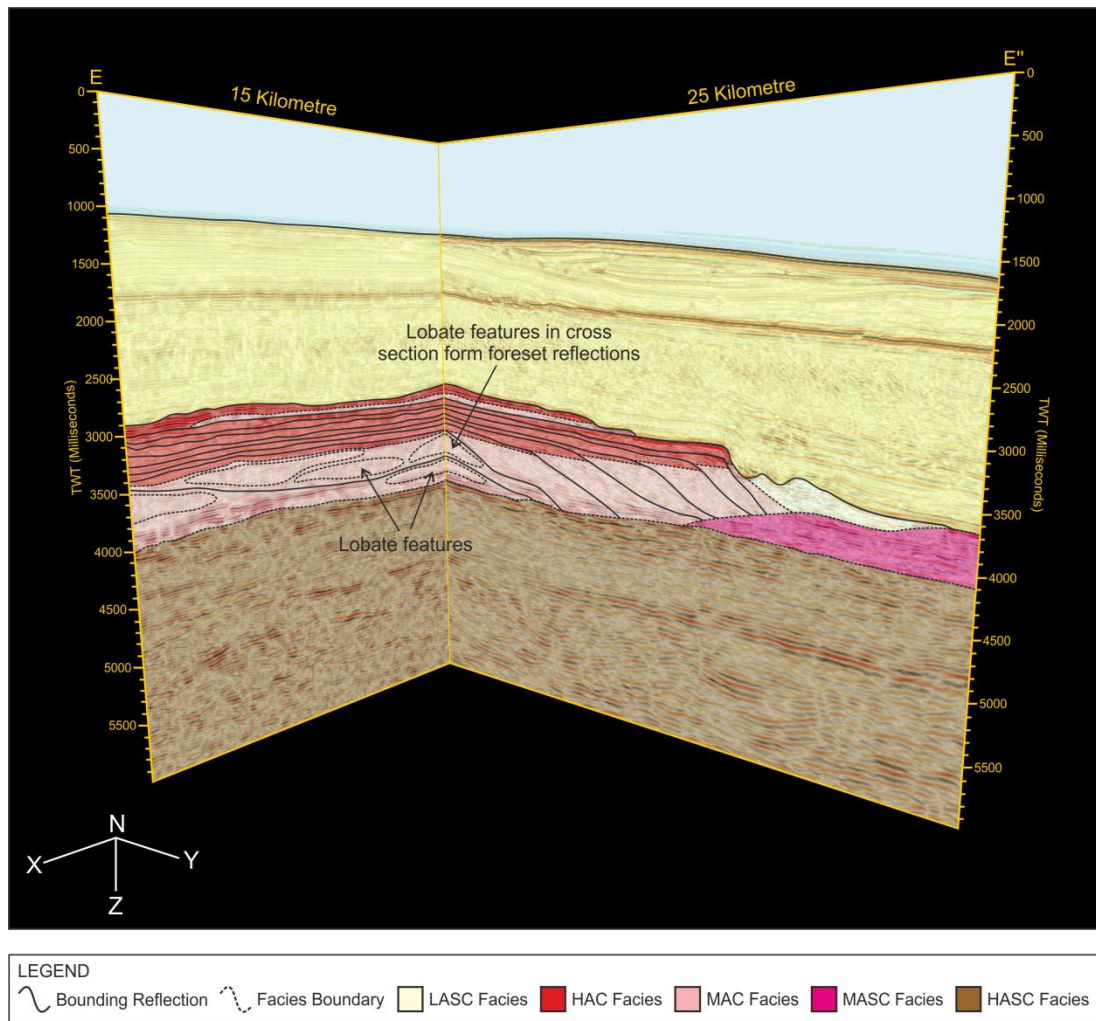
Fig. 4.12. Seismic section E-E'' revealing how the lobate, discontinuous and moderate reflections identified parallel to the offlap break form foreset reflections when imaged perpendicular to offlap break. Scale varies due to perspective. See Fig. 4.5 for location.

The position of the offlap break for the most easterly lying clinoform identifies the limit of the individual seismic reflection unit (Fig. 4.13). The distal limits of the units are inferred, as the thickness of the units thins below seismic resolution and prohibits reliable identification of unit terminations (Fig. 4.14). Seismic reflection units 1 – 11 display 15 – 44 km progradation to the east (Fig. 4.13). The basinward extents of units 1 – 5 are irregular and sinuous, with a northeast–southwest orientation. Units 6 – 11 have a less irregular extent with a smoother, curvi-linear geometry, with localised areas of arcuate, concave upward amplitude anomalies distributed along the offlap break of seismic reflection unit 11. To the north, the offlap break continues to be orientated north-northeast–south-southwest, whereas in the south, the offlap break gradually rotated anticlockwise, becoming orientated north-south. This is caused by variations in the stacking pattern of the units,

with limited progradation and increased aggradation in the north (Fig. 4.15) while there is increased progradation with late aggradation in the south (Fig. 4.16). Seismic reflection units 12 and 13 in contrast record 31 – 75 km retrogradation to the west (Fig. 4.13). Unit 12 has a similar extent and offlap break orientation to unit 11. Unit 13 is located significantly further west towards the Faroe Islands, with an irregular, sinuous extent and northeast–southwest orientated offlap break as displayed by seismic reflection units 1 – 5.
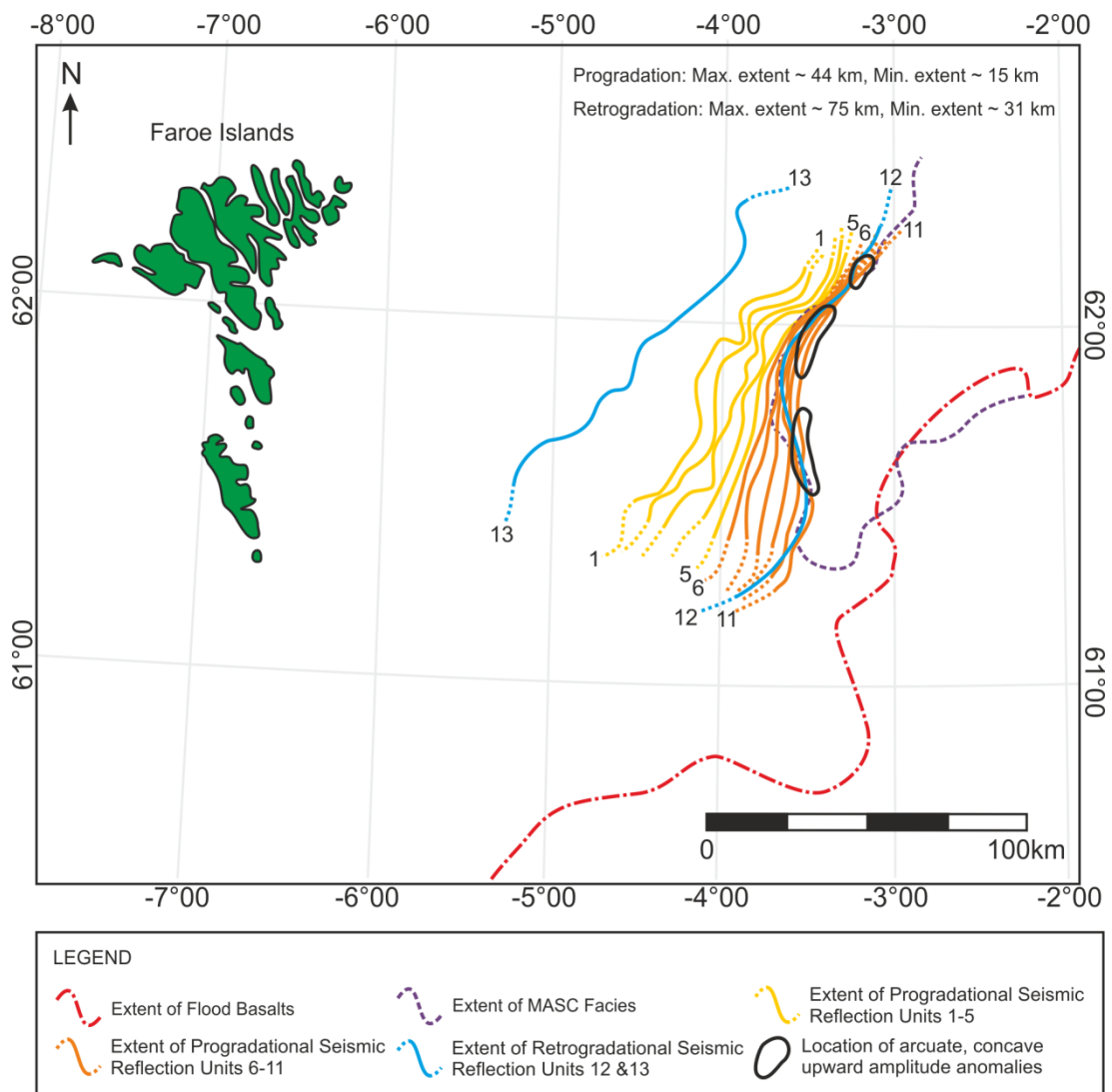
Fig. 4.13. Map of the extent of seismic reflection units, with the position of the offlap break for the most easterly lying clinoform within each unit identified and distribution of arcuate, concave upward geometries associated with seismic reflection unit 11. Distal limits of individual units are inferred with a dotted line, as the thickness of the units thins below seismic resolution and prohibits reliable identification of unit terminations. Map displays the anticlockwise rotation of the offlap break.
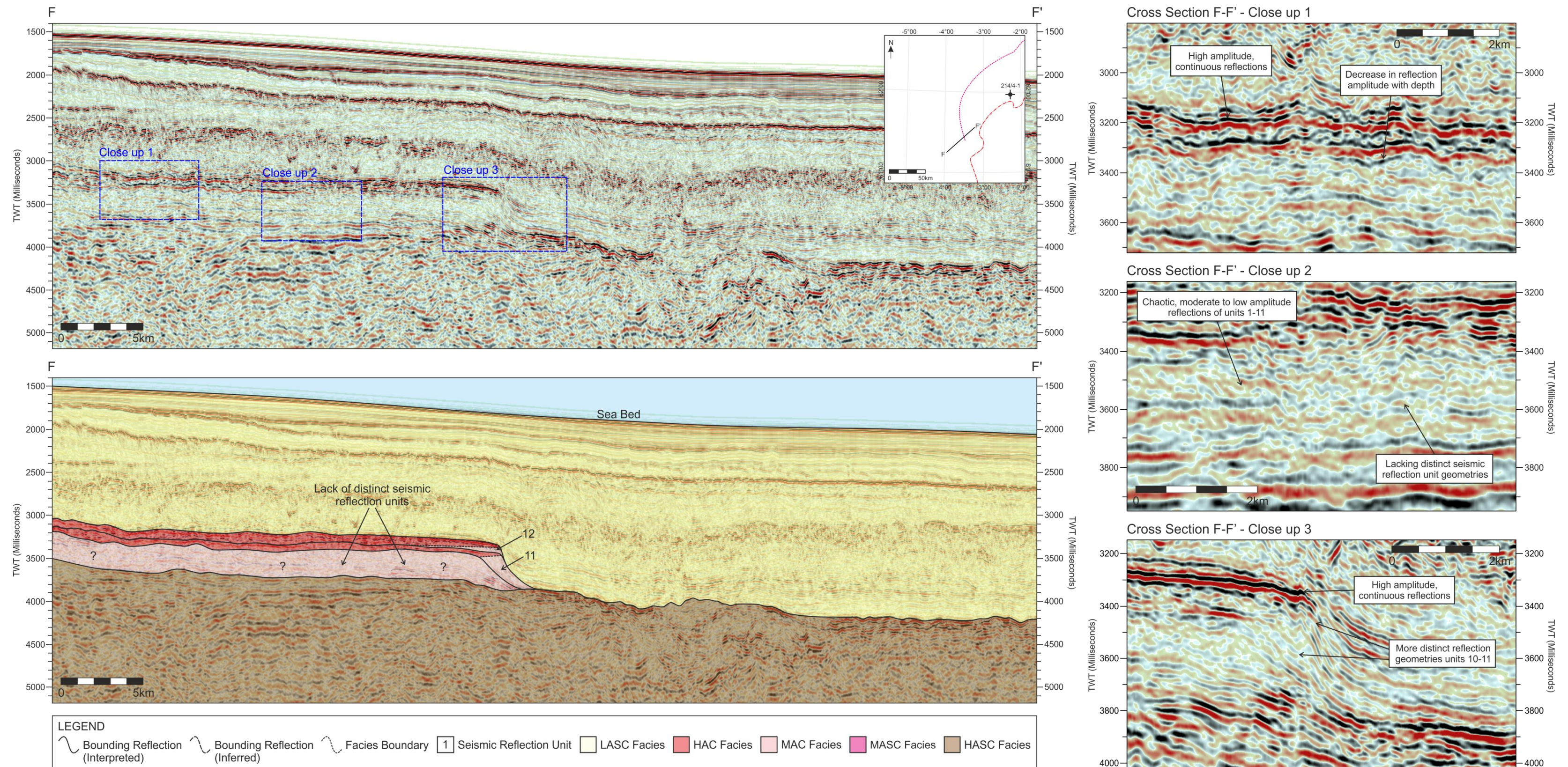
Fig. 4.14. Seismic section F-F' images the southerly extent of the Faroe-Shetland Escarpment, with close-up sections identifying the main features. Close-up 1 is of the high amplitude topsets that define the top of the flood basalts. Close-up 2 is of where the seismic reflection units 1 – 10 are below seismic resolution and prohibits reliable identification of unit terminations. Close-up 3 is of seismic reflection units 11 and 12. The interpreted section includes the seismic reflection units and bounding reflections, distribution of seismic facies and the thinning of the seismic reflection units below seismic resolution, prohibiting the identification of unit terminations shown in Fig. 4.13. See Fig. 4.5 for location.
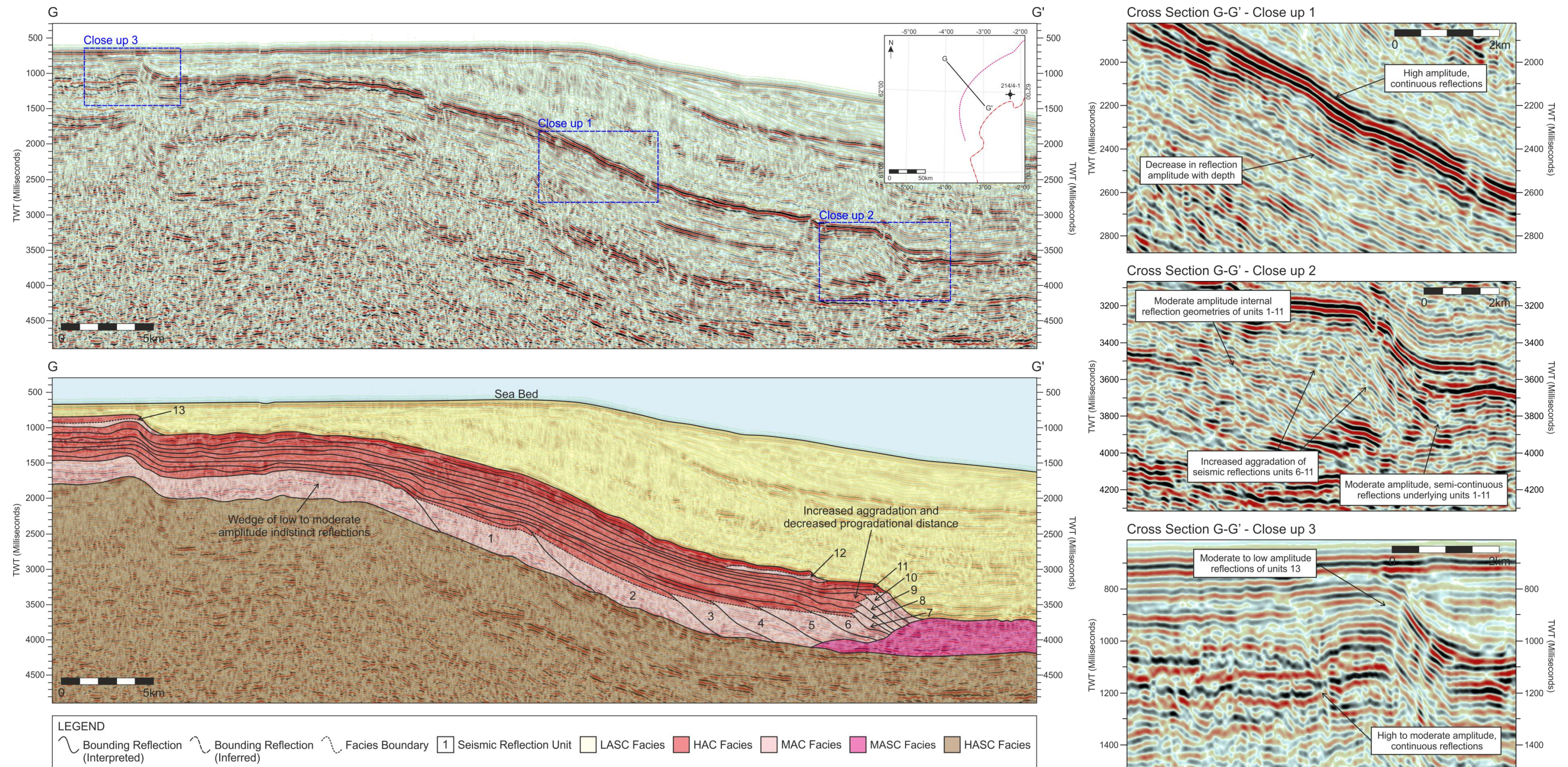
Fig. 4.15. Seismic section G-G' images the Faroe-Shetland Escarpment perpendicular to the curved escarpment edge, with close-up sections identifying the main features. Close-up 1 is of the continuous, high amplitude topsets that define the top of the flood basalts. Close-up 2 is of increased aggradation of seismic reflection units 7 – 11. Close-up 3 is of the basinward extent of seismic reflection unit 13. The interpreted section includes the seismic reflection units and bounding reflections, distribution of seismic facies and the decrease in progradational distance in the north that contributes to the anticlockwise rotation of the delta front shown in Fig. 4.13. See Fig. 4.5 for location.
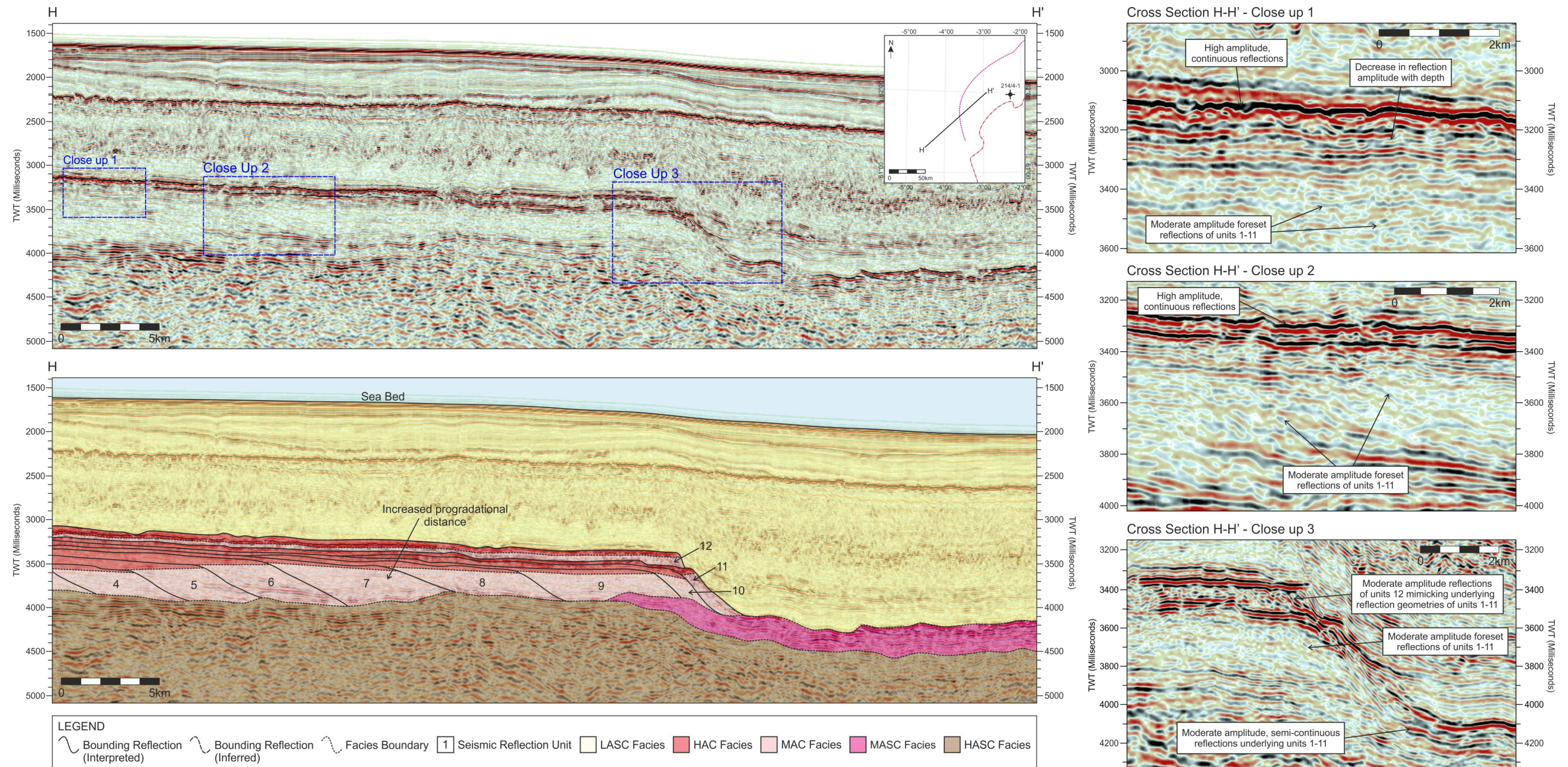
Fig. 4.16. Seismic section H-H' images the Faroe-Shetland Escarpment perpendicular to the curved escarpment edge, with close-up sections identifying the main features. Close-up 1 is of the high amplitude topsets that define the top of the flood basalts. Close-up 2 is of the internal prograding reflections in seismic reflection units 1 – 11. Close-up 3 is of increased progradation with late aggradation in seismic reflection units 1 – 11. The interpreted section includes the seismic reflection units and bounding reflections, distribution of seismic facies and the increase in progradation distance in the south that contributes to the anticlockwise rotation of the delta front shown in Fig. 4.13. See Fig. 4.5 for location.

4.5 Interpretations

4.5.2 Seismic Facies

Interpretation of the seismic facies is based on the reflection characteristics and distinct spatial distributions (Kiørboe, 1999; Planke *et al.*, 1999; West *et al.*, 2002), and comparison to lithologies within lava-fed deltas described in the published literature (Jones & Nelson, 1970; Porebski & Gradzinski, 1990). The uppermost facies within the Faroe-Shetland Escarpment is the HAC facies, which is located at the top of each of the seismic reflection units. The high amplitude, continuous nature and lateral extent suggest that the facies is composed of pāhoehoe lava flows and are lava flow topsets that fed the delta (Fig. 4.17; Planke *et al.*, 1999; Spitzer *et al.*, 2008; Jerram *et al.*, 2009).

Located below and basinward of the HAC facies is the MAC facies, with the reflections displaying progradation into the basin and the transition from the HAC to the MAC facies identified by the offlap break. The facies is interpreted to be foresets composed of hyaloclastic breccias, which record the flow of lava directly into the offshore basin (Fig. 4.17; Spitzer *et al.*, 2008; Jerram *et al.*, 2009). The foresets become increasingly steeper towards the front of the escarpment body and is interpreted to be due to the development of sufficient water depth and therefore, accommodation (Postma, 1990; 1995). The LASC facies has a limited lateral distribution along the delta front and is interpreted to be the product of remobilisation of the MAC facies (Fig. 4.17). The reflections of the LASC facies display a semi-continuous nature that indicates that the delta front may have been semi-consolidated during collapse, which is reflected in the limited distance that the remobilised material travelled downslope (Porebski &Gradzinski, 1990; Planke *et al.*, 2000).

The lava-fed delta system is underlain by two different facies. The first is the MASC facies which has been identified beneath seismic reflection units 6 – 11, appearing to thin and disappear beneath unit 5. The boundary between the MASC facies and overlying MAC facies varies from distinct to ambiguous downlap of the MAC on to the MASC facies. The exact nature and relationship of the MASC to the overlying MAC facies is difficult to discern. Previous interpretations are that the MASC facies is genetically related to the overlying MAC facies and represents delta toesets composed of broken lava flows and hyaloclastic breccias (Kiørboe, 1999; Planke *et al.*, 1999, 2000). The similarities in lithology may account for the indistinct boundary between the MASC and MAC facies, with compaction of the MASC facies beneath the thicker parts of the delta causing the apparent

pinch-out beneath the delta body. Deposition of the hyaloclastic breccias is interpreted to be rapid, quickly becoming consolidated due to the welding of partial molten clasts and the transformation of fine grained glass into clays with depth (Furnes, 1974; Skilling, 2002; Schiffman e*t al.*, 2006). Therefore any toesets at the base of the delta would likely have a fairly limited extent and would not account for the extensive nature of the facies and the penetration by exploration well 214/4-1 which is located ~65 km distance away from the delta front (see Fig. 4.7).

Extensive deposits of interbedded broken lava flows and hyaloclastic breccias are identified in large scale, submarine landslides, such as the Hilina slump identified on Hawaii (Moore *et al.*, 1989; Smith *et al.*, 1999). These landslides are often controlled by faults systems that run parallel to the front of the landslide and extend up to a few hundred kilometres downslope away from the shoreline (Moore *et al.*, 1989; 1995). It is possible that the MASC facies represents remobilised volcanic material that slumped off earlier phases of delta construction and travelled long distances from the delta front, with compaction by subsequently deposited seismic reflection units causing the apparent wedge pinch-out beneath the delta body. However it could be expected that such extensive remobilised material would produce disrupted and chaotic seismic reflections, which differ from the moderate amplitude, horizontal and semi-continuous reflections that define the MASC facies and indicate coherent and layered rocks.

Alternatively the MASC facies may represent the influx of volcanic material from a different source within the basin. Earlier eruptive phases from subaerial volcanic centres have been recognised within the Faroe-Shetland Basin (e.g. the Erlend Complex and Brendans Dome; Gatliff *et al.*, 1984; Ritchie & Hitchen, 1996; Jolley & Bell, 2002). These centres erupted lava flows and hyaloclastic breccias into subaerial to brackish environments that often formed significant topographic structures (Naylor *et al.*, 1999; Jolley & Bell, 2002). The MASC facies is intersected by well 214/ 4-1, which identified hyaloclastic breccias and pāhoehoe lava flows (see Fig. 4.7). This succession has been interpreted accordingly as interbedded lava flows and hyaloclastic breccias that formed a volcanically related topographic structure that subsequent deposition of the lava-fed delta system prograded over. However, definitive conclusions on the lithology and formation of the MASC cannot be achieved without more data, such as high resolution geochemical and wireline data through the MASC close to the Faroe-Shetland Escarpment.

The second facies that underlies the lava-fed delta system is the HASC facies which has been identified to extend beneath the entire delta and the MASC facies, and east into the Faroe-Shetland Basin. This facies is interpreted to be part of the basin-fill before the onset of lava-fed delta deposition and therefore may contain subaerially eroded volcanic material (e.g. Brendans Dome) or minor volcanic intrusions.
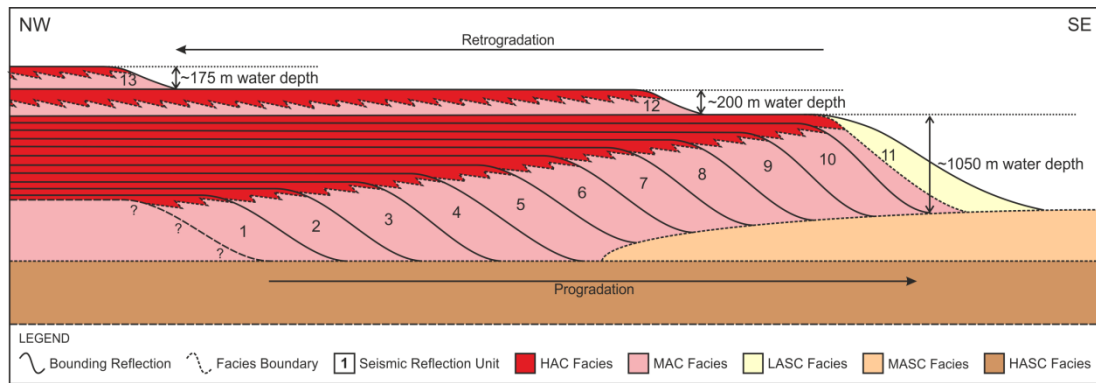
Fig. 4.17. Schematic cross section through the lava-fed delta, including seismic reflection units and distribution of seismic facies (not to scale).

4.5.1 Seismic Reflection Units

The idea that the Faroe-Shetland Escarpment was formed as the front of a prograding lava-fed delta, where subaerial lava flows became marine hyaloclastic breccias is well established (e.g. Smythe, 1983; Smythe *et al.*, 1983; Ritchie *et al.*, 1999; Spitzer *et al.*, 2008). The seismic reflection units identified in this study are interpreted to record continuous emplacement during discrete periods of active volcanism. The seismic reflection units appear to have been deposited sequentially, with the gross stacking pattern revealing variations in the available accommodation, relative sea level rise and the supply of volcanic material. As in conventional delta systems, the height of the delta-front clinoforms may be a proxy for water depth at the time of delta deposition (Schmincke *et al.*, 1997; Kiørboe, 1999; Spitzer *et al.*, 2008).

Prior to the deposition of distinct seismic reflection units, initial deposition of the flood basalts resulted in a wedge of hyaloclastic breccias which underlies the Faroe-Shetland Escarpment and extends back towards the Faroe Islands (Fig. 4.17). The onset of flood basalt volcanism is often recorded by thick basal deposits of volcaniclastic and hyaloclastic material which underlie the thick flood basalt lava flows (Usktins Peate *et al.*, 2003; Ross *et al.*, 2005; Jerram *et al.*, 2009). In the Faroe-Shetland Basin, the volcanic material was most likely sourced from the erosion of the developing volcanic hinterland to the northwest of

the Faroe-Shetland Basin (Dore *et al.*, 1999; Naylor *et al.*, 1999). The volcanic material preceded the continental flood basalt emplacement, infilling the basin until flood basalt lava flows reached the palaeo-shoreline and lava-fed delta deposition commenced. Deposition was likely controlled by large volumes of erupted lava entering the basin and infilling the available accommodation, with the initial stacking pattern of the delta one of progradation as seismic reflection units 1 – 11 extended progressively further into the basin (Fig. 4.17). The seismic reflection units display an increasingly aggradational component with the deposition of units 6 – 11. This is interpreted to be the product of a gradual increase in accommodation due to compaction and syn-volcanic subsidence during active delta construction (Mattox & Mangan, 1997; Kauahikaua *et al.*, 2003). The increased aggradation of the delta is also coincident with the underlying MASC facies (Fig. 4.16).

The south-easterly extent of lava-fed delta progradation into the basin is defined by seismic reflection unit 11. The unit is disrupted by a series of high amplitude, arcuate and concave upward amplitude anomalies. Initially these amplitude anomalies were thought to be processing artefacts, caused by high amplitude structures in the overburden. However recognition of multiple amplitude anomalies distributed in distinct areas along the lateral extent of seismic reflection unit 11, together with the lack of structures in the overburden suitable to create such a processing artefact, indicate that these structures are real. Arcuate, concave-upwards structures are a familiar feature in the Faroe-Shetland Basin as saucer-shaped sills which are commonly found within the deeper subsurface, below the flood basalts (Hansen & Cartwright, 2006; Thomson & Hutton, 2004; Thomson & Schofield, 2008). However these structures display no evidence of a magmatic feeder system or the typical climbing structure associated with intrusive sill complexes.

Arcuate, concave-up structures have been previously recognised in lava-fed delta systems (e.g. Skilling, 2002; Sansone & Smith, 2006; Smellie *et al.*, 2008). These include modern Hawaiian lava-fed deltas where large scale collapse escarpments (up to kilometres across) result from the subsidence of the delta (Mattox & Mangan, 1997; Heliker & Mattox, 2003; Kauahikaua *et al.,* 2003). During active delta deposition, the unconsolidated delta front subsides, causing fractures to propagate up through the delta front. The area located basinward of these fractures is known as a 'lava bench' and can be inherently unstable due to the unconsolidated nature of the material (Heliker & Mattox, 2003; Kauahikaua *et al.,* 2003). During full or partial bench collapses, explosive interactions between hot lava and sea water can occur, resulting in the catastrophic collapse of the delta front (Mattox &

Mangan, 1997; Heliker & Mattox, 2003). The arcuate structures along seismic reflection unit 11 are interpreted to be analogous to these collapse structures. They most likely resulted from a prolonged hiatus or decrease in the supply of new material, which left the delta front prone to erosion and reworking by tides, waves and storms (cf. Skilling, 2002; Sansone & Smith, 2006). The foreset reflection beneath the collapse structures display a variety of reflection geometries and form a low angle wedge composed of shallow, lower amplitudes that has a limited lateral extent. The semi-continuous nature of the reflections within the low angle wedge suggests that the remobilised volcanic material was semi-consolidated, with limited transport away from the delta front.

The stacking pattern of the delta changed from progradation to retrogradation during the deposition of seismic reflection units 12 and 13. The units are located directly above, and downlap onto, the top bounding reflection of seismic reflection unit 11 (Fig. 4.17). They consist of high amplitude, continuous topsets and moderate amplitude, progradational foresets which mimic the reflection geometries of larger seismic reflection units 1 – 11. Seismic reflection units 12 and 13 are interpreted to be later stages of delta deposition, where a decrease in volcanic supply resulted in the limited infill of the available accommodation above the previously deposited seismic reflection units and a progressive step back towards the Faroe Islands (see Fig. 4.13). The accumulation of accommodation above the main delta body is inferred to be caused by volcanic loading and subsidence during reoccurring periods of little to no delta activity (Moore, 1970; Lipman, 1995; Lipman & Moore, 1996). The recommencement of volcanic supply infilled the additional accommodation but never reached the extent of the previous phase of delta construction (Fig. 4.17).

The front of the delta is identified basinward of the offlap break, where reflection geometries change from subhorizontal to inclined. The offlap break is also interpreted as the location of the palaeo-shoreline and the position of relative sea level during delta deposition (Kiørboe, 1999; Spitzer *et al.*, 2008; Ellefsen *et al.*, 2010). Mapping of the offlap break is widely used in siliciclastic seismic stratigraphy to define shoreline trajectory and identify changes in the position of the palaeo-shoreline (e.g. Helland-Hansen & Martinsen, 1996; Helland-Hansen & Hampson, 2009). In the Faroe-Shetland Basin, the lava-fed delta prograded a considerable distance to the southeast, with a gradual anticlockwise rotation from northeast-southwest to north-south, during the deposition of seismic reflection units 1 – 11 (see Fig. 4.13). The height of the individual seismic reflection units displays little

variation across the delta front, while the progradational distance of the units varying from 1 – 2 km in the north to 3 – 5 km in the south. This increase in the filled accommodation caused the delta front to migrate further in the south than the north and the anticlockwise rotation of the delta front. Following deposition of unit 11, the delta underwent retrogradation during deposition of unit 12, migrating between 1 and 6 km to the northeast and with a similar distribution as unit 11. The greatest retrogradation occurred during the deposition of seismic reflection unit 13, where the delta front migrated ~31 km in the north and ~75 km in the south, causing a sharp clockwise rotation of the delta front from north-south to northeast-southwest (see Fig. 4.13).

The distal extents of the lava-fed delta system are difficult to define, as the escarpment thins below seismic resolution. To the south of the delta system, the thickness of the delta decreases to less than 400 m high and appears to lack any distinct internal architecture (see Fig. 4.14). Such a change in delta height indicates that there was much lateral variation in water depth and emplacement environment, with transition from a relatively deep marine (>1 km in depth) to more shallow marine environment (<100 m). As such, the lava-fed delta system appears to mark the edge of a marine basin, with a lack of hyaloclastic deposition and a return to subaerial volcanic emplacement at the edges of the basin (Smythe, 1983; Smythe *et al.*, 1983; Naylor *et al.*, 1999). Where the lava-fed delta does accumulate a sufficient thickness, it is possible to identify clear delta-front clinoforms which, when imaged perpendicular to the delta front, prograde basinward. When imaged parallel to the delta front, the clinoforms exhibit chaotic reflections that form lobate features. These lobate features are interpreted to be the location where a subaerial lava lobe entered the basin and fragmented into a wedge of hyaloclastic breccia along the palaeo-shoreline (Keszthelyi & Self, 1998; Umino *et al.*, 2006). The presence of multiple lobes within a single seismic reflection unit suggests that lava flows entered the basin at discrete points, with each lobe building a wedge of hyaloclastic material that merged into a continuous delta body through the migration of the depositing lava flow lobe along the palaeo-shoreline (Self *et al.*, 1997; Heliker *et al.*, 1998; Passey & Bell, 2007).

4.5.3 Correlation to Onshore Stratigraphy

The eruption of the Faroe Island Basalt Group was broken in to distinct episodes by pauses or migration of the volcanic centres with the identification of seven distinct formations (Passey & Bell, 2007; Jerram *et al.*, 2009). Correlation of the lava-fed delta system to known onshore volcanic successions is based on the nature of the formations, their key volcanic

facies and their stratigraphic position (e.g. Jerram *et al.*, 2009; Nelson *et al.*, 2009b). Interpretation of seismic facies analysis and onshore stratigraphy suggests that the lava flows that fed the delta system were pāhoehoe in nature and are likely to be the offshore equivalent of the Beinisvørð Formation (Smythe *et al.*, 1983; Ritchie *et al.*, 1999). The Beinisvørð Formation is composed of pāhoehoe lava flows that were emplaced through inflation and lobe coalescing, during extensive fissure eruptions in the vicinity of the modern Faroe Islands with relatively continuous supply of lava during each eruption (Boldreel *et al.*, 1994; Dore *et al.*, 1999; Naylor *et al.*, 1999). The structure of these lava flows may account for the distance that the lava would have had to travel before reaching the palaeo-shoreline and forming hyaloclastic breccias (Self *et al.*, 1997; Jerram & Widdowson, 2005; Passey & Bell, 2007).

4.5.4 Lava-Fed Delta Duration

Flood basalt volcanism is characterised by repetitive, long-lived eruptions (weeks to tens of years) that are capable of producing large volumes (>1 km^3) of lava, with the overall duration of volcanism lasting over a few (1 – 5) million years (e.g. Coffin & Eldholm, 1994; Eldholm & Grue, 1994; Bryan *et al.*, 2010). The onset of flood basalt volcanism is characterised by relatively low volume eruptions, controlled by pre-existing topography and location of erupting fissures or vents. The main phase of flood basalt activity is typified by a rapid increase in the erupted volume, with high intensity volcanic eruptions (e.g. 10^{11} kgs^{-1}; Bryan *et al.*, 2010). The end of flood basalt volcanism is signified by a gradual decrease in eruption volumes and the development of widely distributed localised volcanic centres (Jerram & Widdowson, 2005; Bryan *et al.*, 2010). Dating durations of volcanism can be difficult and relies on the preservation of erosional surfaces, deposition of non-volcanic units, palynology and geochemical fingerprinting of different eruptive units. In offshore settings, it can be extremely difficult to obtain this information, especially if the volcanic succession is undrilled.

However, it is possible to estimate the duration of volcanic eruptions using lava flow thickness. Hon *et al.* (1994) calculated the length of time a lava flow takes to inflate and cool based on the thickness of the flow crust, by the empirical equation:

$$t = 164.8C^2 \qquad \textbf{Eq. 4.1}$$

where *t* is time in hours, 164.8 is an empirically determined constant and *C* is the thickness of lava flow crust in metres, as determined by the depth of inflation cracks. Inflation cracks

can only propagate through the brittle part of a lava flow, which at the time of inflation is the upper crust, and serve as a proxy for the thickness of the upper crust. The information used in this equation has been constrained by observing the development of pāhoehoe sheets through time as sheet flows, which inflated due to a sustained input of lava during a long-lived eruption (Hon *et al.*, 1994). There is precedent for its use in calculating ancient lava flows, with Passey & Bell (2007) having used this equation to estimate the duration of individual flow lobes on the Faroe Islands. Their results varied from 10.3 hours for small, isolated lobes to 22.2 days for the better developed lobes that display inflation structures such as defined vesicle zones.

Onshore exposures of the Beinisvørð Formation suggest that the average flow lobe thickness is ~25 m (Ellis *et al.*, 2002; Passey & Bell, 2007; Passey & Jolley, 2009) and is composed of ~40% crust (Nelson et al., 2009b). Use of the empirical equation (Hon *et al.*, 1994) estimates it took 1.88 years for an individual lava flow lobe to inflate to 25 m. Further to this, it has been estimated the average total flow thickness for the seismic reflection units 1 – 13 using two-way travel time from the seismic data and assuming velocities of ~5500 kms^{-1} recorded for pāhoehoe lava flows from boreholes on the Faroe Islands (Table 4.2; Boldreel, 2006; Nelson *et al.*, 2009b). The total thickness of lava flows feeding each seismic reflection unit will be composed of multiple flow lobes. These most likely have a similar thickness to the onshore exposures of the Beinisvørð Formation but are below resolution in the seismic data. In order to calculate the thickness of crust *C*, core to crust ratios from Nelson *et al.* (2009), who plotted the core proportions of onshore Faroes lava flows identified within the Vestmanna-1, Glyvursnes-1 and Lopra-1/1A boreholes. By using data based on lava flows from equivalent onshore stratigraphy, an accurate assessment of lava thicknesses where the core to crust ratio has been well constrained statistically (Nelson *et al.*, 2009b).

The lava flows feeding the hyaloclastic breccias in seismic reflection units 1 – 11 have an average total thickness of 275 m, with 40% crust equating to 110 m (Table 4.2). The average duration (*t*) for each unit is 227.63 years, culminating in the active progradation of units 1 – 11 occurring over 2503.93 years. In contrast, the lava flows feeding the hyaloclastic breccias in seismic reflection units 12 and 13 have a much smaller average thickness of 137.5 m, with 40% crust equating to 55 m (Table 4.2). The average duration (*t*) for each unit is 56.91 years, culminating in total active retrogradation of units 12 and 13

over 113.82 years. The sum of the duration (*t*) for all the units (1 – 13) gives a value of 2617.75 years of active delta deposition and lava flow emplacement.

Seismic Reflection Unit	Average Total Flow Thickness (m)	*C* (m)	*t* (hrs)	*t*/24 = days	*t*/24/365 = yrs
1 – 11	275	110	1994080	83086.67	227.63
12 – 13	137.5	55	498520	20771.67	56.91

Table 4.2. Average thickness for lava flows feeding the seismic reflections units and the calculated time taken to inflate to the total flow thickness (values to 2 decimal places).

If these calculations are correct, it suggests that active lava-fed delta emplacement was relatively short-lived and fast-paced, occurring during ~2.6 ky. However geochemical and isotopic dating of the Beinisvørð Formation suggests that emplacement occurred during 3.3 Ma, between 60.1 ± 0.6 and 56.8 ± 0.6 Ma (Waagstein *et al.*, 2002; Storey *et al.*, 2007), while palynological and seismic stratigraphic analysis suggest emplacement occurred during 1.9 Ma, between 56.8 and 54.9 Ma (Ellis *et al.*, 2002; Jolley & Bell, 2002; Jolley, 2009). This discrepancy could be due to a number of potential issues with the equation of Hon *et al*. (1994). The first is that this equation relies on the assumption that, after the upper crust of a lava flow forms, cools and becomes rigid, it remains horizontal and acts as insulating cover for the molten lava moving beneath it (Hon *et al*., 1994; Self *et al*., 1998). Over time the flow inflates through the injection of addition liquid lava into the flow core, the upper crust thickens as material is added to the base of the crust and cools. This equation does not account of any deformation or deflation of flow (Self *et al*., 1998).

Secondly, it is only possible to calculate the duration of active lava flow emplacement, which does not include any periods of volcanic quiescence between eruptive events. These periods of volcanic quiescence could have varied from 10 to 10^4 years, culminating in a much longer total duration of volcanic activity, although not as long as the radiometric dates suggest (Coffin & Eldholm, 1994; Jerram & Widdowson, 2005). It is difficult to constrain the effects of erosion, which are not resolvable on seismic reflection data and well data are required to provide information on erosional surfaces, intra-volcanic sedimentary deposition and biostratigraphy. If erosion has removed a significant portion of the lava flows, it would reduce the thickness of the upper crust of the lava flows and give an underestimate of the time taken for them to inflate and cool, potentially accounting for the anomalously fast rates of delta construction and changes in relative sea level (Eldholm & Grue, 1994).

Alternatively, the lava-fed delta may only record part of Beinisvørð Formation, rather than the whole. This is possible given the ~100 km distance the delta is from the suspected fissure systems close to the Faroe Islands. Without accurate dating evidence, it is impossible to say which assumption is correct and exactly how much of the Beinisvørð Formation the delta records. Despite these problems, this equation is the only tool available for determining the duration of lava emplacement and can give a minimum estimate of the duration of volcanic eruptions, but should be used with caution (Self *et al.*, 1998; Thordanson & Self, 1998; Passey & Bell, 2007).

4.6 Discussion

4.6.1 Seismic Reflection Units

Interpretation of the seismic reflection units has been based on the seismic facies associations, stratigraphic position and the juxtaposition of one unit against another. I suggest that each unit represents an individual volcanic succession created by a discrete period of active volcanism, with the internal clinoform reflections recording the continuous deposition of hyaloclastic breccias (Schmincke *et al.*, 1997; Kiørboe, 1999). The inference that each seismic reflection unit represents a period of active volcanism also suggests that each period of activity was followed by a period of little or no volcanic activity. During these hiatal periods no new lava flows or hyaloclastic breccias were deposited over the previous unit, leaving them prone to erosion, remobilisation and redeposition. We propose the bounding reflections are surfaces produced during such hiatuses.

In a subaerial environment, weathering and erosion of subaerial lava flows forms volcanogenic soils. Genesis of a soil from basaltic lava parent material is slower than that for scoria or ash of the same composition, and is much slower than for unconsolidated sedimentary deposits such as sand or glacial deposits (Dan & Singer, 1973; Pillans, 1997). Rates of soil genesis are difficult to estimate due to a wide range of factors that influence soil formation, such as climate, temperature and mechanisms of erosion including weathering and leaching. However, it has been estimated that genesis of a volcanogenic soil can take as little as 45-70 years in a tropical climate and up to 500 years in a cool climate (Corbett, 1968; Buol *et al.*, 1989). In a number of onshore outcrops, siliciclastic deposits, often with associated plant material, were deposited after the previous phase of lava-fed delta deposition and indicate the re-emergence of a pre-existing sedimentary

regime during periods of volcanic inactivity (Porebski & Gradzinski, 1990; Yamagishi, 1991; Trodeson & Smellie, 2002; Jolley *et al.*, 2009).

In a submarine environment, erosion can result from reworking by tides, waves and/or storms and are the equivalent of the subaerial palaeosols and erosional surfaces, with coastal sandstones and deeper marine mudstones accumulating during periods of volcanic inactivity (Furnes & Fridleifsson, 1974; Bergh & Sigvaldason, 1991). Submarine erosional surfaces may also occur due to the avulsion of the actively depositing lava lobe during periods of volcanism. Avulsion occurs when the feeder systems shifts location, causing construction of the active delta lobe to cease and the build-out of a new lobe to occur at another location which is usually in close proximity along shore (Coleman, 1988; Correggiari *et al.*, 2005). The bounding reflectors that define the seismic stratigraphic units are interpreted to represent hiatal surfaces at the top of each volcanic succession. It is likely that there are thin, fine grained siliciclastic interbeds between each volcanic succession, which provides a great enough seismic velocity contrast to produce an acoustic impedance which is visible on seismic reflection data.

4.6.2 Lava-Fed Delta Development

The stacking pattern of the seismic reflection units is a function of the interaction between lava supply, relative sea level and available accommodation, and it records how these parameters affected deposition of the lava-fed delta system. It is clear that lava supply to the delta varied, with emplacement occurring during periods of active volcanism and no emplacement during volcanic hiatuses. Volcanic systems are known to have a pulsed or cyclic nature, with variations in distribution, volume and geochemistry of erupted products (Paterne & Guichard, 1993; Knight *et al.*, 2004; Jerram & Widdowson, 2005). Variations in extent can also occur during a waning of the eruption rate, migration of the vent or location switching of the depositing lava tube or inflation lobe (Self *et al.*, 1997; Heliker *et al.*, 1998; Passey & Bell, 2007). Importantly, any significant hiatuses in volcanism are likely, depending on slope angle and preservation potential, to be recorded by degradation and collapse of the delta front as the shoreline is eroded.

The subaerially erupted lava flows of the delta system are suggested to be extensive pāhoehoe flows that coalesced and formed from large inflating sheet flows (e.g. Self *et al.*, 1997). Evidence from lavas in onshore exposures in the Faroes and in the British Palaeogene point to the pāhoehoe nature of the subaerial flows (Single & Jerram, 2004;

Passey & Bell, 2007), while 'a'a lava flows, comprised largely of autoclastic breccias are rare in most flood basalt provinces (Brown *et al.*, 2011). The lava-fed delta system of the Faroe-Shetland Basin was most likely fed by individual lava flows along the palaeo-shoreline with each location building a wedge of hyaloclastic material that eventually merged into one continuous delta body, as seen where modern lava flows enter the ocean (Moore *et al.*, 1973; Mattox *et al.*, 1993; Kauahikaua *et al.*, 2003). Significant, high volume eruptions would be recorded as prolonged episodes of delta progradation, such as in the deposition of seismic reflection units 1 – 11. Variations in lateral extent and progradational distance of these units may indicate the location of increased distribution of volcanic sources. Lower volume eruptions may represent a waning of volcanism or the location of lobe switching, with emplacement removed to another site. This is seen in the more limited deposition of seismic reflection units 12 and 13, which suggests that volcanism was waning and becoming more sporadic.

Variations in the apparent position of relative sea level and the volume of accommodation are also evident. Aggradation of the seismic reflection units is seen to increase through the stratigraphic succession and is defined by the migration of the offlap break in units 1 – 11 (Fig. 4.17). This is interpreted to be an increase in accommodation by the syn-volcanic subsidence of the growing delta system (Moore, 1970; Boldreel & Andersen, 1994). Studies of modern lava-fed deltas on Hawaii have identified that lava-fed deltas flex and subside as they form, with the greatest subsidence during active emplacement (Kauahikaua *et al.*, 2003). Geodetic monitoring of active lava-fed deltas on Hawaii has recorded subsidence of up to 7 cm a month (Mattox & Mangan, 1997; Kauahikaua *et al.*, 2003). Such syn-volcanic subsidence would have been localised, with the greatest subsidence occurring during active delta construction. The more regional subsidence seen within the basin is a product of the underlying rift architecture at the time of extension (Dean *et al.*, 1999; Lamers & Carmichael, 1999; Davies *et al.*, 2004). Deposition of seismic reflection units 12 and 13 towards the Faroe Islands are interpreted to be during the latter stages of delta development when there was a decrease in volcanic supply. The retrogradation of the delta front records an increase in accommodation by volcanic loading and subsidence of the delta during reoccurring periods of lava-fed delta inactivity, rather than an increase in relative sea level, as the calculated durations of these units are too short for a relative sea level increase (Moore, 1970; Lipman, 1995; Lipman & Moore, 1996).

4.6.3 Comparison to Outcrop Analogues

Volcaniclastic units in flood basalt and volcanic margin settings are not as well studied as lava flows, but recent work has shown that they can occur in a variety of settings and are particularly important at the onset of flood volcanism (e.g. Jerram & Stollhofen, 2002; Ukstins Peate *et al.*, 2003; Ross *et al.*, 2005). The majority of known lava-fed deltas have been recognised in outcrop. These include those recognised on the west coast of Greenland where significant volumes of volcanic rocks were erupted at ~65 Ma during the rifting and subsequent continental break up that created the NE Atlantic Margin (Larsen *et al.*, 1992). The lava-fed deltas developed in lacustrine settings, as erupted lava flows dammed indigenous drainage systems and infilled large lake bodies. These lava-fed deltas are contemporaneous to those of the Faroe-Shetland Escarpment and consist of extremely large (1 – 2 km), wedge-shaped bodies composed of hyaloclastite breccias overlain by multiple, thick and extensive lava flows and interbedded with thin sedimentary successions (Fig. 4.18; Pedersen *et al.*, 1997; Dam *et al*., 1998; Pedersen *et al.*, 1998; Ukstins Peate *et al.*, 2003). These large-scale outcrop examples are close to seismic-scale, and feed directly into the observations made within this study, as it displays similar thicknesses, external geometries and proportions of differing lithologies.

Finer-scale features have been identified in more accessible outcrops, such as on the Antarctica Peninsula where volcanism has occurred over the last 6 Ma as relatively short lived basaltic eruptions (Saunders & Tarney, 1982; Skilling, 2002; Smellie *et al*., 2008). The lava-fed deltas developed during glacial periods beneath extensive ice sheets and were deposited in englacial lacustrine and submarine environments. The deltas are much smaller (100 – 200 m), with the transition of individual lava flows into foresets of hyaloclastic breccias and interactions with contemporaneous sedimentary successions easily identified (Fig. 4.19; Porebski & Gradzinski, 1990; Skilling, 2002; Troedson *et al*., 2002; Smellie *et al.*, 2006; 2008). Such observations are typically below seismic resolution, but are none the less useful, as they provide insights into depositional processes, internal geometries and small-scale lithological heterogeneities that, although seemingly insignificant, in aggregate may produce seismically resolvable effects.
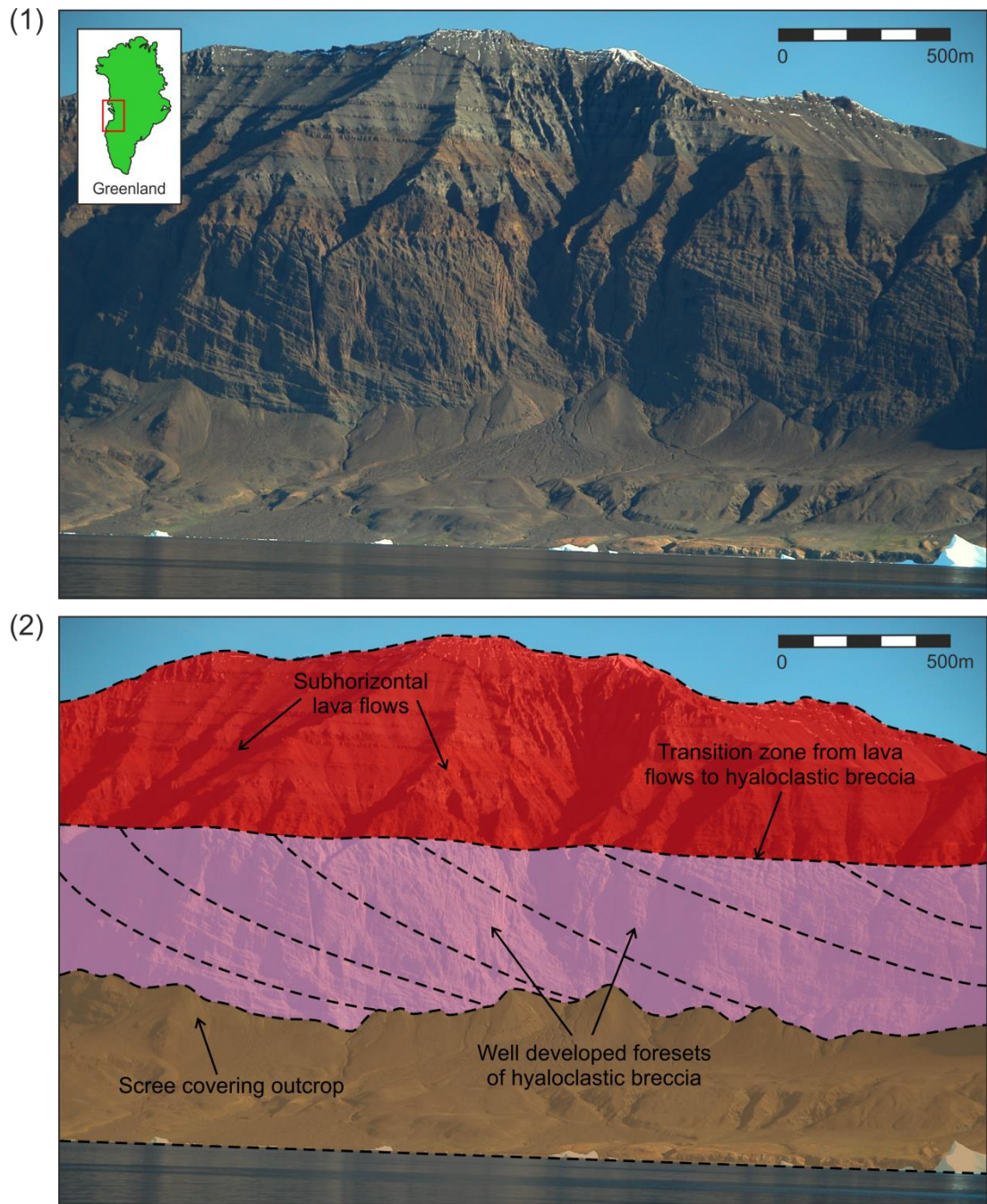
Fig. 4.18. (1) Outcrop of subaerial lava flow topsets feeding thick, well developed foresets of hyaloclastic breccias, West Greenland. (2) Interpreted outcrop. The height of the outcrop is ~ 1.5 km. Photo courtesy of Ken McCaffrey, Durham University.
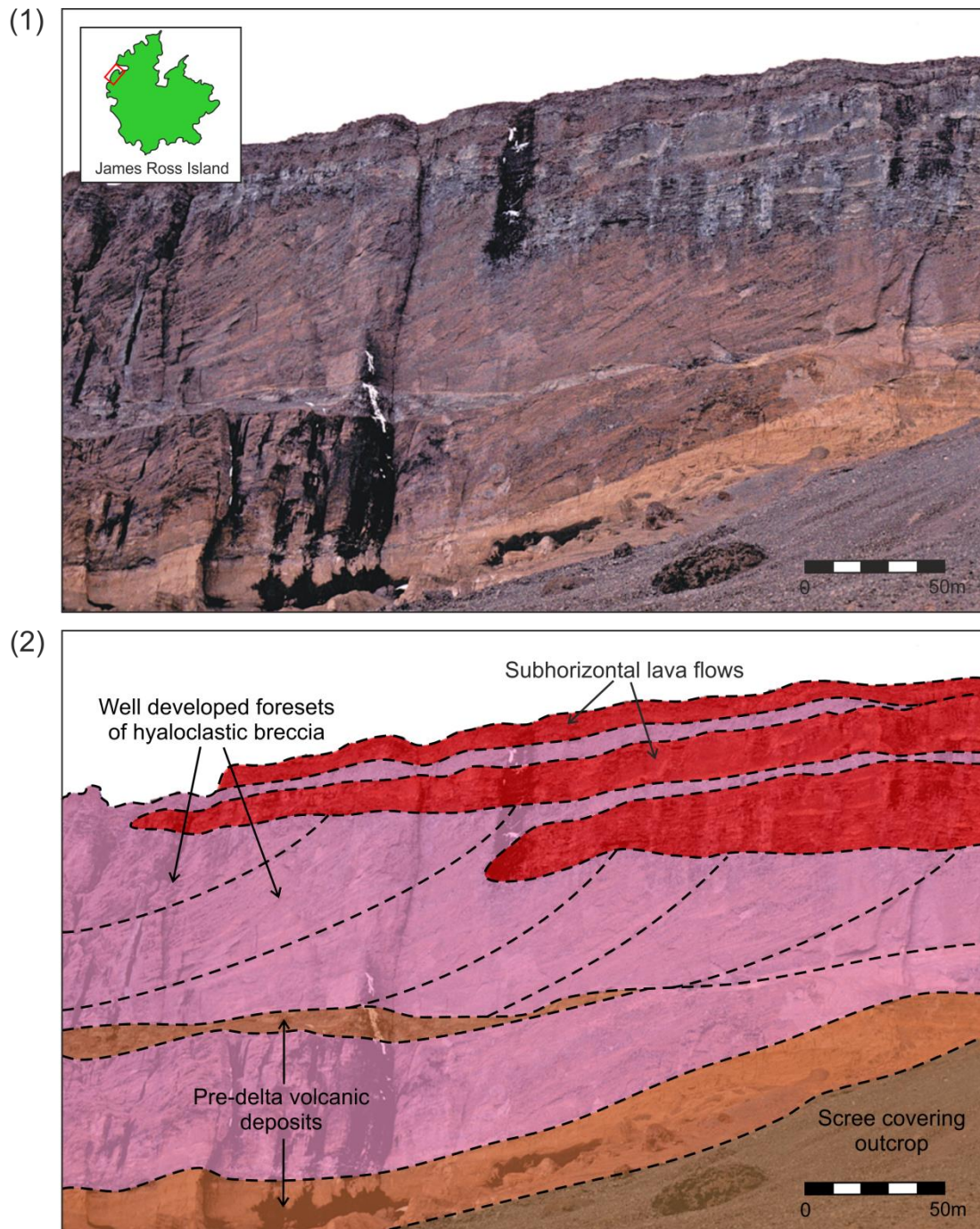
Fig. 4.19. (1) Outcrop of subaerial lava flow topsets feeding well developed foresets of hyaloclastic breccias and a pre-delta succession of volcaniclastic material, James Ross Island, Antarctica. (2) Interpreted outcrop. The stacking pattern of the delta exhibits progradation with a minor aggradational element. The height of the outcrop is ~150 m. Image modified from Smellie *et al.* (2008).

However, the most studied examples of lava-fed deltas are on Hawaii, where multiple lava flows enter the sea from a number of discrete vents and fissures, forming extensive hyaloclastite deposits in an offshore apron along the eastern coastline (Fig. 4.20; Moore *et al.*, 1973; Mattox *et al.*, 1993; Heliker *et al.*, 1998). Hawaiian lava flows are predominantly emplaced as pāhoehoe flows which can travel 0.2 – 50 km from source to shoreline (Malin, 1980, Pieri & Baloga, 1986), and are similar in emplacement style to continental flood basalts (Self *et al.*, 1997; Kauahikaua *et al.*, 1998). The Pu'u 'O'o vent on Hawaii has been erupting almost continuously since 1983 in a series of distinct eruptive episodes that on average continue for 3 – 4 years (Fig. 4.19; Heliker & Mattox, 2003; Kauahikaua *et al.*, 2003). Many of the lava flows are over 12 km long, and extend towards the coast where they have constructed lava-fed deltas at Kalapana and Kamoamoa bays with rates of build-out of ~38,500 and ~18,500 m^2/day (see Table 4.3 and Fig.4.20; Heliker *et al.*, 1998; Heliker & Mattox, 2003). Although the lava flows that feed the deltas were erupted over a number of years, active delta construction only lasted a few months with multiple pauses between eruptions (Mattox *et al.*, 1993; Mattox & Mangan, 1997). Such construction rates would provide an ideal check on the estimates of delta duration in this study. However, quantitative data on the growth of historic lava-fed deltas in the published literature are rather limited due to the lack of detailed records and the inherent difficulties in measuring active lava flow emplacement and delta deposition (Umino *et al.*, 2006). Without a large enough dataset to compare with, no significant correlation can be made.

Hawaiian Name	Duration (months)	Rate (m^2/day)	Length (m)	Width (m)	Depth (m)	Literature Reference
Kalapana/ Kaimū Bay	~11	~38,500	~700	~300	10-20	Mattox *et al.*, 1993; 1997; Umino *et al.*, 2006
Kamoamoa Bay	~24	~18,500	~2900	~500	-	Mattox *et al.*, 1997; Heliker *et al.*, 1998; Kauahikaua *et al.*, 2003

Table 4.3. Duration, growth rates and dimensions of historic, Hawaiian lava-fed deltas taken from the published literature.

Intermittently shifting lava streams have also been identified along the delta front, where the lava tubes feeding the flow of material become blocked and the flow only resumed once a new tube has formed (Kauahikaua *et al.*, 1998; Crown *et al.*, 1999; Peterson *et al.*, 1994). These shifting flows behave in a similar manner to distributary channels as seen in river deltas, where the delta builds out as a lobe that is sourced from the delta mouth, and then shifts its lateral position (Moore *et al.*, 1973; Mattox *et al.*, 1993). In between

eruptions, little or no volcanic activity occurred (Mattox *et al.*, 1993; Heliker *et al.*, 1998). With no new lava flows, erosion of the previously deposited flows commences through both chemical and mechanical mechanisms with a current rate of 11.9 t km^{-2} yr^{-1} (Dessert *et al.*, 2003; Navarre-Sitchler & Brantley, 2007). Onshore, the product of weathering and erosion is often volcanogenic soils which form on the top surface of the lava flow. Offshore, mass wasting of the hyaloclastic delta front can occur, forming a debris field consisting of fine sand to large boulder fragments of volcanic glass, basaltic material and pillow breccias (Smith *et al*., 1999; Sansone & Smith, 2006). The rapid re-establishment of coral communities that were submerged by lava flows have also been widely documented (Grigg & Maragos, 1974).
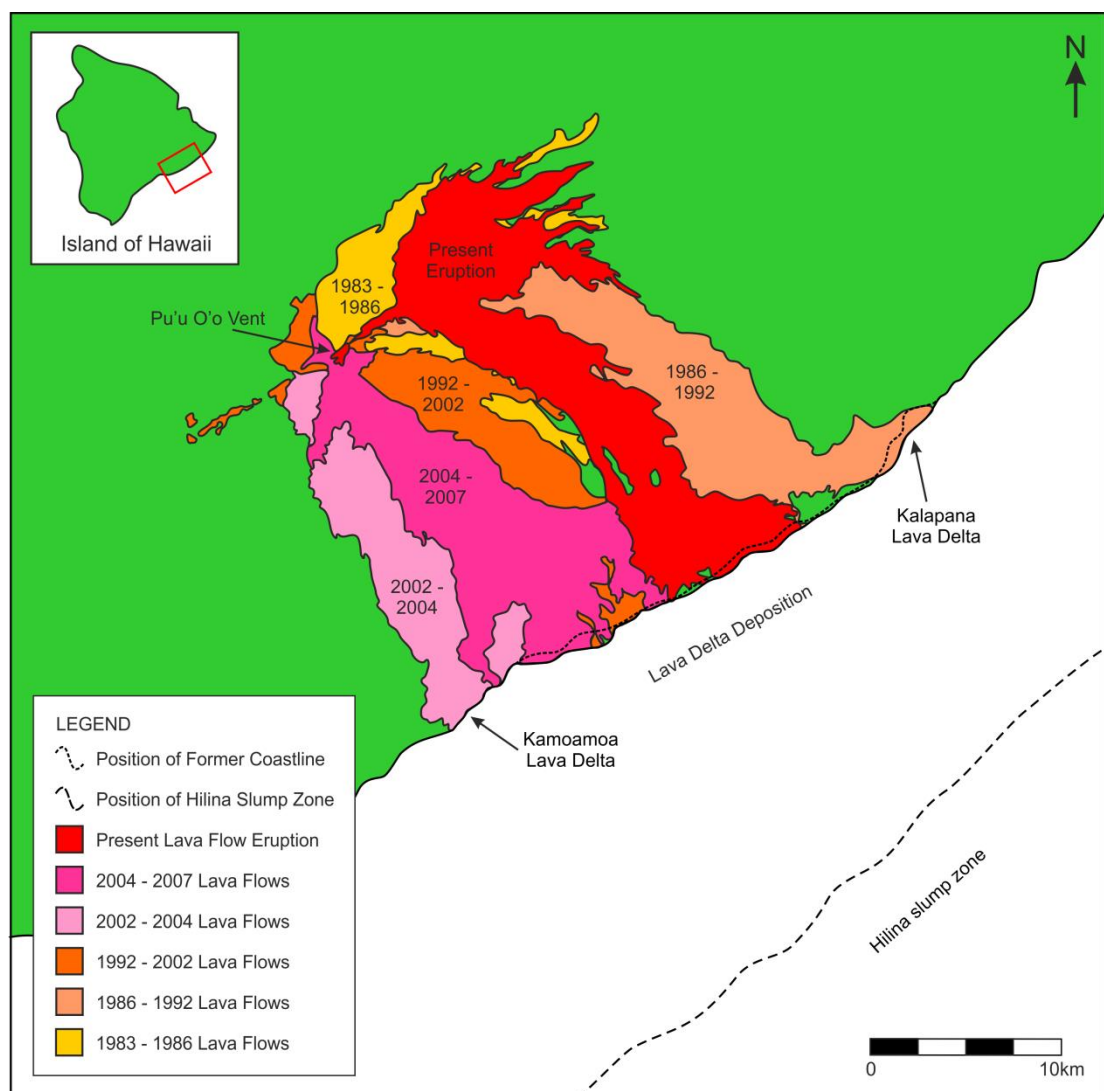
Fig. 4.20. Distribution and ages of lava flows originating from the Pu'u O'o volcano on the southeast side of Hawaii. Modified from Mattox & Mangan (1997), Heliker *et al.* (1998),

Smith *et al.* (1999), Heliker & Mattox (2003), Kauahikaua *et al.* (2003) and Sansone & Smith (2006).

4.7 Conclusions

This study demonstrates the utility in using seismic stratigraphic concepts to reconstruct the volcanic sediment basin-fill history of rifted margins. Detailed analysis of reflection geometries has identified a series of seismic reflection units that record the evolution of the Faroe-Shetland Escarpment during discrete periods of volcanism. Overall, the resulting lava-fed delta system shows a major period of progradation due to high volume eruptions of lava overwhelming the basin, during which the shoreline migrated a maximum distance of ~44 km in an east-southeast direction (away from the Faroes). The later stages of delta deposition were dominated by smaller volume eruptions coupled with increased accommodation through volcanic loading and subsidence. This caused the retrogradation of the delta, during which the shoreline migrated a maximum distance of ~75 km in a north-northwest direction (towards the Faroes). The data have revealed the encroachment of flood basalts into the basin, with the migration of the palaeo-shoreline recorded by the deposition of a lava-fed delta system over several thousand years. Importantly, this study highlights how the preservation of ancient volcanic systems in offshore settings has the potential to record key aspects of basin development, including the histories of relative sea level, volcanic supply and available accommodation, when more conventional depositional systems were absent.

CHAPTER 5: 3D SEISMIC GEOMORPHOLOGY OF THE GROWTH AND COLLAPSE OF A LAVA-FED DELTA SYSTEM, FAROE-SHETLAND BASIN

5.1 Introduction

Lava-fed delta systems can be a volumetrically important component of sedimentary basins and have been identified in a number of locations around the world, including the Faroe-Shetland Basin, West Greenland and Antarctica (e.g. Symthe, 1983; Pedersen *et al.*, 1997; Skilling, 2002). They preserve the transition from subaerial to submarine strata and often display geometries similar to siliciclastic delta systems (Jones & Nelson, 1970; Moore *et al.*, 1973). Understanding the geomorphology of these systems can be difficult, because the majority of outcrop examples have been highly eroded (Porębski & Gradzinski, 1990; Dam, 2002; Rohrman, 2007) or have been buried beneath thick sedimentary successions currently located in bathymetrically deep offshore regions, such as the Faroe-Shetland Basin in the North Atlantic Igneous Province (Stoker *et al*. 1993; Archer *et al.*, 2005; Thomson, 2005).

Growing interest in hydrocarbon exploration and production from offshore basins affected by thick volcanic successions has resulted in the acquisition of extensive 3D seismic reflection surveys in a bid to better constrain the underlying structure and associated hydrocarbon accumulations. These datasets offer a unique opportunity to study volcanic rocks that would otherwise not be accessible at the surface (Cartwright & Huuse, 2005; Davies & Posamentier, 2005; Posamentier *et al.*, 2007). Previously, 3D seismic reflection data have largely been used to study intrusive igneous bodies, which are well imaged due to the high contrast in acoustic impedance between the igneous body and the surrounding sedimentary rocks (e.g. Trude, 2004; Schofield *et al*, 2012). Applying 3D seismic visualisation techniques to buried volcanic structures will allow for investigation and analysis in a manner similar to outcrop, aerial photography or satellite based data (Cartwright & Huuse, 2005; Davies & Posamentier, 2005; Posamentier *et al.*, 2007).

The availability of a high resolution 3D seismic reflection dataset over a lava-fed delta in the Faroe-Shetland Basin has allowed earlier hypotheses about the stratigraphic relationships and internal architecture interpreted from 2D seismic reflection data to be tested (see Chapter 4). This study offers the first description of geomorphological structures associated

with the development and evolution of the lava-fed delta. Previous 2D seismic stratigraphic interpretation has identified bounding seismic reflections delineating units of volcanic deposition (see Chapter 4). These reflections represent potential hiatal surfaces, formed between each eruptive event and recording the end of a phase of volcanic deposition and any subsequent marine deposition. Such an extensive volcanic system has not been studied in 3D before and this dataset gives unparalleled access to morphological structures that potentially have not been seen in outcrop analogues. Understanding how these volcanic systems evolve in time and space, their inherent complexities and preserved distributions may prove to be a valuable resource in hydrocarbon exploration in volcanic rifted settings (Thomson, 2005; Cartwright & Huuse, 2005; Zhang *et al*., 2011).

5.2 Lava-fed Deltas and their Seismic Reflectivity

Lava-fed deltas occur globally and can form where subaerial lava flows enter a body of water. The lava quenches and fragments into hyaloclastic breccias, which are transported down slope under gravity to form inclined foresets (Jones & Nelson, 1970; Kokelarr, 1986; Fisher & Schmincke, 1994). The majority of known lava-fed deltas have been recognised from outcrop, where depositional environments vary from lava flowing into glacial lakes (e.g. Antarctica, Porębski & Gradzinski, 1990; Skilling, 2002; Iceland, Furnes *et al*., 1974; Watton *et al*., 2013) to the flow of flood basalts in to marine basins (e.g. Greenland, Pedersen *et al*, 1997; Columbia River Flood Basalt Province, Fuller, 1931; Shervais *et al*., 2002). Most documented examples of modern lava-fed deltas are on Hawaii, where multiple pāhoehoe lava flows enter the sea from a number of discrete vents and fissures, forming relatively small hyaloclastite deposits along the east coastline (e.g. Moore *et al*, 1973; Mattox *et al*., 1993).

With increased hydrocarbon exploration in rifted basins and improved seismic imaging techniques, a number of lava-fed deltas have been documented in offshore regions, including Western Australia (e.g. Symonds *et al*., 1998; Planke *et al*., 2000), the West Indian Margin (e.g. Calvès *et al*., 2011) and the North Atlantic (e.g. Berndt *et al*., 2001; Spitzer *et al*., 2008). Lava-fed deltas can occur in continental flood basalt provinces where they are often deposited during the early stages of the province eruption when the erupted volumes are greatest and the lavas are more extensive (Jerram & Widdowson, 2005; Ross *et al*., 2005). The volcanic nature of these delta systems is indicated in seismic data by the

large contrast in acoustic impedance between volcanic lithologies and overlying sedimentary rocks. The deltas typically consist of high amplitude topsets and escarpments composed of moderate to low amplitude foresets, with the offlap break a proxy for the position of relative sea level during deposition (Planke *et al.*, 2000; Berndt *et al.*, 2001).

Previously acquired seismic data in the Faroe-Shetland Basin has enabled the identification of an extensive lava-fed delta system that records the encroachment of continental flood basalt lavas across the basin and a significant syn-volcanic migration of the palaeo-shoreline (e.g. Smythe, 1983; Symthe *et al.*, 1983; Kiørboe, 1999). The volcanic delta system is part of the North Atlantic Igneous Province and was constructed through many successive phases of active volcanism during the Palaeocene (Kiørboe, 1999; Spitzer *et al.*, 2008; Ellefsen *et al.*, 2010). The resulting stacking geometry of the volcanic successions reflects the interaction between lava supply, accommodation and relative sea level. The geometry of the delta system was primarily driven by lava supply; with large volumes of lava overwhelming the basin and causing the delta to prograde (see Chapter 4). A decrease in the eruption volume of the continental flood basalt eruptions was recorded by the retrogradation of the delta.

5.3 Geological Setting

The Faroe-Shetland Basin formed through multiple phases of rifting during the Mesozoic to early Cenozoic (Boldreel & Andersen, 1994; Dean *et al.*, 1999). Continental break-up at the adjacent Atlantic continental margin and the onset of seafloor spreading was accompanied by extensive flood basalt volcanism. Significant volumes of subaerial lava were erupted on or close to the Faroe Islands (e.g. Passey & Bell, 2007), together with the intrusion of sills (e.g. Thomson & Schofield, 2008; Hansen *et al.*, 2011) and the formation of individual volcanic centres, including the Erlend Complex and Brendans Dome (e.g. Gatliff *et al.*, 1984; Ritchie & Hitchen, 1996; Jolley & Bell, 2002). The subaerial lava flowed southeast, in-filling pre-existing topography before reaching the palaeo-shoreline and forming a prograding body of hyaloclastic breccias (Smythe, 1983; Smythe *et al.*, 1983; Kiørboe, 1999; Ritchie *et al.*, 1999). Volcanism within the basin ceased when sea floor spreading became established in the Atlantic, north of the Faroe-Shetland Basin. Post-rift subsidence and late Cenozoic compression created the tilted and folded structures that are visible today (Ritchie *et al.*, 2003; Sørensen, 2003; Davies *et al.*, 2004; Praeg *et al.*, 2005).

5.4 Data and Methodology

This study focuses on the interpretation of a 20 km x 40 km 3D seismic reflection survey located over the most distal part of a lava-fed delta system in the central Faroe-Shetland Basin (Fig. 5.1). The survey images the flood basalt succession of the Faroe-Shetland Basin at an average horizontal resolution of ~50 m and an average vertical resolution of ~25 m, with an average velocity of 4000 ms^{-1}. The lava-fed delta is composed of high amplitude and strongly continuous topset reflections that overlie a wedge-shaped body of moderate to low amplitude, inclined and prograding reflections. It has been divided into 13 discrete and seismically resolvable units that were identified on the basis of seismic facies associations, internal reflection geometries and bounding reflections (Chapter 4, Fig. 4.3; Vail *et al.,* 1977b; Posamentier & Vail, 1988; Kiørboe, 1999). The seismic reflection units have been numbered in stratigraphic order, with 1 being the oldest and 13 being the youngest, with each unit interpreted to record continuous volcanic deposition during discrete periods of active volcanism (Fig. 5.2; see Chapter 4). In addition, an exploration well which penetrated the distal extent of the flood basalts was used. Exploration well 214/4-1 encountered approximately ~100 m of basalt overlying at least ~300 m of hyaloclastite and was been used to calibrate the seismic response to the volcanic lithologies (Chapter 4, Fig. 4.4; Davies *et al*., 2002; 2004; Sørensen, 2003).

The 3D seismic reflection data image seismic reflection units 5 – 12, with use of the previously interpreted 2D seismic reflections surveys to guide interpretation of the 3D survey (Fig. 5.3; see Chapter 4). Initial analysis of the 3D survey indicated good correlation between these data and the previously interpreted 2D seismic data. Interpretation was undertaken through mapping the seismic reflection units that constructed the lava-fed delta. They form a wide platform and consist of a positive, high amplitude and strongly continuous topset reflection that overlie a wedge-shaped body of moderate to low amplitude, inclined and prograding clinoform reflections (Fig. 5.3). In addition, distinct seismic reflection successions have been recognised below and above the delta system, and have been termed "pre-delta" and "post-delta" successions respectively (Fig. 5.3).
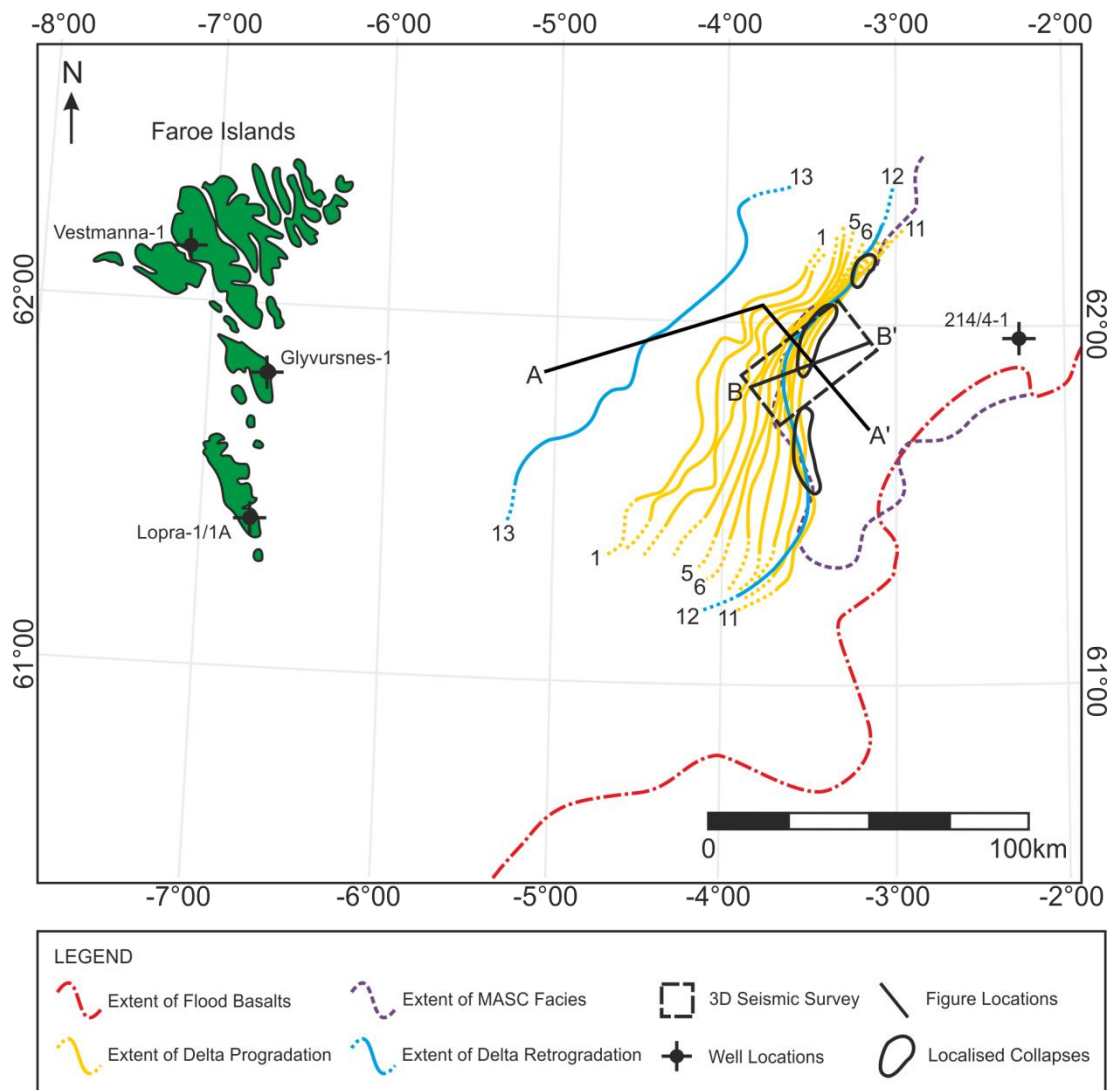
Fig. 5.1. Map showing the location of the 3D seismic survey and the developmental stages of the lava-fed delta which formed the Faroe-Shetland Escarpment in the central Faroe-Shetland Basin. Extent of flood basalts and Faroe-Shetland Escarpment modified from Ritchie *et al.* (1996, 1999), Ellis *et al.* (2002) and Sørensen (2003).
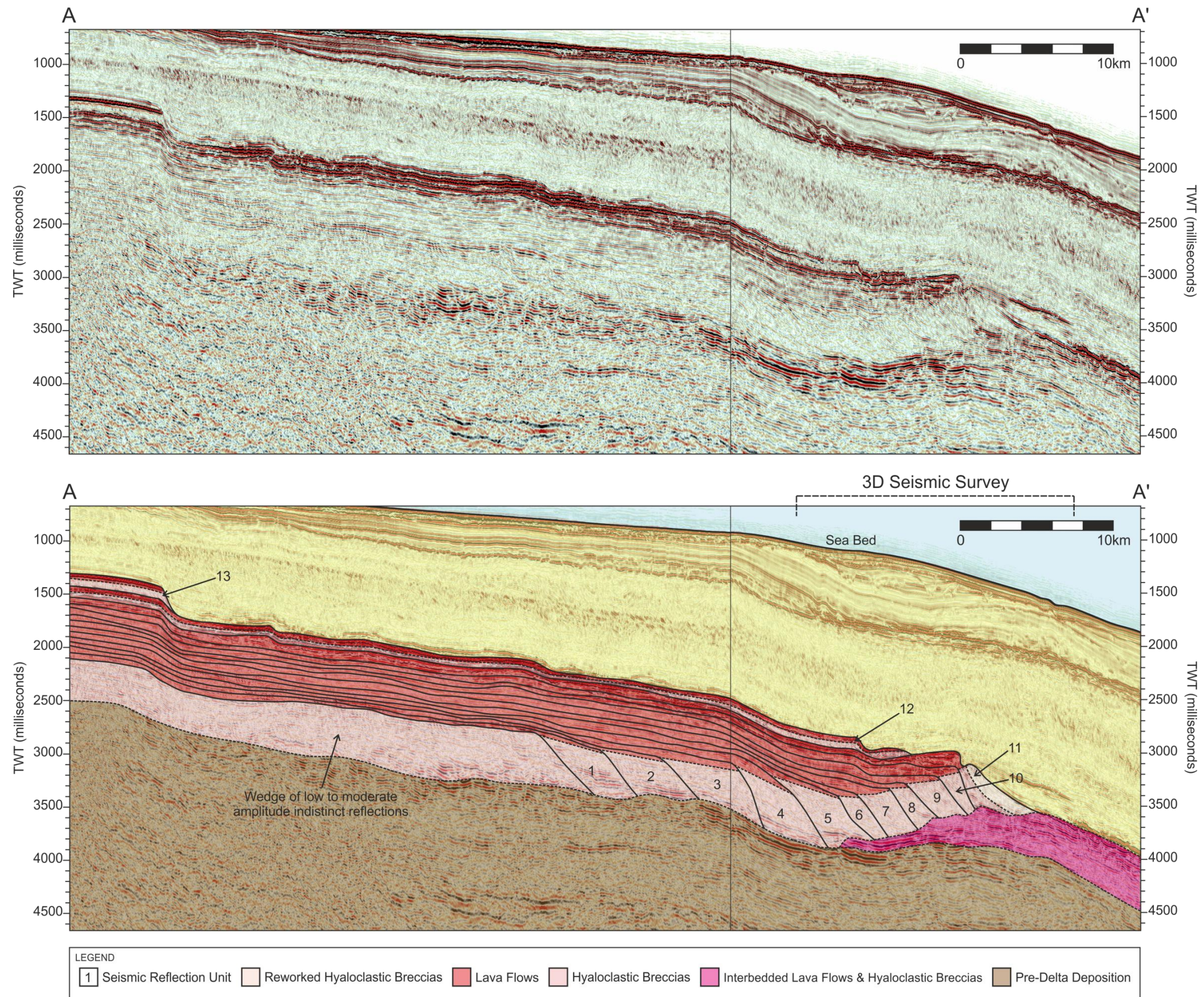
Fig. 5.2. 2D seismic section A-A' which images the internal structure of the Faroe-Shetland Escarpment which is divided into 13 seismic reflection units, with 1 being the oldest and 13 being the youngest. Interpreted section includes bounding reflections of the seismic reflection units, distribution of seismic facies and the extent of the escarpment imaged by the 3D seismic reflection survey (see Chapter 4). See Figure 5.1 for location.
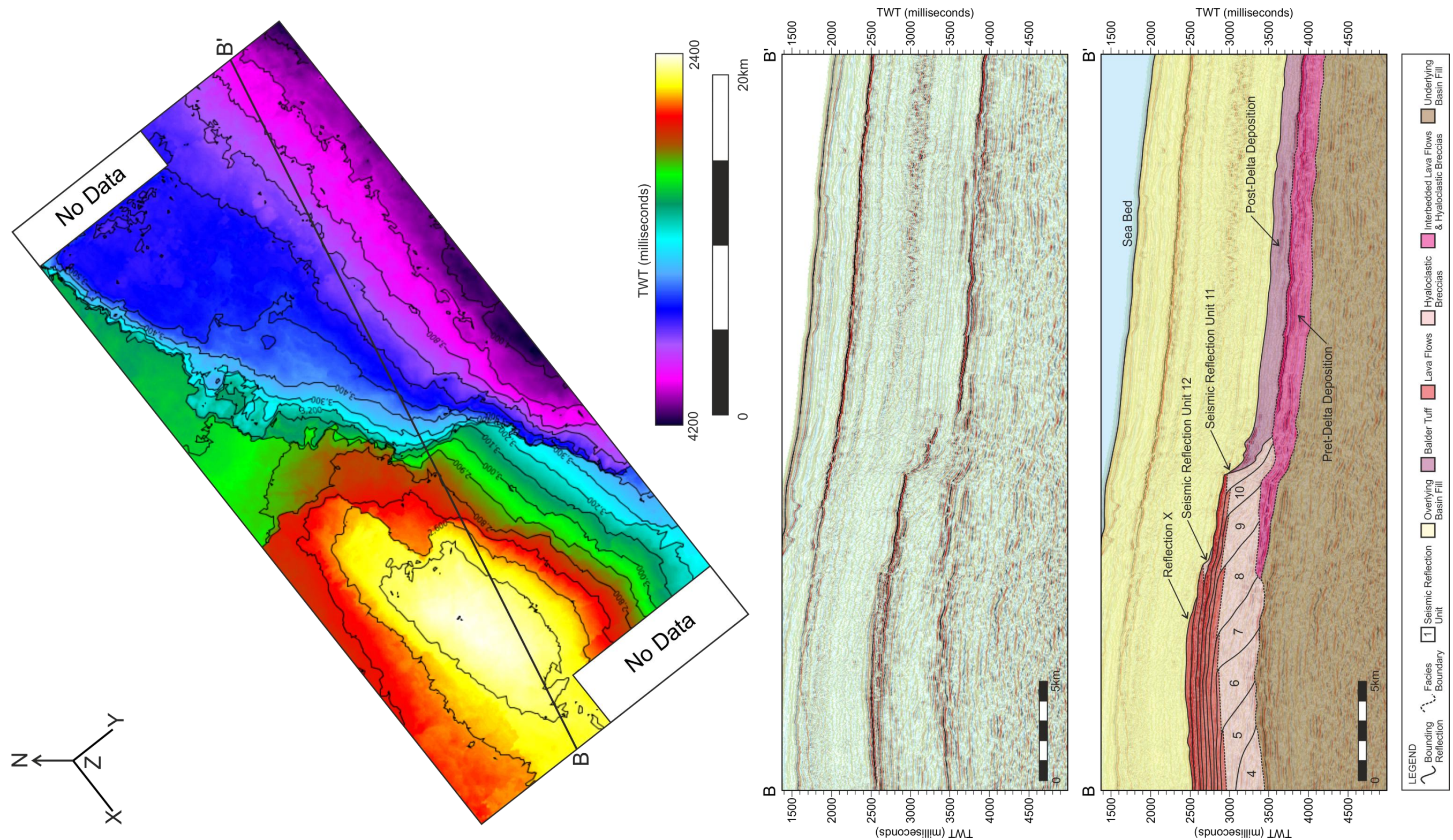
Fig. 5.3. Two-way time reflection surface of the top continental basalts imaged within the 3D survey. Reflection surface has been contoured at 100 millisecond intervals. The lava-fed delta forms a wide platform in the west of the survey, elevated ~1050 m above a lower plateau in the east of the survey. Representative seismic section B-B' through the lava-fed delta imaged in the 3D survey. Interpreted section includes the pre-delta, delta and post-delta succession that have been identified within this study, the extent of the seismic reflection units and the distribution of seismic facies (see Chapter 4). See Figure 5.1 for location.

5.5 Observations

5.5.1 Pre-Delta Succession

Within the 3D survey, a succession has been identified to pre-date the construction of the lava-fed delta (see Fig. 5.3). This succession is composed of semi-continuous, moderate to low amplitude, parallel to hummocky reflections which have velocities of 4000 – 5000 ms^{-1} and an average thickness of ~300 m. This succession has been identified beyond the survey using 2D seismic data and is penetrated by exploration well 214/4-1 between 3978m and 4350 m MD (see Chapter 4; Davies *et al.*, 2002; 2004). RMS amplitude maps of the top of the succession reveal broad, terraced slabs with distinct edges (Fig. 5.4). The terraced slabs vary from high amplitude, smooth and rugose textures to lower amplitude, irregular and hummocky textures (Fig. 5.5). The high amplitude, relatively continuous reflections easily identify the top of pre-delta succession whereas the western extent of the succession is difficult to determine beneath the overlying delta succession (Fig. 5.6). The western extent of the pre-delta succession appears to wedge out beneath the escarpment is based on where the seismic facies changes from continuous, moderate amplitude, inclined reflections to semi-continuous, moderate to low amplitude, parallel to hummocky reflections (Fig. 5.6).
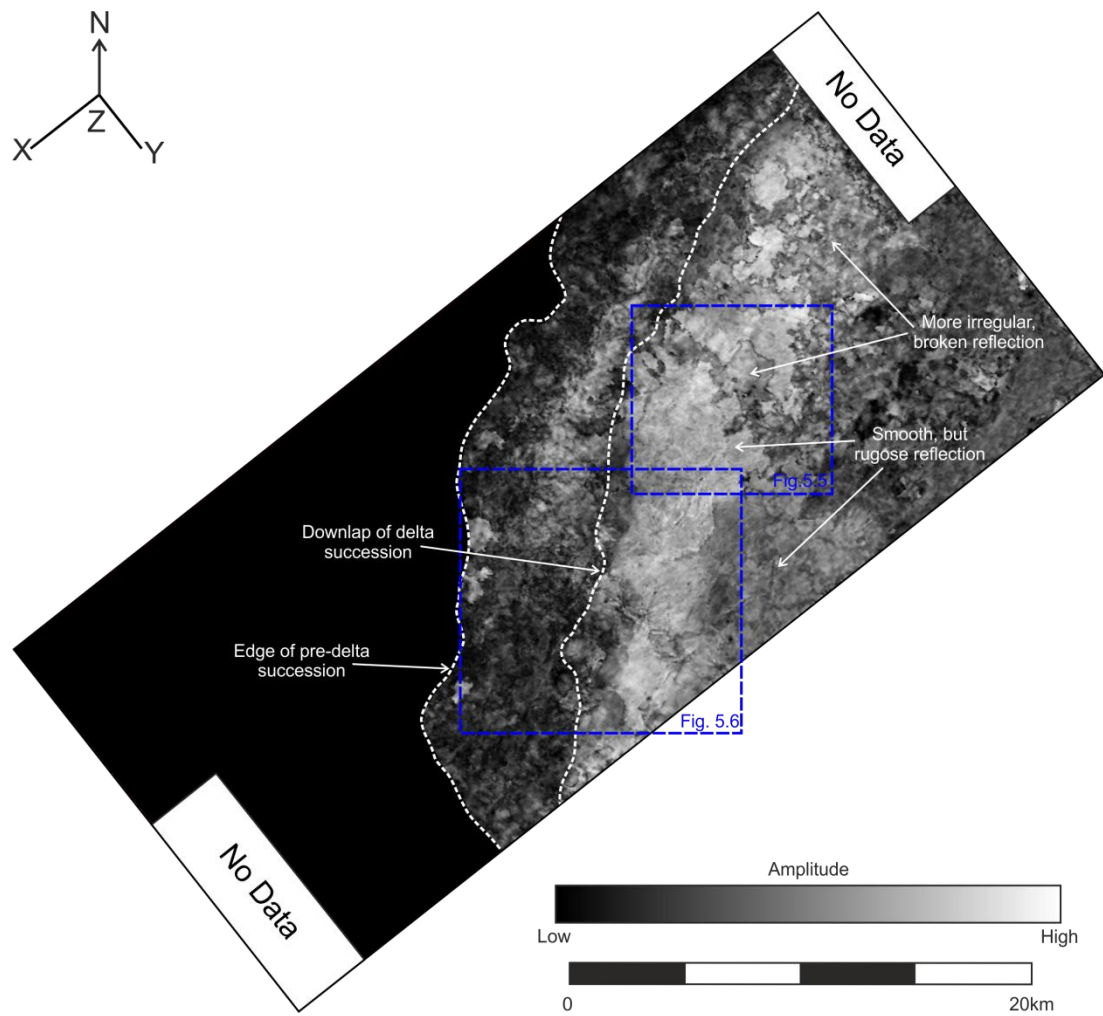
Fig. 5.4. RMS seismic amplitude map with a 5 millisecond window of the top of the pre-delta succession (see Fig. 5.3). The map images the variations in surfaces geometries and the downlap of the overlying delta succession. Location boxes refer to Fig. 5.5 and 5.6.
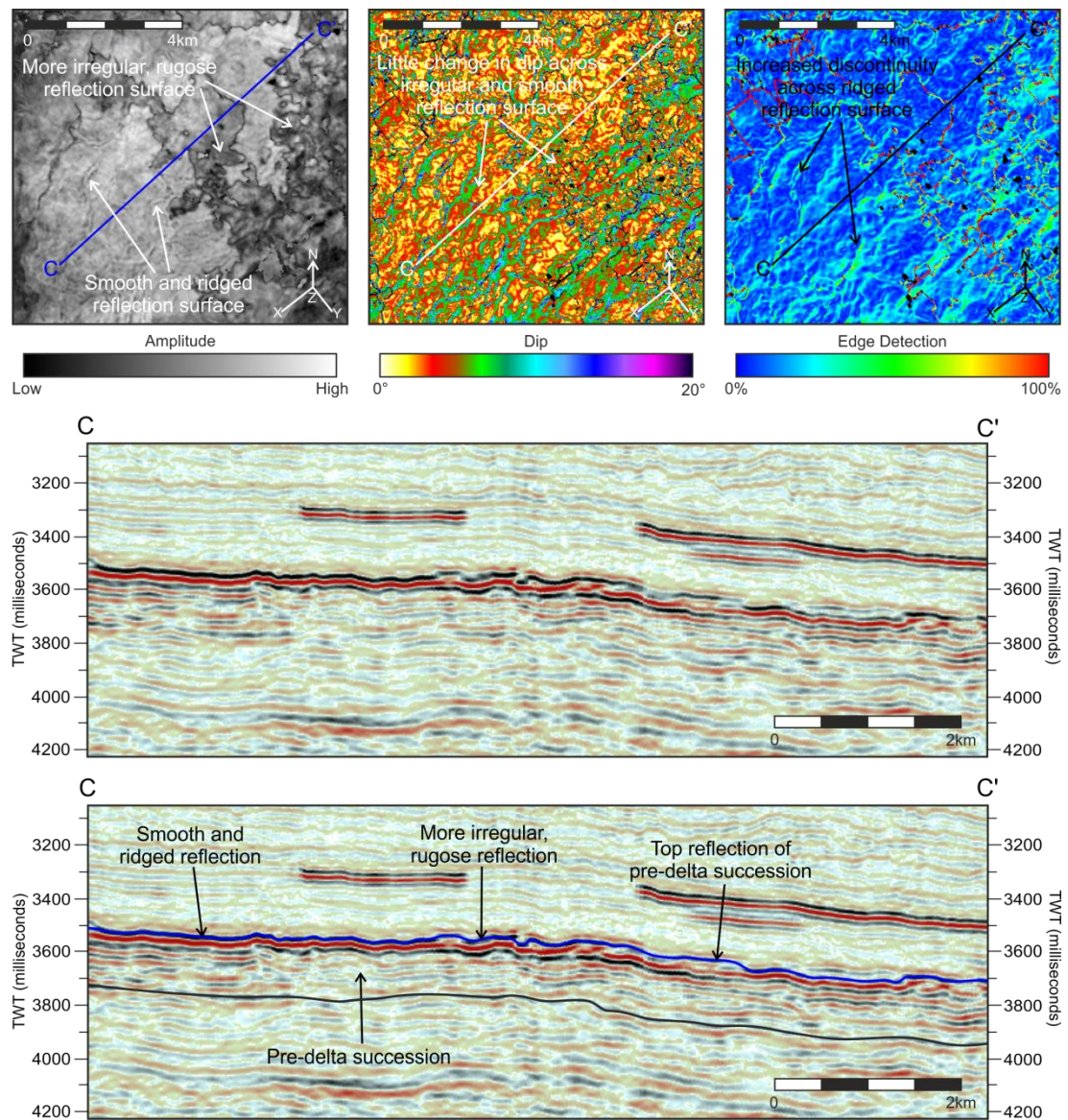
Fig. 5.5. Seismic section C-C' images the pre-delta succession and the broad terraces with high amplitude, smooth and rugose reflection geometries .Seismic attribute maps including amplitude, dip and edge detection maps with a 5 millisecond window of the top of the pre-delta succession. The seismic amplitude map images the variations in surface geometry from smoothed and ridged to more irregular and rugose. The dip map reveals that there is little change in dip across the irregular and smooth reflection surface. The edge detection map shows increased discontinuities across the smooth, ridged reflection surface. For location see Fig. 5.4.
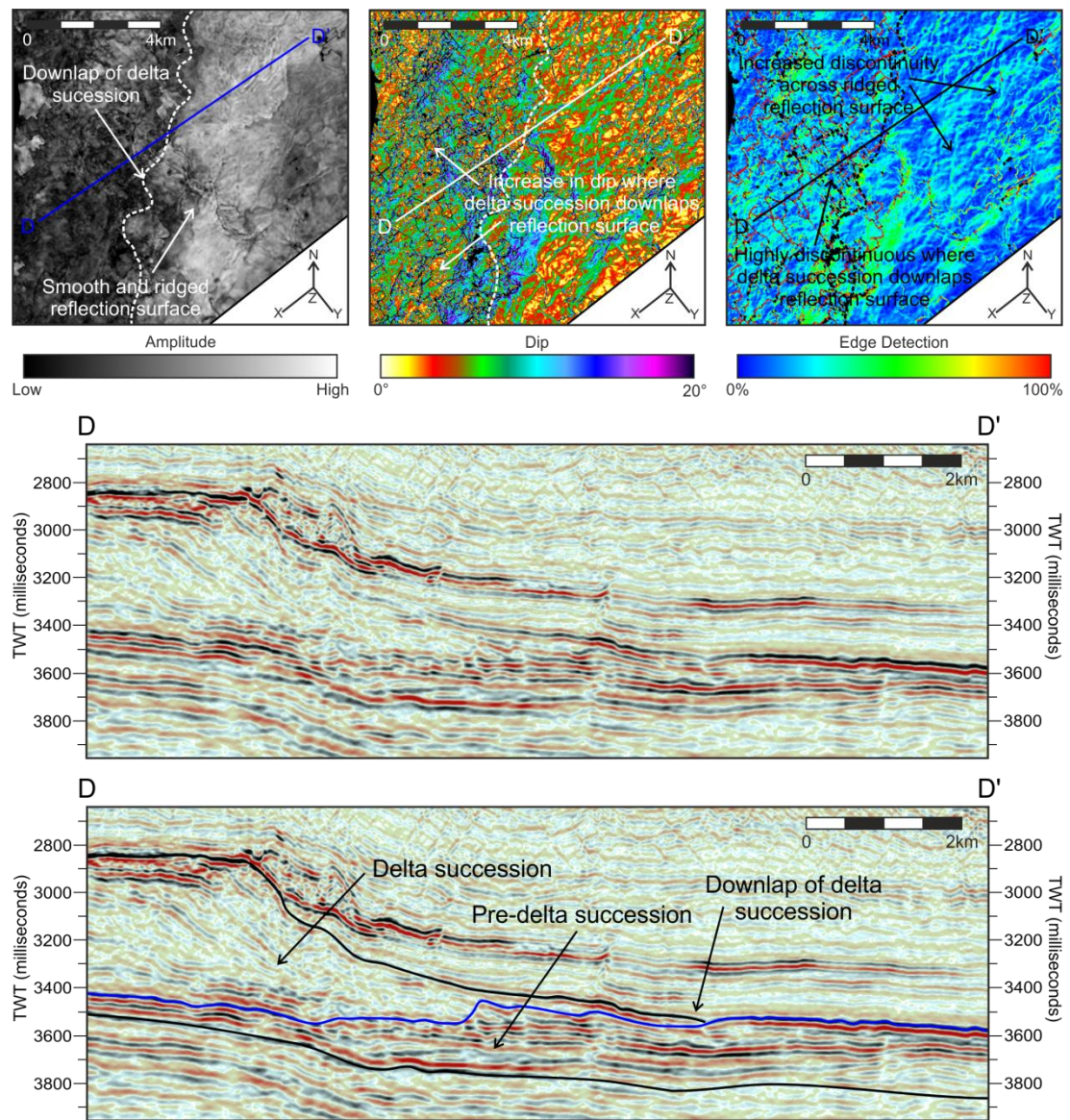
Fig. 5.6. Seismic section D-D' images the pre-delta succession and downlap of the overlying delta succession. Seismic attribute maps including amplitude, dip and edge detection maps with a 5 millisecond window of the top of the pre-delta succession. The seismic amplitude map images the decrease in amplitude caused by the downlap of the overlying delta succession. The dip map shows an increase in dip where the delta succession downlaps on to the top of the pre-delta succession. The edge detection map reveals an increased discontinuity across the smooth, ridged reflection surface. For location see Fig. 5.4.

5.5.2 Delta Succession

The overlying delta succession is composed of high amplitude, sub-horizontal topsets that overlie a prograding body of moderate amplitude, inclined foresets (see Fig. 5.3). The succession of reflection have velocities of 4000 – 5000 ms^{-1} and average thickness of ~1050

m. The 3D seismic survey encountered 8 of the 13 seismic reflection units previously identified using 2D seismic data, with good correlation between the datasets allowing identification of the delta's internal stratigraphic relationships. The best imaged part of the delta is the top surface due to high acoustic impedance contrast produced by the overlying sedimentary rocks. The top surface of the lava-fed delta is actually composed of two seismic reflection units; units 11 and 12. Seismic reflection unit 11 records the final phase of progradation while seismic reflection unit 12 records the first phase of retrogradation. Seismic reflection unit 11 displays high amplitude, sub-horizontal topsets overlying moderate amplitude, inclined foresets (see Fig. 5.3).

Extraction of RMS amplitude maps of the top surface of the delta reveal that the majority of the topsets produce broad, gently dipping, smooth to hummocky lobes while the foresets producing a smooth to hummocky slope (Fig. 5.7). The largest of the topset lobes have been identified along the delta front of seismic reflection unit 11, ranging from 1 – 3.6 km wide and producing a sinuous delta front (Fig. 5.7). Cross-cutting the lobes are a series of branching depressions 150 – 400 m wide and 2 – 5 km long, which are orientated largely perpendicular to the delta front and exhibit lower seismic amplitudes than the surrounding high amplitude lava flows (Fig. 5.8). In the north of the survey area, the RMS seismic amplitude maps reveal the delta front is disrupted by arcuate, concave upwards amplitude anomalies (Fig. 5.9; see Chapter 4). Detailed mapping of these amplitude anomalies revealed chaotic foreset slopes and topsets lacking the broad, smooth to hummocky lobes previously described (Fig. 5.9).

A total of 8 distinct arcuate features have been identified and measure 300 – 740 m in width and 230 – 320 m in height, cutting back into the delta succession between 680 – 1500 m (Fig. 5.9; see Appendix II for individual dimensions). These features are orientated perpendicular to the delta front and are often separated by angular ridges close to the delta front that decrease in size and angularity down slope (Fig. 5.10). The underlying foreset reflections become disrupted, forming low angle wedges composed of shallow, lower amplitudes and that has a limited lateral extent. Downslope the foreset reflections become chaotic and disrupted, extending 4.2 – 4.9 km away from the delta front, widening and flattening out to form an irregular and hummocky surface (Fig. 5.10; see Appendix II for individual dimensions).

The top surface of the lava-fed delta is downlapped by a single, low amplitude, semi-continuous reflection (Reflection X, see Fig. 5.3). Extraction of RMS amplitude maps reveals

that the reflection has a hummocky surface with a limited distribution and a simple branching morphology (Fig. 5.11). The edges of the reflection display irregular, incised edges 100 – 250 m wide and 400 – 600 m long (Fig. 5.11). In contrast to the top surface of the lava-fed delta, imaging the internal structure of the delta is complicated by the internal heterogeneity of the volcanic succession, which causes scattering and attenuation of the seismic wave (Shaw *et al*. 2008; Nelson *et al*., 2009). Despite this, it is possible to recognise the lobate delta front of the deeper seismic reflection units and the distinct progradational phases of delta formation (Fig. 5.12).
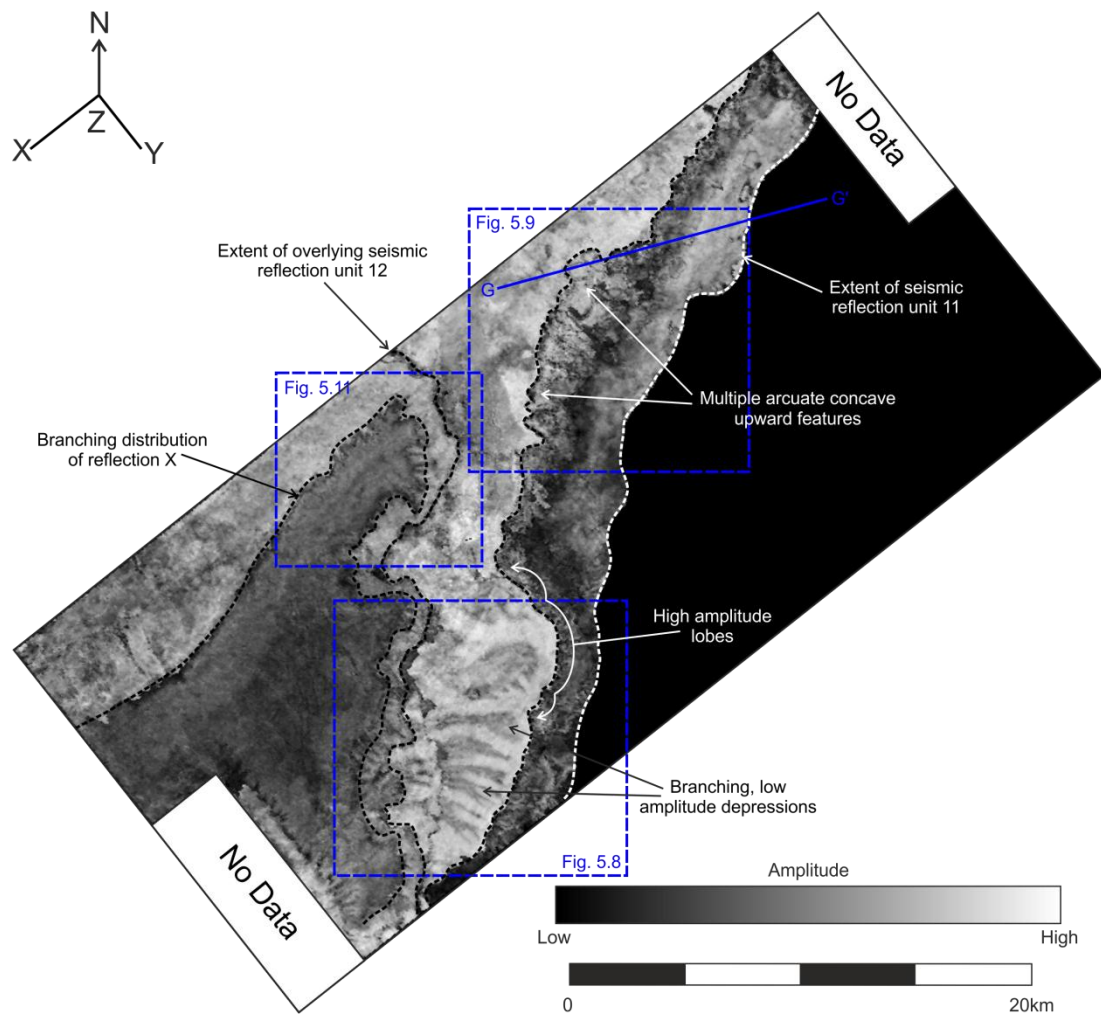
Fig. 5.7. RMS seismic amplitude map with a 5 millisecond window of the top of the lava-fed delta which is composed of seismic reflection units 11 and 12 (see Fig. 5.3). The map images the high amplitude, lobate delta front geometries and the arcuate, concave-up geometries that disrupt the delta front. Location boxes refer to Fig. 5.8, 5.9 and 5.11. Cross section G-G' corresponds to Fig. 5.10.
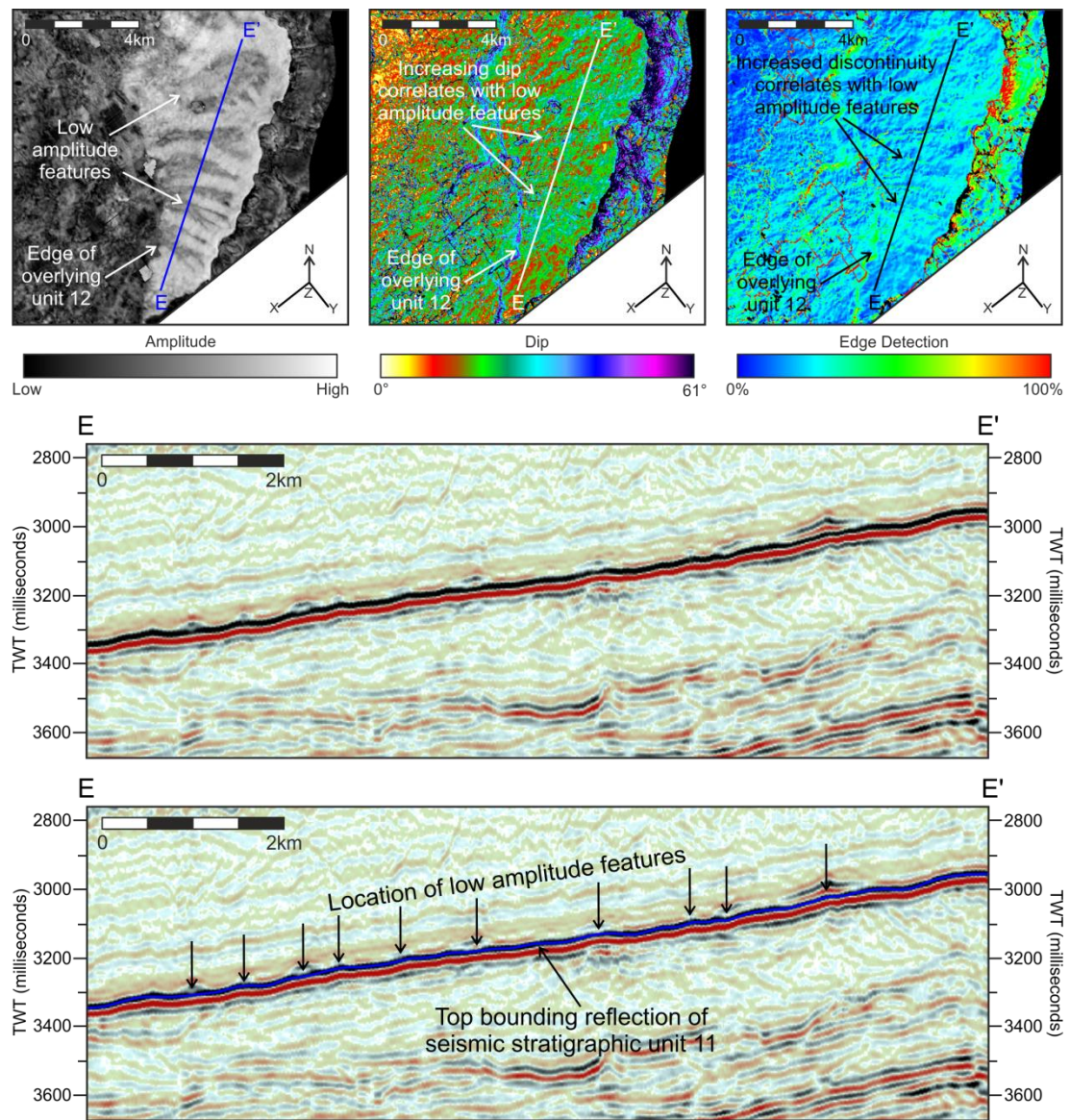
Fig. 5.8. Seismic section E-E' images seismic reflection unit 11 and the low amplitude depressions that are orientated largely perpendicular to the delta front, as is the seismic section. Seismic attribute maps including amplitude, dip and edge detection maps with a 5 millisecond window of the top of the seismic reflection unit 11. The seismic amplitude map images the high amplitude lobes and the low amplitude depressions that cross-cut them. The dip map reveals increases in dip that correspond to the position of the low amplitude, cross-cutting features. The edge detection map shows increased discontinuities that delineate the low amplitude, cross-cutting features. For location see Fig. 5.7.
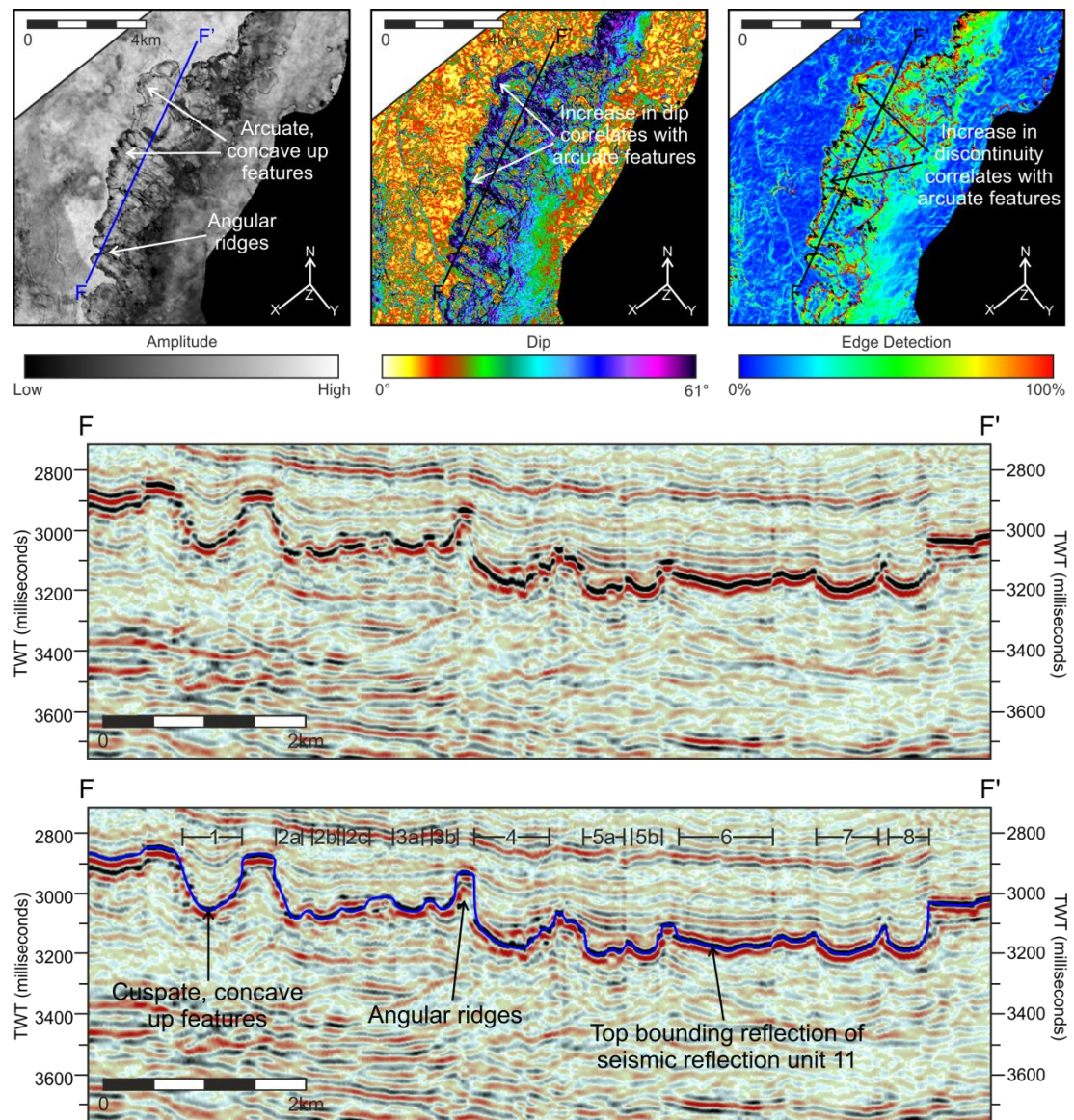
Fig. 5.9. Seismic section F-F' images seismic reflection unit 11 and the arcuate, concave upwards geometries that disrupt the unit. Seismic attribute maps including amplitude, dip and edge detection maps with a 5 millisecond window of the top of the seismic reflection unit 11. The seismic amplitude map images the arcuate, concave upwards features that disrupt the delta front. The dip map reveals a rapid increase in dip that corresponds to the position of the arcuate features. The edge detection map shows a marked increase in discontinuities that corresponds to the position of the arcuate features. For location see Fig. 5.7.
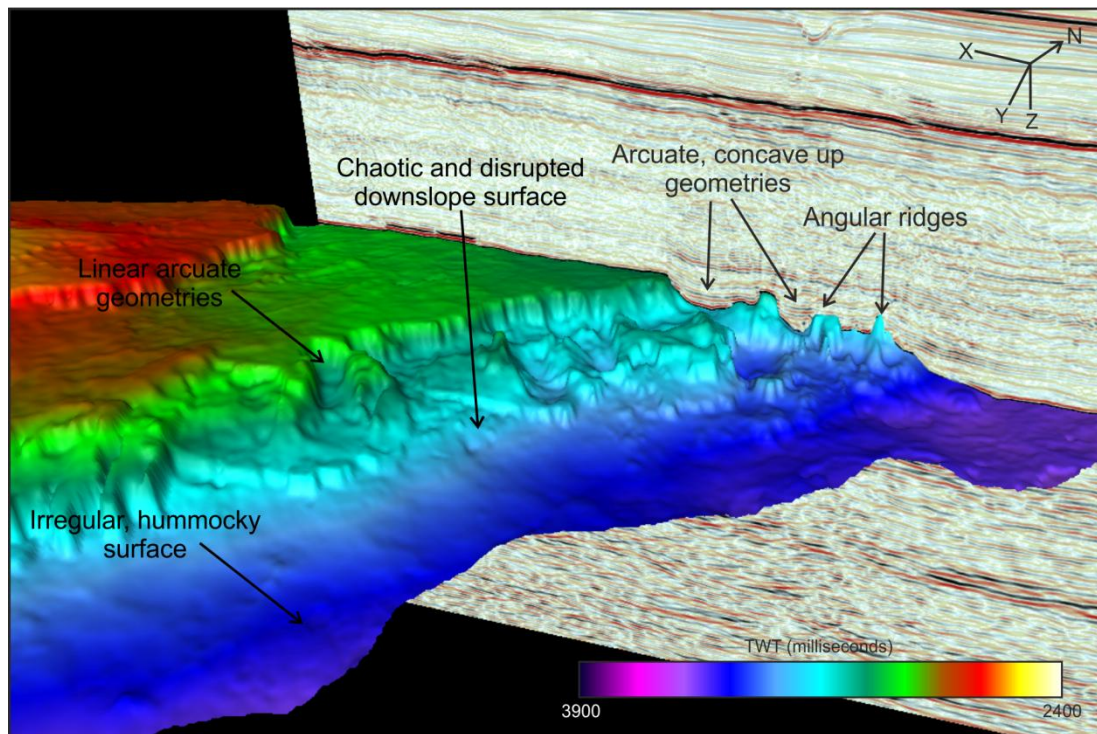
Fig. 5.10. Two-way time reflection surface and seismic section G-G' that image the arcuate, concave-up geometries that intersect the delta succession and the irregular and hummocky delta slope. For cross section location see Fig. 5.7.
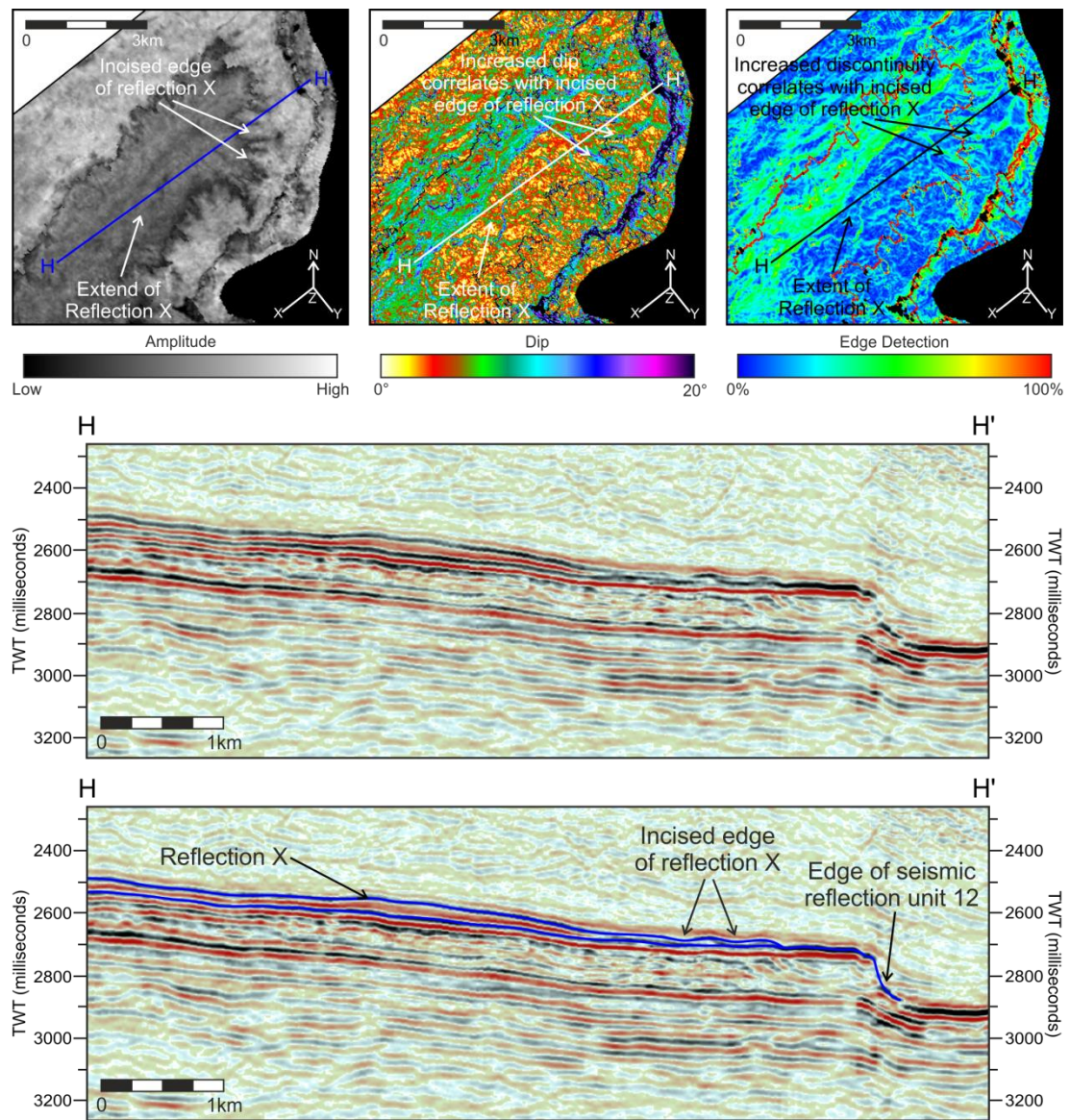
Fig. 5.11. Seismic section H-H' images the downlap of Reflection X on to seismic reflection unit 12. Seismic attribute maps including amplitude, dip and edge detection maps with a 5 millisecond window of the top of seismic reflection unit 12 and Reflection X. The seismic amplitude map images the dark amplitudes and the incised edges of Reflection X against the top surface of seismic reflection unit 12. The dip map reveals an increase in dip that corresponds to the position of the incised edge features of Reflection X. The edge detection map shows a marked discontinuity that corresponds to the extent of Reflection X. For location see Fig. 5.7.
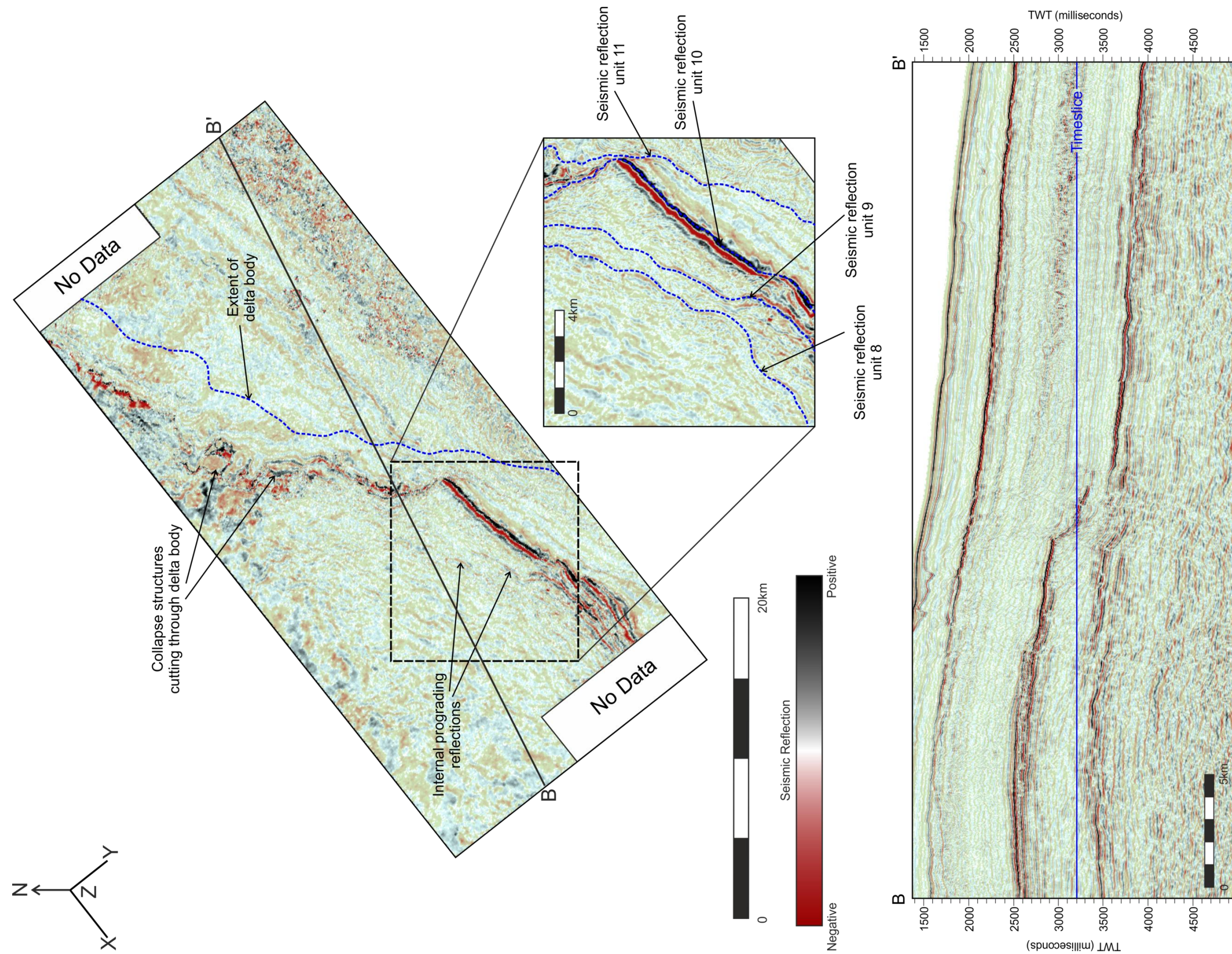
Fig. 5.12. A time-slice through the 3D seismic survey that images the lobate, sinuous delta front of progradational seismic reflection units 8 to 11. Seismic section B-B' indicates the position of the timeslice at 3200 milliseconds.

The extent of the internal seismic reflection units 5 – 10 were also mapped through the correlation of the 3D seismic survey with the previously interpreted 2D seismic reflection surveys. However the resulting RMS seismic amplitude maps are poor, with decreased resolution the deeper the seismic reflection unit was within the delta body. This is due to heterogeneity of the volcanic rocks causing scattering and absorption of the seismic energy (see Chapter 3). The lack of resolution and distinct reflections geometries hampered interpretation of the extracted RMS amplitude maps, with largely moderate to low amplitude, irregular and chaotic reflection surfaces. Seismic reflection units 5 – 10 are not shown in this chapter but can be found in Appendix II.

5.5.3 Post-Delta Succession

Onlapping the delta front is a succession of continuous, moderate to low amplitude reflections which have velocities of 2500 – 4000 ms^{-1} and an average thickness of ~180 m, thinning to ~0 m on the delta slope (see Fig. 5.3). RMS amplitude maps extracted sequentially through the post-delta succession reveal a number of constrained, high amplitude, stacked and interconnected lobes which strongly contrast with the surrounding low amplitude background reflection (Fig. 5.13). Individual lobes vary from 1.2 – 4.5 km in width, and consist of multiple, smaller overlapping lobes (Fig. 5.14). The bulbous lobes extent ~25 km away from the delta front and appear to be fed by a 1.2 – 2.5 km wide channel-like feature that extends from the top of the delta succession (Fig. 5.14).
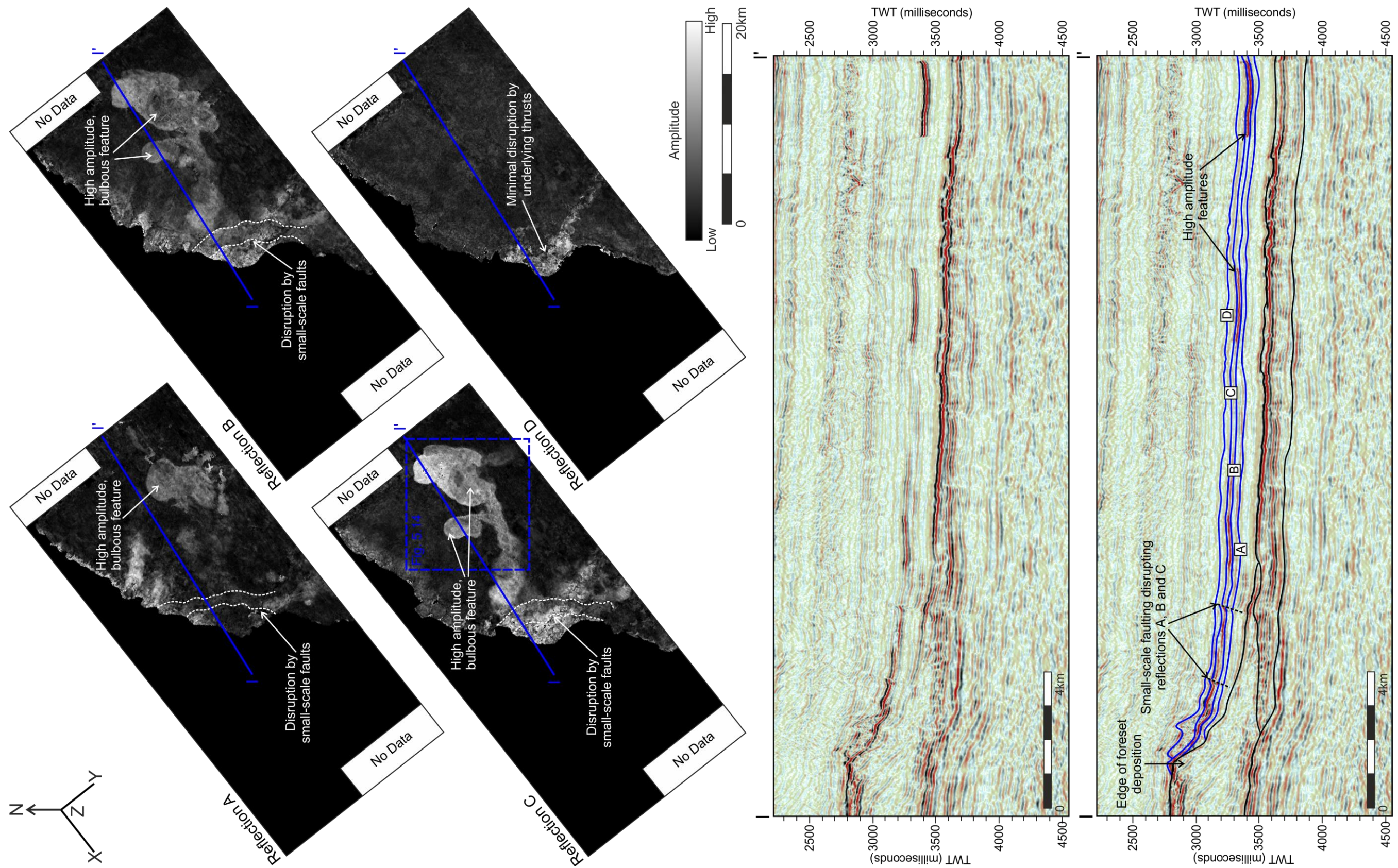
Fig. 5.13. RMS seismic amplitude maps and seismic section K-K' which images the internal reflections of the post-delta succession (see Fig. 5.3). Reflections A-D images a number of high amplitude, stacked and interconnected lobes with limited distributions that becomes increasingly apparent up through the succession. Location box refers to Fig. 5.14.
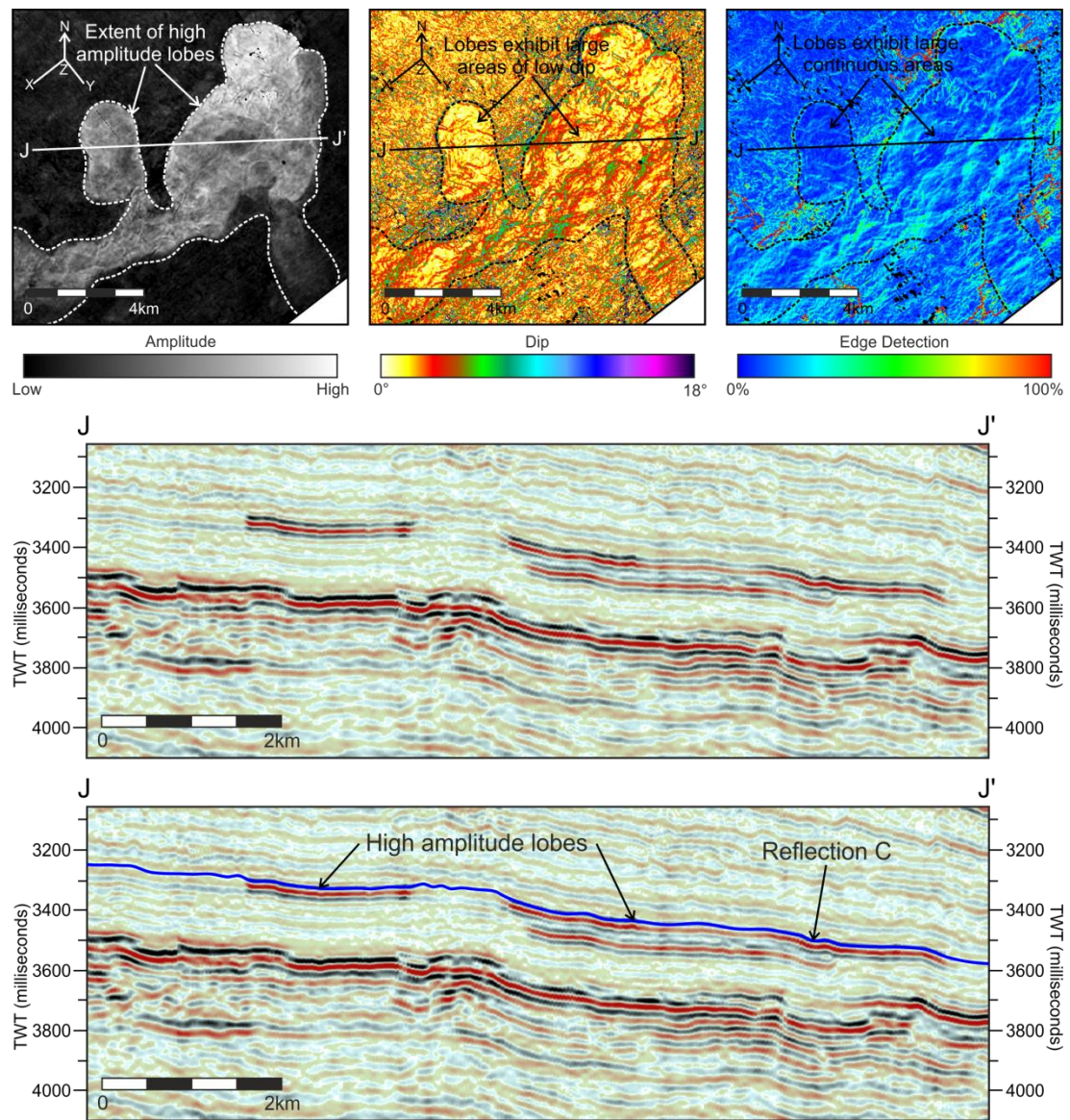
Fig. 5.14. Seismic section J-J' images reflection C of the post-delta succession and the extent of the high amplitude, stacked lobes. Seismic attribute maps including amplitude, dip and edge detection maps with a 5 millisecond window of the top of reflection C. The seismic amplitude map images the high amplitude, bulbous lobes that are contain within reflection C. The dip map reveals the lobes have low dips and are relatively continuous and smooth compared to the surrounding reflection background. The edge detection map shows the lobes are continuous, with few discontinuities. For location see Fig. 5.13.

5.6 Interpretations

5.6.1 Pre-Delta Succession

Early eruptive phases of the North Atlantic Igneous Province have been identified within the Faroe-Shetland Basin, often with subaerial volcanic eruptions that produced significant topographic structures (e.g. the Erlend Complex and Brendans Dome; Gatliff *et al.*, 1984; Ritchie & Hitchen, 1996; Naylor *et al.*, 1999; Jolley & Bell, 2002). These early volcanic rocks are interpreted to pre-date the construction of the lava-fed delta, and have been recognised beneath the main body of the delta as a succession of high amplitude, parallel to hummocky reflections (see Chapter 4). The upper ~400 m of this succession was penetrated by well 214/4-1, which is located ~65 km east of the delta and encountered pāhoehoe lava flows overlying hyaloclastic breccias (Davies *et al.*, 2002; 2004). This succession has been interpreted accordingly as interbedded lava flows and hyaloclastic breccias. The top reflection surface displays broad, terraced slabs with ropy morphologies (see Fig. 5.15) which have been interpreted as multiple thin pāhoehoe lava flows where the crust of the lava flow buckled due to deflation as gas is lost through cracks in the crust (Swanson, 1973; Guest *et al.*, 1984). The western edge of the succession is complicated by the overlying delta succession, where hyaloclastites are thought to downlap the succession (Fig. 5.15). The top of the unit is identified by a high amplitude reflection, with the lateral extent of the succession within the 3D survey has been taken to be where there is a seismic facies change.

5.6.2 Delta Succession

The eruption of significant volumes of lava as flood basalt volcanism became established in the northwest is recorded in the delta succession. The sub-horizontal, high amplitude topsets are interpreted as subaerial pāhoehoe lava flows which flowed southeast until they reached the palaeo-shoreline. At the shoreline the lava flows quenched into hyaloclastic breccias which are recorded in the prograding body of moderate amplitude, inclined foresets (Smythe, 1983; Smythe *et al.*, 1983; Ritchie *et al.*, 1999; Spitzer *et al.*, 2008). The offlap break marks this transition and is a proxy for the position of relative sea level during deposition. The lava flows feeding the delta front can be mapped back to the Faroese shelf and have been correlated with the Beinisvørð Formation, which outcrop in the Faroe Islands and consist of thick, coalesced lobes of pāhoehoe lava (Jerram & Widdowson, 2005; Passey & Bell, 2007).

Where the delta front is intact within the 3D survey, the lava flow topsets display broad, relatively smooth lobes, with each lobe interpreted as an area of hyaloclastite formation (Fig. 5.15). The branching depressions cross-cutting the lobes, and are identified by lower seismic amplitudes than the surrounding high amplitude lava flows. These could be intra-lobe lava-inflation clefts formed during differential rates of inflation and coalescing of pāhoehoe lava flow lobes (Walker, 1991; Anderson *et al*., 1999; Guilbaud *et al*., 2005; Umino *et al*., 2006), which were later infilled by eroded volcaniclastic material. Such features have been recognised in lava flows feeding a lava-fed delta system in the North Rockall Trough. Thomson (2005) identified gently dipping, flat topped lava flows with narrow valleys up ~100m wide between the flows. Alternatively, the depressions could be furrows formed by erosion, where the transport of material from the hinterland to the palaeo-shoreline exploited any minor topographic depression between inflating lobes.
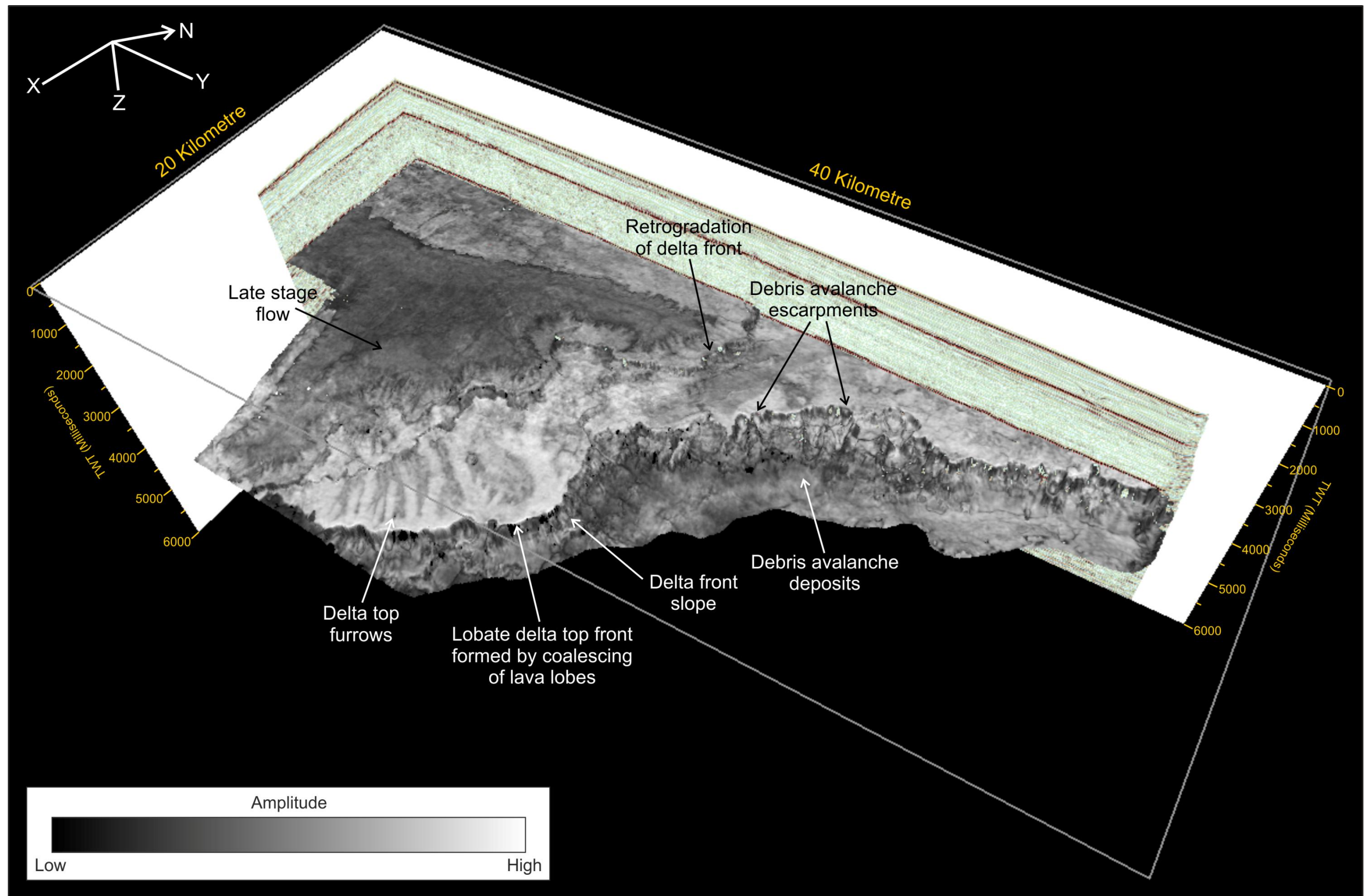
Fig. 5.15. Two-way time reflection surface with RMS amplitude overlay which images the top surface of the lava-fed delta (seismic reflection unit 11 and 12, and reflection X; see Fig. 5.3) and main morphological features. Scale varies due to perspective.

Where the delta front is disrupted by a series of arcuate, concave upwards features, the lava flow lobe structures are missing and have been interpreted to have been removed by erosive processes (Fig. 5.16). The arcuate features are interpreted as collapse escarpments which developed along the delta front during a prolonged hiatus or as lava supply decreased, leaving the delta front prone to erosion (Skilling, 2002; Sansone & Smith, 2006). A total of 8 collapse escarpments have been identified, with a number of escarpments composed of small-scale escarpments that merge into one downslope (escarpments 2, 3 and 5; see Fig. 5.16). The escarpments are interpreted to remobilise hyaloclastic material which produce deposits 250 – 530 m wide and 630 – 950 m high, which thin away from the delta front to form an irregular and hummocky surface (Fig. 5.16; see Appendix II for individual dimensions). The width of individual deposits is only a minimum estimate as there is probably a degree of overlap but this is below the resolution of the data set.
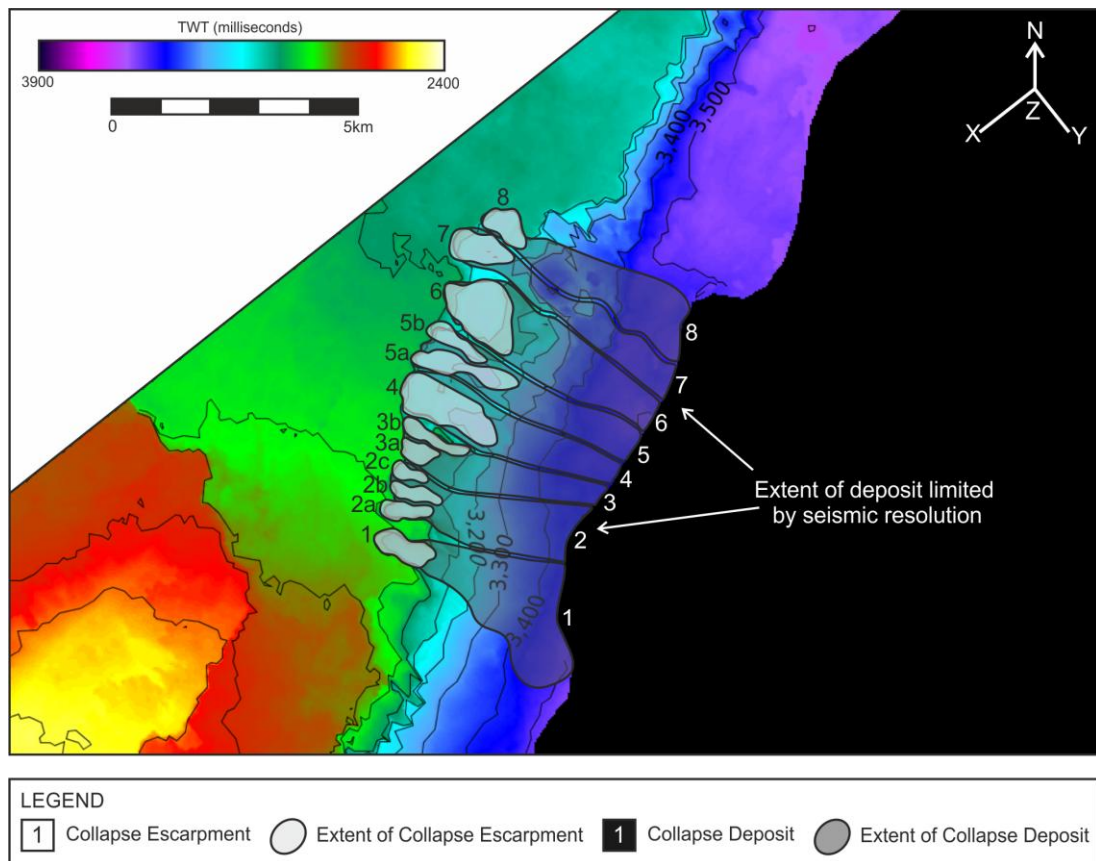
Fig. 5.16. Two-way time reflection surface contoured at 100 millisecond intervals with extents of debris avalanche escarpments and deposits.

Downlapping the top of the delta succession is a single, low amplitude, semi-continuous reflection with a distinct branching morphology (Fig. 5.15). Although understanding of the extent of this reflection is limited by the 3D survey area, the reflection has been identified

on a number of 2D seismic lines which extend back towards the Faroe Islands, suggesting they may have originated from a similar source to the rest of the delta succession. The reflection is interpreted as a late stage lava flow that meandered across the top of the delta system towards the palaeo-shoreline but did not reach the water's edge (Fig. 5.15). The distribution of this lava flow mimics that of the underlying seismic reflection unit 12 and may have erupted from a pre-existing feeder system that was active during deposition of unit 12. The low amplitudes and irregular, incised edges suggest the flow was left above sea level for a period of time, allowing subaerial erosion (Fig. 5.15).

5.6.3 Post-Delta Succession

Flood basalt volcanism continued after construction of the lava-fed delta ceased. In the 3D survey, this has been recognised in the post-delta succession that onlaps the delta front. The succession is stratigraphically contemporaneous with the regionally mapped Balder Formation (Ritchie *et al.*, 1999; Smallwood & Gill, 2002). The majority of the succession is composed of continuous, low to mid amplitude reflections that has been mapped across the basin using 2D seismic surveys and was correlated with the Balder Formation in well 214/4-1 (Davies *et al.*, 2004). The Balder Formation is composed of predominantly deep water siliciclastic rocks and volcanic tuffs which represent the final phase of volcanism in the Faroe-Shetland Basin (Underhill, 2001; Ellis *et al.*, 2002; Smallwood & Gill, 2002; Spitzer *et al.*, 2008). The high amplitude nature of the lobes may indicate that they are volcanic in origin, and they are interpreted to have been actively emplaced during Balder deposition. The extent of the post-delta succession becomes increasingly visible as the reflections onlap the delta front, which is consistent with the progressively northwest onlap of the Balder Formation on to the flood basalts (Smallwood, 2008).

5.7 Discussion

5.7.1 Lava Flow Morphologies

The lava-fed delta system of the Faroe-Shetland Escarpment has long been thought to be fed by pāhoehoe lava flows which reached a palaeo-shoreline and formed hyaloclastic breccias (Smythe *et al.*, 1983; Kiørboe, 1999; Spitzer *et al.*, 2008). Previous use of 2D seismic data has only revealed the extent of this Faroe-Shetland Escarpment and some of the internal stratigraphic relationships. The 3D seismic reflection data in this study has taken understanding of these systems further by providing access to detailed surface

morphologies and internal geometries of the lava-fed delta. The resulting RMS seismic reflection surfaces do not represent the true geological boundaries between volcanic and non-volcanic lithologies. The reflection is the product of acoustic impedance contrasts between multiple, interbedded or closely space lava flows and sedimentary beds (Barton *et al.*, 1997). Therefore, the seismic reflection surfaces are an approximation to the surface of the lava flows.

The majority of the topsets in the survey area produce lobate seismic reflection surfaces edges and are interpreted to have formed through the coalescing of inflating pāhoehoe lava flows (Hon *et al.*, 1994; Self et al., 1997; 1998; Umino *et al.*, 2006). Where the lava flows reached the palaeo-shoreline they produce a sinuous delta front, with each lobe an area of hyaloclastite formation (see Fig. 5.15). Lobate lava flow morphologies are typically formed through relatively high local flow rates, while branching morphologies as displayed by Seismic Reflection X are commonly formed through relatively low local flow rates (see Fig. 5.15; Swanson, 1973; Crown & Baloga, 1999; Duraiswami *et al.*, 2004; Mitchell *et al.*, 2008). The change in morphology of the lava flow indicates a change in the supply rate, most likely during a waning of an eruption, while the top of the delta system was still subaerially exposed. Variations in supply rate and resulting depositional extent can also occur due to migration of the vent or switching of the depositing lava tube or inflation lobe (Self *et al.*, 1997; Heliker *et al.*, 1998; Passey & Bell, 2007).

5.7.2 Collapse of the Delta Front

Interpretation of the 3D seismic data has revealed that the lava-fed delta underwent a least one period of catastrophic gravitational collapse during or shortly after active construction. Large scale gravitational collapses are known to be an integral part of the evolution of many volcanic structures and oceanic island volcanoes across the world (e.g. Hawaii, Lipman *et al.*, 1988; Smith *et al.*, 1999; Canary Islands, Urgeles *et al.*, 1999; Masson *et al.*, 2002; Reunion Islands, Oehler *et al.*, 2004; 2008). These collapse features commonly exhibit arcuate amphitheatre geometries and are thought to be closely linked with geological processes such as earthquakes, high sedimentation rates, shoreline oversteepening or submergence (Siebert, 1984; Moore *et al.*, 1994; Hampton *et al.*, 1996; Morgan *et al.*, 2003).

There are typically two types of gravitational collapse processes that can cause the destruction of a volcanic structure or edifice. The first are slumps, which can affect a

significant thickness of an edifice, creating arcuate escarpments that are wide relative to their length. Slumps are thought to be relatively slow-moving events, involving the creep of the slump deposit over an extended period of time. The deposits are relatively coherent masses of material that typically become deformed during slumping to produce scarps, folds and ridges on the upper surface of the deposit (Moore *et al.*, 1989; Masson *et al.*, 2002). In comparison, debris avalanches are more superficial, affecting the sedimentary cover or upper level of the volcanic edifice (Siebert, 1984; Moore *et al.*, 1994; Masson *et al.*, 2002). They are rapidly emplaced and can occur as a series of discrete events. Debris avalanches form narrow, arcuate escarpments and thick deposits, with large unsorted blocks close to the escarpment and hummocky terrain downslope. Debris avalanche deposits have steep marginal levees and are relatively elongate, with the downslope length greater than the width (Siebert, 1984; Lipman *et al.*, 1988; Masson *et al.*, 2002; Mitchell, *et al.*, 2002).

The collapse escarpments identified in this study have narrow (average of ~325 m), arcuate and concave up geometries which transect the lava flow topsets, disrupting the underlying hyaloclastite breccia foresets. The escarpments feed elongated deposits of remobilised hyaloclastic material that are chaotic and blocky when close to the escarpment and more irregular and hummocky when downslope. The damage zone created by the slope failure is relatively superficial, affecting the upper 300 m of the delta front and limited to the delta front. These escarpments have previously been interpreted to be large scale lava benches which developed syn- or post-deposition (see Chapter 4). Use of 3D seismic data has revealed the exact size and distribution of the escarpments and in resultant deposits, giving a greater understanding of the features and leading to the conclusion that they are sector collapses which produced multiple debris avalanches and occurred during sudden failure and rapid emplacement.

Multiple debris avalanche flows are often initiated by a single failure (Bugge *et al.*, 1987; Lipman *et al.*, 1988; Hampton *et al.*, 1996; Urgeles *et al.*, 1999). Each of the escarpments identified in this study is thought to represent a single episode of rapid failure during a prolonged hiatus or a decrease in the supply of lava (Moore *et al.*, 1989; Masson *et al.*, 2002; Sansone & Smith, 2006). The exact location of initial failure is impossible to detect, but it is likely that it propagated through the delta front and caused a domino effect with multiple failures. The volume of debris avalanche escarpments, such as identified offshore of the Canary Islands, can range from $50 - 500$ km^3 with the resulting debris avalanche

deposits able to extend up to 130 km and cover several thousand km^2 (Moore *et al.*, 1989; Carracedo *et al.*, 1999; Masson *et al.*, 2002). The volume of the escarpments identified in this study, and a likely indicator of the volume of the resulting deposits, varies from 0.004 – 0.039 km^3 (see Appendix II for individual dimensions). These are relatively small and are likely a function of the height of the escarpment as those previously mentioned offshore Canary Islands often have escarpment heights of >15 km (e.g. Carracedo *et al.*, 1999). The volumes of the deposits are much harder to assess because the deposits have a limited extent of 4.2 – 4.9 km, at which they thin below seismic resolution.

5.7.3 Post-Delta Remobilisation

The high amplitude, stacked and interconnected lobes within the post-delta succession of the Balder Formation have not been previously described. However horizons with anomalously high amplitude features have previously been identified within the Balder Formation and have been caused by small gas accumulations in the Lower Eocene Hildassay sandstone, situated just above the flood basalts in the east of the Faroe-Shetland Basin (Sørensen, 2003; Smallwood & Kirk, 2005). Despite this, it is unlikely that the high amplitude, interconnected lobes identified in the 3D survey contain gas, as there is no accumulation in the crest of the delta slope, migration of the lobes upslope or conformance to structure. There is also a lack of escape structures such as pockmarks and gas chimneys that would signify a viable fluid migration pathway (Sørensen, 2003; Smallwood & Kirk, 2005).

Alternatively, the stacked and interconnected lobes could be interpreted as intrusive features, which propagated up through the succession. The flow displays overlapping lobate protuberances and arcuate ridges similar to surface morphologies of a very shallow sill as identified by Trude (2004). These morphologies formed as a direct result of the propagation of viscous magma into soft, waterlogged sediments. However there is no evidence of a magmatic feeder system and the lobes do not display the typical climbing, saucer-shaped lobes documented in sill complexes of the Faroe-Shetland Basin (Hansen & Cartwright, 2006; Thomson & Hutton, 2004; Thomson & Schofield, 2008). The stacked and interconnected lobes are stratigraphically constrained and may be depositional in origin. The lobes appear to be sourced from the delta front via a 1.2 – 2.5 km wide, channel-like system and have very high amplitudes compared to the surrounding stratigraphy. Localized, gravity-driven high density slurries of volcaniclastic material have previously been identified in subaqueous to deep marine settings. These were deposited into, and on

top of, water saturated sediment, forming smooth to hummocky, lobate sheets of hyaloclastite with abrupt edges (Maicher *et al*., 2000; White, 2000). The high amplitudes and morphological similarities with the lobes identified in this study suggest that they are composed of volcaniclastic-rich sediment, most likely derived from the local erosion of the delta front and delta plain as it is the closest source of volcanic material and emplaced as high density slurries.

5.7.4 Comparison to Outcrop Analogues

The structures interpreted in this study are based on the identification of similar morphologies in seismic data to those recognised in outcrop and in the published literature. It is critical to ground truth seismic observations with outcrop analogues where possible, to identify which features are consistent across scale and highlight smaller scale structures which are below seismic resolution (Cartwright & Huuse, 2005; Davies & Posamentier, 2005; Posamentier *et al*., 2007). A number of lava-fed deltas have been recognised in outcrop, with similar geomorphological structures identified in Iceland, Greenland and in the Columbia River Flood Basalt Province (e.g. Porębski & Gradzinski, 1990; Skilling, 2002; Pedersen *et al*, 1997; Shervais *et al*., 2002). In Iceland, the Sølkatla lava-fed delta formed in a melt water lake when the Sølkatla volcano erupted adjacent to the Langjökull glacier (Piper, 1973; Sigurdsson, *et al*., 1978; Rossi, 1996). The eastern edge of the Sølkatla delta is formed of lobate lava flows 800 – 1400 m wide, although the delta front has been modified by subsequent erosion and may have originally been more extensive (Fig. 5.17).

Although the Sølkatla lava-fed delta formed in a glacial lake environment and the Faroe-Shetland Escarpment formed in a marine environment, the resulting lava-fed delta systems exhibit comparable features of similar scales to those interpreted in this 3D study. Both deltas display sinuous delta fronts constructed by lobate, kilometre-wide pāhoehoe lava flows (see Fig. 5.15). The debris avalanche escarpments recognised to affect the Faroe-Shetland Escarpment also displays remarkably similar geometries on a comparable scale to the arcuate collapse escarpments and the resulting hummocky, remobilised hyaloclastic deposits identified in the Sølkatla delta (see Fig. 5.15). The presence of comparable features suggests similar emplacement processes occurred in both settings, suggesting such features may not be constrained to continental flood basalt provinces.
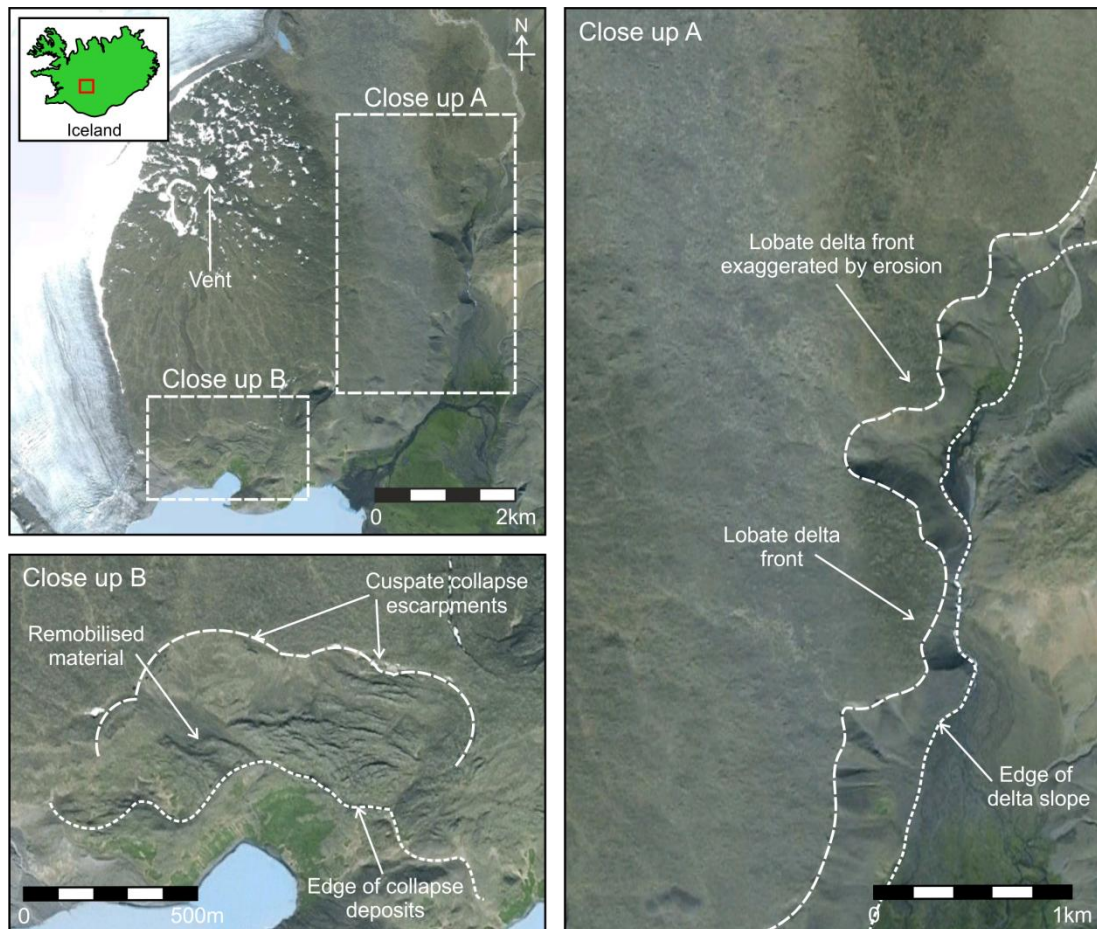
Fig. 5.17. The Sølkatla volcano is located at the eastern edge of the Langjökull glacier and erupted in to a melt water lake, forming a lava-fed delta. Close up A focuses on the lobate delta front geometries. Close up B focuses on the arcuate, concave up collapse escarpments which have affected the delta front.

5.8 Conclusions

Analysis of a 3D seismic reflection survey over the Faroe-Shetland Escarpment has revealed at least 3 phases of volcanic-related activity during the flood basalt eruptions of the North Atlantic Igneous Province. Initial volcanism within the survey area occurred as thin pāhoehoe lava flows and interbedded hyaloclastic breccias were erupted from a localised volcanic centre not imaged within the survey area and which constructed a topographic feature. This was followed by the eruption of significant volumes of lava is recorded in the deposition of the lava-fed delta succession, with active delta development fed from the west by the thick, kilometre-scale pāhoehoe lava flows. The delta system was constructed through many successive phases of active volcanism and records significant syn-volcanic

migration of the palaeo-shoreline. It is composed of at least 13 distinct seismic reflection units and stacking architecture records variations in lava supply, accommodation and relative sea level. The use of 3D seismic reflection data has indicated that the resulting bounding seismic reflection surfaces have a stratigraphic significance, recording the eruptive styles and erosional processes. Lava flow geometries vary significantly over a relatively small (800 km^2) area from lobate morphologies which are typically formed through relatively high local flow rates to branching morphologies which are commonly formed through relatively low local flow rates.

Erosional processes during or just after delta deposition caused the instability or oversteepening of the delta front. This produced gravity-driven debris avalanches that remobilise the hyaloclastic material and greatly modify the delta front. The final phase of volcanic-related activity occurred after lava-fed delta construction had ceased, with high density slurries of volcaniclastic material derived from the local erosion of the delta front deposited during the Balder Formation. The results of this study show that it is possible to map thick successions of volcanic rocks and builds on the methodology used to identify and map the lava-fed delta of the Faroe-Shetland Escarpment as shown in Chapter 4. In particular, the use of 3D seismic data has allowed the imaging of surface morphologies and internal structures that are consistent with subaerial outcrop exposures and are indicative of emplacement process. Detailed analysis of offshore flood basalts using 3D seismic data can provide important information about the evolution of the volcanic activity in frontier petroleum basins.

CHAPTER 6: AN EVALUATION OF THE VOLCANIC STRATIGRAPHY OF THE ROSEBANK FIELD, FAROE-SHETLAND BASIN

6.1 Introduction

Hydrocarbon exploration is becoming increasingly focused on sedimentary basins that contain significant volumes of volcanic rocks, including the North Atlantic, Western Australia, Brazil and China (e.g. Filho *et al.*, 2008; Cukur, *et al.*, 2010; Davison *et al.*, 2010; Zou *et al.*, 2010; Holford *et al.*, 2012). This has resulted in the acquisition of extensive 2D and 3D seismic surveys in an attempt to better constrain the underlying structure and associated hydrocarbon accumulations. Such datasets offer a unique opportunity to study large-scale, buried volcanic structures that are not necessarily accessible at the surface due to limited 3D exposure or outcrop erosion (Archer *et al.*, 2005; Cartwright & Huuse, 2005; Davies & Posamentier, 2005; Posamentier *et al.*, 2007). However seismic imaging and interpretation can be greatly complicated by the internal structure and lithological heterogeneity of volcanic deposits (e.g. Planke *et al.*, 2000; Nelson *et al.*, 2009a), resulting in less established stratigraphic and facies models for volcanic and volcaniclastic-siliciclastic systems than for siliciclastic and carbonate systems.

During the opening of the North Atlantic, significant volumes of continental flood basalts were erupted into the Faroe-Shetland Basin, emplacing thick successions of lava into subaerial to submarine environments (White, 1989; Lamer *et al.*, 1999; Ellis *et al.*, 2002). During the eruption and emplacement of continental flood basalts, the deposition of indigenous sedimentary systems stopped or was diverted, with deposition resuming during periods of volcanic quiescence (Naylor *et al.*, 1999; Jolley & Bell, 2002). In marginal environments at the distal edges of the flood basalts, the emplacement of lava was in direct competition with the sedimentary systems and produced complex, multi-facies successions. These preserved volcanic-sedimentary deposits provide important information about the evolution of the palaeo-environment (Naylor *et al.*, 1999; Jolley & Bell, 2002; Brown *et al.*, 2009).

Hydrocarbon exploration in the Faroe-Shetland Basin has been largely confined beyond the south-easterly extent of the flood basalts, where seismic imaging is not hampered by thick successions of volcanic rocks (Lamers *et al.*, 1999; Sørensen, 2003; Loizou *et al.*, 2006). The

increased understanding of the relationship between volcanic and siliciclastic systems has identified a number of potential plays within the distal reaches of the flood basalt succession, where hydrocarbon traps have formed through a combination of stratigraphic pinch-outs and structural dip closures (Jowitt *et al*., 1999; Naylor *et al*., 1999; Rohrman, 2007). These include the Rosebank field, which was discovered in 2004 during drilling of a four-way inversion structure below the flood basalts. The oil and gas reservoirs in the Rosebank field are composed of intra-basalt siliciclastic fluvial and shallow marine deposits (Naylor *et al*., 1999; Scotchman *et al*., 2006; Nelson *et al*., 2009a; Larsen *et al*., 2010).

This study uses an extensive 3D seismic reflection survey located over the distal edge of the flood basalts to investigate the emplacement of volcanic rocks in a marginal environment, where the transient eruptive system was in competition with the indigenous depositional system. Several exploration wells have penetrated the entire thickness of the volcanic succession in this area, providing detailed information on the volcanic horizons and helping to constrain regional seismic interpretations. This is vital because the morphology of subaerial lava flows can vary over relatively small areas and can be difficult to correlate (Soule *et al.,* 2005; Thomson, 2005). An understanding of the interplay between volcanism and sedimentation can help constrain the spatial and temporal distribution of volcanic facies and help reconstruct the depositional environment. This may prove to be a valuable resource in hydrocarbon exploration in volcanic rifted settings, with implications for potential reservoir deposits (Naylor *et al*., 1999; Cartwright & Huuse, 2005; Thomson, 2005; Zhang *et al*., 2011).

6.2 Geological Setting

The Faroe-Shetland Basin was formed by multiple phases of rifting and subsequent continental break up between Greenland and Eurasia throughout the Mesozoic to early Cenozoic (Stoker *et al*., 1993; Boldreel & Andersen, 1994; England *et al*., 2005). Continental breakup produced the volcanism of the North Atlantic Igneous Province, which was characterised by the extensive subaerial basaltic lavas (e.g. Passey & Bell, 2007), the intrusion of sills (e.g. Thomson & Schofield, 2008; Hansen *et al*., 2011) and the formation of several volcanic centres (e.g. Gatliff *et al*., 1984; Ritchie & Hitchen, 1996). Volcanism ceased when sea floor spreading became established to the north of the basin and was followed by post-rift thermal subsidence (Nadin *et al.,* 1997; Dean *et al*., 1999; Smallwood *et al*.,

2004). Although parts of the basin became uplifted during the late Palaeocene, increased subsidence followed in the Eocene, with Neogene compression creating the tilted and folded structures identified today (Ritchie *et al*., 2003; Sørensen, 2003; Davies *et al*., 2004; Praeg *et al*., 2005).

Flood basalt volcanism is interpreted to be sourced from fissures located close to what is now the Faroese platform (Dore *et al*., 1999; Naylor *et al*., 1999). The subaerial flood basalt lava flows extended far into the Faroe-Shetland Basin, thinning in the centre of the basin over the Corona Ridge which has been interpreted as a basement fault block (Dean *et al.* 1999; Naylor *et al.* 1999). The Corona Ridge was probably an active structural high at the time of deposition, with coarse clastic sediment sourced from the southeast and deposited into a series of sag and fault controlled sub-basins and onlapping the ridge (Jowitt *et al*., 1999; Lamers *et al*., 1999; Naylor *et al*., 1999; Sørensen, 2003). Periodic emplacement of lava flows resulted in an interbedded succession of volcanic and siliciclastic rocks (Larsen *et al*., 1999; Naylor *et al*., 1999; Davies *et al*., 2002; Jolley & Morton, 2007).

6.3 Data and Methodology

Seismic interpretation has focused on a 50 x 60 km section of the 3D PGS MegaSurvey located over the distal edge of the flood basalt succession in the middle of the Faroe-Shetland Basin (Fig. 6.1). The 3D survey images the flood basalt succession at an average vertical resolution of ~30 m and an average horizontal resolution between 40 – 60 m, with velocities of 5000 – 7000 ms^{-1}. The top surface of the flood basalts is identified by a positive, high amplitude and strongly continuous reflection which defines the upper limit of a succession of high to moderate amplitude, subhorizontal and continuous reflections. Many of these reflections have been mapped extending from the Faroes shelf into the centre of the basin where they thin and disappear. The strong reflectivity of the top surface and the internal heterogeneity within the volcanic succession presents a challenge for seismic imaging, particularly identifying and understanding the intra- and sub-basalt siliciclastic depositional successions.
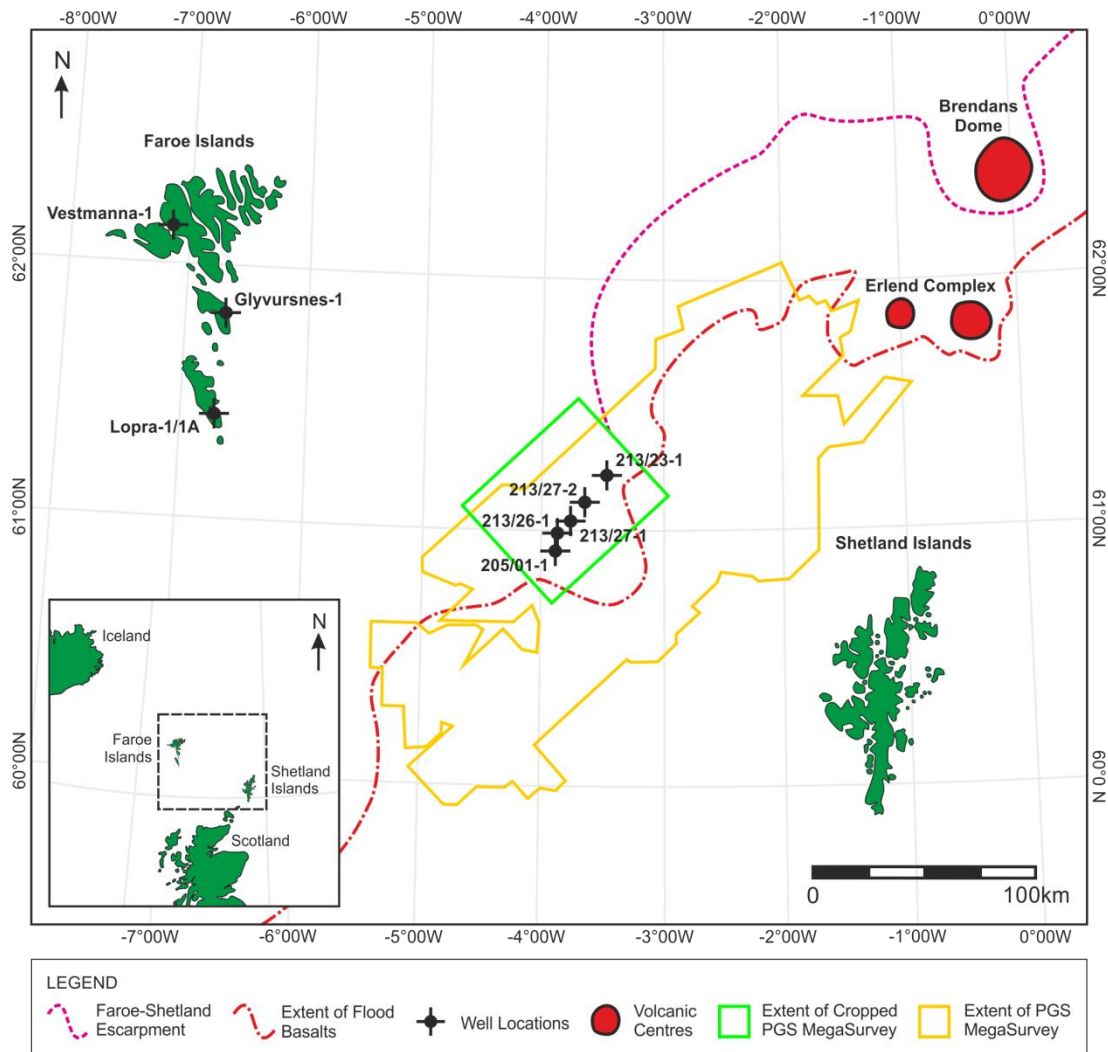
Fig. 6.1. Map of Faroe-Shetland Basin showing the study area, extent of the 3D seismic survey and distribution of wells. Extent of flood basalts and Faroe-Shetland Escarpment modified from Ritchie *et al.* (1996, 1999), Ellis *et al.* (2002) and Sørensen (2003).

Well control within the Faroe-Shetland Basin is limited, with the majority of wells in the southeast of the basin, past the flood basalts and where the hydrocarbon-rich sedimentary sequences have been discovered. The proximal flood basalts are penetrated by three boreholes on the Faroe Islands, where the flood basalts have a stratigraphic thickness of at least ~6.6 km and have been subdivided on the basis of lithology, geochemistry and flow structure (see Chapter 2, Fig. 2.3; Ellis *et al*., 2002; Passey & Bell, 2007; Passey & Jolley, 2009). The distal extent of the flood basalts has been penetrated by a number of exploration wells, towards the centre and southeast of the basin where hydrocarbon-rich sedimentary rocks have been discovered (see Chapter 2, Fig. 2.10; Lamers & Carmichael, 1999; Davies *et al*., 2004; Smallwood *et al*., 2004; 2005).

In the survey area, the distal flood basalts have been penetrated by several wells which were drilled to investigate the hydrocarbon potential of a four-way inversion structure (Fig. 6.2). The wells extend into and beneath the basalts and encountered inter-bedded volcanic and siliciclastic rocks (Fig. 6.3; Larsen *et al.*, 1999; Davies *et al.*, 2002; Jolley & Morton, 2007). The siliciclastic rocks within the Faroe-Shetland Basin are the subject of much debate and have been well documented (e.g. Jolley & Morton, 2007; Mansurbeg *et al.*, 2008). Therefore the focus of this study is the volcanic rocks and their interaction with the developing depositional environment. Seismic stratigraphic division of the volcanic succession into a series of units is based on the recognition of relatively conformable reflections and the identification of systematic discordances or reflection terminations (Mitchum *et al.*, 1977a; Van Wagoner *et al.*, 1988). Interpretation of the volcanic succession is primarily through analysis of the seismic reflection geometries. Additional use of wireline interpretation and seismic facies analysis with characterisation in terms of amplitude, continuity and configuration are used to define the gross stratigraphic architecture of the volcanic deposits (Mitchum *et al.*, 1977b; Sangree & Widmier, 1977; Cross & Lessenger, 1988).
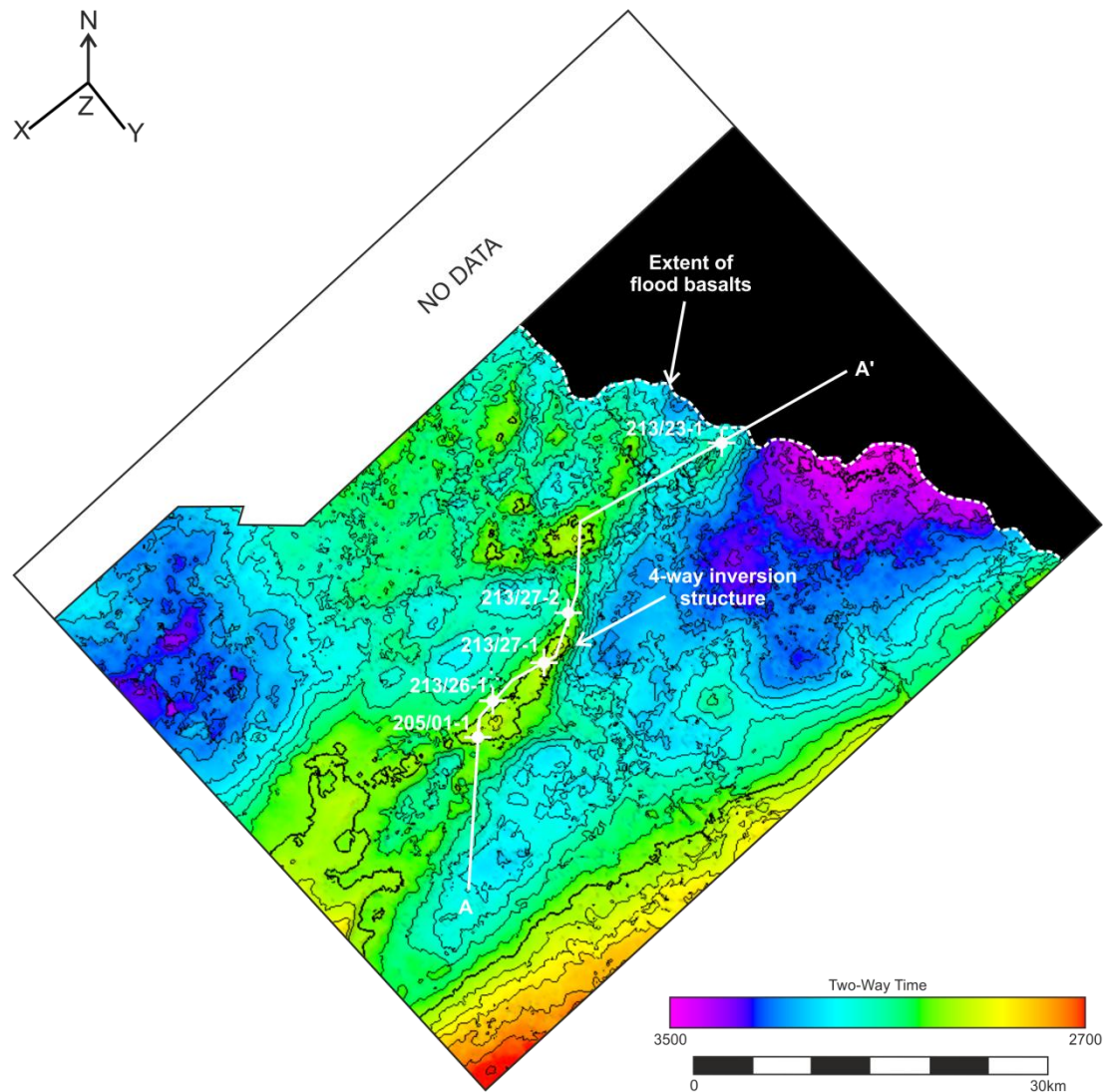
Fig. 6.2. TWT surface and extent of top flood basalts, contoured at 50 millisecond intervals. Location of exploration wells penetrating the Rosebank structure and cross section A-A'.

6.4 Exploration Wells

6.4.1 Wireline Interpretation

This study has used five exploration wells which penetrated the volcanic rocks in and around the Rosebank field (see Fig. 6.2). Although multiple logging tools were deployed in each well, this study has focused on the resistivity, velocity, bulk density, gamma-ray and porosity logs as they are of greatest use in distinguishing volcanic and non-volcanic rocks. Pāhoehoe lava flows typically exhibit a three-part internal structure, consisting of a thin, lower flow base, a thick, dense flow core and a thick, vesicular and fractured upper flow

crust (see Chapter 3, Fig. 3.19; Self *et al.*, 1997; 1998; Nelson *et al.*, 2009b). This produces an asymmetrical, cyclic pattern which is observed across the log signatures and relates directly to the vertical variations in vesicle and fracture distribution, geochemistry and crystalline structure (see Chapter 3, Fig. 3.20; Planke, 1994; Planke *et al.*, 2000; Boldreel, 2006).

Analysis of wireline data is based on the evaluation of all the individual log responses together and has identified at least four volcanic successions. Each succession contains one or more lava flows which are typically identified by low neutron porosity and gamma-ray log values, moderate bulk density log values and high resistivity and velocity log values. Variations in log signature can occur at the crystalline base and vesicular and fracture crust of the lava flows (see Chapter 3, Fig. 3.20; Planke, 1994; Planke *et al.*, 2000; Boldreel, 2006). The volcanic successions often contain and are separated by sedimentary interbeds which typically have higher neutron porosity and gamma-ray log values and low to moderate bulk density, resistivity and velocity log values compared to the volcanic lithologies. The volcanic successions have been numbered in stratigraphic order, with 1 being the oldest and 4 being the youngest (Fig. 6.3; see Appendix III for additional wells).

Volcanic succession 1 is stratigraphically the oldest unit identified and varies from 10 – 40 m thick. It is composed of a volcaniclastic bed between 10 – 40 m thick which is often capped by a thin lava flow ~15 m thick. The succession is separated from the overlying volcanic succession 2 by a series of sedimentary beds with a gross thickness of 7 – 70 m. Volcanic succession 2 is 15 – 90 m thick and is composed of 2 – 6 separate lava flows between 8 – 35 m thick, with sedimentary interbeds 5 – 20 m thick. The succession is overlain by a thin series of sedimentary beds 10 – 45 m thick. Volcanic succession 3 is 35 – 95 m thick and is composed of 3 – 6 separate lava flows that vary from 5 – 20 m thick, with few sedimentary interbeds 3 – 15 m thick. Volcanic succession 3 is overlain by a succession of sedimentary beds 20 – 75 m. Volcanic succession 4 is 25 – 255 m thick and is composed of between 4 and 11 separate lava flows that vary from 5 – 55 m thick and sedimentary interbeds 5 – 15 m thick.
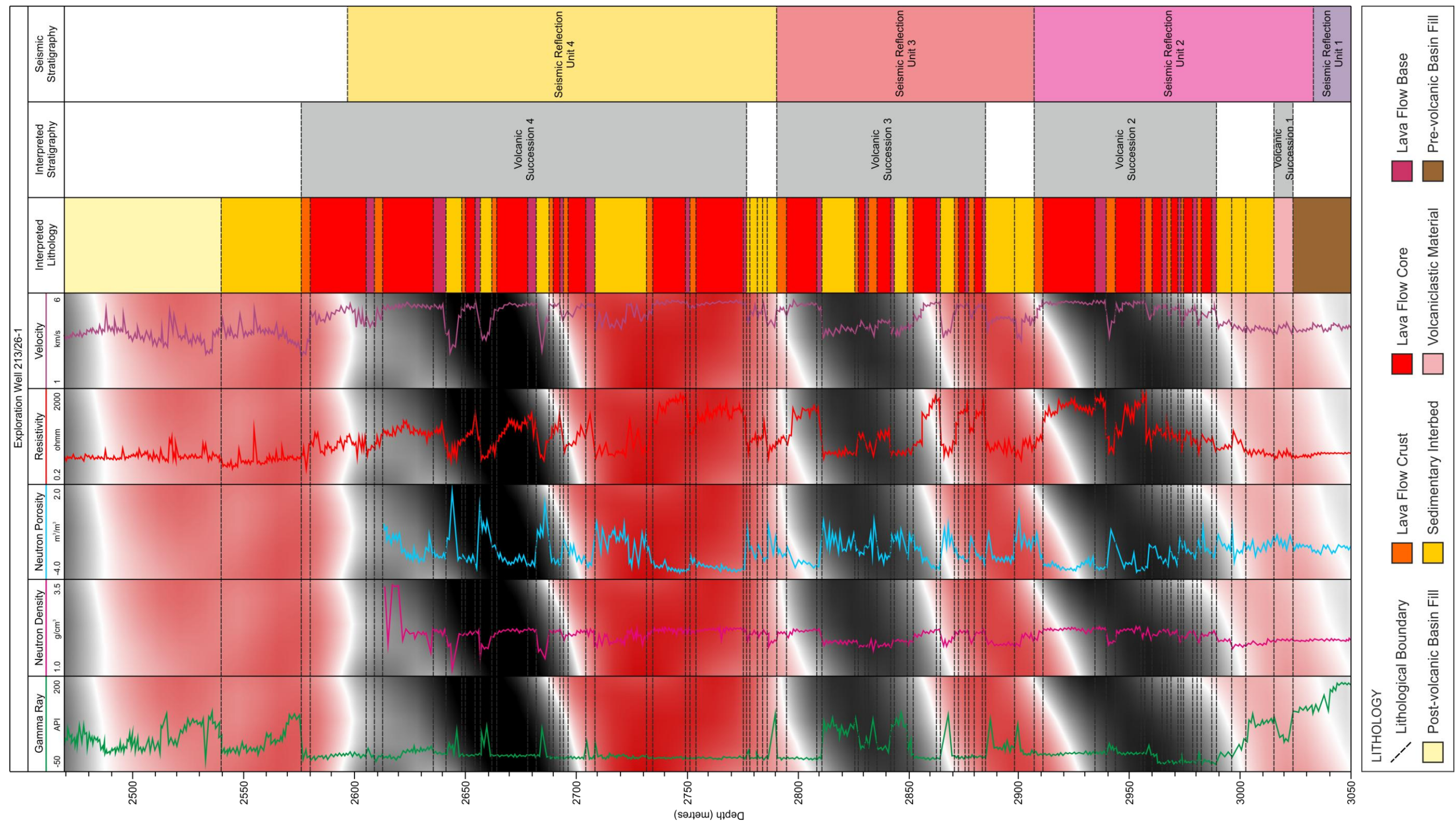
Fig. 6.3. Exploration well 213/26-1 with the wireline log data displayed on the seismic reflection data coincident with the well path. Interpretation of lithology is based on the identification of individual lava flows, volcaniclastic and sedimentary beds by analysis the suite of wireline log responses (see Chapter 3, Fig. 20). Interpretation of volcanic stratigraphy is based on the gross interpreted lithology. Interpretation of seismic stratigraphy is based on the correlation of the interpreted lithology and volcanic stratigraphy with the seismic data. See Fig. 6.2 for location.

6.4.2 Well to Seismic Correlation

The correlation of wireline to seismic data is typically through the creation of synthetic seismograms (see White & Simm, 2003). A synthetic seismogram is a one dimensional model of the predicted seismic reflectivity and is produced by convolving the velocity and density logs with a wavelet derived from the seismic data (see Chapter 3, Fig. 3.18; Sheriff & Geldart, 1995; Bacon *et al.*, 2007; Ashcroft, 2011). In this study, the synthetic seismograms created proved to be poor, with little correlation between the predicted and real seismic reflectivity (see Appendix III for synthetic seismograms). This discrepancy is interpreted to be due to the use of a high resolution wavelet derived from defined from the seismic reflection data above the volcanic succession. This wavelet has not been affected by a loss of energy through the scattering and attenuation of the seismic wave by the interbedded volcanic and sedimentary successions (Ogilvie *et al.*, 2001; Shaw *et al.* 2008; Nelson *et al.*, 2009a). This led to the creation of a synthetic seismogram with a higher resolution than that of the seismic reflection data, and therefore the creation of mis-ties between the predicted and real seismic reflectivity (Maresh & White, 2005; Maresh *et al.*, 2006).

Despite this, the exploration wells have provided a robust control on seismic interpretation. Comparison of wireline data with the real seismic reflection data aided in the identification of the seismic reflections that appear to be directly related to the volcanic stratigraphy. The resolution of the wireline data is greater than that of the seismic reflection data, with multiple lava flows identified in wireline logs forming one seismic reflection (Fig. 6.3). The seismic reflectivity within the volcanic succession is the product of a complex interference pattern generated by the acoustic impedance contrasts between multiple, interbedded lava flows and sedimentary beds and the closely spaced lava flows (Barton *et al.*, 1997). Comparison between the well and seismic data has confirmed the presence of 4 volcanic successions that are seismically resolvable and that have been mapped, extending away from the wells used in this study (Fig. 6.4).
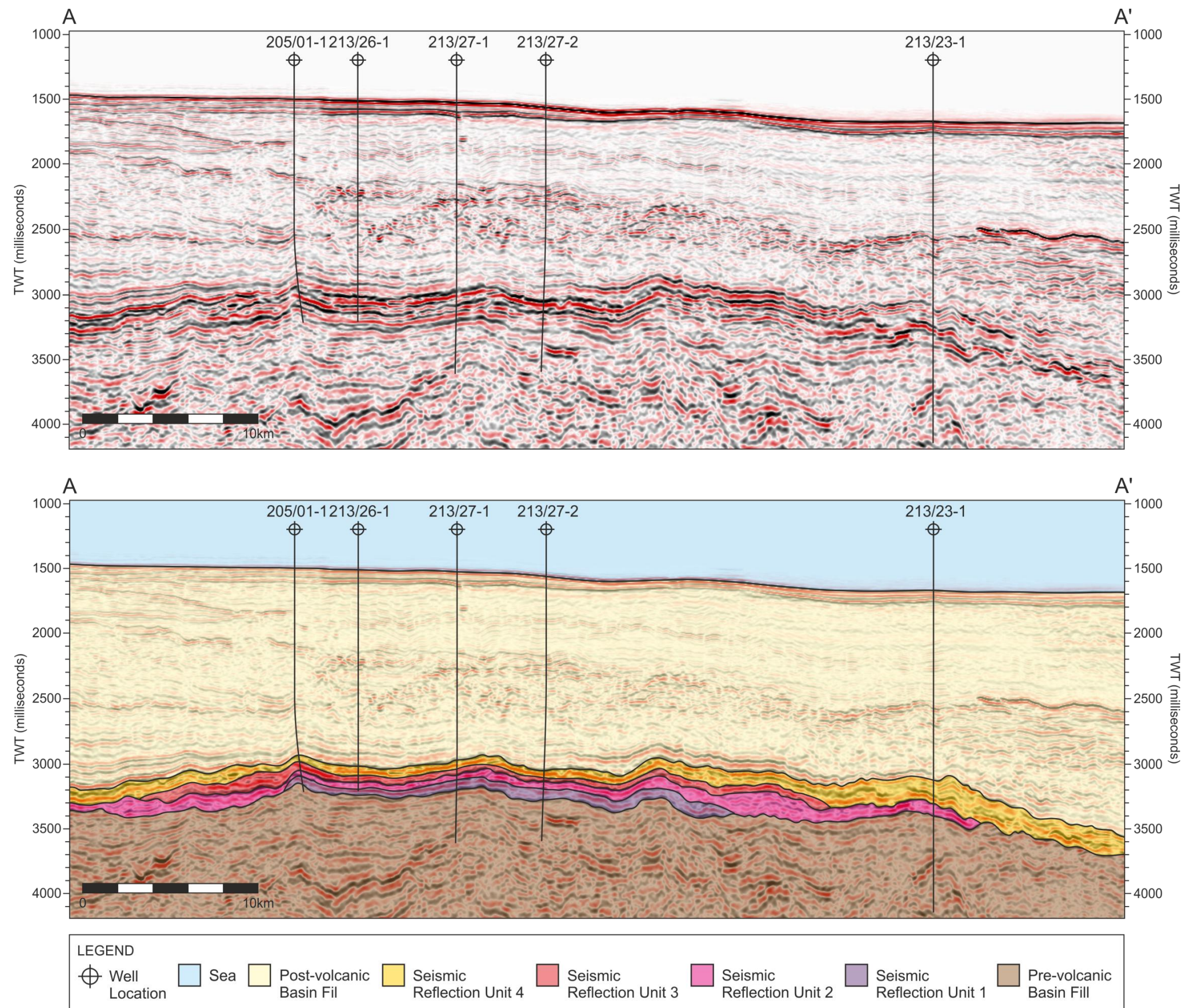
Fig. 6.4. Seismic section A-A' through the exploration wells and Rosebank structure. Interpreted section includes the extent of seismic reflection units as identified on both seismic data and wireline log data. For location of exploration wells and cross section see Fig. 6.2.

6.5 Seismic Observations

6.5.1 Seismic Reflection Unit 1

The first volcanic succession identified in the wells correlate to localised and semi-continuous, moderate to low amplitude reflections in the seismic data (Fig. 6.3). RMS amplitude extraction maps across the top of the reflection unit reveal a reflection surface that consists of broad, hummocky areas of moderate to low amplitudes with an irregular, lobate extent (Fig. 6.5). The unit has a limited distribution, with southeast extent of the unit coincident with, and onlapping the underlying four-way basement inversion structure that the exploration wells were drilled to investigate, while the northwest extent of the unit thins below seismic resolution (Fig. 6.6).
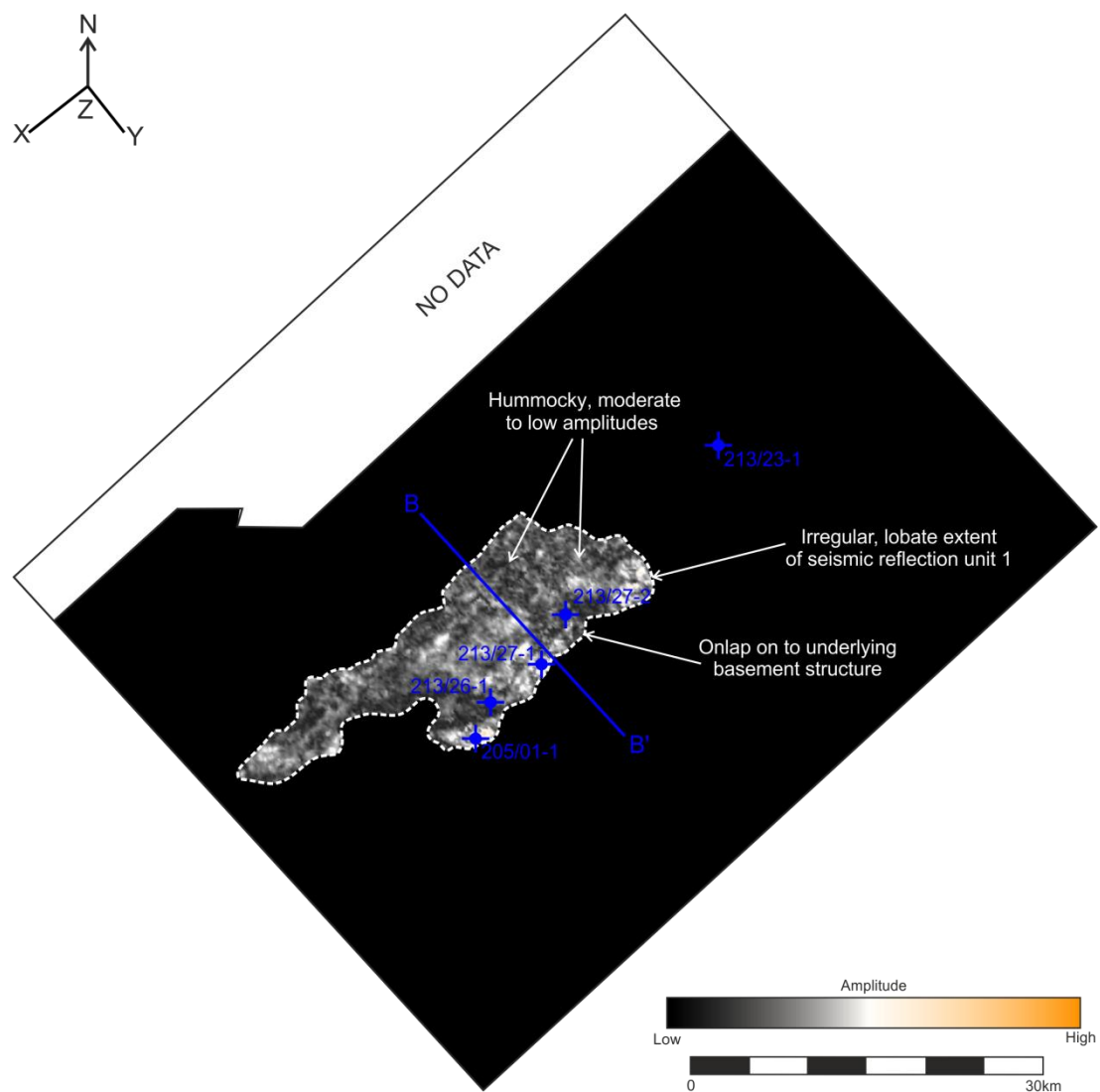
Fig. 6.5. RMS amplitude extraction map with a 5 millisecond window over the top of seismic reflection unit 1. The map images the irregular, lobate extent of unit and hummocky nature of reflection surface. Cross section B-B' corresponds to Fig. 6.6.
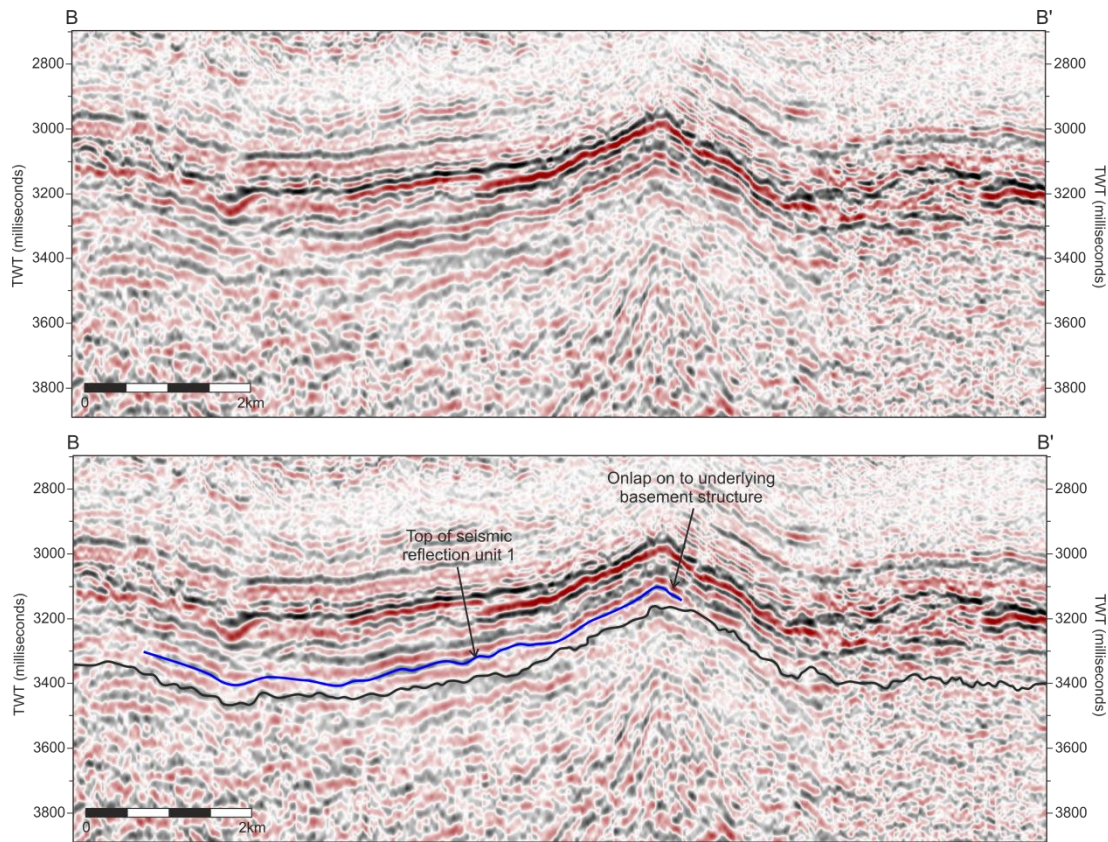
Fig. 6.6. Seismic section B-B' which images the extent of seismic reflection unit 1 and downlapping relationship of the unit with the underlying structure. For location of cross section see Fig. 6.5.

6.5.2 Seismic Reflection Unit 2

The second volcanic succession recognised across all of the wells is represented by regional, laterally extensive, high amplitude and continuous reflections in the seismic data (Fig. 6.3). RMS amplitude extraction maps across the top of the unit reveal a reflection surface that consists of large coherent areas of high amplitude surrounded by hummocky areas of moderate to low amplitudes (Fig. 6.7). The unit has an irregular, lobate extent (Fig. 6.7). Cross-cutting the surface is a series of sinuous, low amplitude features are orientated largely northeast to southwest and appear to run largely parallel with the edges of coherent and continuous high amplitudes areas (Fig. 6.8). In cross section they are 200 – 350 m wide, subtle and low amplitude depressions (Fig. 6.8).
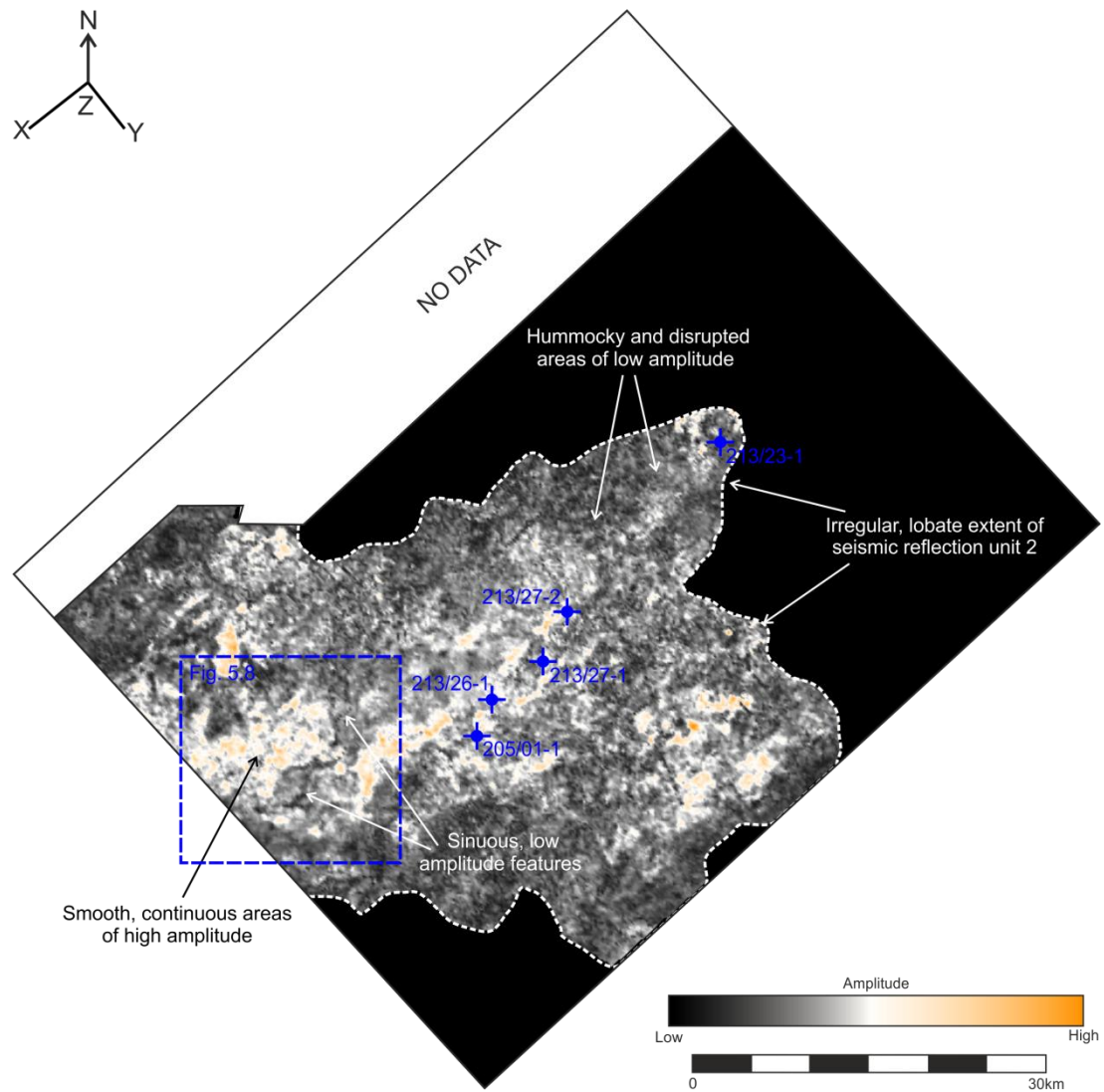
Fig. 6.7. RMS amplitude extraction map with a 5 millisecond window over the top of seismic reflection unit 2 (see Fig. 6.4). The map images the irregular, lobate extent of unit, variations in the reflection surface and the sinuous, low amplitude features. Location box refers to Fig. 6.8.
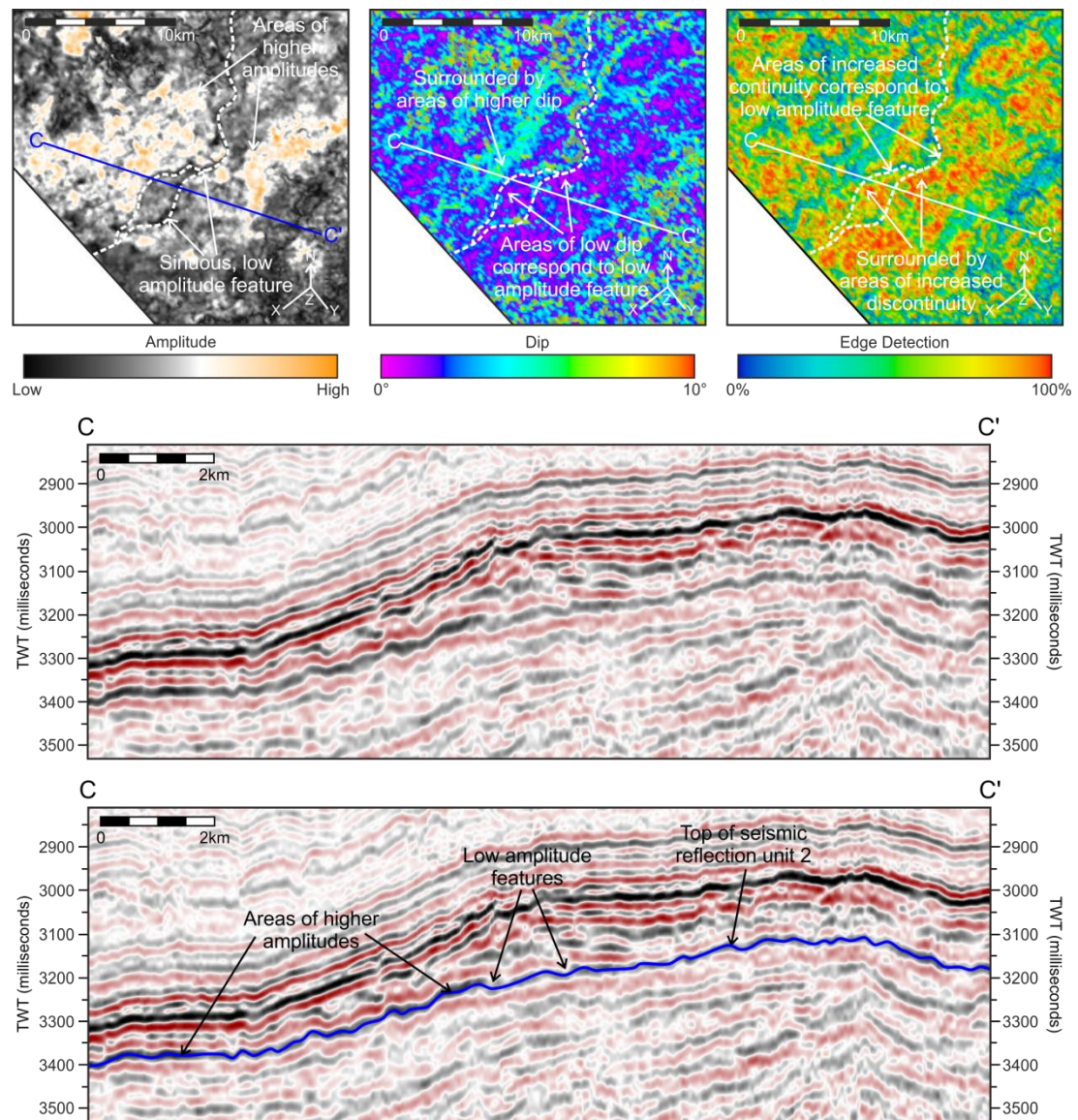
Fig. 6.8. Seismic section C-C' images the top of seismic reflection unit 2 and the location of subtle, low amplitude troughs which correspond with the sinuous features identified on the seismic attribute maps. Seismic attribute maps including RMS amplitude, dip and edge detection maps with a 5 millisecond window of the top of seismic reflection unit 2. The amplitude extraction map reveals the sinuous feature exhibits low amplitudes and runs parallel to two areas of higher amplitudes. The dip map shows a decrease in dip that corresponds to the low amplitude feature. The edge detection map indicates that the sinuous feature is located in an area of low discontinuity surrounded by areas of much higher discontinuity. For location see Fig. 6.7.

6.5.3 Seismic Reflection Unit 3

The third volcanic succession that has been identified in the wells corresponds to semi-regional and semi-continuous, high to moderate amplitude reflections in the seismic data (Fig. 6.3). RMS amplitude extraction maps across the top of the unit reveal a reflection surface that consists of patchy, hummocky areas of moderate to low amplitudes interspersed with small areas of higher amplitudes (Fig 6.9). The unit has a very irregular, lobate extent with many protuberances along its edge (Fig 6.9). The surface is cross-cut by sinuous, low amplitude features orientated largely northeast to southwest. In cross section the features are subtle, low amplitude depressions 300 – 500 m wide (Fig. 6.10).
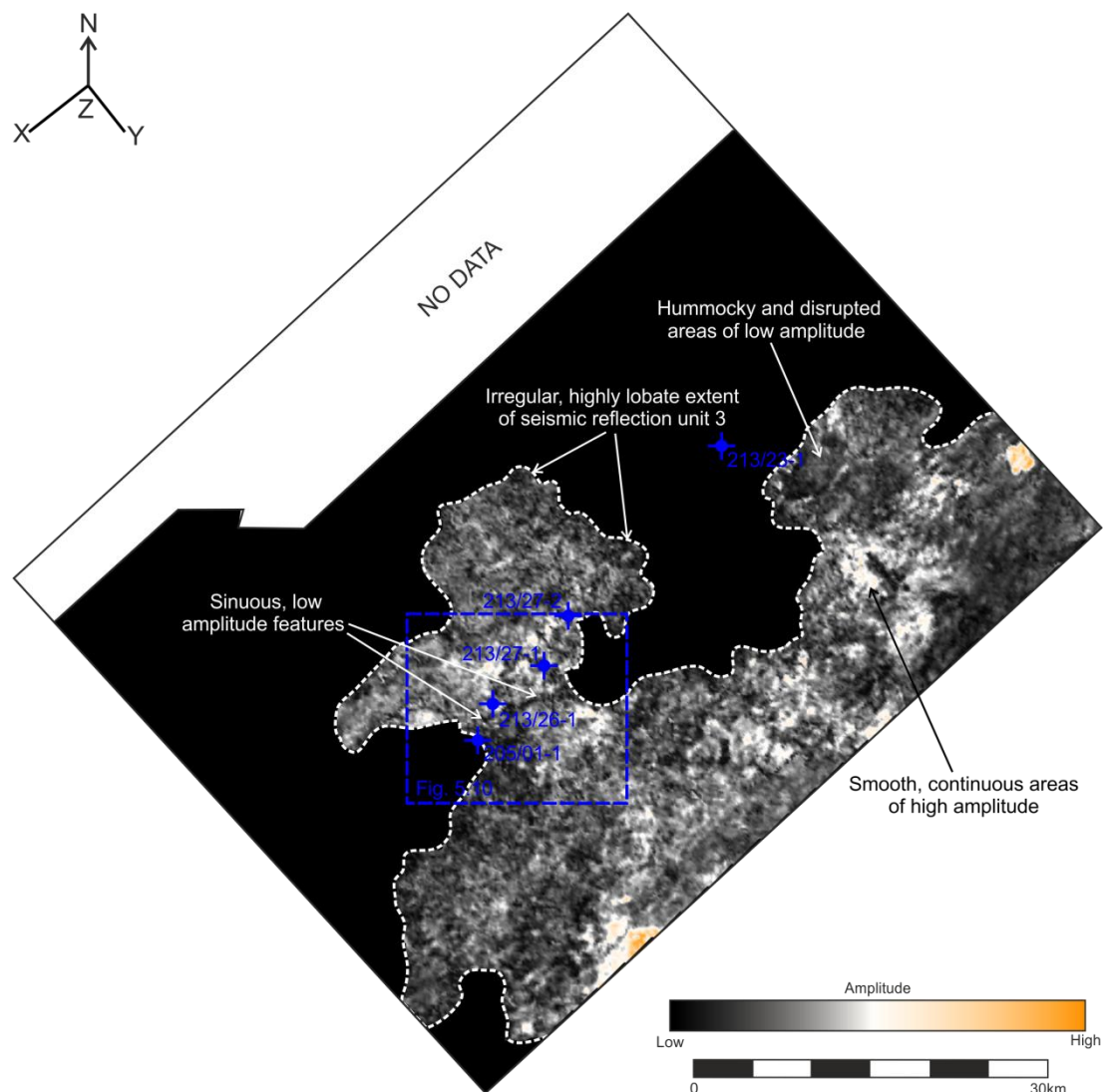
Fig. 6.9. RMS amplitude extraction map with a 5 millisecond window over the top of seismic reflection unit 3 (see Fig. 6.4). The map images the highly irregular, lobate extent of unit, variations in reflection surface and location of the sinuous, low amplitude feature. Location box refers to Fig. 6.10.
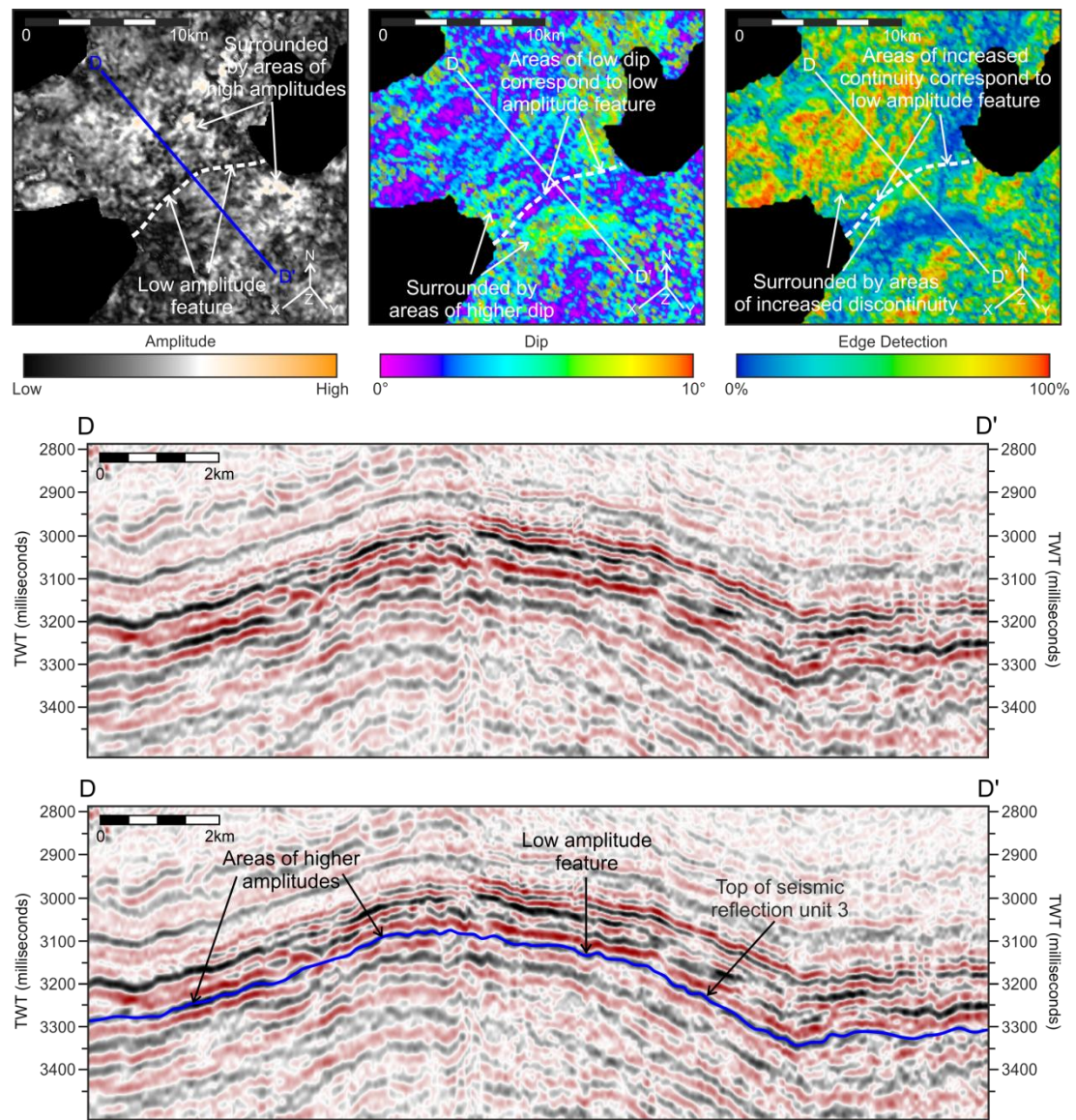
Fig. 6.10. Seismic section D-D' images the top of seismic reflection unit 3 and the location of a subtle, low amplitude trough which correspond with the sinuous features identified on the seismic attribute maps. Seismic attribute maps including RMS amplitude, dip and edge detection maps with a 5 millisecond window of the top of seismic reflection unit 3. The amplitude extraction map reveals that a sinuous low amplitude feature. The dip map shows that the sinuous feature corresponds to an area of very low dip. The edge detection map indicates that the sinuous feature is located in an area of low discontinuity surrounded by areas of much higher discontinuity. For location see Fig. 6.9.

6.5.4 Seismic Reflection Unit 4

The final volcanic succession recognised in the wells is represented by regional, laterally extensive and continuous, high to moderate amplitude reflections in the seismic data (Fig. 6.11). RMS amplitude extraction maps across the top of the unit reveal a reflection surface that consists of very large coherent areas of high amplitude surrounded by hummocky areas of moderate amplitudes (Fig. 6.11). The unit has an irregular, lobate extent, with a gradual decrease in amplitude across the survey in an eastward direction, with the reflection becoming increasingly hummocky in nature (Fig. 11). The reflection surface is cut by sinuous, low amplitude feature that is orientated largely northeast to southwest and runs between two areas of high amplitudes (Fig. 6.12). In cross section, this feature is a low amplitude depression 500 – 750 m wide (Fig. 6.12).

The reflection surface is also disrupted by two low amplitude and circular structures at the edges of areas of high amplitude (Fig. 11). The structures are composed of sloping circular to sub-circular mounds with a basal diameter of ~1500 m, a central circular depression of ~1000 m wide and a relief of between 100 – 200 m high (see Fig. 6.13 and 6.14). Analysis of the seismic data has revealed that seismic reflection 4 is downlapped by a continuous, very high amplitude reflection in the northwest of the survey area (see Reflection X, Fig. 6.15). The reflection has a limited extent and has not been penetrated by any of the wells used in this study. RMS amplitude extraction maps across the top of the unit reveal a reflection surface that consists of coherent areas of very high amplitude surrounded by hummocky areas of moderate amplitudes, with an irregular, lobate edge (Fig. 6.11).
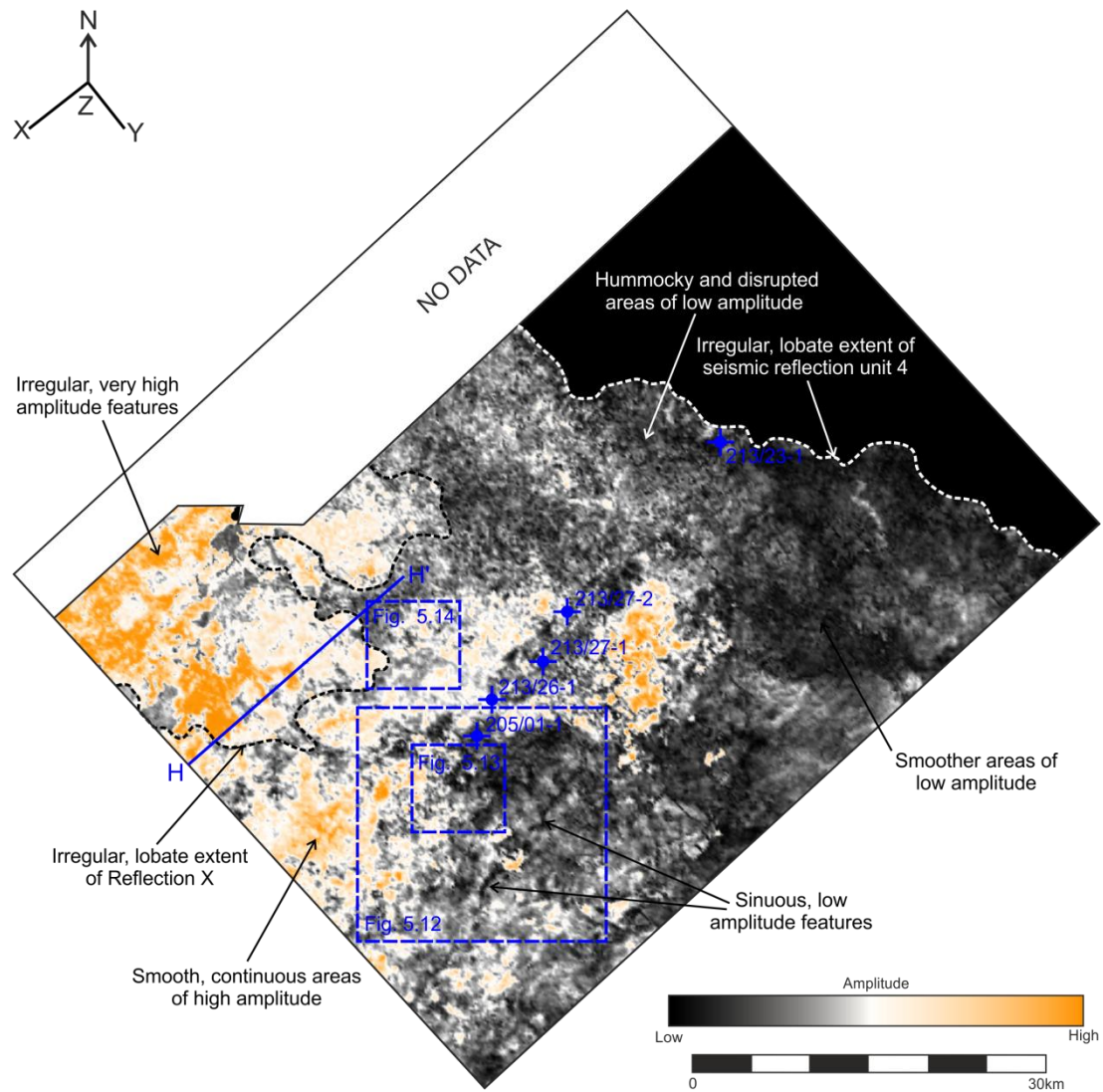
Fig. 6.11. RMS amplitude extraction map with a 5 millisecond window over the top of seismic reflection unit 4 and reflection X. The map images the irregular, lobate extent of unit 4 and the overlying reflection X, variations in the reflection surface and location of the sinuous, low amplitude features. Location box refers to Fig. 6.12, 5.13 and 5.14. Cross section H-H' corresponds to Fig. 6.15.
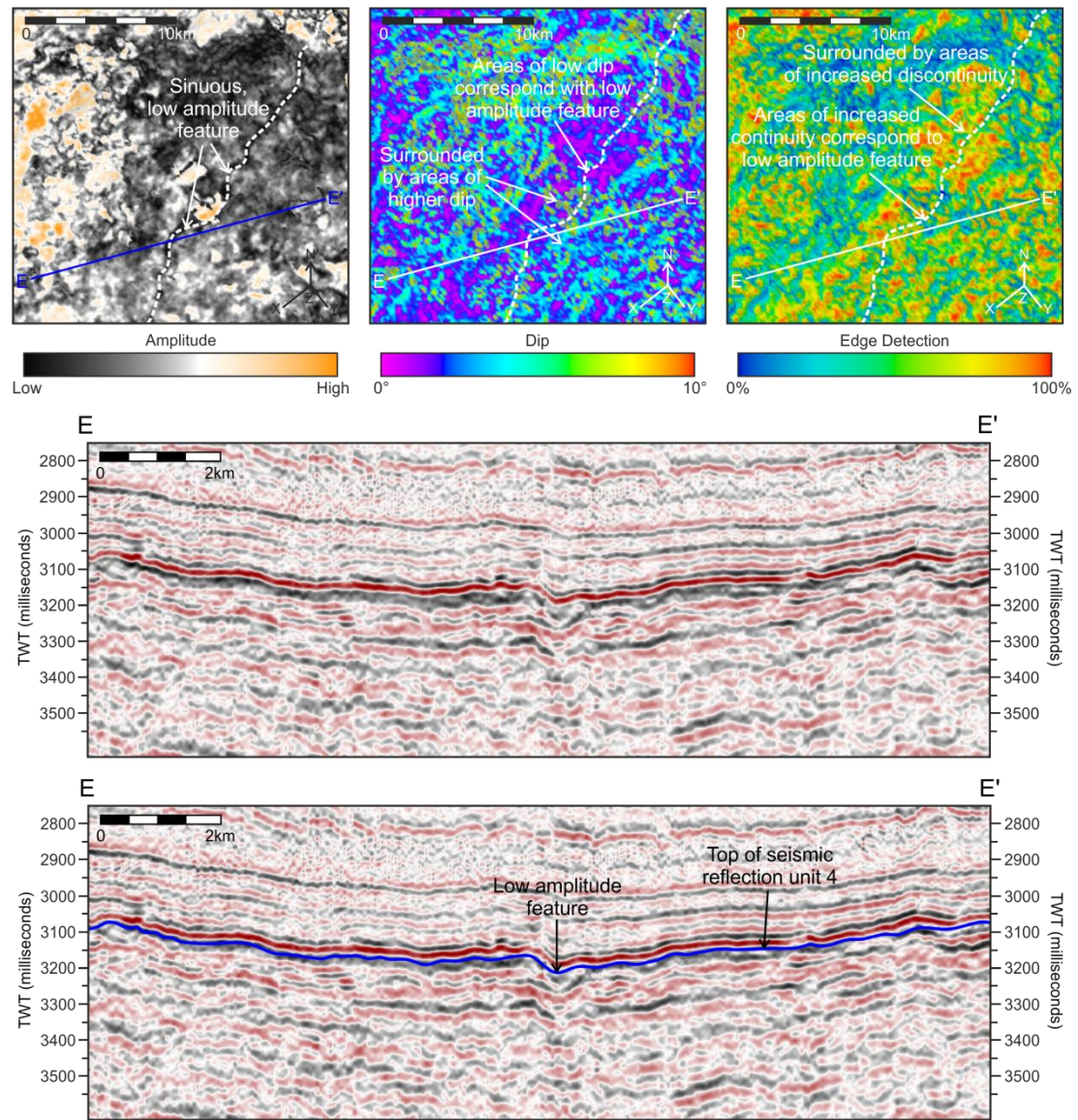
Fig. 6.12. Seismic section E-E' images the top of seismic reflection unit 4 and the location of a subtle, low amplitude trough which correspond with the sinuous features identified on the seismic attribute maps. Seismic attribute maps including RMS amplitude, dip and edge detection maps with a 5 millisecond window of the top of seismic reflection unit 4. The amplitude map reveals that the sinuous feature exhibits low amplitudes and is located between areas of relatively higher amplitudes. The dip map reveals that the sinuous feature corresponds to an area of very low dip. The edge detection map shows that the sinuous feature is located in an area of low discontinuity surrounded by areas of much higher discontinuity. For location see Fig. 6.11.
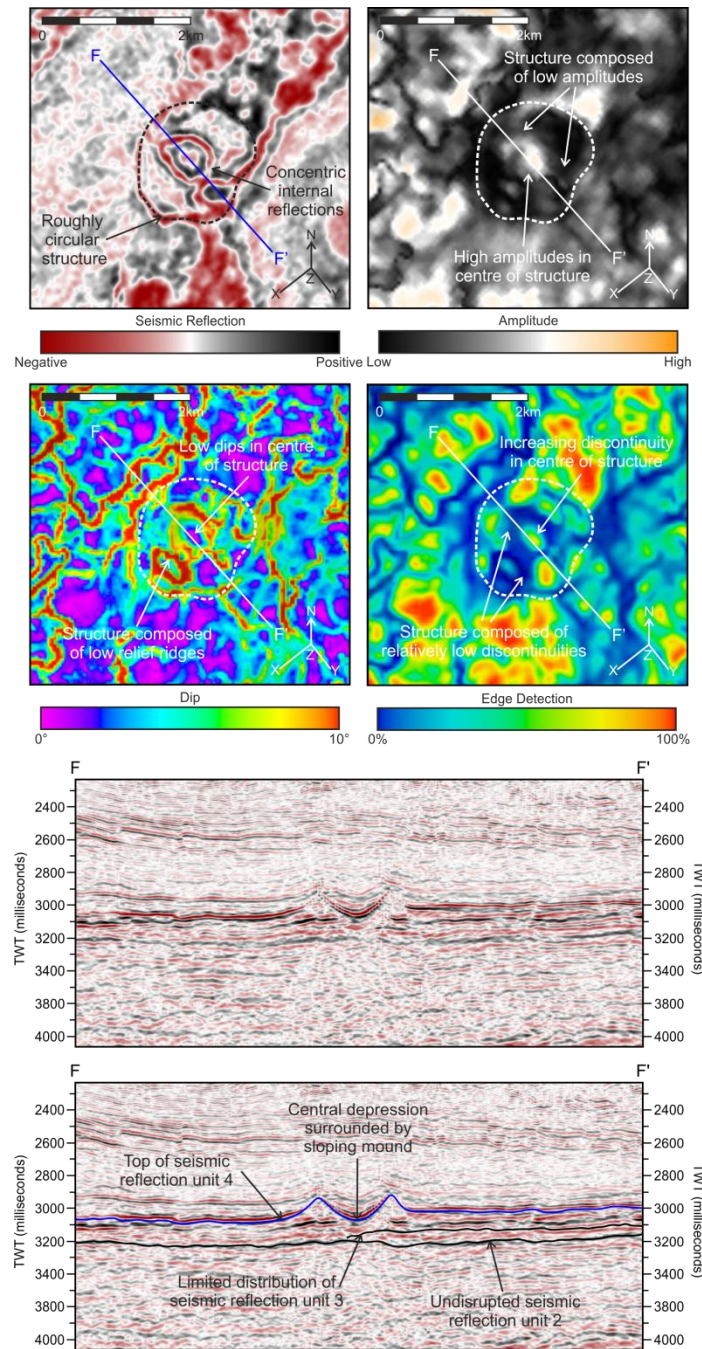
Fig. 6.13. Seismic section F-F' images the first and most obvious circular structure that disrupts seismic reflection unit 4. The timeslice reveals that the concentric internal structures of the structure while the seismic attribute maps including RMS amplitude, dip and edge detection maps with a 5 millisecond window of the top of seismic reflection unit 4. The amplitude map reveals that the circular feature is composed of low amplitude with a central area of high amplitude. The dip map shows that the circular structure is composed of concentric ridges of higher dips with a central area of lower dips. The edge detection map indicates that the circular structure is located in an area of low discontinuity with a centre area that has an increased discontinuity. For location see Fig. 6.11.
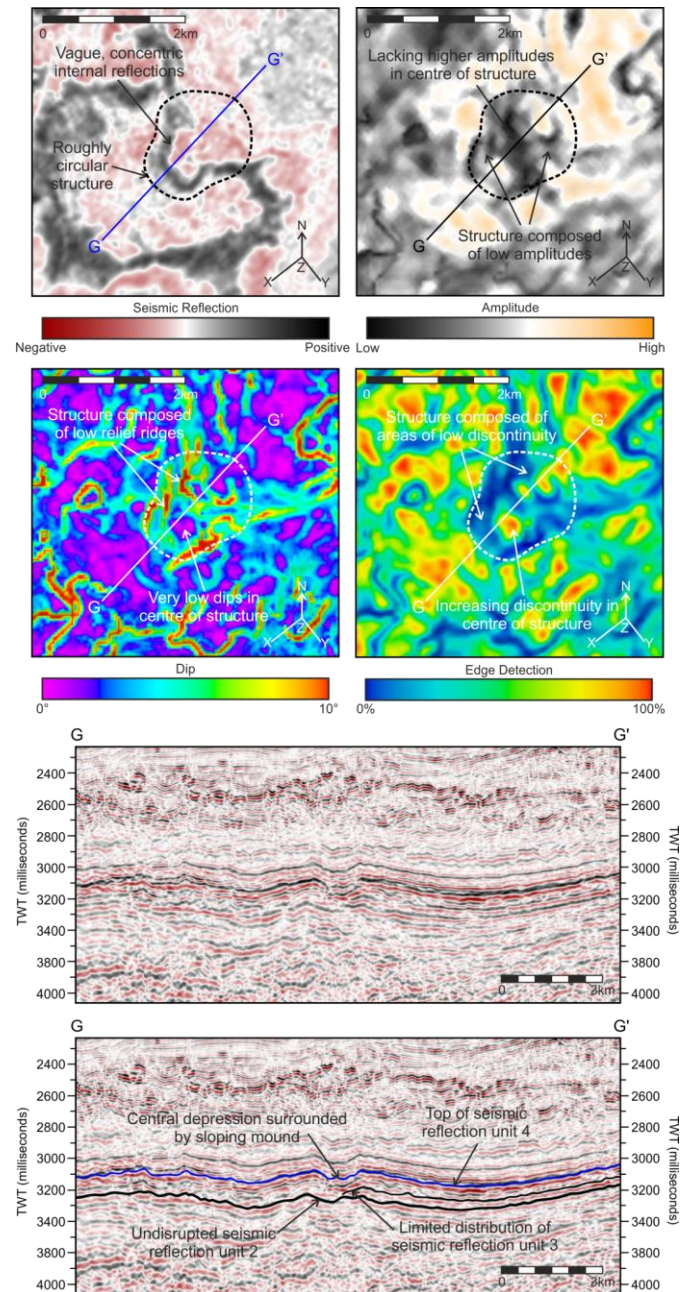
Fig. 6.14. Seismic section G-G' images the second, and less obvious, sub-circular structure that disrupts seismic reflection unit 4. The timeslice reveals that the vague, roughly concentric internal structures of the structure while the seismic attribute maps including RMS amplitude, dip and edge detection maps with a 5 millisecond window of the top of seismic reflection unit 4. The amplitude map reveals that the circular feature is composed of low amplitude but lacks the central area of high amplitude as seen in the first circular structure. The dip map shows that the circular structure is composed of irregular ridges of high dips with a central area of lower dips. The edge detection map indicates that the circular structure is located in an area of low discontinuity with a centre area that has an increased discontinuity. For location see Fig. 6.11.
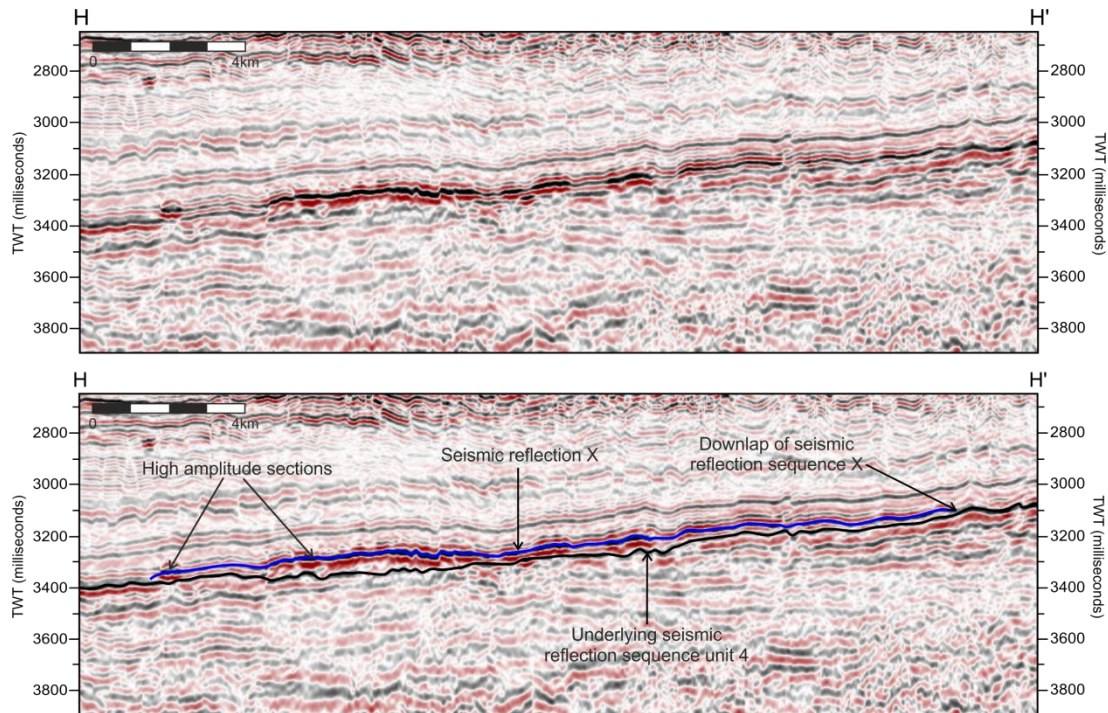
Fig. 6.15. Seismic section H-H' which images the extent of reflection X and downlapping relationship of the reflection with the underlying seismic reflection unit 4. For location of cross section see Fig. 6.11.

6.6 Interpretations

6.6.1 Seismic Reflection Units

The seismic reflection units identified in this study are based on detailed wireline and seismic reflection configuration analysis. Each unit is interpreted to record the emplacement of multiple lava flows during a period of flood basalt eruption. The units appear to have been deposited sequentially and record variations in the source and supply of volcanic material, the available accommodation and the effect of syn-volcanic topography. The initial eruption of the continental flood basalts is recorded by seismic reflection unit 1. The semi-continuous, moderate to low amplitude reflections of the unit 1 broadly correlate with beds of volcaniclastic material and intermittent capping lava flows of volcanic succession 1 identified in the wireline data (see Fig. 6.3; Appendix III). The localised distribution, onlapping geometry and the lithology of the unit has led to the interpretation of a shallowly dipping wedge of volcanic derived material prior to the onset of continental flood basalt emplacement (Roberts *et al.*, 2005; Spitzer *et al.*, 2008). This material was likely sourced from the erosion of the developing volcanic hinterland to the northwest of

the Faroe-Shetland Basin, where the fissure systems that fed the continental flood basalts are interpreted to be located (Dore *et al.*, 1999; Naylor *et al.*, 1999). Transportation may have been via debris flows that formed at, and were shed off the front of the eastward flowing body of continental flood basalt lava.

The emplacement of the flood basalts continued with seismic reflection unit 2 (Fig. 6.16). The high amplitude and continuous reflections of unit 2 correlate with the multiple, interbedded lava flows and sedimentary beds of volcanic succession 2 identified in wireline data (see Fig. 6.3; Appendix III). The unit is interpreted to represent a series of laterally extensive, stacked and overlapping lava flows that formed an extensive lava flow field sourced from the fissures systems to the northwest of the basin. The regional extent of unit 2 indicates that the lava flows were most likely emplaced during voluminous eruptions.
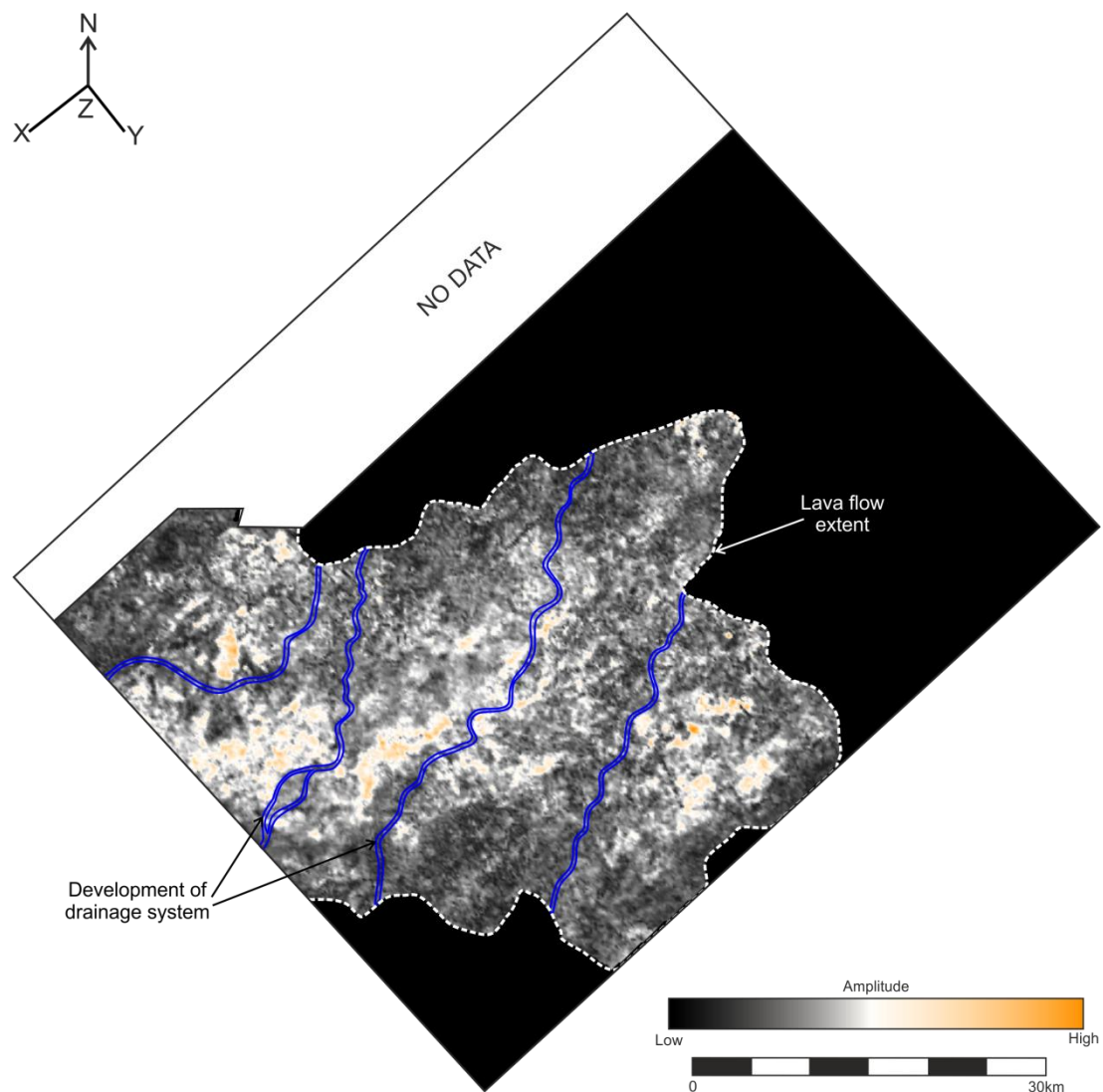
Fig. 6.16. Interpreted RMS amplitude extraction map of the reflection surface of seismic reflection unit 2. The unit was emplaced during high volume eruptions, after which incising

drainage channels developed in a northeast to southwest trend and were constrained by the lava flow field.

When volcanic activity resumed, it was with the emplacement of seismic reflection unit 3 (Fig. 6.17). The semi-continuous, high to moderate amplitude reflections of unit 3 correlate with the multiple, relatively thin interbedded lava flows and sedimentary beds of volcanic succession 3 identified in wireline data (see Fig. 6.3; Appendix III). Seismic reflection unit 3 is interpreted to represent a lava flow field composed of stacked and overlapping lava flows. The unit has a semi-regional and constrained extent suggests that the lava flow field may have been erupted during smaller volumes eruptions. The flow field has a number of irregular lobate protuberances that are largely face northwest and is interpreted to have developed through budding and coalescing lava flow lobes across the survey. The source direction of the seismic reflection unit has been interpreted to be from somewhere to the southeast of the survey area, and therefore differs from that of the previous 2 seismic reflection units (Fig. 6.17). Volcanic centres with localised lava flows have previously been identified in the Faroe-Shetland Basin (e.g. the Erlend Complex and Brendans Dome; Gatliff *et al.*, 1984; Ritchie & Hitchen, 1996).
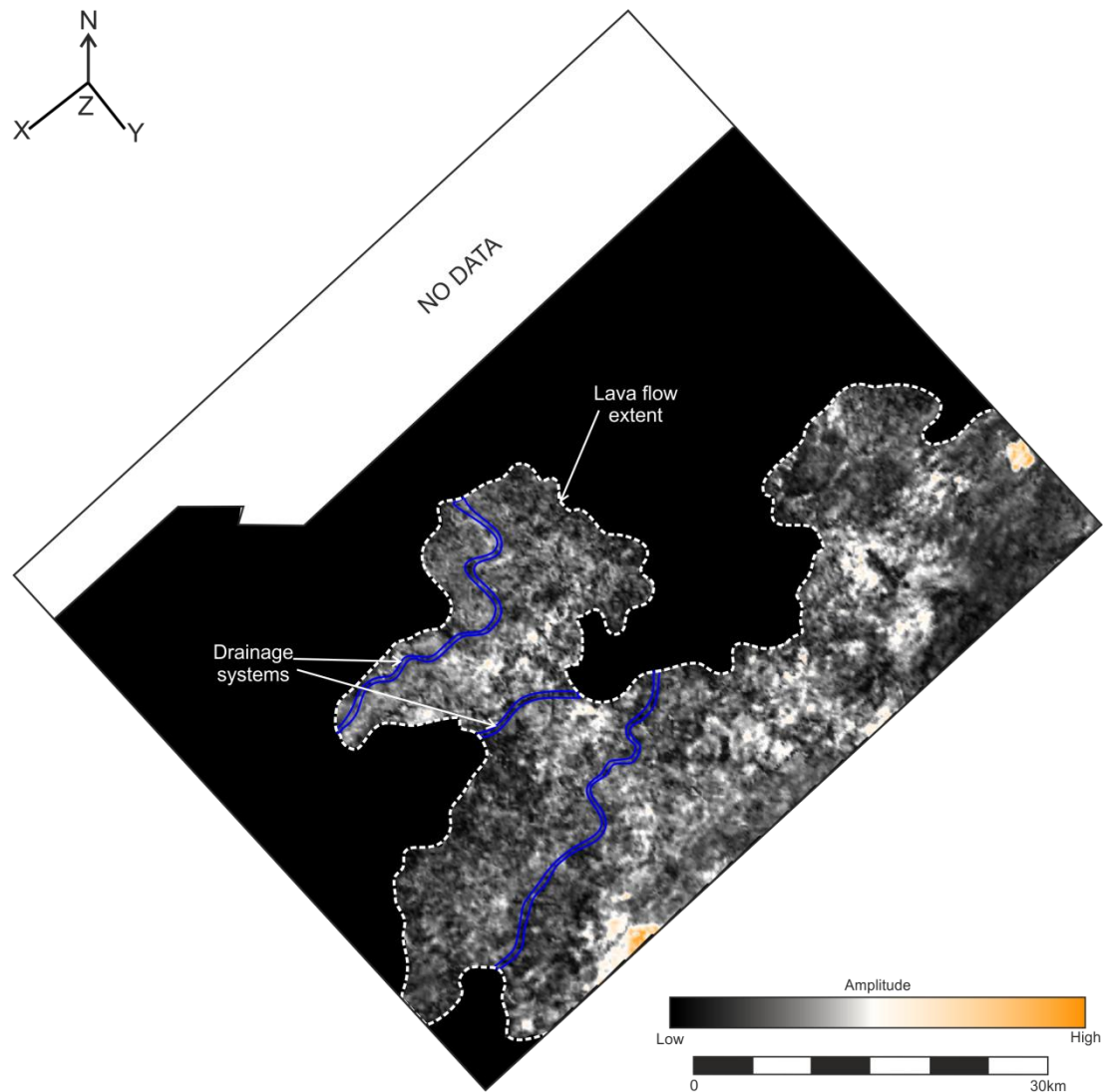
Fig. 6.17. Interpreted RMS amplitude extraction map of the reflection surface of seismic reflection unit 3. The unit was emplaced during lower volume eruptions. After lava flow field emplacement, incising drainage systems developed across the top of the lava flow fields in a northeast to southwest trend.

The final phase of volcanic activity is marked by the renewed lava flow emplacement of seismic reflection unit 4 (Fig. 6.18). The continuous, high to moderate amplitude reflections of seismic reflection unit 4 correlates with the multiple, relatively thick interbedded lava flows and sedimentary beds of volcanic succession 4 identified in wireline data (see Fig. 6.3; Appendix III). Seismic reflection unit 4 is interpreted to represent a laterally extensive lava flow field composed of thick, stacked and overlapping lava flows. The source of the lava flows appears to have reverted back to the northwest of the basin, with the regional extent indicating that the lava flow field was emplaced during voluminous eruptions (Fig. 6.18). The seismic reflection surface gradually decreases in amplitude in an eastward direction

across the survey area, with a vague, lobate edge defining the transition for moderate to low amplitude, hummocky reflection surface (Fig. 6.18). This could indicate a change in the lava flow field morphology, with a decrease in the thickness or distribution of overlapping lava flow lobes producing lower amplitudes. Alternatively, the decrease in reflection amplitude may represent a change in lithology, with the lava flow field becoming increasingly volcaniclastic or hyaloclastic in nature and forming a lobate palaeo-shoreline (Fig. 6.18). However, without greater well control in the survey area, it is difficult to prove for certain.

Seismic reflection 4 is downlapped by a very high amplitude reflection in the northwest of the survey. The reflection is interpreted to represent late stage lava flows sourced from the northwest much the same as unit 4 (Fig. 6.18). The lava flows were likely erupted when volcanic activity was waning or switching to more localised sources. However the exact nature of this reflection is unclear because so little of the unit is recognised within the survey and the reflection is not penetrated by any of the wells.
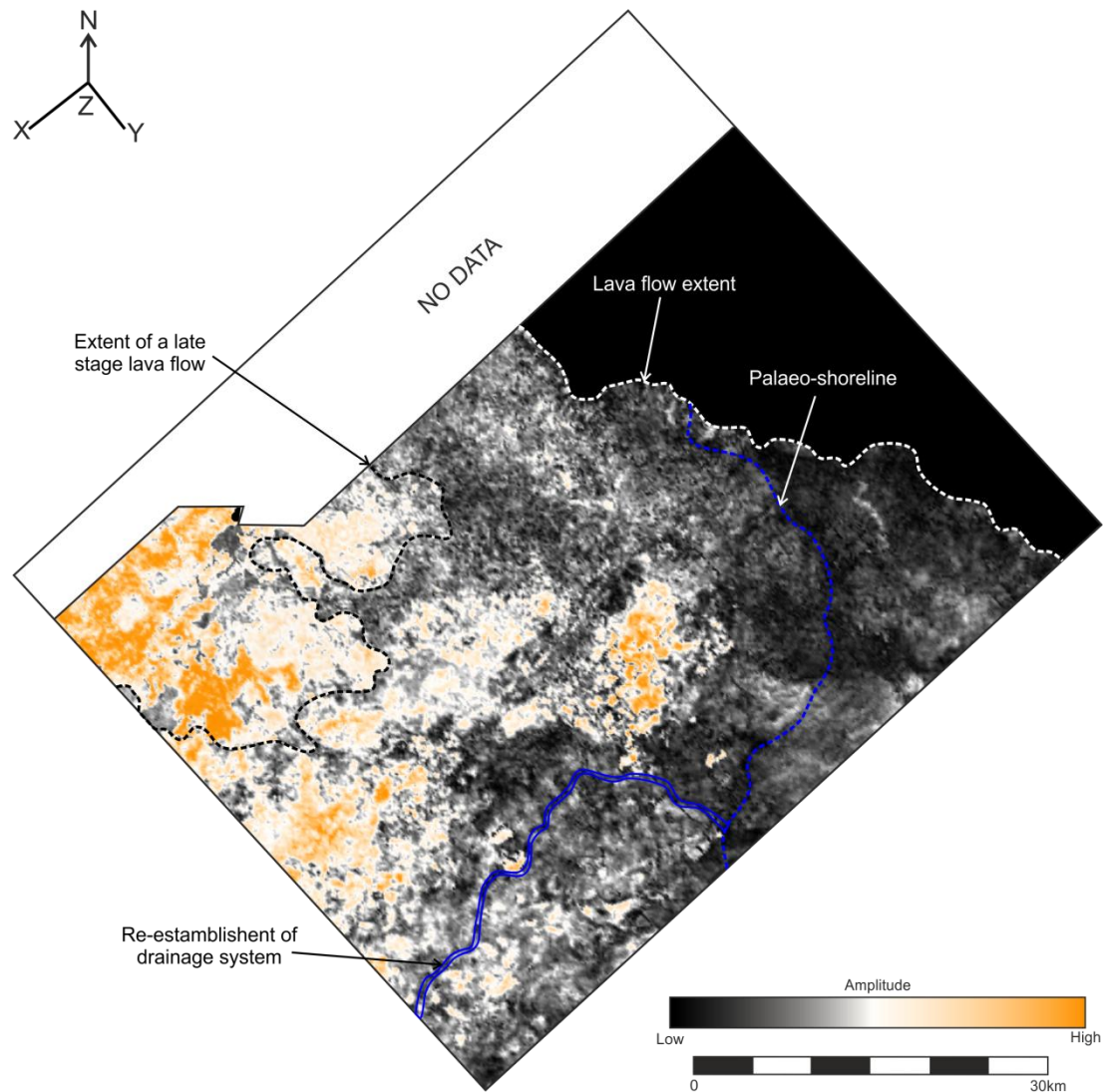
Fig. 6.18. Interpreted RMS amplitude extraction map of the reflection surface of seismic reflection unit 4 which was emplaced during high volume eruptions. Incising drainage channels developed in a northeast to southwest trend after the eruptions ceased and were constrained by the lava flow field. Potential development of a palaeo-shoreline has also been identified in the east of the survey.

6.6.2 Sinuous Low Amplitude Features

Linear features in seismic reflection data, whether curved, straight or sinuous, can indicate a number of geological structures. These include faults, intrusions, channels and the edges of depositional environments. In this study a series of sinuous, low amplitude features have been identified cross-cutting the reflection surfaces of seismic reflection units 2, 3 and 4. In cross section, these features correspond to low amplitude depressions that affect the top of the reflection unit (see Fig 6.8, 6.10 and 6.12). The features display a consistent

northeast to southwest orientation, with the position and sinuosity of the features varying across each of the affected seismic reflection units (see Fig. 6.16, 6.17 and 6.18). The lack of subsurface discontinuity identified by reflection terminations suggests the features are not caused by faults or intrusions, while the continuations of seismic facies across the features indicate the features do not mark the boundary between two different depositional environments (Brown, 2005; Bacon *et al.*, 2007; Ashcroft, 2011). The low amplitude features are interpreted to represent incised channels that developed across the top of the lava flow field after emplacement during a period of volcanic quiescence. The majority of these channels are confined by the distribution of areas of coherent, high amplitudes, which are interpreted to be the location of thick and coherent, stacked lava flows that constrained the development of the drainage channels.

6.6.3 Circular Mound Structures

Circular, mound-like structures are common features in volcanic environments (Francis & Oppenheimer, 2004; White, 1991). They can occur due to a range of eruptive processes and at a range of scales, from relatively small-scale rootless cones, tuff rings and hydrothermal vents, 50 – 1500 m wide and 50 – 300 m high, to large-scale volcanoes, several kilometres high and wide (e.g. Lorenz, 1986; White, 1991; Hamilton *et al.*, 2010; Ross *et al.*, 2011). All of these volcanically-related structures have been recognised across the North Atlantic Igneous Province (e.g. Gatliff *et al.*, 1984; Archer *et al.*, 2005; Planke *et al.*, 2005; Larsen *et al.*, 2006). The two individual circular to sub-circular mounds recognised in this study are 1 – 1.5 km wide and 100 – 200 m high (see Fig. 6.13 and 6.14). The occurrence of individual mounds and not multiple overlapping mounds suggest that they are monogenetic and created by a single eruptive event, rather than polygenetic and created by multiple eruptive events (Walker, 1991; White, 1991; Németh, 2010).

The lack of lava flows recognised extending from the central depression, may suggest that the volcanic eruptions were triggered by hydrovolcanic (water-magma interaction) processes and produced volcaniclastic material rather than molten lava flows. However, the mounds appear to be too large to be rootless cones (see Hamilton *et al.*, 2010) and are at the extreme end of the scale for maars and tuff rings (see Lorenz, 1986; Ross *et al.*, 2011). This may indicate that the mounds are better classified as small-scale volcanoes that produced sub-seismic scale lava flows. The formation of volcanoes requires a feeder system, where molten volcanic rock is fed by sub-vertical dykes and fissures or deep-seated magma chambers located beneath the growing volcanic edifice (Magee *et al.*, 2013). The

mounds are at the edge of seismic resolution and any feeder system would therefore be below seismic resolution. As no feeder systems have been recognised below the mounds, it is assumed that any feeder system is likely composed of sub-seismic scale dykes. In addition to the disruption of seismic reflection unit 4, the central depressions of the mounds are coincident with the distal extent of the underlying seismic reflection unit 3 (Fig. 6.19). Although the exact relationship (if any) between the distributions of the seismic reflection units and the mounds is unknown, the overlapping nature of the units may have had an effect on the path of any feeder systems and the position of the erupting volcanic cones.
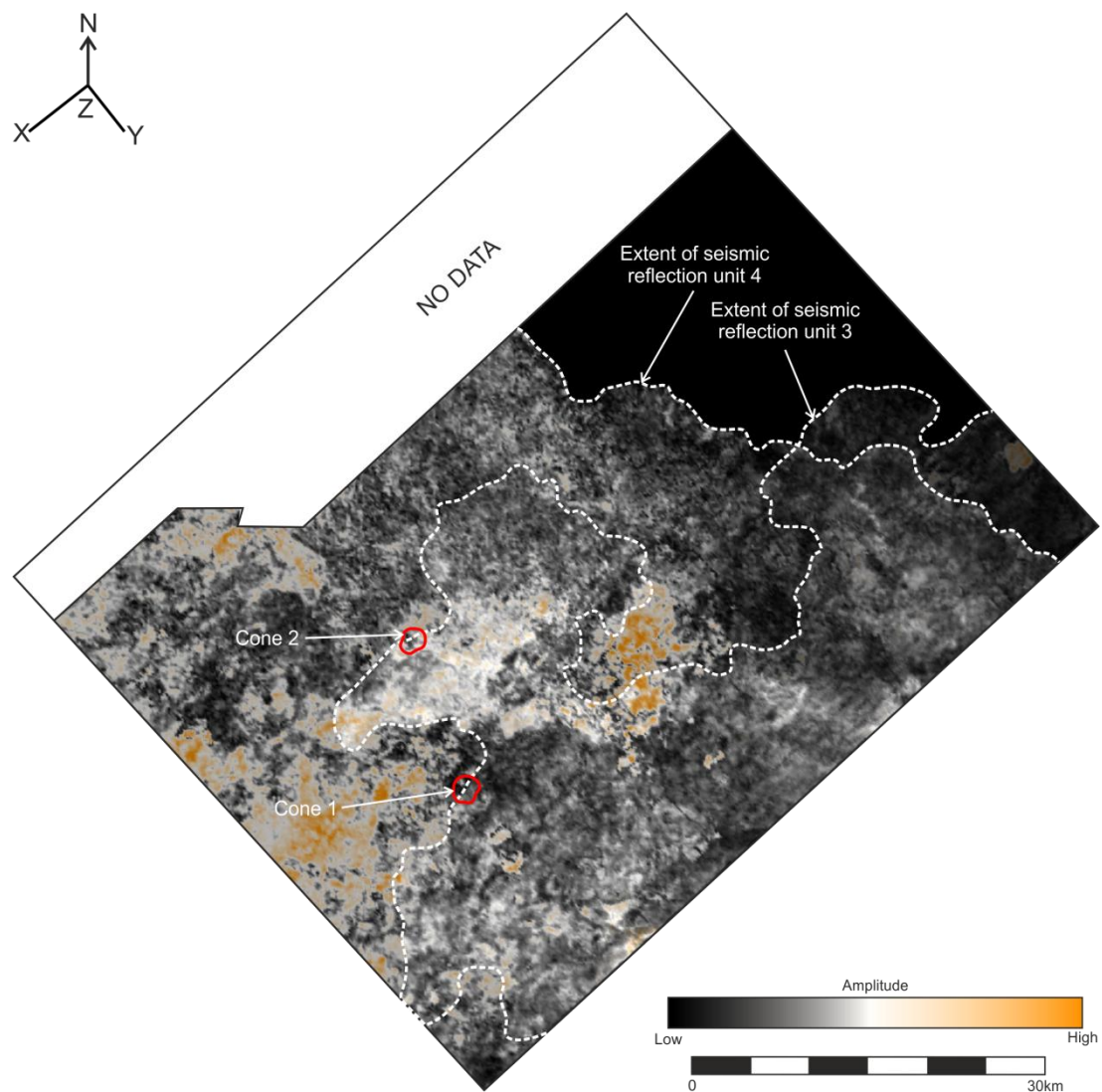
Fig. 6.19. RMS amplitude extraction map of seismic reflection unit 3 overlain with a transparent RMS amplitude extraction map of seismic reflection unit 4 and the locations of the volcanic cones.

6.6.4 Correlation to Onshore Stratigraphy

Although correlation of onshore and offshore volcanic successions is difficult, especially without high resolution geochemistry or biostratigraphy, it is possible to make broad interpretations based on lava flow field extent, source and morphology. On the Faroe Islands, the evolution of the flood basalts is recorded by the eruption of four volcanic formations, with three inter-basalt sedimentary formations that record periods of quiescence between the volcanic eruptions (see Chapter 2, Fig. 2.3; Ellis *et al*., 2002; Passey & Bell, 2007; Passey & Jolley, 2009). Initiation of flood basalt volcanism is often recorded by thick basal deposits of volcaniclastic and hyaloclastic material that have been previously identified in many emergent volcanic settings (Gamberi, 2001; Usktins Peate *et al*., 2003; Ross *et al*., 2005; Jerram *et al*., 2009). On the Faroe Islands this is recorded by thick basal deposits of hyaloclastic breccias and lava flows of the Lopra Formation (Ellis *et al*., 2002; Passey & Bell, 2007; Passey & Jolley, 2009). In the study area, seismic reflection unit 1 consists of a thin succession of volcaniclastic material and lava. This unit has been recognised at the base of the volcanic succession, underlying the subsequent lava flow fields and recording the initiation of volcanism in the survey area .

Volcanism continued with the emplacement of the Beinisvørð Formation which is composed of thick and extensive subaerial lava flows. The lava flows are interpreted to be emplaced as multiple lava flow lobes which coalesced to form a single lava flow field, with a continuous supply of magma from extensive fissure systems allowing the flows to spread out laterally over a wide area (Self *et al.*, 1996; 1998; Jerram & Widdowson, 2005; Passey & Bell, 2007). The majority of the lava flows emplaced offshore of the Faroe Islands are interpreted to be the equivalent of the Beinisvørð Formation (Smythe *et al.*, 1983; Kiørboe, 1999; Ritchie *et al.*, 1999). In this study, the lava flow fields of seismic reflection units 2 and 4 are interpreted to be the offshore equivalent of the Beinisvørð Formation. The laterally extensive, stacked and overlapping lava flows that formed the lava flow fields reflect the continuous supply of magma from extensive fissure systems to the northwest. Onshore the Beinisvørð Formation is composed of multiple eruptive phases often separated by palaeosols (Ellis *et al*., 2002; Passey & Bell, 2007; Passey & Jolley, 2009). Although multiple eruptions have been recognised in the study area they are not at the same frequency. Seismic reflection units 2 and 4 are most likely composites of multiple periods of eruption, rather than individual periods of active volcanism, with only the most significant periods of volcanic quiescence and fluvial incision recorded. In addition to the offshore equivalent of

the Beinisvørð Formation, the influx of lava flows most likely erupted from localised volcanic centre in the southeast of the Faroe-Shetland Basin is recorded with the emplacement of the lava flow fields of seismic reflection unit 3. The change in source location and areal extent of the seismic reflection unit may reflect a change in eruption style changed from fissure fed to vent fed, however the exact relationship between the localised volcanic eruptions and the Beinisvørð Formation is unknown.

6.7 Discussion

6.7.3 Emplacement of Lava Flow Fields

Continental flood basalt provinces are dominated by multiple, thick pāhoehoe lava flows erupted from long-lived fissure and vent systems with a continuous supply of magma (Self *et al.*, 1996; 1997). Initially, lava flows are emplaced as a series of lobes which coalesce to form broad, extensive and relatively flat-lying sheet flows, often with interconnect lava flow cores (Fig. 6.20). The emplacement of multiple sheet lobes form lava flow fields and are an aggregate product of the lava flows from a single eruptive event (Fig. 6.20; Hon *et al.*, 1994; Self *et al.*, 1996; 1997; 1998; Anderson *et al.*, 1999). Flood basalt provinces are typically composed of numerous stacked lava flow fields each 20 – 100 m thick (Self *et al.*, 1997; 1998). Active lava flows are also subject to the effects of gravity as they flow, as they are composed of partially molten rock (Griffiths, 2000). They can be affected by pre-existing topography while successively erupted lava flows can be affected by any minor construction relief formed during the inflation of the previous flow field (Hulme, 1974; Hon *et al.*, 1994; Self *et al.*, 1996).

The majority of the flood basalts in the Faroe-Shetland Basin were erupted from extensive fissure systems (Dore *et al.*, 1999; Naylor *et al.*, 1999), while localised volcanic vents erupted lava flows on the periphery of the basin (Gatliff *et al.*, 1984; Ritchie & Hitchen, 1996). In the survey area, the flood basalt eruptions were recorded by the emplacement of a series of stacked lava flow fields in which the effects of pre-existing topography and flow field relief have been recognised. This is recognised in the emplacement of the flow fields of seismic reflection unit 3, which was affected by the minor surface relief created through the accumulation of stacked lava flows of the underlying seismic reflection unit 2 (Fig. 6.21). This surface relief influenced the emplacement of the flow fields of unit 3, with the

lava flows constrained by minor topographic highs and diverted into topographic lows (Fig. 6.22).

Variations in volcanic source have also been interpreted. The majority of the lava flows in the Faroe-Shetland Basin are interpreted to be sourced from the fissure systems that are interpreted to be located in the northwest of the basin, close to the Faroe Islands (Dore *et al*., 1999; Naylor *et al*., 1999). This includes the flow fields of seismic reflection units 1, 2 and 4. In contrast, the flow fields of seismic reflection unit 3 differ in source location, with the unit appearing to have flowed across the survey area from a south/southeast direction (see Fig. 6.17). This change in source location indicates the influx of both proximal and distal volcanic sources into the same area. The eruption of unit 3 from a more localised volcanic source, such as a volcano with restricted lava flows, may explain the more localised areal extent. The cause of the variations in volcanic source, supply and extent between the seismic reflection units are unknown, but may reflect changes in eruption rate or the migration of the eruption site through time (Self *et al.*, 1997; Heliker *et al.*, 1998; Passey & Bell, 2007).
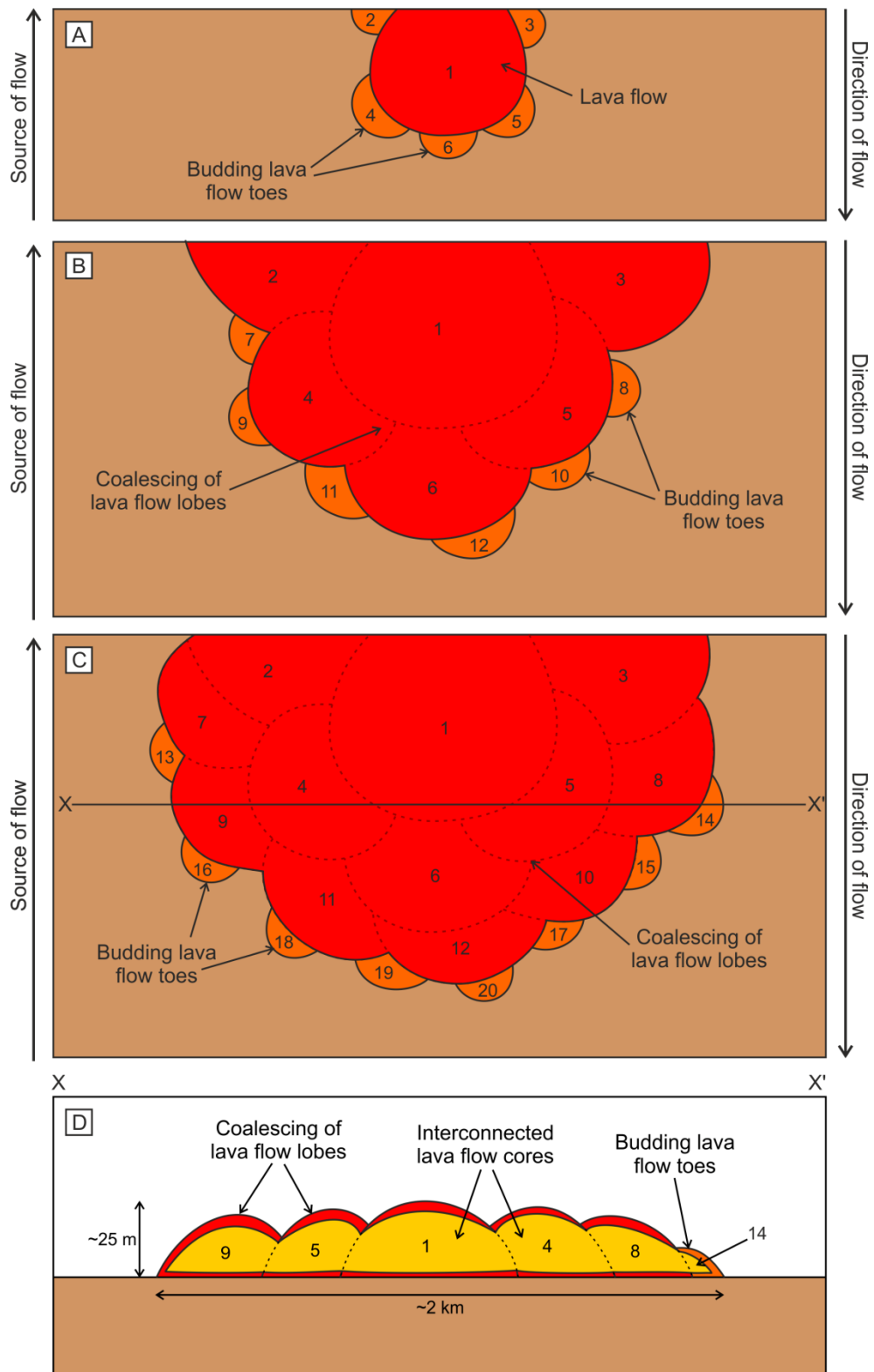
Fig. 6.20. Schematic diagram and cross section through the development of a lava flow field. Figures A to C shows the development of a lava flow field through time as individual flow lobes coalesce. Cross section in figure D reveals the potential internal geometry of the coalesced lava flow core, modified after Rowland *et al*. (1990), Self *et al*. (1996; 1998) and Thordarson & Self (1998).
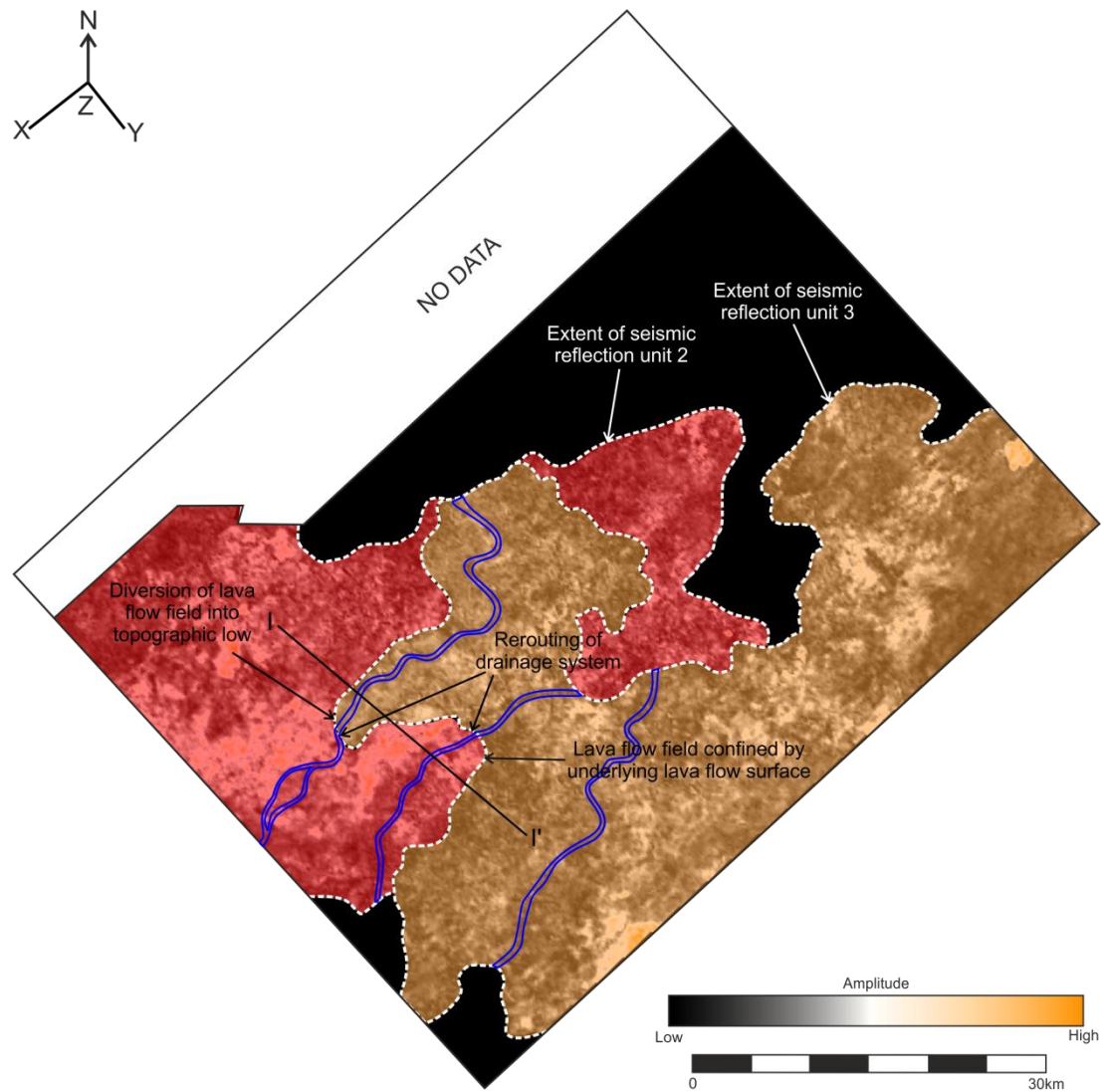
Fig. 6.21. Interpreted RMS amplitude extraction map of the extent of seismic reflection unit 2 overlain with the extent of seismic reflection unit 3 and the location of the incising drainage systems across both reflection surfaces. The drainage channels that developed across the surface of unit 2 can be seen to have been diverted around the distal extents of unit 3. Cross section I-I' corresponds to Fig. 6.22.
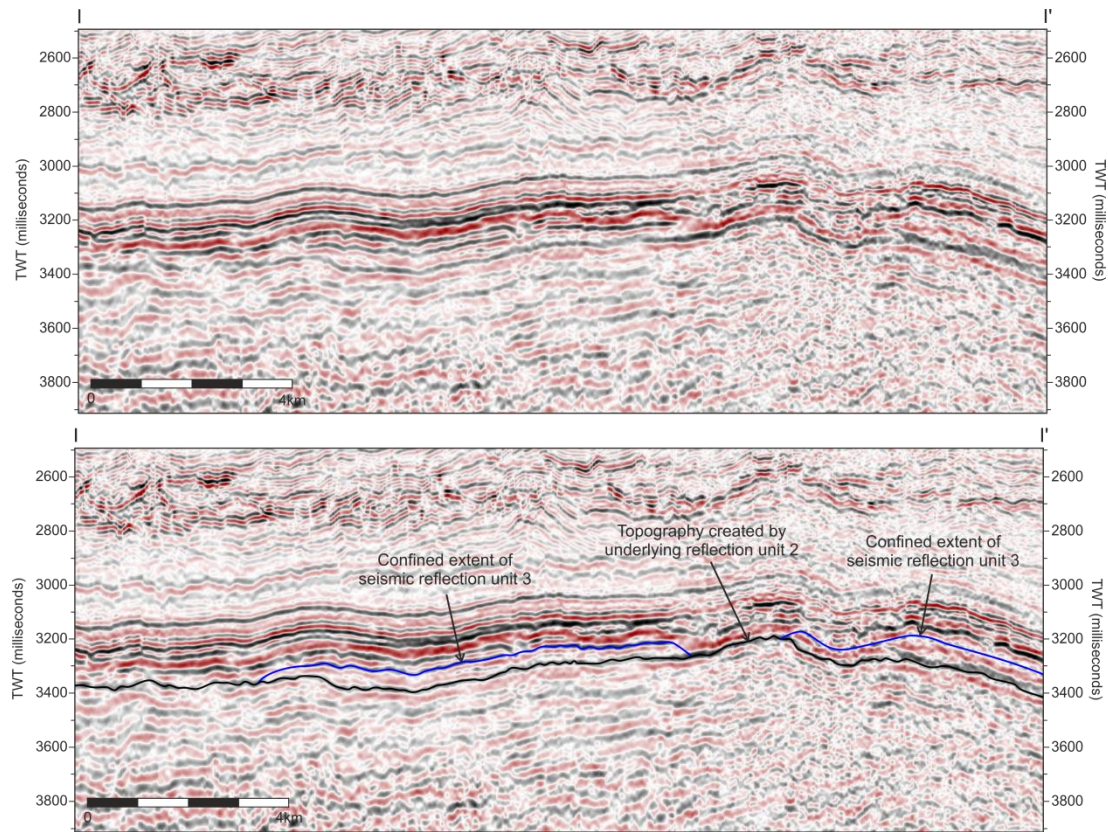
Fig. 6.22. Seismic section I-I' images the limited extent of seismic reflection unit 3 and the downlapping relationship of the unit with the underlying seismic reflection unit 2. For location of cross section see Fig. 6.21.

6.7.2 Development of Drainage Systems

Indigenous sedimentary systems can be greatly affected by flood basalt volcanism, with tectonic activity caused by thermal uplift of the crust often enhancing fluvial incision and sediment supply (Smith, 1987; 1988; Dam, 1998; 2002). The emplacement of flood basalt lava flows can also cause drainage systems to stop or become diverted, resuming only during periods of volcanic quiescence, and often tens of thousands of years after flow emplacement (Wells *et al*., 1985; Inbar *et al*., 1994; Stollhofen & Stanistreet, 1994; Ollier *et al*., 1995). The development of incising fluvial systems across lava flow fields is initially controlled by the morphology of the upper surface of the flows, distribution of flow features and constructional relief created by the inflation of the lava flow lobes (Wells *et al*., 1985; Dohrenwend *et al*., 1987; Inbar *et al*., 1994). Fluvial systems commonly exploit areas of weakness or topography, often incising along the edges of lava flows or between lava flow lobes (Inbar *et al*., 1994).

Multiple drainage systems have been recognised incising the top reflection surfaces of seismic reflection units 2, 3 and 4, while the lack of drainage systems across the surface of seismic reflection 1 indicates the unit was subaerially exposed for a relatively short period of time. The distribution of drainage systems have been constrained by minor topographical and surface relief of the lava flow fields (Fig. 6.21). The channels have also been influenced by the emplacement of subsequent lava flow fields, with the emplacement of seismic reflection unit 3 having dammed and diverted the pre-existing channels that had incised into the underlying seismic reflection unit 2 (Fig. 6.21). The drainage systems likely transported a mixture of siliciclastic sediments sourced from the Scottish hinterland to the south and volcaniclastic derived material sourced from volcanic hinterland to the northwest (Mudge & Bujak, 2001; Sørensen, 2003; Jolley *et al.*, 2005; Brown *et al.*, 2009).

The channels display a broadly northeast to southwest trend. This is consistent with the main regional stress regime produced by the rifting of the North Atlantic during the Mesozoic-Cenozoic rifting (see Chapter 2, Fig. 2.1; Dore *et al.*, 1999; Ritchie *et al.*, 2003; 2008). It is also of a similar orientation to that of the Faroe-Shetland Escarpment, a thick and regional extensive lava-fed delta system that marked the palaeo-shoreline of a marine basin (see Chapter 4; Smythe, 1983; Smythe *et al.*, 1983; Kiørboe, 1999; Naylor *et al.*, 1999). The escarpment gradually thinned towards the south due to decreasing water depths (Mitchell *et al.*, 1993; Lamers *et al.*, 1999; Naylor *et al.*, 1999). The transition from open marine to more restricted marine and non-marine conditions is recorded by the deposition of cyclic, fluvial to shallow marine siliciclastic sediments sourced from the Scotland-Shetland hinterland (Van Den Akker *et al.*, 2000; Mudge & Bujak, 2001; Sørensen, 2003; Jolley *et al.*, 2005).

6.7.3 Comparison to Outcrop Analogues

As with all remote sensing techniques, it is critical to ground-truth seismic observations with outcrop analogues (Cartwright & Huuse, 2005; Davies & Posamentier, 2005; Posamentier *et al.*, 2007). The seismic observations in this study are based on the identification of similar morphologies recognised in outcrop and the published literature. Although flood basalt provinces have been recognised across the world, there are currently no active examples. Therefore comparisons must be made with ancient flood basalts where lava flow emplacement can be observed. This includes the lava flows of the Columbia River Flood Basalt Province, Washington USA, which is an onshore Large Igneous Province,

erupted from a series of fissure and vents between 17-6 Ma (Thompson & Gibson, 1991; Camp, 1995).

The lava flows of the Columbia River Flood Basalt Province were emplaced as a series of inflated, stacked and overlapping flow fields 20-100 m thick (Swanson *et al.*, 1975; Reidel *et al.*, 1992; Self *et al.*, 1996; 1997). Where these lava flow fields are exposed in outcrop, they display thick, undulating and interconnected lava flows with massive to columnar jointed flow cores (Fig. 6.23). Many of the lava flow fields are interbedded with weakly consolidated, lacustrine sedimentary rocks that developed across the top surfaces of the lava flows during periods of volcanic quiescence (Fig. 6.23; Camp, 1981; Long & Wood, 1986; Smith, 1988). There is also fluvial incision into the underlying volcanic and sedimentary rocks, with channels migrated around the edge of the lava flows and eroding into the softer sedimentary beds (Camp, 1981; Ely *et al.*, 2012). Channel incision is followed by deposition of interbedded lacustrine, fluvial and volcaniclastic sediments as the channel became established (Tolan & Beeson, 1984; Smith, 1998; Lyle, 2000). Once volcanism resumed, these canyons were dammed by lava flows, which progressively infilled then overflowed over the incised canyon (Fig. 6.24; Tolan & Beeson, 1984; Lyle, 2000; Ely *et al.*, 2012). In outcrop, these intra-canyon lava flows are obvious when juxtaposed next to the canyon walls or occur as positive topographic features as the surrounding sedimentary rocks that form the canyon walls are softer than the volcanic rocks, and are preferentially eroded (Fig. 6.24; see Tolan & Beeson, 1984; Lyle, 2000; Ely *et al.*, 2012).

The subaerial emplacement environment of the Columbia River Flood Basalt Province provides an analogue for the Faroe-Shetland Basin with extensive subaerial lava flows and interbedded siliciclastic and volcaniclastic rocks. The extensive lava flow fields recognised in this 3D study display comparable features on similar scales to those of the Columbia River Flood Basalt Province, suggesting similar emplacement processes occurred. These include the multiple, stacked pāhoehoe lava flows and kilometre-wide lobate flow geometries. The interpreted drainage systems that developed across the flow fields in the study area are also remarkably similar to the incised channels and lava-filled palaeo-canyons that developed across the lava flows of Columbia River Flood Basalt Province. In addition, the intra-canyon lava flows are analogous to the constrained emplacement of the flow fields and diverted channel of seismic reflection 3 by the minor surface relief and location of incised channels of the underlying seismic reflection unit 2 (see Fig. 6.21).
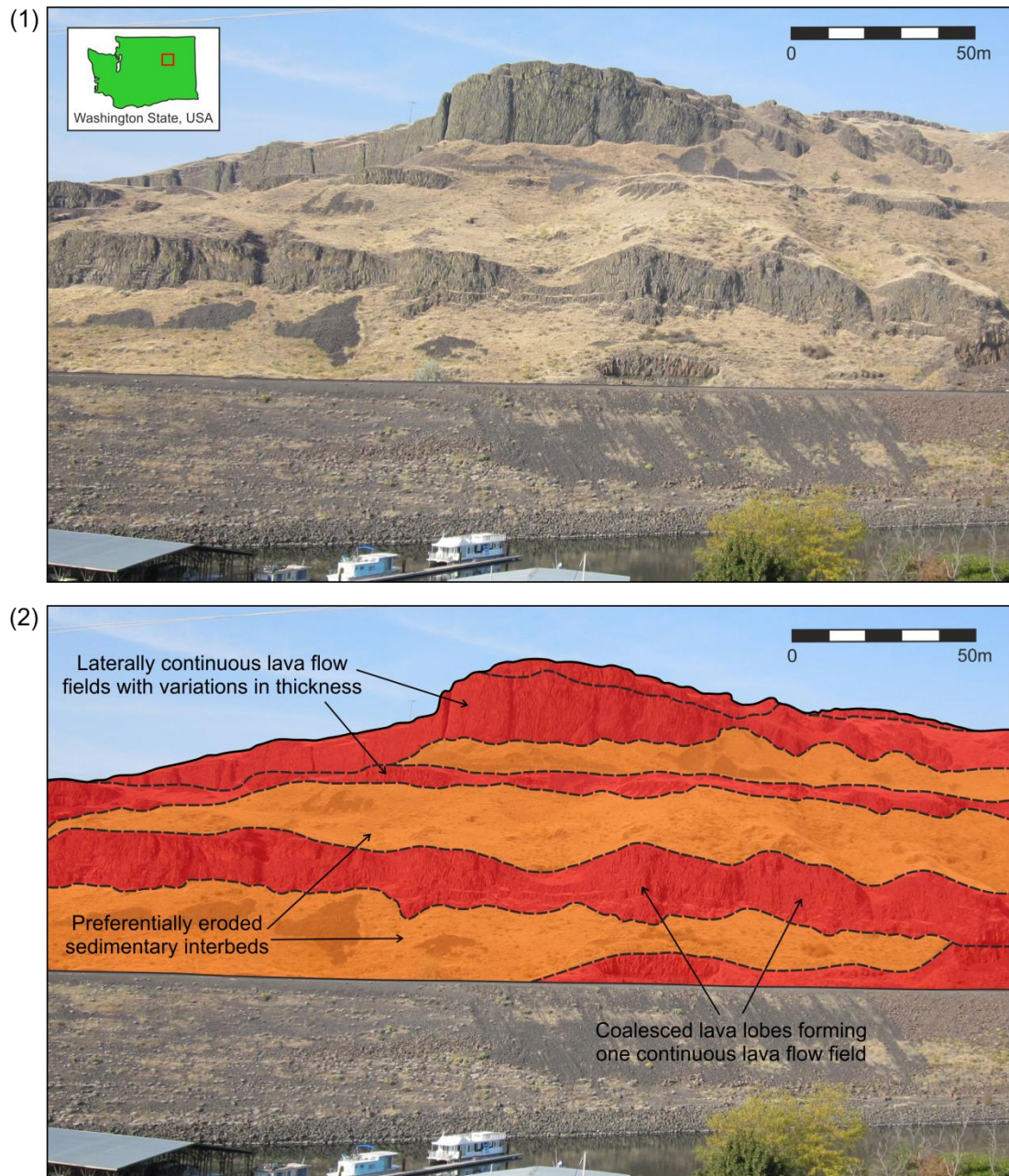
Fig. 6.23. Outcrop exposures of interconnected lava flow cores in multiple, stacked lava flow field and interbedded sedimentary beds, Columbia River Flood Basalt Province, Washington, USA. Height of the outcrop is ~200 m. Photo taken on field trip to the Columbia River Flood Basalt Province, September 2012.
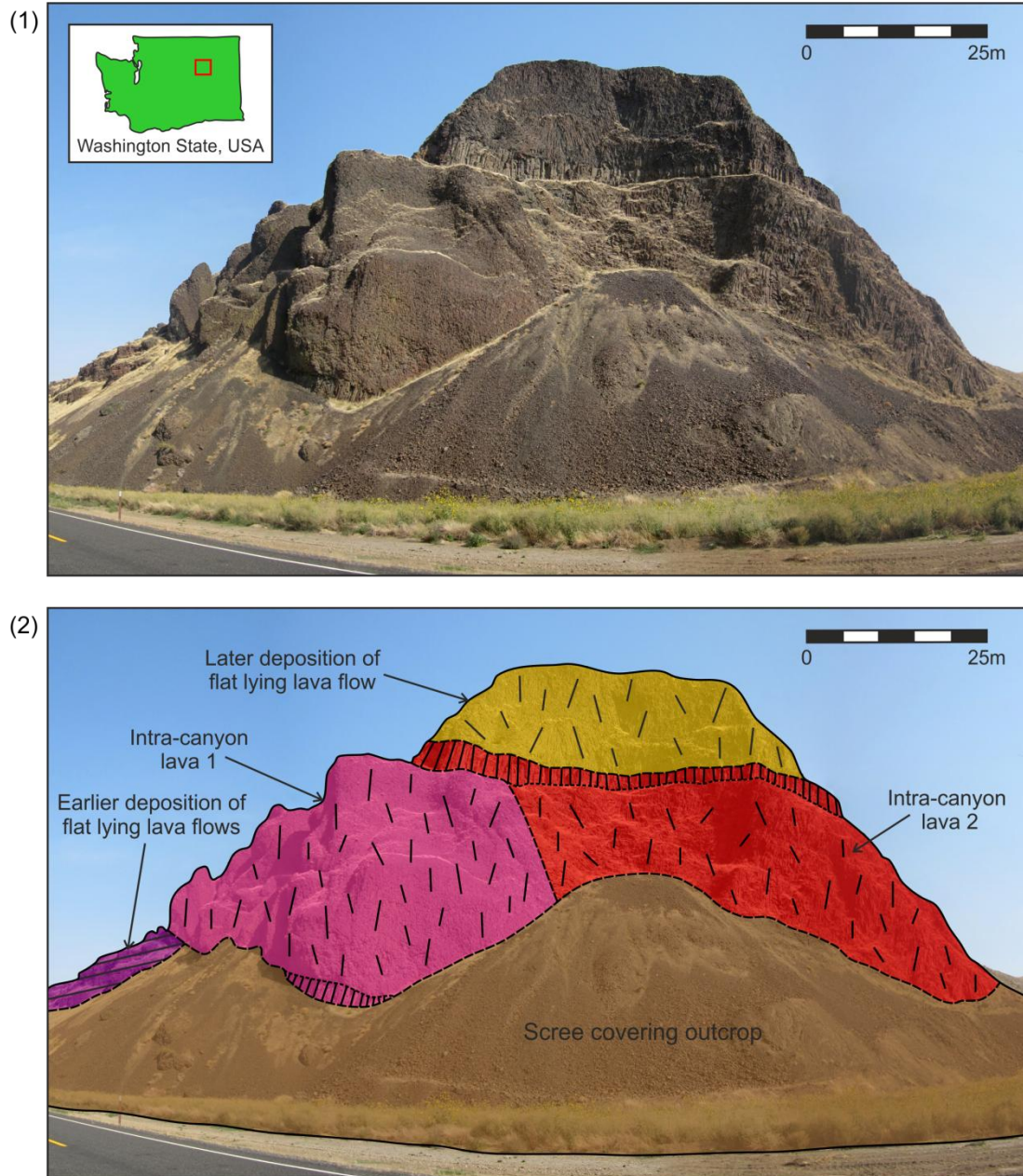
Fig. 6.24. Outcrop exposure of intra-canyon lava flows infilling an ancient incised river system, Columbia River Flood Basalt Province, Washington, USA. Height of the outcrop is ~100 m. Photo taken on field trip to the Columbia River Flood Basalt Province, September 2012.

6.8 Conclusions

The detailed examination of an extensive 3D seismic reflection survey and five exploration wells has revealed at least four phases of volcanic emplacement that document emplacement process, volcanic source and supply. The initial phase of volcanism in the survey area is recorded by the emplacement of a shallowly dipping wedge of volcaniclastic rocks sourced from the erosion of the developing onshore volcanic hinterland to the northwest of the Faroe-Shetland Basin. Volcanism continued with the emplacement of laterally extensive, stacked and overlapping lava flows that formed an extensive lava flow field sourced from the fissures systems to the northwest of the basin during voluminous eruptions. The source of volcanism appeared to switch to a more localise source, with the emplacement of less extensive, more confined lava flow field from the southeast. The development of the flow field was affected by minor topography of the underlying flow field, with lava flows constrained by minor topographic highs and diverted into topographic lows. The final phase of volcanic activity is marked by renewed volcanic supply from the northwest with the emplacement on an extensive lava flow field and the development of late stage lava flows.

Multiple incising drainage systems have been identified across the top of each of the flow fields and are interpreted to have developed during periods of volcanic quiescence. The channels display a broadly northeast to southwest trend and were constrained by minor topographical and surface relief of the lava flow fields. Without access to 3D data, these subtle features would not have been recognised. This study allowed the reconstruction of continental flood basalts in a marginal environment, which is characterised by repeated phases of extensive lava flow emplacement and fluvial incision during periods of volcanic quiescence. Many of the morphological features recognised from the data are directly comparable to documented subaerial outcrop exposures and are indicative of the emplacement processes. Such detailed analysis of offshore flood basalts can provide important information about the evolution of volcanism in otherwise unknown volcanic basins.

CHAPTER 7: DISCUSSIONS AND CONCLUSIONS

7.1 Introduction

Using a variety of 2D and 3D seismic reflection data, this thesis investigated whether the emplacement of volcanic rocks produced depositional successions that recorded temporal and spatial variations of the basin into which they were emplaced. Based on the hypothesis that these successions can be delineated by bounding reflection surfaces that record periods of volcanic quiescence and/or sedimentary deposition, seismic stratigraphy provides a suitable framework in which to interpret volcanic rocks. The work presented in Chapters 4, 5 and 6 examines the seismic reflection configurations of thick continental flood basalts that were emplaced into subaerial to marine environments within the Faroe-Shetland Basin. Although each chapter investigates a different aspect of the development of the volcanic basin-fill, the stratigraphic relationships, emplacement processes and surface morphologies are intrinsically linked.

Chapter 4 introduced the use of seismic reflection data to study volcanic rocks on a scale of hundreds to thousands of meters in an offshore, volcanically rifted margin. The chapter examined the seismic reflection geometries and seismic facies associations exhibited by an extensive lava-fed delta system in the Faroe-Shetland Basin, UK Atlantic Margin. In a bid to understand the development of the subaerial flood basalts and the resulting marine lava-fed delta, seismic stratigraphic concepts were applied to the volcanic rocks using multiple 2D seismic reflection surveys. Analysis of the data revealed that it is possible to recognise successions of volcanic depositional units that record variations in lava supply and accommodation. In addition, the units are interpreted to be bounded by hiatal surfaces which may record a lack of volcanic activity through erosion and the potential deposition of thin, siliciclastic rocks.

Chapter 5 built upon the research undertaken in Chapter 4 and used a 3D seismic reflection survey over the distal extent of the lava-fed delta in the central Faroe-Shetland Basin. This chapter examined in detail the internal structure and surface geomorphology of the seismic reflection units of the lava-fed delta, as well as volcanically related activity below and above the delta. This included the identification of pre-delta volcanic activity, most likely sourced from a localised volcanic centre to the east and post-delta redeposition of volcanic rocks. Interpretation of the data revealed many morphological features that are consistent with subaerial outcrop exposures and are indicative of emplacement process. The delta

was fed from the west by thick, kilometre-scale pāhoehoe lava flows which produced steep foresets composed of hyaloclastic breccias. The delta front was also modified by at least two phases of remobilisation, with the first forming steep, arcuate escarpments and hummocky debris avalanche deposits, and the second creating high density slurries of volcaniclastic material which emplaced hummocky, lobate sheets of hyaloclastite with abrupt edges.

Chapter 6 investigated the emplacement of continental flood basalts south of the lava-fed delta system studied in Chapters 4 and 5. This chapter used an extensive 3D seismic reflection survey and five exploration wells in the south of the Faroe-Shetland Basin to analyse the distribution of subaerial lava flows in a marginal environment. The exploration wells provided a robust control on the seismic interpretation of multiple successions of volcanic rocks. The morphological features recognised from the data are directly comparable to documented subaerial outcrop exposures and are indicative of the emplacement processes. The volcanic rocks were emplaced as a succession of thick, stacked and interconnected lava flow fields that document emplacement process, source and supply of the volcanic rocks. Flow field surface topography affected the emplacement of subsequent flow field and fluvial channels incised into the top surfaces of the flood basalts during periods of volcanic quiescence.

This discussion chapter summarizes the principal findings of the research undertaken in this thesis, with regards to the initial aims and objectives. This chapter also discusses the main questions arising from this work, the implications and major uncertainties, and where additional data is required. The main conclusions for this thesis, both the fundamental concepts and those relating directly to the case study are presented, including a new seismic stratigraphic model for volcanic rocks and the development of volcanic rocks in the Faroe-Shetland Basin. Finally, potential avenues for further work are suggested.

7.2 Fundamental Concepts

In order to study volcanic rocks in seismic reflection data, a systematic description and interpretation approach is required. In siliciclastic and carbonate environments this is provided by the well-established method of seismic stratigraphy. In contrast, volcanic rocks are relatively poorly defined, and at present only margin-scale structures have been recognised. By applying seismic stratigraphy to volcanic rocks, this thesis attempts to gain

some insight into temporal and spatial variations of the basin into which the volcanic rocks are emplaced. In order to achieve this, the fundamental objectives were;

− To calibrate the response of seismic reflection data to volcanic lithologies and explore the validity of using seismic stratigraphy to interpret the emplacement and distribution of the volcanic rocks

− To recognise cycles of volcanic activity, in particular how the emplacement of volcanic rocks record variations in accommodation, supply and relative sea level.

− To identify unique volcanic morphological features and relate them to volcanic processes, such as lava-water interaction, erosion and remobilisation.

− To suggest suitable outcrop analogues that exhibit similarities to the stratigraphic geometries and geomorphological features identified in seismic data.

7.2.1 Seismic Interpretation of Volcanic Rocks

Key to the work presented in this thesis is the hypothesis that the emplacement of volcanic rocks can produce depositional successions that record temporal and spatial variations of the basin into which they emplaced. Therefore volcanic depositional successions should be recognisable in seismic reflection data through the application of seismic stratigraphic concepts, similar to that used for sedimentary successions. The volcanic successions in this study were defined by the systematic analysis of seismic reflection terminations and geometries. This resulted in the identification of cycles of volcanic deposition bounded by seismic reflection surfaces that are considered to record periods of volcanic quiescence and subsequent erosion and/or sedimentary deposition.

In Chapter 4, at least 13 cycles of volcanic activity were recognised through the identification of seismic reflection units using 2D seismic reflection data. Each unit is interpreted to record continuous emplacement during discrete periods of active volcanism. The seismic reflection units appear to have been deposited sequentially, revealing initial deposition was progradational and controlled by large volumes of lava entering the basin and infilling accommodation. An increasingly apparent aggradational element is introduced as accommodation started to increase due to compaction and syn-volcanic subsidence during active delta construction. A decrease in volcanic supply caused a change from progradation to retrogradation, with delta deposition infilling limited volumes of accommodation above the previously deposited seismic reflection units. The accumulation

of accommodation above the main delta body is inferred to be caused by a continuation of volcanic loading and subsidence of the delta during reoccurring periods of little to no delta activity.

The seismic reflection units are defined by bounding reflections which are interpreted to represent hiatal surfaces and may have a time-stratigraphic significance. Each bounding reflection are not a single surface but are an approximation of multiple lava flows at the end of volcanic deposition and the following period of volcanic quiescence. Greater understanding of the seismic reflection units and the bounding reflection surfaces is difficult through seismic data alone, and could only be achieved with high resolution wireline and biostratigraphic calibration, which are currently lacking in offshore volcanic provinces. However, where the bounding reflection surfaces were imaged using 3D seismic reflection data in Chapter 5, there was evidence of minor subaerial erosional processes on the topsets and remobilisation of the foresets. 3D seismic imaging of the seismic reflection units revealed a variety of geomorphologies that are indicative of constructive and destructive depositional processes.

The interpretation of volcanic rocks in Chapter 6 was aided by five exploration wells which penetrated the volcanic succession within the 3D seismic reflection survey. However the volcanic succession was thinner than that in Chapters 4 and 5 with less distinct internal reflections. Volcanism was largely subaerial and the four seismic reflection units identified were deposited sequentially. The seismic reflection units display a simple stacking pattern, with variations produced by the effects of topography and the differing lateral extents of the units. The seismic reflection units recognised in Chapter 6 are most likely composites of multiple periods of eruption and emplacement of extensive, overlapping lava flow fields, rather than individual periods of active volcanism as identified in Chapters 4 and 5. The bounding reflection surfaces not only record the periods of active emplacement but also significant volcanic quiescence and the incision of fluvial channels.

7.2.2 Seismic Stratigraphy of Volcanic Rocks

The depositional patterns recognised using seismic stratigraphy are products of variations in sediment supply, relative sea level and accommodation (e.g. Mitchum *et al*., 1977a; 1977b; Posamentier & Vail, 1988). Traditionally, the dominant control is thought to be relative sea level change on accommodation (Fig. 7.1; see Chapter 3). Delta systems that are largely driven by sea level fluctuations are referred to as "accommodation-driven

deltas" (Schlager, 1993; Porębski & Steel, 2006; Carvajal *et al.*, 2009). However if significant variations in sediment supply occur, the depositional patterns will reflect changes in supply and accommodation, rather than sea level (Schlager, 1993). Despite this, the influence of sediment supply is often overlooked due to the difficulty of quantifying supply in ancient depositional systems (Carvajal *et al.*, 2009). Recent studies of modern deltas have recognised that given sufficiently high sediment supply, deltas are capable of continuous progradation despite fluctuations in sea level and accommodation. These deltas are referred to as "supply-driven deltas" (Schlager, 1993; Burgess & Hovius, 1998; Porębski & Steel, 2006; Carvajal *et al.*, 2009).

This study has recognised that the depositional patterns produced during volcanic activity are primarily driven by volcanic supply (Fig. 7.1). It is fluctuations in supply, rather than sea level that appear to be the dominant control on delta architecture and location within the basin (Schlager, 1993; Porębski & Steel, 2006; Carvajal *et al.*, 2009). During deposition of volcanic supply-driven deltas, accommodation is rapidly infilled by progradational and aggradational successions. If volcanic supply is high enough, progradation will occur throughout the entire sea level cycle, overwriting all but the largest eustatic sea level changes (Fig. 7.1; Schlager, 1993; Porębski & Steel, 2006; Carvajal *et al.*, 2009). This makes it difficult to identify exactly where in the sea level cycle volcanic deposition occurred, relying on additional siliciclastic deposition to indicate position. The deposition of volcanic rocks can also affect accommodation, with an increase in subsidence causing aggradation. Subsidence will often be at a higher rate than eustatic fluctuations in sea level, with any rise in eustatic sea level contributing to an increase in accommodation (Fig. 7.1; Moore, 1970; Lipman, 1995). Subsidence will be the result of syn-volcanic subsidence during active volcanic deposition and the continued effects of loading during periods of little or no volcanic deposition (Moore, 1970; Lipman, 1995; Mattox & Mangan, 1997; Heliker & Mattox, 2003; Kauahikaua *et al.*, 2003).

Additionally, there may be a depositional bias towards volcanic depositional systems. Siliciclastic rocks lithify slowly, with depositional systems prone to erosion and remobilisation that often alters the original depositional geometries (Schlager, 1991; 1993). In contrast, volcanic rocks lithify much faster and depositional systems are potentially less likely to be affected by erosion and remobilisation, except during significant subaerial exposure or prolonged periods of non-deposition (Fisher & Schmincke, 1994). Combined

with increased subsidence during deposition, volcanic depositional systems may be preferentially preserved.

The very nature of volcanic supply-driven deltas may lead to a lack of depositional patterns recognised in traditional seismic stratigraphy. This could include little to no evidence of a fall in eustatic sea level that is faster than subsidence which led to a fall in relative sea level (see Chapter 3; Porębski & Steel, 2006; Carvajal *et al.*, 2009). The lack of a fall in relative sea level may prohibit the development of a sequence boundary, which marks the lowest position of sea level and the greatest extent of subaerial exposure and erosion (see Chapter 3; Posamentier & Vail, 1988; Van Wagoner *et al.*, 1988; Van Wagoner *et al.*, 1990). In volcanic supply-driven deltas, a lack of sequence boundaries is hypothesised to be because there is rarely any true sediment by-pass as lava flows are emplaced as they flow and inflate. Any transition from falling to rising relative sea level will be recorded by an aggradational turnaround from a basinward to a more landward direction (Fig. 7.1; Porębski & Steel, 2006). Despite the potential lack of sequence boundaries, there will be many local erosion surfaces due to the waning of the eruption rate, migration of the vent or location switching of lava tubes (Self *et al.*, 1997; Heliker *et al.*, 1998; Porębski & Steel, 2006).

Assumptions about the depositional patterns of volcanic supply-driven deltas are based upon high and continuous supply rates (Fig. 7.2). However volcanic supply is controlled by duration and volume of the volcanic eruptions, which can be highly variable (Coffin & Eldholm, 1994; Eldholm & Grue, 1994; Bryan *et al.*, 2010). Flood basalt eruptions, such as those that fed the lava flows of the Faroe-Shetland Basin, are characterised by repetitive, long-lived, high flux eruptions separated by periods of short-lived, low flux eruptions and volcanic quiescence. Volcanic supply can also be affected by migration of the erupting source or location switching of the depositing lava flow (Self *et al.*, 1997; Heliker *et al.*, 1998; Passey & Bell, 2007). Where there is a decrease in volcanic supply, the depositional patterns more closely resemble those of traditional seismic stratigraphy (Fig. 7.2). Such variations in volcanic supply would account for the mix of depositional patterns recognised in Chapter 4, from the significant progradational geometries produced by high volume supply to the retrogradational geometries caused by lower volume supply. Therefore interpretation of volcanic systems requires knowledge and understanding of the potential switching between supply-driven and accommodation-driven depositional regimes.
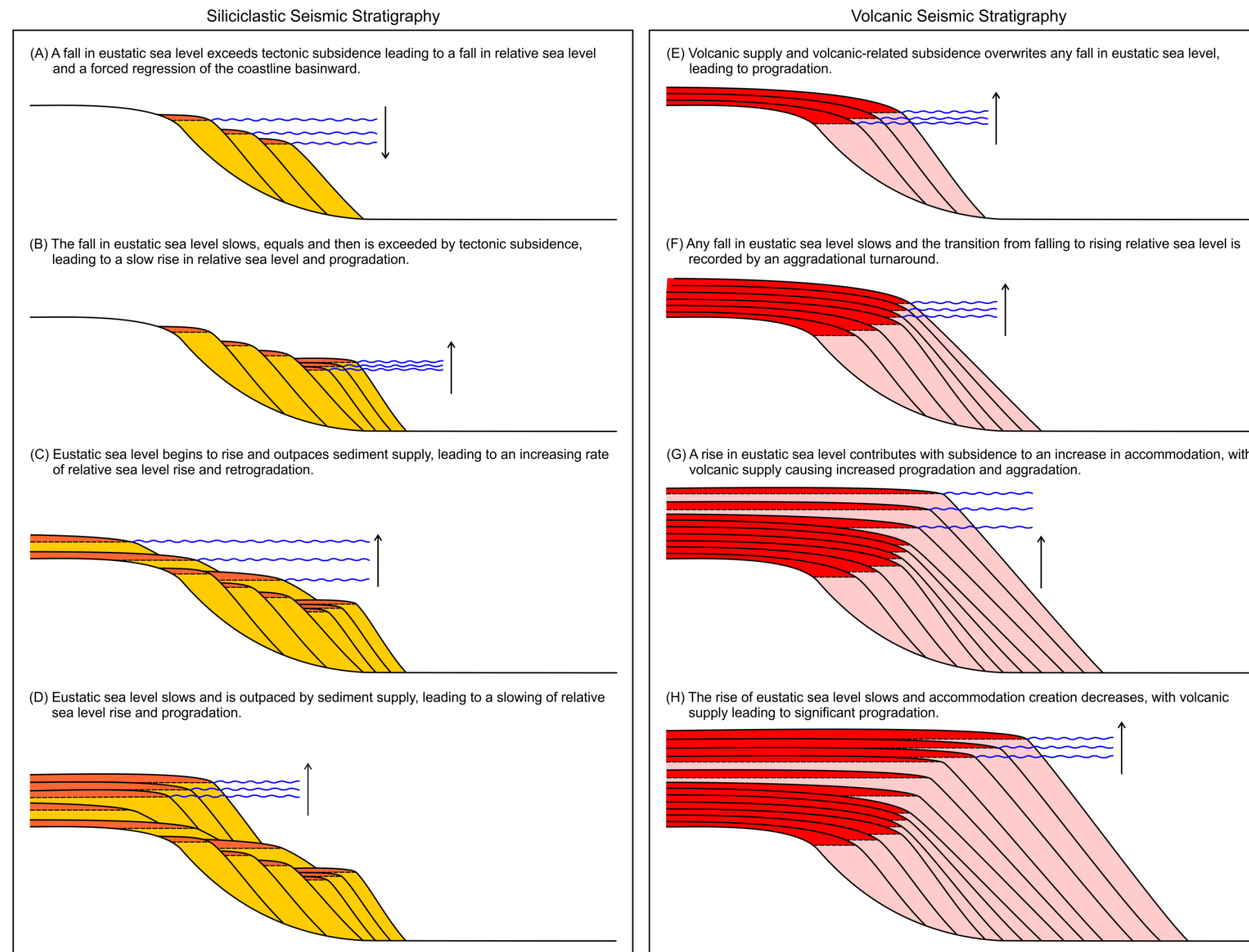
Fig. 7.1. Potential differences in seismic stratigraphy between siliciclastic depositional systems (A – D) and volcanic depositional systems (E-H). (A) A fall in eustatic sea level exceeds tectonic subsidence, leading to a fall in relative sea level. This causes a forced regression as the coastline is forced to build out into the basin. (B) The fall in eustatic sea level slows, equals and then is exceeded by tectonic subsidence, leading to a slow rise in relative sea level and progradation. (C) Eustatic sea level begins to rise and outpaces sediment supply, leading to an increasing rate of relative sea level rise. This causes retrogradation towards the hinterland. (D) Eustatic sea level slows and is outpaced by sediment supply, leading to a slowing of relative sea level rise and progradation. (E) Volcanic supply coupled with volcanic-related subsidence drives progradation and overwrites any fall in sea level. (F) Although sea level fall is not recognised, the transition from falling to rising relative sea level is recorded by an aggradational turnaround from a basinward to a more landward direction. (G) The rise in eustatic sea level contributes to an increase in accommodation, with volcanic supply causing the progradational and aggradation infill of accommodation. (H) The rise of eustatic sea level slows and volcanic supply leads to significant basinward progradation. Based on this study and after Posamentier & Vail (1988), Van Wagoner *et al*. (1988), Van Wagoner *et al*. (1990), Schlager (1993), Porębski & Steel (2006) and Carvajal *et al*. (2009).

7.2.3 Limitations and Uncertainties

As with any study based on seismic reflection data, there are certain interpretation limitations and uncertainties because seismic data are only a representation of the subsurface (Vail *et al*., 1977c; Sheriff & Geldart, 1995). Seismic reflection data are typically good at imaging the subsurface when it consists of layered sedimentary rocks. However the presence of volcanic rocks can have a significant effect on the quality of seismic reflection data (Roberts *et al*., 2005; Gallagher & Dromgoole, 2008; Nelson *et al*., 2009a). Imaging volcanic rocks in seismic reflection data is difficult due to the absorption and attenuation of the seismic waves. When coupled with compaction at depth and the loss of higher frequencies in the volcanic rocks, the resolution within volcanic successions is typically poor (Ogilvie *et al*., 2001; Shaw *et al*. 2008; Nelson *et al*., 2009a).

The seismic reflectivity within volcanic successions is the product of a complex interference pattern generated by the acoustic impedance contrasts between multiple, interbedded lava flows and sedimentary beds and the closely spaced lava flows (Barton *et al*., 1997). Therefore seismic reflection data can only provide low-resolution proxies for individual geological interfaces (Vail *et al*., 1977c; Sheriff & Geldart, 1995). This can affect the interpretation of the seismic data, with limited information and a lack of distinct reflections. The interpretation of seismic reflection data can also be affected by different processing techniques, different stacking velocities and the suppression or enhancement of specific frequencies (Yilmaz & Doherty, 1987; Sheriff & Geldart, 1995; Kearey *et al*., 2002). The data in this thesis were provided already processed and as no in-depth processing reports were supplied, it is impossible to say for certain if, and how, the interpretation would differ. However it should be noted that interpretation of the same area of the subsurface using a variety of data with different input parameters will produce slightly different results.

Much of this thesis is based solely on the interpretation of seismic reflection data and therefore can only provide a certain level of detail. The use of 3D seismic reflection data improved resolution and confidence in the interpretations, with the identification of subsurface structures that were not apparent in 2D seismic data. Access to wireline log data provided more rigorous controls on the seismic reflection data and continued to increase confidence in the interpretations. The work presented in Chapters 4 and 5 used exploration wells that penetrated the distal flood basalts calibrate the response of seismic reflection data to volcanic lithologies. There are currently no exploration wells that

penetrate the lava-fed delta system, but if such data were to become available in the future, it would be possible to provide more detailed information on the ages of the volcanic rocks and the nature of the bounding surfaces of the seismic reflection units. In contrast, the work presented in Chapter 6 was aided by access to closely spaced, high resolution wireline data which provided high resolution calibration of the seismic reflection data.

7.2.4 Use of Field Analogues

Due to the reliance of this study on seismic reflection data, and the resolution limits that are inherent within such datasets, it is critical to ground-truth, where possible, seismic observations with outcrop analogues. Typically structures recognised in seismic reflection data are an order of magnitude larger than those seen in outcrop (Kearey *et al*., 2002; Nelson *et al*., 2009a). However, comparisons between seismic and outcrop observations allow the discrimination of structures which are real from those that may be data artefacts, as well as structures that are likely to be present, but are below seismic resolution. In addition, a number of structures can be process-related and scale-independent. There are no currently active continental flood basalt eruptions, so comparisons have been made with outcrop exposures of ancient flood basalt provinces or with smaller, modern day eruptions where the active emplacement of lava flows have been observed. In this thesis many comparisons have been made between the seismic observations and outcrop analogues, and are based on either field data or the published literature.

The lava-fed delta system investigated in Chapter 4 is first compared to known lava-fed delta outcrops in Greenland and Antarctica which display a variety of seismic and sub-seismic scale features, before focusing on comparisons with the modern lava-fed deltas on the Island of Hawaii. Lava-fed deltas on Hawaii provided suitable outcrop analogues as the extensive pāhoehoe lava flows are similar in emplacement style to continental flood basalts (Hon *et al*., 1994; Self *et al.*, 1997; Kauahikaua *et al.*, 1998). The deltas on Hawaii also undergo subaerial erosion and subaqueous mass-wasting between and during the eruptive phases, and produce features similar to those recognised in Chapter 4. However, due to differences in scale between the lava-fed delta in this study and those on Hawaii, not all the features were comparable. For example, the collapse escarpments originally identified in Chapter 4 were thought to be large-scale lava-bench collapses. With access to the 3D seismic reflection data in Chapter 5, the collapse escarpments were quickly resolved to be much larger in scale and comparable to debris avalanches similar to the catastrophic

gravitational collapse processes that affect large composite volcanoes and ocean island volcanoes (e.g. Siebert, 1984; Lipman *et al.*, 1988; Moore *et al.*, 1994; Oehler *et al.*, 2008).

In addition to resolving the details about the debris avalanche structures and deposits, the surface structures examined in Chapter 5 using 3D seismic reflection data are comparable to those seen in lava-fed deltas in Iceland. The Sølkatla lava-fed delta developed in a glacial melt-water lake in Iceland and provided a suitable outcrop analogue as the thick inflated pāhoehoe lava flows were emplaced from a number of discrete vents and fissures before entering a standing body of water (Piper, 1973; Sigurdsson, *et al.*, 1978; Rossi, 1996). Despite obvious differences in depositional environment, the Sølkatla delta exhibited a number of features recognised from the data used in Chapter 5, including lobate lava flows at the delta front that suggest that the features identified in this study are dependent on process rather than environment.

The lava flows recognised in 3D seismic reflection data Chapter 6 were compared to the Columbia River Basalt Province, where thick successions of subaerial lava flows and interbedded siliciclastic rocks provide suitable outcrop analogues, as they are often large enough to be considered seismic scale. The lava flows of the Columbia River Basalt Province were emplaced as a series of stacked, overlapping flow lobes and coalesced to form continuous lava flow fields (Swanson *et al.*, 1975; Reidel *et al.*, 1992; Self *et al.*, 1996; 1997). Similarities in kilometre-wide lobate flow geometries suggest similar emplacement processes occurred in the Faroe-Shetland Basin. Multiple phases of fluvial incision and siliciclastic deposition across the top of the lava flow fields occurred during periods of volcanic quiescence. Direct comparisons were made where the development of subsequent lava flow fields were affected by the topography of the underlying lava flow field and drainage system, with the emplacement of intra-canyon lava flows damming pre-existing channels and diverting both lava flows and drainage systems (Tolan & Beeson, 1984; Lyle, 2000; Ely *et al.*, 2012).

7.3 The Faroe-Shetland Basin

The continental flood basalts of the Faroe-Shetland Basin provide an excellent case study to test the hypothesis that volcanic rocks produced depositional successions that recorded temporal and spatial variations of the basin into which they were emplaced. The Faroe-Shetland Basin has been extensively imaged, its geological history relatively well defined

and the onshore exposures well documented. The volcanic rocks in the basin have previously been characterised on a regional scale (e.g. Planke *et al*., 2000; Berndt *et al*., 2001), leaving scope for more detailed studies to understand the distribution, internal structure and lateral variations of the flood basalts. In order to gain a greater understanding of continental flood basalts emplacement processes in the Faroe-Shetland Basin, the objectives were;

- To define and map key volcanic successions within the Faroe-Shetland Basin using seismic reflection data to interpret gross distribution, variations in source and supply and pre-existing basin topography.

- To reconstruct the depositional environment of the Faroe-Shetland Basin during the eruption of the continental flood basalts.

- To correlate, where possible, the key volcanic successions identified offshore with the known onshore stratigraphy of the Faroe Island Basalt Group.

7.3.1 Reconstruction of the Depositional Environment

Detailed analysis of multiple 2D and 3D seismic reflection surveys across the Faroe-Shetland Basin has shown that it is possible to identify and interpret the volcanic basin-fill. By constraining the temporal and spatial distribution of key volcanic facies and horizons, it is possible to identify multiple phases of volcanism, variations in volcanic source and supply and to reconstruct the depositional environment. The continental flood basalts of the Faroe-Shetland Basin were emplaced in a subaerial to marine basin that gradually deepened to the north. Initiation of flood basalt volcanism is recorded by the deposition of basal deposits of volcaniclastic and hyaloclastic material (Usktins Peate *et al*., 2003; Ross *et al*., 2005; Jerram *et al*., 2009). Such deposits have been previously identified in many emergent volcanic settings and form volcaniclastic aprons around, and thinning away from, the volcanic sources (Gamberi, 2001; Casalbore *et al*., 2010).

In the Faroe-Shetland Basin this is interpreted to have produced a volcaniclastic fan that preceded the emplacement of the thick continental flood basalts from the Faroese shelf. In the north this fan developed a substantial thickness where the basin was deepest (Fig. 7.2; see Chapter 4 and 5), while in the south the fan was thin and discontinuous as the developing basin remained shallow (Fig. 7.2; see Chapter 6). Early volcanism was also characterised by the eruption of individual volcanic centres in the east and southeast of the basin (e.g. the Erlend Complex, Brendans Dome; Gatliff *et al*., 1984; Ritchie & Hitchen,

1996; Naylor *et al*., 1999; Jolley & Bell, 2002). The volcanic centres erupted lava flows, hyaloclastic breccias and volcaniclastic material into subaerial to brackish environments created significant terrestrial topography in the developing basin (Fig. 7.2; see Chapters 4 and 5; Gatliff *et al*., 1984; Jolley & Bell, 2002).

Flood basalt volcanism became established with the emplacement of thick and extensive lava flow fields from fissures in the northwest, close to what is now the Faroese platform (Dorè *et al*., 1999; Naylor *et al*., 1999). The majority of lava flows were supplied by continuous to multiple, long lived eruption events that aided in their extensive coverage. In the north, an extensive lava-fed delta system developed in the deepest part of the basin (Fig. 7.2; see Chapters 4 and 5). In the south, development of the lava flow fields remained subaerial, with multiple phases of lava flow emplacement (Fig. 7.2; see Chapter 6). During periods of volcanic quiescence, fluvial drainage systems developed across the top of flow fields in a broadly northeast to southwest orientation. The incised channels were constrained by the underlying flow field topography, often incising along the edges of lava flows or between lava flow lobes (Inbar *et al*., 1994). Fluvial incision has not been recognised in the more marine lava fed delta system and it is likely that mass-wasting and fine grained sedimentary deposits accumulated during periods of volcanic quiescence. Erosion and fluvial incision may have occurred on the subaerial lava flows that supplied the delta front and which extend back towards the Faroe Islands but is not resolvable on the 2D seismic reflection data available.

Not all volcanism appears to have been sourced from the fissure systems to the northwest, with the influx of more locally lava flows recorded in the south (Fig. 7.2; see Chapter 6). These lava flow fields were heavily influenced by the surface topography of the underlying lava flow fields and the location of incised drainage systems. The subsequently emplaced lava flows were constrained by minor topographic highs and diverted into topographic lows, re-routing the pre-existing fluvial channels (see Chapter 6). How long this phase of volcanic activity lasted is unknown and no equivalent volcanism has been recognised in the north. Despite this, the majority of lava flows were sourced from voluminous eruptions close to the Faroe Islands. In the north of the basin, this caused extensive progradation, with the palaeo-shoreline migrating up to ~44 km in a south-southeast direction, away from the Faroe Islands and rotating anticlockwise (Fig. 7.2; see Chapter 4). Coincident with this rotation of the delta front are the emplacement of the most extensive subaerial lava

flow fields in the south and the development of a potential palaeo-shoreline (Fig. 7.2; see Chapter 6).

Volcanic activity was followed by a prolong hiatus or decrease in lava supply, that facilitating fluvial incision and left the delta front prone to erosion and reworking by tides, waves and storms (Skilling, 2002; Sansone & Smith, 2006). Gravity-driven debris avalanches modified the delta front with the creation of large arcuate collapse escarpments and low angle deposits of remobilised hyaloclastites (Fig. 7.2; see Chapter 5). When volcanism resumed, it was characterised by decreased supply and more limited extent. This primarily affected the lava-fed delta system in the north of the basin, with retrogradation of the delta front and migration of the palaeo-shoreline up to ~75 km in a north-northwest direction, towards the Faroe Islands and rotating clockwise (Fig. 7.2; see Chapter 4). In the south, thin lava flows have been recognised but have a limited extent (see Chapter 6). Volcanism is known to have continued but was located to the west close to the Faroe Islands and to the north where sea floor spreading was initiating. The end of volcanic activity in the Faroe-Shetland Basin is recognised by the deposition of the Balder Formation. The Balder Formation is composed of predominantly deep water siliciclastic rocks and reworked volcanic tuffs and records a marine transgression across the whole basin (Underhill, 2001; Ellis *et al*., 2002; Smallwood & Gill, 2002; Spitzer *et al*., 2008). Along the lava-fed delta this coincided with the remobilisation of volcaniclastic sediment in to localized, gravity-driven high density slurries (see Chapter 4).
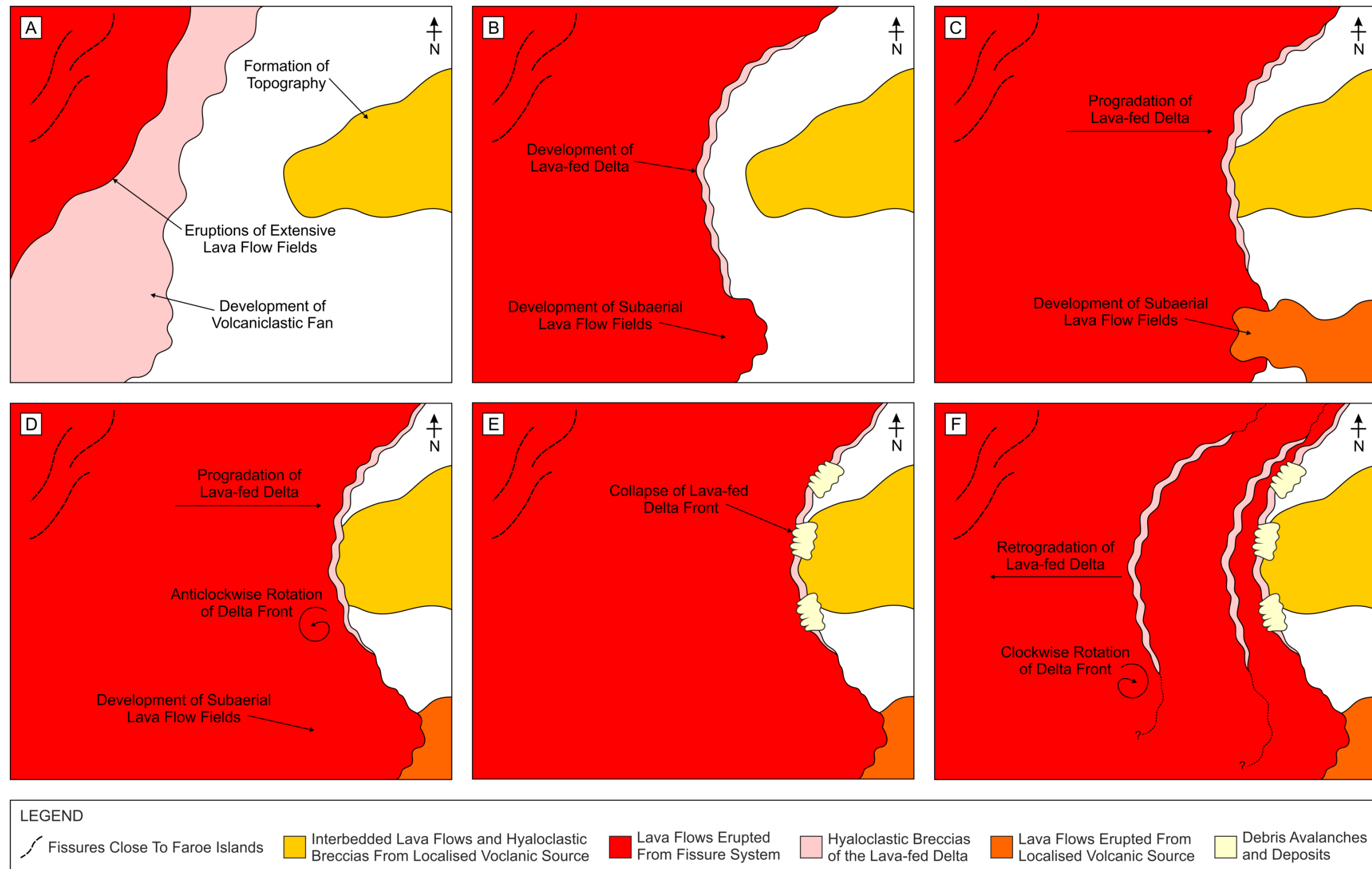
Fig. 7.2. Schematic palaeogeographic reconstruction of the development of the volcanic rocks in the Faroe-Shetland Basin based on this study. (A) Initiation of flood basalt volcanism produced a volcaniclastic fan that preceded the emplacement of the continental flood basalts. In addition, the eruption of individual volcanic centres created significant terrestrial topography in the developing basin. (B) Flood basalt volcanism became established with the emplacement of thick and extensive lava flow fields in the south and development of an lava-fed delta system in the north of the basin (C) The influx of more locally erupted lava flows in the south during a period of volcanic quiescence. (D) Continued volcanic activity cause the anticlockwise progradation of the lava-fed delta system in the north and the emplacement of lava flow fields in the south. (E) A decrease or hiatus in volcanic activity lead to the collapse and modification of the lava-fed delta front by gravity-driven debris avalanches. (F) Volcanism resumed with decreased supply, leading to retrogradation of delta and limited lava flows in south. Based on this study and after Stoker *et al*. (1993), Naylor *et al*. (1999) and Ellis *et al*. (2002).

7.3.2 Correlation to Onshore Stratigraphy

The reconstruction of emplacement history of continental flood basalts in the Faroe-Shetland Basin and correlation with onshore stratigraphy is based on key volcanic facies and seismic reflection relationships. On the Faroe Islands, the flood basalts are known to have a stratigraphic thickness of at least ~6.6 km and have been subdivided on the basis of lithology, geochemistry and lava flow structure (see Chapter 2, Fig. 2.3). The evolution of the flood basalts is recorded by the eruption of four volcanic formations, with three inter-basalt sedimentary formations that record periods of quiescence between the volcanic eruptions (Fig. 7.3; Ellis *et al.*, 2002; Passey & Bell, 2007; Passey & Jolley, 2009). The volcanic rocks recognised in this study likely only represent a small part of the continental flood basalts that were erupted in the Faroe-Shetland Basin. Initial volcanism in the Faroe-Shetland Basin is recorded by thick basal deposits of subaqueous hyaloclastic breccias and lava flows of the Lopra Formation (Ellis *et al.*, 2002; Passey & Bell, 2007; Passey & Jolley, 2009). Volcaniclastic and hyaloclastic material has been inferred at the base of the volcanic successions in the both marine basin examined in Chapters 4 and 5, as well as the subaerial to shallow marine depositional environment in Chapter 6.

On the Faroe Islands, the Lopra formation is overlain by the Beinisvørð Formation. The Beinisvørð Formation is composed of thick, subaerial pāhoehoe lava flows that signify the establishment of extensive, voluminous flood basalt volcanism. The flows were emplaced as multiple lava flow lobes which coalesced to form lava flow fields, with a continuous supply of magma from extensive fissure systems close to the Faroe Island facilitating the extensive nature of the formation (Self *et al.*, 1996; 1998; Jerram & Widdowson, 2005; Passey & Bell, 2007). The majority of the lava flows emplaced offshore of the Faroe Islands are interpreted to be the equivalent of the Beinisvørð Formation (Smythe *et al.*, 1983; Kiørboe, 1999; Ritchie *et al.*, 1999). In the north of the basin, the Beinisvørð Formation is interpreted to have constructed an extensive lava-fed delta system when the lava flows reached the palaeo-shoreline. Onshore the formation is composed of multiple eruptive phases often separated by palaeosols, while offshore multiple phase of delta construction have been recognised (see Chapter 4 and 5; Smythe *et al.*, 1983; Kiørboe, 1999; Ritchie *et al.*, 1999; Passey & Bell, 2007; Passey & Jolley, 2009). In the south of the basin, the Beinisvørð Formation is interpreted to have been emplaced as a series of extensive and overlapping subaerial lava flow fields (see Chapter 6). Here the offshore formation appears to be composed of fewer eruptive phases. This discrepancy is because to the south the

seismic reflection units of the lava-fed delta thin below seismic resolution and cannot be correlated with the seismic reflection units of the subaerial lava flow fields. This indicates that each of the seismic reflection units identified in Chapter 6 is a composite of multiple eruptive phases that formed individual seismic reflection units in Chapters 4 and 5.

In the offshore volcanic successions, periods of active volcanism are interpreted to have been followed by periods of limited or no volcanism, similar to those recognised in the onshore exposure of the Beinisvørð Formation (Ellis *et al.*, 2002; Passey & Bell, 2007; Passey & Jolley, 2009). This has been recognised in the erosion and collapse of the lava-fed delta front (see Chapters 4 and 5) and fluvial incision of the fluvial incision of the subaerial lava flow fields (see Chapter 6). In addition, localised subaerial eruptions within the Faroe-Shetland Basin have been identified in both the marine basin to the north and the subaerial to shallow marine basin in the south (see Chapters 4, 5 and 6). The exact relationship between the localised volcanic eruptions and the Beinisvørð Formation is unknown. Without more extensive seismic reflection data and robust geochemical or biostratigraphical well data, the precise correlation of onshore and offshore volcanic stratigraphy is difficult.
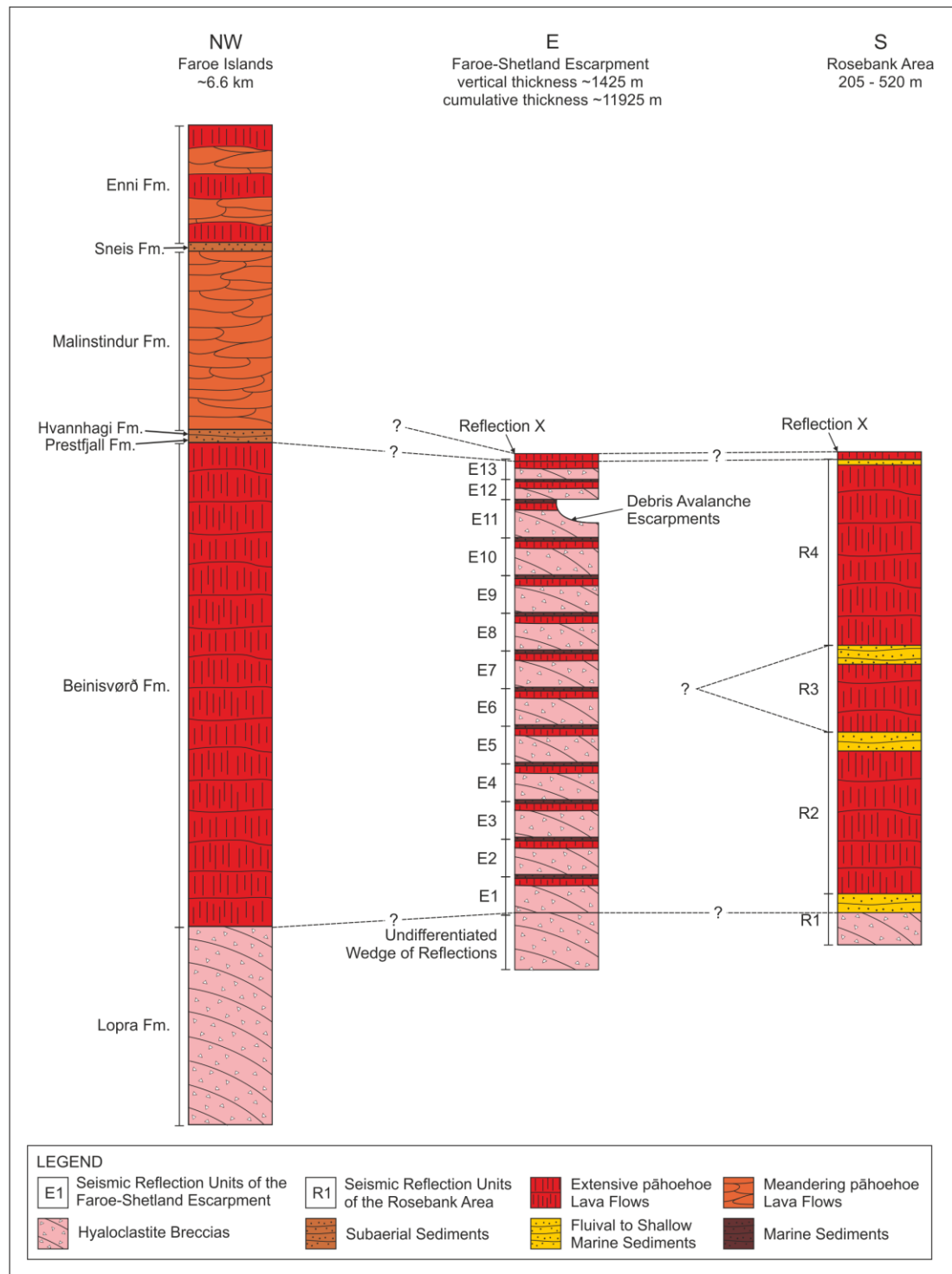
Fig. 7.3. Schematic diagram showing the potential correlation of volcanic stratigraphy of the onshore Faroe Islands and the offshore volcanic stratigraphy recognised in this study (see Chapters 4, 5 and 6). Average thicknesses are given, with both the vertical thickness and cumulative lateral thickness of the Faroe-Shetland Escarpment. Onshore stratigraphy modified from Ellis *et al*. (2002), Passey & Bell (2007) and Passey & Jolley (2009).

7.3.3 Implications for Hydrocarbon Exploration

The data used in this thesis was used by the petroleum industry to interpret the subsurface in order to reduce the risk of failure during hydrocarbon exploration (Nestvold, 1996; Hart, 1999; Stewart & Holt, 2004; Rohrman, 2007). Volcanic rocks are typically not of economic importance and were previously not interpreted in detail. However in the exploration of volcanically-rifted margins, knowledge of the temporal and spatial distribution of volcanic rocks is essential because they can significantly impact the methods used for exploration (e.g. acquisition of seismic reflection data and drilling of exploration wells), the complexity of the hydrocarbon system, and the quality and distribution of reservoir rocks. Therefore significant attention was given to the interpretation of volcanic rocks imaged in the seismic data across the Faroe-Shetland Basin, with the aim that knowledge of the temporal and spatial distribution of volcanic rocks may be of use for future exploration, including;

- Lava flows are gravity-driven and are affected by the underlying topography, potential putting volcanic deposition in competition with siliciclastic deposition, resulting in complex depositional successions (see Chapter 6).

- Where incising fluvial systems develop across the lava flow fields, there is the potential for the channels to be dominated by volcaniclastic material. The inclusion of volcaniclastic material can drastically reduce primary porosity of the siliciclastic reservoirs through the alteration of volcanic glass into clay (Vernik, 1990; Mathisen & McPherson, 1991; Petford, 20).

- If the primary porosity of lava flow crust is preserved at depth, the highly vesicular and fractured lava flow crusts can act as aquifers or migration pathways. In the Columbia River Flood Basalt Province, upper crusts of lava flows are extremely good aquifers with water flow and recharge controlled by intra-flow structures and regional stratigraphy (e.g. Hansen *et al.*,1994; Tolan *et al.*, 2009; Lindsey *et al.*, 2011).

- Alternatively, the dense, highly crystalline lava flow cores are impermeable at depth (despite cooling joints and fractures) they may serve as seals if they are laterally extensive.

7.4 Conclusions

The research presented in this thesis provides valuable insights into the seismic interpretation of volcanic rocks. By examining in detail the character, structure and extent of volcanic rocks in seismic reflection data and how the emplacement of volcanic rocks recorded the spatial and temporal evolution of the basin. In particular, this study has utilised 2D and 3D seismic reflection data from the Faroe-Shetland Basin to provide specific examples of volcanic structures and the development of the depositional environment during continental flood basalt emplacement. The extensive mapping and detailed characterisation of the seismic reflections carried out in this study have enhanced the understanding of the emplacement of continental flood basalts in subaerial to marine environments. Whilst this study has only focused on the Faroe-Shetland Basin, it is anticipated that the results are relevant to the volcanic rocks of other volcanically rifted margins.

7.4.1 Fundamental Conclusions

With increasing understanding of the distribution of flood basalts, the identification of outcrop analogues and improved seismic imaging techniques, the emplacement of volcanic rocks can now be recognised as a record of basin development. The following conclusions are based on the fundamental aims and objectives of this thesis;

− The acquisition of extensive 2D and 3D seismic reflection data, in a bid to understand basin structure and hydrocarbon accumulations, offers a unique opportunity to study large-scale, buried volcanic structures that are not necessarily accessible at the surface due to limited 3D exposure or outcrop erosion.

− It is possible to characterise volcanic rocks in seismic reflection data in their reflection geometries and terminations and through the application of seismic stratigraphic concepts, it is possible to understand the development history of the basin and the emplacement environment of volcanic rocks. However volcanic systems are primarily controlled by lava supply and can produce different depositional patterns to more conventional sedimentary basin-fill. An increase in volcanic supply has the potential to overwrite any changes in sea level, while a decrease in volcanic supply will produce depositional geometries close to traditional siliciclastic seismic stratigraphy.

－ The emplacement of volcanic rocks results in distinct depositional successions bounded by reflection surfaces that may have a time-stratigraphic significance. Definitive conclusions concerning the exact nature of the depositional successions and the bounding seismic reflections can only be achieved with high resolution wireline and biostratigraphic calibration, which is currently lacking in offshore volcanic provinces.

－ The correlation of volcanic horizons within different areas of a basin is difficult. This is because volcanic rocks can vary greatly over relatively small distances. Limited correlation can be done using the assumption that seismic reflections are chronostratigraphic but robust correlations can only be done using high resolution geochemical and biostratigraphic well data, which was not available to this study.

－ Many of the morphological structures interpreted from the seismic reflection data are directly comparable to interpretations of outcrop analogues which have proven useful in interpreting the emplacement environment. A number of the structures also appear to be process-related and scale-independent, indicating that similar processes that occur during both small-volume and large-volume eruptions.

7.4.2 Case Study Conclusions

By undertaking detailed seismic analysis of the volcanic rocks of the Faroe-Shetland Basin, and correlating them with high resolution well data where available, it has been possible to reconstruct the volcanic basin-fill, an essential first-step in understanding how volcanic rocks have impacted the depositional environment and for helping future hydrocarbon exploration. The following conclusions are based on the case study aims and objectives of this thesis;

－ The lava flows in the Faroe-Shetland Basin were derived from multiple sources, including extensive pāhoehoe lava flows from high volume eruptions interpreted to be fed from fissure systems close to the Faroese shelf and from less widespread lava flows from low-volume eruptions fed from individual volcanic centres within the basin.

－ In the north of the basin the lava flows constructed an extensive lava-fed delta system. The gross architecture of the lava-fed delta records variations in lava supply and the creation of accommodation. Overall, the lava-fed delta system shows up to ~44 km of progradation in an east-southwest direction due to large-

volume eruptions of lava filling the basin. The later stages of the delta were dominated by smaller-volume eruptions coupled with an increase in accommodation, which caused the retrogradation of the delta of up to ~75 km north-northwest direction.

− The delta system also underwent two phases of remobilisation; the first occurred during or just after delta deposition and greatly modified the delta front. These have been interpreted as gravity-driven debris avalanches and are comparable to the gravitational collapse processes that occur at large composite volcanoes and ocean island volcanoes. The second phase occurred after delta growth and emplaced high density slurries of volcaniclastic material derived from the local erosion of the delta front during deposition of the Balder Formation.

− South of the lava-fed delta system the lava flows were emplaced in a subaerial to shallow marine environment. Volcanism was characterised by multiple periods of extensive lava flow field emplacement, with subsequent lava flow emplacement affected by the topography of the underlying lava flow field. During periods of volcanic quiescence, incising drainage systems developed across the top of the lava flow fields in broadly northeast to southwest orientation and were constrained by the underlying lava flow field topography.

− The volcanic rocks within this study have been correlated to the Lopra and Beinisvørð Formation of the Faroe Island Basalt Group, which record the early stages of the North Atlantic Igneous Province. However correlation has been limited and would be improved with access to more extensive seismic reflection data and robust geochemical or biostratigraphical well data.

7.4.3 Recommendations for Further Work

The conclusions of this thesis have helped define future research pathways that would aid in a more comprehensive understanding of continental flood basalts, both in the Faroe-Shetland Basin and other Large Igneous Provinces. The outlined research avenues would provide better constraints on the distributions and variations of volcanic rocks and may be able to quantify unknown elements such as rates of syn-volcanic subsidence, durations of lava-fed delta development and correlation with onshore volcanic stratigraphy. These include;

－ Comparison of the seismic observations of the volcanic rocks in this study with volcanic rocks located in other volcanic basins, such as the western coast of Australia, offshore Deccan traps or Hawaii. This would clarify which volcanic structures are commonly associated with continental flood basalts and how the emplacement of volcanic rocks differs depending on the basin geometry, volcanic supply and eruption source (fissure verses volcano).

－ Access to more extensive seismic reflection data and integration of high resolution geochemical and biostratigraphical well data of the thicker volcanic successions, especially those close to the lava-fed delta system of the Faroe-Shetland Basin. This would provide more insight into the nature of the volcanic depositional successions and the bounding reflection surfaces. These data would also help to understand variations in volcanic source and supply, constrain durations and better correlation the offshore volcanic stratigraphy across the basin and with the known onshore stratigraphy.

－ Greater knowledge of outcrop analogues in order to understand lithological variations of volcanic rocks and the nature of the foreset reflections of the lava-fed delta system. For example, the extensive lava-fed deltas recognised on Greenland and Antarctica are well known but there are limited studies done on their lithological variations and the effect this has on seismic reflection data.

－ Quantitative analysis of the use of the equation of Hon *et al*. (1994) to determine duration of lava flow emplacement in the Faroe-Shetland Basin. In addition, comparison of the progradational rates calculated using this equation with the known progradational rates of historical lava-fed deltas. This requires more a detailed examination of historical lava-fed deltas than is currently available in the currently available literature.

－ The use of isostatic loading modelling the amount of volcanic-related subsidence associated with the emplacement of the continental flood basalts, in particular the lava-fed delta system, in order to resolve how it affects the creation of accommodation.

BIBLIOGRAPHY

A

Allen, R.M., Nolet, G., Morgan, W.J., Vogfjörd, K., Nettles, M., Ekström, G., Bergsson, B.H., Erlendsson, P., Foulger, G.R., Jakobsdóttir, Julian, B.R., Pritchard, M., Ragnarsson, S. & Stefánsson, R. (2002). Plume-driven plumbing and crustal formation in Iceland. *Journal of Geophysical Research*, 107 (B8), 2163-2182.

Andersen, M.S. (1988). Late Cretaceous and early Tertiary extension and volcanism around the Faeroe Islands. In: *Early Tertiary Volcanism and the Opening of the NE Atlantic* (edited by A.C. Morton & L.M. Parson). The Geological Society of London Special Publications, 39, 115-122.

Anderson, D.L. (1994). The sublithospheric mantle as the source of continental flood basalts; the case against the continental lithosphere and plume head reservoirs. *Earth and Planetary Science Letters*, 123, 269-280.

Anderson, S.W., Stofan, E.R., Smrekar, S.E., Guest, J.E. & Wood, B. (1999). Pulsed inflation of Pāhoehoe lava flows: implications for flood basalt emplacement. *Earth and Planetary Science Letters*, 168, 7-18.

Andersen, M.S., Nielsen, T., Sørensen, A.B., Boldreel, L.O. & Kuijpers, A. (2000). Cenozoic sediment distribution and tectonic movements in the Faroe region. *Global and Planetary Change*, 24, 239-259.

Asquith, G., Krygowski, D., Henderson, S. & Hurley, N. (2004). *Basic Well Log Analysis*, 2nd Edition. American Association of Petroleum Geologists Methods in Exploration Series, 16, pp. 244.

Archer, S.G., Bergman, S.C., Iliffe, J., Murphy, C.M. & Thornton M. (2005). Palaeogene igneous rocks reveal new insights into the geodynamic evolution and petroleum potential of the Rockall Trough, NE Atlantic Margin. *Basin Research*, 17, 171-201.

Ashcroft, W. (2011). *A Petroleum Geologist's Guide to Seismic Reflection*. Wiley-Blackwell, pp. 157.

B

Bacon, M., Simm, R. & Redshaw, T. (2007). *3-D Seismic Interpretation*. Cambridge University Press, pp. 225.

Barton, A.J. & White, R.S. (1997). Volcanism on the Rockall continental margin. *Journal of the Geological Society of London*, 154, 531-536.

Bell, B.R. & Jolley, D.W. (1997). Application of palynological data to the chronology of the Palaeogene lava fields of the British Province: implications for magmatic stratigraphy. *The Journal of the Geological Society of London*, 154, 701-708.

Bell, B.R. & Butcher, H. (2002). On the emplacement of sill complexes: evidence from the Faroe-Shetland Basin. In: *The North Atlantic Igneous Province: Stratigraphy, Tectonic, Volcanic and Magmatic Processes* (edited by D.W. Jolley & B.R. Bell). The Geological Society of London Special Publications, 197, 307-329.

Bergh, S.F. & Sigvaldason, G.E. (1991). Pleistocene mass-flow deposits of basaltic hyaloclastite on a shallow submarine shelf, South Iceland. *Bulletin of Volcanology*, 53 (8), 597-611.

Berndt, C., Planke, S., Alvestad, E., Tsikalas, F. & Rasussen, T. (2001). Seismic volcanostratigraphy of the Norwegian Margin: constraints on tectonomagmatic break-up processes. *Journal of the Geological Society of London*, 158, 413-426.

Berndt, C., Bünz, S., Clayton, T., Mienert, J. & Saunders, M. (2004). Seismic character of bottom simulating reflectors: examples from the mid-Norwegian margin. *Marine and Petroleum Geology*, 21, 723-733.

Blatt, H. & Jones, R.L. (1975). Proportions of Exposed Igneous, Metamorphic, and Sedimentary Rocks. *Geological Society of America Bulletin*, 86 (8), 1085-1088.

Bojesen-Koefoed, J.A., Christiansen, F.G., Nytoft, H.P. & Pedersen, A.K. (1999). Oil seepage onshore West Greenland: evidence of multiple source rocks and oil mixing. In: *Petroleum Geology of Northwest Europe: Proceedings of the 5th Conference* (edited by A.J. Fleet & S.A.R. Boldy). The Geological Society of London, 305-314.

Boldreel, L.O. & Andersen, M.S. (1993). Late Paleocene to Miocene compression in the Faeroe-Rockall area. In: *Petroleum Geology of Northwest Europe: Proceedings of the 4th Conference* (edited by J.R. Parker). The Geological Society of London, 1025-1034.

Boldreel, L.O. & Andersen, M.S. (1994). Tertiary development of the Faeroe-Rockall Plateau based on reflection seismic data. *Bulletin of the Geological Society of Denmark*, 41, 162-180.

Boldreel, L.O. (2006). Wire-line log-based stratigraphy of flood basalts from the Lopra-1/1A well, Faroe Islands. In: *Scientific results from the deepened Lopra-1 borehole, Faroe Islands* (edited by J.A. Chalmers & R. Waagstein). Geological Survey of Denmark and Greenland Bulletin, 9, 7-22.

Brown, A.R. (2005). *Interpretation of Three-Dimensional Seismic Data*, 6th edition. American Association of Petroleum Geologists Memoir 42 & Society of Economic Geologists, Investigations in Geophysics 9, pp. 646.

Brown, D.J., Holohan, E.P. & Bell, B.R. (2009). Sedimentary and volcano-tectonic processes in the British Paleocene Igneous Province: a review. *Geological Magazine*, 146 (3), 326-352.

Brown, R.J., Blake, S., Bondre, N.R., Phadnis, V.M. & Self, S. (2011). 'A'ā lava flows in the Deccan Volcanic Province, India, and their significance for the nature of continental flood basalt eruptions. *Bulletin of Volcanology*, 73 (6), 737-752.

Bryan, S.E., Riley, T.R., Jerram, D.A., Stephans, C.J. & Leat, P.T. (2002). Silicic volcanism: An undervalued component of large igneous provinces and volcanic rifted margins. In: *Volcanic Rifted Margins* (edited by M.A. Menzies, S.L. Klemperer, C.J. Ebinger, & J. Baker). The Geological Society of America Special Paper, 362, 99–120.

Bryan, S.E. & Ernst, R.E. (2008). Revised definition of Large Igneous Provinces (LIPs). *Earth-Science Reviews*, 86, 175-202.

Bryan, S.E., Uktins Peate, I., Peate, D.W., Self, S., Jerram, D.A., Mawby M.R., Marsh, J.S. & Miller, J.A. (2010). The largest volcanic eruptions of Earth. *Earth Science Reviews*, 102, 207-229.

Bubb, J.N. & Hatlelid, W.G. (1977). Seismic Stratigraphy and Global Changes of Sea Level, Part 10: Seismic Recognition of Carbonate build-ups. In: *Seismic Stratigraphy – Applications to Hydrocarbon Exploration* (edited by C.E. Payton). American Association of Petroleum Geologists Memoirs, 26, 185-204.

Bugge, T., Befring, S., Belderson, R.H., Eidvin, T., Jasen, E., Kenyon, N.H., Holtedahl, H. & Sejrup, H.P. (1987). A Giant Three-Stage Submarine Slide Off Norway. *Geo-Marine Letters*, 7, 191-198.

Buol, S.W., Hole, F.D. & McCracken, R.J. (1989). *Soil Genesis and Classification*, 3rd ed. Iowa State University Press, pp. 494.

Burgess, P.M. & Hovius, N. (1998). Rates of delta progradation during highstands: consequences for timing of deposition in deep-marine systems. *Journal of the Geological Society of London*, 155, 217-222.

Burke, K. & Torsvik, T.H. (2004). Derivation of Large Igneous Provinces of the past 200 million years from long-term heterogeneities in the deep mantle. *Earth and Planetary Science Letters*, 227, 531-538.

C

Calvès, G., Schwab, A.M., Huuse, M., Cliff, P.D., Gaina, C., Jolley, D., Tabrez, A.R. & Inam, A. (2011). Seismic volcanostratigraphy of the western Indian rifted margin: The pre-Deccan igneous province. *Journal of Geophysical Research*, 116, 1-28.

Camp, V.E. (1981). Geologic studies of the Columbia Plateau: Part II. Upper Miocene basalt distribution, reflecting source locations, tectonism, and drainage history in the Clearwater embayment, Idaho. *Geological Society of American Bulletin*, 92 (9), 669-678.

Camp, V.E. (1995). Mid-Miocene propagation of the Yellowstone mantle plume head beneath the Columbia River basalt source region. *Geology*, 23 (5), 435-438.

Campbell, I.H. & Griffiths, R.W. (1990). Implications of mantle plume structure for the evolution of flood basalts. *Earth and Planetary Science Letters,* 99, 79-93.

Carracedo, J.C., Day, S.J., Gullou, H.G. & Gravestock, P. (1999). Later stages of volcanic evolution of La Palma, Canary Islands: Rift evolution, giant landslides, and the genesis of the Caldera de Taburiente. *Geological Society of America Bulletin,* 111 (5), 755-768.

Carracedo Sánchez, M., Sarrionandia, F., Juteau, T. & Gill Ibarguchi. J.I. (2012). Structure and organization of submarine basaltic flows: sheet flow transformation into pillow lavas in shallow submarine environments. *International Journal of Earth Science*, 101 (8), 2201-2214.

Cartwright, J. & Huuse, M. (2005). 3D seismic technology: the geological 'Hubble'. *Basin Research*, 17, 1–20.

Carvajal, C., Steel, R. & Petter,A. (2009). Sediment supply: The main driver of shelf-margin growth. *Earth Science Reviews*, 96, 221-248.

Casalbore, D., Romagnoli, C., Chiocci, F. & Frezza, V. (2010). Morpho-sedimentary characteristics of the volcaniclastic apron around Stromboli volcano (Italy). *Marine Geology*, 269, 132-148.

Catuneanu, O., Abreu, V., Bhattacharya, J.P., Blum, M.D., Dalrymple, R.W., Eriksson, P.G., Fielding, C.R., Fisher, W.L., Galloway, W.E., Gibling, M.R., Giles, K.A., Holbrook, J.M., Jordan, R., Kendall, C.G.St.C., Macurda, B., Martinsen, O.J., Miall, A.D., Neal, J.E., Nummedal, D., Poma, L., Posamentier, H.W., Pratt, L., Sarg, J.F., Shanley, K.W., Steel, R.J., Strasser, A., Tucker, M.E. & Winker, C. (2009). Towards the standardization of sequence stratigraphy. *Earth-Science Reviews*, 92, 1-33.

Catuneanu, O. (2002). Sequence stratigraphy of clastic systems: concepts, merits, and pitfalls. *Journal of African Earth Sciences*, 35, 1-43.

Catuneanu, O., Bhattacharya, J.P., Blum, M.D., Dalrymple, R.W., Eriksson, P.G., Fielding, C.R., Fisher, W.L., Galloway, W.E., Gianolla, P., Gibling, M.R., Giles, K.A., Holbrook, J.M., Jordan, R., Kendall, C.G.St.C., Macurda, B., Martinsen, O.J., Miall, A.D., Nummedal, D., Posamentier, H.W., Pratt, B.R., Shanley, K.W., Steel, R.J., Strasser, A. & Tucker, M.E. (2010). Sequence stratigraphy: common ground after three decades of development. *First Break*, 28, 21-34.

Catuneanu, O., Galloway, W.E., Kendall, C.G.St.C., Miall, A.D., Posamentier, H.W., Strasser, A. & Tucker, M.E. (2011). Sequence Stratigraphy: Methodology and Nomenclature. *Newsletters on Stratigraphy*, 44 (3), 173-245.

Ceramicola, S. Stoker, M., Praeg, D., Shannon, P.M., De Santis, L., Hoult, R., Hjelstuen, B.O., Laberg, S. & Mathiesen, A. (2005). Anomalous Cenozoic subsidence along the 'passive' continental margin from Ireland to mid-Norway. *Marine and Petroleum Geology*, 22, 1045-1067.

Chalmers, J.A. & Westerm, P.G. (1979). A Tertiary igneous centre north of the Shetland Islands. S*cottish Journal of Geology*, 15, 333-341.

Chalmers, J.A. & Waagstein, R. (2006). Scientific results from the deepened Lopra-1 borehole, Faroe Islands. *Geological Survey of Denmark and Greenland Bulletin*, 9, pp. 160.

Chropra, S. & Marfurt, K.J. (2007). *Seismic Attributes for Prospect Identification and Reservoir Characterization*. Society of Economic Geologists Geophysical Developments, 11, pp. 464.

Coffin, F.M. & Eldhom, O. (1992). Volcanism and continental break-up: a global compilation of large igneous provinces. In: *Magmatism and the Causes of Continental Break-up* (edited by B. C. Storey, T. Alabaster & R. J. Pankhurst). The Geological Society of London Special Publication, 68, 17-30.

Coffin, F.M. & Eldhom, O. (1994). Large Igneous Provinces: Crustal structure, dimensions, and external consequences. *Reviews of Geophysics*, 32(1), 1-36.

Coleman, J.M. (1988). Dynamic changes and processes in the Mississippi River delta. G*eological Society of America Bulletin*, 100, 999-1015.

Cooper, M.M., Evans, A.C., Lynch, D.J., Neville, G. & Newley, T. (1999). The Foinaven Field: managing reservoir development uncertainty prior to start-up. In *Petroleum Geology of Northwest Europe: Proceedings of the 5th Conference* (edited by A.J. Fleet & S.A.R. Boldy). The Geological Society of London, 675-682.

Corbett, J.R. (1968). The Genesis of some Basaltic Soils in New South Wales. *European Journal of Soil Science*, 19(1), 174-185.

Correggiari, A., Cattaneo, A. & Trincardi, F. (2005). The modern Po Delta system: Lobe switching and asymmetric prodelta growth. *Marine Geology*, 222-223, 49-74.

Courtillot, V., Jaupart, C., Manighettic, I., Tapponnier, P. & Besse, J. (1999). On causal links between flood basalts and continental breakup. *Earth and Planetary Science Letters*, 166, 177-195.

Courtillot, V. & Renne, P.R. (2003). On the ages of flood basalt events. *Comptes Rendus Geoscience*, 335, 113-140.

Cross, T.A. & Lessenger, M.A. (1988). Seismic Stratigraphy. *Annual Review of Earth and Planetary Sciences*, 16, 19-54.

Crown, D.A. & Baloga, S.M. (1999). Pahoehoe toe dimensions, morphology, and branching relationships at Mauna Ulu, Kilauea Volcano, Hawai'i. *Bulletin of Volcanology*, 61 (5), 288-305.

Cukur, D., Horozal, S., Kim, D.C., Lee, G.H., Han, H.C. & Kang, M.H. (2010). The distribution and characteristics of the igneous complexes in the northern East China Sea Shelf Basin and their implications for hydrocarbon potential. *Marine Geophysical Research*, 31, 299-313.

D

Dam, G., Larsen, M. & Sønderholm, M. (1998). Sedimentary response to mantle plumes: Implications from Paleocene onshore successions, West and East Greenland. *Geology*, 26 (3), 207-210.

Dam, G. (2002). Sedimentology of magmatically and structurally controlled outburst valleys along rifted volcanic margins: examples from the Nuussuaq Basin, West Greenland. *Sedimentology*, 49, 505–532.

Dan, J. & Singer, A. (1973). Soil Evolution on basalt and Basic Pyroclastic Materials in the Golan Heights. *Geoderma*, 9, 165-192.

Davies, R.J., Bell, B.R., Cartwright, J.A. & Shoulders, S. (2002). Three-dimensional seismic imaging of Paleogene dike-fed submarine volcanoes from the northeast Atlantic margin. *Geology*, 30 (3), 223-226.

Davies, R.J., Cloke, I., Cartwright, J., Robinson, A. & Ferrero, C. (2004). Post-breakup compression of a passive margin and its impact on hydrocarbon prospectivity: An example from the Tertiary of the Faeroe–Shetland Basin, United Kingdom. *American Association of Petroleum Geologists Bulletin*, 88 (1), 1–20.

Davies, R.J. & Posamentier, H.W. (2005). Geologic processes in sedimentary basins inferred from three-dimensional seismic imaging. *GSA Today*, 15 (10), 4-9.

Davison, I., Stasiuk, S., Nuttall, P. & Keane, P. (2010). Sub-basalt hydrocarbon prospectivity in the Rockall, Faroe-Shetland and Møre basins, NE Atlantic. In: *Petroleum Geology: From Mature Basins to New Frontiers - Proceedings of the 7th Conference* (edited by B.A. Vining & S.C. Pickering). The Geological Society of London, 1025-1032.

Dean, K., Mclachlan, K. & Chambers, A. (1999). Rifting and the Development of the Faeroe-Shetland Basin. In *Petroleum Geology of Northwest Europe: Proceedings of the 5th Conference* (edited by A.J. Fleet & S.A.R. Boldy). The Geological Society of London, 533-544.

Dessert, C., Dupre, B., Gaillardet, J., Francois, L.M. & Allegre, C.J. (2003). Basalt weathering laws and the impact of basalt weathering on the global carbon cycle. *Chemical Geology*, 202, 257-273.

Dohrenwend, J.C., Abrahams, A.D.& Turrin, B.D. (1987). Drainage development on basaltic lava flows, Cima volcanic field, southeast California, and Lunar Crater volcanic field, south-central Nevada. *Geological Society of America Bulletin*, 99, 405-413.

Duraiswami, R.A., Bondre, N. & Dole, G. (2004). Possible lava tube system in a hummocky lava flow at Daund, western Deccan Volcanic Province, India. *Proceedings of the Indian Academy of Sciences, Earth and Planetary Sciences*, 113 (4), 819-829.

E

Eldhome, O. & Grue, K. 1994. North Atlantic volcanic margins: Dimensions and production rates. *Journal of Geophysical Research*, 99 (B2), 2955-2968.

Ellefsen, M., Boldreel, L.O. & Larsen, M. (2010). Intra-basalt units and base of the volcanic succession east of the Faroe-Islands exemplified by interpretation of offshore 3D seismic data. In: *Petroleum Geology: From Mature Basins to New Frontiers - Proceedings of the 7th Conference* (edited by B.A. Vining & S.C. Pickering). The Geological Society of London, 1033-1042.

Ellis, D., Bell, B.R., Jolley, D.W. & O'Callaghan, M. (2002). The stratigraphy, environment of eruption and age of the Faroes Lava Group, NE Atlantic Ocean. In: *The North Atlantic Igneous Province: Stratigraphy, Tectonic, Volcanic and Magmatic Processes* (edited by D.W. Jolley & B.R. Bell). The Geological Society of London Special Publications, 197, 253-269.

Ellis, D., Jolley, D.W., Passey, S.R. & Bell, B.R. (2009). Transfer zones: The application of new geological information from the Faroe Islands applied to the offshore exploration of intra basalt and sub-basalt strata. In: *Faroe Islands Exploration Conference:*

Proceedings of the 2nd Conference (edited by H. Ziska & T. Varming). Annales Societatis Scientarum Faroensis, Supplement 50, 205-226.

Ely, L.L., Brossy, C.C., House, P.K., Safran, E.B., O'Connor, J.E., Champion, D.E., Fenton, C.R., Bondre, N.R., Orem, C.A., Grant, G.E., Henry, C.D. & Turrin, B.D. (2012). Owyhee River intracanyon lava flows: Does the river give a dam? *Geological Society of America Bulletin*, 124, 1667-1687.

Embry, A.F. (1995). Sequence boundaries and sequence hierarchies: problems and proposals. In: *Sequence Stratigraphy on the Northwest European Margin* (edited by R.J. Steel, V.L. Felt, E.P. Johannessen & C. Mathieu). Norwegian Petroleum Society Special Publication, 5, 1-11.

Emery, D. & Myers, K.J. (1996). *Sequence Stratigraphy*. Blackwell Science Ltd, pp.297.

England, R.W., Mcbride, J.H. & Hobbs, R.W. (2005). The role of Mesozoic rifting in the opening of the NE Atlantic; evidence from deep seismic profiling across the Faroe-Shetland Trough. *Journal of the Geological Society of London*, 162, 661-673.

F

Filho, A.T., Pimentel Mizusaki, S.M., Antonioli, L. (2008). Magmatism and petroleum exploration in the Brazilian Paleozoic basins. *Marine and Petroleum Geology*, 25, 143-151.

Fisher, R.V. (1984). Submarine volcaniclastic rocks. In: *Marginal Basin Geology: Volcanic and Associated Sedimentary and Tectonic Processes in Modern and Ancient Marginal Basins* (edited by B. P. Kokelaar & M. F. Howells). The Geological Society of London Special Publications, 16, 5-27.

Fisher, R.V. & Schmincke, H.-U. (1994). Volcaniclastic sediment transport and deposition. In: *Sediment Transport and Depositional Processes* (edited by K. Pye). Blackwell Scientific Publication, 351-388.

Fliedner, M.M. & White, R.S. (2001). Sub-basalt imaging in the Faroe-Shetland Basin with large-offset data. *First Break*, 19, 247-252.

Francis, P. & Oppenheimer, C. (2004). *Volcanoes*, 2nd edition. Oxford University Press, pp. 521.

Fuller, R.E. (1931). The aqueous chilling of basaltic lava on the Columbia River Plateau. *American Journal of Science*, Series 5 (21), 281-320.

Furnes, H. (1974). Volume Relations between Palagonite and Authigenic Minerals in Hyaloclastites, and Its Bearing on the Rate of Palagonitization. *Bulletin of Volcanology*, 38 (1), 173-186.

Furnes, H. & Fridleifsson, I.B. (1974). Tidal Effects on the Formation of Pillow Lava/Hyaloclastic Deltas. *Geology*, 2, 381-384.

G

Gallagher, J.W. & Dromgoole, P.W. (2008). Seeing below the basalt – offshore Faroes. *Geophysical Prospecting,* 56, 33-45.

Galloway, W.E. (1989a). Genetic Stratigraphic Sequences in Basin Analysis I: Architecture and genesis of Flooding-Surface Bounded Depositional Units. *American Association of Petroleum Geologist Bulletin*, 73 (2), 125-142.

Galloway, W.E. (1989a). Genetic Stratigraphic Sequences in Basin Analysis I: Application to Northwest Gulf of Mexico Cenozoic Basin. *American Association of Petroleum Geologist Bulletin*, 73 (2), 143-154.

Gamberi, F. (2001). Volcanic facies associations in a modern volcaniclastic apron (Lipari and Vulcano offshore, Aeolian Island Arc). *Bulletin of Volcanology*, 63, 264-273.

Ganerød, M., Smethurst, M.A., Torsvik, T.H., Prestvik, T., Rousse, S., McKenna, C., van Hinsbergen, D.J.J. & Hendriks, B.W.H. (2010). The North Atlantic Igneous Province reconstructed and its relation to the Plume Generation Zone: the Antrim Lava Group revisited. *Geophysical Journal International*, 182, 183-202.

Gatliff, R.W., Hitchen, K., Ritchie, J.D. & Smythe, D.K. (1984). Internal structure of the Erlend Tertiary volcanic complex, north of Shetland, revealed by seismic reflection. *Journal of the Geological Society of London*, 141, 555-562.

Geoffroy, L. (2005). Volcanic passive margins. *Comptes Rendus Geoscience*, 337, 1395-1408.

Goodchild, M.W., Henry, K.L., Hinkley, R.J. & Imbus, S.W. (1999). The Victory gas field, West of Shetland. In: *Petroleum Geology of Northwest Europe: Proceedings of the 5th Conference* (edited by A.J. Fleet & S.A.R. Boldy). The Geological Society of London, 713-724.

Gordon, A., Younis, T., Bernard-Graille, C., Urruty, J.M., Ben-Brahim, L., Navarre, J.C., Paternoster, B. & Evers, G. (2010). Laggan; a mature understanding of an undeveloped discovery, more than 20 years old. In: *Petroleum Geology: From Mature Basins to New Frontiers - Proceedings of the 7th Conference* (edited by B.A. Vining & S.C. Pickering). The Geological Society of London, 279-297.

Griffiths, R.W. (2000). The Dynamics of Lava Flows. *Annual Review of Fluid Mechanics*, 32, 477-518.

Grigg, R.W. & Maragos, J.E. (1974). Recolonization of Hermatypic Corals on Submerged Lava Flows in Hawaii. *Ecology*, 55 (2), 387-395.

Guest, J.E., Wood, C. & Greeley, R. (1984). Lava Tubes, Terraces and Megatumuli on the 1614-24 Pahoehoe Lava Flow Field, Mount Etna, Sicily. *Bulletin of Volcanology*, 47 (3), 635-648.

Guilbaud, M.N., Self, S., Thordarson, T. & Blake, S. (2005). Morphology, surface structures, and emplacement of lavas produced by Laki, A.D. 1783 -1784. *The Geological Society of America Special Papers*, 396, 81-102.

H

Hamilton, C.W., Thordarson, T. & Fagents, S.A. (2010). Explosive lava–water interactions I: architecture and emplacement chronology of volcanic rootless cone groups in the 1783–1784 Laki lava flow, Iceland. *Bulletin of Volcanology*, 72, 449-467.

Hampton, M.A., Lee, H.J. & Locat, J. (1996). Submarine Landslides. *Review of Geophysics*, 44 (1), 33-59.

Hansen Jr., A.J., Vaccaro, J.J. & Bauer, H.H. (1994). Ground-water flow simulation of the Columbia Plateau Regional Aquifer System, Washington, Oregon and Idaho. *U.S. Geological Survey, Water-Resources Investigations Report 91-4187*, pp. 87

Hansen, D.M., Cartwright, J.A. & Thomas, D. (2004). 3D seismic analysis of the geometry of igneous sills and sill junction relationships. In: *3D Seismic Technology: Application to the Exploration of Sedimentary Basins* (edited by R.J. Davies, J.A. Cartwright, S.A. Stewart, M. Lappin & J.R. Underhill). The Geological Society of London Memoirs, 29, 199-208.

Hansen, D.M. (2006). The morphology of intrusion-related vent structures and their implications for constraining the timing of intrusive events along the NE Atlantic margin. *Journal of the Geological Society of London*, 163, 789-800.

Hansen, D.M. & Cartwright, J.A. (2006a). Saucer-shaped sill with lobate morphology revealed by 3D seismic data: implications for resolving a shallow-level sill emplacement mechanism. *Journal of the Geological Society of London*, 163, 509-523.

Hansen, D.M. & Cartwright, J.A. (2006b). The three-dimensional geometry and growth of forced folds above saucer-shaped igneous sills. *Journal of Structural Geology*, 28, 1520-1535.

Hansen, J., Jerram, D.A., McCaffery, K. & Passey, S.R. (2009). The onset of the North Atlantic Igneous Province in a rifting perspective. *Geological Magazine*. 146, 309–325.

Hansen, J., Jerram, D.A., Mccaffery, K. & Passey, S.R. (2011). Early Cenozoic saucer-shaped sills of the Faroe Islands: an example of intrusive styles in basaltic lava piles. *Journal of the Geological Society*, 168, 159-178.

Hart, B.S. (1999). Definition of subsurface stratigraphy, structure and rock properties from 3-D seismic data. *Earth-Science Reviews*, 47, 189-218.

Hart, B.S. (2008). Stratigraphically significant attributes. *The Leading Edge*, 27 (3). 320-324.

Heliker, C.C., Mangan, M.T., Mattox, T.N., Kauahikaua, J.P. & Helz, R.T. (1998). The character of long-term eruptions: inferences from episodes 50–53 of the Puʻu ʻŌ ʻō-Kūpaianaha eruption of Kilauea Volcano. *Bulletin of Volcanology*, 59 (6), 381-393.

Heliker, C.C. & Mattox, T.N. (2003). The First Two Decades of the Puʻu ʻŌʻō-Kūpaianaha Eruption: Chronology and Selected Bibliography. *U.S. Geological Survey Professional Paper 1676*, 1-28.

Helland-Hansen, W. & Martinsen, O.J. (1996) Shoreline trajectories and sequences: description of variable depositional-dip scenarios. *Journal of Sedimentary Research*, 66 (4), 670-688.

Helland-Hansen, W. & Hampson, G.J. (2009). Trajectory analysis: concepts and applications. In: *Trajectory Analysis in Stratigraphy* (edited by S. Henriksen, G.J. Hampson W. Helland-Hansen, E.P. Johannessen & R.J. Steel). *Basin Research*, 21, 454-483.

Helm-Clark, C.M., Rodgers, D.W. & Smith, R.P. (2004). Borehole geophysical techniques to define stratigraphy, alteration and aquifers in basalt. *Journal of Applied Geophysics*, 55, 3-38.

Herries, R., Poddubiuk, R. & Wilcockson, P. (1999). Solan, Strathmore and the back basin play, West of Shetland. In *Petroleum Geology of Northwest Europe: Proceedings of the 5th Conference* (edited by A.J. Fleet & S.A.R. Boldy). The Geological Society of London, 693-712.

Holford, S.P., Schofield, N., MacDonald, J.D., Duddy, I.R. & Green, P.F. (2012). Seismic Analysis of Igneous Systems in Sedimentary Basins and their Impacts on Hydrocarbon Prospectivity: Examples from the Southern Australian Margin. *The Australian Petroleum Production & Exploration Association Journal*, 52, 229-252.

Hon, K., Kauahikaua, J.P., Denlinger, R. & Mackay, K. (1994). Emplacement and inflation of pāhoehoe sheet flows: Observations and measurements of active lava flows on Kilauea Volcano, Hawaii. *Geological Society of America Bulletin*, 106, 351-370.

Hulme, G. (1974). The Interpretation of Lava Flow Morphology. *Geophysical Journal of the Royal Astronomical Society*, 39 (2), 361-383.

I

Inbar, M., Hubp, J.L. & Ruiz, V. (1994). The geomorphological evolution of the Paricutin cone and lava flows, Mexico, 1943-1990. *Geomorphology*, 9, 57-76.

Ireland, M.T., Davies, R.J., Goulty, N.R. & Carruthers, D. (2011). Structure of a silica diagenetic transformation zone: the Gjallar Ridge, offshore Norway. *Sedimentology*, 58, 424-441.

J

Japsen, P., Andersen, M.S., Boldreel, L.O., Waagstein, R., White, R.S. & Worthington, M. (2004). Seismic and petrohysical properties of Faroe Islands basalts: the SeiFaBa project. *Geological Survey of Denmark and Greenland Bulletin*, 4, 53-65.

Jerram, D.A. & Stollhofen, H. (2002). Lava/sediment interaction in desert settings; are all peperite-like textures the result of magma-water interaction? *Journal of Volcanology and Geothermal Research*, 114, 231-249.

Jerram, D.A. & Widdowson, M. (2005). The anatomy of Continental Flood Basalt Provinces: geological constraints on the processes and products of flood volcanism. *Lithos*, 79, 385-405.

Jerram, D.A., Single, R.T., Hobbs, R.W. & Nelson, C.E. (2009). Understanding the offshore flood basalt sequence using onshore volcanic facies analogues: an example from the Faroe–Shetland basin. *Geological Magazine*, 146, 353-367.

Jervey, M.T. (1988). Quantitative geological modeling of siliciclastic rock sequences and their seismic expression. In: *Sea Level Changes – An Integrated Approach* (edited by C.K. Wilgus, B.S. Hastings, C.G Kendal, H.W. Posamentier, C.A. Ross & J.C. Van Wagoner). Society for Sedimentary Geology Special Publications, 42, 47-69.

Jolley, D.W. (1997). Palaeosurface palynofloras of the Skye lava field and the age of the British Tertiary volcanic province. In: *Palaeosurfaces: Recognition, Reconstruction and Palaeoenvironmental Interpretation* (edited by M. Widdowson). The Geological Society of London Special Publications, 197, 67-94.

Jolley, D.W. & Bell, B.R. (2002). Genesis and age of the Erland Volcano, NE Atlantic Margin. In: *The North Atlantic Igneous Province: Stratigraphy, Tectonic, Volcanic and Magmatic Processes* (edited by D.W. Jolley & B.R. Bell). The Geological Society of London Special Publications, 197, 95-110.

Jolley, D.W., Morton, A.C. & Prince, I. (2005). Volcanogenic impact on phytogeography and sediment dispersal patterns in the NE Atlantic. In: *Petroleum Geology of Northwest Europe: Proceedings of the 6th Conference* (edited by A.G. Dore & B.A. Vining). The Geological Society of London, 969-975.

Jolley, D.W. & Morton, A.C. (2007). Understanding basin sedimentary provenance: evidence from allied phytogeographic and heavy mineral analysis of the Palaeocene of the NW Atlantic. *Journal of the Geological Society of London*, 164, 553-563.

Jolley, D.W. (2009). Palynofloral evidence for the onset and cessation of eruption of the Faroe Islands lava field. In: *Faroe Islands Exploration Conference: Proceedings of the 2nd Conference* (edited by T. Varming & H. Ziska). Annales Societatis Scientiarum Færoensis, Supplementum 48, 149-166.

Jolley, D.W., Bell, B.R., Williamson, I.T & Prince, I. (2009). Sun-eruption vegetation dynamics, paleosurfaceas and structural controls on lava field vegetation: An example from the Palaeogene Staffa Formation, Mull Lava Field, Scotland. *Review of Palaeobotany and Palynology*, 153, 19-33.

Jones, J.G. & Nelson, P.H.H. (1970). The flow of basalt lava from air into water – its structural expression and stratigraphic significance. *Geological Magazine*, 107(1), 13-19.

Jurado-Chichay, Z., Rowland, S.K. & Walker, G.P.L. (1996). The formation of circular littoral cones from tube-fed pāhoehoe: Mauna Loa, Hawai'i. *Bulletin of Volcanology*, 57, 471-482.

K

Kauahikaua, J.P., Cashman, K.V., Mattox, T.N., Heliker, C.C., Hon, K.A., Mangan, M.T., & Thornber, C.R. (1998). Observations on basaltic lava streams in tubes from Kilauea Volcano, island of Hawai'i. *Journal of Geophysical Research*, 103 (B11), 27,303-27,323.

Kauahikaua, J.P., Sherrod, D.R., Cashman, K.V., Heliker, C.C., Hon, K., Mattox, T.N. & Johnson, J.A. (2003). Hawaiian Lava-Flow Dynamics during the Puʻu ʻŌ ʻō-Kūpaianaha Eruption: A Tale of Two Decades. *U.S. Geological Survey Professional Paper 1676*, 63-88.

Kearey, P., Brooks, M. & Hill, I. (2002). *An Introduction to Geophysical Exploration*, 3rd edition. Blackwell Science Ltd, pp. 262.

Kimbell, G.S., Gatliff, R.W., Ritchie, J.D., Walker, A.S.D. & Williamson, J.P. (2004). Regional three-dimensional gravity modelling of the NE Atlantic margin. *Basin Research*, 16, 259-278

King, S.D. & Anderson, D.L. (1995). An alternative mechanism of flood basalt formation. *Earth and Planetary Science Letters*, 136, 269-279.

Kiørboe, L., (1999). Stratigraphic relationships of the Lower Tertiary of the Faroe Basalt Plateau and the Faeroe-Shetland Basin. In: *Petroleum Geology of Northwest Europe: Proceedings of the 5th Conference* (edited by A.J. Fleet & S.A.R. Boldy). The Geological Society of London, 559-572.

Knight, K.B., Nomade, S., Renne, P.R., Marzolic, A., Bertrand, H. & Youbi, N. (2004). The Central Atlantic Magmatic Province at the Triassic–Jurassic boundary: paleomagnetic and 40Ar/39Ar evidence from Morocco for brief, episodic volcanism. *Earth and Planetary Science Letters*, 228, 143– 160.

Kokelarr, P. (1986). Magma-water interactions in subaqueous and emergent basaltic volcanism. *Bulletin of Volcanology*, 48 (5), 275-289.

L

Lamers, E. & Carmichael, S.M.M. (1999). The Paleocene deepwater sandstone play West of Shetland. In: *Petroleum Geology of Northwest Europe: Proceedings of the 5th Conference* (edited by A.J. Fleet & S.A.R. Boldy). The Geological Society of London, 645-659.

Larsen, L.M., Pedersen, A.K., Pedersen, G.K. & Piasecki, S. (1992). Timing and duration of Early Tertiary volcanism in the North Atlantic: new evidence from West Greenland. In: *Magmatism and the Causes of Continental Break-up* (edited by B.C. Storey, T. Alabaster & R.J. Pankhurst). The Geological Society of London Special Publications, 68, 321-333.

Larsen, L.M., Waagstein, R., Pedersen, A.K. & Storey, M., (1999). Trans-Atlantic correlation of the Palaeogene volcanic successions in the Faeroe Islands and East Greenland, *Journal of the Geological Society of London*, 156, 1081–1095.

Larsen, L.M., Pedersen, A.K. & Pedersen, G.K. (2006). A subaqueous rootless cone field at Niuluut, Disko, Paleocene of West Greenland. *Lithos*, 92, 20–32.

Larsen, M., Rasmussen, T. & Hjelm, L. (2010). Cretaceous revisited: exploring the syn-rift play of the Faroe–Shetland Basin. In: *Petroleum Geology: From Mature Basins to New Frontiers - Proceedings of the 7th Conference* (edited by B.A. Vining & S.C. Pickering). The Geological Society of London, 953-962.

Leach, H.M., Nerbert, N., Los, A. & Smith, R.L. (1999). The Schiehallion development. In: *Petroleum Geology of Northwest Europe: Proceedings of the 5th Conference* (edited by A.J. Fleet & S.A.R. Boldy). The Geological Society of London, 683-692.

Lindsey, K., Porcello, J., Tolan, T., Hammond, T. & Royer, P. (2011). *Evidence for Hydrogeologic Compartmentalization in the Columbia River Basalt Aquifer System, Columbia Basin Ground Water Management Area of Adams, Franklin, Grant, and Lincoln Counties, Washington*. GSI Water Solutions Inc report (www.cbgma.org), pp. 86.

Lipman, P.W., Normark, W.R., Moore, J.G.,Wilson, J.B. & Gutmacher, C.E. (1988). The Giant Submarine Alika Debris Slide, Mauna Loa, Hawaii. *Journal of Geophysical Research*, 93 (B5), 4279-4299.

Lipman, P.W. (1995). Declining Growth Of Mauna Loa During The Last 100,000 Years: Rates of Lava Accumulation vs. Gravitational Subsidence. In: *Mauna Loa Revealed: Structure, Composition, History, and Hazards* (edited by J.M. Rhodes and J.P. Lockwood). American Geophysical Union Monograph, 92, 45-80.

Lipman, P.W. & Moore, J.G. (1996). Mauna Loa lava accumulation rates at the Hilo drill site: Formation of lava deltas during a period of declining overall volcanic growth. *Journal of Geophysical Research*, 101 (B5), 11,631-11,641.

Loizou, N., Andrews, I.J., Stoker, S.J. & Cameron, D. (2006). West of Shetland revisited: the search for stratigraphic traps. In: *The Deliberate Search for the Stratigraphic Trap* (edited by M.R. Allen, G.P. Goffey, R.K. Morgan & I.M. Walker). The Geological Society of London Special Publications, 254, 225-245.

Long, P.E. & Wood, B.J. (1986). Structures, textures, and cooling histories of Columbia River basalt flows. *Geological Society of America Bulletin*, 97 (9), 1144-1155.

Lorenz, V. (1986). On the growth of maars and diatremes and its relevance to the formation of tuff rings. *Bulletin of Volcanology*, 48, 265-274.

Lundin, E.R. & Doré, A.G. (1997). A tectonic model for the Norwegian passive margin with implications for the NE Atlantic: Early Cretaceous to break-up*. Journal of the Geological Society*, 154, 545-550.

Lyle, P. (2000). The eruption environment of multi-tiered columnar basalt lava flows. *Journal of the Geological Society*, 157, 715-722.

M

Magee, C., Hunt-Stewart, E. & Jackson, C.A.-L. (2013). Volcano growth mechanisms and the role of sub-volcanic intrusions: Insights from 2D seismic reflection data. *Earth and Planetary Science Letters*, 373, 41-53.

Maicher, D., White, J.D.L. & Batiza, R. (2000). Sheet hyaloclastite: density-current deposits of quench and bubble-burst fragments from thin, glassy sheet lava flows, Seamount Six, Eastern Pacific Ocean. *Marine Geology*, 171, 75-94.

Malin, M.C. (1980). Lengths of Hawaiian lava flows. *Geology*, 8, 306-308.

Mansurbeg, H., Morad, S., Salem, A., Marfil, R., El-ghali, M.A.K., Nystuen, J.P., Caja, M.A., Amorosi, A., Garcia, D. & la Iglesia, A. (2008). Diagenesis and reservoir quality evolution of palaeocene deep-water, marine sandstones, the Shetland-Faroes Basin, British continental shelf. *Marine and Petroleum Geology*, 25, 514-543.

Maresh, J. & White, R.S. (2005). Seeing through a glass, darkly: strategies for imaging through basalt. *First Break*, 23, 27-33.

Maresh, J., White, R.S., Hobbs, R.W. & Smallwood, J.R. (2006). Seismic attenuation of Atlantic margin basalts: Observations and modelling. *Geophysics*, 71 (6), B211-B221.

Masson, D.G, Watts, A.B., Gee, M.J.R., Urgeles, R., Mitchell, N.C., Le Bas, T.P. & Canals, M. (2002). Slope failures on the flanks of the western Canary Islands*. Earth-Science Reviews*, 57, 1-35.

Mathisen, M.E. & McPherson, J.G. (1991). Volcaniclastic Deposits: Implications for Hydrocarbon Exploration. In: *Sedimentation in Volcanic Settings* (edited by R.V. Fisher & G.A. Smith). Society for Sedimentary Geology Special Publications, 45, 27-36.

Mattox, T.N., Heliker, C.C., Kauahikaua, J.P. & Hon, K.A. (1993). Development of the 1990 Kalapana Flow Field, Kilauea Volcano, Hawaii. *Bulletin of Volcanology*, 55 (6), 407-413.

Mattox, T.N. & Mangan, M.T. (1997). Littoral hydrovolcanic explosions: a case study of lava-seawater interaction at Kilauea Volcano. *Journal of Volcanology and Geothermal Research*, 75, 1-17.

Mitchum, R.M. (1977). Seismic Stratigraphy and Global Changes of Sea Level, Part 11: Glossary of Terms used in Seismic Stratigraphy. In: *Seismic Stratigraphy – Applications to Hydrocarbon Exploration* (edited by C.E. Payton). American Association of Petroleum Geologists Memoirs, 26, 205-212.

Mitchum, R.M., Vail, P.R. & Thompson III, S. (1977a). Seismic Stratigraphy and Global Changes of Sea Level, Part 2: The Depositional Sequence as a Basic Unit for

Stratigraphic Analysis. In: *Seismic Stratigraphy – Applications to Hydrocarbon Exploration* (edited by C.E. Payton). American Association of Petroleum Geologists Memoirs, 26, 53-62.

Mitchum, R.M., Vail, P.R. & Sangree, J.B. (1977b). Seismic Stratigraphy and Global Changes of Sea Level, Part 6: Stratigraphical Interpretation of Seismic Reflection Patterns in Depositional Sequence. In: *Seismic Stratigraphy – Applications to Hydrocarbon Exploration* (edited by C.E. Payton). American Association of Petroleum Geologists Memoirs, 26, 117-133.

Mitchum, R.M. & Vail, P.R. (1977). Seismic Stratigraphy and Global Changes of Sea Level, Part 7: Seismic Stratigraphic Interpretation Procedure. In: *Seismic Stratigraphy – Applications to Hydrocarbon Exploration* (edited by C.E. Payton). American Association of Petroleum Geologists Memoirs, 26, 135-143.

Mitchell, S.M., Beamish, G.W.J, Wood, M.V., Malacek, S.J., Armentrout, J.A., Damuth,J.E. & Olson, H.C. (1993). Paleogene sequence stratigraphic framework of the Faeroe Basin. In: *Petroleum Geology of Northwest Europe: Proceedings of the 4th Conference* (edited by J. R. Parker). The Geological Society of London, 1011-1023.

Mitchell, N.C., Masson, D.G., Watts, A.B., Gee, M.J.R. & Urgeles, R. (2002). The morphology of the submarine flanks of volcanic ocean islands, a comparative study of the Canary and Hawaiian hotspot islands. *Journal of Volcanology and Geothermal Research*, 115, 83-107.

Moore, J.G. (1970). Relationship between Subsidence and Volcanic Load, Hawaii. *Bulletin of Volcanology*, 34 (2), 562-276.

Moore, J.G., Phillips, R.L., Grigg, R.W., Peterson, D.W. & Swanson, D.A. (1973). Flow of Lava into the Sea, 1969-1971, Kilauea Volcano, Hawaii. *Geological Society of America Bulletin*, 84, 537-546.

Moore, J.G., Clague, D.A., Holcomb, R.T., Lipman, P.W., Normark, W.R. & Torresan, M.E. (1989). Prodigious Submarine Landslides on the Hawaiian Ridge. *Journal of Geophysical Research*, 94 (B12), 17-465-17,484.

Moore, J.G. & Clague, D.A. (1992). Volcano growth and evolution of the Island of Hawaii. *Geological Society of America Bulletin*, 104, 1471-1484.

Moore, J.G., Normark, W.R. & Holcomb, R.T. (1994). Giant Hawaiian Landslides. *Annual Review of Earth Planetary Science*, 22, 119-144.

Moore, J.G. & Chadwick Jr., W.W. (1995). Offshore Geology of Mauna Loa and Adjacent Areas, Hawaii. In: *Mauna Loa Revealed: Structure, Composition, History, and Hazards*

(edited by J.M. Rhodes and J.P. Lockwood). American Geophysical Union Monograph, 92, 21-44.

Morgan, J.K., Moore, G.F. & Clague, D.A. (2003). Slope failure and volcanic spreading along the submarine south flank of Kilauea volcano, Hawaii. *Journal of Geophysical Research*, 108 (B9), 2415-2430.

Moy, D.J. & Imber, J. (2009). A critical analysis of the structure and tectonic significance of rift-oblique lineaments ('transfer zones') in the Mesozoic-Cenozoic succession of the Faroe -Shetland Basin, NE Atlantic margin. *Journal of the Geological Society*, 166, 831-844.

Mudge, D.C.& Bujak, J.P. (2001). Biostratigraphic evidence for evolving palaeoenvironments in the Lower Paleogene of the Faroe-Shetland Basin. *Marine and Petroleum Geology*, 18, 577-590.

Muto, T. & Steel, R.J. (2000). The accommodation concept in sequence stratigraphy: some dimensional problems and possible redefinition. *Sedimentary Geology*, 130, 1-10.

N

Naylor, P.H., Bell, B.R., Jolley, D.W., Durnall, P. & Fredsted, P. (1999). Palaeogene magmatism in the Faeroe-Shetland Basin: influences on uplift history and sedimentation. In: *Petroleum Geology of Northwest Europe: Proceedings of the 5th Conference* (edited by A.J. Fleet & S.A.R. Boldy). The Geological Society of London, 545-558.

Navarre-Sitchler, A. & Brantley, S. (2007). Basalt weathering across scales. *Earth and Planetary Science Letters*, 261, 321-334.

Neal, J. & Abreu, V. (2009). Sequence stratigraphy hierarchy and the accommodation succession method. *Geology*, 37, 779-782.

Nelson, C.E., Jerram, D.A., Single, R.T. & Hobbs, R.W. (2009a). Understanding the facies architecture of flood basalts and volcanic rifted margins and its effect on geophysical properties. In: *Faroe Islands Exploration Conference: Proceedings of the 2nd Conference* (edited by T. Varming & H. Ziska). Annales Societatis Scientiarum Færoensis, Supplementum 48, 76-95.

Nelson, C.E., Jerram, D.A. & Hobbs, R.W. (2009b). Flood basalt facies from borehole data: implications for prospectivity and volcanology in volcanic rifted margins. *Petroleum Geoscience,* 15, 313-324.

Németh, K. (2010). Monogenetic volcanic fields: Origin, sedimentary record, and relationship with polygenetic volcanism. *The Geological Society of America Special Paper*, 470, 43-66.

Nestvold, E.O. (1996). The Impact of 3-D Seismic Data on Exploration, Field Development, and Production. In: *Applications of 3-D seismic data to exploration and production* (edited by P. Weimer & T.L. Davis). Association of Petroleum Geologists, Studies in Geology, 42 & Society of Economic Geologists, Geophysical Developments Series, 5, 1-8.

Nielsen, P.H., Stefánsson, V. & Tulinius, H. (1984). Geophysical logs from Lopra-1 and Vestmanna-1. In: *The deep drilling project 1980–1981 in the Faeroe Islands* (edited by O. Berthelsen, A. Noe-Nygaard, & J. Rasmussen). Annales Societatis Scientiarum Faeroensis, Supplementum **IX**, 115–135.

O

Oehler, J.F., Labazuy, P. & Lénat, J.F. (2004). Recurrence of major flank landslides during the last 2-Ma-history of Reunion Island. *Bulletin of Volcanology*, 66, 585-598.

Oehler, J.F., Lénat, J.F. & Labazuy, P. (2008). Growth and collapse of the Reunion Island volcanoes. *Bulletin of Volcanology*, 70, 171-742.

Ogilvie, J.S., Crompton, R. & Hardy, N.M. (2001). Characterization of volcanic units using detailed velocity analysis in the Atlantic Margin, West of Shetlands, United Kingdom. *The Leading Edge*, 20 (1), 34-50.

Ollier, C.D. (1995). Tectonics and landscape evolution in southeast Australia. *Geomorphology*, 12, 37-44.

P

Parkin, C.J., Lunnon, Z.C., White, R.S., Christie, P.A.F. & iSIMM Team (2007). Imaging the pulsing Iceland mantle plume through the Eocene. *Geology*, 35 (1), 93-96.

Parnell, J., Carey, P.F., Green, P. & Duncan, W. (1999). Hydrocarbon migration history, West of Shetland: integrated fluid inclusion and fission track studies. In: *Petroleum Geology of Northwest Europe: Proceedings of the 5th Conference* (edited by A.J. Fleet & S.A.R. Boldy). The Geological Society of London, 613-625.

Passey, S. & Bell, B.R. (2007). Morphologies and emplacement mechanisms of the lava flows of the Faroe Islands Basalt Group, Faroe Islands, NE Atlantic Ocean. *Bulletin of Volcanology*, 70 (2), 139-156.

Passey, S. & Jolley, D.W. (2009). A revised lithostratigraphic nomenclature for the Palaeogene Faroe Islands Basalt Group, NE Atlantic Ocean. *Earth and Environmental Science Transactions of the Royal Society of Edinburgh*, 99, 127-158.

Paterne, M. & Guichard, F. (1993). Triggering of Volcanic Pulses in the Campanian Area, South Italy, by Periodic Deep Magma Influx. *Journal of Geophysical Research*, 98 (B2), 1861-1873.

Payton, C.E. (1977). *Seismic Stratigraphy – Applications to Hydrocarbon Exploration*. American Association of Petroleum Geologists Memoirs, 26, pp. 516.

Pedersen, A.K., Watt, M., Watt, W.S. & Larsen, L.M. (1997). Structure and stratigraphy of the Early Tertiary basalts of the Blosseville Kyst, East Greenland. *The Journal of the Geological Society of London*, 154, 565-570.

Pedersen, G.K., Larsen, L.M., Pedersen, A.K. & Hjortkjær, B.F. (1998). The syn-volcanic Naajaat lake, Paleocene of West Greenland. *Palaeogeography, Palaeoclimatology, Palaeoecology*, 140, 271-287.

Peterson, D.W., Holcomb, R.T., Tilling, R.I. & Christiansen, R.L. (1994). Development of lava tubes in the light of observations at Mauna Ulu, Kilauea Volcano, Hawaii. *Bulletin of Volcanology*, 56, 343-360.

Petford, N. (2003). Controls on primary porosity and permeability development in igneous rocks. In: *Hydrocarbons in Crystalline Rocks* (edited by N. Petford & K. J. W. McCaffrey). The Geological Society of London Special Publications, 214, 93-107.

Pieri, D.C. & Baloga, S.M. (1986). Eruption Rate, Area, and Length Relationships for Some Hawaiian Lava Flows. *Journal of Volcanology and Geothermal Research,* 30, 29-45.

Pillans, B. (1997). Soil Development at a snail's pace: evidence from a 6 Ma soil chronosequence on basalt in north Queensland, Australia. *Geoderma*, 80, 117-128.

Piper, J.D.A. (1973). Volcanic History and Tectonics of the North Langjökull Region, Central Iceland. *Canadian Journal of Earth Science*, 10, 164-179.

Planke, S. (1994). Geophysical response of flood basalts from analysis of wire line logs: Ocean Drilling Program Site 642, Vøring volcanic margin. *Journal of Geophysical Research*, 99 (B5), 9279-9296.

Planke, S. & Cambray, H. (1998). Seismic Properties of Flood Basalts from Hole 917A Downhole Data, Southeast Greenland Volcanic Margin. In: *Leg 152 - Scientific Results; East Greenland Margin, Sites 914-919* (edited by A.D. Saunders, H.C. Larsen & S.W. Wise Jr). Proceedings of the Ocean Drilling Program, Scientific Results, 152, 453-462.

Planke, S. & Alvestad, E. (1999). Seismic Volcanostratigraphy of the Extrusive Breakup Complexes in the Northeast Atlantic: Implications from ODP/DSDP Drilling. In: Leg 163 - *Scientific Results; Southeast Greenland, Sites 988-990* (edited by H.C. Larsen, R.A. Duncan, J.F. Allan & K. Brooks). Proceeding of the Ocean Drilling Program, Scientific Results, 163, 3-16.

Planke, S., Alvestad, E. & Eldholm, O. (1999). Seismic characteristics of basaltic extrusive and intrusive rocks. *The Leading Edge*, 18 (3), 342-348.

Planke, S., Symonds, P.A., Alvestad, E. & Skogseid, J. (2000). Seismic volcanostratigraphy of large-volume basaltic extrusive complexes on rifted margins. *Journal of Geophysical Research*, 105 (B8), 19,335-19,351.

Planke, S., Rasmussen, T., Rey, S.S.& Myklebust, R. (2005). Seismic characteristics and distribution of volcanic intrusions and hydrothermal vent complexes in the Vøring and Møre basins. In: *Petroleum Geology of Northwest Europe: Proceedings of the 6th Conference* (edited by A.G. Dore & B.A. Vining). The Geological Society of London, 833-844.

Porębski, S.J. & Gradzinski, R. (1990). Lava Gilbert-type delta in the Polonez Cove Formation (Lower Oligocene), King George Island, West Antarctica. In: *Coarse Grained Deltas* (edited by A. Colella & D.B. Prior). Special Publication of the International Association of Sedimentologists, 10, 335-351.

Porębski, S.J. & Steel, R.J. (2006). Deltas and Sea-Level Change. *Journal of Sedimentary Research*, 76, 390-403.

Posamentier, H.W. & Vail, P.R. (1988). Eustatic Controls on Clastic Deposition II – Sequences and System Tract Models. In: *Sea Level Changes – An Integrated Approach* (edited by C.K. Wilgus, B.S. Hastings, C.G Kendal, H.W. Posamentier, C.A. Ross & J.C. Van Wagoner). Society for Sedimentary Geology Special Publications, 42, 125-154.

Posamentier, H.W., Jervey, M.T. & Vail, P.R. (1988). Eustatic Controls on Clastic Deposition I – Conceptual framework. . In: *Sea Level Changes – An Integrated Approach* (edited by C.K. Wilgus, B.S. Hastings, C.G Kendal, H.W. Posamentier, C.A. Ross & J.C. Van Wagoner). Society for Sedimentary Geology Special Publications, 42, 110-124.

Posamentier, H.W., Davies, R.J., Cartwright, J.A. & Wood, L. (2007). Seismic geomorphology - an overview. In: *Seismic Geomorphology: Applications to Hydrocarbon Exploration and Production* (edited by R.J. Davies, H.W. Posamentier, L. Wood & J.A. Cartwright). The Geological Society of London Special Publications, 277, 1-14.

Postma, G. (1990). Depositional architectures and facies of river and fan deltas: a synthesis. In: *Coarse Grained Deltas* (edited by A. Colella & D.B. Prior). Special Publication of the International Association of Sedimentologists, 10, 13-27.

Postma, G. (1995). Sea-Level related architectural trends in coarse-grained delta complexes. *Sedimentary Geology*, 98, 3-12.

Praeg, M., Stoker, M.S., Shannon, P.M., Ceramicola, S., Hjelstuen, B., Laberg, J.S. & Mathiesen, a. (2005). Episodic Cenozoic tectonism and the development of the NW European 'passive' continental margin. *Marine and Petroleum Geology*, 22, 1007-1030.

Q

R

Reidel, S.P. & Tolan, T.L. (1992). Eruption and emplacement of flood basalt: An example from the large-volume Teepee Butte Member, Columbia River Basalt Group. *Geological Society of America Bulletin*, 104, 1650-1671.

Richardson, K.R., White, R.S., England, R.W. & Fruehn, J. (1999). Crustal structure east of the Faroe Islands: mapping sub-basalt sediments using wide-angle seismic data. *Petroleum Geoscience*, 5, 161-172.

Rider, M.H. (1991). *The Geological Interpretation of Well Logs*, 2nd Edition. Whittles Publishing, pp 175.

Ritchie, J.D. & Hitchen, K. (1996). Early Palaeogene offshore igneous activity to the northwest of the UK and its relationship to the North Atlantic Igneous Province. In: *Correlation of the Early Palaeogene in Northwest Europe* (edited by R.W.O'B Knox, R.M. Corfield & R.E. Dunay). The Geological Society of London Special Publications, 101, 63-78.

Ritchie, J.D., Gatliff, R.W., Richards, P.C., Fleet, A.J. & Boldy, S.A.R. (1999). Early Tertiary magmatism in the offshore NW UK margin and surrounds. In: *Petroleum Geology of Northwest Europe: Proceedings of the 5th Conference* (edited by A.J. Fleet & S.A.R. Boldy). The Geological Society of London, 573-584.

Ritchie, J.D., Johnson, H. & Kimbell, G.S. (2003). The nature and age of Cenozoic contractional deformation within the NE Faroe-Shetland Basin. *Marine and Petroleum Geology*, 20, 399-409.

Ritchie, J.D., Johnson, H, Quinn, M.F. & Gatliff, R.W.(2008). The effects of Cenozoic compression within the Faroe–Shetland Basin and adjacent areas. In: *The Nature and*

Origin of Compression in Passive Margins (edited by H. Johnson, A. G. Doré, R. W. Gatliff, R. Holdsworth, E.R. Lundin, & J.D. Ritchie). The Geological Society of London Special Publications, 306, 121-136.

Roberts, A. W., White, R. S., Lunnon, Z. C., Christie, P. A. F., Spitzer, R. & iSIMM TEAM (2005). Imaging magmatic rocks on the Faroes Margin. In: *Petroleum Geology of Northwest Europe: Proceedings of the 6th Conference* (edited by A.G. Dore & B.A. Vining). The Geological Society of London, 755-766.

Roberts, A. W., White, R. S. & Christie, P. A. F. (2009). Imaging igneous rocks on the North Atlantic rifted continental margin. *Geophysical Journal International*, 179**,** 1024-1038.

Rohrman, M. (2007). Prospectivity of volcanic basins: Trap delineation and acreage de-risking. *American Association of Petroleum Geologists Bulletin*, 91 (6), 915-939.

Ross, P.S., Ukstins Peate, I., Mcclintock, M.K., Xu, Y.G., Skilling, I.P., White, J.D.L. & Houghton, B.F. (2005). Mafic volcaniclastic deposits in flood basalt provinces: A review. *Journal of Volcanology and Geothermal Research*, 145, 281-314.

Ross, P.-S., Delpit, S., Haller, M.J., Németh, K. & Corbella, H. (2011). Influence of the substrate on maar–diatreme volcanoes — An example of a mixed setting from the Pali Aike volcanic field, Argentina. *Journal of Volcanology and Geothermal Research*, 201, 253-271.

Rossi, M.J. (1996). Morphology and mechanism of eruption of postglacial shield volcanoes in Iceland. *Bulletin of Volcanology*, 57, 530-540.

S

Sangree, J.B. & Widmier, J. (1977). Seismic stratigraphy and global changes in sea-level, part 9: seismic stratigraphic interpretation of clastic depositional facies. In: *Seismic Stratigraphy – Applications to Hydrocarbon Exploration* (edited by C.E. Payton). American Association of Petroleum Geologists Memoirs, 26, 1165-1184.

Sansone, F.J. & Smith, J.R. (2006). Rapid mass wasting following nearshore submarine volcanism on Kilauea volcano, Hawaii. *Journal of Volcanology and Geothermal Research*, 151, 133-139.

Sarg, J.F. (1988). Carbonate Sequence Stratigraphy. In: *Sea Level Changes – An Integrated Approach* (edited by C.K. Wilgus, B.S. Hastings, C.G Kendal, H.W. Posamentier, C.A. Ross & J.C. Van Wagoner). Society for Sedimentary Geology Special Publications, 42, 155-182.

Saunders, A.D. & Tarney, J. (1982). Igneous activity in the southern Andes and northern Antarctic Peninsula: a review. *Journal of the Geological Society of London*, 139, 691-700.

Saunders, A.D., Jones, S.M., Morgan, L.A., Pierce, K.L., Widdowson, M. & Xu, Y.G. (2007). Regional uplift associated with continental large igneous provinces: The roles of mantle plumes and the lithosphere. *Chemical Geology*, 241, 282-318.

Schiffman, P., Watters, R.J., Thompson, N. & Walton, A.W. (2006). Hyaloclastites and the slope stability of Hawaiian volcanoes: Insights from the Hawaiian Scientific Drilling Project's 3-km drill core. *Journal of Volcanology and Geothermal Research*, 151, 217-228.

Schlager, W. (1991). Depositional bias and environmental change-important factors in sequence stratigraphy. *Sedimentary Geology*, 70, 109-130.

Schlager, W. (1993). Accommodation and supply – a dual control on stratigraphic sequences. *Sedimentary Geology*, 86, 111-136.

Schmincke, H.-U., Behncke, B., Grasso, M. & Raffi, S. (1997). Evolution of the northwestern Iblean Mountains, Sicily: uplift, Pliocene/Pleistocene sea-level change, palaeoenvironment, and volcanism. *Geol Rundsch*, 86, 637-669.

Schofield, N., Heaton, L., Holford, S.P., Archer, S.G., Jackson, C.A.-L. & Jolley, D.W. (2012). Seismic imaging of 'broken bridges': linking seismic to outcrop-scale investigations of intrusive magma lobes. *Journal of the Geological Society of London*, 169, 421-426.

Schopka, H.H., Gudmundsson, M.T. & Tuffen, H. (2006). The formation of Helgafell, southwest Iceland, a monogenetic subglacial hyaloclastite ridge: Sedimentology, hydrology and volcano–ice interaction. *Journal of Volcanology and Geothermal Research*, 152, 359-377.

Scotchman, I.C., Carr, A.D. & Parnell, J. (2006). Hydrocarbon generation modelling in a multiple rifted and volcanic basin: a case study in the Foinaven Sub-basin, Faroe–Shetland Basin, UK Atlantic margin. *Scottish Journal of Geology*, 42 (1), 1-19.

Self, S., Thordarson, T., Keszthelyi, L., Walker, G.P.L., Hon, K., Murphy, M.T., Long, P. & Finnemore, S. (1996). A new model for the emplacement of Columbia River basalts as large, inflated pahoehoe lava flow fields. *Geophysical Research Letters*, 23 (19), 2689-2692.

Self, S., Thordarson, T. & Keszthelyi, L. (1997). Emplacement of continental flood basalt lava flows. In: Large Igneous Provinces: Continental, Oceanic, and Planetary Flood Volcanism. *Geophysical monograph*, 100, 381-410.

Self, S., Keszthelyi, L. & Thordarson, T. (1998). The importance of Pāhoehoe. Annual *Review of Earth and Planetary Sciences*, 26, 81-110.

Serra, O. (1984). *Fundamentals of well-log interpretation - 1. The acquisition of logging data*. Elsevier, pp. 423.

Serra, O. (1986). *Fundamentals of well-log interpretation - 2. The interpretation of logging data*. Elsevier, pp. 684.

Shaw, F., Worthington, M.H., White, R.S., Andersen, M.S., Petersen, U.K. & Seifaba Group (2008). Seismic attenuation in Faroe Islands basalts. *Geophysical Prospecting,* 56, 5-20.

Sheriff, R.E. (1977). Limitations on Resolution of Seismic Reflections and Geological Detail; Derivable from Them. In: *Seismic Stratigraphy – Applications to Hydrocarbon Exploration* (edited by C.E. Payton). American Association of Petroleum Geologists Memoirs, 26, 3-14.

Sheriff, R.E. & Geldart, L.P. (1995). *Exploration Seismology*. Cambridge University Press, pp. 628.

Shervais, J.W., Shroff, G., Vetter, S.K., Matthews, S., Hanan, B.B. & McGee, J.J. (2002). Origin and Evolution of the Western Snake River Plain: Implications From Stratigraphy, Faulting, and the Geochemistry of Basalts Near Mountain Home, Idaho. In: *Tectonic and Magmatic Evolution of the Snake River Plain Volcanic Province* (edited by B. Bonnichsen, C.M. White & M. McCurry). Idaho Geological Survey Bulletin 30, 343-361.

Sheth, H.C. (1999). Flood basalts and large igneous provinces from deep mantle plumes: fact, fiction, and fallacy. *Tectonophysics*, 311, 1-29.

Siebert, L. (1984). Large Volcanic Debris Avalanches: Characteristics of Source Areas, Deposits, and Associated Eruptions. *Journal of Volcanology and Geothermal Research*, 22, 163-197.

Sigurdsson, H., Schilling, J.G. & Meyer, P.S.(1978). Skagi and Langjökull Volcanic Zones in Iceland: 1. Petrology and Structure. *Journal of Geophysical Research*, 83 (B8), 3971-3982.

Single, R.T. & Jerram, D.A. (2004). The 3D facies architecture of flood basalt provinces and their internal heterogeneity: examples from the Palaeogene Skye Lava Field. *Journal of the Geological Society of London*, 161, 911-926

Sinton, C.W., Hitchen, K. & Duncan, R.A. (1998). ^{40}Ar–^{39}Ar geochronology of silicic and basic volcanic rocks on the margins of the North Atlantic. *Geological Magazine*, 135, 161-170.

Skilling, I.P. (2002). Basaltic pāhoehoe lava deltas: large-scale characteristics, clast generation, emplacement processes and environmental discrimination. In: *Volcano-ice Interaction on Earth and Mars* (edited by J.L. Smellie, & M.G. Chapman). The Geological Society of London Special Publications, 202, 91-113.

Skogseid, J., Planke, S., Faleide, J.I., Pedersen, T., Eldholm, O. & Neverdal, F. (2000). NE Atlantic continental rifting and volcanic margin formation. In: *Dynamics of the Norwegian Margin* (edited by A. Nøttvedt). The Geological Society of London Special Publication, 167, 29-326.

Sloss, L.L., Krumbein, W.C. & Dapples, E.C. (1949). Integrated facies analysis. In: *Sedimentary Facies in Geologic History* (edited by C.R. Longwell). Geological Society of America Memoir, 39, 91-124.

Smallwood, J.R. & Gill, C. (2002). The rise and fall of the Faroe-Shetland Basin: evidence from seismic mapping of the Balder Formation. *Journal of the Geological Society of London*, 159, 627-630.

Smallwood, J.R. & Maresh, J. (2002). The properties, morphology and distribution of igneous sills: modelling, borehole data and 3D seismic from the Faroe-Shetland area. In: *The North Atlantic Igneous Province: Stratigraphy, Tectonic, Volcanic and Magmatic Processes* (edited by D.W. Jolley & B.R. Bell). The Geological Society of London Special Publications, 197, 271-306.

Smallwood, J.R. & White, R.S. (2002). Ridge-plume interaction in the North Atlantic and its influence on continental breakup and seafloor spreading. In: T*he North Atlantic Igneous Province: Stratigraphy, Tectonic, Volcanic and Magmatic Processes* (edited by D.W. Jolley & B.R. Bell). The Geological Society of London Special Publications, 197, 15-37.

Smallwood, J.R., Prescott, D. & Kirk, W. (2004). Alternatives in Paleocene exploration Wes of Shetland: a case study. *Scottish Journal of Geology*, 40 (2), 131-143.

Smallwood, J.R. & Kirk, W.J. (2005). Paleocene exploration in the Faroe–Shetland Channel: disappointments and discoveries. In: *Petroleum Geology: North-West Europe and Global Perspectives: Proceedings of the 6th Conference* (edited by A.G. Dore & B.A. Vining). The Geological Society of London, 977–991.

Smallwood, J.R. (2008). Uplift, compression and the Cenozoic Faroe–Shetland sediment budget. In: *The Nature and Origin of Compression in Passive Margins* (edited by H.

Johnson, A.G. Doré, R.W. Gatliff, R. Holdsworth, R. Lundin & J.D. Ritchie The Geological Society of London Special Publications, 306, 137–152.

Smellie, J.L., McArthur, J.M, Mcintosh, W.C. & Esser R. (2006). Late Neogene interglacial events in the James Ross Island region, northern Antarctic Peninsula, dated by Ar/Ar and Sr-isotope stratigraphy. *Palaeogeography, Palaeoclimatology, Palaeoecology*, 242, 169-187.

Smellie, J.L., Johnson, J.S., Mcintosh, W.C., Esser R., Gudmundsson, M.T., Hambrey, M.J. & Van Wyk De Vries, B. (2008). Six million years of glacial history recorded in volcanic lithofacies of the James Ross Island Volcanic Group, Antarctic Peninsula. *Palaeogeography, Palaeoclimatology, Palaeoecology*, 260, 122-148.

Smith, G.A. (1987). Sedimentology of Volcanism-Induced Aggradation in Fluvial Basins: Examples from the Pacific Northwest, U.S.A. In: *Recent Developments in Fluvial Sedimentology* (edited by F.G. Ethridge, R.M. Flores & M.D. Harvey). Society for Sedimentary Geology Special Publications, 39, 217-228.

Smith, G.A. (1988). Neogene synvolcanic and syntectonic sedimentation in central Washington. *Geological Society of America Bulletin*, 100, 1479-1492.

Smith, J.R., Malahoff, A. & Shor, A.N. (1999). Submarine geology of the Hilina slump and morpho-structural evolution of Kilauea volcano, Hawaii. *Journal of Volcanology and Geothermal Research*, 94, 59-88.

Smythe, D.K. (1983). Faeroe-Shetland escarpment and continental margin north of the Faeroes. In: *Structure and Development of the Greenland-Scotland Ridge* (edited by M. H. P. Bott, S. Saxov, M. Talwani & J. Thiede). Plenum Publishing Corporation, 109-119.

Smythe, D.K., Chalmers, J.A., Skuce, A.G., Bobinson, A. & Mould, A.S. (1983). Early opening history of the North Atlantic – I. Structure and origin of the Faroe-Shetland Escarpment. *Geophysical Journal of the Royal Astronomical Society*, 72, 373-398.

Soule, S.A., Cashman, K.V. & Kauahikaua, J.P. (2004). Examining flow emplacement through the surface morphology of three rapidly emplaced, solidified lava flows, Kilauea Volcano, Hawaii. *Bulletin of Volcanology*, 66, 1-14.

Søager, N. & Holm, P.M. (2009). Extended correlation of the Paleogene Faroe Islands and East Greenland plateau basalts. *Lithos*, 107, 205-215.

Sørensen, A.B. (2003). Cenozoic basin development and stratigraphy of the Faroes area. *Petroleum Geoscience*, 9, 189-207.

Spencer, A.M., Birkeland, Ø., Knag, G.Ø & Fredsted, R. (1999). Petroleum systems of the Atlantic margin of northwest Europe. In: *Petroleum Geology of Northwest Europe: Proceedings of the 5th Conference* (edited by A.J. Fleet & S.A.R. Boldy). The Geological Society of London, 231-246.

Spitzer, R., White, R.S. & iSIMM Team (2005). Advances in seismic imaging through basalts: a case study from the Faroe–Shetland Basin. *Petroleum Geoscience*, 11**,** 147-156.

Spitzer, R., White, R.S. & Christie, P.A.F. (2008). Seismic characterization of basalt flows from the Faroes margin and the Faroe-Shetland basin. *Geophysical Prospecting*, 56, 21-31.

Stewart, S.A. & Holt, J. (2004). Improved drilling performance through integration of seismic, geological and drilling data. In: *3D Seismic Technology: Application to the Exploration of Sedimentary Basins* (edited by R.J. Davies, J.A. Cartwright, S.A. Stewart, M. Lappin & J.R. Underhill). The Geological Society of London Memoirs, 29, 303-310.

Stoker, M.S., Hitchen, K. & Graham, C.C. (1993). *United Kingdom Offshore Regional Report: The geology of the Hebrides and West Shetland shelves, and adjacent deep-water areas*. British Geological Survey, pp. 149.

Stollhofen, H. & Stanistreet, I.G. (1994). Interaction between bimodal volcanism, fluvial sedimentation and basin development in the Permo-Carboniferous Saar- Nahe Basin (south-west Germany). *Basin Research*, 6, 245-267.

Storey, M., Duncan, R.A. & Tegner, C. (2007). Timing and duration of volcanism in the North Atlantic Igneous Province: Implications for geodynamics and links to the Iceland hotspot. *Chemical Geology*, 241, 264-281.

Sullivan, M., Coombes, T., Imbert, P. & Ahamdach-Demars, C. (1999). Reservoir quality and petrophysical evaluation of Paleocene sandstones in the West of Shetland area. In: *Petroleum Geology of Northwest Europe: Proceedings of the 5th Conference* (edited by A.J. Fleet & S.A.R. Boldy). The Geological Society of London, 627-633.

Swanson, D.A. (1973). Pahoehoe Flows from the 1969-1971 Mauna Ulu Eruption, Kilauea Volcano, Hawaii. *Geological Society of America Bulletin*, 84, 615-626.

Swanson, D.A., Wright, T.L. & Helz, R.T. (1975). Linear Vent Systems and Estimated Rates of Magma Production and Eruption for the Yakima Basalt on the Columbia Plateau. *America Journal of Science*, 275, 877-905.

Symonds, P.A., Planke, S., Frey, O. & Skogseid, J. (1998). Volcanic evolution of the Western Australian continental margin and its implications for basin development. In: *The*

Sedimentary Basins of Western Australia 2: Proceedings of the PESA Symposium, (edited by P. G. R. R. Purcell). Petroleum Exploration Society of Australia, 33-54.

T

Thomson, K. (2005). Volcanic features of the North Rockall Trough: application of visualisation techniques on 3D seismic reflection data. *Bulletin of Volcanology*, 67 (2), 116-128.

Thomson, K. & Schofield, N. (2008). Lithological and structural controls on the emplacement and morphology or sills in sedimentary basins. In: *Structure and emplacement of High-Level Magmatic Systems* (edited by K. Thomson & N. Petford). The Geological Society of London Special Publications, 302, 31-44.

Thompson, R.N. & Gibson, S.A. (1991). Subcontinental mantle plumes, hotspots and pre-existing thinspots. *Journal of the Geological Society*, 148, 973-977.

Thordarson, T. & Self, S. (1998). The Roza Member, Columbia River Basalt Group: A gigantic pahoehoe lava flow field formed by endogenous processes? *Journal of Geophysical Research*, 103 (B11), 27,411-27,445.

Thouret, J.-C. (1999). Volcanic geomorphology - an overview. *Earth Science Reviews*, 47, 95-131.

Tipper, J.C. (1993). Do seismic reflections necessarily have chronostratigraphic significance? *Geological Magazine*, 130 (1), 47-55.

Tolan, T. & Beeson, M.H. (1984). Intracanyon flows of the Columbia River Basalt Group in the lower Columbia River Gorge and their relationship to the Troutdale Formation. *Geological Society of America Bulletin*, 95, 463-477.

Tolan, T., Lindsey, K. & Porcello, J. (2009). *A Summary of Columbia River Basalt Group Geology and its Influence on the Hydrogeology of the Columbia River Basalt Aquifer System: Columbia Basin ground Water Management Area of Adams, Franklin, Grant and Lincoln Counties*. GSI Water Solutions Inc (www.cbgma.org), pp. 65.

Torsvik, T.H., Smethurst, M.A., Burke, K. & Steinberger, B. (2006). Large igneous provinces generated from the margins of the large low-velocity provinces in the deep mantle. *Geophysical Journal International*, 167, 1447-1460.

Trodeson, A.L. & Smellie, J.L. (2002). The Polonez Cove Formation of King George Island, Antarctica: stratigraphy, facies and implications for mid-Cenozoic cryosphere development. *Sedimentology*, 49, 277-301.

Trude, J., Cartwright, J., Davies, R.J. & Smallwood, J. (2003). New technique for dating igneous sills. *Geology*, 31, 813-816.

Trude, K.J. (2004). Kinematic indicators for shallow level igneous intrusions from 3D seismic data: evidence of flow direction and feeder location. In: 3D *Seismic Technology: Application to the Exploration of Sedimentary Basins* (edited by R.J. Davies, J.A. Cartwright, S.A. Stewart, M. Lappin & J.R. Underhill). The Geological Society of London Memoirs, 29, 209-217.

U

Ukstins Peate, I., Larsen, M. & Lesher, C.E. (2003). The transition from sedimentation to flood volcanism in the Kangerlussuaq basin, East Greenland: basaltic pyroclastic volcanism during initial Palaeogene continental break-up. *Journal of the Geological Society of London*, 160, 759-722.

Umino S., Nonaka, M. & Kauahikaua, J. (2006). Emplacement of subaerial pahoehoe lava sheet flows into water: 1990 Kūpaianaha flow of Kilauea volcano at Kaimū Bay, Hawai`i. *Bulletin of Volcanology*, 69 (2), 125-139.

Underhill, J.R. (2001). Controls on the genesis and prospectivity of Paleogene palaeogeomorphic traps, East Shetland Platform, UK North Sea. *Marine and Petroleum Geology*, 18, 259-281.

Urgeles, R., Masson, D.G., Canals, M., Watts, A.B. & Le Bas, T. (1999). Recurrent large-scale landsliding on the west flank of La Palma, Canary Islands. *Journal of Geophysical Research*, 104 (B11), 25331-25348.

V

Vail, P.R., Mitchum, R.M. & Thompson III, S. (1977a). Seismic Stratigraphy and Global Changes of Sea Level, Part 3: Relative Changes of Sea Level from Coastal Onlap. In: *Seismic Stratigraphy – Applications to Hydrocarbon Exploration* (edited by C.E. Payton). American Association of Petroleum Geologists Memoirs, 26, 63-81.

Vail, P.R., Mitchum, R.M. & Thompson III, S. (1977b). Seismic Stratigraphy and Global Changes of Sea Level, Part 4: Global Cycles of Relative Changes in Sea Level. In: *Seismic Stratigraphy – Applications to Hydrocarbon Exploration* (edited by C.E. Payton). American Association of Petroleum Geologists Memoirs, 26, 83-97.

Vail, P.R., Todd, R.G. & Sangree, J.B. (1977c). Seismic Stratigraphy and Global Changes of Sea Level, Part 5: Chronostratigraphic Significance of Seismic Reflections. In: *Seismic Stratigraphy – Applications to Hydrocarbon Exploration* (edited by C.E. Payton). American Association of Petroleum Geologists Memoirs, 26, 99-116.

Van Den Akker, T.J.H.A., Kaminski, M.A., Gradstein, F.M. & Wood, J. (2000). Campanian to Palaeocene biostratigraphy and palaeoenvironments in the Foula Sub-basin, west of the Shetland Islands, UK. *Journal of Micropalaeontology*, 19, 23-43.

Van Wagoner, J.C., Posamentier, H.W., Mitchum, R.M., Vail, P.R., Sarg, J.F., Loutit, T.S. & Hardenbol, J. (1988). An Overview of the Fundamentals of Sequence Stratigraphy and Key Definitions. In: *Sea Level Changes – An Integrated Approach* (edited by C.K. Wilgus, B.S. Hastings, C.G. Kendal, H.W. Posamentier, C.A., Ross & J.C. Van Wagoner). Society for Sedimentary Geology Special Publications, 42, 39-46.

Van Wagoner, J.C., Mitchum, R.M., Campion, M.K. & Rahmanian, V.D. (1990). Siliciclastic Sequence Stratigraphy in Well Logs, Core and Outcrop: Concepts for High Resolution Correlation of Time and Facies. *American Association of Petroleum Geologists, Methods in Exploration Series*, 7, pp. 55.

Vernik, L. (1990). A new type of reservoir rock in volcaniclastic sequences. *American Association of Petroleum Geologists Bulletin*, 74 (6), 830-836.

Verstralen, I. & Hurst, A. (1994). Sedimentology, reservoir characteristics and exploration potential of the Rona Sandstone, west of Shetland. *First Break*, 12, 11-20.

Vink, G.E. (1984). A Hotspot Model for Iceland and the Vøring Plateau. *Journal of Geophysical Research*, 89 (B12), 9949-9959.

W

Waagstein, R., Guise, P. & Rex, D. (2002). K/Ar and ^{39}Ar/^{40}Ar whole-rock dating of zeolite facies metamorphosed flood basalts: the upper Paleocene basalts of the Faroe Islands, NE Atlantic. In: *The North Atlantic Igneous Province: Stratigraphy, Tectonic, Volcanic and Magmatic Processes* (edited by D.W. Jolley & B.R. Bell). The Geological Society of London Special Publications, 197, 219-252.

Walker, G.P.L. (1991). Structure, and origin by injection of lava under surface crust, of tumuli, "lava rises", "lava-rise pits", and "lava-inflation clefts" in Hawaii. *Bulletin of Volcanology*, 53, 546-558.

Walker, G.P.L. (1993). Basaltic-volcano systems. In: *Magmatic Processes and Plate Tectonics* (edited by H.M. Prichard, T. Alabaster, N.B.W. Harris & C.R. Neary). The Geological Society of London Special Publications, 76, 3-38.

Watton, T.J., Jerram, D.A., Thordarson, T. & Davies, R.J. (2013). Three-dimensional lithofacies variations in hyaloclastite deposits. *Journal of Volcanology and Geothermal Research*, 250, 19-33.

Wells, S.G., Dohrewend, J.C., McFadden, L.D., Turrin, B.D. & Mahrer, K.D. (1985). Late Cenozoic landscape evolution on lava flow surfaces of the Cima volcanic field, Mojave Desert, California. *Geological Society of America Bulletin,* 96 (12), 1518-1529.

West, B.P., May, S.R., Eastwood, J.E. & Rossen, C. 2002. Interactive seismic facies classification using textural attributes and neural networks. *The Leading Edge*, 21 (10), 1042-1049.

Widdowson, M. (1997). Tertiary palaeosurfaces of the SW Deccan, Western India: implications for passive margin uplift. In: *Palaeosurfaces: Recognition, Reconstruction and Palaeoenvironmental Interpretation* (edited by M. Widdowson). The Geological Society of London Special Publications, 197, 221-248.

Wilgus, C.K., Hastings, B.S., Kendal, C.G, Posamentier, H.W., Ross, C.A. & Van Wagoner, J.C. (1988). *Sea Level Changes – An Integrated Approach*. Society for Sedimentary Geology Special Publications, 42, pp. 535.

White, R.S. & Mckenzie, D. (1989). Magmatism at Rift Zones: The Generation of Volcanic Continental Margins and Flood Basalts. *Journal of Geophysical Research*, 94 (B6), 7685-7729.

White, J.D.L. (1991). The depositional record of small monogenetic volcanoes within terrestrial basins. In: *Sedimentation in Volcanic Settings* (edited by R.V. Fisher & G.A. Smith). Society for Sedimentary Geology Special Publications, 45, 155-171.

White, N. & Lovell, B. (1997). Measuring the pulse of a plume with the sedimentary record. *Nature*, 387, 888-891.

White, R. S., Fruehn, J., Richardson, K.R., Cullen, E., Kirk, W., Smallwood, J.R. & Latkiewicz, C. (1999). Faeroes Large Aperture Research Experiment (FLARE): imaging through basalt. In: *Petroleum Geology of Northwest Europe: Proceedings of the 5th Conference* (edited by A.J. Fleet & S.A.R. Boldy). The Geological Society of London, 1243-1252.

White, J.D.L. (2000). Subaqueous eruption-fed density currents and their deposits. *Precambrian Research*, 101, 97-109.

White, R. & Simm, R. (2003). Tutorial: Good practice in well ties. *First Break*, 21, 75-83.

White, R.S., Smallwood, J.R., Fliedner, M.M., Boslaugh, B., Maresh, J. & Fruehn, J. (2003). Imaging and regional distribution of basalt flows in Faeroe-Shetland Basin: Sub-basalt imaging. *Geophysical Prospecting*, 51, 215-231.

White, R. S., Spitzer, R., Christie, P. A. F., Roberts, A., Lunnon, Z., Maresh, J. & iSIMM Working Group (2005). Seismic imaging through basalt flows on the Faroes Shelf. In:

Faroe Islands Exploration Conference: Proceedings of the 1ˢᵗ Conference (edited by H. Ziska, T. Varming & D. Blotch). Faroe Islands Exploration Conference: Proceedings of the 1ˢᵗ Conference, Annales Societatis Scientiarum Færoensis, Supplementum 43, 11-31.

Witt, A.J., Fowler, S.R., Kjelstadli, R.M., Draper, L.F., Barr, D. & McGarrity, J.P. (2010). Managing the start-up of a fractured oil reservoir: development of the Clair field, West of Shetland. In: *Petroleum Geology: From Mature Basins to New Frontiers - Proceedings of the 7th Conference* (edited by B.A. Vining & S.C. Pickering). The Geological Society of London, 299-313.

X

Y

Yamagishi, H. (1991). Morphological and sedimentological characteristic of the Neogene submarine coherent lavas and hyaloclastites in Southwest Hokkaido, Japan. *Sedimentary Geology*, 74, 5-23.

Yilmaz, Ö. & Doherty, S.M. (1987). *Seismic data processing*. Society of Exploration Geophysicists, Tulsa, pp. 526.

Z

Zhang, K., Marfurt, K.J., Wan, Z. & Zhan, S. (2011). Seismic attribute illumination of a igneous reservoir in China. *The Leading Edge*, 30 (3), 266-270.

Zhong, S. & Watts, A.B. (2002). Constraints on the dynamics of mantle plumes from uplift of the Hawaiian Islands. *Earth and Planetary Science Letters*, 203, 105-116.

Ziolkowski, A., Hanssen, P., Gatliff, R., Jakubowicz, H., Dobson, A., Hampson, G., Li, X-Y. & Liu, E. (2003). Use of low frequencies for sub-basalt imaging. *Geophysical Prospecting*, 51, 169-182.

Zou, C., Zhu, R., Zhao, W., Jia, C., Zhang, G., Yian, X, Zhao, X. & Wen, B. (2010). Geological Characteristic of Volcanic Hydrocarbon Reservoirs and Exploration Directions in China. *Acta Geologica Sinica*, 84 (1), 194-205.

APPENDIX I: SUPPORT MATERIAL FOR CHAPTER 4

This appendix contains supporting evidence for Chapter 4: *Application of Sequence Stratigraphic Concepts to a Lava-fed Delta System in the Faroe-Shetland Basin*. It includes a location map (see Fig. A1.1), the 2D seismic sections used in Chapter 4 without the close-ups (see A1.2 – A1.7) and additional 2D seismic sections which transect the Faroe-Shetland Escarpment (see Fig. A1.8 – A1.15). All 2D seismic section have been interpreted to display the seismic reflection units, bounding reflections and distribution of seismic facies.
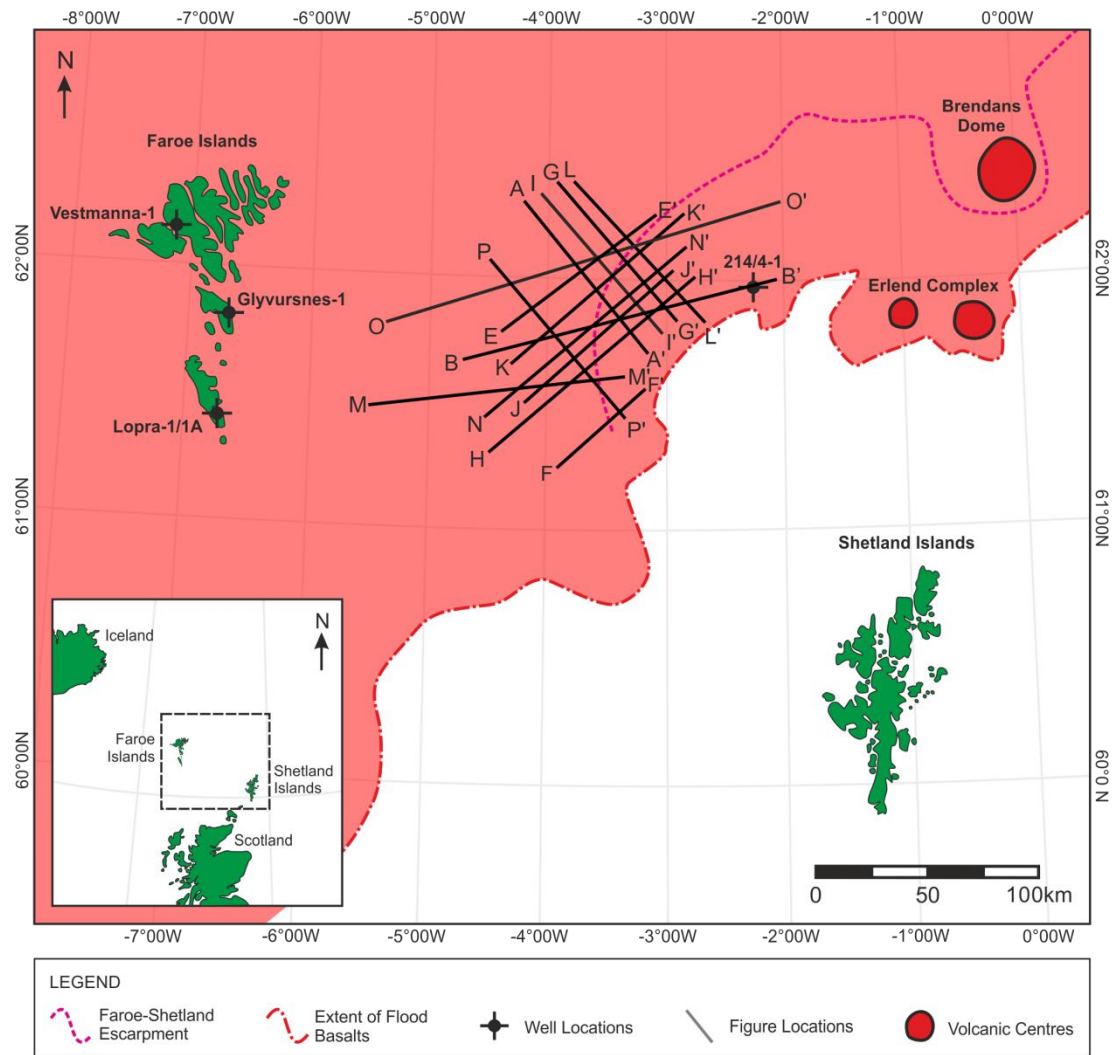
Fig. A1.1. Map of the study area and the location of cross sections shown in Figures A1.2 to A1.15, with a continuation of identifying letter from Chapter 4. Extent of flood basalts and Faroe-Shetland Escarpment modified from Ritchie *et al.* (1996, 1999), Ellis *et al.* (2002) and Sørensen (2003).
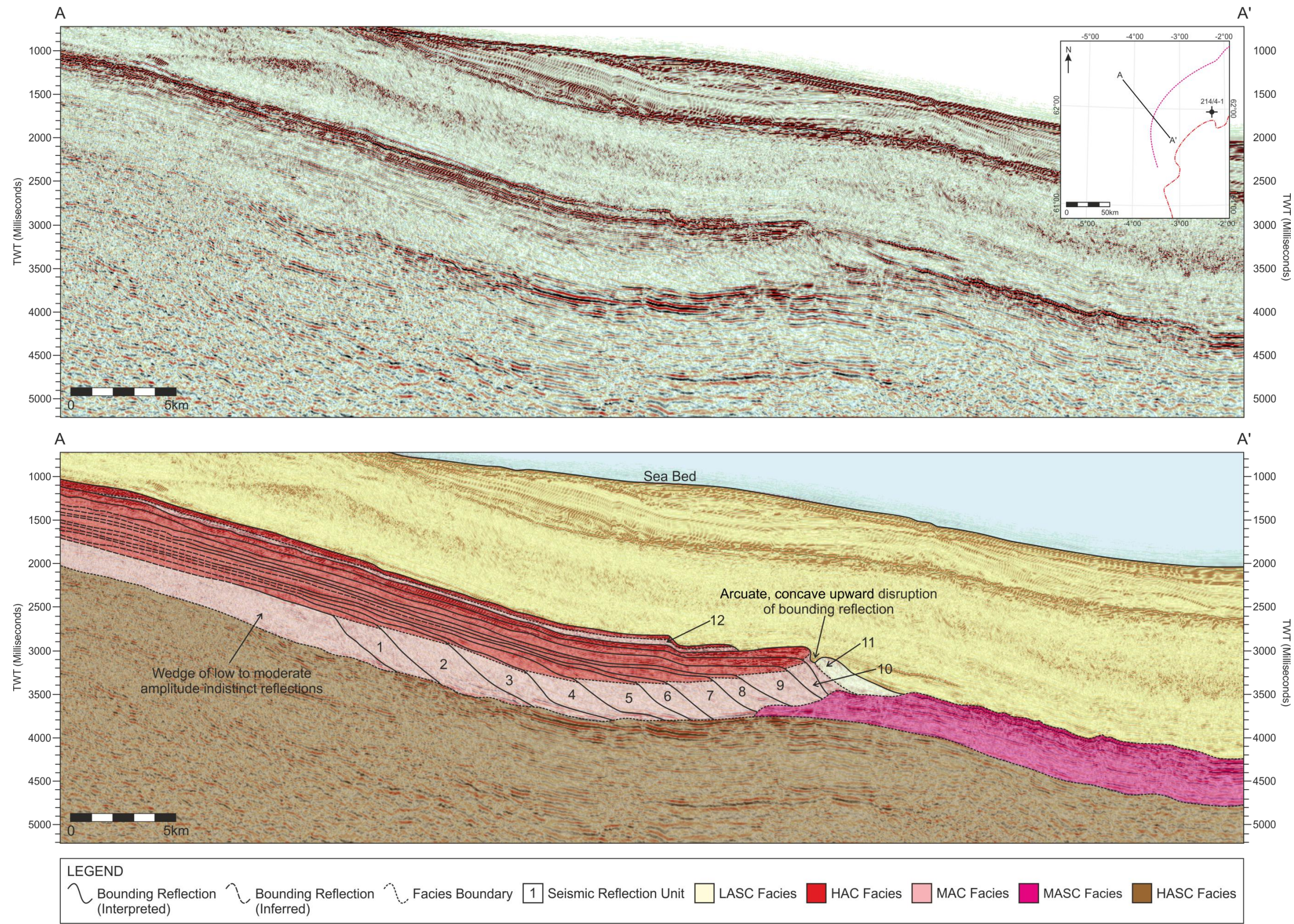
Fig. A1.2. Seismic section A-A' images the Faroe-Shetland Escarpment perpendicular to the curved escarpment edge. The interpreted section includes the seismic reflection units and bounding reflections, distribution of seismic facies and disruption of seismic reflection unit 11 with shallow, semi-continuous internal reflections and a curved, concave-up upper bounding reflection. See Fig. A1.1. for location.
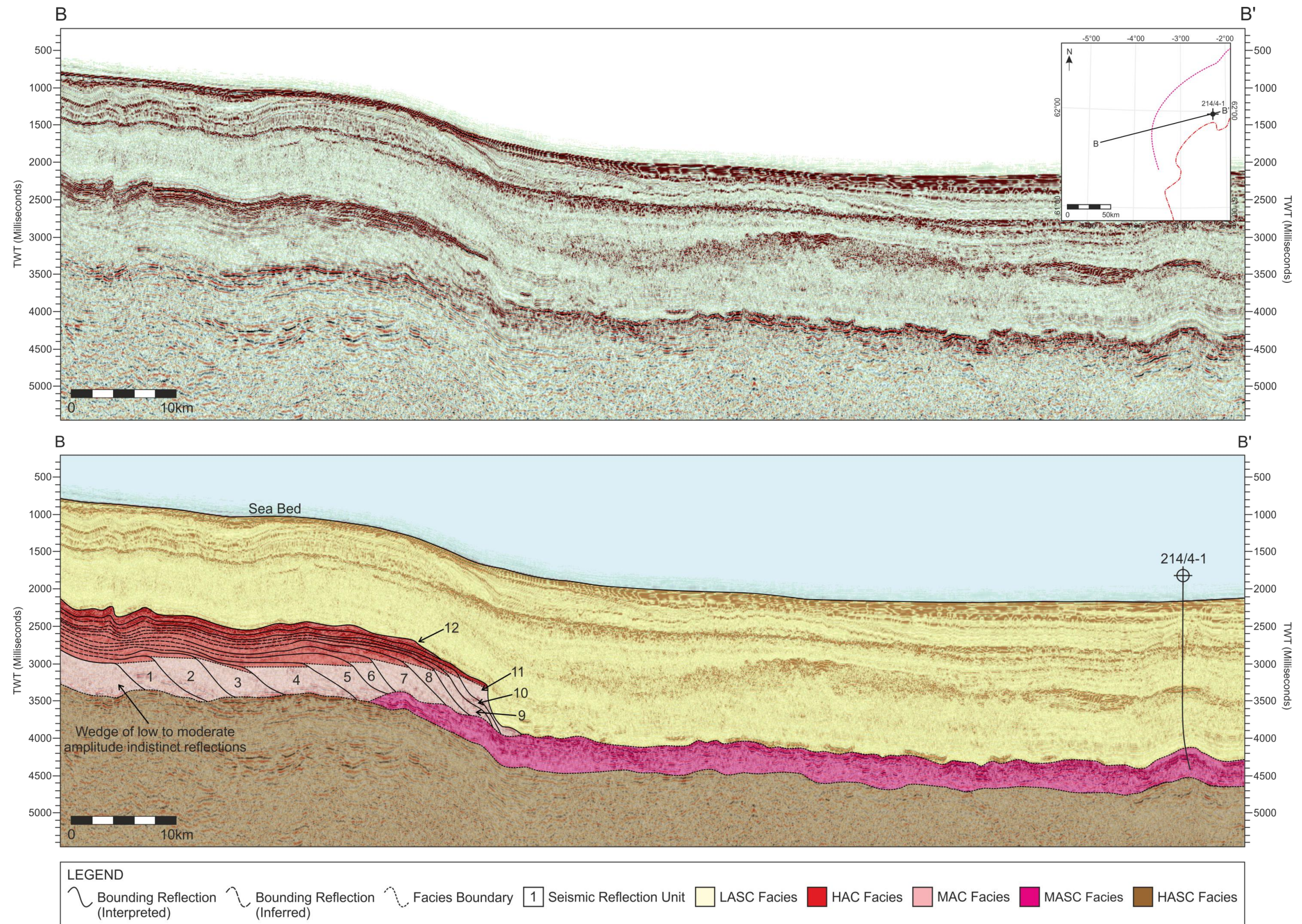
Fig. A1.3. Seismic section B-B' images the Faroe-Shetland Escarpment perpendicular to the curved escarpment edge and the location of exploration well 214/4-1. The interpreted section includes the seismic reflection units and bounding reflections, distribution of seismic facies and the path of intersecting well 214/4-1. See Fig. A1.1. for location.

Fig. A1.4. Seismic section E-E' images the Faroe-Shetland Escarpment largely parallel to curved escarpment edge. The interpreted section includes the seismic reflection units and bounding reflections, distribution of seismic facies and ellipsoid seismic reflection unit which is shown in greater detail in Figure 4.11. See Fig. A1.1. for location.
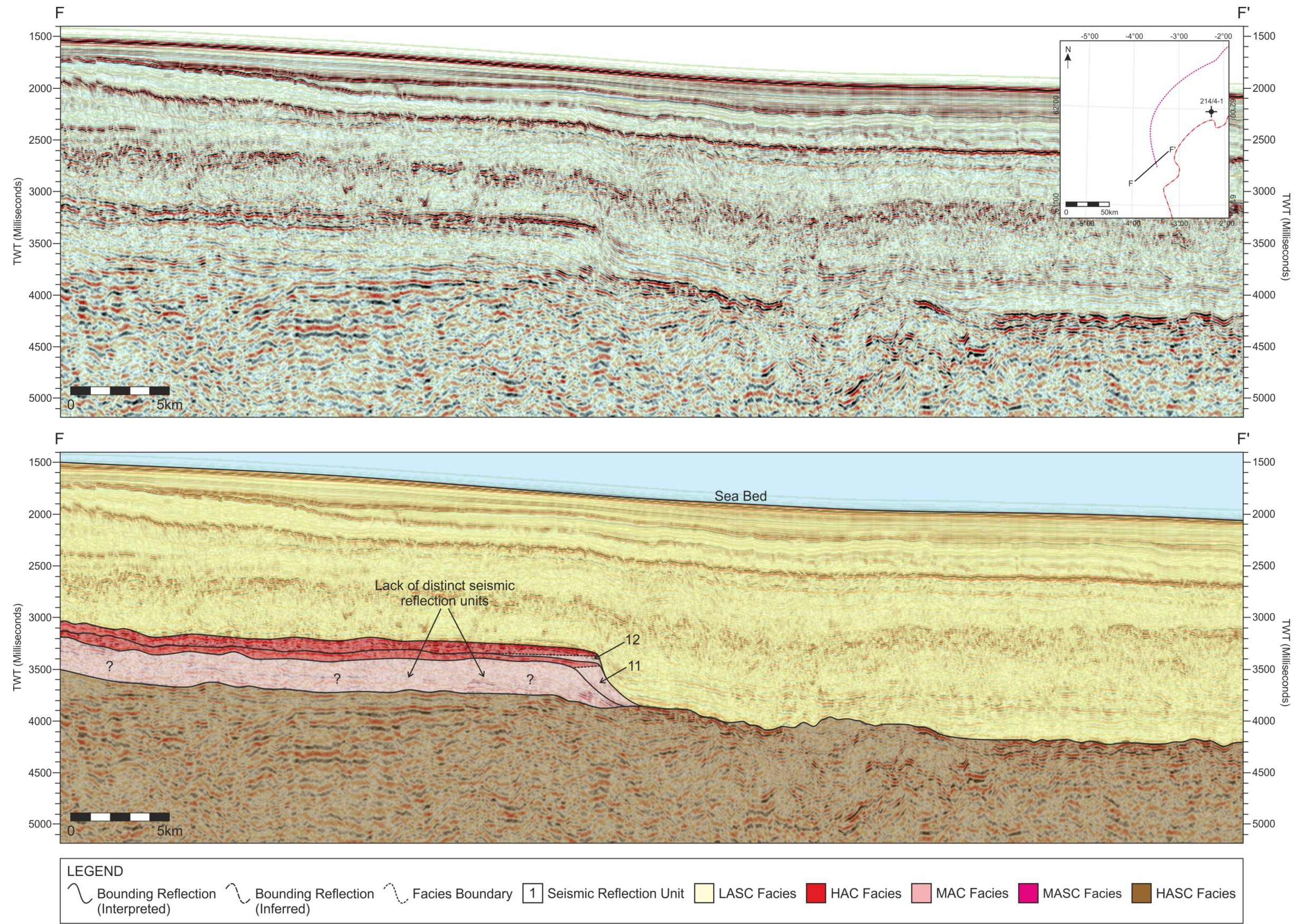
Fig. A1.5. Seismic section F-F' images the southerly extent of the Faroe-Shetland Escarpment. The interpreted section includes bounding reflections of the seismic reflection units, distribution of seismic facies and the thinning of the seismic reflection units below seismic resolution, prohibiting the identification of unit terminations. See Fig. A1.1. for location.
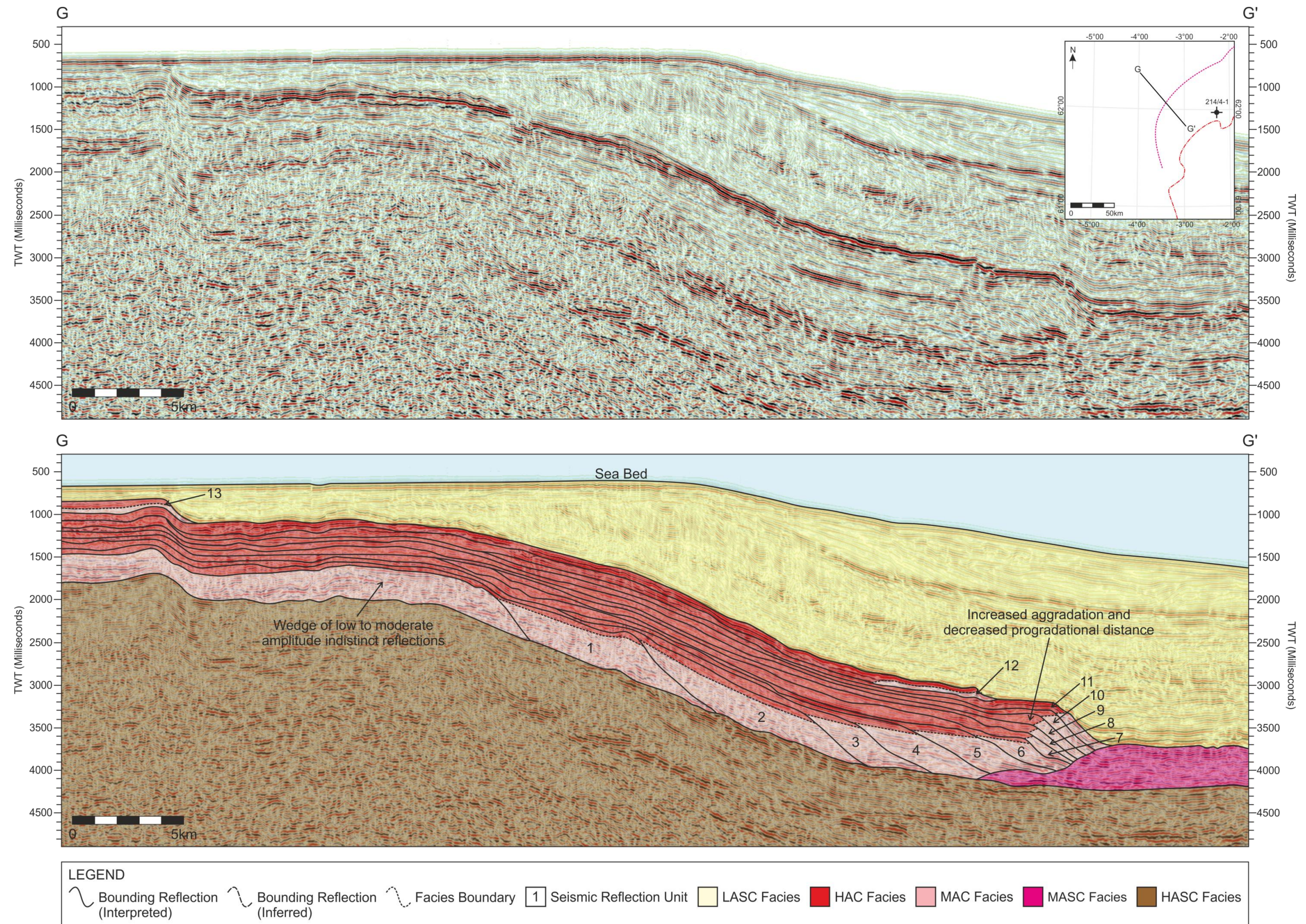
Fig. A1.6. Seismic section G-G' images the Faroe-Shetland Escarpment perpendicular to the curved escarpment edge. The interpreted section includes the seismic reflection units and bounding reflections, distribution of seismic facies and the decrease in progradational distance in the north that contributes to the anticlockwise rotation of the delta front. See Fig. A1.1. for location.
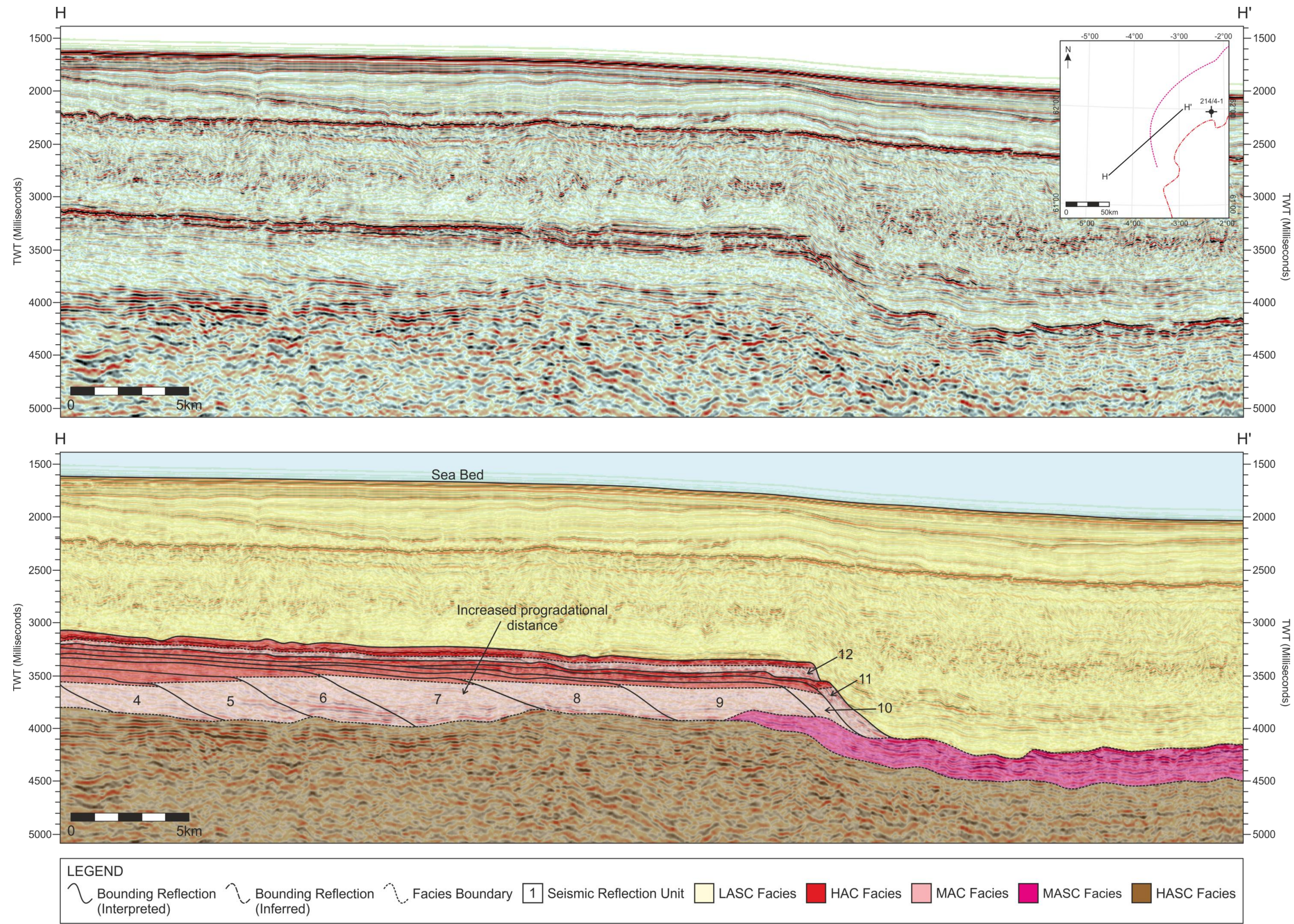
Fig. A1.7. Seismic section H-H' images the Faroe-Shetland Escarpment perpendicular to the curved escarpment edge. The interpreted section includes the seismic reflection units and bounding reflections, distribution of seismic facies and the increase in progradational distance in the south that contributes to the anticlockwise rotation of the delta front. See Fig. A1.1. for location.
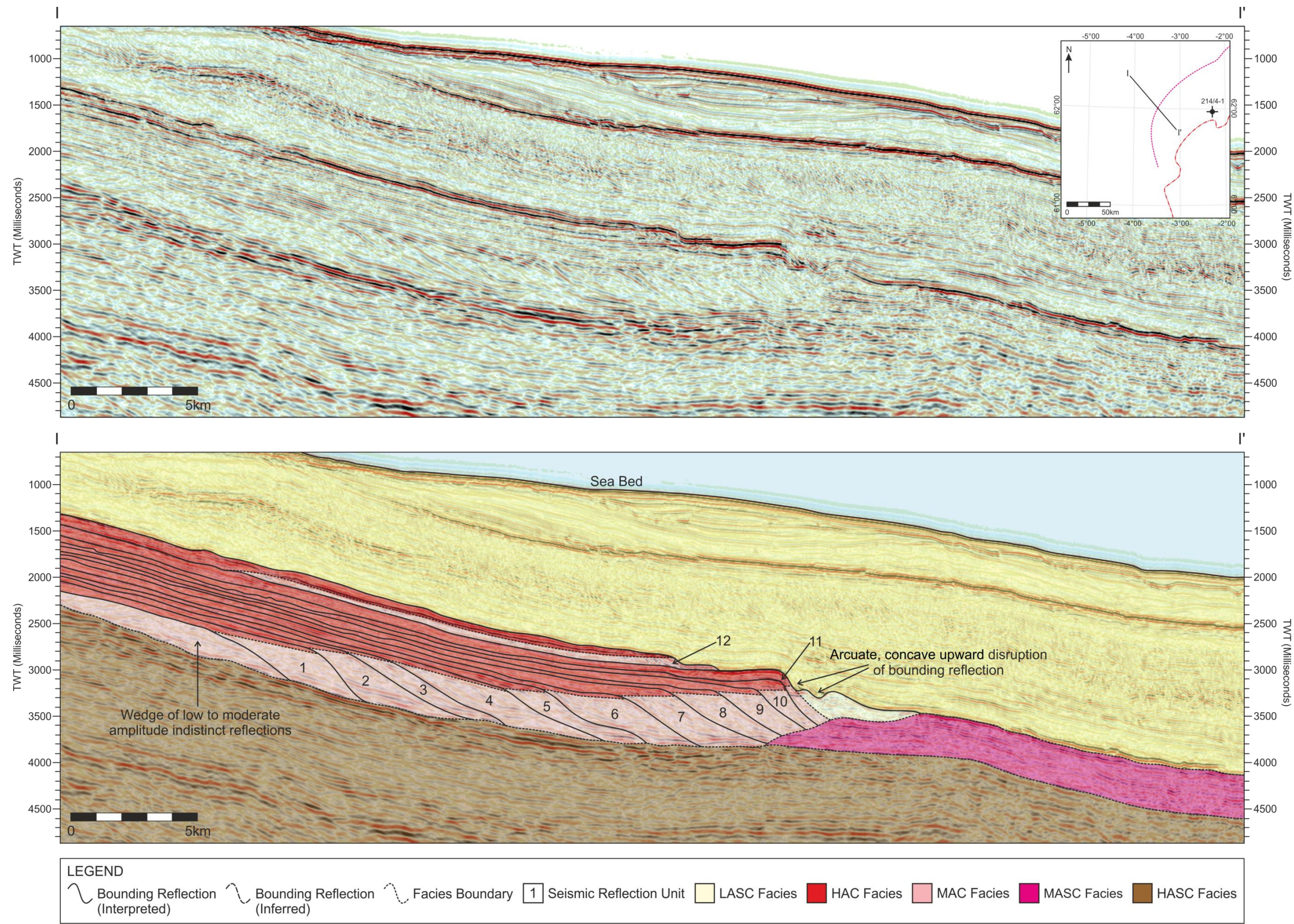
Fig. A1.8. Seismic section I-I' images the Faroe-Shetland Escarpment perpendicular to the curved escarpment edge. The interpreted section includes the seismic reflection units and bounding reflections, distribution of seismic facies and disruption of seismic reflection unit 11 with shallow, semi-continuous internal reflections and a curved, concave-up upper bounding reflection. See Fig. A1.1. for location.
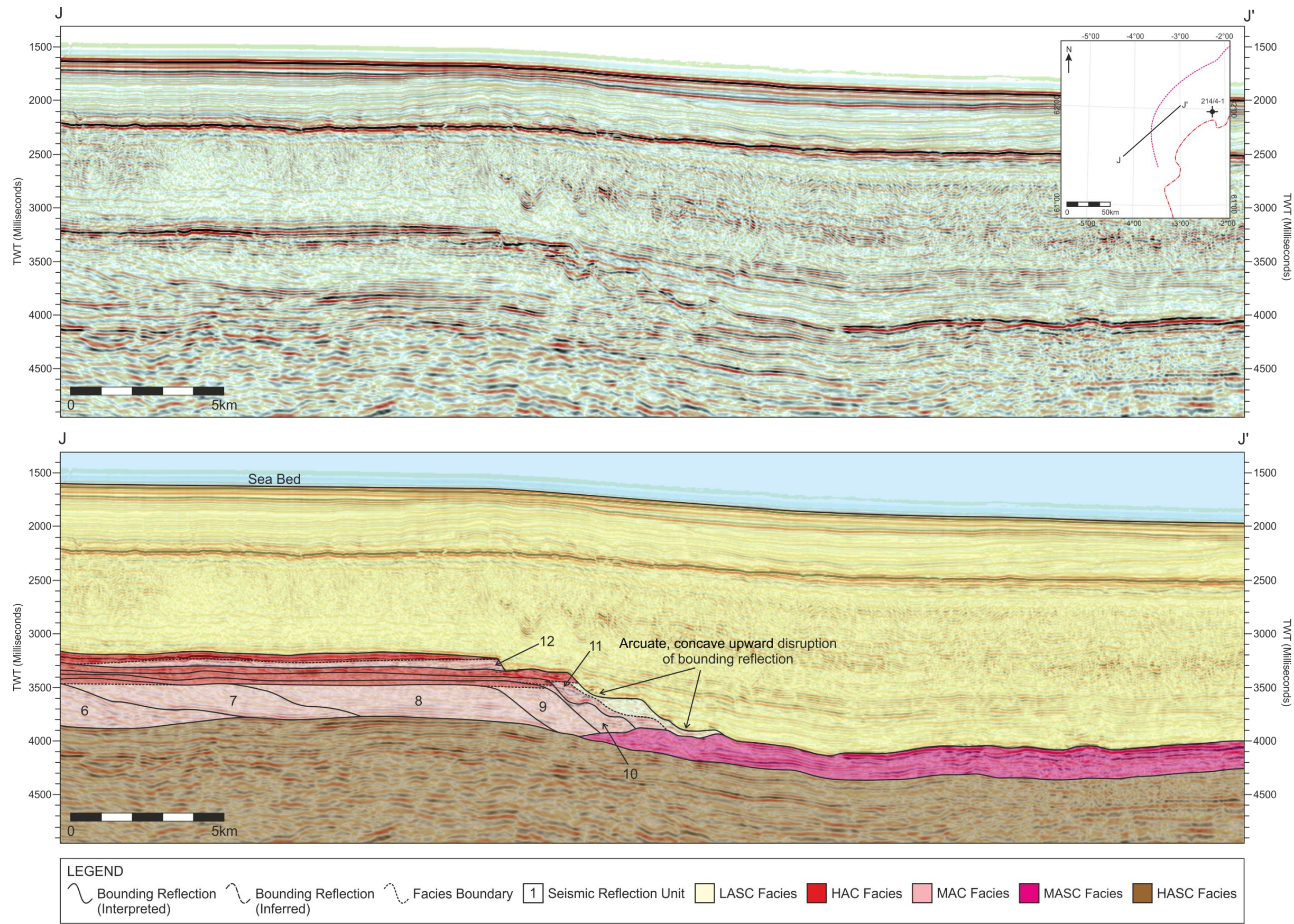
Fig. A1.9. Seismic section J-J' images the Faroe-Shetland Escarpment perpendicular to parallel with the curved escarpment edge. The interpreted section includes the seismic reflection units and bounding reflections, distribution of seismic facies and disruption of seismic reflection unit 11 with shallow, semi-continuous internal reflections and a curved, concave-up upper bounding reflection. See Fig. A1.1. for location.
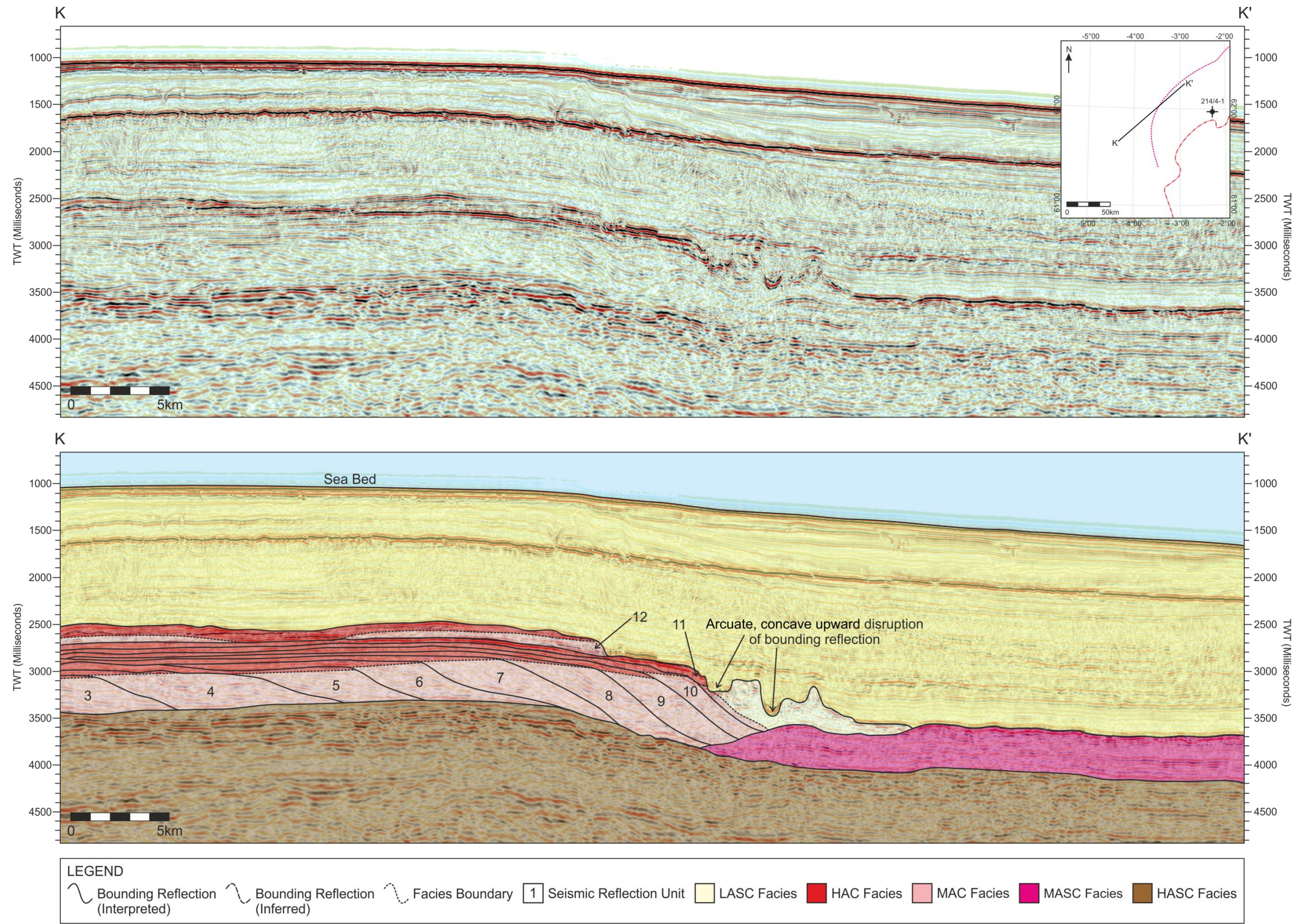
Fig. A1.10. Seismic section K-K' images the Faroe-Shetland Escarpment perpendicular to parallel with the curved escarpment edge. The interpreted section includes the seismic reflection units and bounding reflections, distribution of seismic facies and disruption of seismic reflection unit 11 with shallow, semi-continuous internal reflections and a curved, concave-up upper bounding reflection. See Fig. A1.1. for location.
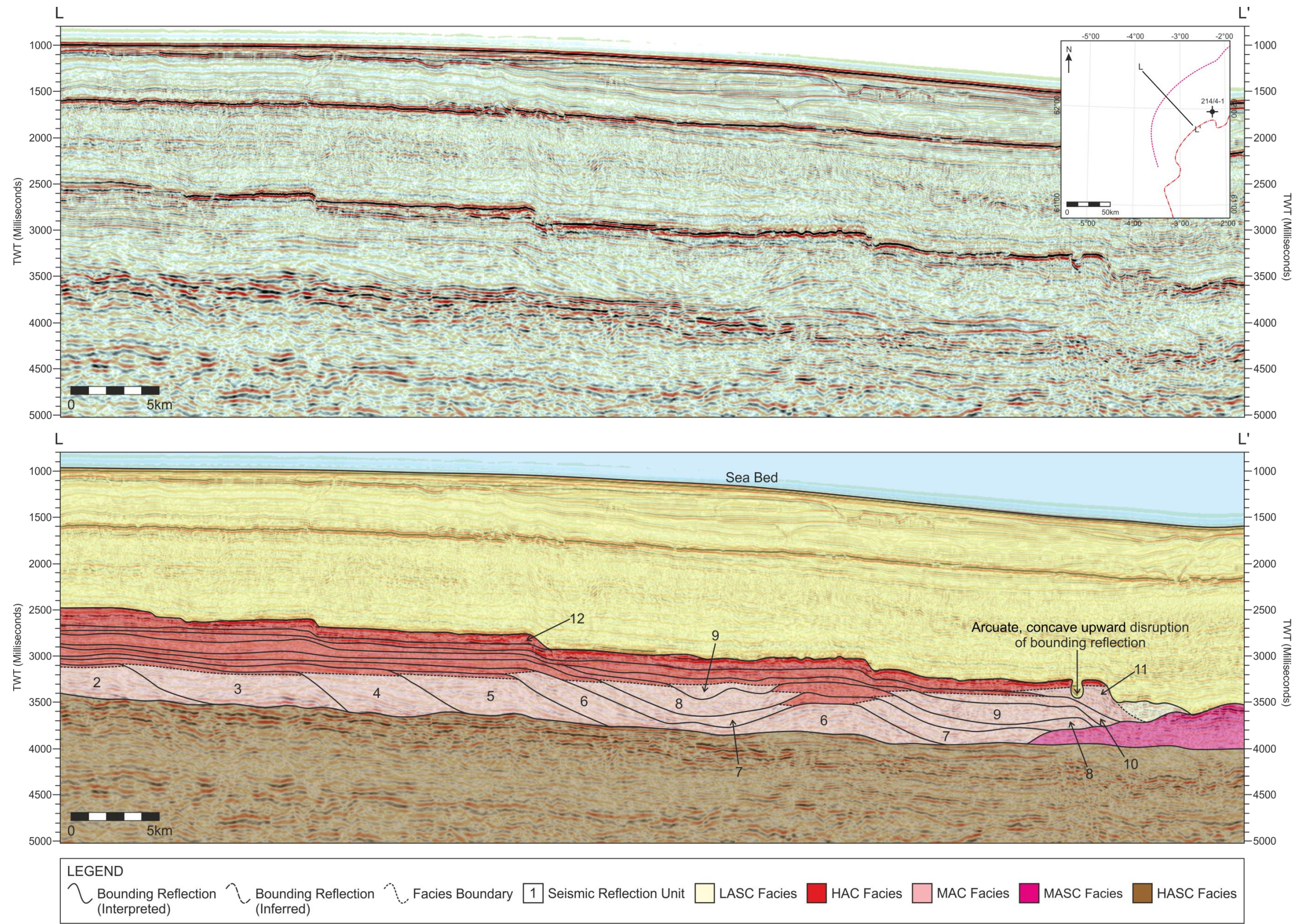
Fig. A1.11. Seismic section L-L' images the Faroe-Shetland Escarpment perpendicular to the curved escarpment edge. The interpreted section includes the seismic reflection units and bounding reflections, distribution of seismic facies and variations in a wedge to ellipsoid shape of the seismic reflection units. See Fig. A1.1. for location.
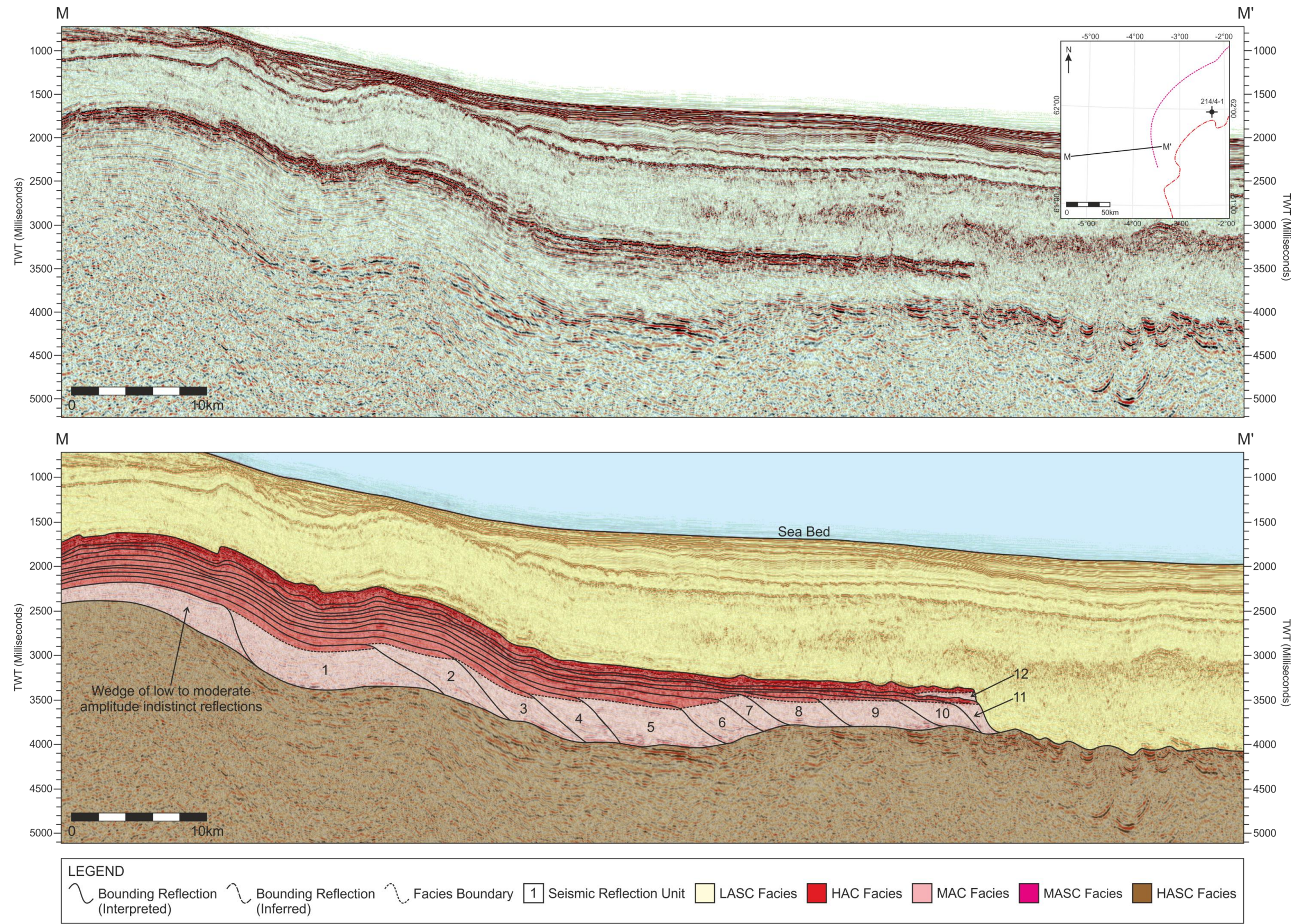
Fig. A1.12. Seismic section M-M' images the Faroe-Shetland Escarpment perpendicular to the curved escarpment edge. The interpreted section includes the seismic reflection units and bounding reflections and distribution of seismic facies, with a lack of MASC facies underlying the escarpment. See Fig. A1.1. for location.
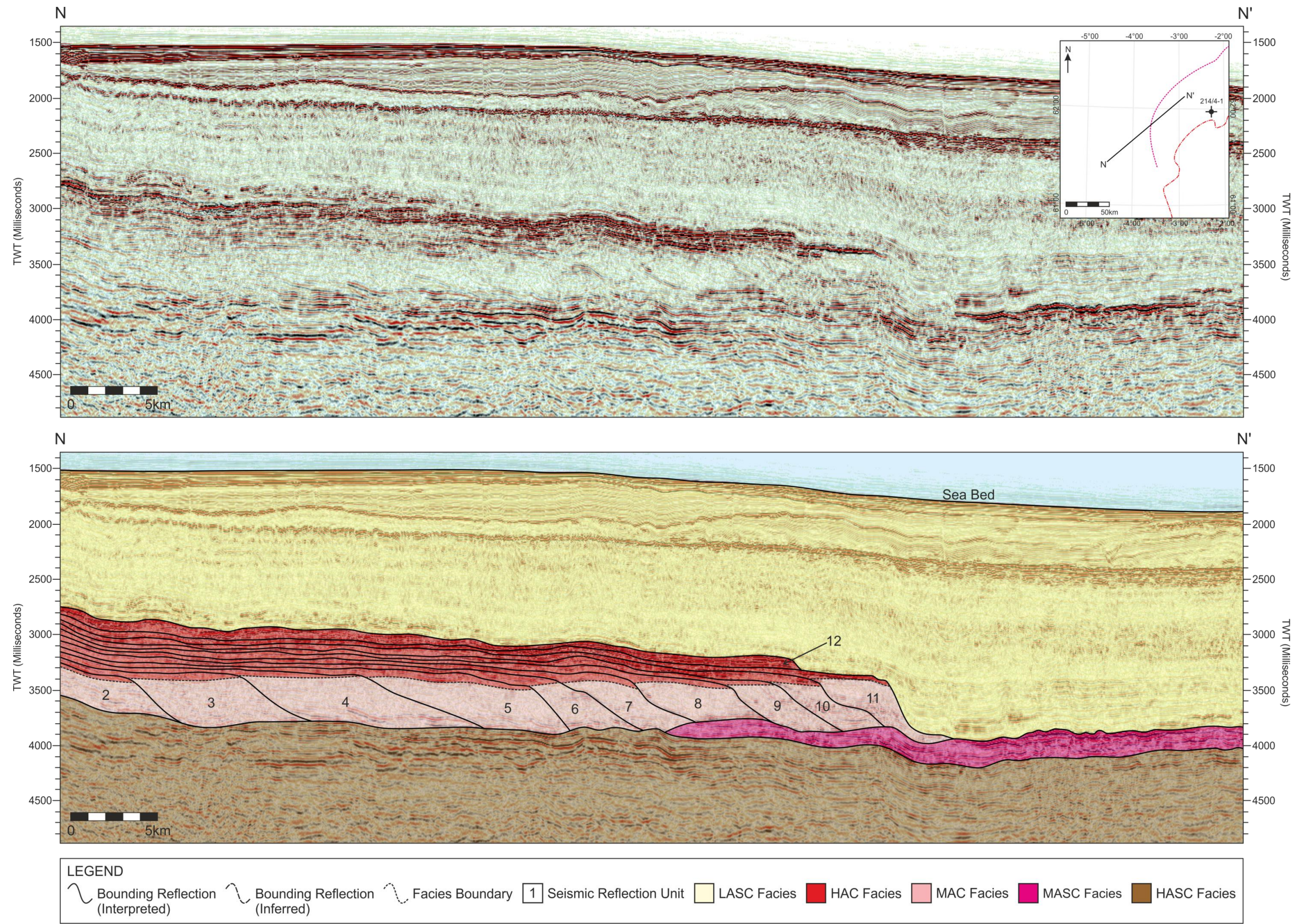
Fig. A1.13. Seismic section N-N' images the Faroe-Shetland Escarpment perpendicular to parallel with the curved escarpment edge. The interpreted section includes the seismic reflection units and bounding reflections and distribution of seismic facies. See Fig. A1.1. for location.
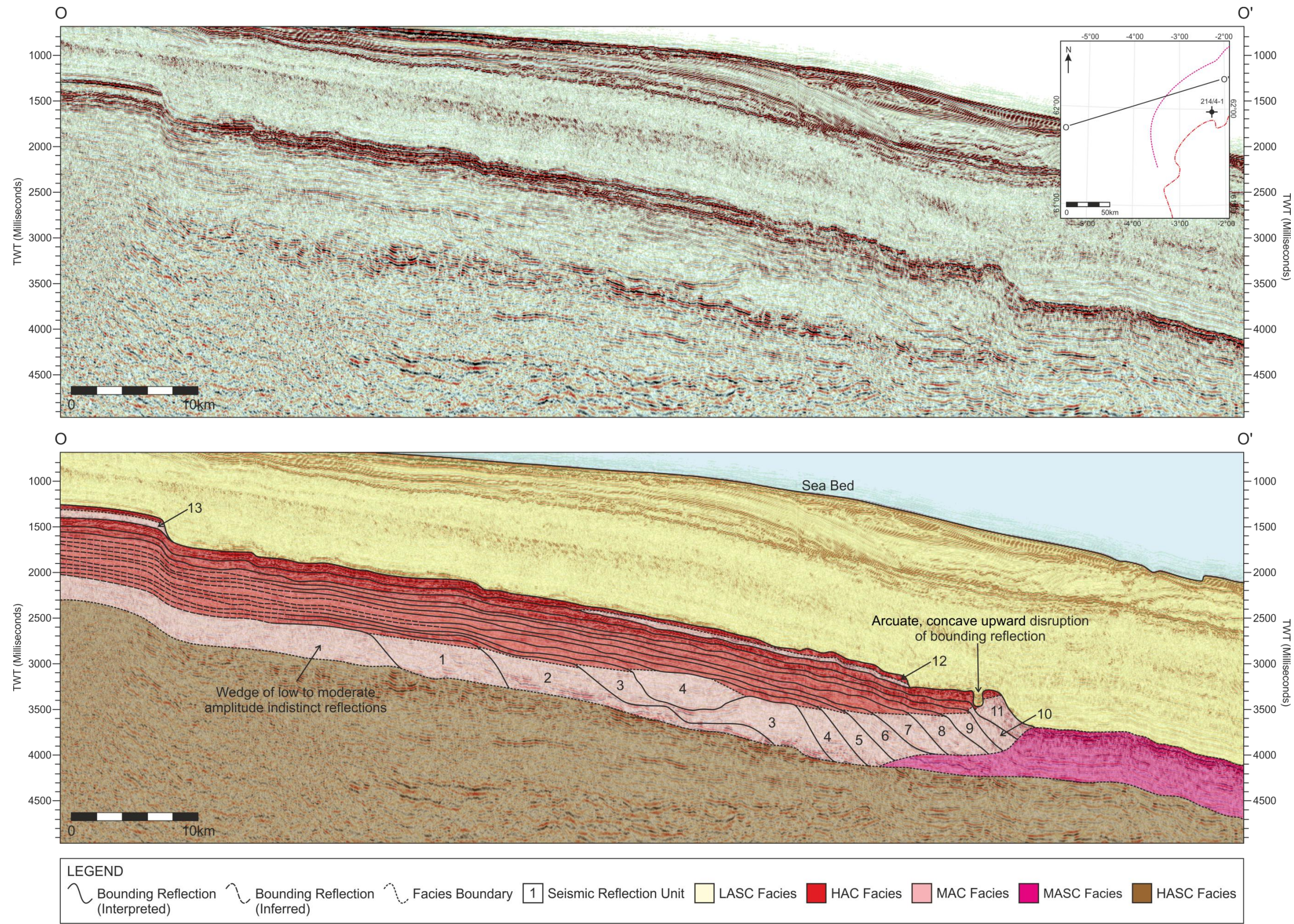
Fig. A1.14. Seismic section O-O' images the Faroe-Shetland Escarpment parallel to perpendicular to the curved escarpment edge. The interpreted section includes the seismic reflection units and bounding reflections, distribution of seismic facies and variations in a wedge to ellipsoid shape of the seismic reflection units. See Fig. A1.1. for location.
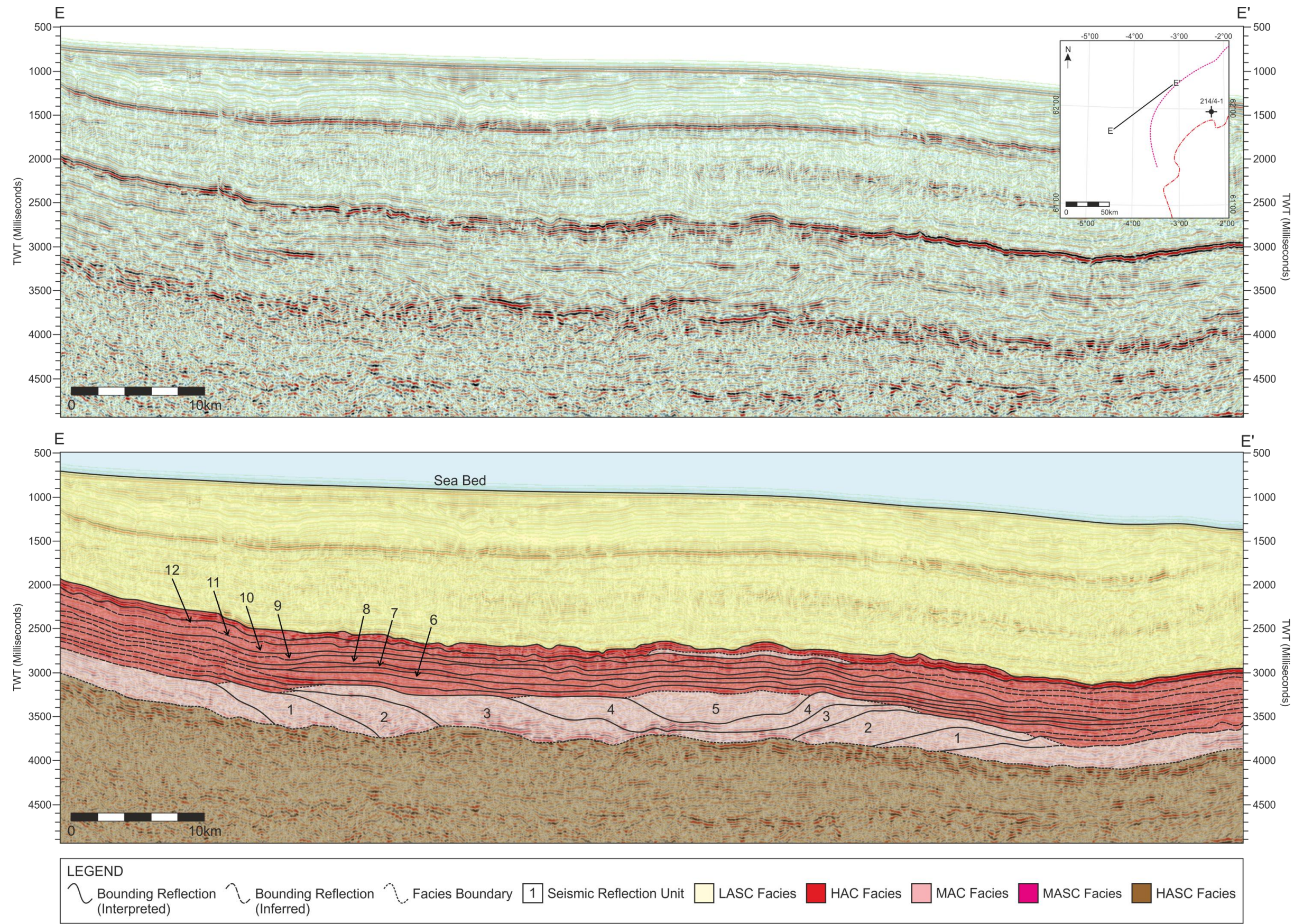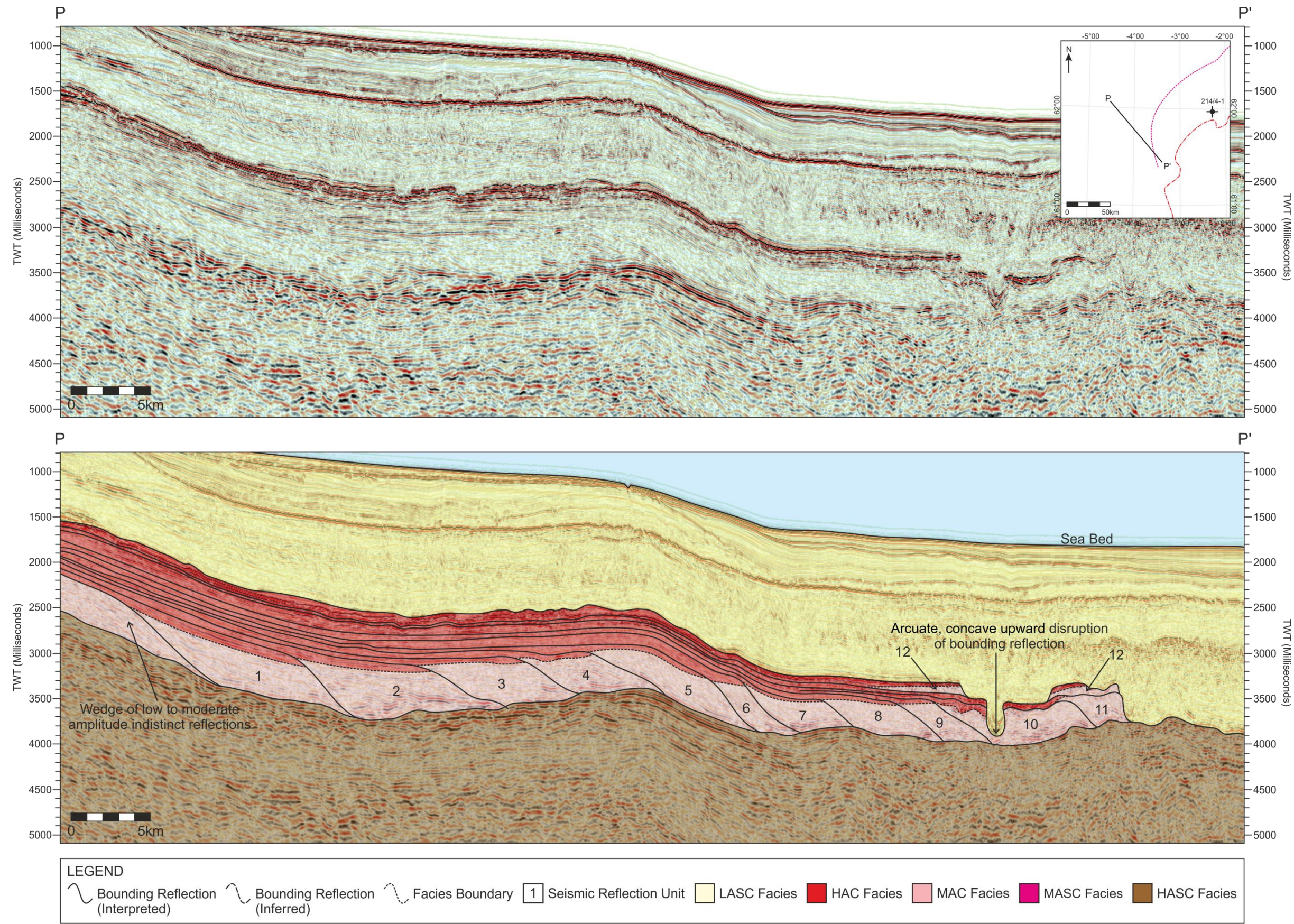
Fig. A1.15. Seismic section P-P' images the Faroe-Shetland Escarpment perpendicular to the curved escarpment edge. The interpreted section includes the seismic reflection units and bounding reflections, distribution of seismic facies and disruption of seismic reflection unit 11 with a curved, concave-up upper bounding reflection. Also note the lack of MASC facies underlying the escarpment See Fig. A1.1. for location.

APPENDIX II: SUPPORT MATERIAL FOR CHAPTER 5

This appendix contains supporting evidence for Chapter 5: *3D Seismic Geomorphology of the Growth and Collapse of a Lava-fed Delta System, Faroe-Shetland Basin*. It includes descriptions of the methodology used to measure the debris avalanche escarpments and deposits (see Fig. A2. 1 – A2.3) with tables of the individual dimensions (see Tables A2.1 – A2.3). RMS amplitude extration maps without the location of close-up figures and RMS amplitude extration maps of the seismic reflection units within the delta succession that are discussed but not shown in Chapter 5 are provided (see Fig. A2.4 – A2.16). The appendix also includes full versions of dip and edge detection attribute maps used in Chapter 5 (see Fig. A2. 17 – A2.42).
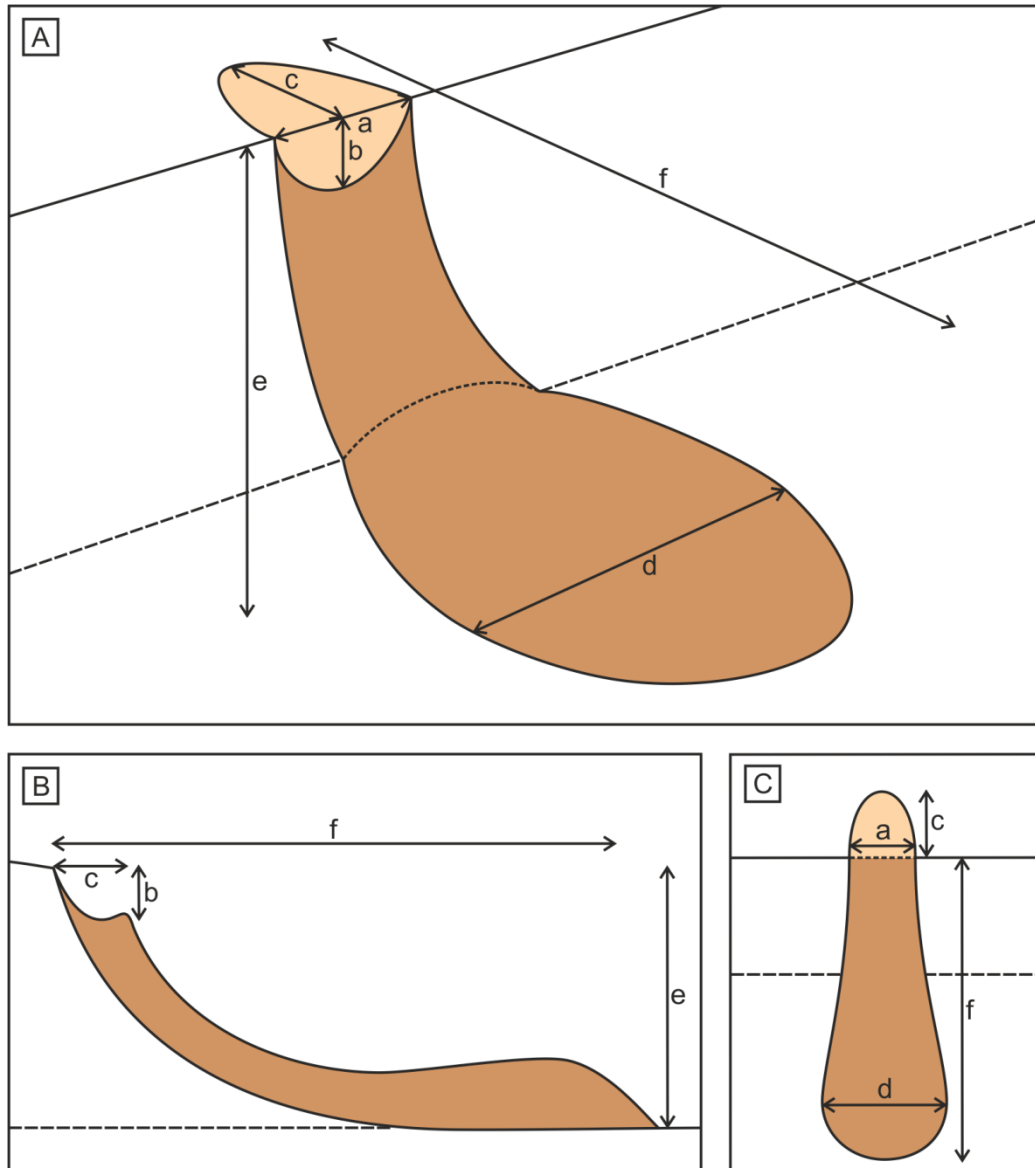
Fig. A2.1. Methodology to measure the dimensions of the debris avalanche escarpments and deposits identified to affect seismic reflection unit 11. (a) Height of the collapse escarpment. (b) Width of the collapse escarpment. (c) Depth of the collapse escarpment. (d) Height of the collapse deposit. (e) Width of the collapse deposit. (f) Length of the collapse deposit.

Debris Avalanche Escarpment	(a) Width (km)	(b) Height (km)	(c) Depth (km)	Areal Extent (km^2)
1	0.50	0.30	1.15	0.59
2a	0.13	0.30	0.80	0.35
2b	0.20	0.27	1.20	0.39
2c	0.17	0.30	0.70	0.20
3a	0.23	0.24	0.76	0.29
3b	0.14	0.23	1.00	0.36
4	0.55	0.27	0.68	1.51
5a	0.26	0.32	0.76	0.71
5b	0.20	0.30	1.05	0.39
6	0.73	0.27	1.50	1.53
7	0.49	0.24	1.05	0.71
8	0.30	0.23	0.70	0.30

Table A2.1. Dimensions of the debris avalanche escarpment in kilometres (values to 2 decimal places).

Debris Avalanche Deposit	(d) Width (km)	(e) Height (km)	(f) Length (km)	Areal Extent (km^2)
1	2.53	0.95	4.55	5.54
2a		0.91	4.70	
2b	1.37*	0.79	4.20	4.36*
2c		0.77	4.22	
3a	0.75*	0.84	4.71	2.48*
3b		0.91	4.90	
4	0.87	0.75	4.88	3.37
5a	1.06*	0.74	4.70	3.52*
5b		0.63	4.80	
6	1.25	0.78	4.25	4.48
7	0.97	0.79	4.96	3.56
8	1.10	0.82	4.50	3.53

Table A2.2. Dimensions of the debris avalanche deposits in kilometres (values to 2 decimal places). Width of deposit measured at the widest point parallel to the offlap break. *denotes where debris avalanche deposits merge and cannot be measured as an individual deposit.
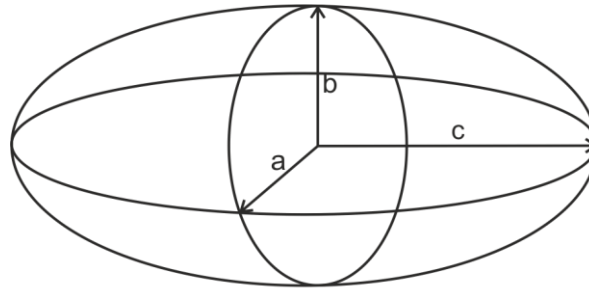
Volume of Ellipsoid = $\frac{3}{4}\pi$ abc   **Eq. A2.1**

Fig. A2.2. Methodology to calculate the volume of an ellipsoid, where a is the radius along the x axis, b is the radius along the y axis and c is the radius along the z axis.
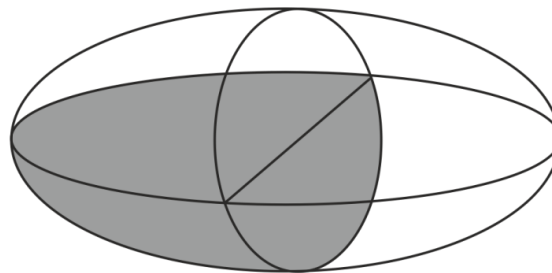
Volume of Escarpment = $\dfrac{\text{Volume of Ellipsoid}}{4}$ **Eq. A2.2**

Fig. A2.3. Methodology to calculate the volume of the collapse escarpments. The escarpments exhibit scoop-shaped geometries which are the equivalent of a quarter of a ellipsoid.

Debris Avalanche Escarpment	(a) Radius along x axis (km)	(b) Radius along y axis (km)	(c) Radius along z axis (km)	Volume of Escarpment (km^3)
1	0.250	0.150	0.575	0.029
2a	0.065	0.150	0.400	0.004
2b	0.100	0.135	0.600	0.008
2c	0.850	0.150	0.350	0.005
3a	0.115	0.120	0.380	0.005
3b	0.070	0.113	0.500	0.004
4	0.275	0.135	0.340	0.013
5a	0.130	0.158	0.380	0.008
5b	0.100	0.150	0.525	0.008
6	0.365	0.135	0.750	0.039
7	0.245	0.120	0.525	0.016
8	0.150	0.116	0.350	0.006

Table A2.3. The radial dimensions of the debris avalanche escarpments and the volume of the escarpments, as determined by calculating the volume of quarter of an ellipsoid (values to 3 decimal places).
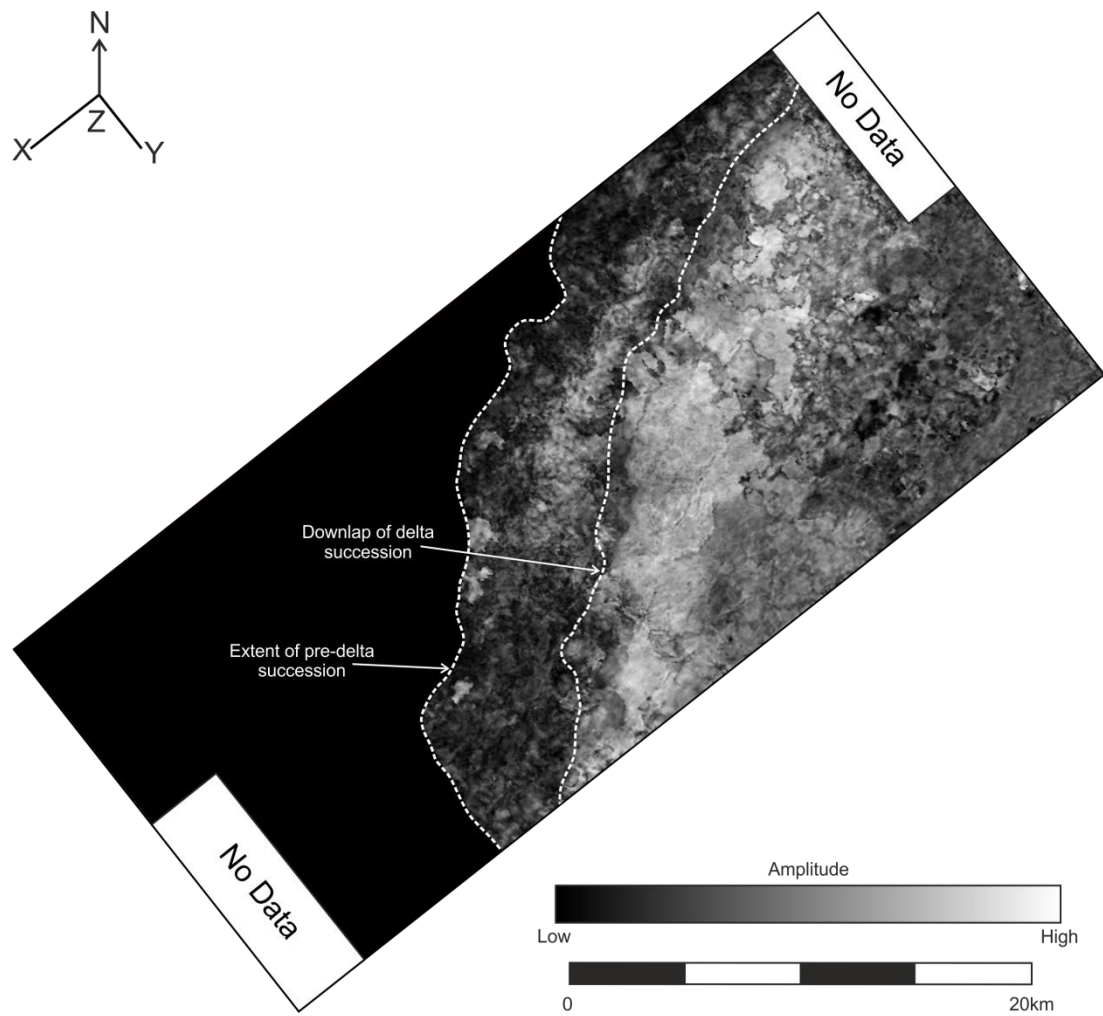
Fig. A2.4. RMS amplitude extraction map with a 5 millisecond window over the top of the pre-delta succession, with extent of succession and downlap of overlying delta succession identified. For location of 3D survey see Chapter 5.
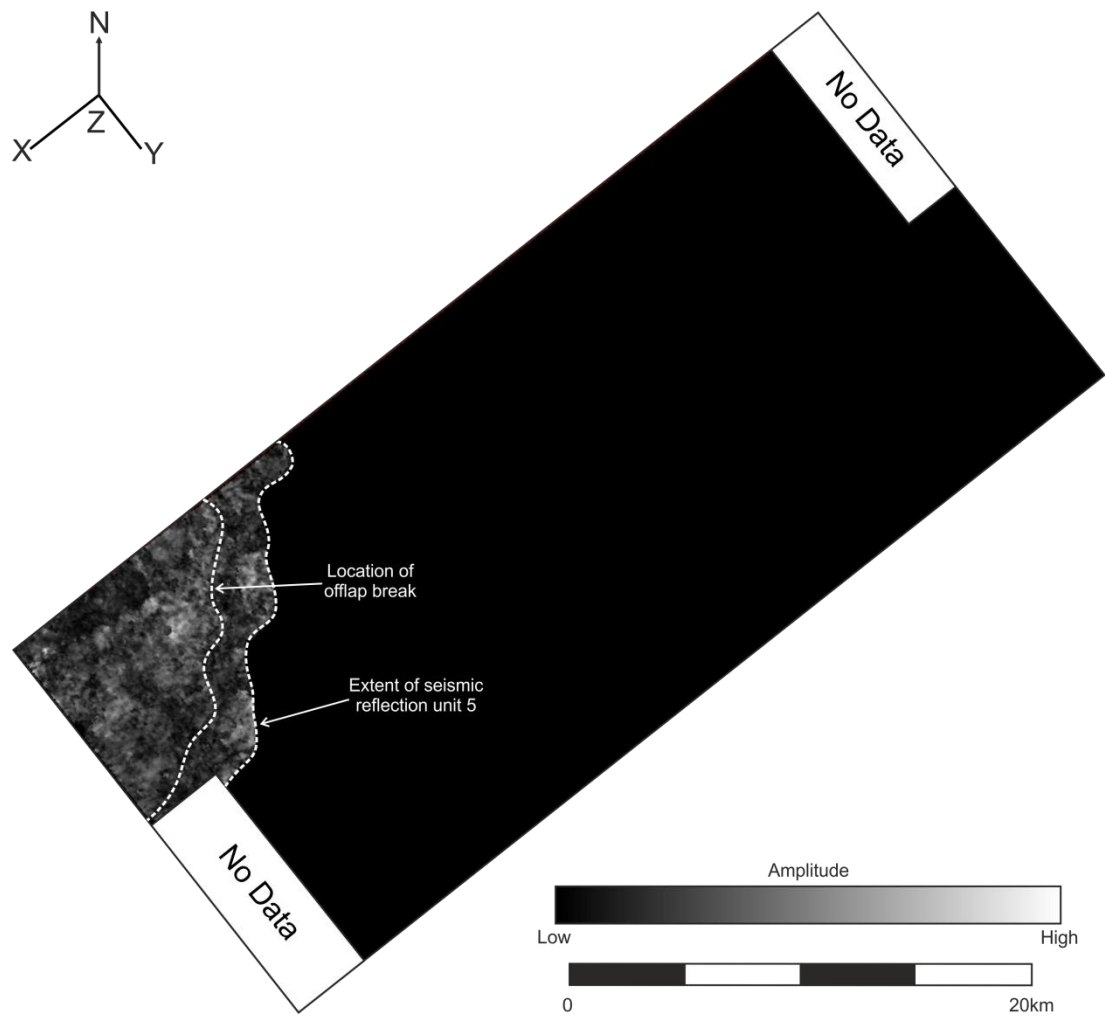
Fig. A2.5. RMS amplitude extraction map with a 5 millisecond window over the top of seismic reflection unit 5 within the delta succession, with extent of seismic reflection unit and offlap break identified. For location of 3D survey see Chapter 5.
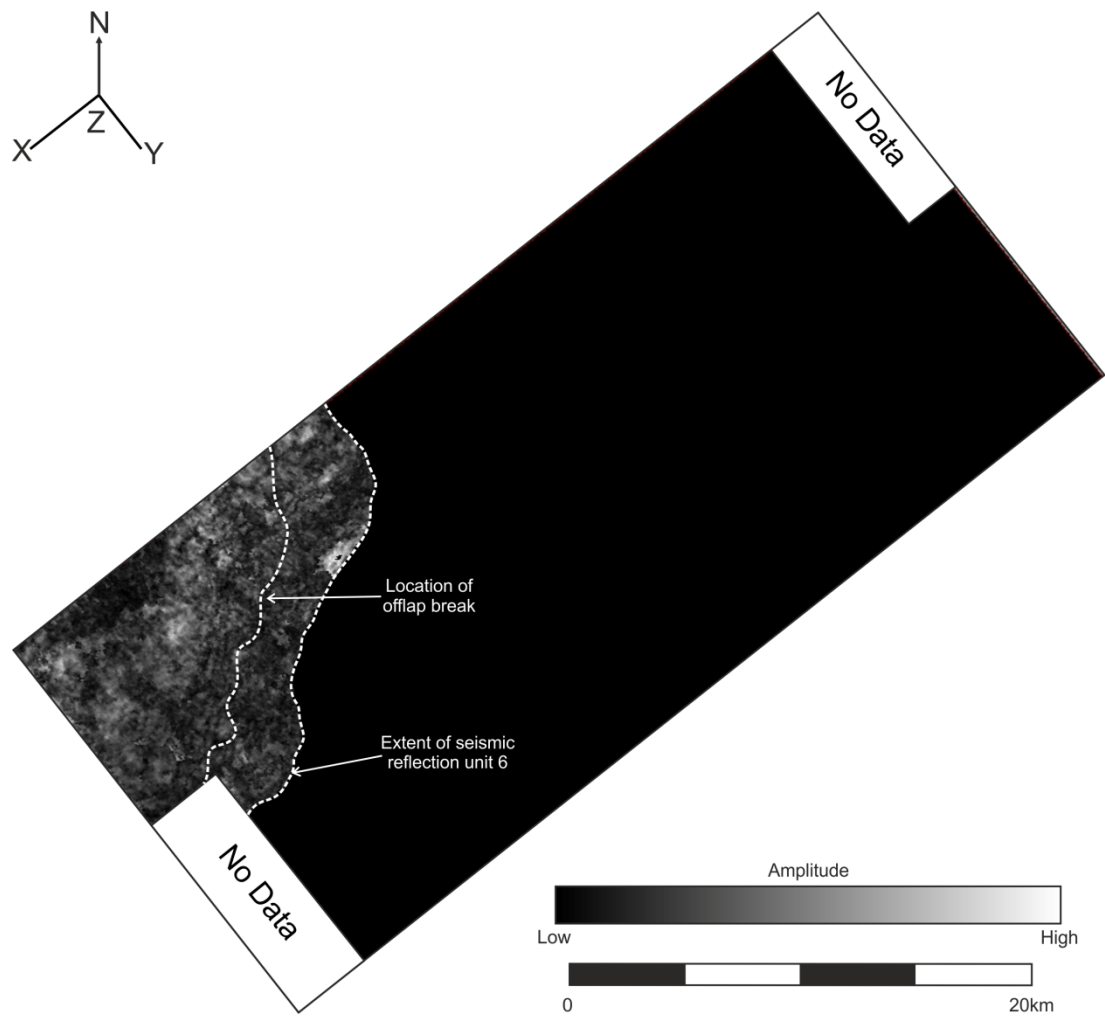
Fig. A2.6. RMS amplitude extraction map with a 5 millisecond window over the top of seismic reflection unit 6 within the delta succession, with extent of seismic reflection unit and offlap break identified. For location of 3D survey see Chapter 5.
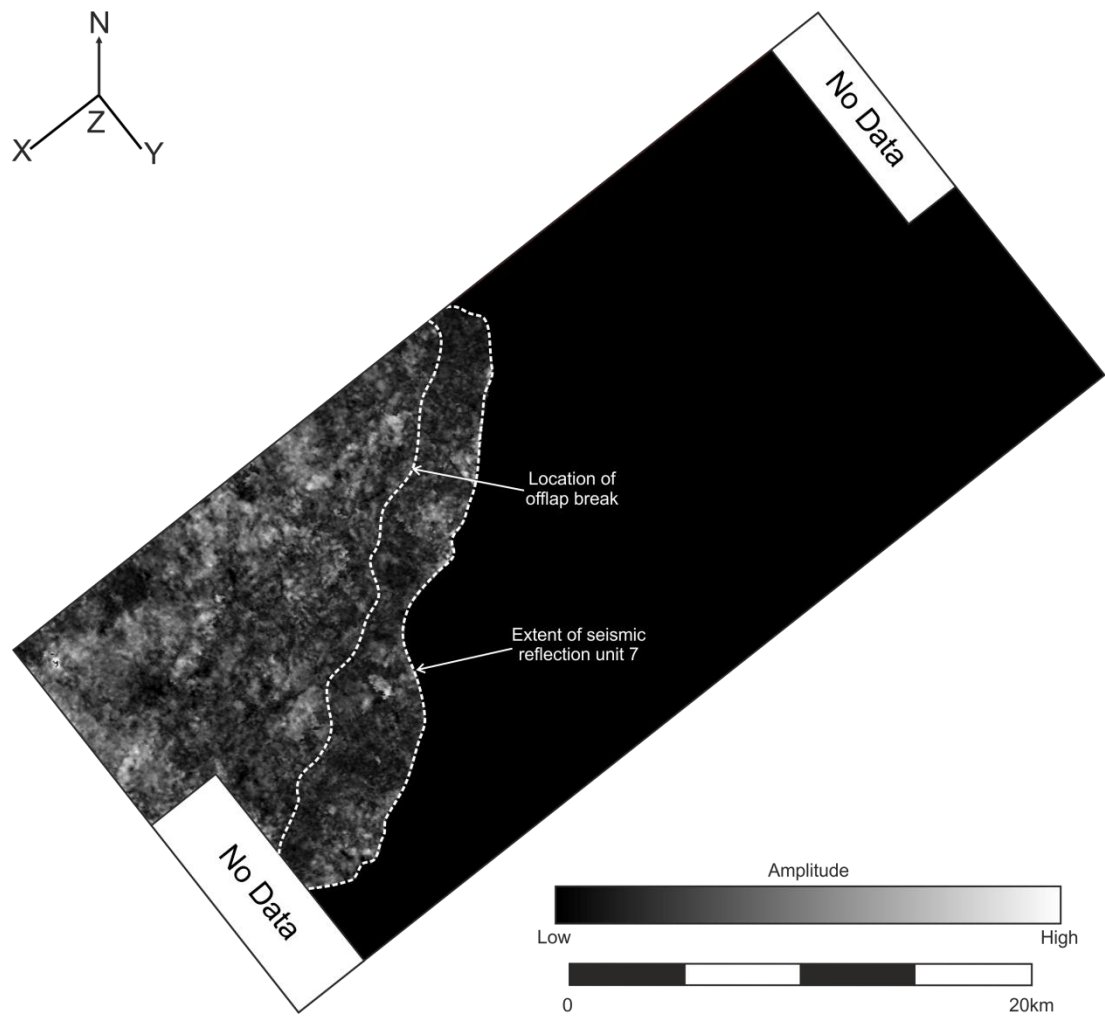
Fig. A2.7. RMS amplitude extraction map with a 5 millisecond window over the top of seismic reflection unit 7 within the delta succession, with extent of seismic reflection unit and offlap break identified. For location of 3D survey see Chapter 5.
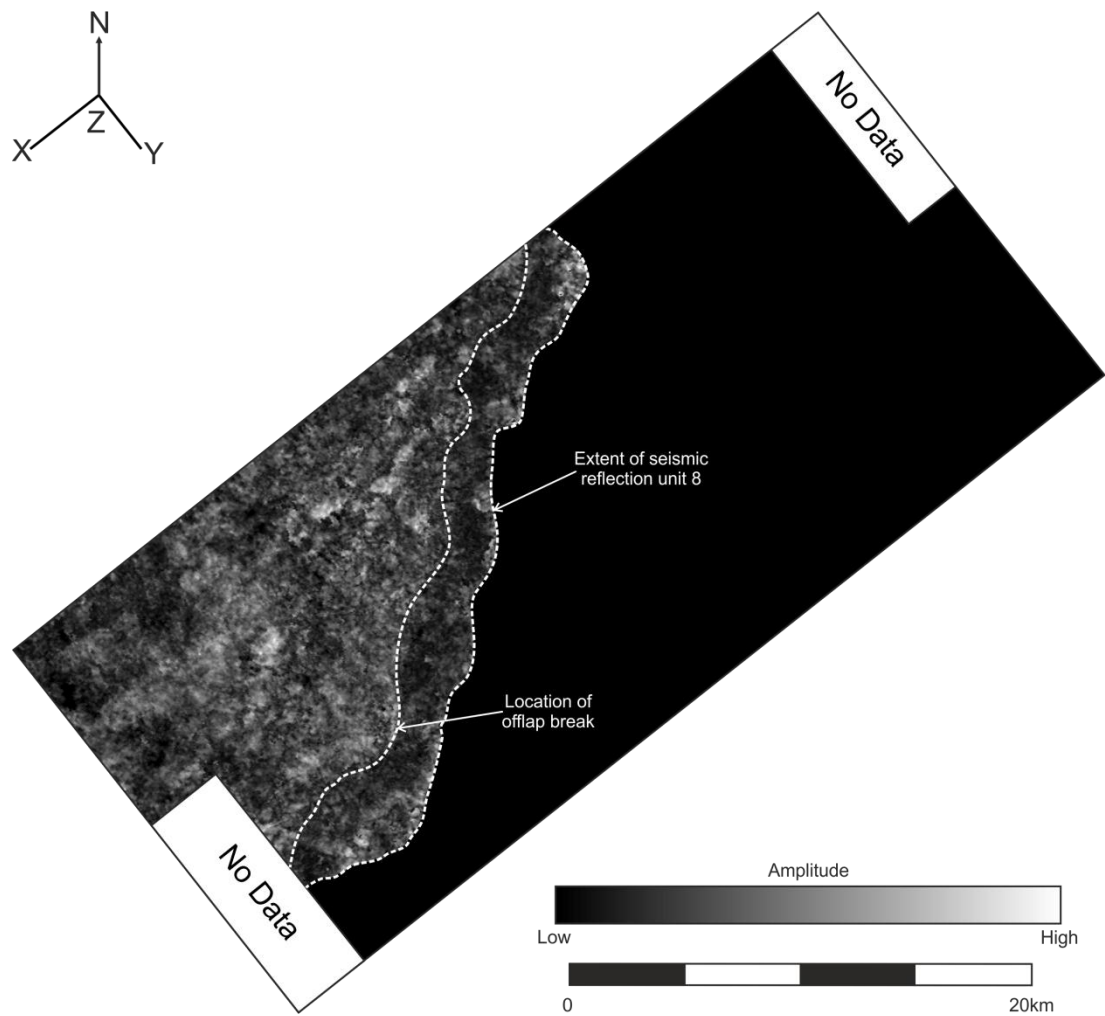
Fig. A2.8. RMS amplitude extraction map with a 5 millisecond window over the top of seismic reflection unit 8 within the delta succession, with extent of seismic reflection unit and offlap break identified. For location of 3D survey see Chapter 5.
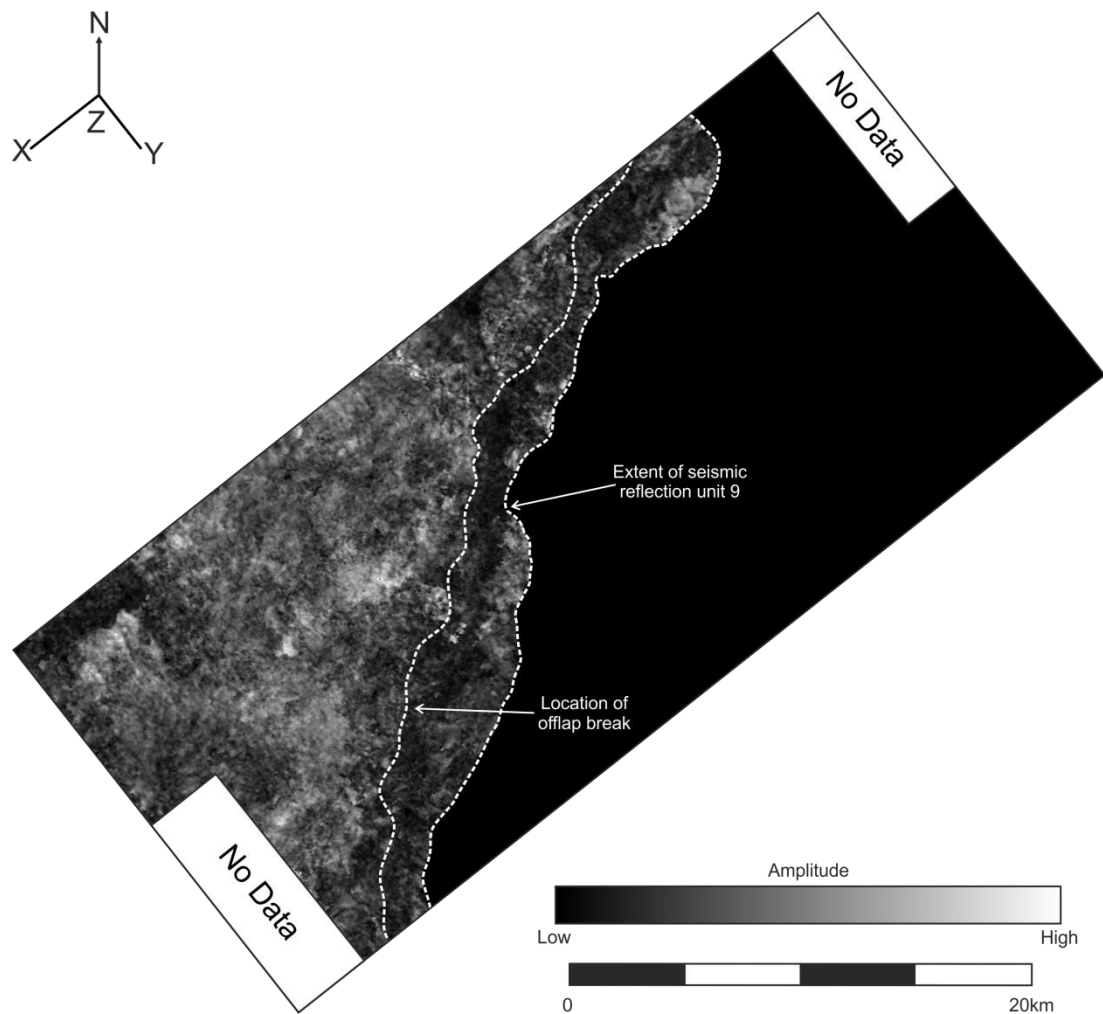
Fig. A2.9. RMS amplitude extraction map with a 5 millisecond window over the top of seismic reflection unit 9 within the delta succession, with extent of seismic reflection unit and offlap break identified. For location of 3D survey see Chapter 5.
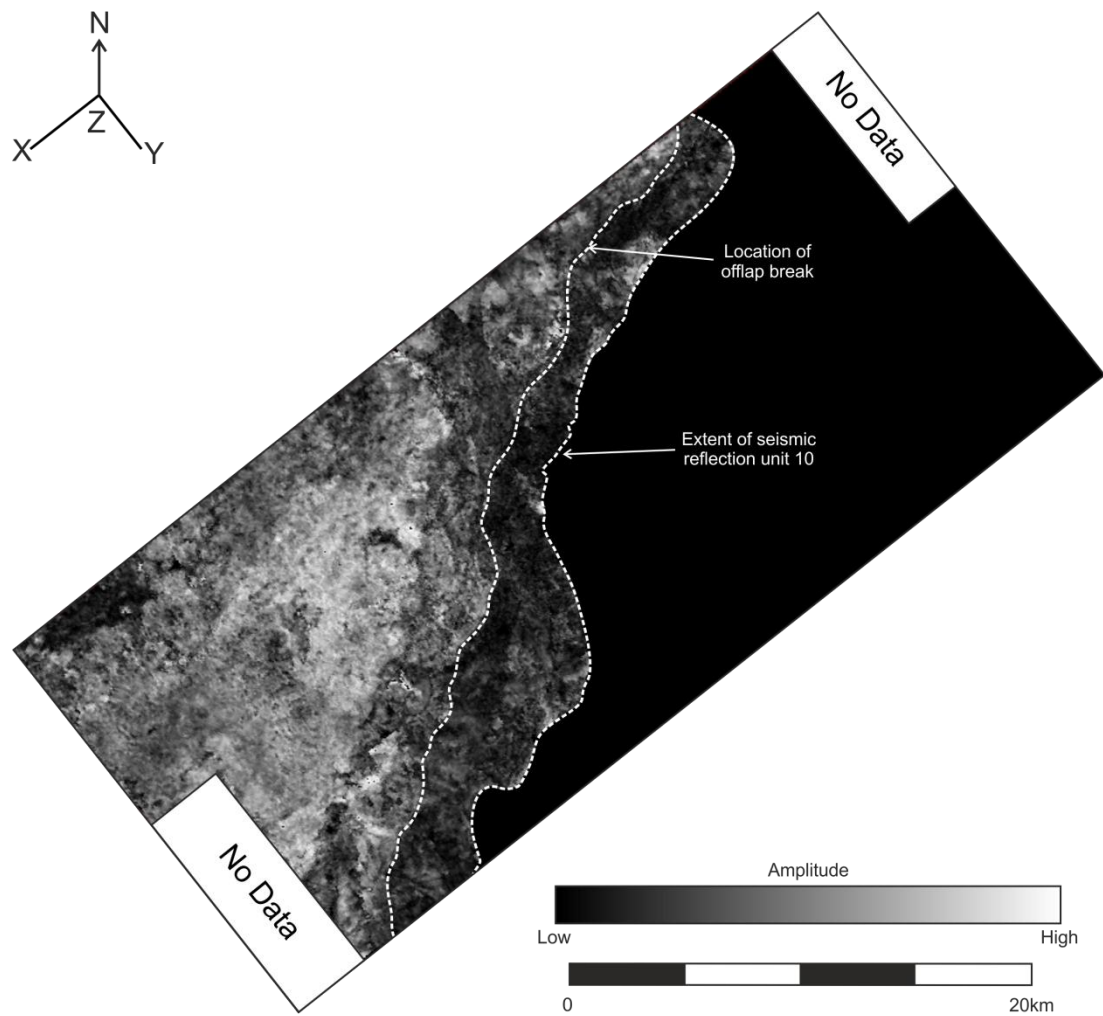
Fig. A2.10. RMS amplitude extraction map with a 5 millisecond window over the top of seismic reflection unit 10 within the delta succession, with extent of seismic reflection unit and offlap break identified. For location of 3D survey see Chapter 5.

Fig. A2.11. RMS amplitude extraction map with a 5 millisecond window over the top of seismic reflection unit 11 within the delta succession, with extent of seismic reflection unit, offlap break and extent of overlying seismic reflection unit 12 identified. For location of 3D survey see Chapter 5.

Fig. A2.12. RMS amplitude extraction map with a 5 millisecond window over the top of seismic reflection unit 12 within the delta succession, with extent of seismic reflection unit, offlap break and extent of reflection X identified. For location of 3D survey see Chapter 5.
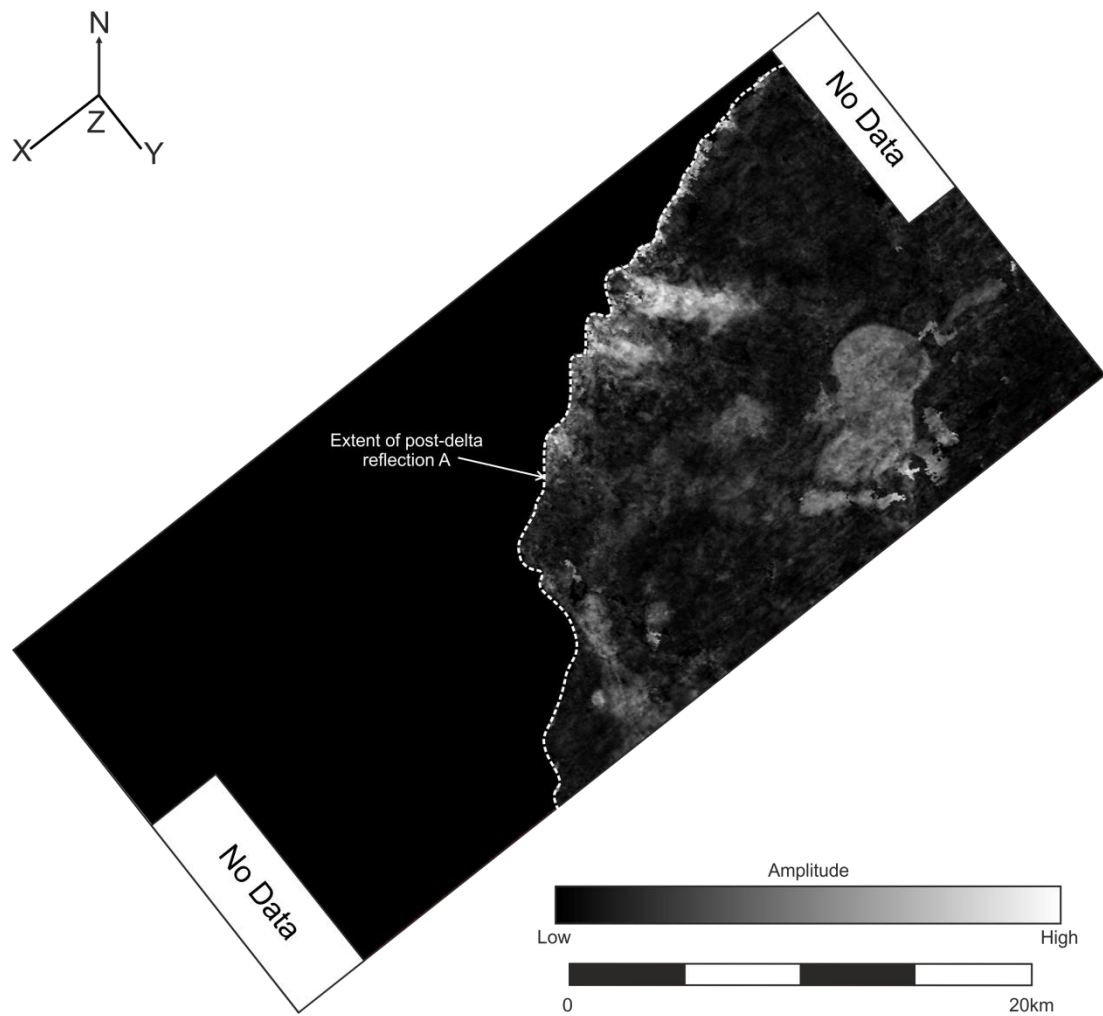
Fig. A2.13. RMS amplitude extraction map with a 5 millisecond window over reflection A within the post-delta succession, with extent of seismic reflection the onlaps the underlying delta succession. For location of 3D survey see Chapter 5.
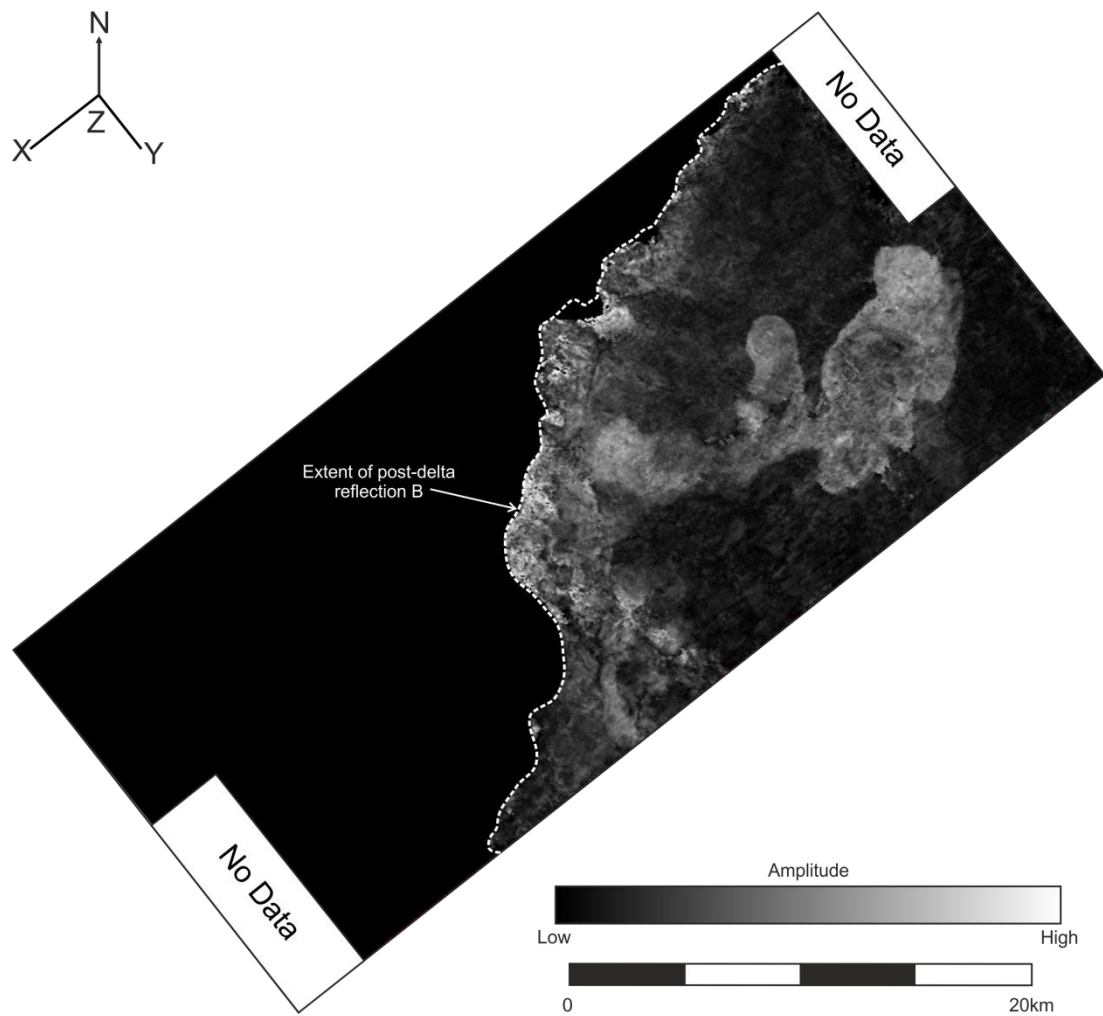
Fig. A2.14. RMS amplitude extraction map with a 5 millisecond window over reflection B within the post-delta succession, with extent of seismic reflection the onlaps the underlying delta succession. For location of 3D survey see Chapter 5.
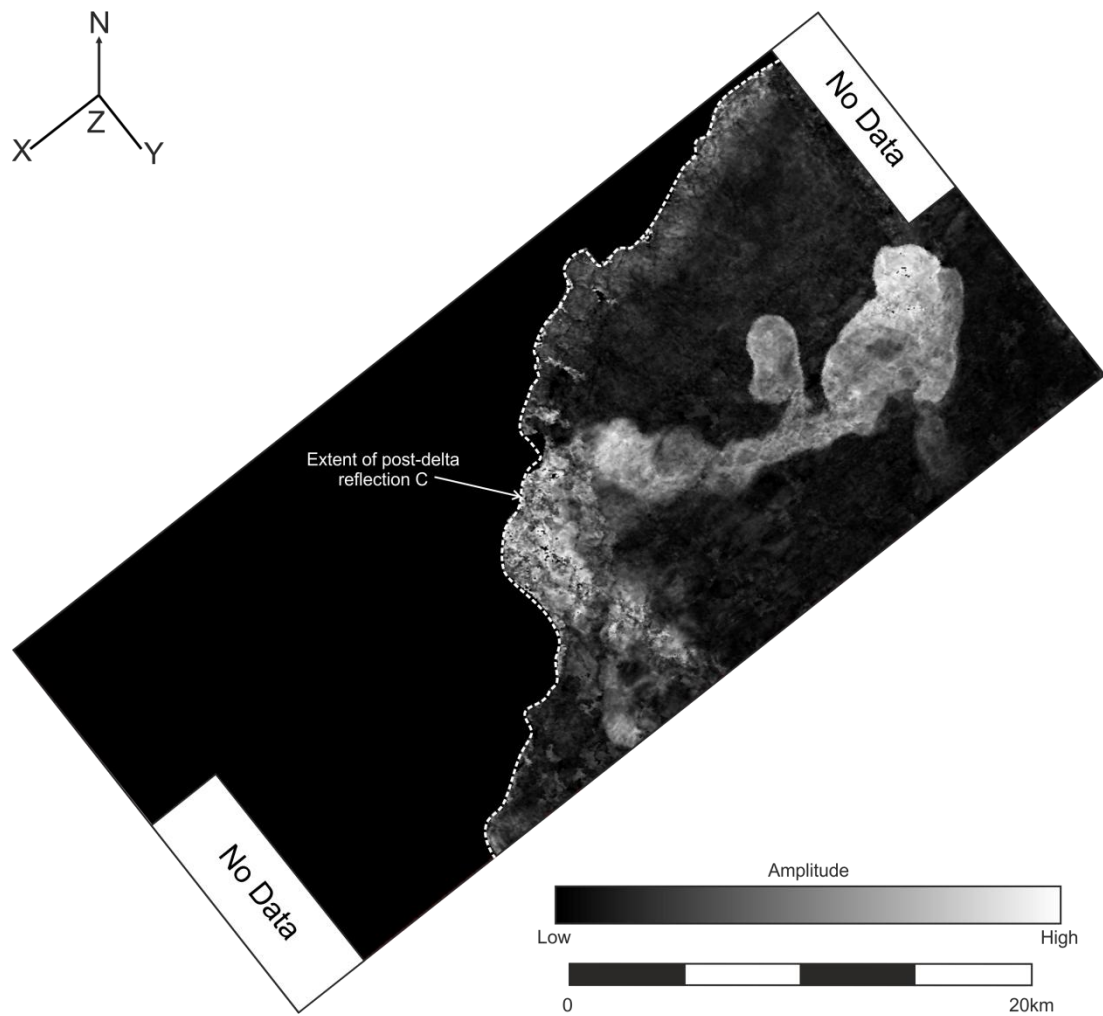
Fig. A2.15. RMS amplitude extraction map with a 5 millisecond window over reflection C within the post-delta succession, with extent of seismic reflection that onlaps the underlying delta succession. For location of 3D survey see Chapter 5.
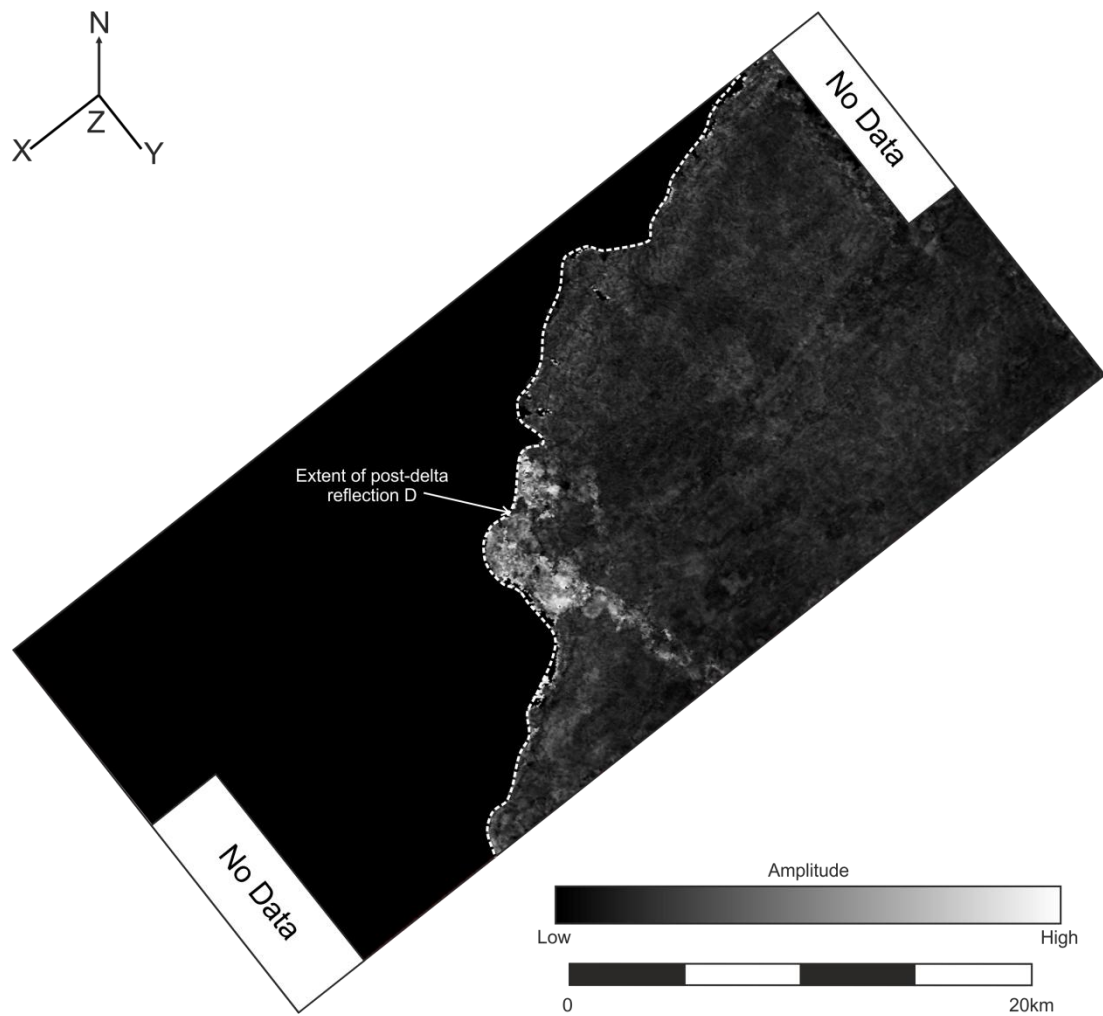
Fig. A2.16. RMS amplitude extraction map with a 5 millisecond window over reflection D within the post-delta succession, with extent of seismic reflection the onlaps the underlying delta succession. For location of 3D survey see Chapter 5.
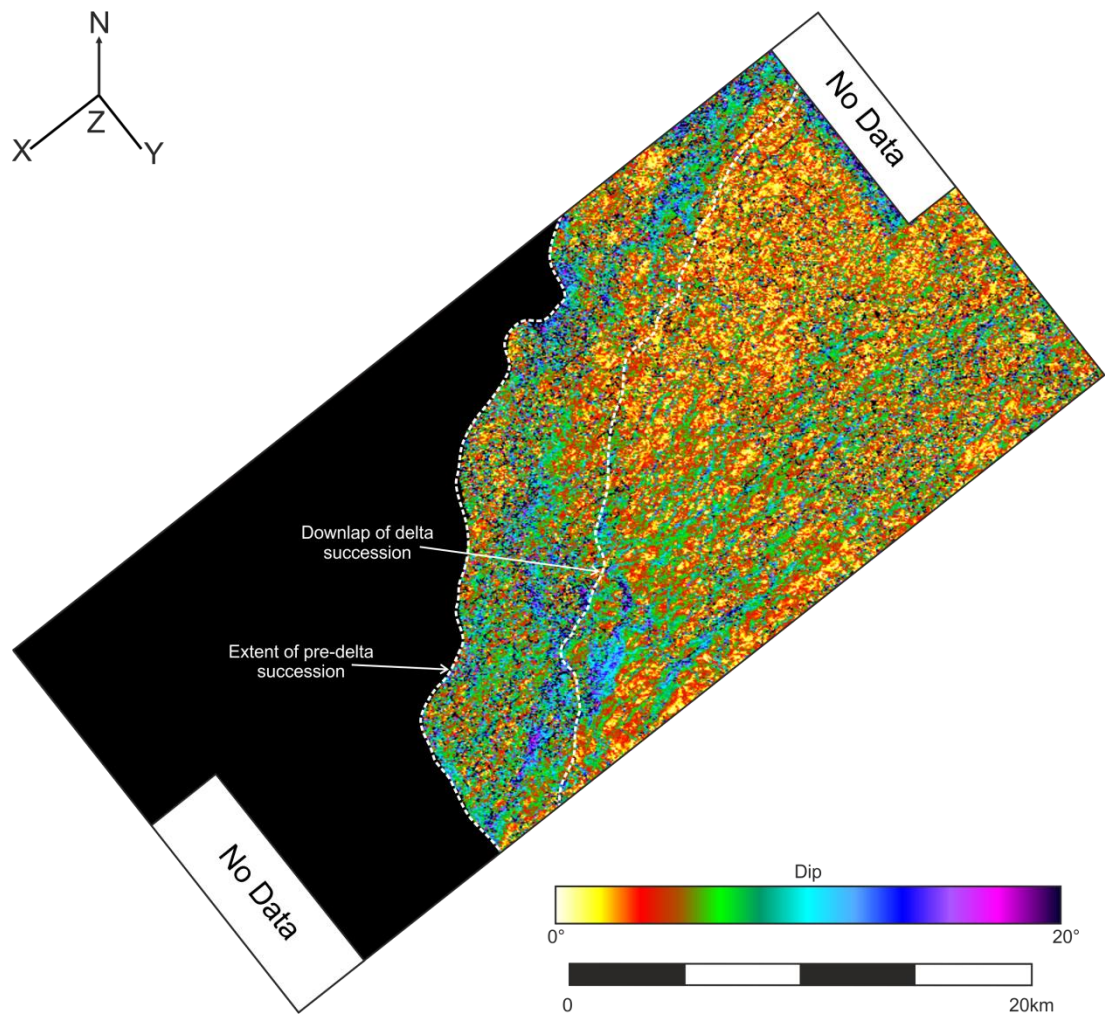
Fig. A2.17. Dip map of pre-delta succession, with extent of succession and downlap of overlying delta succession identified. For location of 3D survey see Chapter 5.
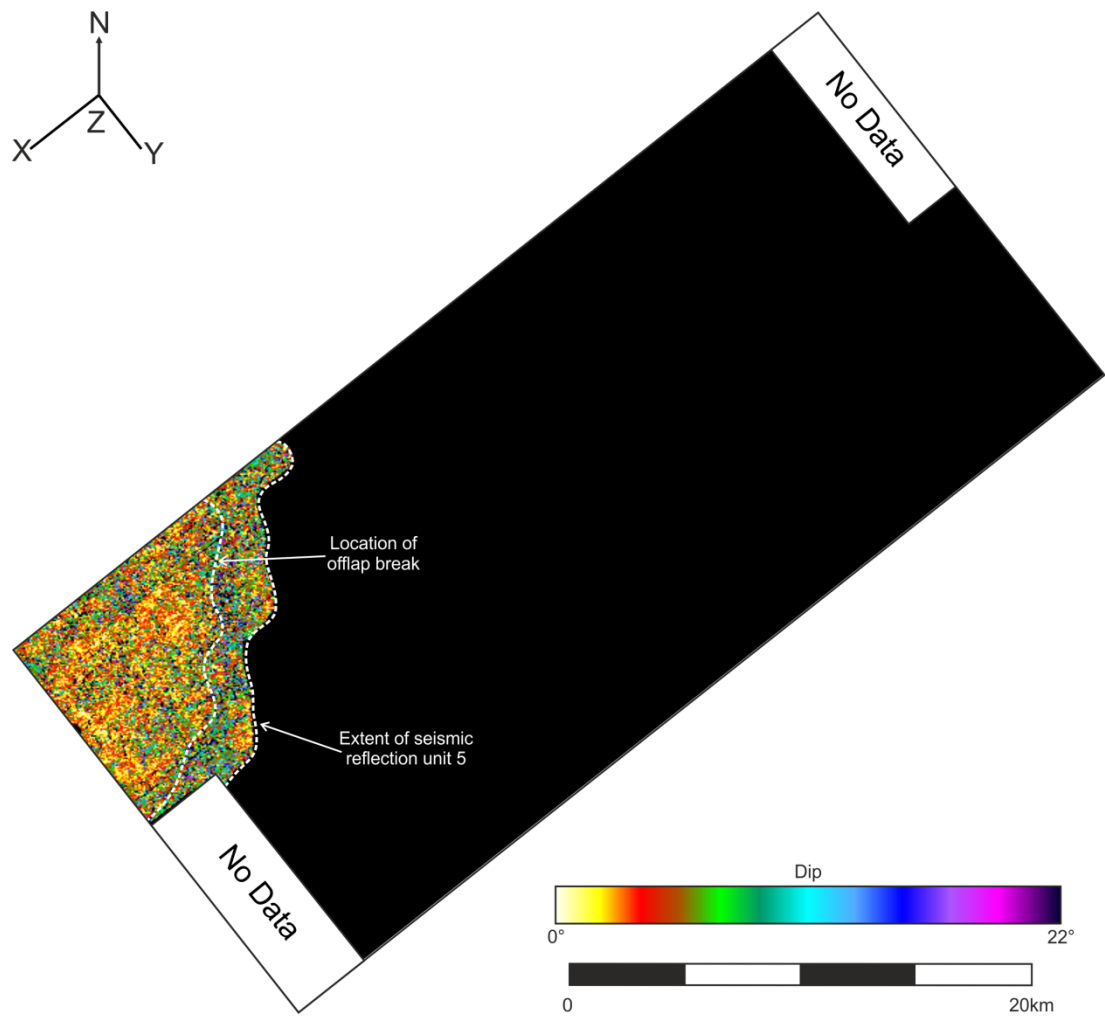
Fig. A2.18. Dip map of seismic reflection unit 5 within the delta succession, with extent of seismic reflection unit and offlap break identified. Lowest dips exhibited by subparallel lava flow topsets and highest dips exhibited by inclined hyaloclastite foresets. For location of 3D survey see Chapter 5.
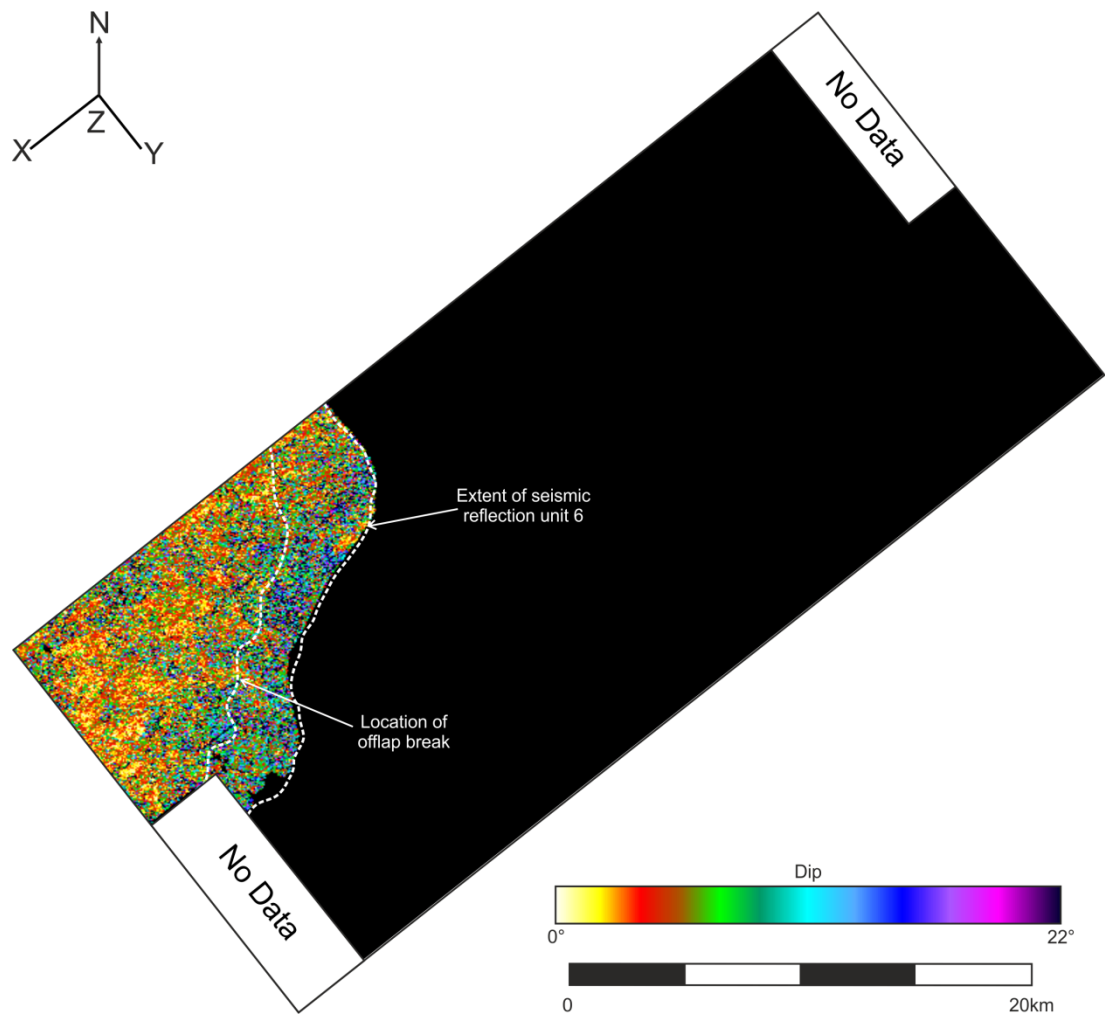
Fig. A2.19. Dip map of seismic reflection unit 6 within the delta succession, with extent of seismic reflection unit and offlap break identified. Lowest dips exhibited by subparallel lava flow topsets and highest dips exhibited by inclined hyaloclastite foresets. For location of 3D survey see Chapter 5.
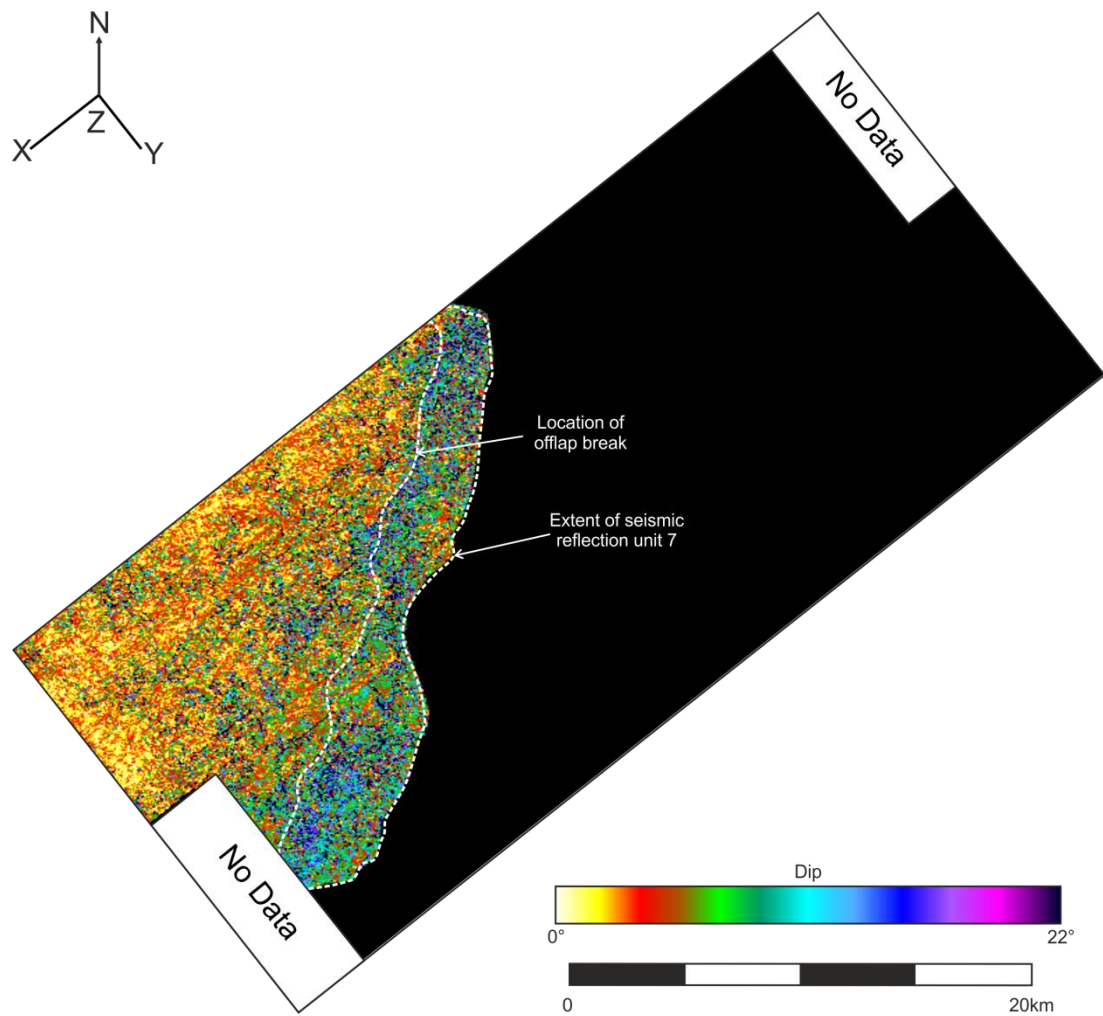
Fig. A2.20. Dip map of seismic reflection unit 7 within the delta succession, with extent of seismic reflection unit and offlap break identified. Lowest dips exhibited by subparallel lava flow topsets and highest dips exhibited by inclined hyaloclastite foresets. For location of 3D survey see Chapter 5.
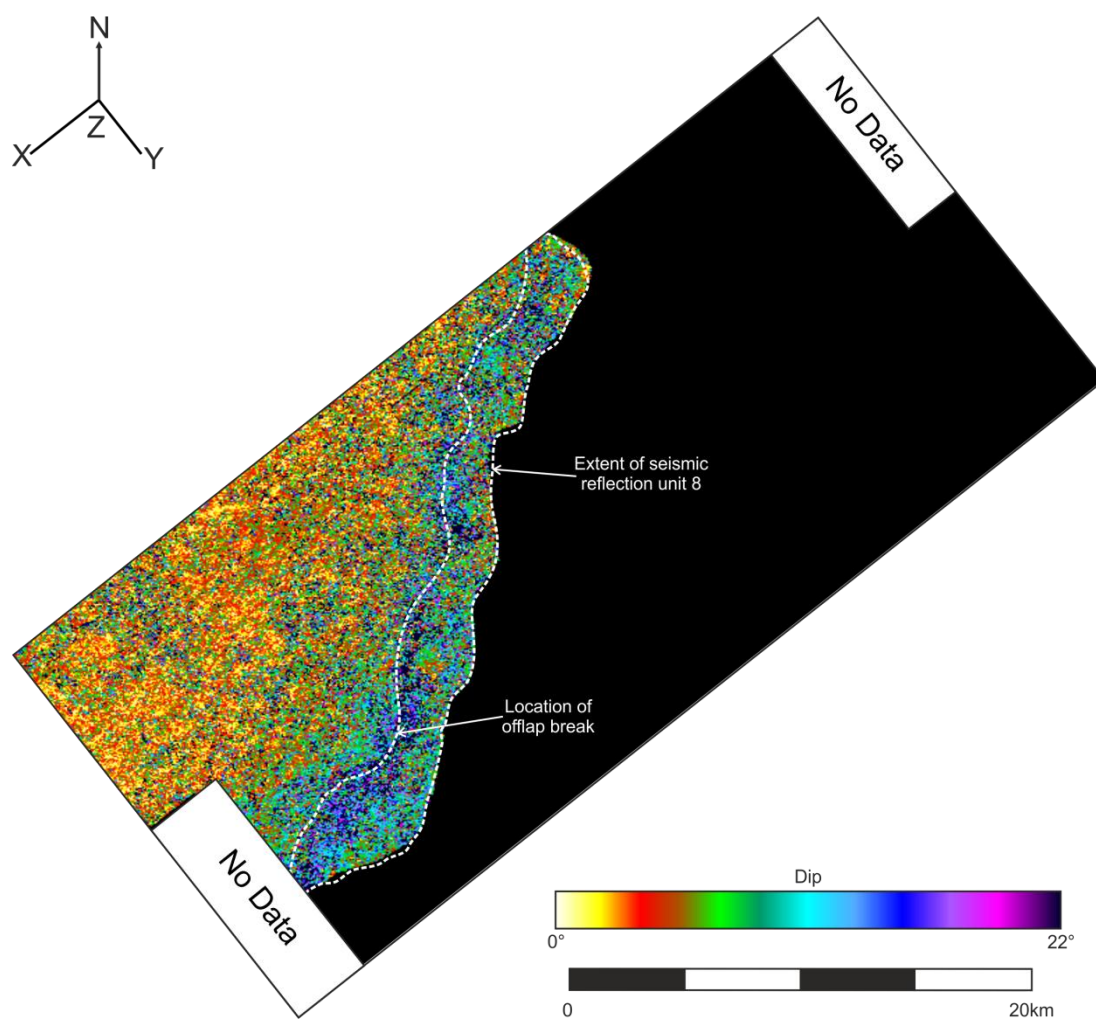
Fig. A2.21. Dip map of seismic reflection unit 8 within the delta succession, with extent of seismic reflection unit and offlap break identified. Lowest dips exhibited by subparallel lava flow topsets and highest dips exhibited by inclined hyaloclastite foresets. For location of 3D survey see Chapter 5.
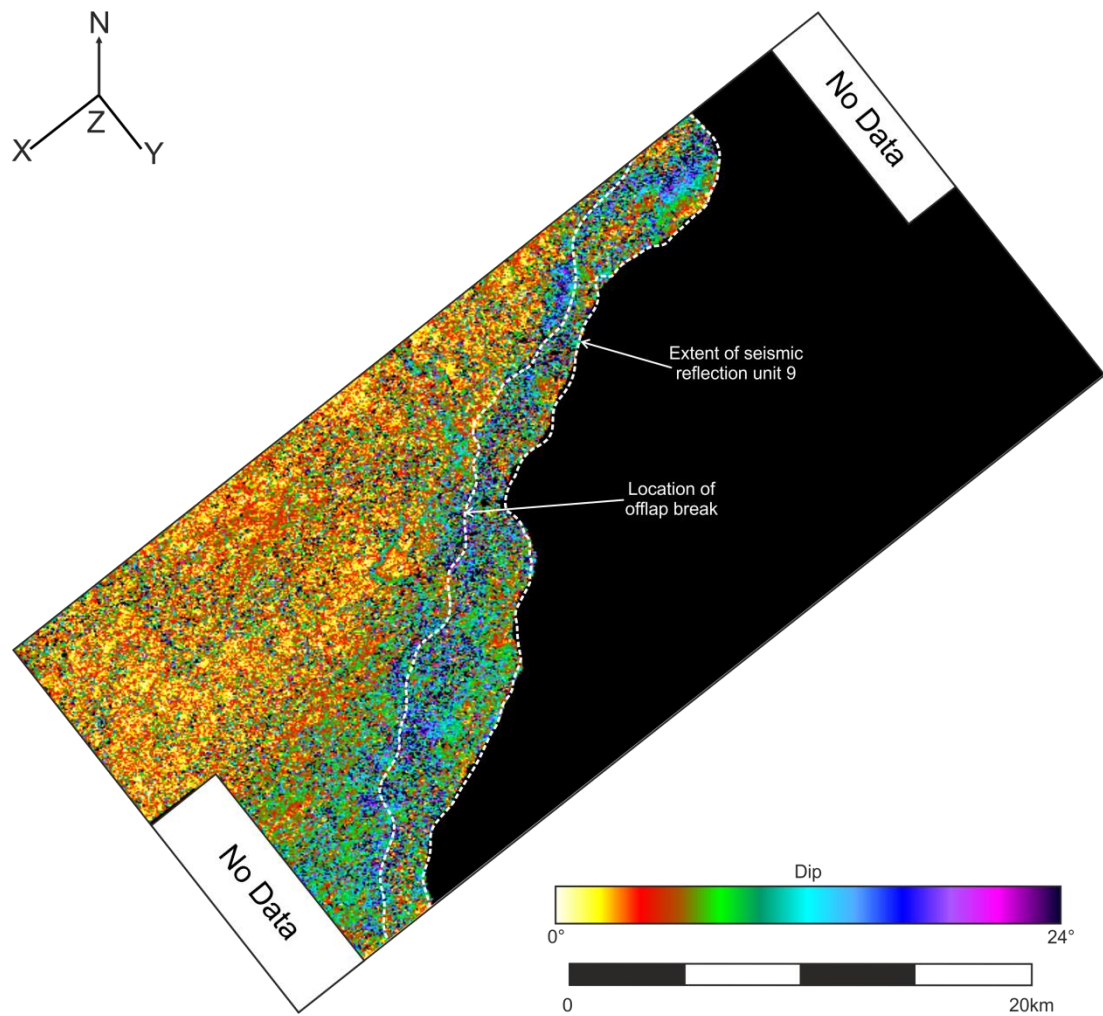
Fig. A2.22. Dip map of seismic reflection unit 9 within the delta succession, with extent of seismic reflection unit and offlap break identified. Lowest dips exhibited by subparallel lava flow topsets and highest dips exhibited by inclined hyaloclastite foresets. For location of 3D survey see Chapter 5.
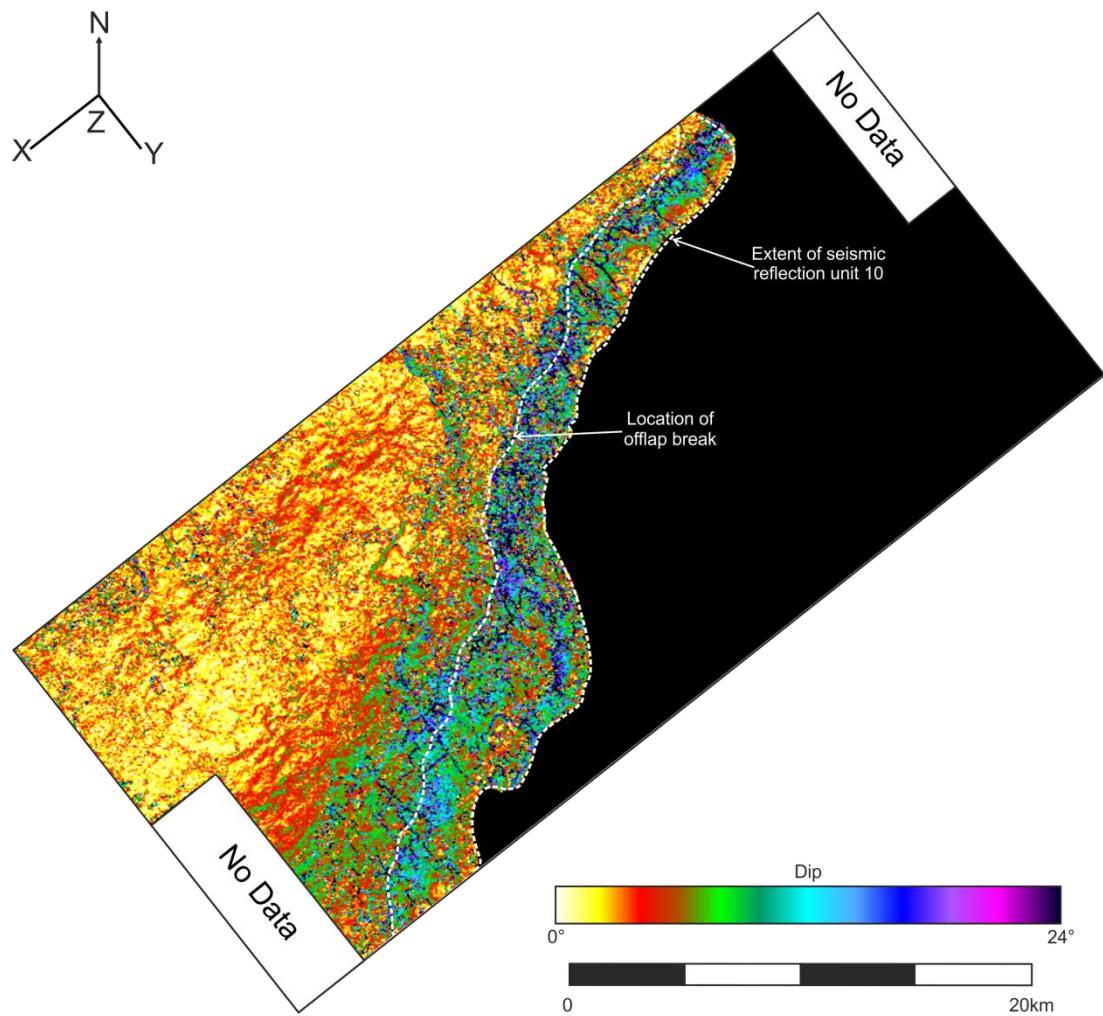
Fig. A2.23. Dip map of seismic reflection unit 10 within the delta succession, with extent of seismic reflection unit and offlap break identified. Lowest dips exhibited by subparallel lava flow topsets and highest dips exhibited by inclined hyaloclastite foresets. For location of 3D survey see Chapter 5.
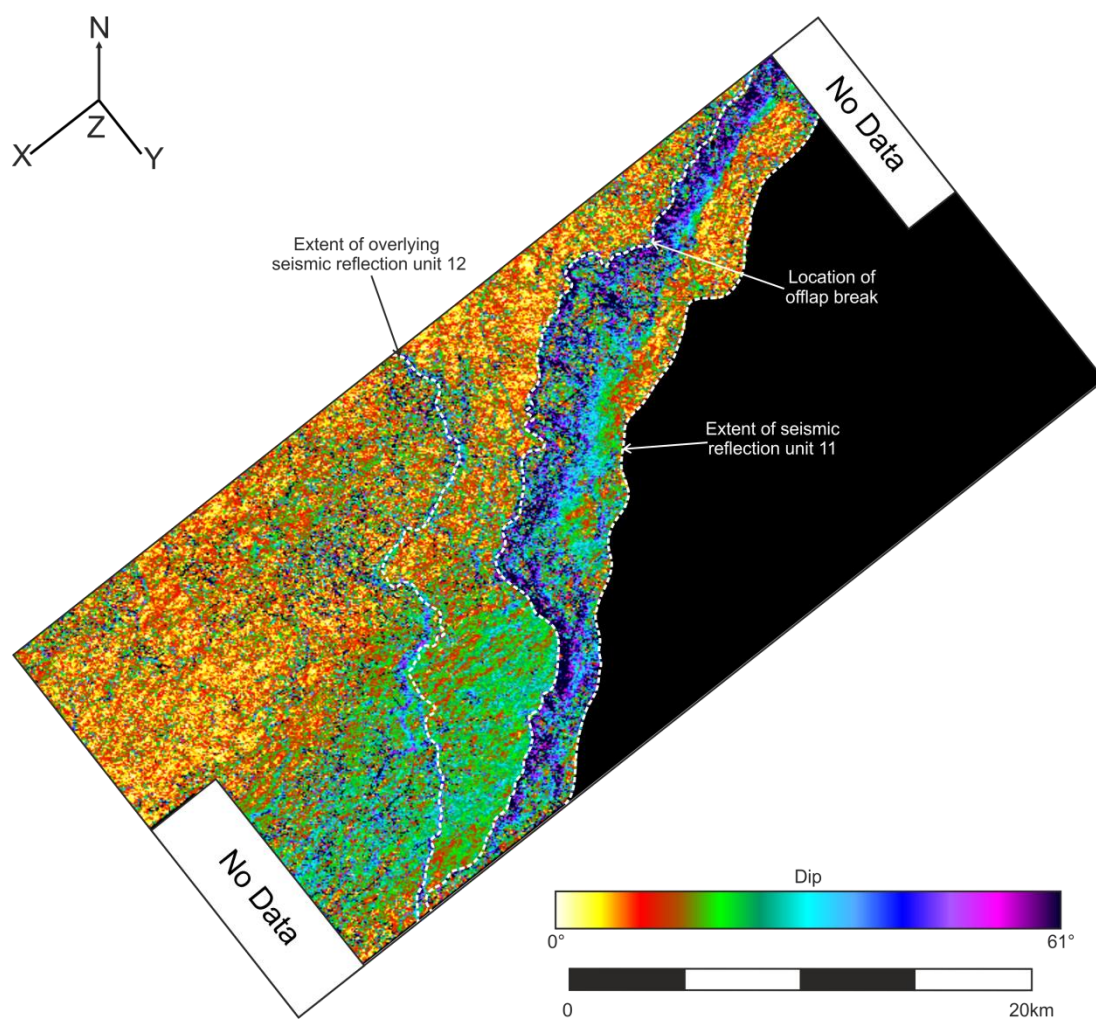
Fig. A2.24. Dip map of seismic reflection unit 11 within the delta succession, with extent of seismic reflection unit, offlap break and extent of overlying seismic reflection unit 12 identified. Lowest dips exhibited by subparallel lava flow topsets and highest dips exhibited by inclined hyaloclastite foresets. Variations in dip highlight lobate delta front geometries. For location of 3D survey see Chapter 5.
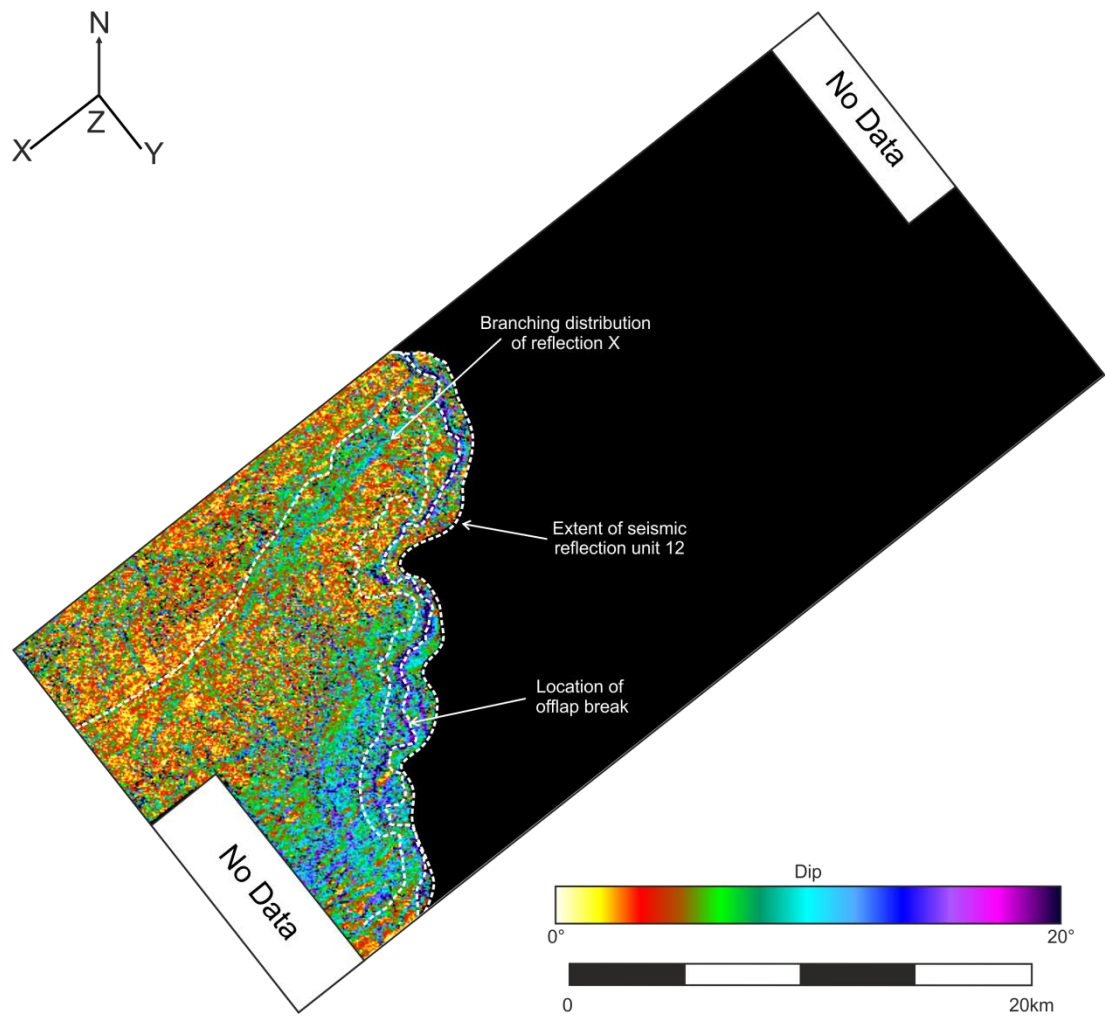
Fig. A2.25. Dip map of seismic reflection unit 12 within the delta succession, with extent of seismic reflection unit, offlap break and extent of reflection X identified. Lowest dips exhibited by subparallel lava flow topsets and highest dips exhibited by inclined hyaloclastite foresets. For location of 3D survey see Chapter 5.
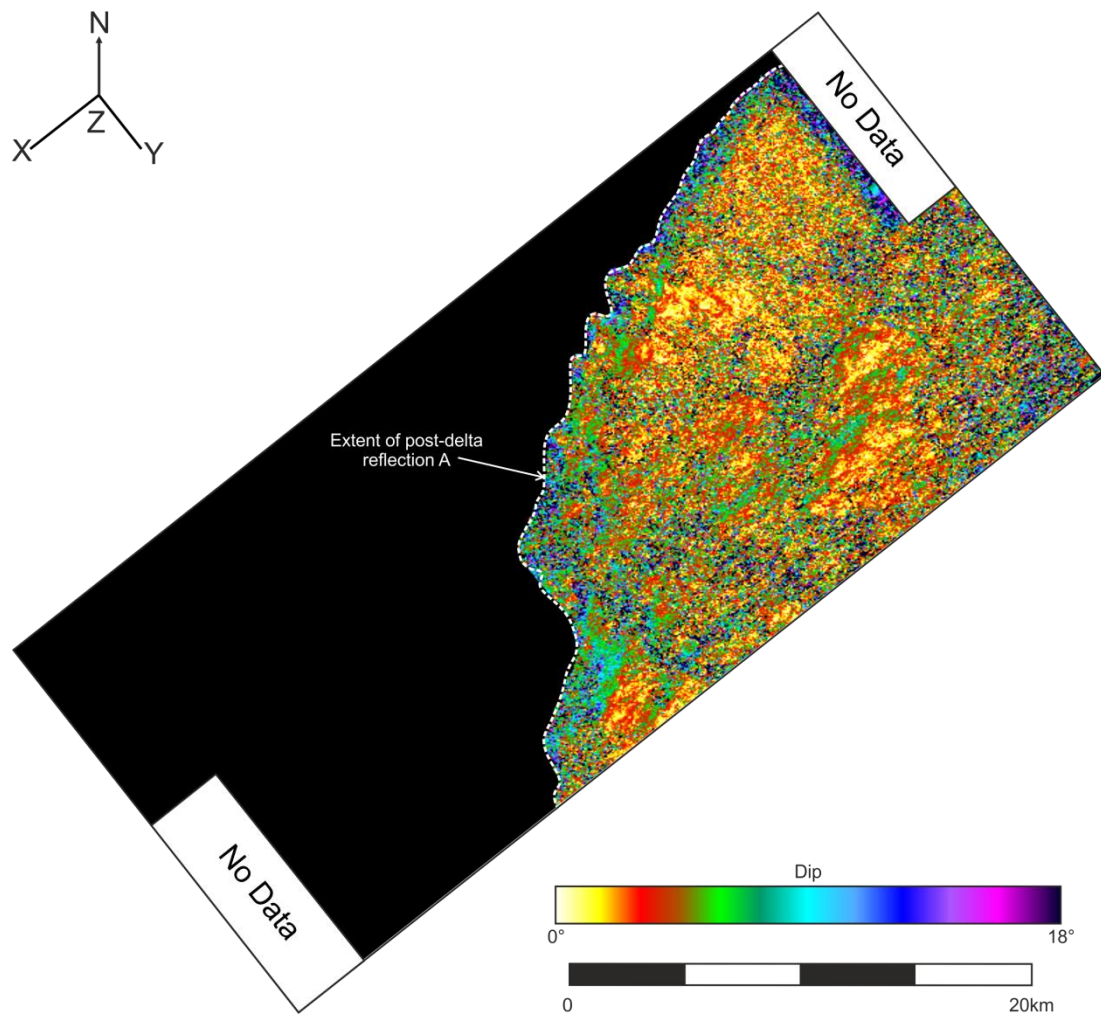
Fig. A2.26. Dip map of reflection A within the post-delta succession, with extent of seismic reflection the onlaps the underlying delta succession. Lowest dips exhibited by flat lying lobate features and highest dips exhibited by delta front onlap. For location of 3D survey see Chapter 5.
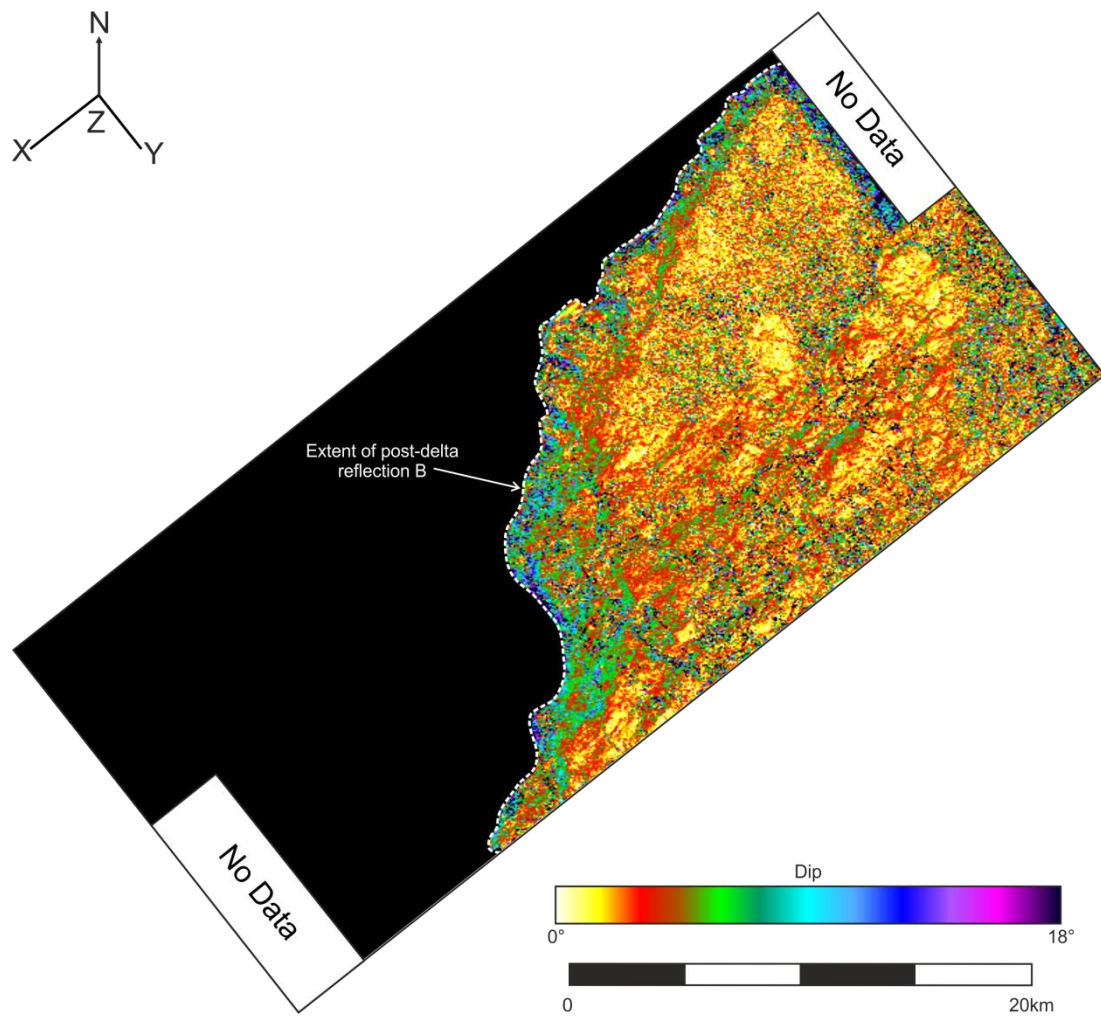
Fig. A2.27. Dip map of reflection B within the post-delta succession with extent of seismic reflection the onlaps the underlying delta succession. Lowest dips exhibited by flat lying lobate features and highest dips exhibited by delta front onlap. For location of 3D survey see Chapter 5.
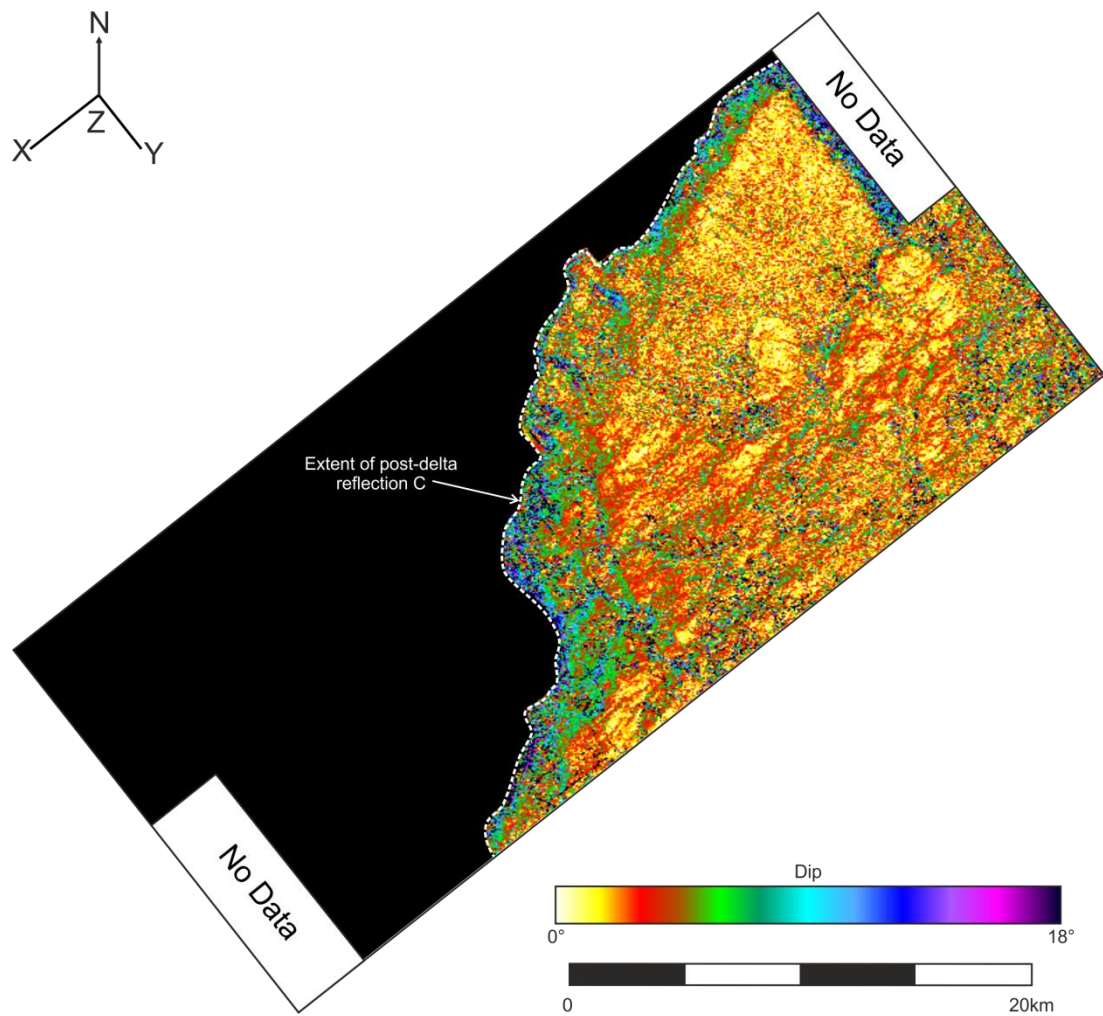
Fig. A2.28. Dip map of reflection C within the post-delta succession, with extent of seismic reflection the onlaps the underlying delta succession. Lowest dips exhibited by flat lying lobate features and highest dips exhibited by delta front onlap. For location of 3D survey see Chapter 5.
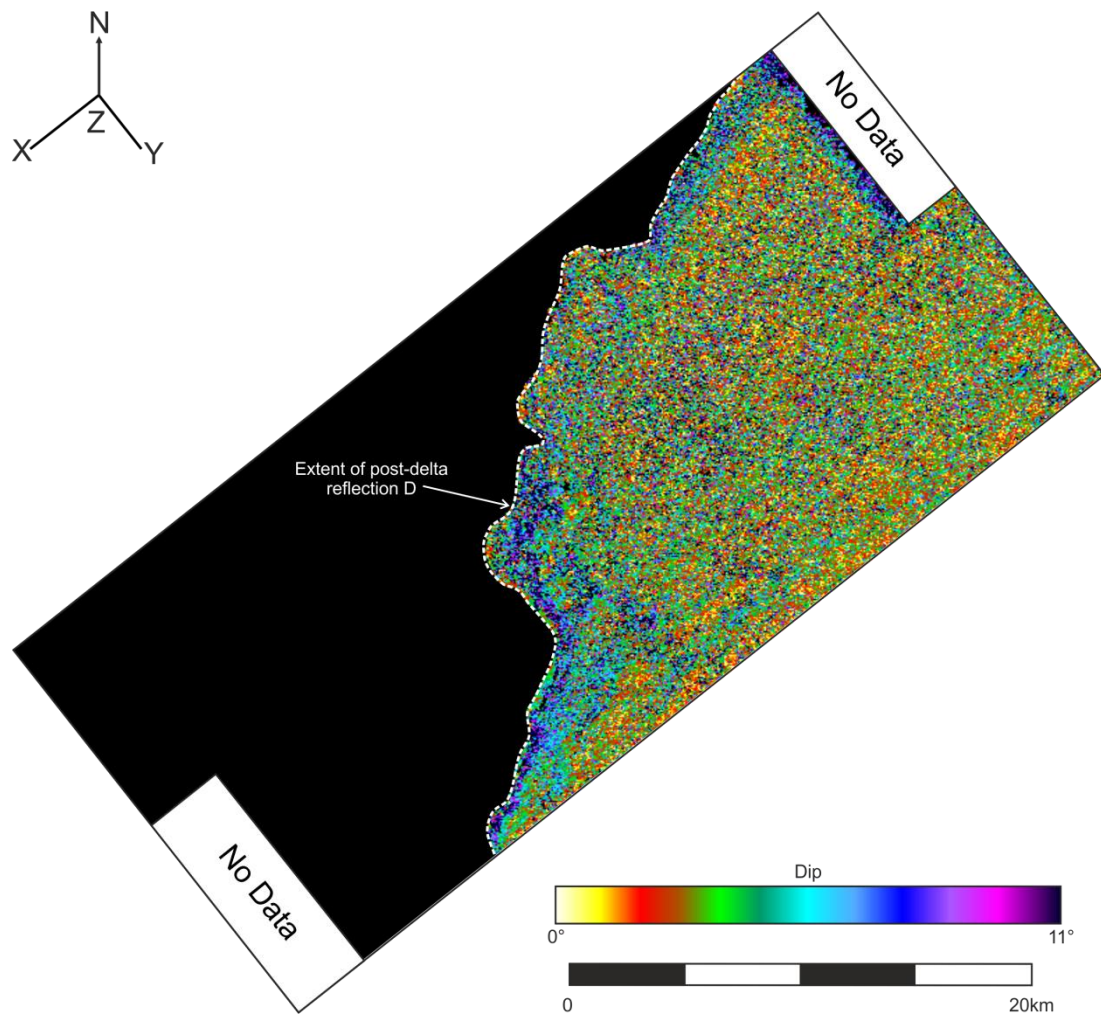
Fig. A2.29. Dip map of reflection D within the post-delta succession with extent of seismic reflection the onlaps the underlying delta succession. For location of 3D survey see Chapter 5.
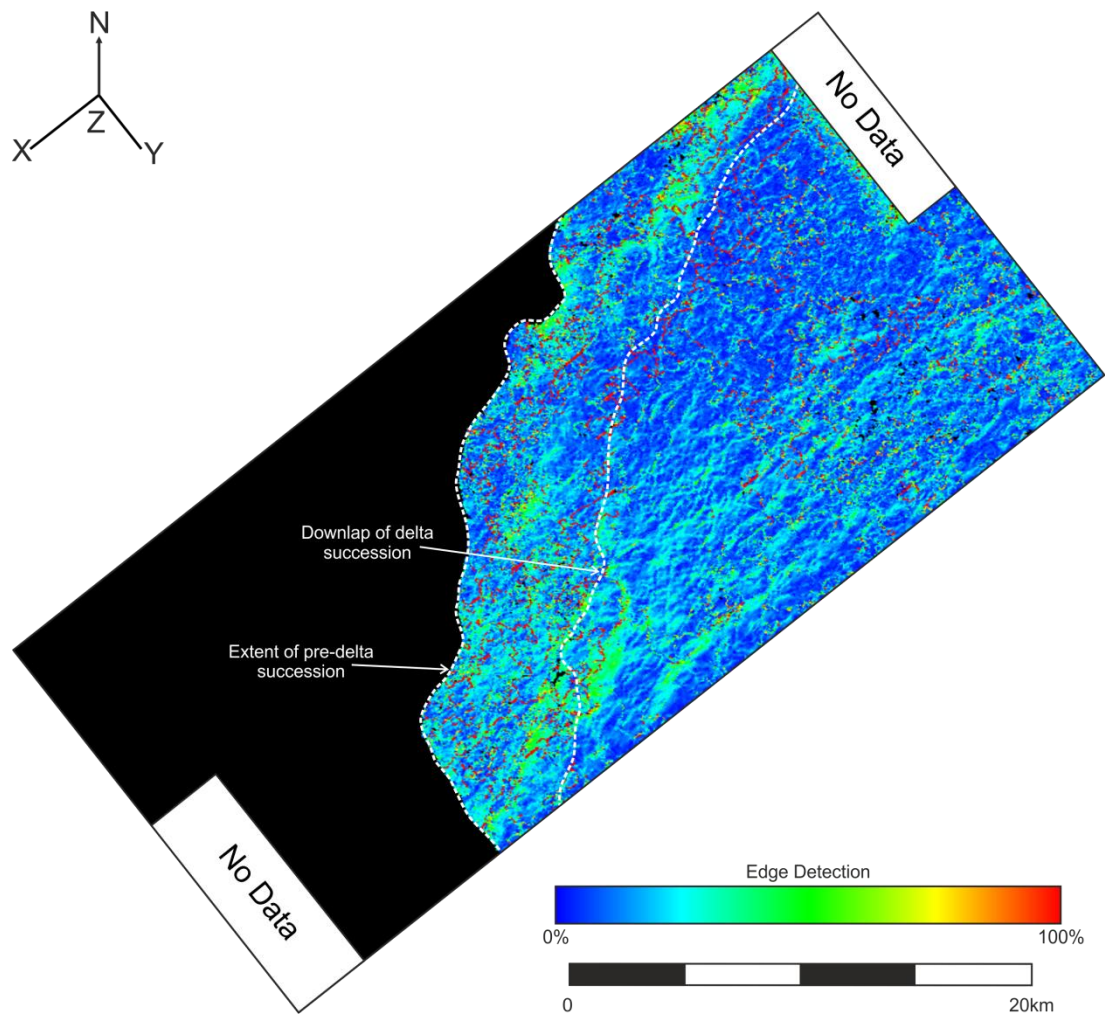
Fig. A2.30. Edge detection map of pre-delta succession, with extent of succession and downlap of overlying delta succession identified. For location of 3D survey see Chapter 5.
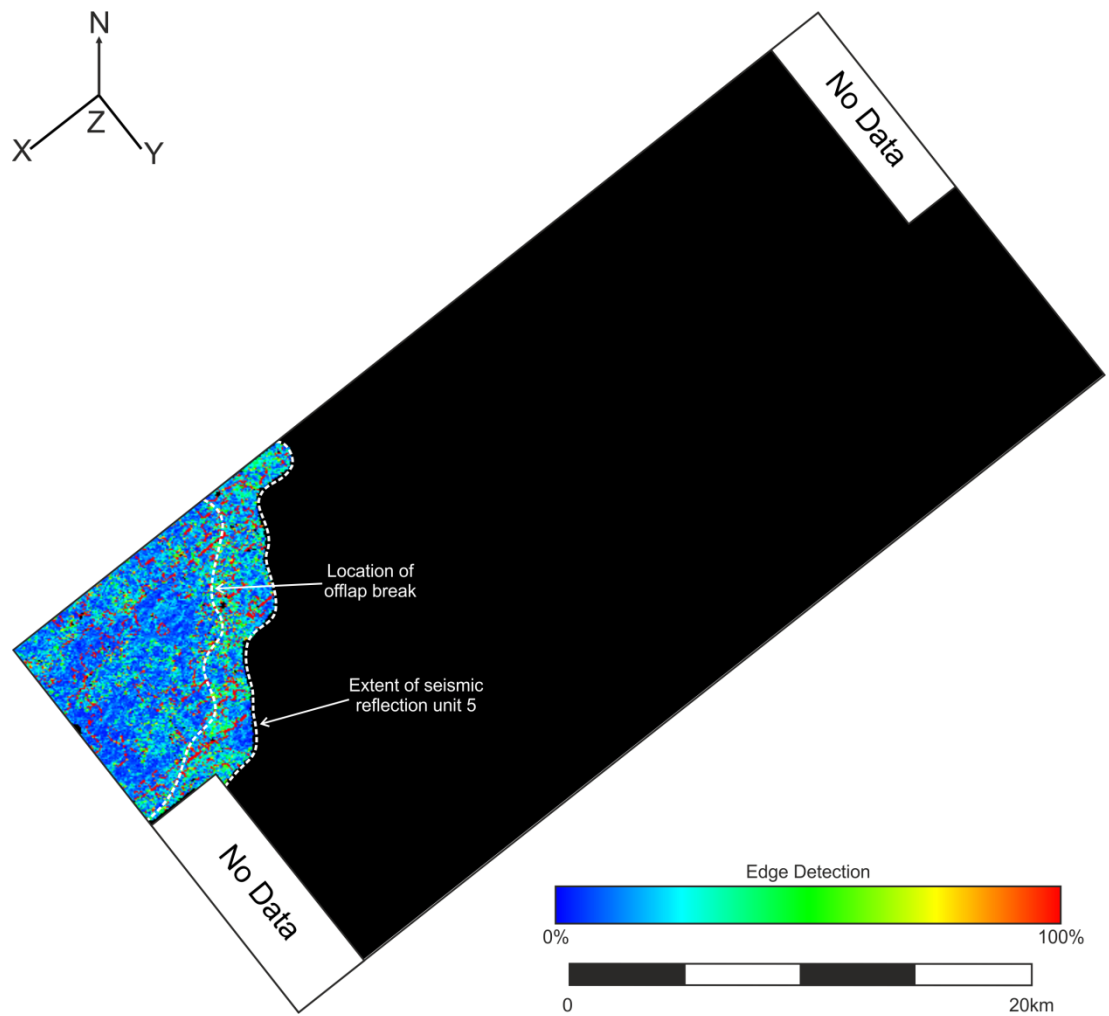
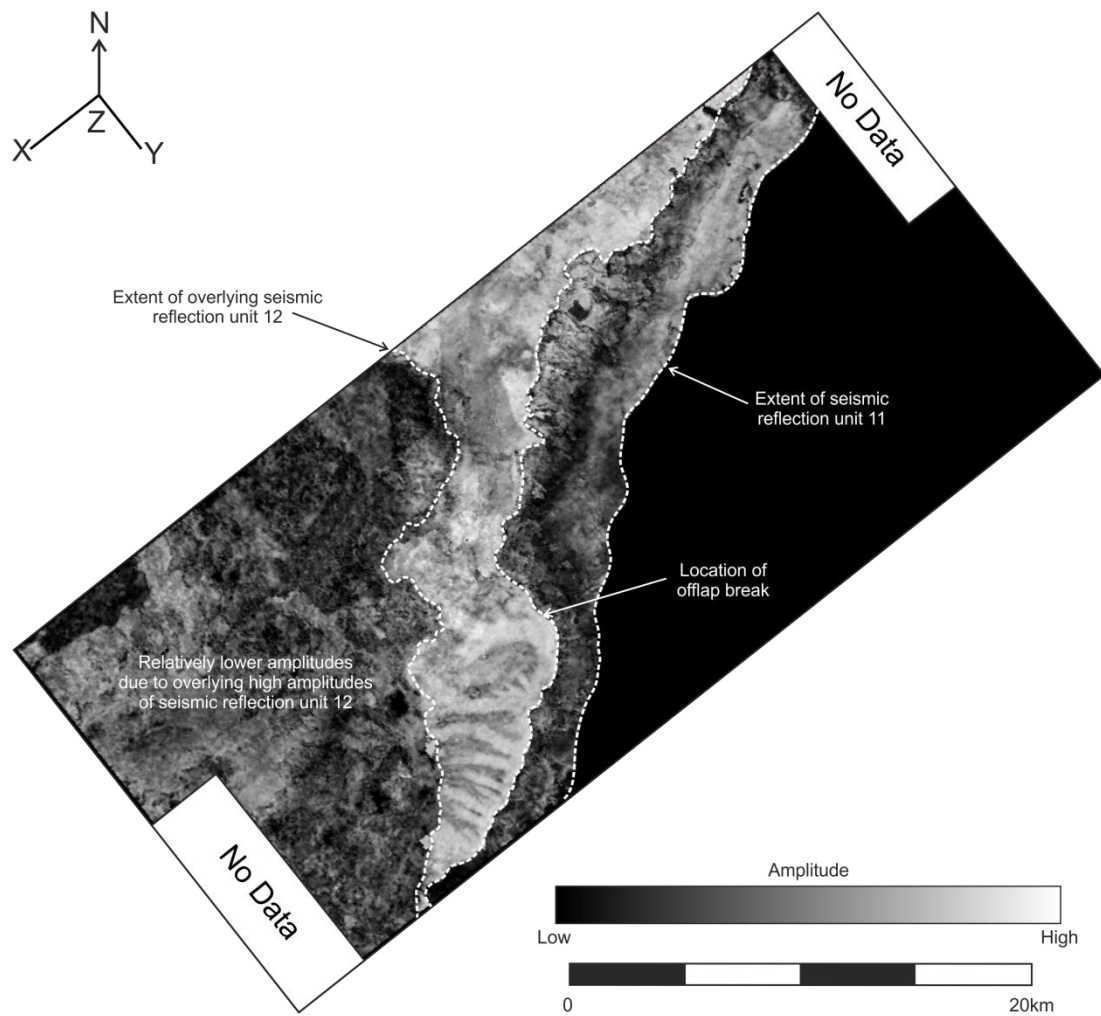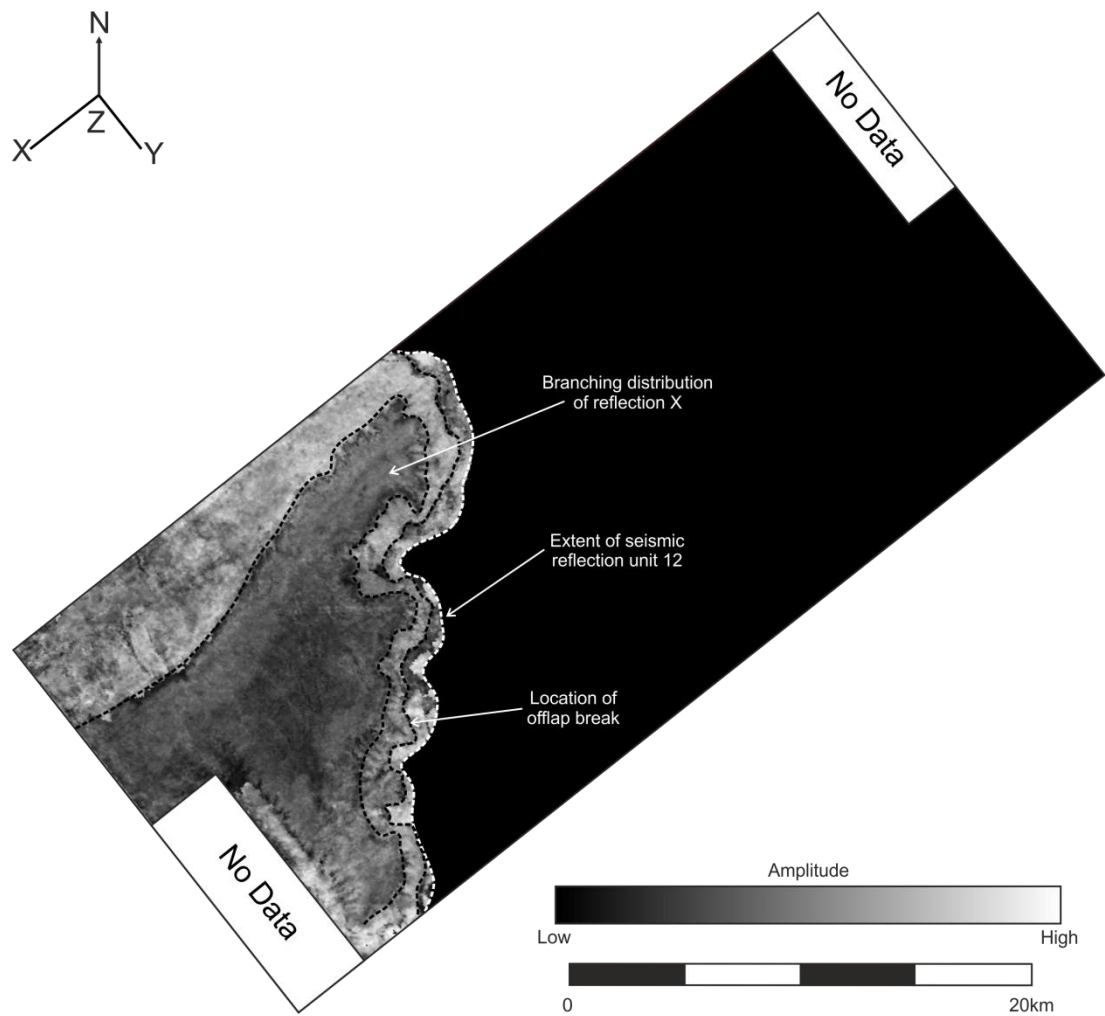**Fig. A2.31.** Edge detection map of seismic reflection unit 5 within the delta succession, with extent of seismic reflection unit and offlap break identified. Low discontinuity exhibited by subparallel lava flow topsets and high discontinuity exhibited by offlap break and inclined hyaloclastite foresets. For location of 3D survey see Chapter 5.
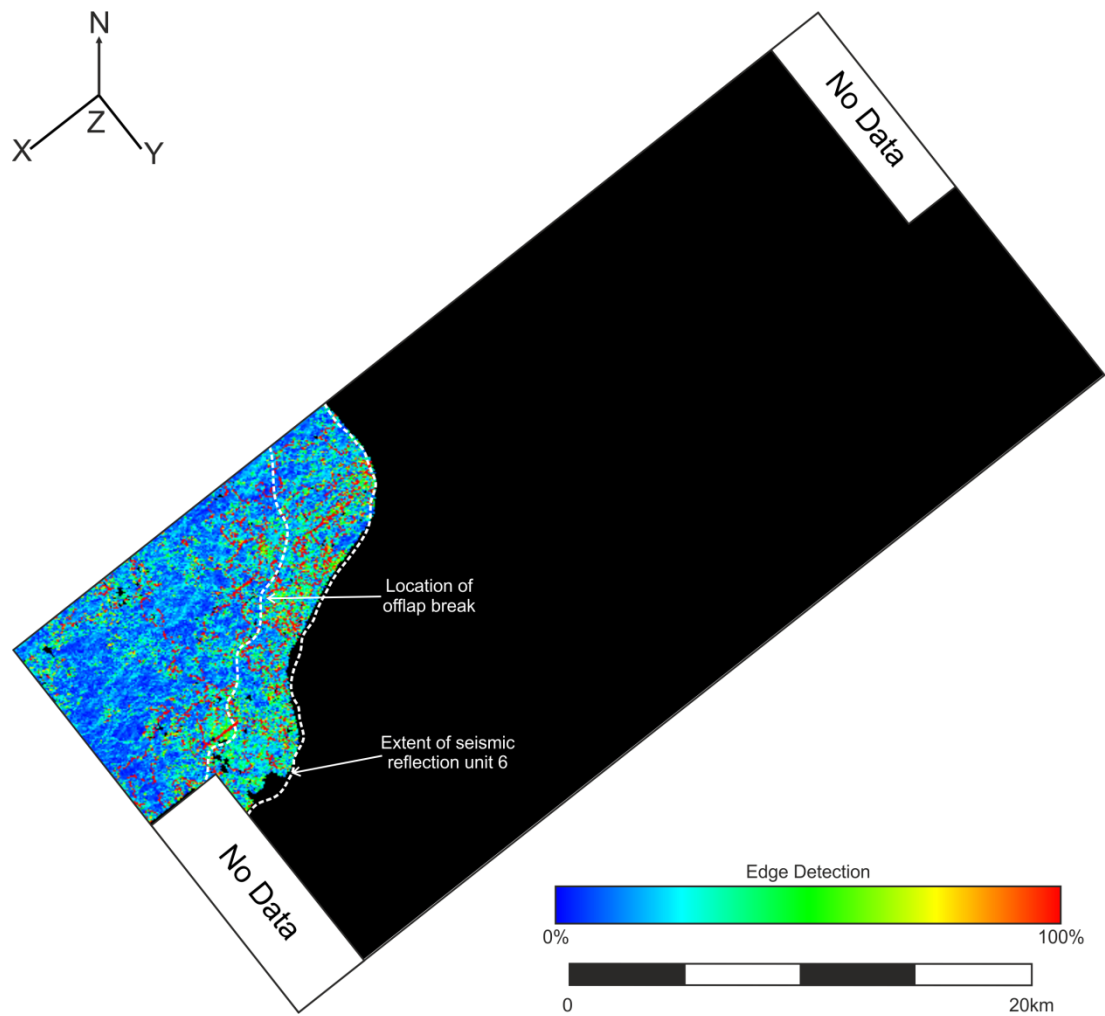
**Fig. A2.32.** Edge detection map of seismic reflection unit 6 within the delta succession, with extent of seismic reflection unit and offlap break identified. Low discontinuity exhibited by subparallel lava flow topsets and high discontinuity exhibited by offlap break and inclined hyaloclastite foresets. For location of 3D survey see Chapter 5.
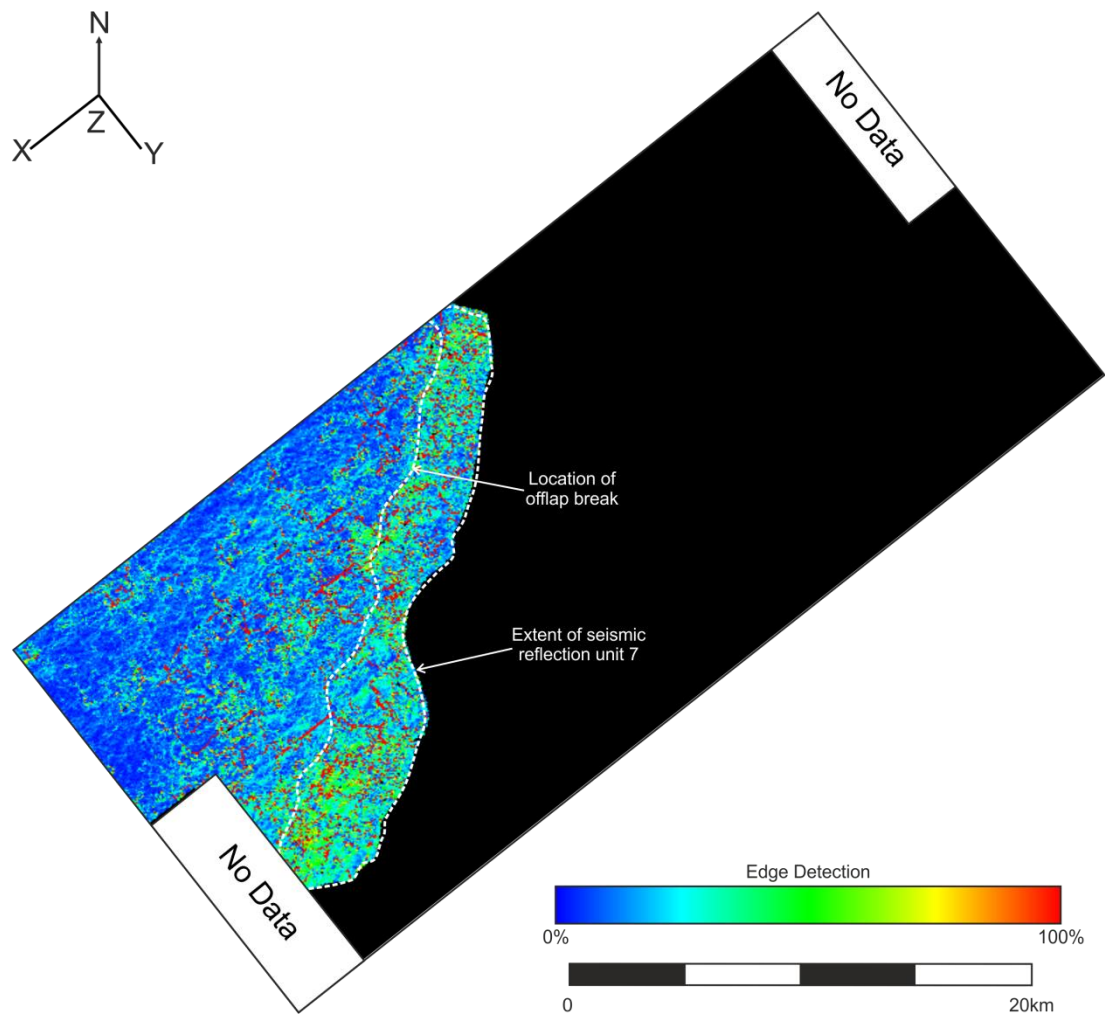
Fig. A2.33. Edge detection map of seismic reflection unit 7 within the delta succession, with extent of seismic reflection unit and offlap break identified. Low discontinuity exhibited by subparallel lava flow topsets and high discontinuity exhibited by offlap break and inclined hyaloclastite foresets. For location of 3D survey see Chapter 5.
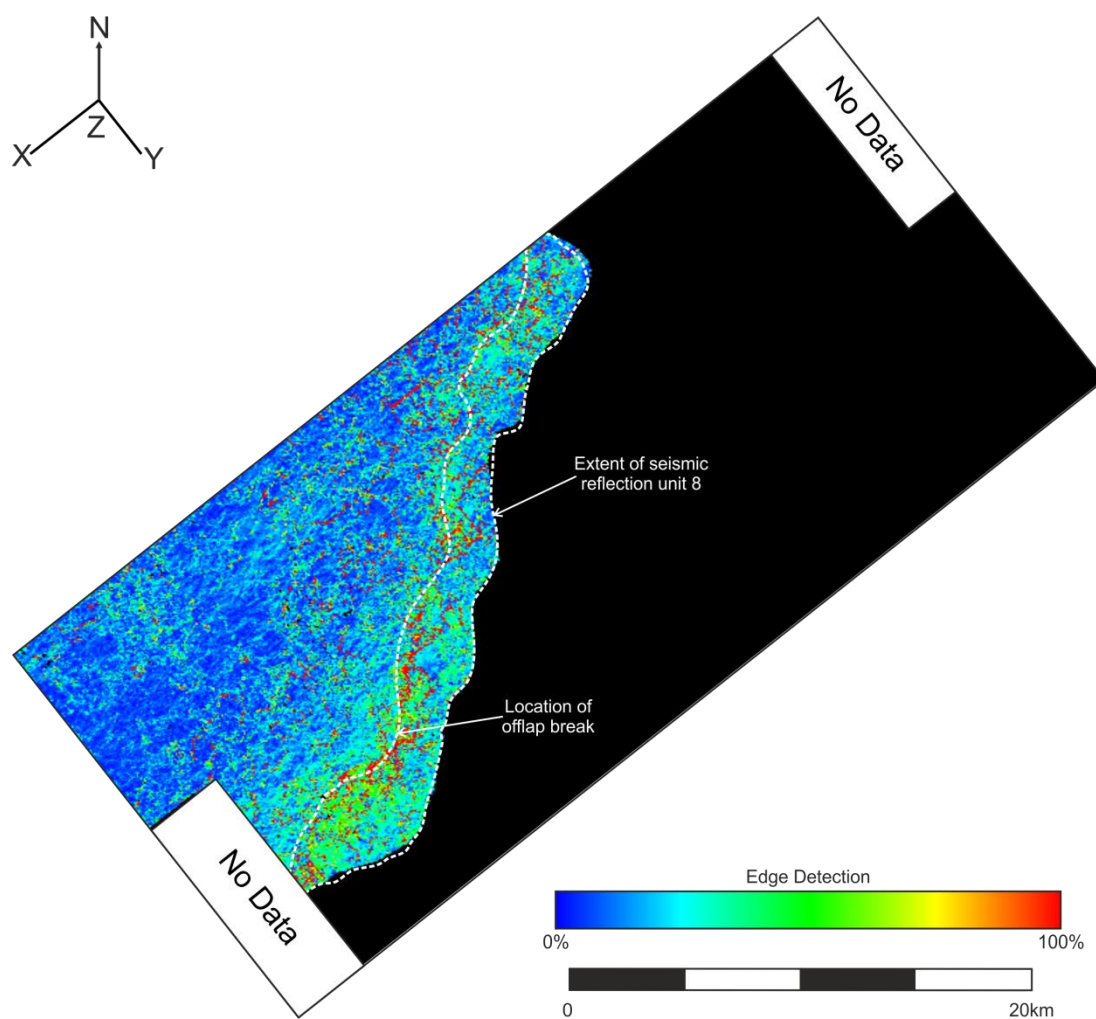
Fig. A2.34. Edge detection map of seismic reflection unit 8 within the delta succession, with extent of seismic reflection unit and offlap break identified Low discontinuity exhibited by subparallel lava flow topsets and high discontinuity exhibited by offlap break and inclined hyaloclastite foresets. For location of 3D survey see Chapter 5.
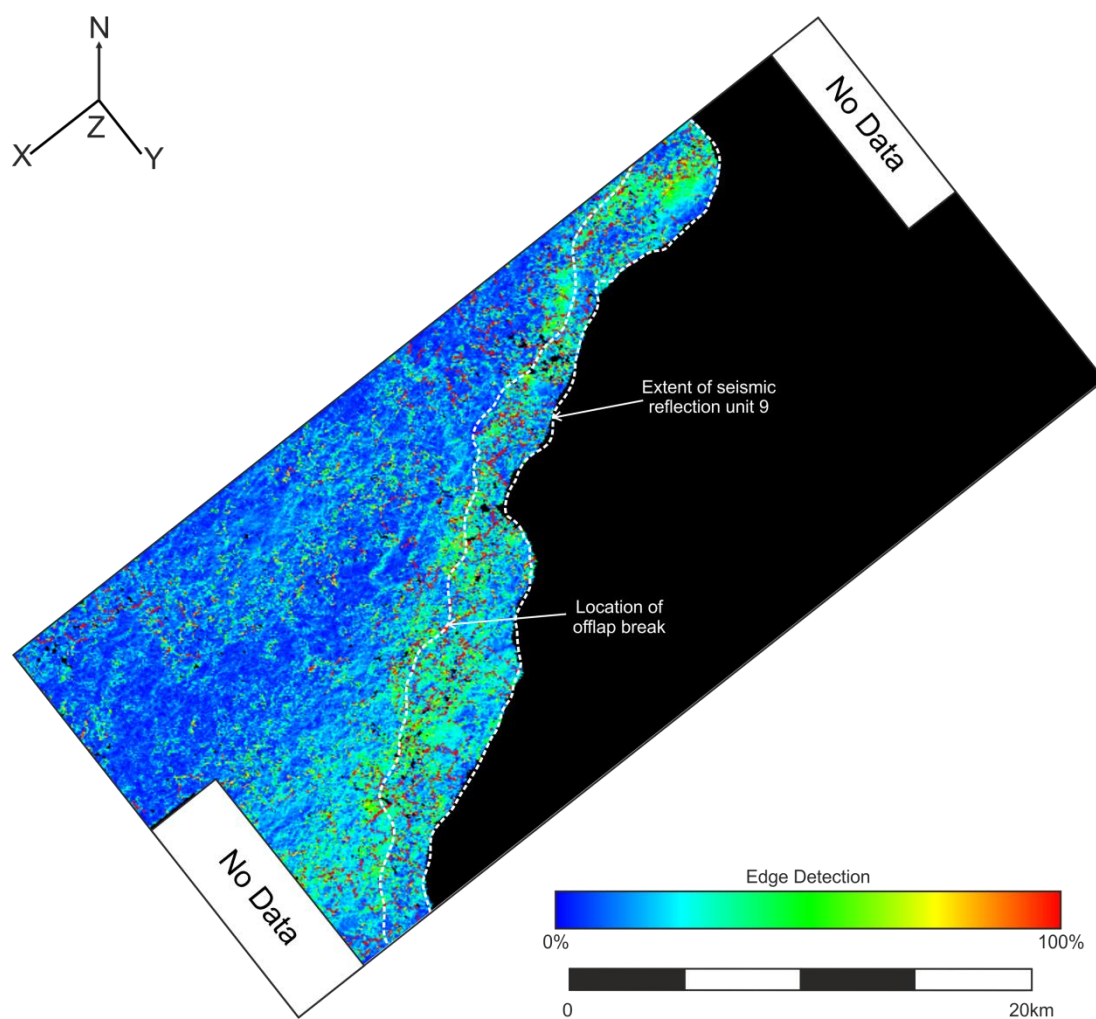
Fig. A2.35. Edge detection map of seismic reflection unit 9 within the delta succession, with extent of seismic reflection unit and offlap break identified. Low discontinuity exhibited by subparallel lava flow topsets and high discontinuity exhibited by offlap break and inclined hyaloclastite foresets. For location of 3D survey see Chapter 5.
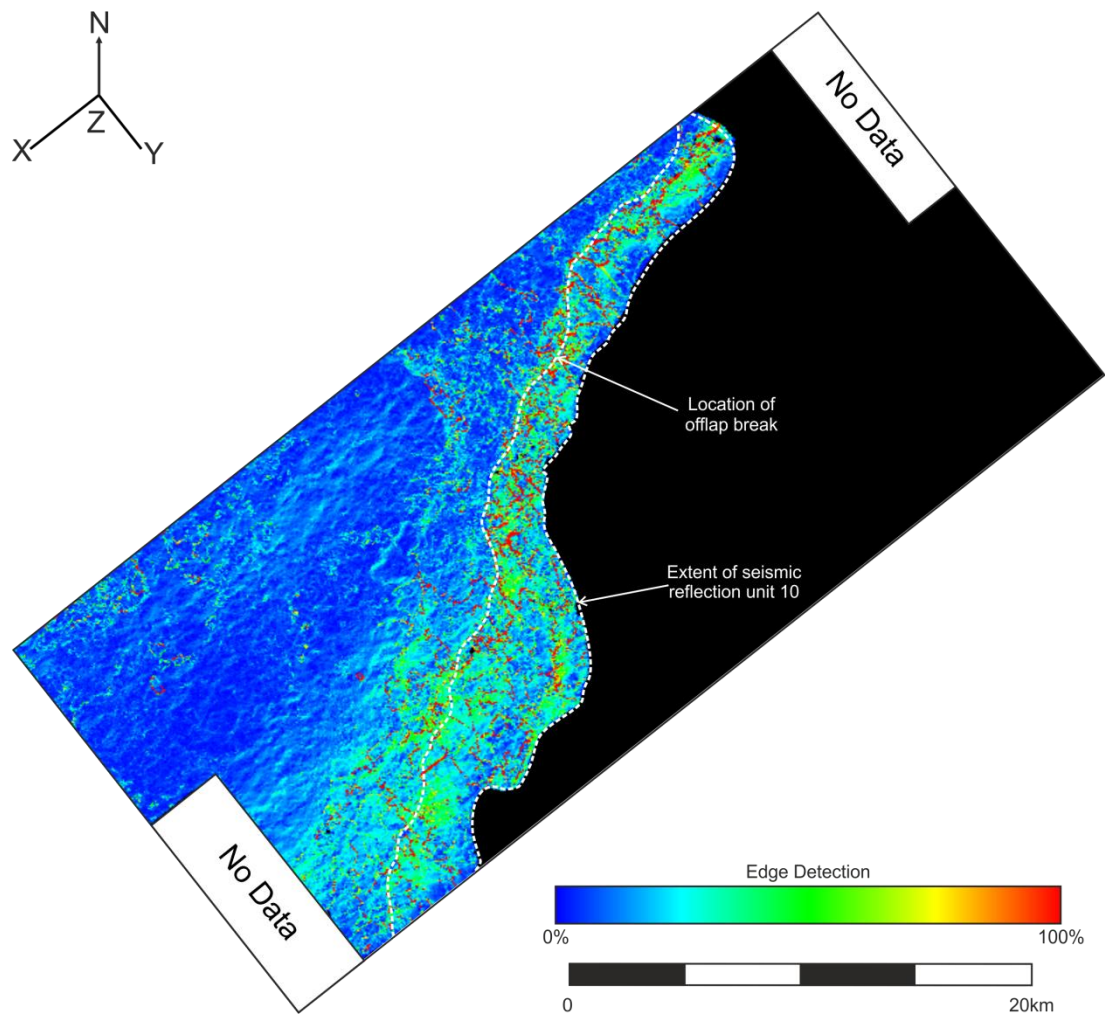
Fig. A2.36. Edge detection map of seismic reflection unit 10 within the delta succession, with extent of seismic reflection unit and offlap break identified. Low discontinuity exhibited by subparallel lava flow topsets and high discontinuity exhibited by offlap break and inclined hyaloclastite foresets. For location of 3D survey see Chapter 5.
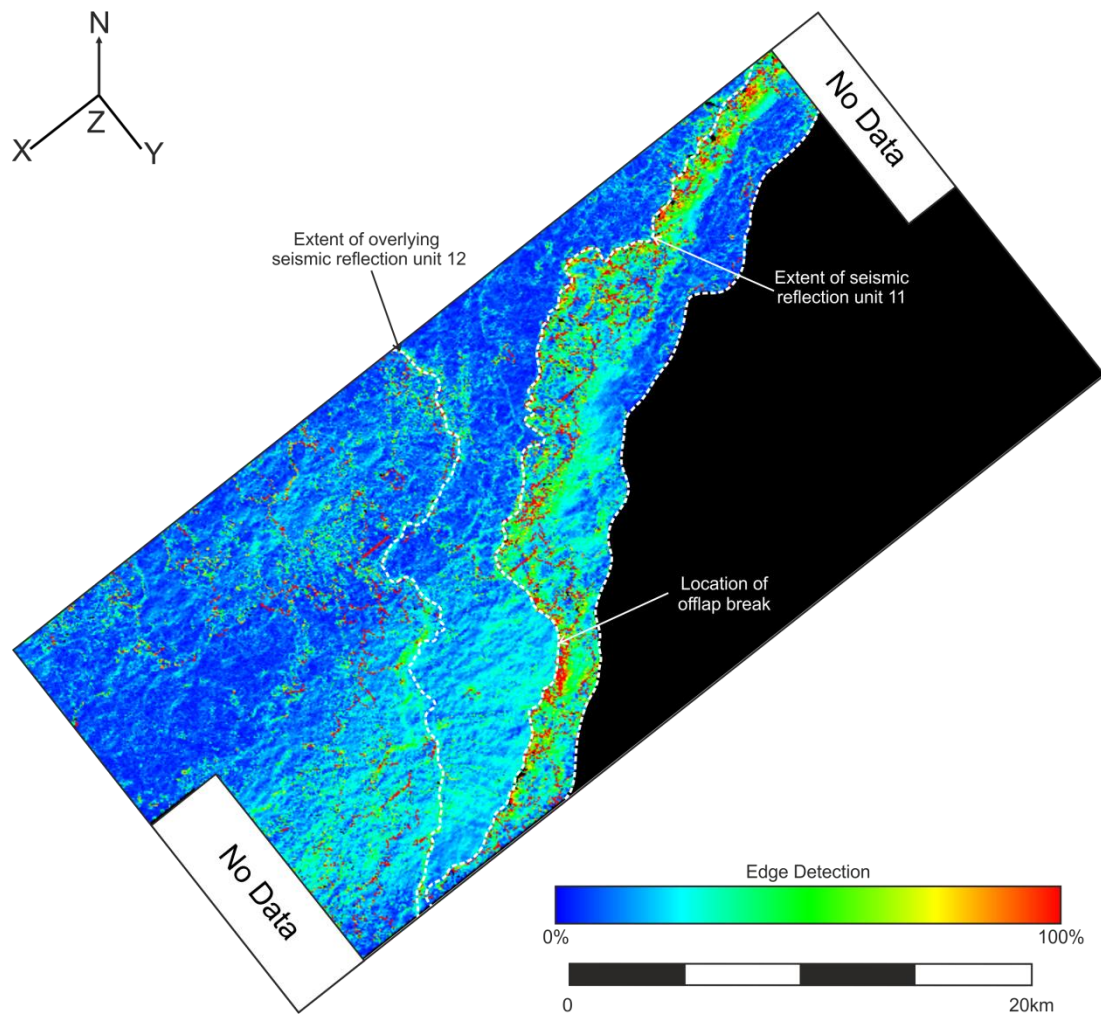
Fig. A2.37. Edge detection map of seismic reflection unit 11 within the delta succession, with extent of seismic reflection unit, offlap break and extent of overlying seismic reflection unit 12 identified. Low discontinuity exhibited by subparallel lava flow topsets and high discontinuity exhibited by offlap break and inclined hyaloclastite foresets. Edge detection attribute highlight debris avalanche escarpments and lava-inflations clefts. For location of 3D survey see Chapter 5.
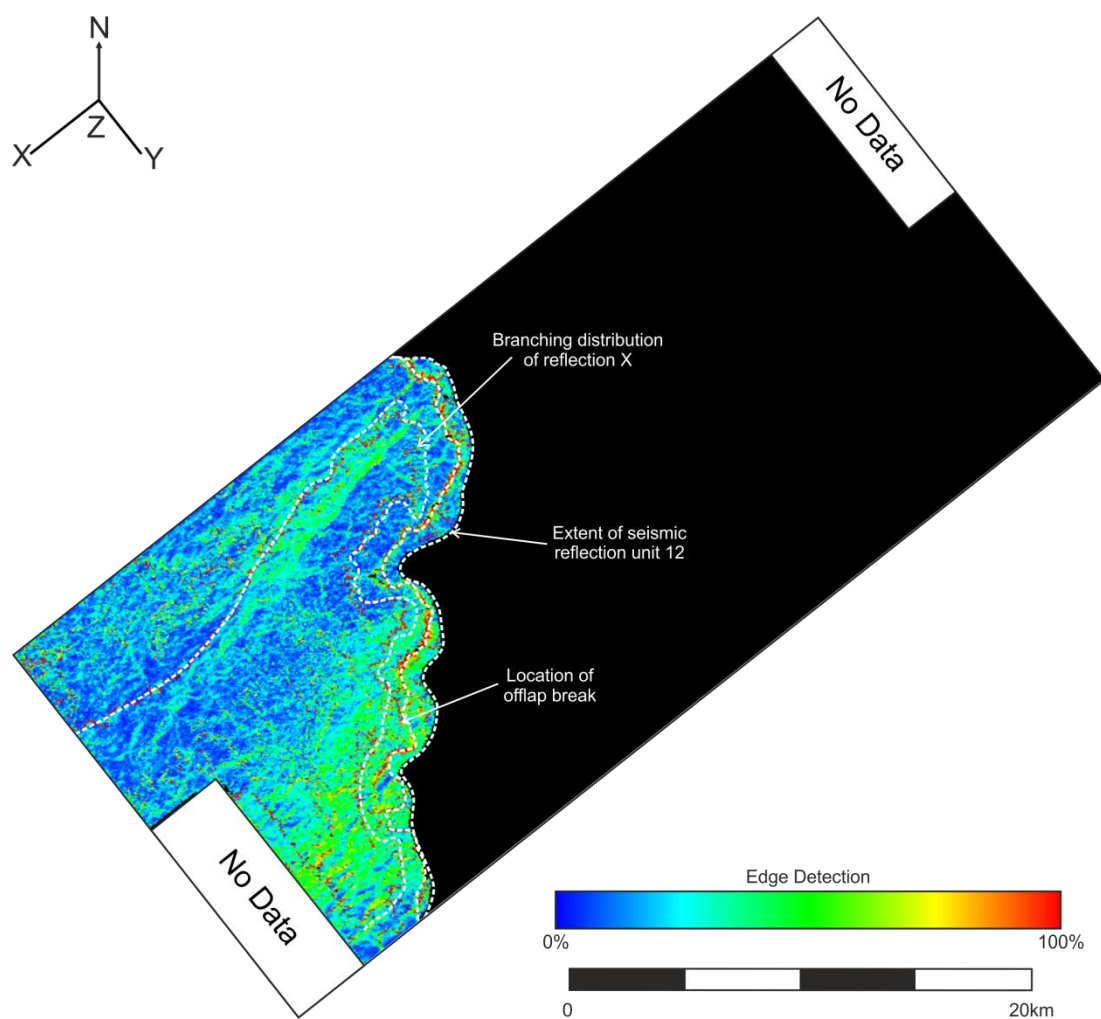
Fig. A2.38. Edge detection map of seismic reflection unit 12 within the delta succession, with extent of seismic reflection unit, offlap break and extent of reflection X identified. Low discontinuity exhibited by subparallel lava flow topsets and high discontinuity exhibited by offlap break and inclined hyaloclastite foresets. For location of 3D survey see Chapter 5.
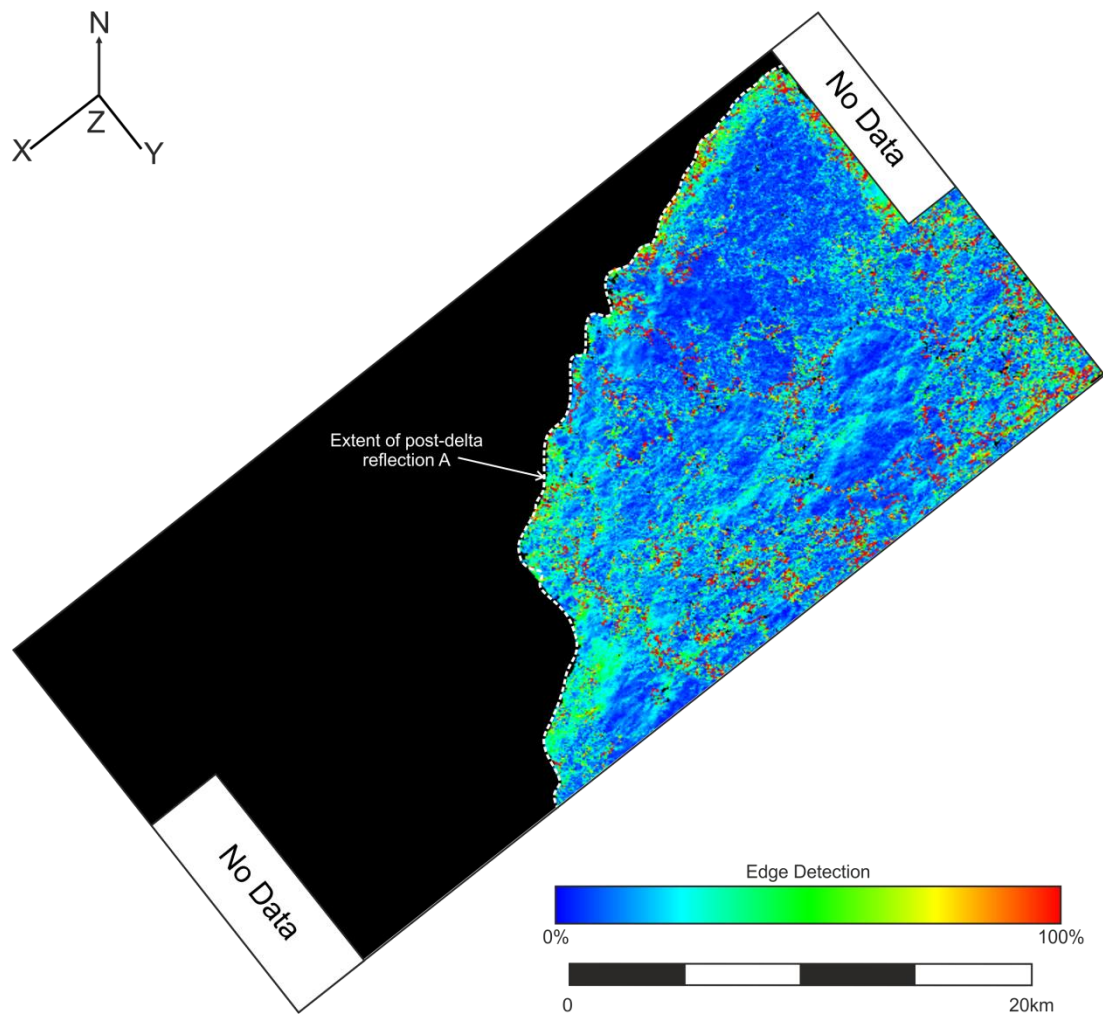
**Fig. A2.39.** Edge detection map of reflection A within the post-delta succession, with extent of seismic reflection the onlaps the underlying delta succession. Low discontinuity exhibited by flat lying lobate features and high discontinuity exhibited by delta front onlap. For location of 3D survey see Chapter 5.
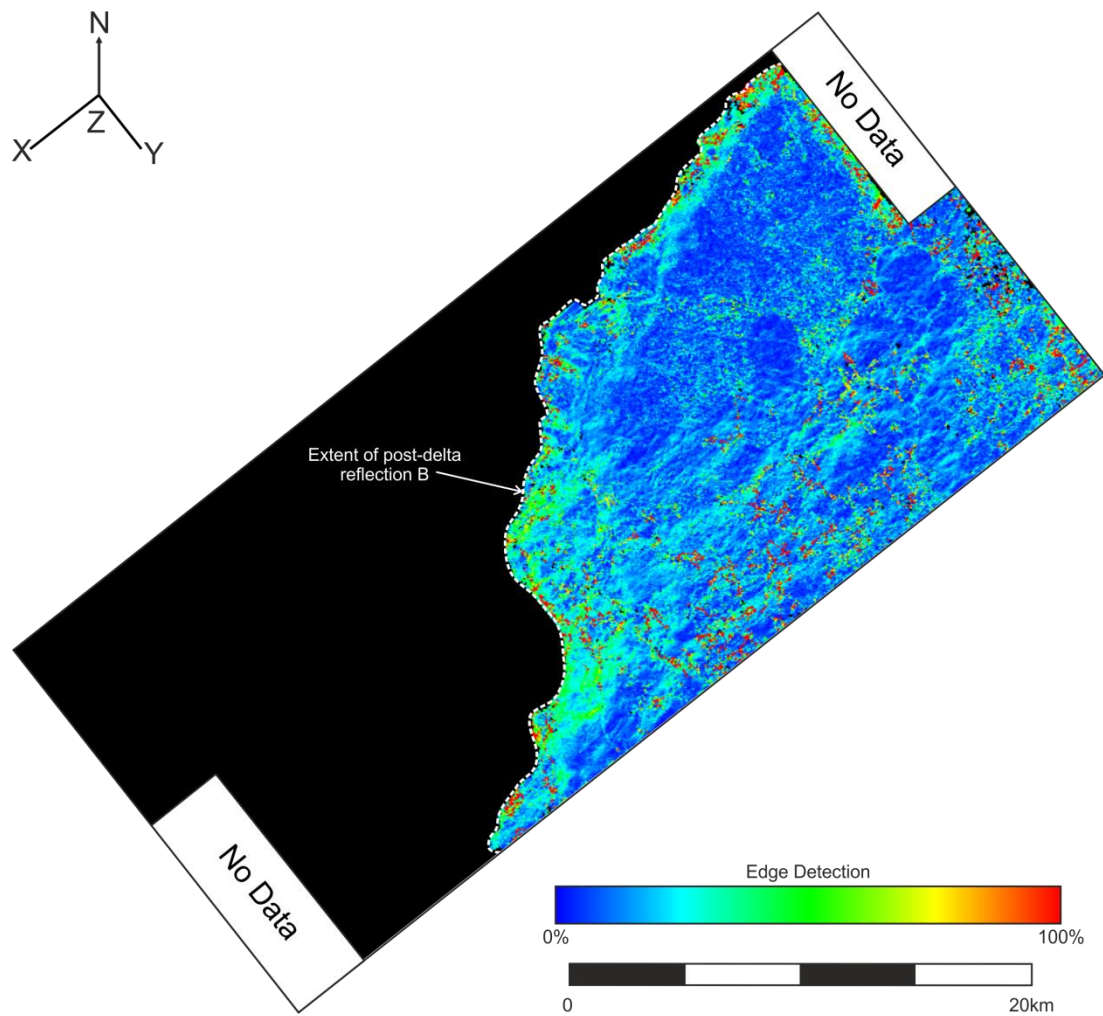
Fig. A2.40. Edge detection map of reflection B within the post-delta succession, with extent of seismic reflection the onlaps the underlying delta succession. Low discontinuity exhibited by flat lying lobate features and high discontinuity exhibited by delta front onlap. For location of 3D survey see Chapter 5.
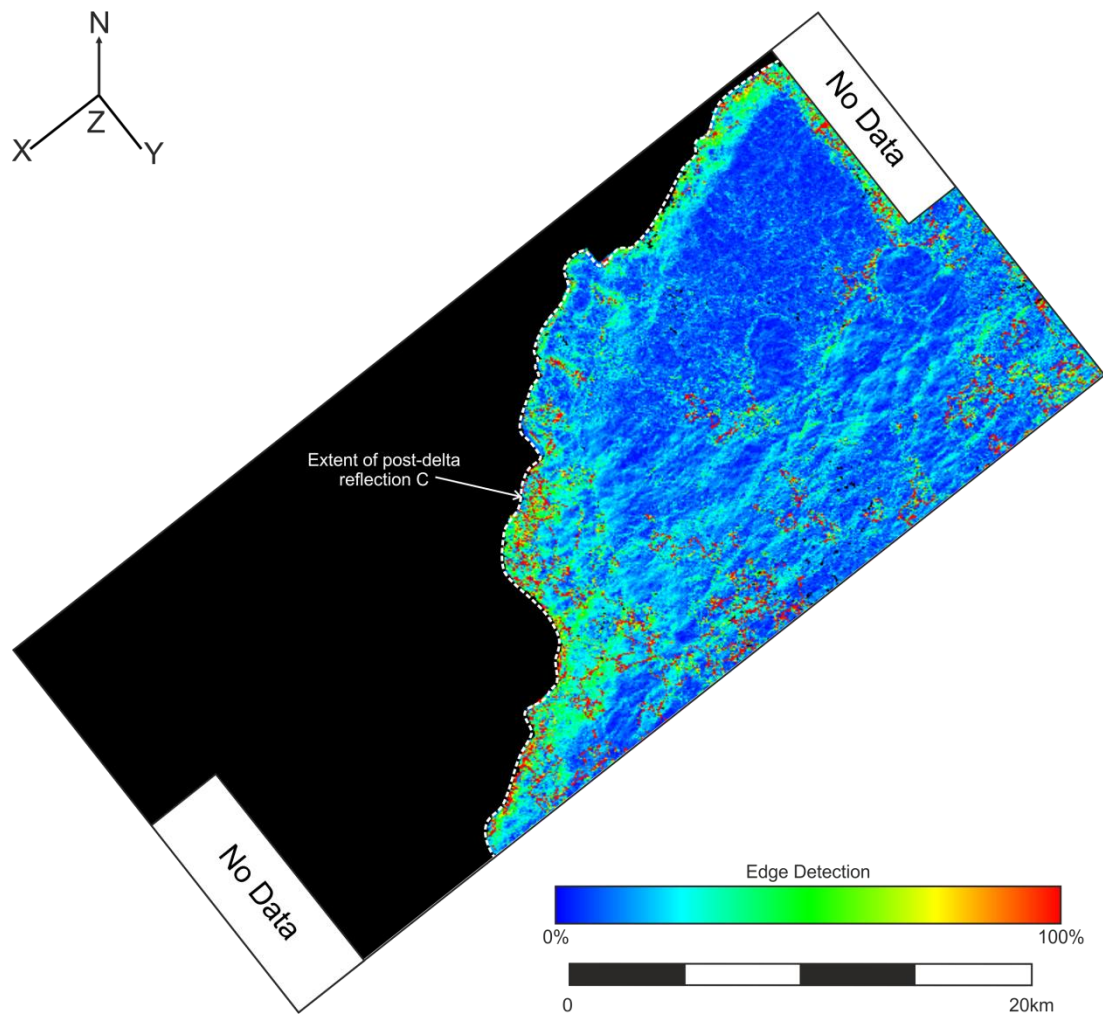
Fig. A2.41. Edge detection map of reflection C within the post-delta succession, with extent of seismic reflection the onlaps the underlying delta succession. Low discontinuity exhibited by flat lying lobate features and high discontinuity exhibited by delta front onlap. For location of 3D survey see Chapter 5.
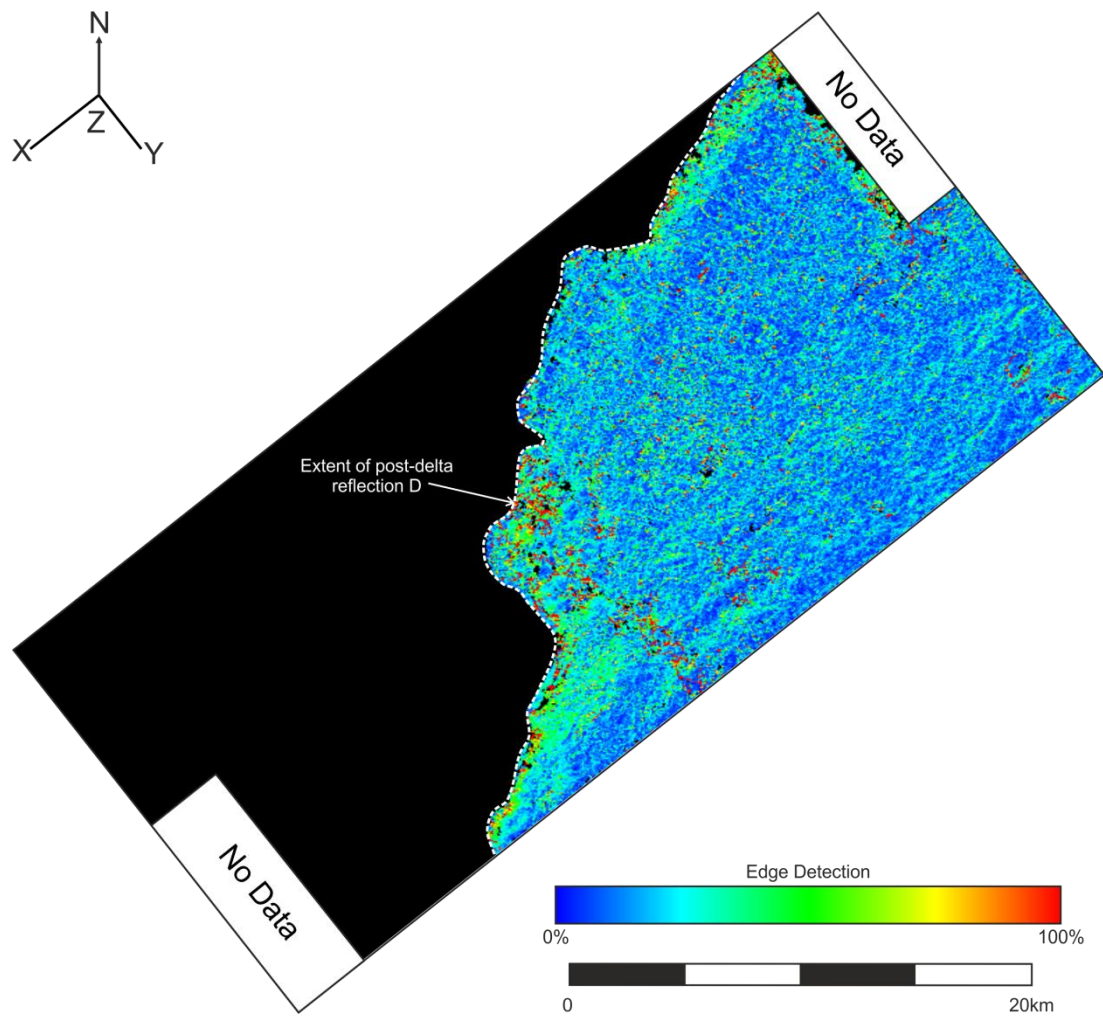
Fig. A2.42. Edge detection map of reflection D within the post-delta succession, with extent of reflection and lack of internal lobate geometries. For location of 3D survey see Chapter 5.

APPENDIX III: SUPPORT MATERIAL FOR CHAPTER 6

This appendix contains supporting evidence for Chapter 6: *An Evaluation of the Volcanic Stratigraphy of the Rosebank Field, Faroe-Shetland Basin*. It includes a location map (see Fig. A3.1), the well data used and the synthetic seismograms discussed but not shown in Chapter 6 (see Fig. A3.2 – A3.6). In addition, seismic sections that display the path of the exploration wells and related seismic reflection units are presented (see Fig. A3.7 – A3. 11). RMS amplitude extraction maps without locations of close-up figures are provided (see Fig. A3.12 – A3.16). This appendix also includes full versions of dip and edge detection attribute maps used in Chapter 6 (see Fig. A3.12 – A3.19).
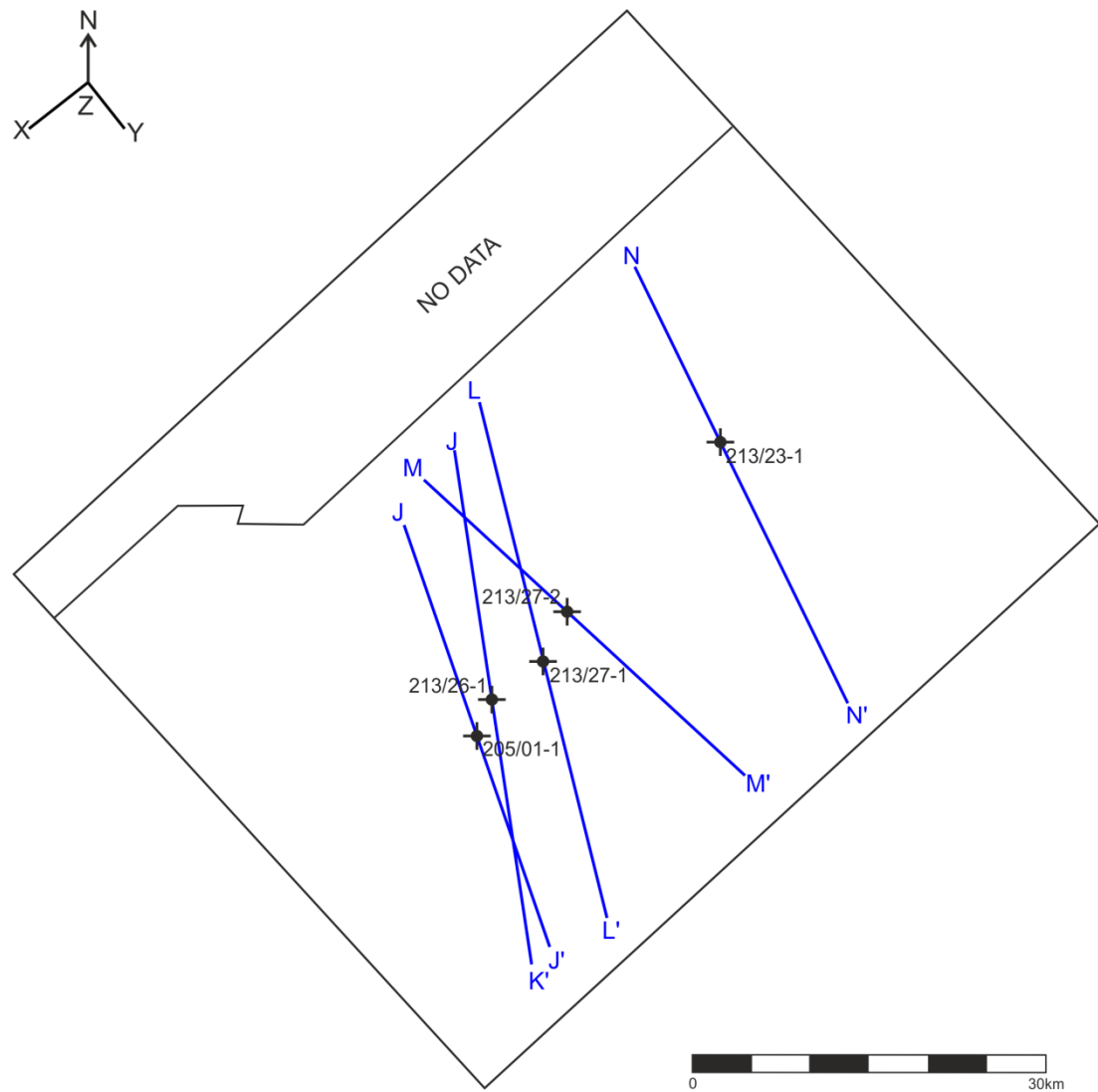
Fig. A3.1. Map of the 3D seismic survey and location of the exploration wells (see Fig. A3.2 to A3.6) and the corresponding seismic sections that intersect the well path (see Fig. A3.7 – A3.11). For location of 3D survey see Chapter 6.
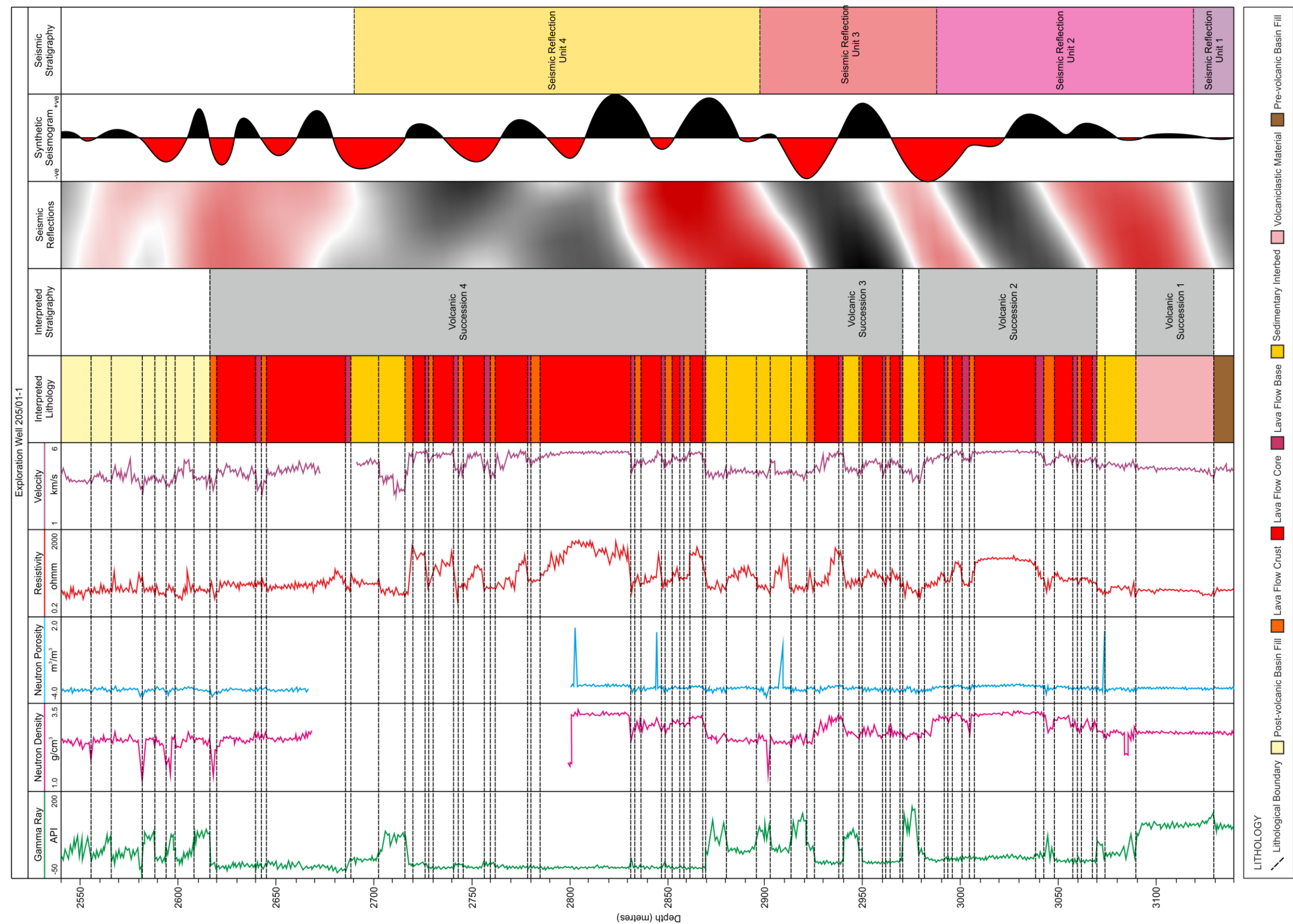
Fig. A3.2. Wireline log data from exploration well 205/01-1, with the seismic reflection data coincident with the well path and the synthetic seismogram. Interpretation of lithology is based on the identification of individual lava flows, volcaniclastic and sedimentary beds by analysis the suite of wireline log responses (see Chapter 3, Fig. 20). Interpretation of volcanic stratigraphy is based on the gross interpreted lithology. Interpretation of seismic stratigraphy is based on the correlation of the interpreted lithology and volcanic stratigraphy with the seismic data. For well location see Fig. A3.1.
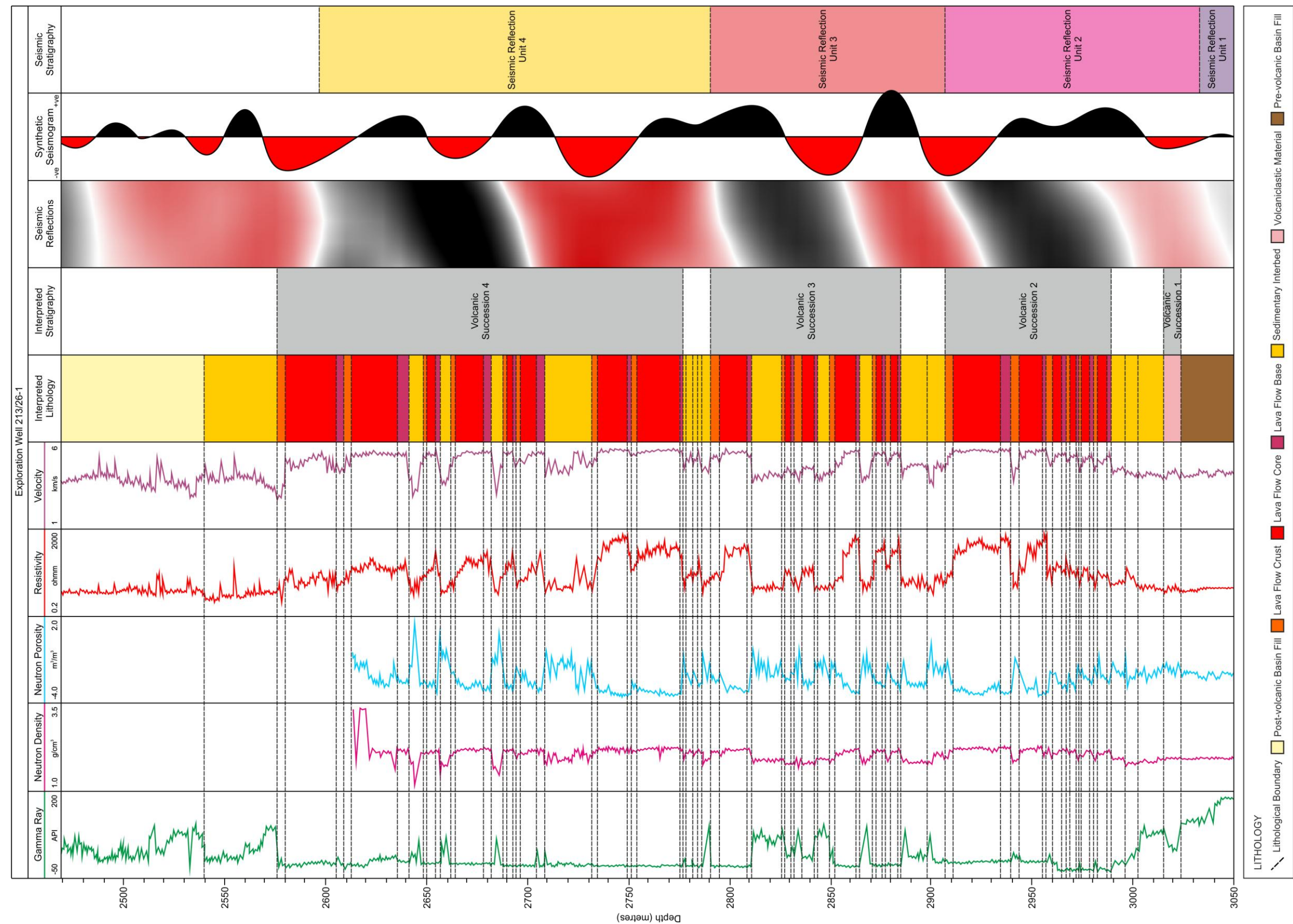
Fig. A3.3. Wireline log data from exploration well 213/26-1, with the seismic reflection data coincident with the well path and the synthetic seismogram. Interpretation of lithology is based on the identification of individual lava flows, volcaniclastic and sedimentary beds by analysis the suite of wireline log responses (see Chapter 3, Fig. 20). Interpretation of volcanic stratigraphy is based on the gross interpreted lithology. Interpretation of seismic stratigraphy is based on the correlation of the interpreted lithology and volcanic stratigraphy with the seismic data. For well location see Fig. A3.1.
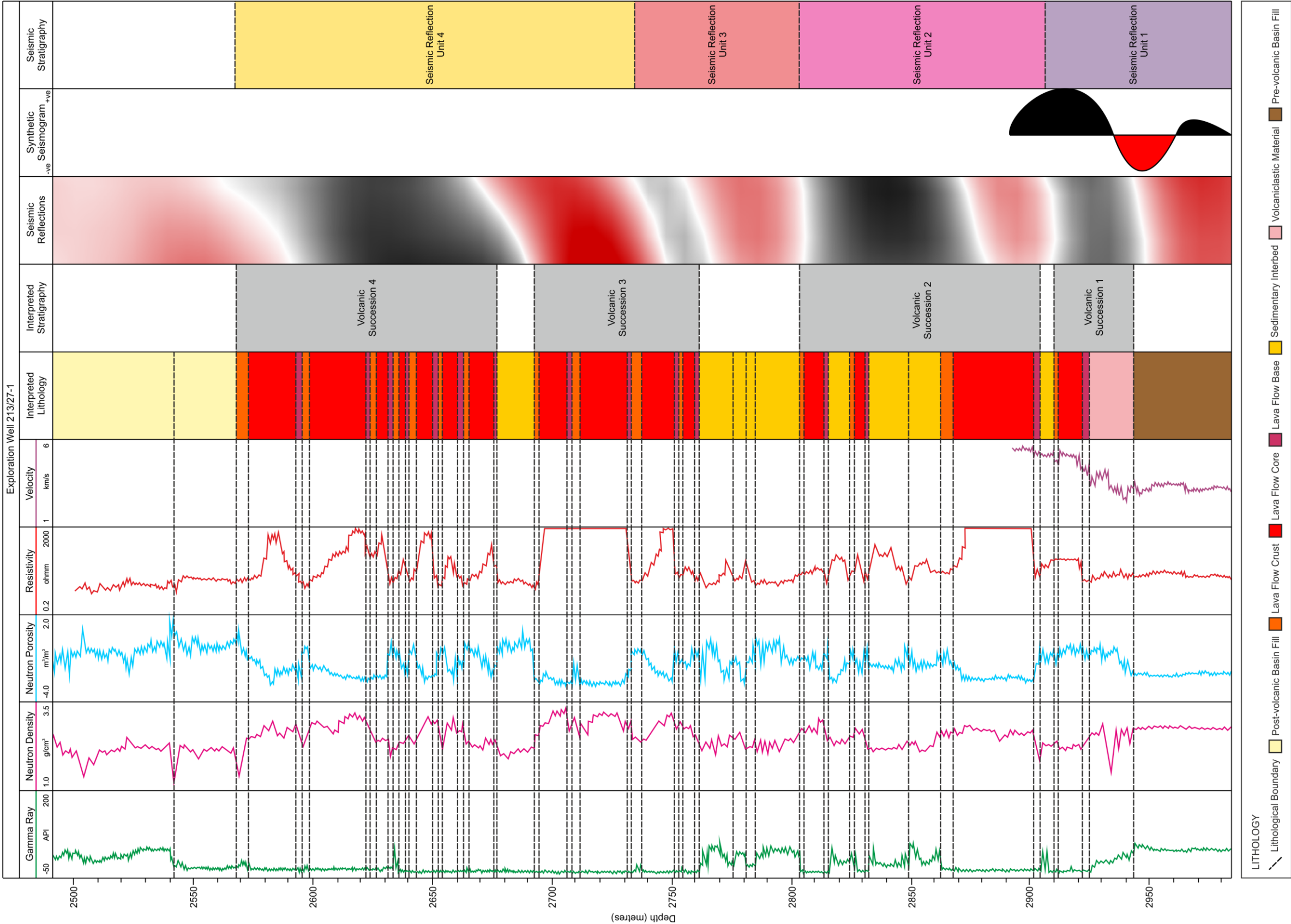
Fig. A3.4. Wireline log data from exploration well 213/27-1, with the seismic reflection data coincident with the well path and the synthetic seismogram. Interpretation of lithology is based on the identification of individual lava flows, volcaniclastic and sedimentary beds by analysis the suite of wireline log responses (see Chapter 3, Fig. 20). Interpretation of volcanic stratigraphy is based on the gross interpreted lithology. Interpretation of seismic stratigraphy is based on the correlation of the interpreted lithology and volcanic stratigraphy with the seismic data. For well location see Fig. A3.1.
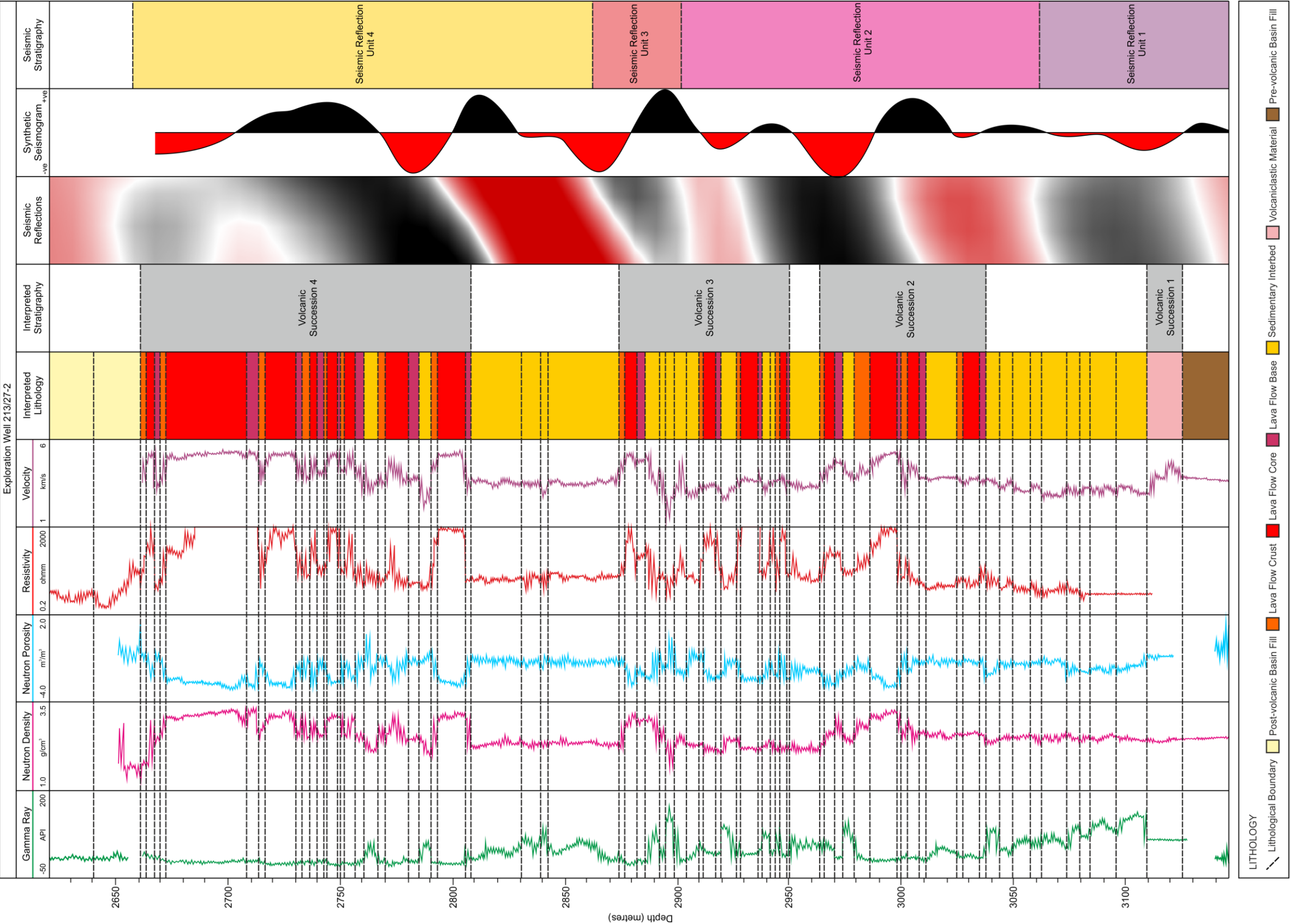
Fig. A3.5. Wireline log data from exploration well 213/27-2, with the seismic reflection data coincident with the well path and the synthetic seismogram. Interpretation of lithology is based on the identification of individual lava flows, volcaniclastic and sedimentary beds by analysis the suite of wireline log responses (see Chapter 3, Fig. 20). Interpretation of volcanic stratigraphy is based on the gross interpreted lithology. Interpretation of seismic stratigraphy is based on the correlation of the interpreted lithology and volcanic stratigraphy with the seismic data. For well location see Fig. A3.1.
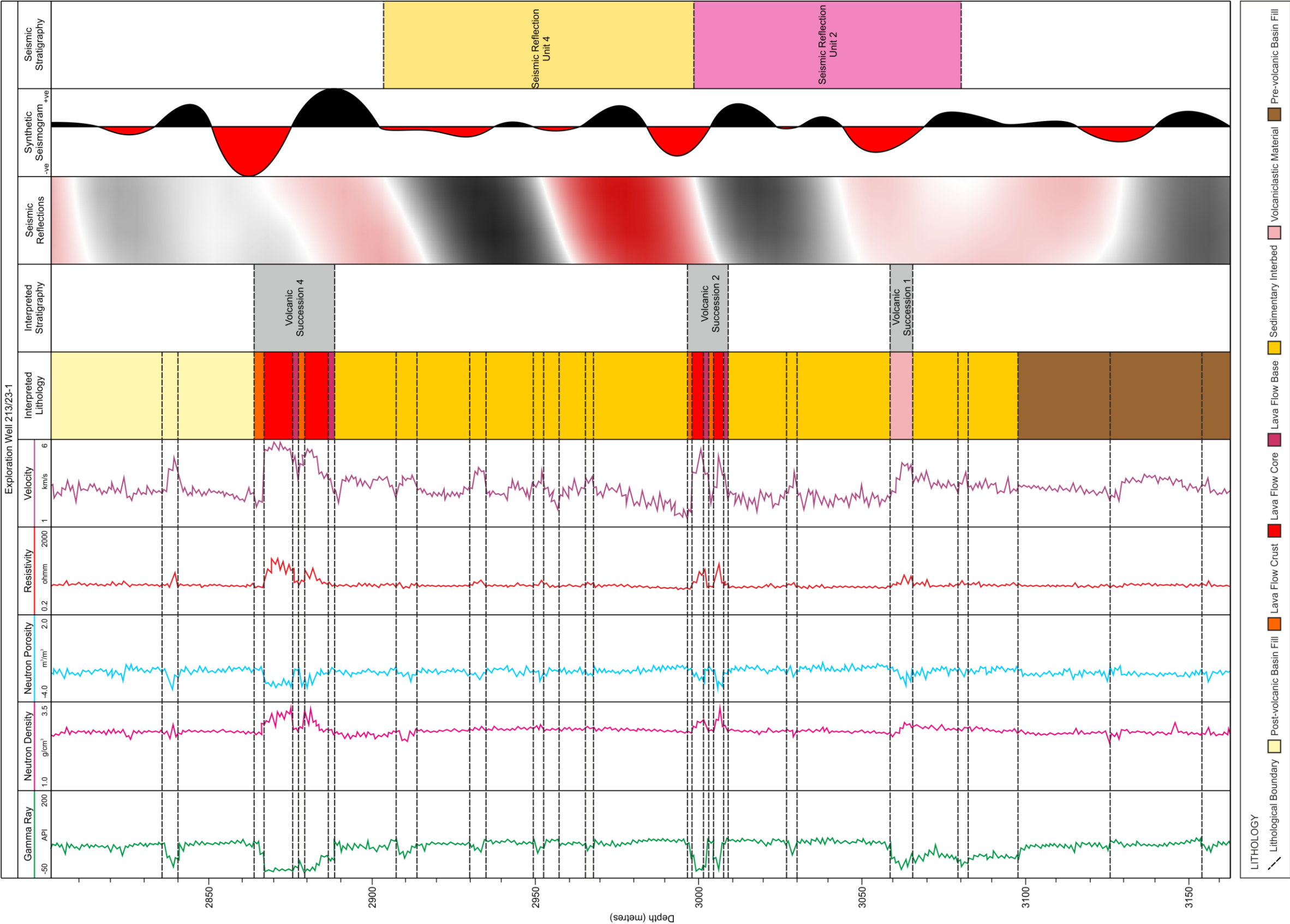
Fig. A3.6. Wireline log data from exploration well 213/23-1, with the seismic reflection data coincident with the well path and the synthetic seismogram. Interpretation of lithology is based on the identification of individual lava flows, volcaniclastic and sedimentary beds by analysis the suite of wireline log responses (see Chapter 3, Fig. 20). Interpretation of volcanic stratigraphy is based on the gross interpreted lithology. Interpretation of seismic stratigraphy is based on the correlation of the interpreted lithology and volcanic stratigraphy with the seismic data. For well location see Fig. A3.1.
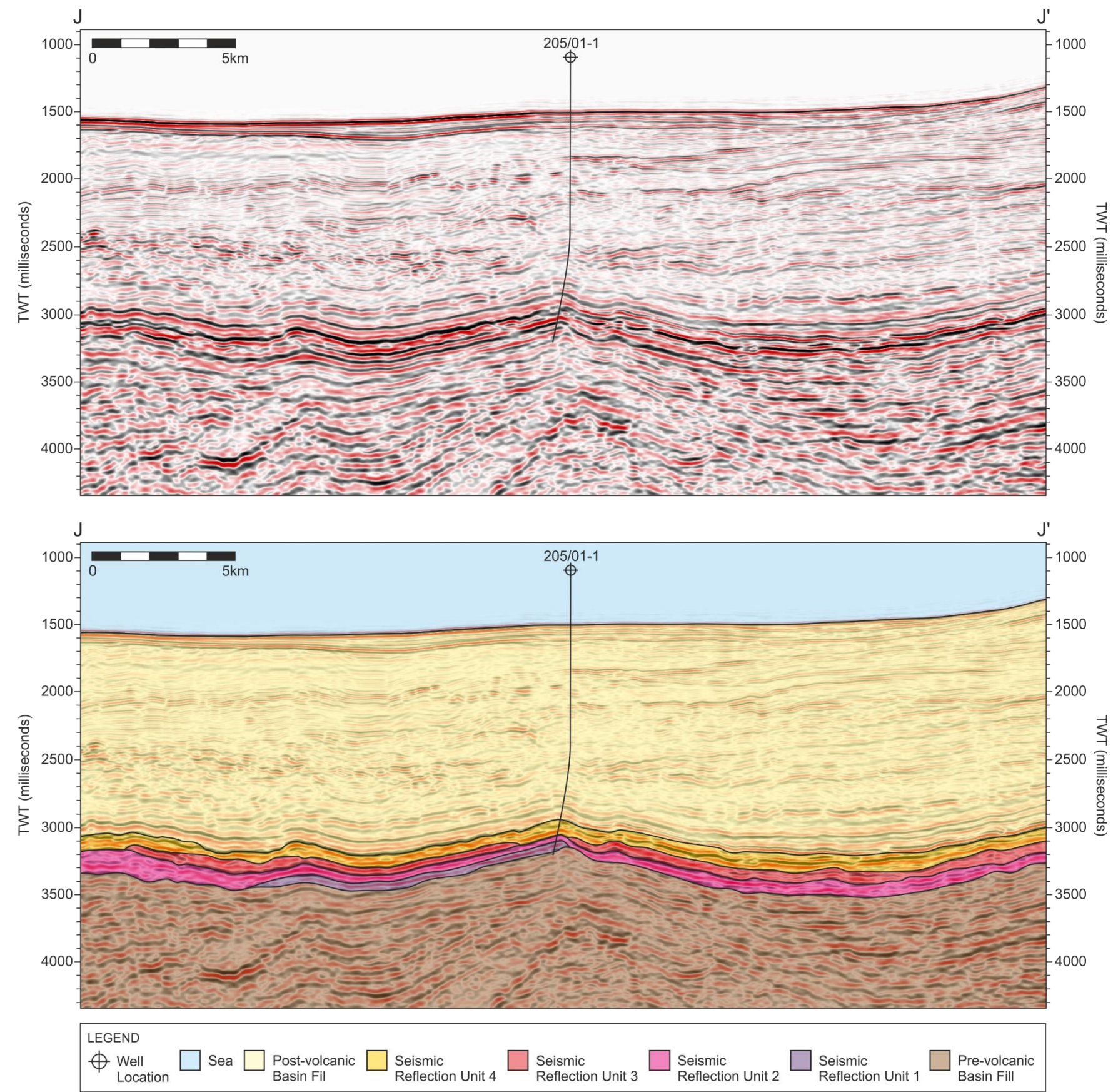
Fig. A3.7. Seismic section J-J' that transects exploration well 205/01-1 and the Rosebank structure. The interpreted section includes the extent of the seismic reflection units as identified in both seismic data and wireline log data. For location see Fig. A3.1.
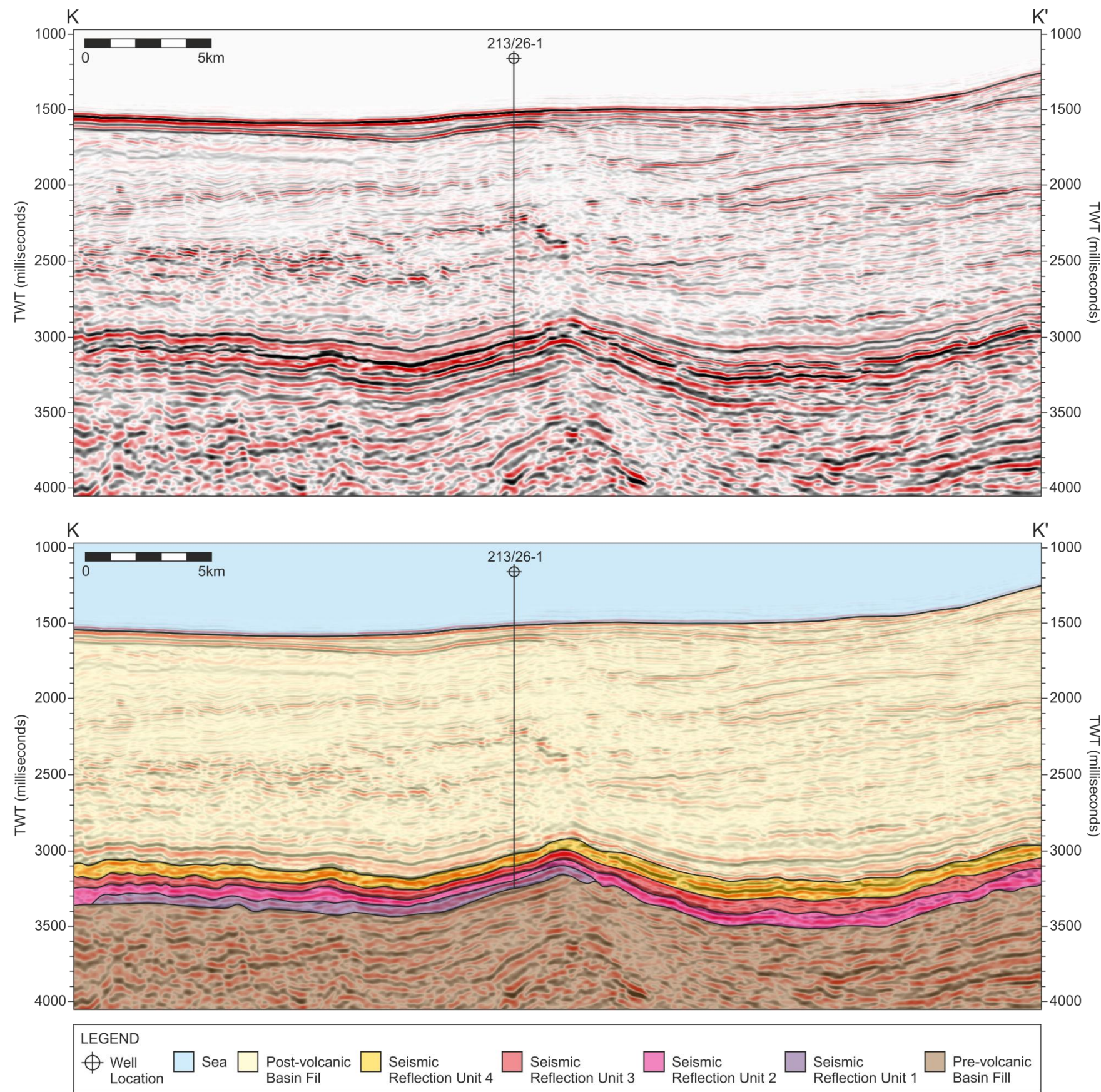
Fig. A3.8. Seismic section K-K' that transects exploration well 213/26-1 and the Rosebank structure. The interpreted section includes the extent of the seismic reflection units as identified in both seismic data and wireline log data. For location see Fig. A3.1.
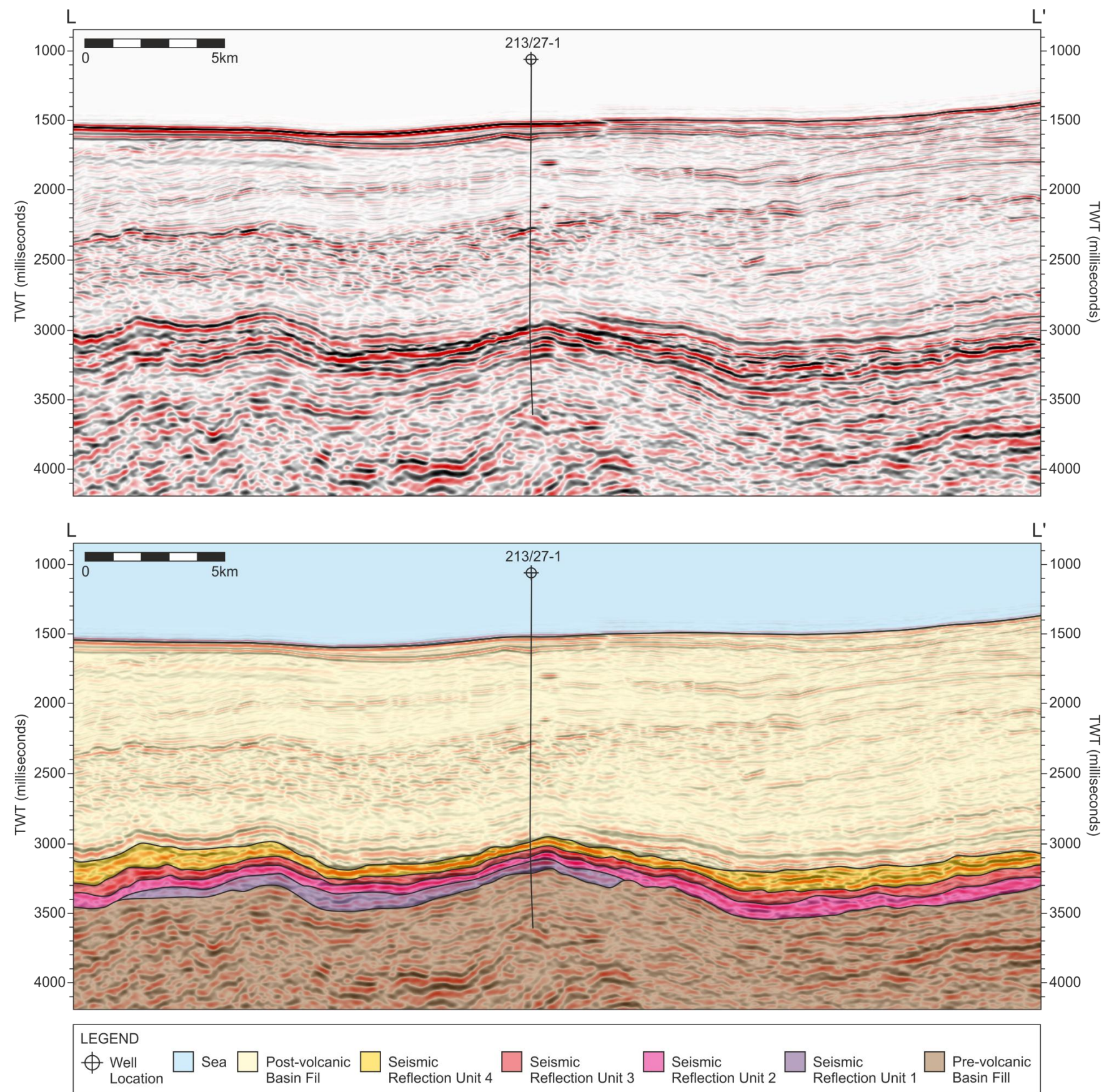
Fig. A3.9. Seismic section L-L' that transects exploration well 213/27-1 and the Rosebank structure. The interpreted section includes the extent of the seismic reflection units as identified in both seismic data and wireline log data. For location see Fig. A3.1.
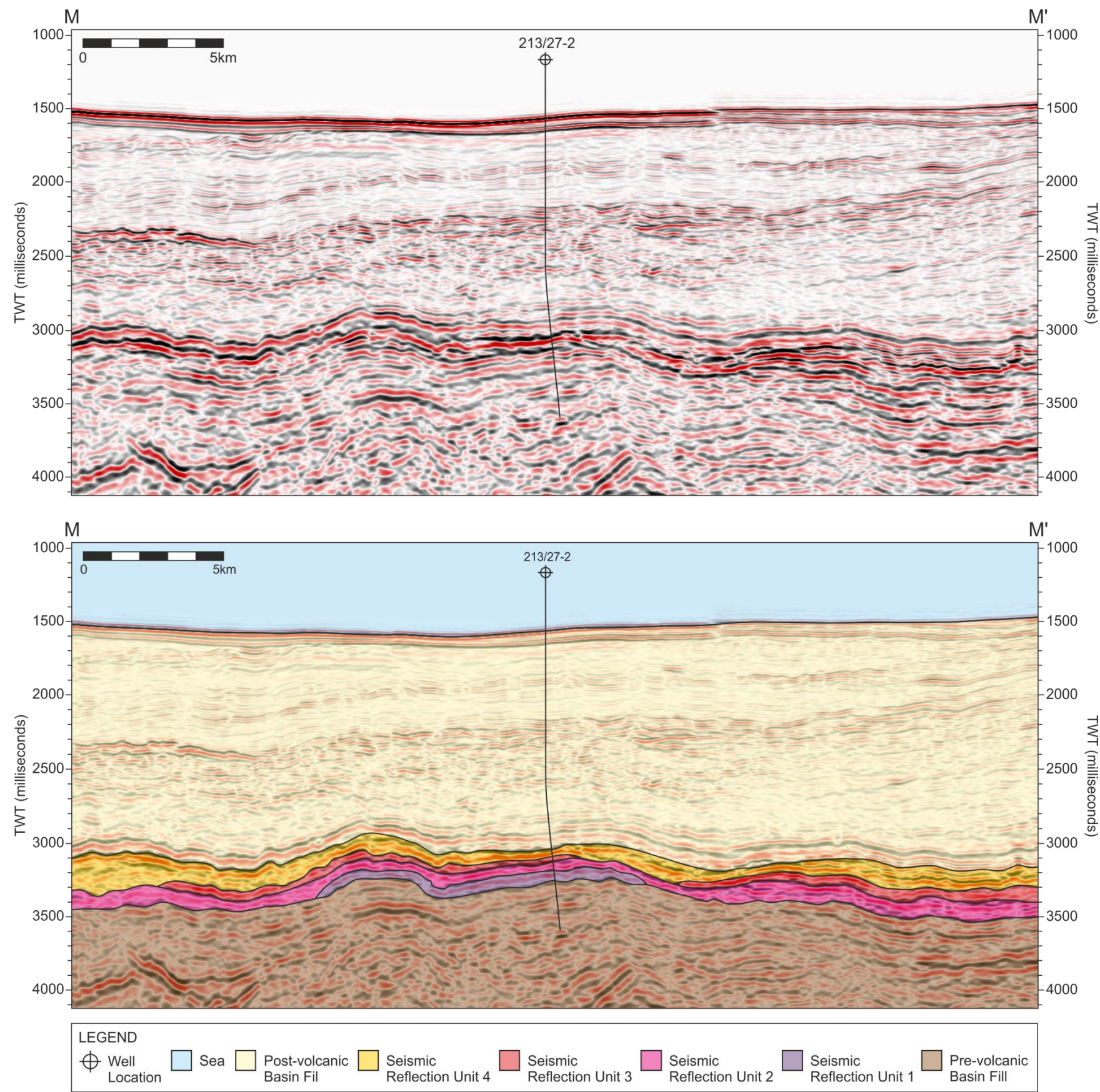
Fig. A3.10. Seismic section M-M' that transects exploration well 213/27-2 and the Rosebank structure. The interpreted section includes the extent of the seismic reflection units as identified in both seismic data and wireline log data. For location see Fig. A3.1.
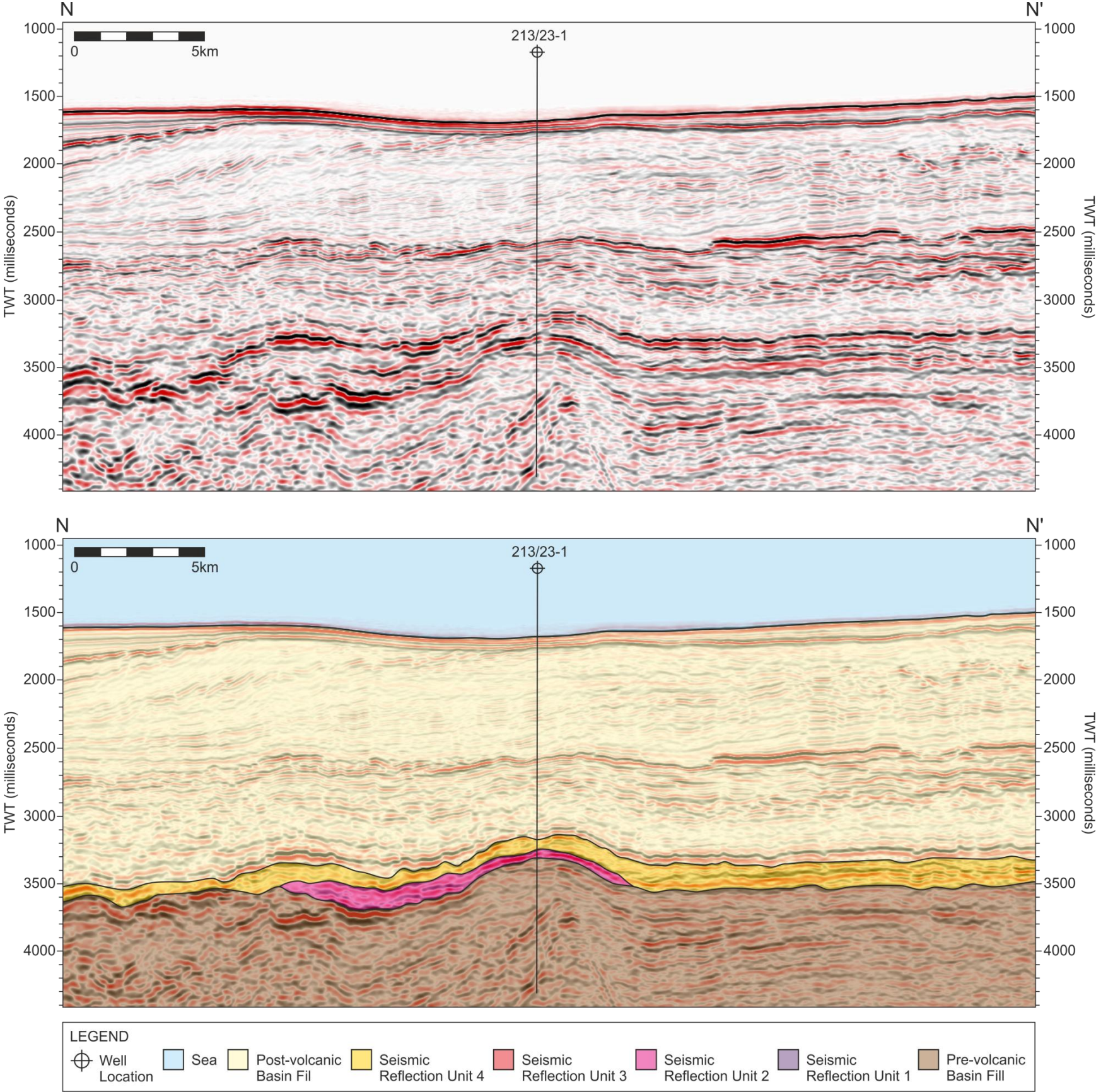
Fig. A3.11. Seismic section N-N' that transects exploration well 213/23-1 and the Rosebank structure. The interpreted section includes the extent of the seismic reflection units as identified in both seismic data and wireline log data. For location see Fig. A3.1.
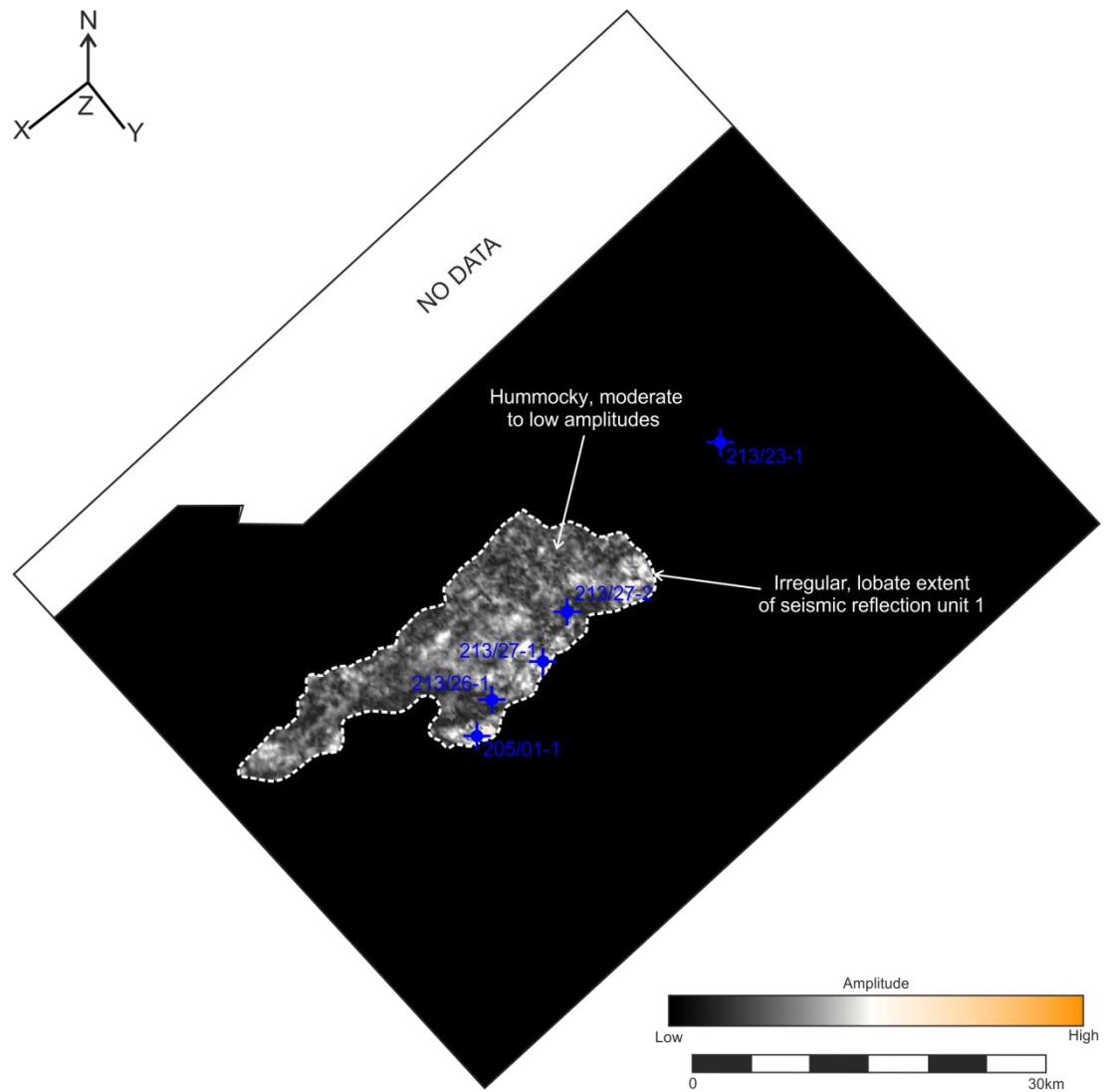
Fig. A3.12. RMS amplitude extraction map with a 5 millisecond window over the top of seismic reflection unit 1, with extent of seismic reflection unit and position of exploration wells identified. For location of 3D survey see Chapter 6.
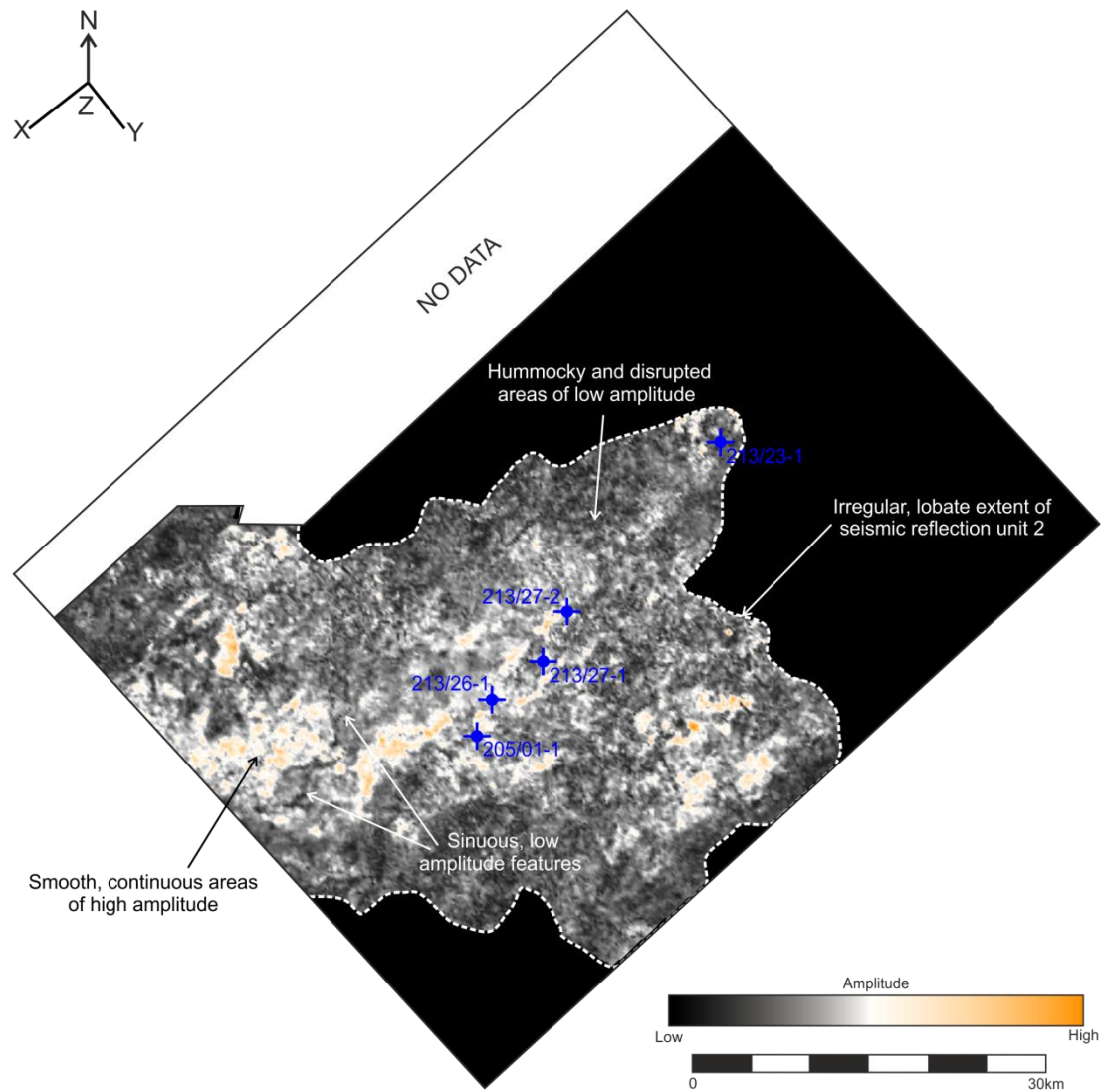
Fig. A3.13. RMS amplitude extraction map with a 5 millisecond window over the top of seismic reflection unit 2, with extent of seismic reflection unit and position of exploration wells identified. For location of 3D survey see Chapter 6.
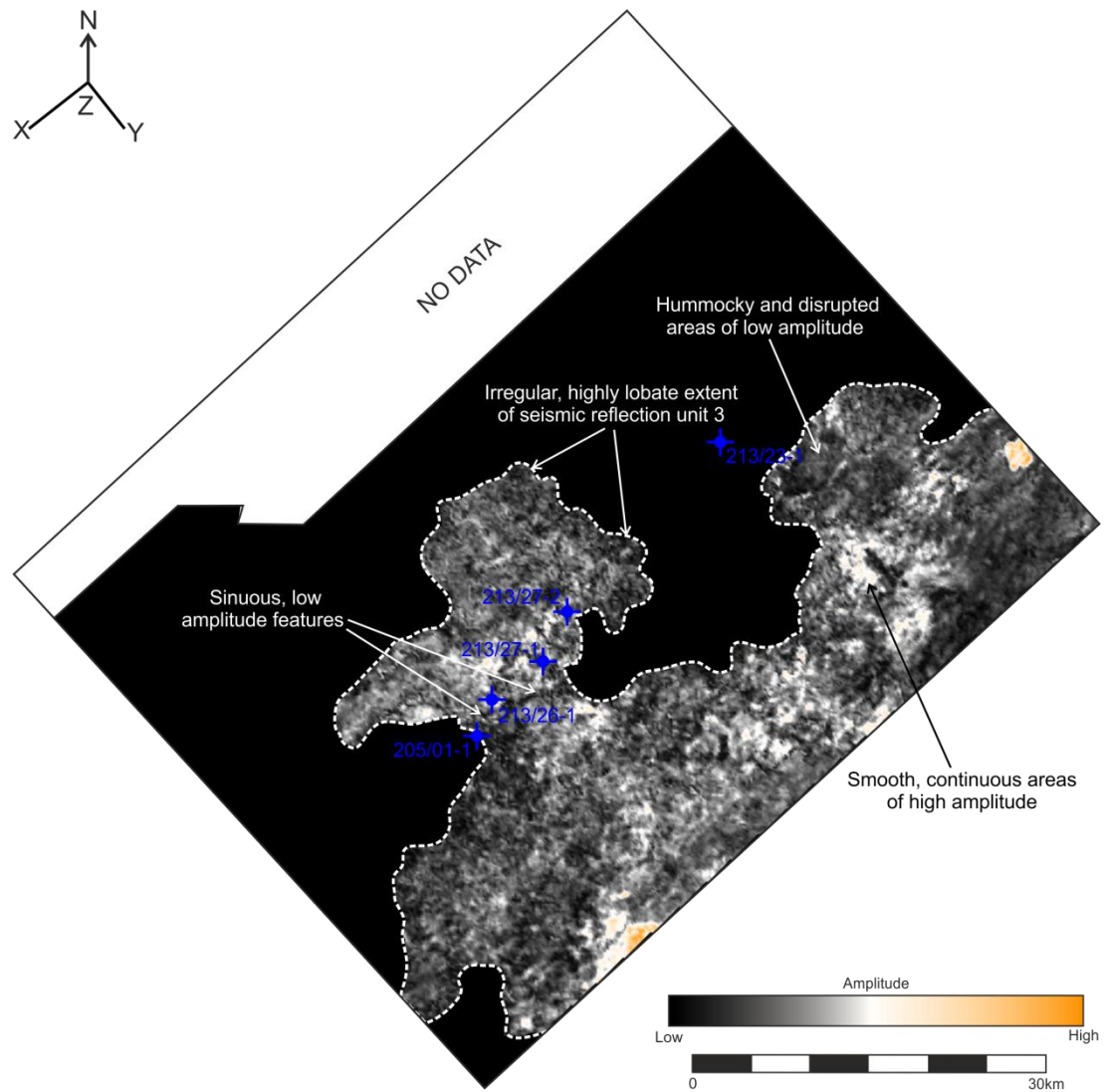
Fig. A3.14. RMS amplitude extraction map with a 5 millisecond window over the top of seismic reflection unit 3, with extent of seismic reflection unit and position of exploration wells identified. For location of 3D survey see Chapter 6.
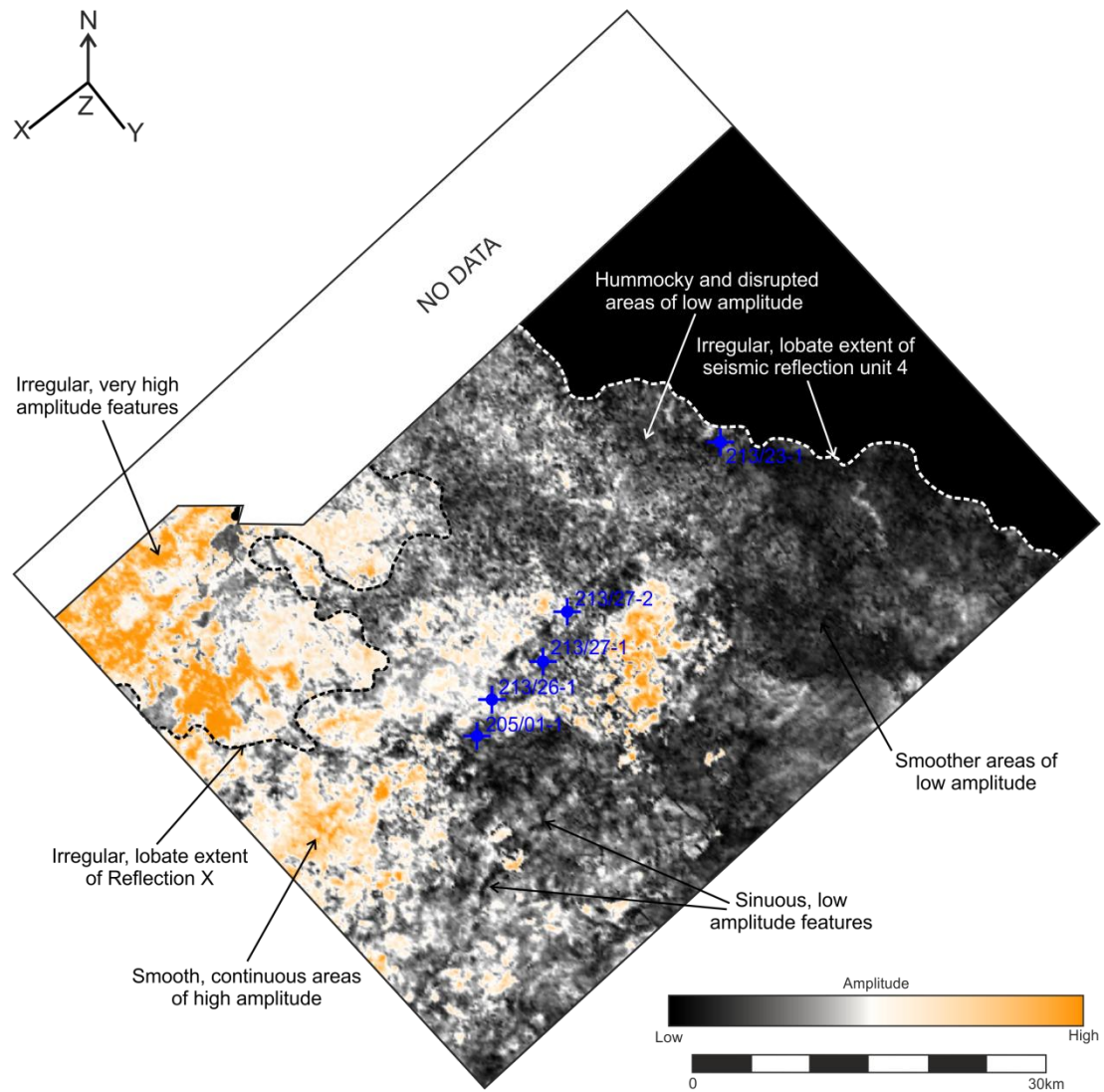
Fig. A3.15. RMS amplitude extraction map with a 5 millisecond window over the top of seismic reflection unit 4 and reflection X, with extent of seismic reflection unit, the extent of reflection X and position of exploration wells identified. For location of 3D survey see Chapter 6.
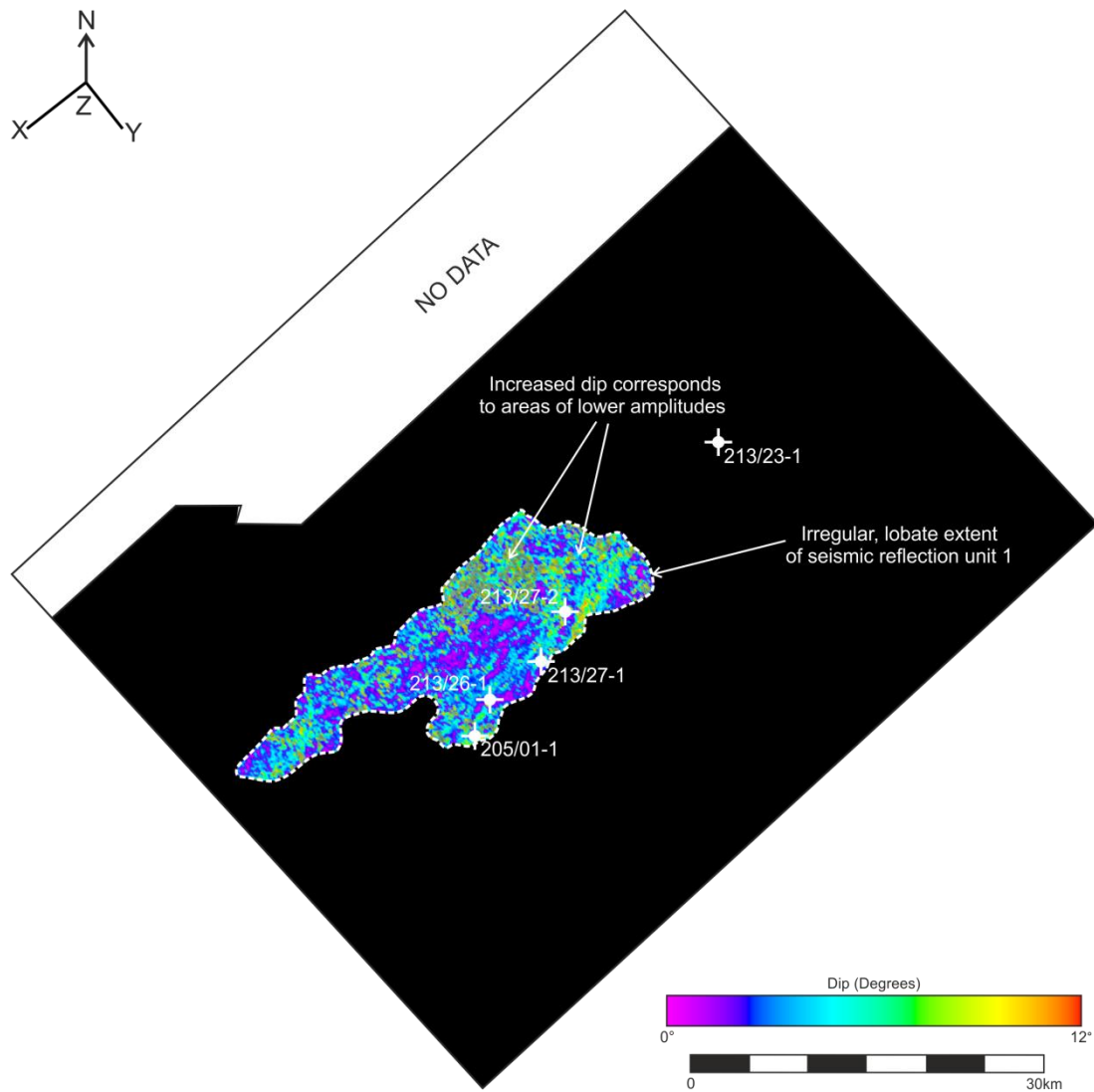
Fig. A3.16. Dip map with a 5 millisecond window over the top of seismic reflection unit 1, with extent of seismic reflection unit and position of exploration wells identified. Amount of dip gradually increases where the unit onlaps the underlying structure. For location of 3D survey see Chapter 6.
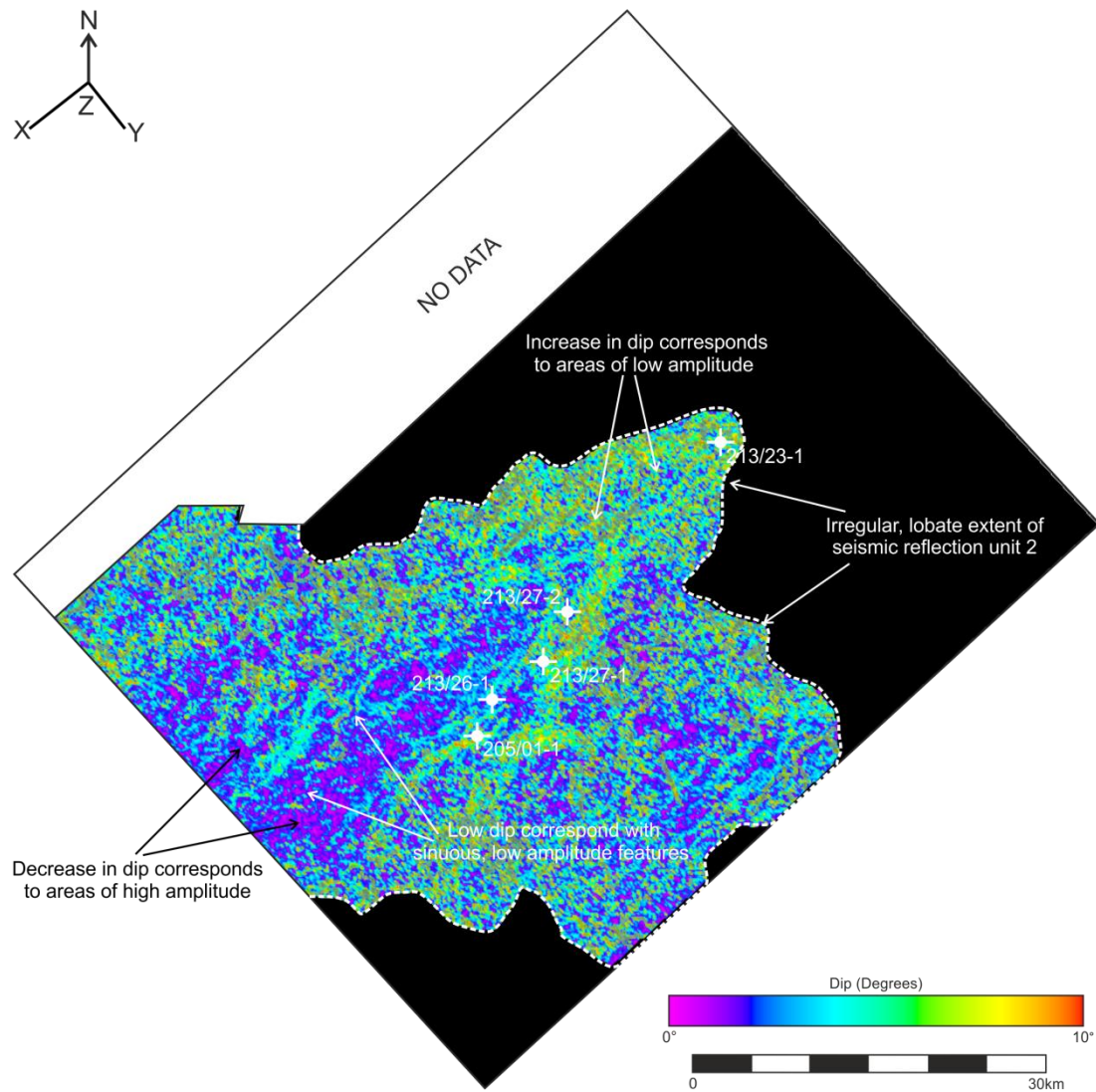
Fig. A3.17. Dip map with a 5 millisecond window over the top of seismic reflection unit 2, with extent of seismic reflection unit and position of exploration wells identified. Highest dips recognised at edges of areas of high amplitudes. For location of 3D survey see Chapter 6.
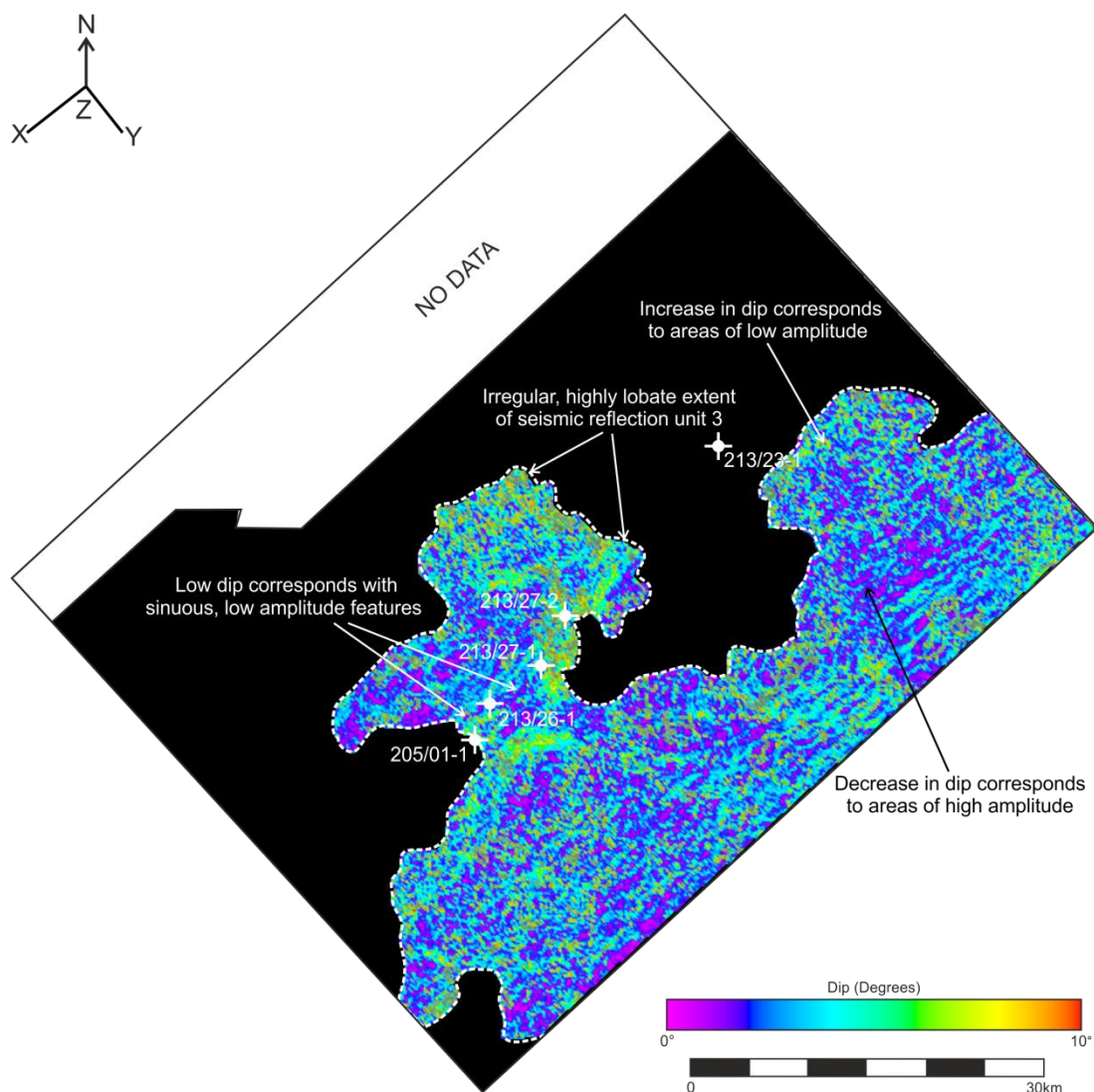
Fig. A3.18. Dip map with a 5 millisecond window over the top of seismic reflection unit 2, with extent of seismic reflection unit and position of exploration wells identified. Highest dips recognised at edges of areas of high amplitudes. For location of 3D survey see Chapter 6.
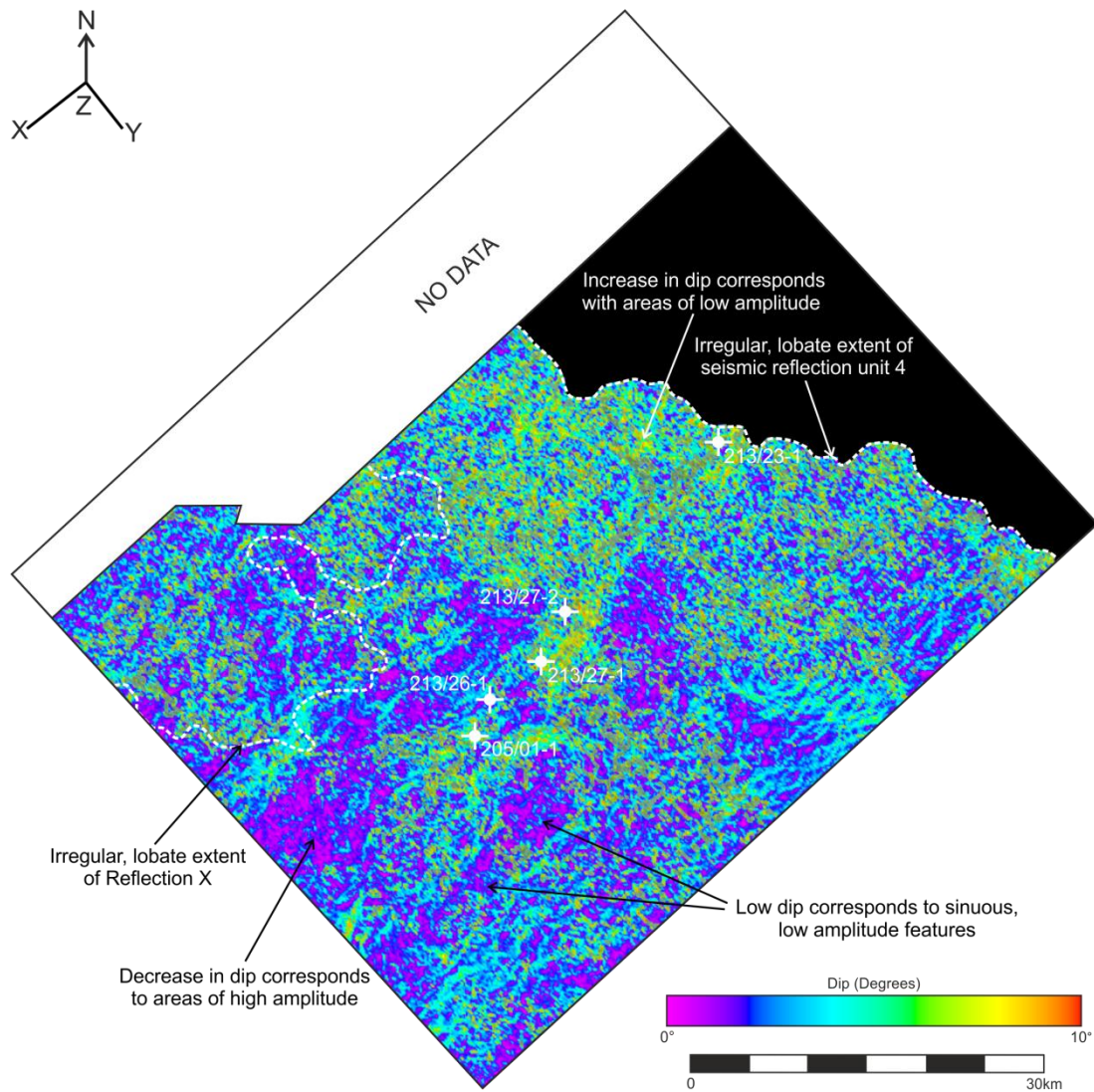
Fig. A3.19. Dip map with a 5 millisecond window over the top of seismic reflection unit 4 and reflection X, with extent of seismic reflection unit, the extent of reflection X and position of exploration wells identified. Highest dips recognised at edges of areas of high amplitudes. For location of 3D survey see Chapter 6.
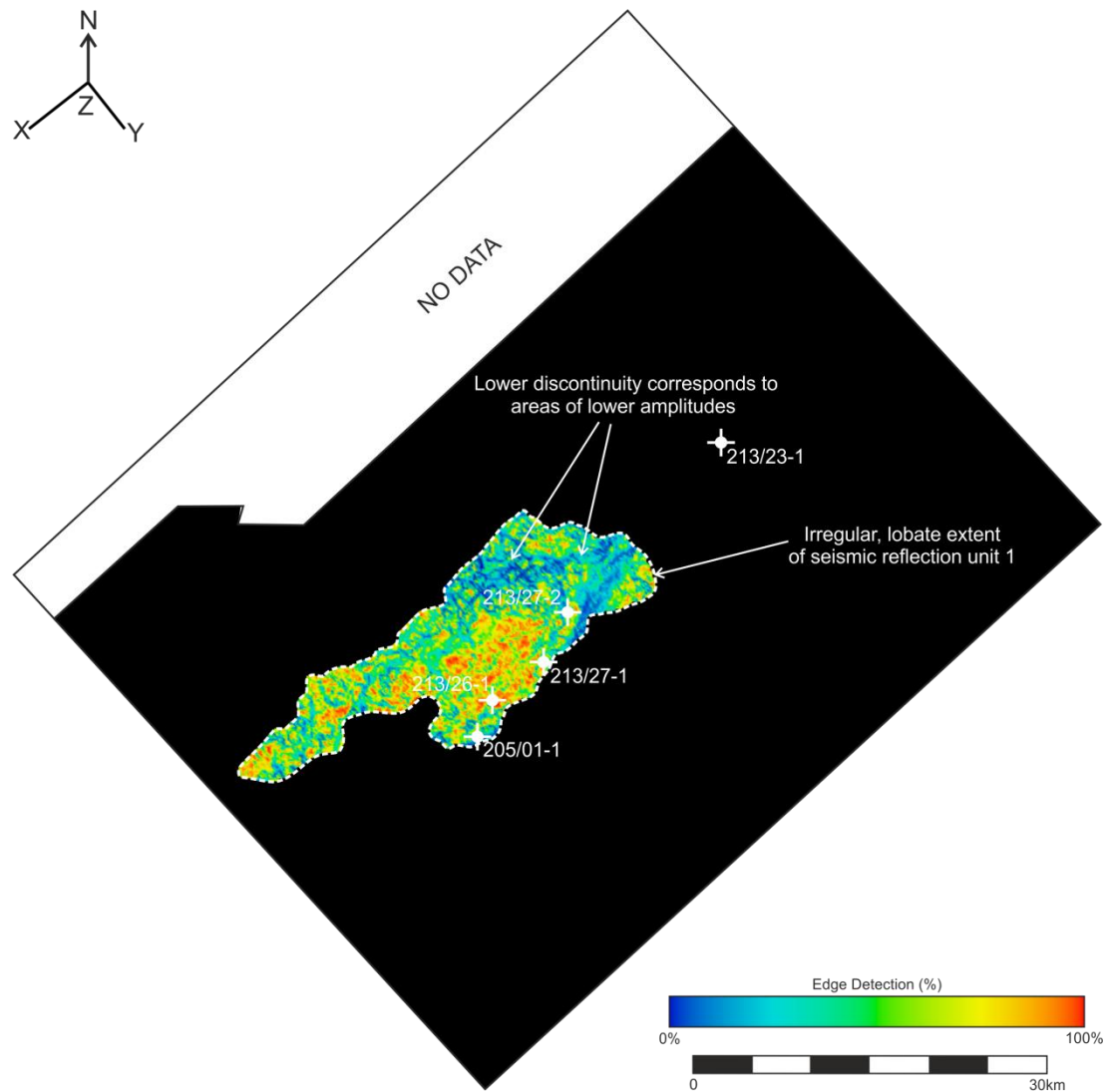
Fig. A3.20. Edge detection map with a 5 millisecond window over the top of seismic reflection unit 1, with extent of seismic reflection unit and position of exploration wells identified. For location of 3D survey see Chapter 6.
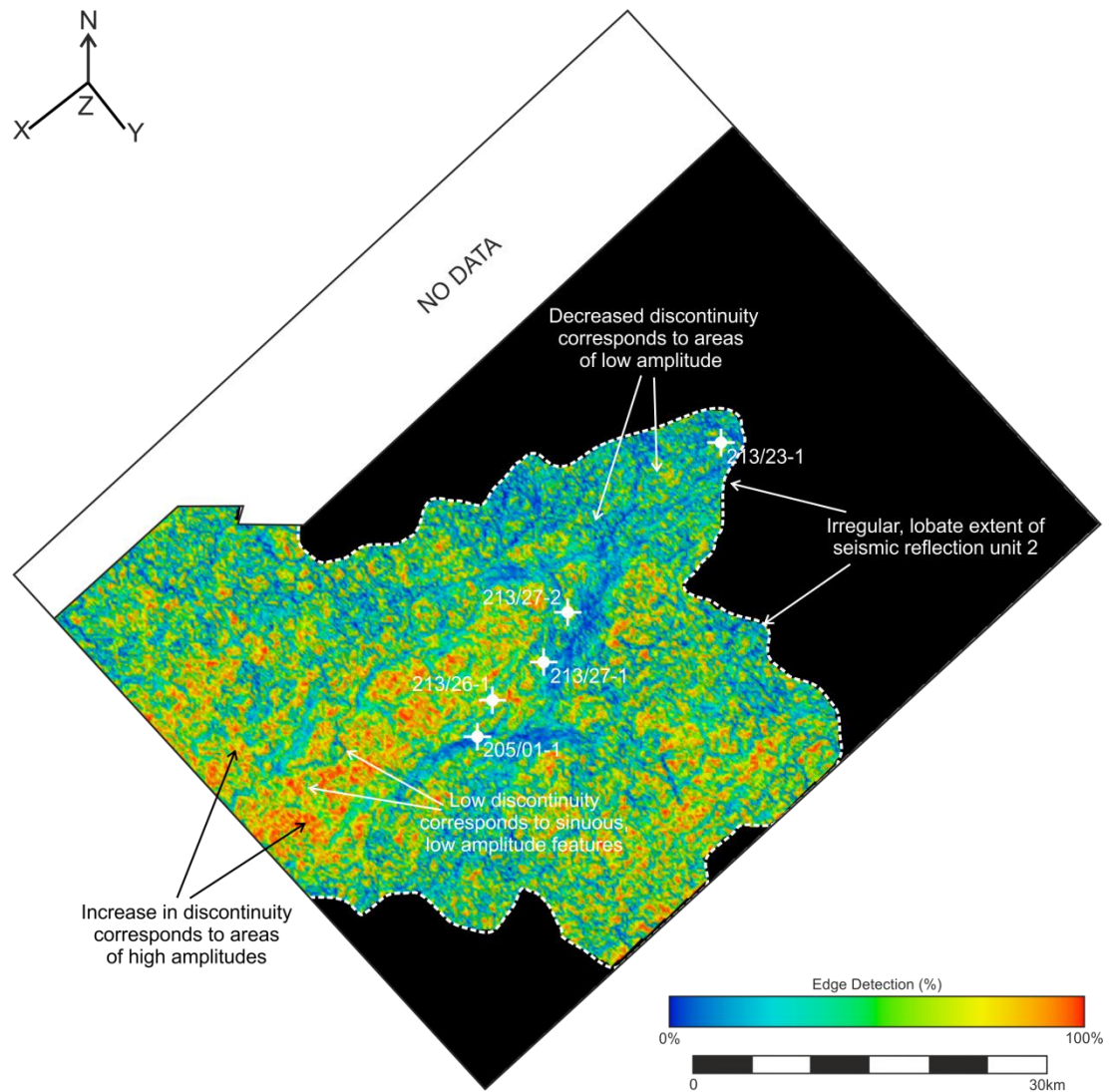
Fig. A3.21. Edge detection map with a 5 millisecond window over the top of seismic reflection unit 2, with extent of seismic reflection unit and position of exploration wells identified. Highest discontinuities correspond to areas of high amplitudes. For location of 3D survey see Chapter 6.
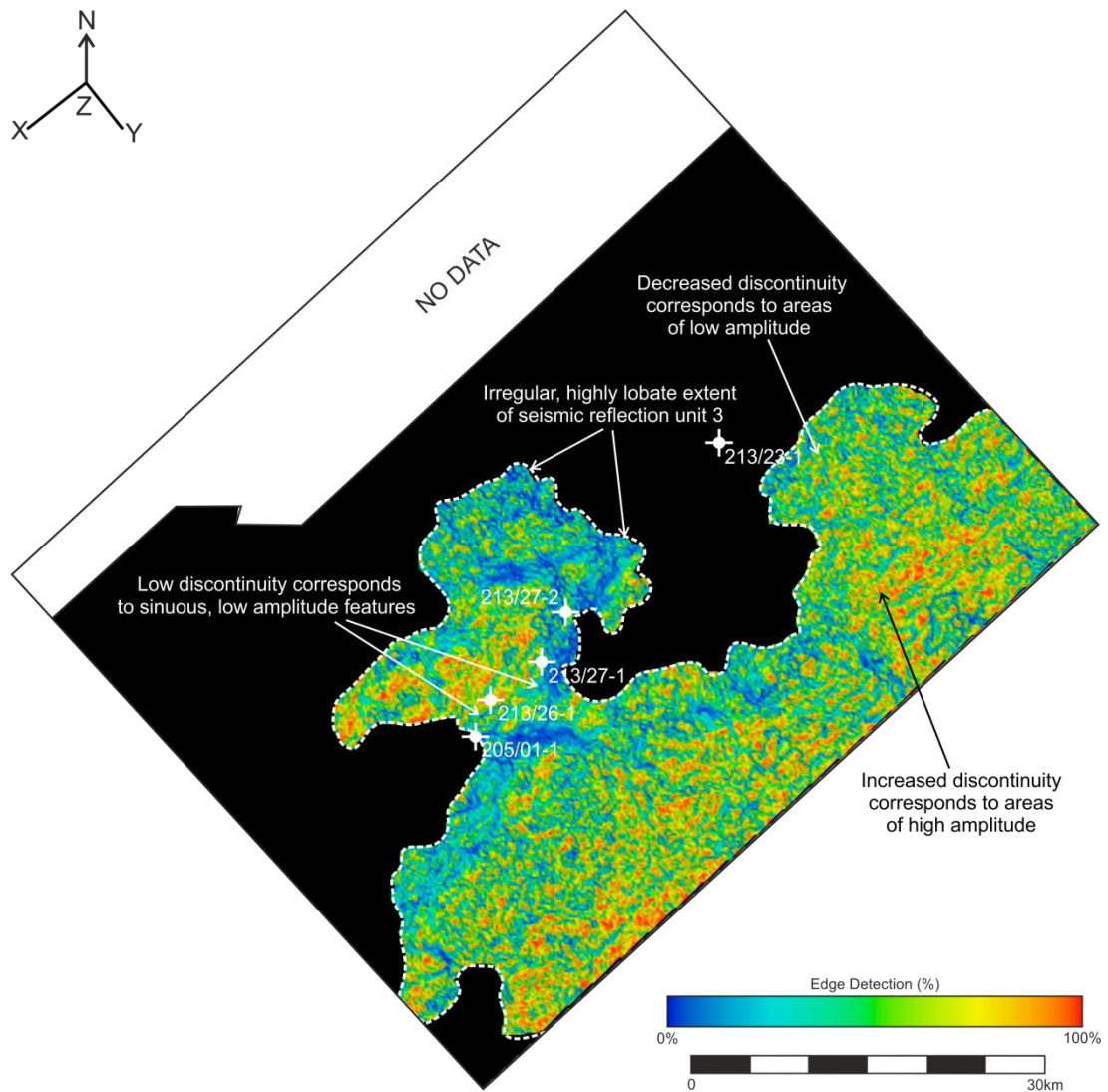
Fig. A3.22. Edge detection map with a 5 millisecond window over the top of seismic reflection unit 3, with extent of seismic reflection unit and position of exploration wells identified. Highest discontinuities correspond to areas of high amplitudes. For location of 3D survey see Chapter 6.
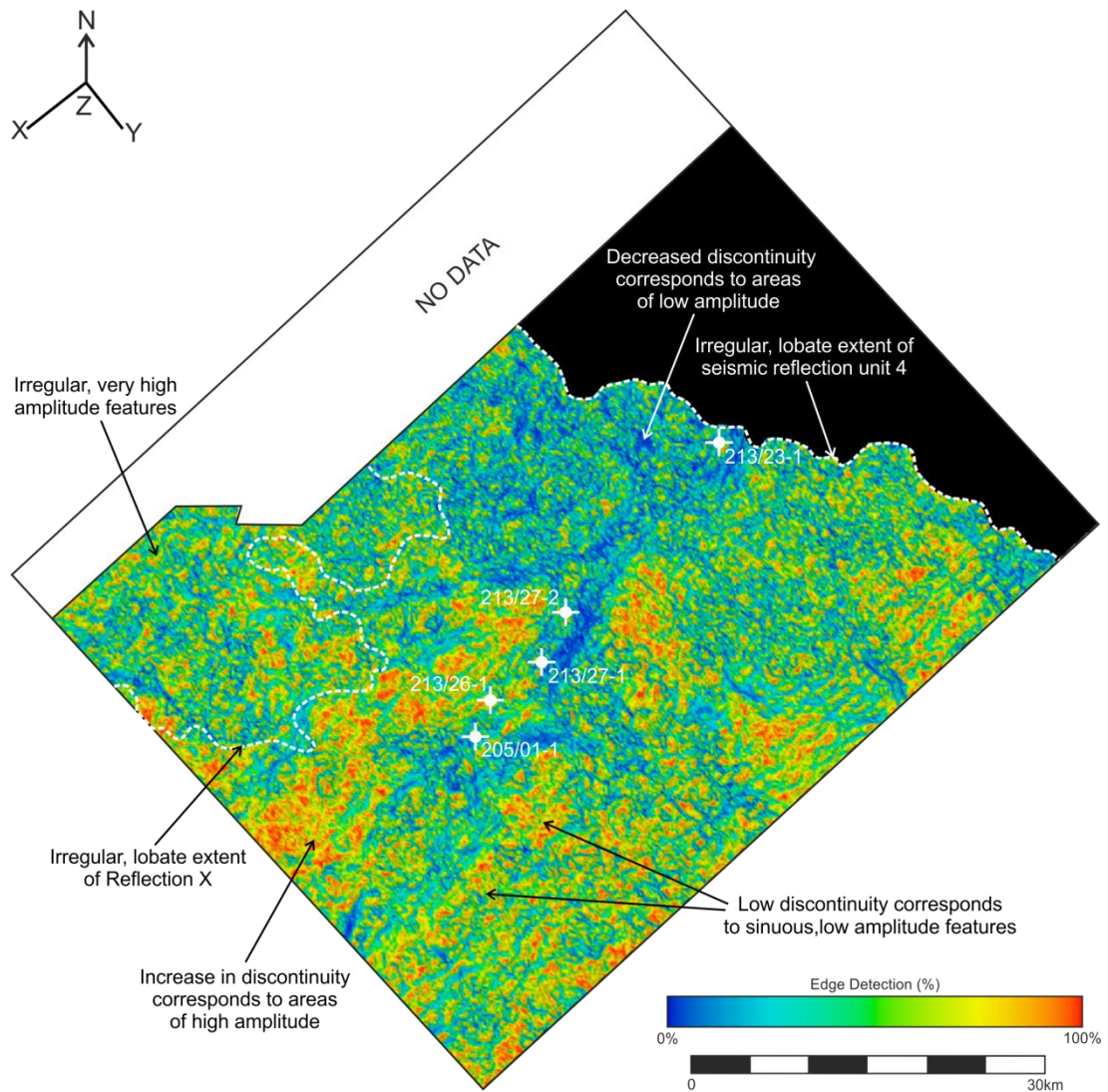
Fig. A3.23. Edge detection map with a 5 millisecond window over the top of seismic reflection unit 4 and reflection X, with extent of seismic reflection unit, the extent of reflection X and position of exploration wells identified. Highest discontinuities correspond to areas of high amplitudes. For location of 3D survey see Chapter 6.

APPENDIX IV: PUBLISHED JOURNAL ARTICLES

This appendix contains published journal articles from this thesis. Chapter 4 has been published as;

Wright, K.A., Davies, R.J., Jerram, D.A., Morris, J. and Fletcher, R. (2012). Application of Seismic and Sequence Stratigraphic Concepts to a Lava-fed Delta System in the Faroe-Shetland Basin, UK and Faroes. *Basin Research*, 24 (1), 91-106.

Application of seismic and sequence stratigraphic concepts to a lava-fed delta system in the Faroe-Shetland Basin, UK and Faroes

K. A. Wright*, R. J. Davies*, D. A. Jerram[‡], J. Morris[†] and R. Fletcher[†]

Centre for Research into Earth Energy Systems (CeREES), Department of Earth Sciences, Durham University, Durham, UK
[†]*Statoil UK Limited, London, UK*
[‡]*Dougalearth Ltd, 12 Nevilles Cross Villas, Durham DH1 4JR, UK*

ABSTRACT

Detailed seismic stratigraphic analysis of 2D seismic data over the Faroe-Shetland Escarpment has identified 13 seismic reflection units that record lava-fed delta deposition during discrete periods of volcanism. Deposition was dominated by progradation, during which the time shoreline migrated a maximum distance of ~44 km in an ESE direction. Localised collapse of the delta front followed the end of progradation, as a decrease in volcanic activity left the delta unstable. Comparison with modern lava-fed delta systems on Hawaii suggests that syn-volcanic subsidence is a potential mechanism for apparent relative sea level rise and creation of new accommodation space during lava-fed delta deposition. After the main phase of progradation, retrogradation of the delta occurred during a basinwide syn-volcanic relative sea level rise where the shoreline migrated a maximum distance of ~75 km in a NNW direction. This rise in relative sea level was of the order of 175–200 m, and was followed by the progradation of smaller, perched lava-fed deltas into the newly created accommodation space. Active delta deposition and the emplacement of lava flows feeding the delta front lasted ~2600 years, although the total duration of the lava-fed delta system, including pauses between eruptions, may have been much longer.

INTRODUCTION

Seismic reflection imagery of sedimentary basins has resulted in the recognition of specific reflection configurations and reflection discordances that have informed the reconstruction of relative sea level changes and an understanding of basin fill histories (e.g. Payton, 1977; Wilgus *et al.*, 1988). The seismic reflection method was initially applied to siliciclastic (e.g. Vail *et al.*, 1977; Posamentier & Vail, 1988) and then carbonate successions (e.g. Bubb & Hatlelid, 1977; Sarg, 1988), and more recently to volcanic rifted margins (e.g. Spitzer *et al.*, 2008; Jerram *et al.*, 2009; Ellefsen *et al.*, 2010). Growing interest in exploration and production of hydrocarbons from offshore successions with a volcanic component has resulted in seismic data being acquired over such areas, including the Møre and Vøring Basins (offshore Norway) and the Faroe-Shetland Basin (UK and Faroes).

Significant volumes of flood basalts were erupted in subaerial to submarine settings in the North Atlantic Region during the Late Palaeocene (e.g. Ellis *et al.*, 2002;

Jerram *et al.*, 2009). The volcanic succession displays a variety of reflection configurations that are indicative of depositional environment and subsequent mass transport. These include parallel bedded reflections that are interpreted to be subaerially erupted plateau lava flows (Boldreel & Andersen, 1994). In contrast, seaward dipping reflections exhibit inclined, smooth to hummocky geometries and are interpreted to be subaerial to shallow submarine lava flows erupted during the early stages of sea floor spreading. They erupted close to, or on the axis of spreading and were later affected by post-rift subsidence, with the greatest inclination seen in the oldest lava flows (Andersen, 1988; Planke *et al.*, 2000; Parkin *et al.*, 2007). Prograding reflections with a steeper inclination ($>20°$) are interpreted to be subaerially erupted lava flows entering the sea, forming steep delta escarpments of hyaloclastic breccias (Smythe *et al.*, 1983; Kiørboe, 1999; Spitzer *et al.*, 2008).

Lava-fed deltas preserve the transition from subaerial to submarine strata, and are a record of the palaeo-shoreline. They often display similarities to siliciclastic delta systems, by filling available accommodation space, reacting to changes in relative sea level and variations in the supply of material (Fig. 1) (Jones & Nelson, 1970; Moore *et al.*, 1973; Jerram *et al.*, 2009). This has led to comparisons of lava-fed deltas with Gilbert-type siliciclastic deltas and

Fig. 1. Schematic cross-section through a developing lava-fed delta. Based on this study, Fuller (1931) and Jones & Nelson (1970).

the identification of comparable facies components (Fuller, 1931; Jones & Nelson, 1970; Porebski & Gradzinski, 1990; Naylor *et al.*, 1999). However, lava-fed delta systems, particularly those formed during flood basalt eruptions, record variations in the supply of volcanic material, which can be much greater than in siliciclastic systems. Huge volumes of lava erupt over geologically short timescales, resulting in the very efficient filling of accommodation space and rapid progradation of the shoreline.

Modern examples of lava flowing into the sea (such as seen on Hawaii), undergo quenching and fragmentation into hyaloclastic breccias which are then rapidly deposited down slope under gravitational processes to form inclined foresets (Kokelarr, 1986; Fisher & Schmincke, 1994). The growth of the delta is through deposition of new lava flows and hyaloclastic breccias, with successive phases of volcanism producing a stacking pattern that is directly related to the interaction of relative sea level, lava supply and available accommodation space. The geometry of the stacking pattern depends on the dominant factor at the time of deposition, making it possible to reconstruct the depositional environment and interpreted the lava-fed delta within a sequence stratigraphic framework (Jones & Nelson, 1970; Gatliff *et al.*, 1984; Kiørboe, 1999).

This paper investigates in detail the reflection geometries of the Faroe-Shetland Escarpment and the applicability of seismic and sequence stratigraphy to define a series of volcanic units that can be interpreted in terms of relative sea level, lava supply and available accommodation space. Understanding how flood basalts develop from a subaerial to submarine environment and the identification of key horizons within the volcanic succession can be used to investigate the onset, development and closing stages of flood basalt volcanism (e.g. Jerram & Widdowson, 2005). It can constrain the spatial and temporal distribution of key volcanic facies (Nelson *et al.*, 2009) and be a valuable resource for exploration in volcanic rifted settings. This allows us to reconstruct in detail the development and evolution of Faroe-Shetland Escarpment and how the palaeo-shore line evolved due to flood volcanism during the break-up of Europe from North America.

GEOLOGICAL SETTING

The Faroe-Shetland Basin is a product of North Atlantic rifting between Greenland and Eurasia during the Mesozoic to early Cenozoic (England *et al.*, 2005; Passey & Bell,

2007). Continental break-up and the onset of seafloor spreading were accompanied by extensive flood basalt volcanism. The main phase of volcanism occurred during the Palaeocene, at 62–54 Ma (e.g. Ritchie & Hitchen, 1996; Hansen *et al.*, 2009; Søager & Holm, 2009) and is characterised by the extrusion of subaerial basaltic lavas (e.g. Passey & Bell, 2007), the intrusion of sills (e.g. Thomson & Schofield, 2008; Hansen *et al.*, 2011) and the formation of individual igneous centres, such as the Erlend Complex and Brendans Dome (e.g. Gatliff *et al.*, 1984; Ritchie & Hitchen, 1996).

To the east of the Faroe Islands, the Faroe-Shetland Escarpment has been identified as the subaerial extension of the flood basalts, which flowed to the southeast infilling pre-existing topography before reaching the palaeo-shoreline (Smythe *et al.*, 1983; Kiørboe, 1999; Ritchie *et al.*, 1999). At the shoreline, a number of the flood basalt flows entered the water and formed a prograding body of hyaloclastic breccias pushing the shoreline basinward. Initial work has shown that the distribution of these systems or deltas can be extensive, recording a significant syn-volcanic migration of the palaeo-shoreline in this region (e.g. Kiørboe, 1999; Spitzer *et al.*, 2008; Jerram *et al.*, 2009). Volcanism within the basin ceased when sea floor spreading became established to the north of the basin, with post-rift subsidence and late Cenozoic compression creating the tilted and folded structures identified today (Ritchie *et al.*, 2003; Sørensen, 2003; Davies *et al.*, 2004; Praeg *et al.*, 2005).

DATA AND METHODOLOGY

This study has used a variety of 2D seismic reflection surveys gathered within the Faroe-Shetland Basin between 1983 and 2005 with large areas of geographical overlap. The greatest concentration of survey lines is located over Faroe-Shetland Escarpment (Fig. 2) and images the flood basalt succession and contemporaneous deep water strata at an average vertical resolution of 20–30 m. Analysis included detailed mapping of > 60 lines that have an average line spacing between 1 and 3 km. The top surface of the flood basalts throughout the basin is identified by a prominent, high amplitude and strongly continuous reflection (Fig. 3). The strong reflectivity of the top surface and the internal heterogeneity within the volcanic succession presents a challenge for imaging, particularly near the base of the succession (e.g. White *et al.*, 2003; Roberts *et al.*, 2005).

Despite these challenges, seismic amplitudes variations and various reflection geometries have been clearly imaged,
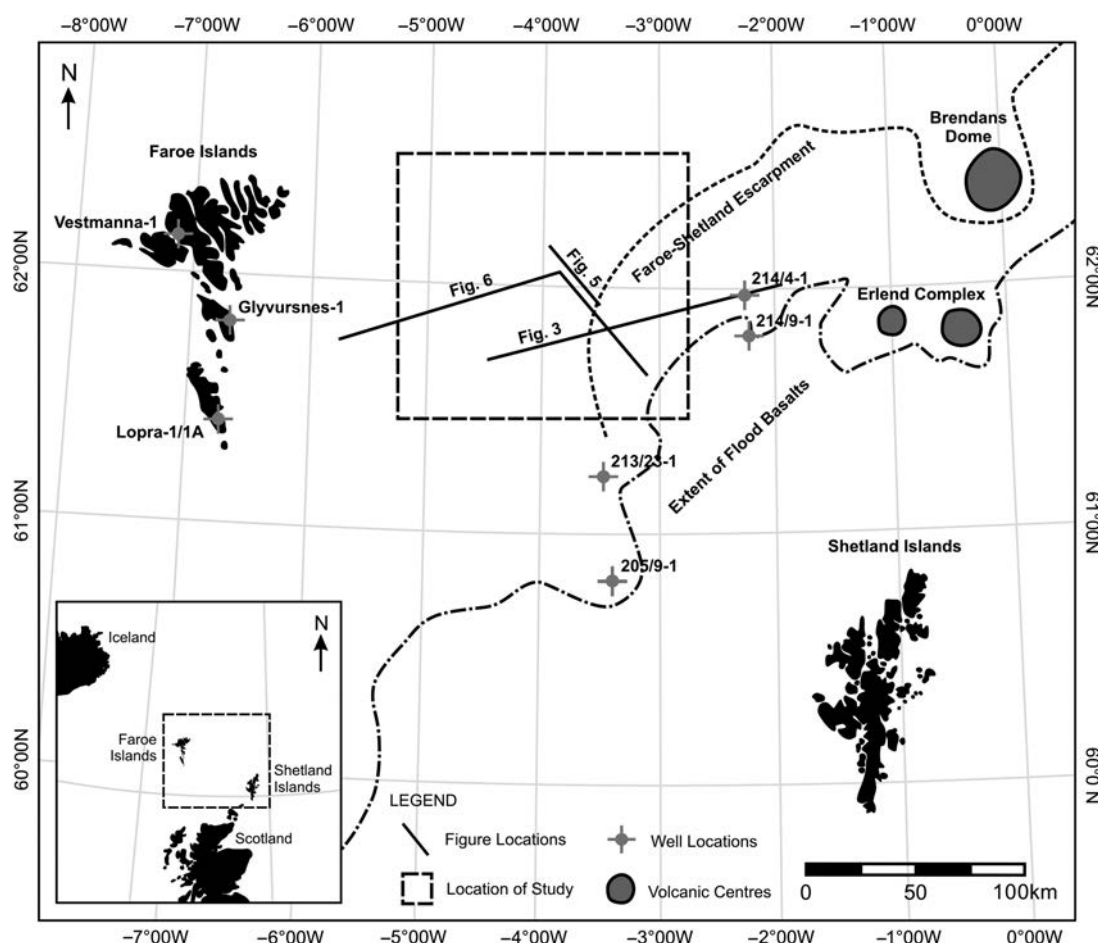
Fig. 2. Map of the Faroe-Shetland Basin showing the study area and location of Figs 3, 5 and 6. Extent of flood basalts and Faroe-Shetland Escarpment modified from Ritchie & Hitchen (1996), Ritchie *et al.* (1999), Ellis *et al.* (2002) and Sørensen (2003).

and with the application of seismic stratigraphy it is possible to define the gross stratigraphic architecture. The recognition of units composed of relatively conformable reflections and bounded by unconformities is through identification of systematic discordances or reflection terminations against the bounding reflection (Mitchum *et al.*, 1977a; Van Wagoner *et al.*, 1988). Additional use of seismic facies analysis with characterisation in terms of amplitude, continuity and configuration can be used to interpret the depositional processes, lithologies and environmental conditions (Mitchum *et al.*, 1977b; Sangree & Widmier, 1977; Cross & Lessenger, 1988).

The majority of wells are located in the south east of the basin, beyond the extent of the Faroe-Shetland Escarpment (Fig. 2), so well control is limited. These wells include 205/9-1 and 213/23-1, which encountered inter-bedded successions of hyaloclastites, lavas and siliciclastic successions of varying thickness (Larsen *et al.*, 1999; Jolley & Morton, 2007). Wells 214/4-1 and 214/9-1 penetrated the most distal flood basalts, with 214/4-1 encountering lava flows overlying a ~1000 m thickness of hyaloclastic breccias, which have been identified to extend some distance beneath the Faroe-Shetland Escarpment (Fig. 3) (Davies *et al.*, 2002).

On the Faroe Islands, the flood basalts have a stratigraphic thickness of at least 6.6 km, which have been sub-

divided into seven formations on the basis of lithology, geochemistry and flow structure (Fig. 4) (Ellis *et al.*, 2002; Passey & Bell, 2007; Jerram *et al.*, 2009). The Lopra Formation is composed of volcaniclastic material thought to have been deposited in an estuarine environment, proximal to the eruption (Ellis *et al.*, 2002; Boldreel, 2006; Passey & Bell, 2007). The Beinisvørð and Malinstindur Formations consist of significant thicknesses of lava with an average flow thickness of 25 and 2 m, respectively. The Enni Formation has thinner, less extensive lava flows with an average flow thickness of 15 m (Ellis *et al.*, 2002; Passey & Bell, 2007; Passey & Jolley, 2009). The Prestfjall, Hvannhagi and Sneis Formations consist of siliciclastic and volcaniclastic interbeds which may record periods of local volcanic quiescence (Passey & Bell, 2007; Jerram *et al.*, 2009).

The onshore volcanic succession is penetrated by three wells, including the Glyvursnes-1 borehole, which reached a depth of 700 m, encountering 450 m of the Malinstindur Formation and 250 m of the Enni Formation (Fig. 4) (Japsen *et al.*, 2004). The Vestmanna-1 borehole, which reached a depth of 660 m, encountered 550 m of the lower part of the Malinstindur Formation and 110 m of the uppermost part of the Beinisvørð Formation (Fig. 4) (Japsen *et al.*, 2004). The oldest flood basalts were penetrated
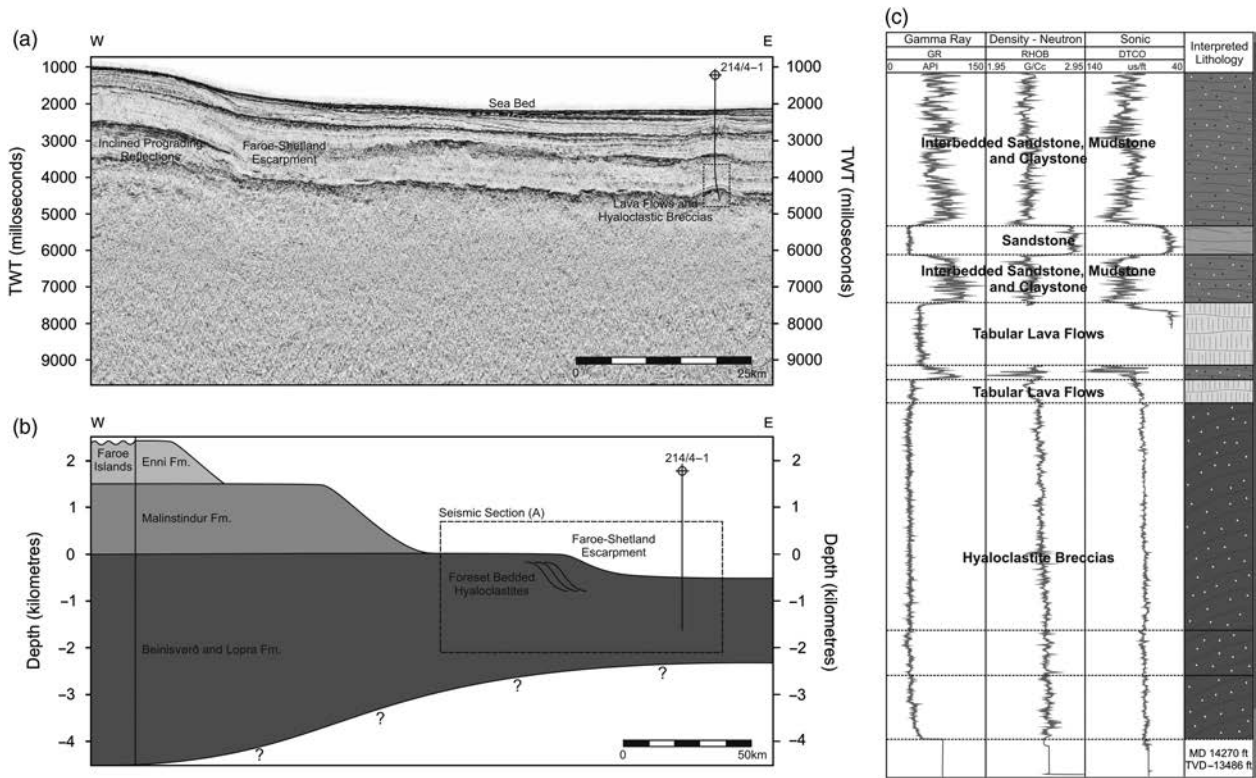
Fig. 3. (a) Regional correlation of seismic reflection configurations and interpreted lithologies identified in well 214/4-1 (see Fig. 2 for location). (b) Schematic correlation of onshore and offshore stratigraphy, modified after Smythe *et al.* (1983) and Ritchie *et al.* (1999). (c) Wireline log responses and interpreted lithologies for the volcanic succession in 214/4-1 (MD, measured depth; TVD, total vertical depth).
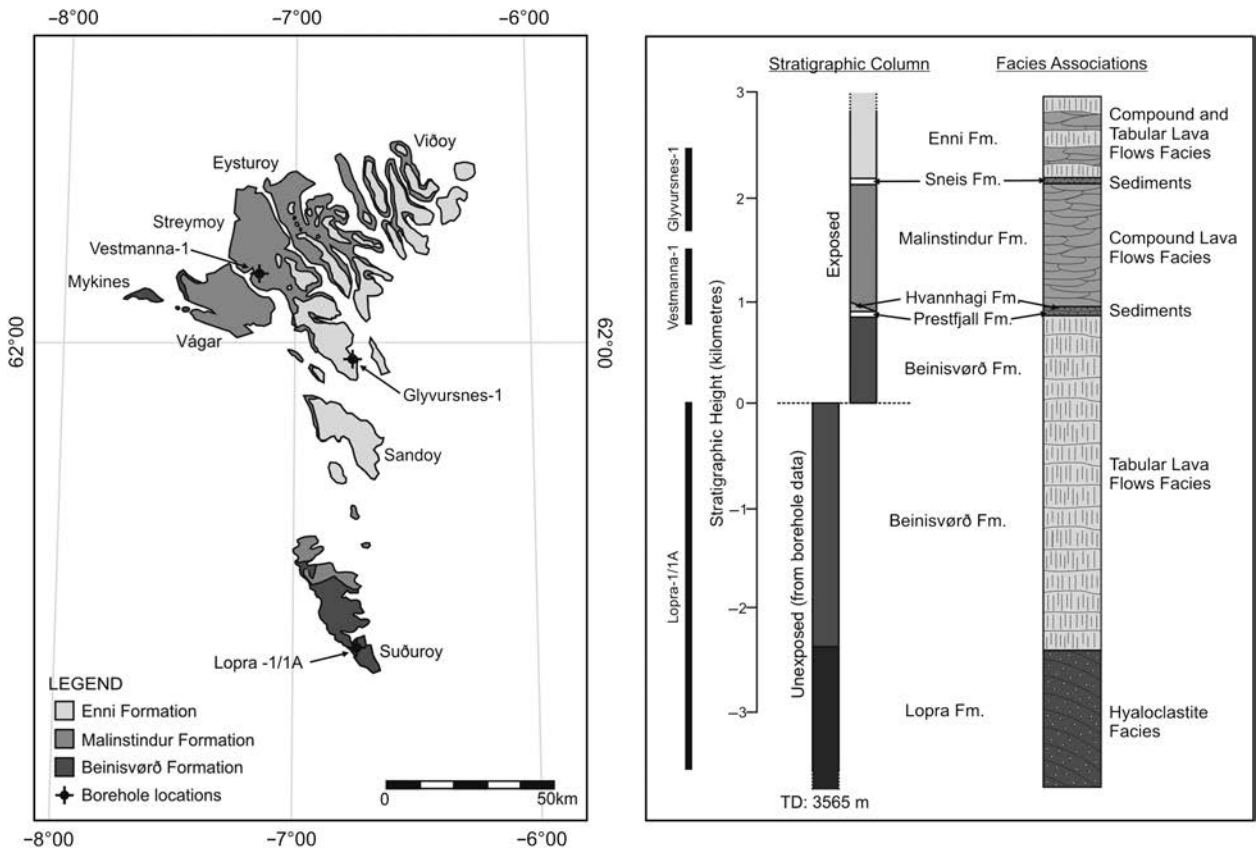
Fig. 4. Distribution of the Faroe Island Basalt Group on the Faroe Islands and stratigraphy compiled from both onshore and borehole data. Modified from Passey & Bell (2007), Jerram *et al.* (2009) and Nelson *et al.* (2009).

by the Lopra-1/1A borehole, which reached a depth of 3.6 km without encountering the base of the volcanic succession. The borehole encountered $> 2500\,m$ of lava flows from the Beinisvørð Formation and $> 1000\,m$ of volcaniclastic material from the Lopra Formation (Fig. 4). The volcanic succession exhibits a variety of velocities which are indicative of the volcanic facies. Tabular lava flows, as identified in the Beinisvørð Formation have high velocities, varying from 4 to $7\,km\,s^{-1}$ with an average of $5.5\,km\,s^{-1}$. Compound lava flows, as identified in the Malinstindur Formation have low velocities, varying between 3 and $6\,km\,s^{-1}$ with an average of $4.5\,km\,s^{-1}$. Hyaloclastite breccias as identified in the Lopra Formation have the lowest velocities, varying between 3 and $5\,km\,s^{-1}$ with an average of $3.5\,km\,s^{-1}$ (Planke, 1994; Boldreel, 2006; Nelson *et al.*, 2009).

OBSERVATIONS

Reflection configuration analysis

The top of the flood basalts is identified by a prominent, high amplitude and strongly continuous reflection that defines the upper limit of a succession of high amplitude, subhorizontal and continuous reflections that decrease in amplitude and continuity with depth (Fig. 5). This succession extends from the Faroes shelf into the Faroe-Shetland Basin, where they rapidly change to inclined, moderate amplitude reflections with the transition marked by a clear offlap break. Basinward of the offlap break, the reflections define units composed of moderate to low amplitude, continuous reflections with prograding, sigmoidal geometries. The reflections often onlap the underlying bounding reflection and vary from downlapping to being terminated by the overlying reflections. The base of each seismic reflection unit is identified by downlap on to deeper reflections (Fig. 5). In total, 13 seismic reflection units with a reflection configuration of high amplitude topsets and low amplitude foresets have been identified (Fig. 6). We have numbered these in stratigraphic order, with 1 being the oldest and 13 being the youngest.

Seismic reflection units 1–11 have a sheet to wedge-like morphology, with heights varying from 700 to 1050 m. The stacking pattern of the units is largely progradational with an aggradational component that becomes increasingly apparent in units 6–11 (Fig. 6). Unit 11 is the most distal
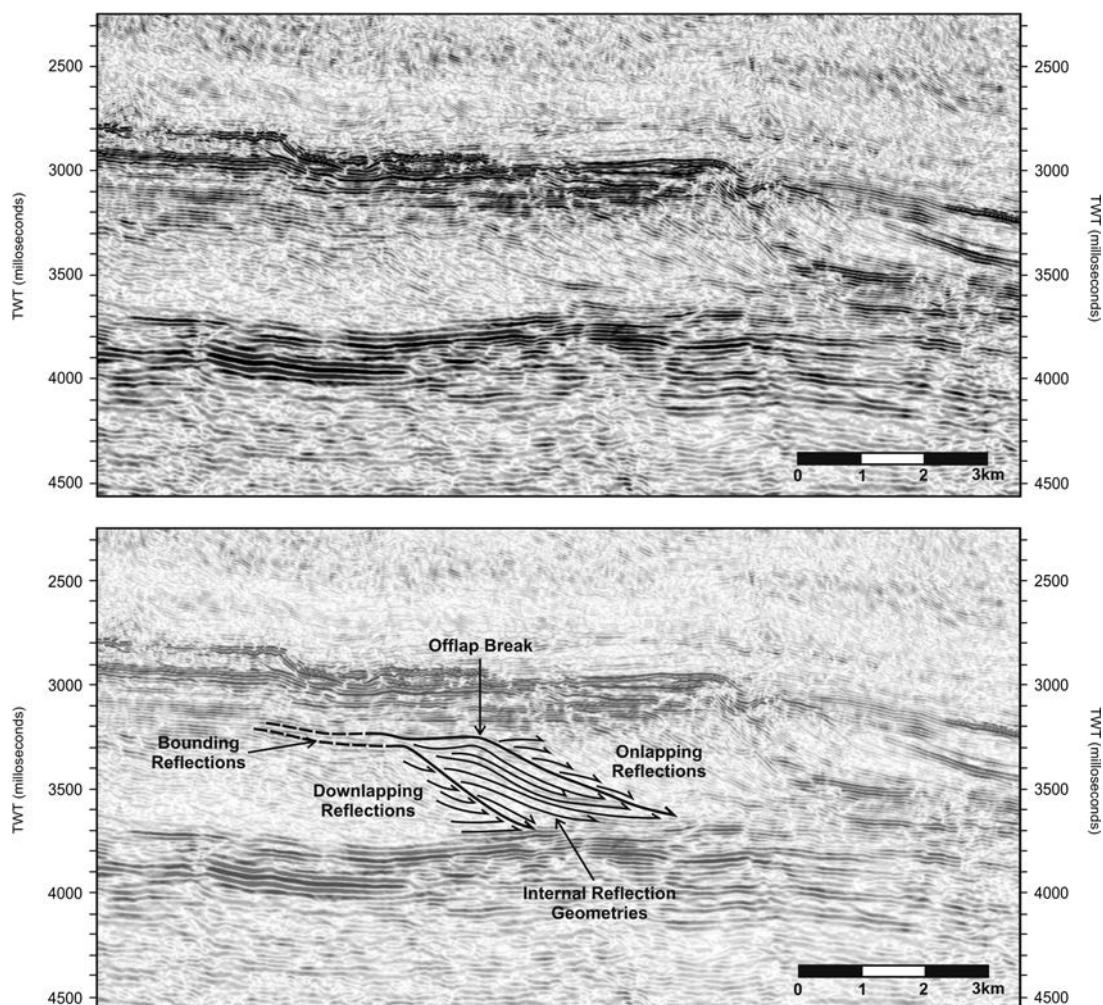
Fig. 5. Seismic stratigraphic methodology used to identify seismic reflection units after Vail *et al.* (1977), Posamentier & Vail (1988) and Kiørboe (1999) (see Fig. 2 for location).
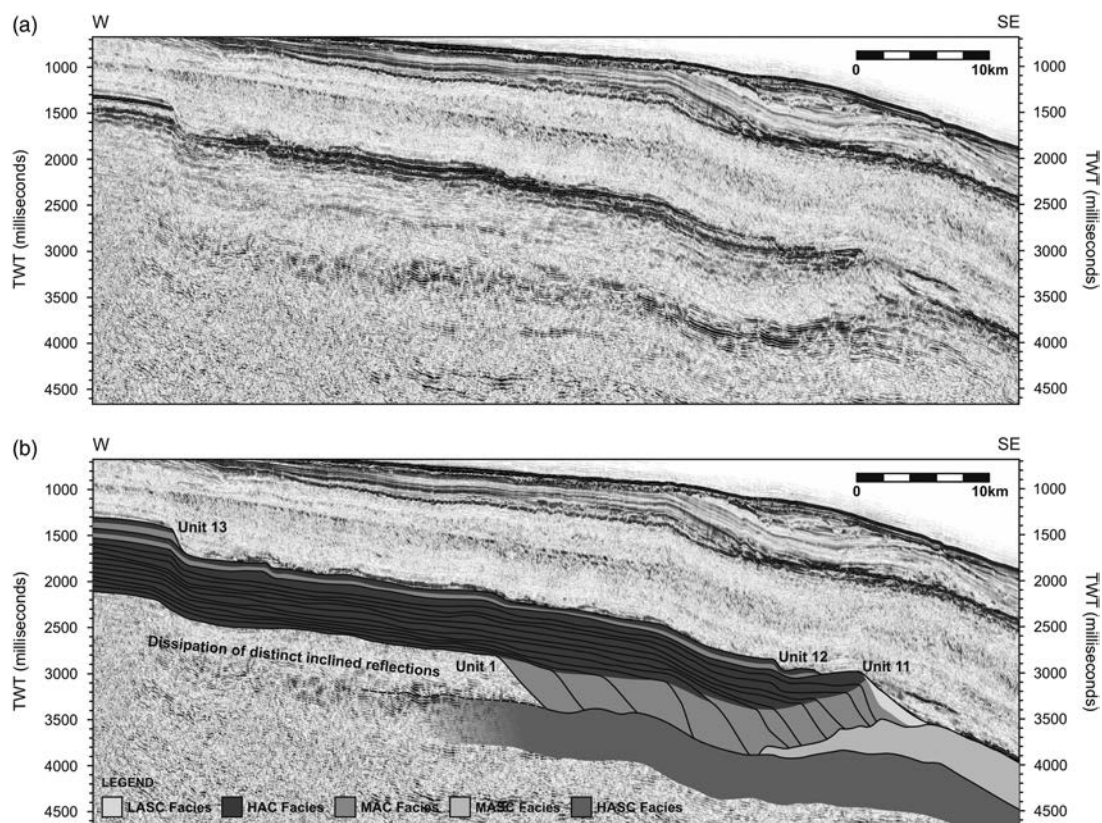
Fig. 6. (a) Uninterpreted seismic sections through the Faroe-Shetland Escarpment. (b) Interpreted seismic section through the Faroe-Shetland Escarpment, displaying bounding reflections of the seismic reflection units and distribution of seismic facies (see Fig. 2 for location).

unit, and displays shallower internal reflections which vary from continuous to semi-continuous, with a locally disrupted and curved upper bounding reflection. Seismic reflection units 12 and 13 have a similar wedge-shaped morphology as units 1–11, with height varying from 175 to 200 m. These units are directly above units 1–11 and display a retrogradational stacking pattern, with the extent of each unit located progressively to the west, towards the Faroe Islands (Fig. 6). Identification of seismic reflection units, in particular the bounding reflections, becomes increasingly difficult deeper within the succession of reflections due to heterogeneity of the system causing scattering and absorption of the seismic energy.

The position of the offlap break for the most easterly lying clinoform identifies the limit of the individual seismic reflection unit (Fig. 7). The distal limits of the units are inferred, as the thickness of the units thins below seismic resolution and prohibits reliable identification of unit terminations. Seismic reflection units 1–11 display progradation to the east. The extent of units 1–5 is irregular and highly sinuous, with an NE–SW orientation. Units 6–11 have a less irregular extent with a smoother, curvi-linear geometry, with unit 11 displaying localised areas of disruption (Fig. 7). To the north, the offlap break continues to be orientated NNE–SSW, whereas in the south, the offlap break gradually rotated anticlockwise, becoming orientated N–S. Seismic reflection units 12 and 13 record retrogradation to the west (Fig. 7). Unit 12 has a similar

extent and offlap break orientation to unit 11, with only minor westerly movement. Unit 13 is located significantly further west towards the Faroe Islands, with a irregular, sinuous extent and NE–SW orientated offlap break as displayed by seismic reflection units 1–5.

Seismic facies analysis

Detailed analysis of the seismic reflection configurations has identified five seismic facies, using key observational criteria such as amplitude and continuity (Table 1), with each facies named according to their distinctive reflection characteristics, as suggested by West *et al.* (2002). The identified facies have distinct distributions and spatial relationships, often with indistinct facies boundaries (Fig. 6). The first and uppermost facies identified is composed of high amplitude, continuous reflections (HAC facies) that extend from the Faroes shelf into the basin. The second facies is composed of moderate amplitude, continuous reflections (MAC facies) that are located basinward of the offlap break. The reflections are inclined and prograde in a south easterly direction. The third seismic facies is composed of low amplitude, semi-continuous reflections (LASC facies) that are located further basinward of the MAC facies. The fourth facies is composed of moderate amplitude, semi-continuous reflections (MASC facies) that extend from the east and terminated half way beneath the body of the MAC facies. The final and deepest facies

Fig. 7. Map of the extent of seismic reflection units, with the position of the offlap break for the most easterly lying clinoform within each unit identified. Distal limits of individual units are inferred with a dotted line, as the thickness of the units thins below seismic resolution and prohibits reliable identification of unit terminations.
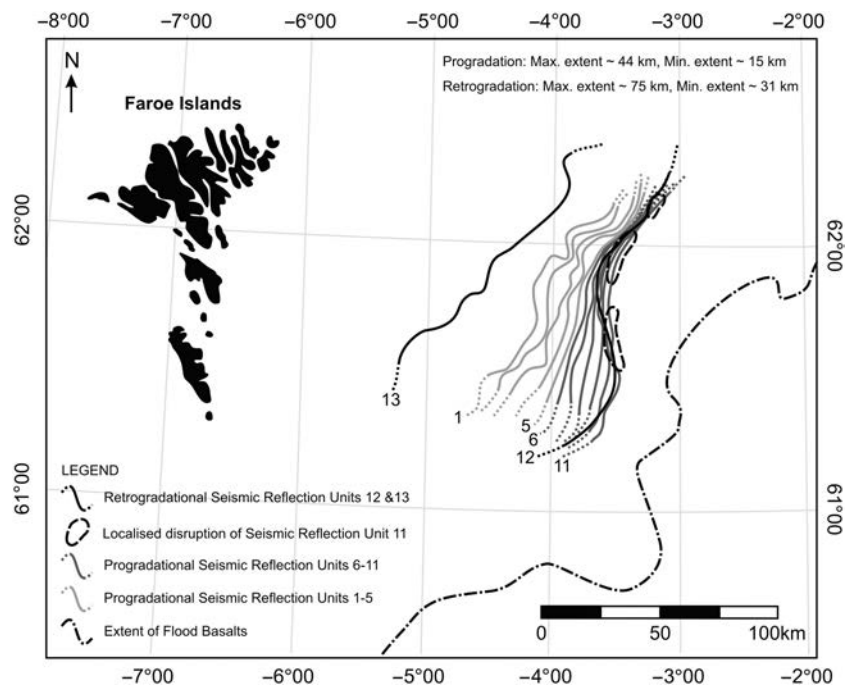
identified is composed of high amplitude, semi-continuous reflections (HASC facies) that are located beneath all of the previously described facies, extending across the basin and towards the Faroe Islands.

INTERPRETATIONS
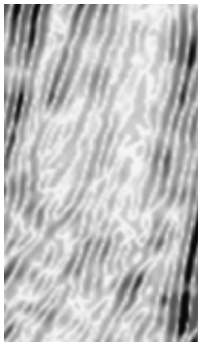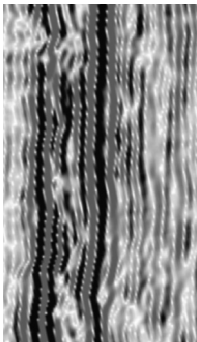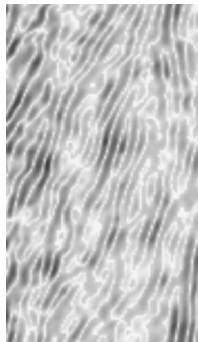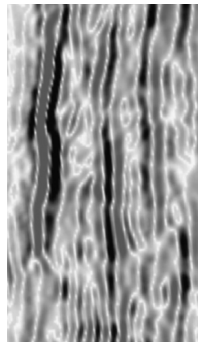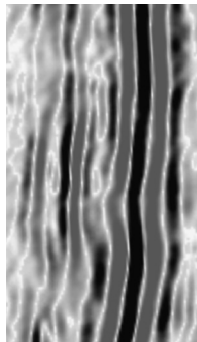
Seismic reflection units

The idea that the Faroe-Shetland Escarpment was formed through the deposition of subaerial lava flows into marine hyaloclastic breccias is well established (e.g. Smythe *et al.*, 1983; Ritchie *et al.*, 1999; Spitzer *et al.*, 2008). We interpret that the seismic reflection units identified in this study record continuous volcanic deposition during discrete periods of active volcanism. The seismic reflection units appear to have been deposited sequentially, with the gross stacking pattern revealing variations in the available accommodation space, relative sea level rise and the supply of volcanic material. As in conventional delta systems, the height of the delta-front clinoforms (MAC and LASC facies) may be a proxy for water depth at the time of delta deposition (Schmincke *et al.*, 1997; Kiørboe, 1999; Spitzer *et al.*, 2008). The initial stacking pattern is progradational, with seismic reflection units 1–11 extending progressively further into the basin (Fig. 8). Deposition was likely controlled by the volumes of erupted lava entering the basin and infilling the available accommodation space. Units 1–5 also display a minor aggradational component, which is interpreted to be the product of a gradual rise in the position of relative sea level. The degree of aggradation increases with the deposition of units 6–11, as the delta front intersects with, and climbs over the MASC facies (Fig. 8).

Seismic reflection unit 11 extends furthest into the basin and defines the extent of progradation of the lava-fed delta. The unit displays a variation of inclinations, including shallowly dipping reflections (LASC facies) which have a limited lateral distribution (Figs 7 and 8). This delta front morphology is interpreted to be controlled by collapse scarps, which developed along the delta front. The collapse of unit 11 resulted from a prolonged hiatus or decrease in the supply of new material, which left the delta front prone to erosion and reworking by tides, waves and storms (cf. Skilling, 2002; Sansone & Smith, 2006). Large scale section collapse scarps (up to 10 km across) may result from the subsidence of the delta, as seen in modern Hawaiian lava-fed deltas identified by Kauahikaua *et al.* (2003) and Mattox & Mangan (1997). During active delta deposition, the unconsolidated delta front subsides, causing fractures to propagate up through the delta front. The area located basinward of these fractures is known as a 'lava bench' and can be inherently unstable due to the unconsolidated material. During full or partial bench collapses, explosive interactions between lava and ocean water can occur, resulting in the catastrophic collapse of the delta front (Mattox & Mangan, 1997; Heliker & Mattox, 2003).

The stacking pattern changes to one of retrogradation during the deposition of seismic reflection units 12 and 13, with each unit located progressively towards the Faroe Islands. The units are located directly above, and downlap onto seismic reflection units 1–11. We interpret that during the hiatus between units 11 and 12, there was a continued syn-volcanic rise in relative sea level, creating a new volume of accommodation space above the previously deposited units. Recommencement of lava supply infilled the newly created accommodation space above seismic reflection units 1–11. Lava supply is inferred to be limited and short lived with deposition of unit 12 rarely reaching

97

Table 1. Description of seismic facies, including observational criteria, external geometry and typical reflection configurations

Seismic facies	Seismic reflections	Geometry	Top reflections	Internal reflections	Base reflections
Low Amplitude Semi-Continuous (LASC)		Wedge	Moderate amplitude inclined and subparallel reflections	Low amplitude, inclined, subparallel, varies between semi-continuous and disrupted reflections	Low amplitude, subhorizontal, subparallel reflections
High Amplitude Continuous (HAC)		Sheet-like	High amplitude, horizontal to subhorizontal, parallel largely continuous with a irregular or undulating reflections	High to moderate amplitude, horizontal to subhorizontal, parallel to subparallel, continuous reflections	Moderate amplitude, subhorizontal, parallel, varies from continuous to disrupted reflections
Moderate Amplitude Continuous (MAC)		Wedge	Moderate amplitude, subhorizontal, parallel to subparallel reflections	Moderate to low amplitude, inclined, parallel to subparallel, continuous to semi-continuous reflections	Low amplitude, parallel to subparallel, semi-continuous reflections
Moderate Amplitude Semi-Continuous (MASC)		Sheet-like to wedge	High amplitude, horizontal to subhorizontal, parallel to subparallel, occasionally rugose reflections	High to moderate amplitude, horizontal to subhorizontal, parallel to subparallel, semi-continuous, hummocky reflections	Moderate to low amplitude, subhorizontal, parallel, varies from semi-continuous to disrupted reflections
High Amplitude Semi-Continuous (HASC)		Sheet-like	High amplitude, horizontal to subhorizontal, largely continuous reflections	High to moderate amplitude, parallel to subparallel, varying continuity with strong layered reflections	Moderate to low amplitude, parallel to subparallel, semi-continuous reflections, difficult to identify

Fig. 8. Schematic cross-section through the lava-fed delta based on Fig. 6, including seismic reflection units and distribution of seismic facies (not to scale).

the extent of unit 11, therefore recording the retrogradation of the delta front (Fig. 8). The syn-volcanic rise in relative sea level continued after the deposition of unit 12, and once again created a new volume of accommodation space above the previously deposited units. When lava supply resumed, deposition was greatly limited, with unit 13 never reaching the extent of unit 12, recording further retrogradation of the delta front (Fig. 8).

The delta front is identified by the position of the offlap break, where reflection geometries change from subhorizontal to inclined. The offlap break is also interpreted to identify the location of the palaeo-shoreline and the position of relative sea level during delta deposition (Kiørboe, 1999; Spitzer *et al.*, 2008; Ellefsen *et al.*, 2010). Mapping of the offlap break is widely used in siliciclastic seismic stratigraphy to define shoreline trajectory and identify changes in the position of the palaeo-shoreline (e.g. Helland-Hansen & Martinsen, 1996; Helland-Hansen & Hampson, 2009).

The lava-fed delta front prograded SE, with a gradual anticlockwise rotation from NE–SW to N–S during deposition of seismic reflection units 1–11 (Fig. 7). The rotation of the delta front was caused by variations in the volume of material filling the available accommodation space. The height of the individual seismic reflection units displays little variation across the delta front, while the width of the units varies from 1–2 km in the north to 3–5 km in the south. This increase in unit width caused the delta front to migrate further in the south than the north, and rotate anticlockwise. Such variation in the filled accommodation space may indicate the location and distribution of volcanic sources, with more fissures located to the south of the Faroe Islands and the Faroese shelf. Following deposition of unit 11, the delta underwent retrogradation during deposition of unit 12, migrating between 1 and 6 km to the NE and with a similar distribution as unit 11. The greatest retrogradation occurred during the final stage of delta construction. During deposition of seismic reflection unit 13 the delta front migrated ~31 km in the north and ~75 km in the south, causing a sharp clockwise rotation of the delta front from N-S to NE–SW (Fig. 7). Deposition of unit 12 and 13 suggests volcanism was waning and becoming more sporadic.

Seismic facies

Interpretation of the facies identified within this study is based on the reflection characteristics and distinct spatial distributions, with comparison to lithologies known to exist within lava-fed delta systems. The uppermost facies within the lava-fed delta system is the HAC facies, which is located at the top of each of the seismic reflection units. The continuous nature and lateral extent suggest that the facies is composed of tabular lava flows that fed the delta (Fig. 8) (Planke *et al.*, 1999; Spitzer *et al.*, 2008; Jerram *et al.*, 2009). The MAC facies is located below and basinward of the HAC facies, with the reflections displaying progradation into the basin and the transition from the HAC to the MAC facies identified by the offlap break. The facies is interpreted to be composed of hyaloclastic breccias, which record the flow of lava directly into the offshore basin (Fig. 8) (Spitzer *et al.*, 2008; Jerram *et al.*, 2009). The LASC facies has a limited lateral distribution along the delta front in unit 11 and is interpreted to be the product of remobilisation of the MAC facies (Fig. 8). The reflections of the LASC facies display a semi-continuous nature that indicates that the delta front may have been semi-consolidated during the period of collapse, which is reflected in the limited distance that the remobilised material travelled downslope and the shallower dip of the delta front (Porebski & Gradzinski, 1990; Planke *et al.*, 2000).

The lava-fed delta system is underlain by two different facies. The first is the MASC facies which has been identified beneath seismic reflection units 6–11, appearing to wedge out beneath unit 5. The boundary between the MAC and MASC facies varies from distinct to more ambiguous downlap of the MAC on to the MASC facies. At times the MAC appears to interdigitise with the MASC facies, with previous studies suggesting the reflections of the MASC are extensive toesets (e.g. Kiørboe, 1999; Planke *et al.*, 1999, 2000). However this interpretation does not account for why the MASC facies is found beneath the later seismic reflection units, rather that all of the units, as would be expected for toesets. The MASC facies extends east out into the basin where it is intersected by well 214/4-1, which identified hyaloclastic breccias capped by tabular lava flows (see Fig. 3).

We have interpreted that the MASC facies was deposited from an easterly volcanic source within the basin, such as the Erlend Complex and Brendans Dome (Fig. 2) that flowed west towards the Faroe Islands. This was followed by the subsequent deposition and progradation of the lava-fed delta system east into the basin. Where the delta system became spatial coincident with the MASC facies, the seismic reflection units traversed over and downlapped on to the MASC facies (Fig. 8). We believe that the cause of the ambiguous downlap of the MAC facies on to the MASC facies is due to the both facies containing hyaloclastic lithologies. The second facies that underlies the lava-fed delta system is the HASC facies which has been identified to extend beneath the entire delta and the MASC facies, and east into the Faroe-Shetland Basin. This facies is interpreted to be part of the basin fill before the onset of lava-fed delta deposition and therefore may contain subaerially eroded volcanic material or minor volcanic intrusions.

Correlation to onshore stratigraphy

The eruption of the Faroe Island Basalt Group was broken into distinct episodes by small pauses or migration of the volcanic centres with the identification of seven distinct formations (Passey & Bell, 2007; Jerram *et al.*, 2009). Correlation of the lava-fed delta system to known onshore volcanic successions is based on the nature of the formations, their key volcanic facies and their stratigraphic position (e.g. Jerram *et al.*, 2009; Nelson *et al.*, 2009). Interpretation from seismic facies analysis and onshore stratigraphy suggests that the lava flows that fed the delta system were tabular in nature and are likely to be the offshore equivalent of the Beinisvørð Formation. The Beinisvørð Formation is composed of tabular lava flows that were emplaced though inflation and lobe coalescing, during fissure eruptions with relatively continuous supply of lava during each eruption. The structure of these lava flows may account for the distance that the lava would have had to travel before reaching the palaeo-shoreline and forming hyaloclastic breccias (Self *et al.*, 1997; Jerram & Widdowson, 2005; Passey & Bell, 2007).

Lava-fed delta duration

Flood basalt volcanism is characterised by repetitive, long-lived eruptions (weeks to 10s years) that are capable of producing large volumes ($> 1 km^3$) of lava, with the overall duration of volcanism lasting over a few (1–5) million years (e.g. Coffin & Eldholm, 1994; Eldholm & Grue, 1994; Bryan *et al.*, 2010). The onset of flood basalt volcanism is characterised by rela-

tively low volume eruptions, controlled by pre-existing topography or stress regime. The main phase of flood basalt activity is typified by an increase in eruption volume with high intensity volcanic flux (e.g. $10^{11} kg s^{-1}$) eruptions. The end of flood basalt volcanism is signified by a rapid decrease in eruption volume and the development of widely distributed localised volcanic centres (Jerram & Widdowson, 2005; Bryan *et al.*, 2010). Relative and absolute dating between eruptions can be difficult and relies on the preservation of erosional surfaces, deposition of non volcanic units, palynology and geochemical fingerprinting of different eruptive units. In offshore settings, it can be extremely difficult to obtain this information, especially if the volcanic succession is undrilled.

Hon *et al.* (1994) calculated the length of time a lava flow has taken to inflate and cool based on the thickness of the flow crust, by the empirical equation:

$$t = 164.8C^2$$

where *t* is time in hours, 164.8 is an empirically determined constant and *C* is the thickness of the flow crust in metres. This information has been constrained by observing the development of pāhoehoe sheets through time (Hon *et al.*, 1994). Passey & Bell (2007) used this equation to estimate the duration of individual flow lobes on the Faroe Islands, with results varying from 10.3 h for small, isolated lobes to 22.2 days for the better developed lobes that display inflation structures such as defined vesicle zones. Onshore exposures of the Beinisvørð Formation suggest that the average flow lobe thickness is 25 m (Ellis *et al.*, 2002; Passey & Bell, 2007; Passey & Jolley, 2009) and will be composed of 40% crust (Nelson *et al.*, 2009). Use of the empirical equation (Hon *et al.*, 1994) estimates it took 1.88 years for a individual lava flow lobe to inflate to 25 m.

Further to this, we have estimated the average total flow thickness for the seismic reflection units 1–13 (Table 2) using two-way travel time from the seismic data and velocities of $5.5 km s^{-1}$ for tabular lava flows gathered from boreholes on the Faroe Islands (Boldreel, 2006; Nelson *et al.*, 2009). The total thickness of lava flows for each unit will be composed of a number of individual flows, most likely with a similar thickness as the onshore exposures of the Beinisvørð Formation but are below seismic resolution. In order to calculate the thickness of crust *C*, we have used core to crust ratios from Nelson *et al.* (2009), who plotted the core proportions of onshore Faroes lava flows identified within the Vestmanna-1, Glyvursnes-1 and Lopra-1/1A boreholes. By using data based on lava flows from equivalent onshore stratigraphy, we have an accurate

Table 2. Average thickness for lava flows feeding the seismic reflections units and the calculated time taken to inflate to the total flow thickness (values to two decimal places).

Seismic reflection unit	Average total flow thickness (m)	C (m)	t (h)	$t/24$ = days	$t/24/365$ = years
1–11	275	110	1 994 080	83 086.67	227.63
12–13	137.5	55	498 520	20 771.67	56.91

assessment of lava thicknesses where the core to crust ratio has been well constrained statistically (Nelson *et al.*, 2009).

Seismic reflection units 1–11 have an average total thickness of 275 m, with 40% crust equating to 110 m (Table 2). The average duration (*t*) for each unit is 227.63 years, culminating in the active progradation of units 1–11 occurring over 2503.93 years. In contrast, seismic reflection units 12 and 13 have a much smaller average thickness of 137.5 m, with 40% curst equating to 55 m (Table 2). The average duration (*t*) for each unit is 56.91 years, culminating in the active retrogradation of units 12 and 13 over 113.82 years. The sum of the duration (*t*) for all the units (1–13) gives a value of 2617.75 years of active delta deposition and lava flow emplacement.

Geochemical and isotopic dating of the Beinisvørð Formation suggests that volcanism occurred between 60.1 ± 0.6 and 56.8 ± 0.6 Ma (Waagstein *et al.*, 2002; Storey *et al.*, 2007), while palynological and sequence stratigraphic analysis suggest volcanism occurred between 56.8 and 54.9 Ma (Ellis *et al.*, 2002; Jolley & Bell, 2002; Jolley, 2009). The calculated total duration of active deposition does not include any periods of volcanic quiescence which could have varied from 10 to 10^4 years (Coffin & Eldholm, 1994; Jerram & Widdowson, 2005). By including extended pauses between volcanic pulses, the duration of delta construction would be in keeping with the timing of the eruption of the Beinisvørð Formation. However, it is difficult to constrain the effects of erosion, which would have reduced the total thickness of the lava flows and therefore give an underestimate of the time taken to inflate and cool (Eldholm & Grue, 1994).

DISCUSSION
Seismic reflection units

Interpretation of the seismic reflection units has been based on the seismic facies associations, stratigraphic position and the juxtaposition of one unit against another. We suggest that each unit represents an individual volcanic succession created by a discrete period of active volcanism, with the internal reflections recording the continuous deposition of hyaloclastic breccias (Schmincke *et al.*, 1997; Kiørboe, 1999). The inference that each seismic reflection unit represents a period of active volcanism also suggests that each period of activity was followed by a period of little or no volcanic activity. During these hiatal periods no new lava flows or hyaloclastic breccias were deposited over the previous unit, leaving them prone to erosion, remobilisation and resedimentation. We propose the bounding reflections are surfaces produced during such hiatuses.

In a subaerial environment, weathering and erosion of subaerial lava flows forms volcanogenic soils. Genesis of a soil from basaltic lava parent material is slower than that for scoria or ash of the same composition, and is much slower than for unconsolidated sedimentary deposits such as sand or glacial deposits (Dan & Singer, 1973; Pillans, 1997). Rates of soil genesis are difficult to estimate due to

a wide range of factors that influence soil formation, such as climate, temperature and mechanisms of erosion including weathering and leaching. However, it has been estimated that genesis of a volcanogenic soil can take as little as 45–70 years in a tropical climate and up to 500 years in a cool climate (Corbett, 1968; Buol *et al.*, 1989). In a number of onshore outcrops, siliciclastic deposits, often with associated plant material were deposited after the previous phase of lava-fed delta deposition and indicate the re-emergence of a pre-existing sedimentary regime during periods of volcanic inactivity (Porebski & Gradzinski, 1990; Yamagishi, 1991; Trodeson & Smellie, 2002; Jolley *et al.*, 2009).

In a submarine environment, erosion can result from reworking by tides, waves and/or storms and are the equivalent of the subaerial palaeosols and erosional surfaces, with coastal sandstones and deeper marine mudstones accumulating during periods of volcanic inactivity (Furnes & Fridleifsson, 1974; Bergh & Sigvaldason, 1991). Submarine erosional surfaces may also occur due to the avulsion of the actively depositing lava lobe during periods of volcanism. Avulsion occurs when the feeder systems shifts location, causing construction of the active delta lobe to cease and the build-out of a new lobe to occur at another location which is usually in close proximity along shore (Coleman, 1988; Correggiari *et al.*, 2005). In the Faroe-Shetland Escarpment area, we interpret the bounding reflectors of the seismic stratigraphic units to represent submarine erosional surfaces at the top of each volcanic succession.

Lava-fed delta development

The stacking pattern of the seismic reflection units is a function of the interaction between lava supply, the position of relative sea level and available accommodation space, and it records how these parameters affected the lava-fed delta system. It is clear that lava supply varied, with deposition occurring during periods of active volcanism and no deposition during volcanic hiatuses. Volcanic systems are known to display a pulsed or cyclic nature, with variations in distribution, volume and geochemistry of erupted products (Paterne & Guichard, 1993; Knight *et al.*, 2004; Jerram & Widdowson, 2005). Variations in depositional extent can also occur during a waning of the eruption rate, migration of the vent or location switching of the depositing lava tube or inflation lobe (Self *et al.*, 1997; Heliker *et al.*, 1998; Passey & Bell, 2007).

The subaerially erupted lava flows of the delta system are suggested to be extensive pāhoehoe flows that coalesced and formed on large inflating sheet flows (e.g. Self *et al.*, 1997). Evidence from lavas in onshore exposures in the Faroes and in the British Palaeogene indeed point to the pāhoehoe nature of the subaerial flows (Single & Jerram, 2004; Passey & Bell, 2007), while 'a'ā lava flows, comprised largely of autoclastic breccias are rare in most flood basalt provinces (Brown *et al.*, in press). It is unlikely that the lava flows of the delta entered the basin simulta-
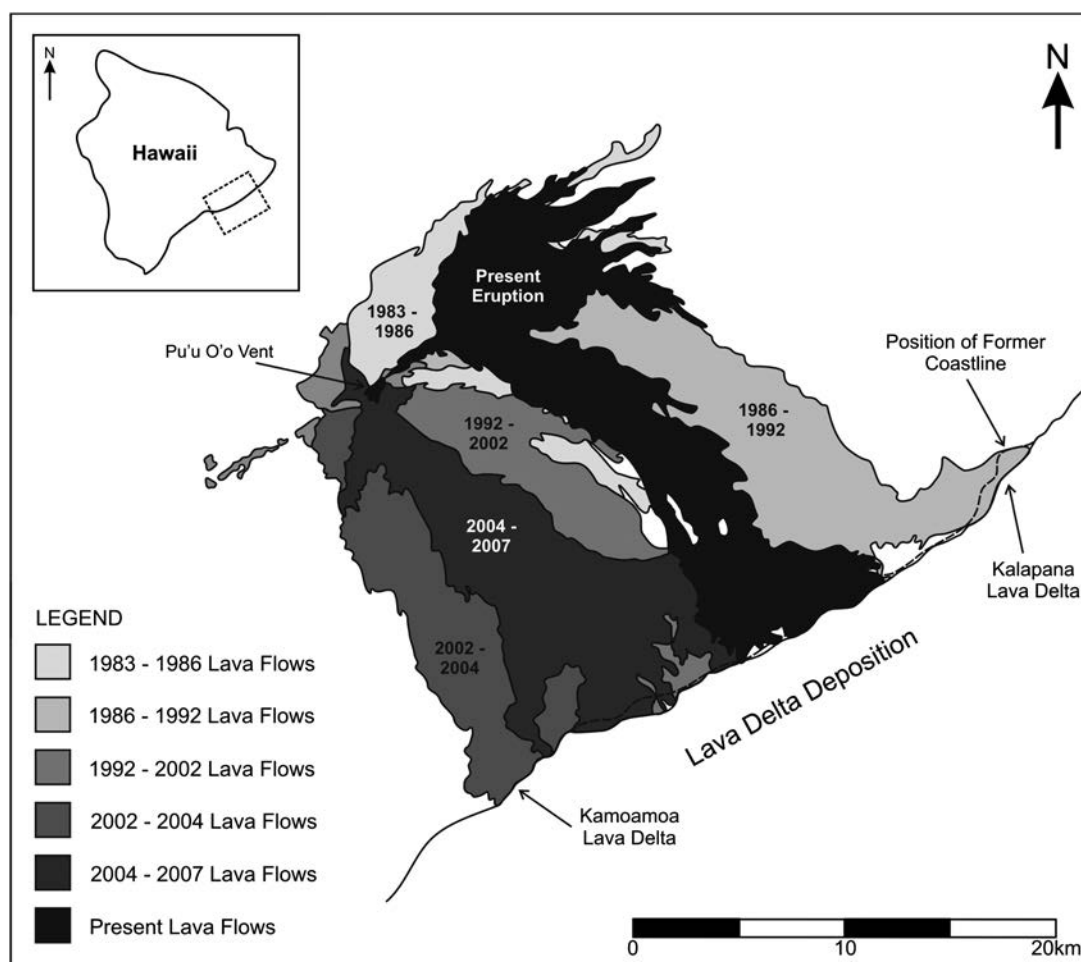
Fig. 9. Distribution and ages of lava flows originating from the Pu'u O'o volcano on the southeast side of Hawaii. Modified from Mattox & Mangan (1997), Heliker *et al.* (1998), Smith *et al.* (1999), Kauahikaua *et al.* (2003), Heliker & Mattox (2003), Sansone & Smith (2006).

neously and fed the entire delta front. The delta system was more likely fed from point sources along the palaeo-shoreline, with each location building a delta that eventually merged into one continuous delta body, as seen where modern lava flows enter the ocean (Moore *et al.*, 1973; Mattox *et al.*, 1993; Kauahikaua *et al.*, 2003). Hiatuses occurring in this system would only record local varia-tions, representing a waning of volcanism closer to the source or sites of lobe switching, with deposition removed to another location. Importantly, any significant hiatuses in volcanism are likely to be recorded by degradation and collapse of parts of the delta front as the sea starts to erode the shoreline. Therefore, periods of significant lava flux would be seen as a prolonged, probably pulsed, period of delta progradation, as seen with the early to middle phases of delta development in this study.

Variations in both the position of relative sea level and the volume of accommodation space are also evident. Ag-gradation of the seismic reflection units is seen to increase through the stratigraphic succession and is defined by the migration of the offlap break in units 1–11 (Fig. 8). This apparent rise in relative sea level is interpreted to be a product of the loading and subsidence of the growing delta system. Studies of modern lava-fed deltas on Hawaii

have identified that deltas subside as they form, with the greatest subsidence during active deposition. Geodetic monitoring of active lava-fed deltas on Hawaii has recorded subsidence of up to 7 cm a month (Mattox & Mangan, 1997; Kauahikaua *et al.*, 2003). Such syn-volcanic subsidence would have been localised, with the greatest subsidence occurring in areas of active deposition. The more regional subsidence seen within the basin (e.g. Dean *et al.*, 1999; Lamers & Carmichael, 1999) is a product of the underlying rift architecture at the time of extension (e.g. Davies *et al.*, 2004). Deposition of the retrogradational seismic reflection units (Fig. 8) occurred after periods of volcanic inactivity when the delta system was no longer actively depositing and subsiding. This retrogradation of the delta front towards the Faroe Islands in the latter stages of delta development records a far more significant rise in relative sea level and the creation of new accom-modation space.

Comparison with modern lava-fed deltas

Volcaniclastic units in flood basalt and volcanic margin settings are not as well studied as the more distinct lava flow units, but recent work has shown that they can occur

in a number of settings and are particularly important at and near the onset of flood volcanism (e.g. Jerram & Stollhofen, 2002; Ukstins Peate *et al.*, 2003; Ross *et al.*, 2005). Indeed, Iceland, Greenland and Antarctica contain documented outcrops of lava fed delta systems similar in thickness and geometry to the one presented in this study (e.g. Furnes & Fridleifsson, 1974; Porebski & Gradzinski, 1990; Pedersen *et al.*, 1997; Smellie *et al.*, 2008). The most well known and studied example of modern lava-fed delta systems is that of the eruptions on the Island of Hawaii. Multiple lava flows enter the sea from a number of discrete vents and fissures, forming extensive hyaloclastite deposits in an offshore apron along the eastern coastline of the Main Island of Hawaii (Fig. 9) (Moore *et al.*, 1973; Mattox *et al.*, 1993; Heliker *et al.*, 1998). Hawaiian lava flows are predominantly emplaced as pāhoehoe flows, which can travel significant distances from source to emplacements (Heliker *et al.*, 1998; Heliker & Mattox, 2003), and are considered as analogues to the way in which continental flood basalts are emplaced with similar mechanisms of emplacement and character of eruptions (Self *et al.*, 1997; Kauahikaua *et al.*, 1998).

The Pu'u 'O'o vent on Hawaii has been erupting almost continuously since 1983 in a series of distinct, eruptive episodes that on average continue for 3–4 years (Heliker & Mattox, 2003; Kauahikaua *et al.*, 2003). Lava-fed deltas have been identified at Kalapana and Kamonamoa bays (Fig. 9), with rates of build out of ∼38 500 and ∼18 500 m^2/day. Although delta construction was over 2 years, active deposition lasted only 11 months in total (Mattox *et al.*, 1993; Mattox & Mangan, 1997). Intermittently shifting lava streams have also been identified along the delta front, where the lava tubes feeding the flow of material become blocked and the flow only resumes when a new tube has formed. These shifting flows behave in a similar manner to distributaries as seen in river deltas, where the delta builds out as a lobe that is sourced from the delta mouth, and then shifts lateral position (Moore *et al.*, 1973; Mattox *et al.*, 1993).

In between, and occasionally during the eruptive episodes, periods of little or no volcanic activity occur with a lack of any new eruptive products (Mattox *et al.*, 1993; Heliker *et al.*, 1998). These periods are likely a function of the plugging of the eruptive vent and/or the injection of new material into the magma chamber, causing a new vent or fissure to open up which is often in close proximity to the previous one. With no new lava flows, erosion of the previously deposited flows commences through both chemical and mechanical mechanisms with a current rate of 11.9 t km^{-2} yr^{-1} (Dessert *et al.*, 2003; Navarre-Sitchler & Brantley, 2007). Onshore, the product of weathering and erosion is often volcanogenic soils or boles that form on the top surface of the lava flow. Offshore, mass wasting of the hyaloclastic delta front can occur, forming a debris field consisting of fine sand to large boulder fragments (Sansone & Smith, 2006). The rapid re-establishment of coral communities that have been submerged by lava flows has also been widely documented (Grigg & Maragos, 1974).

CONCLUSIONS

This study demonstrates the utility in using seismic and sequence stratigraphic concepts to reconstruct the volcanic sediment basin-fill history of rifted margins. Detailed analysis of reflection geometries has identified a series of seismic reflection units that record the evolution of the Faroe-Shetland Escarpment during discrete periods of volcanism. Overall, the resulting lava-fed delta system shows a major period of progradation due to high volcanic lava fluxes during which the shoreline migrated a maximum distance of ∼44 km in an ESE direction (away from the Faroes). The later stages of delta deposition were dominated by reduced volcanic input coupled with basinwide relative sea level rise, which caused retrogradation of the delta during which the shoreline migrated a maximum distance of ∼75 km in a NNW direction (towards the Faroes). We conclude that the encroachment of flood basalts into the basin and the resulting palaeo-shoreline in the central Faroe-Shetland Basin has recorded the deposition of a lava-fed delta system over several thousand years. Importantly, this study highlights how the preservation of ancient volcanic systems in offshore settings has the potential to record key aspects of basin development, including the histories of relative sea level, volcanic sediment supply and available accommodation space, when more conventional depositional systems were absent.

References

ANDERSEN, M.S. (1988) Late Cretaceous and early Tertiary extension and volcanism around the Faeroe Islands. In: *Early Tertiary Volcanism and the Opening of the NE Atlantic* (Ed. by A.C. Morton & L.M. Parson), *Geol. Soc. Spec. Publ.*, **39**, 115–122.

BERGH, S.F. & SIGVALDASON, G.E. (1991) Pleistocene mass-flow deposits of basaltic hyaloclastite on a shallow submarine shelf, South Iceland. *Bull. Volcanol.*, **53**, 597–611.

BOLDREEL, L.O. (2006) Wire-line log-based stratigraphy of flood basalts from the Lopra-1/1A well, Faroe Islands. In: *Scientific Results from the Deepened Lopra-1 Borehole, Faroe Islands* (Ed. by J.A. Chalmers & R. Waagstein), *Geol. Surv. Denmark Greenland Bull.*, **9**, 7–22.

BOLDREEL, L.O. & ANDERSEN, M.S. (1994) Tertiary development of the Faeroe-Rockall Plateau based on reflection seismic data. *Bull. Geol. Soc. Denmark*, **41**, 162–180.

BROWN, R.J., BLAKE, S., BONDRE, N.R., PHADNIS, V.M. & SELF, S. (2011) A'a lava flows in the Deccan Volcanic province, India, and their significance for the nature of continental flood basalt eruptions. *Bull. Volcanol.*, in press. doi:10.1007/s00445-011-0450-7.

BRYAN, S.E., UKTINS PEATE, I., PEATE, D.W., SELF, S., JERRAM, D.A., MAWBY, M.R., MARSH, J.S. & MILLER, J.A. (2010) The largest volcanic eruptions of earth. *Earth Sci. Rev.*, **102**, 207–229.

BUBB, J.N. & HATLELID, W.G. (1977) Seismic stratigraphy and global changes of sea level, part 10: seismic recognition of carbonate build-ups. In: *Seismic Stratigraphy – Applications to Hydrocarbon Exploration* (Ed. by C.E. Payton), AAPG Mem., **26**, 185–204.

BUOL, S.W., HOLE, F.D. & MCCRACKEN, R.J. (1989) *Soil Genesis and Classification*, 3rd edn. Iowa State University Press, Ames, Iowa.

COFFIN, F.M. & ELDHOLM, O. (1994) Large igneous provinces: crustal structure, dimensions, and external consequences. *Rev. Geophys.*, **32**, 1–36.

COLEMAN, J.M. (1988) Dynamic changes and processes in the Mississippi River delta. *Geol. Soc. Am. Bull.*, **100**, 999–1015.

CORBETT, J.R. (1968) The genesis of some Basaltic soils in New South Wales. *Eur. J. Soil Sci.*, **19**, 174–185.

CORREGGIARI, A., CATTANEO, A. & TRINCARDI, F. (2005) The modern Po Delta system: lobe switching and asymmetric pro-delta growth. *Mar. Geol.*, **222–223**, 49–74.

CROSS, T.A. & LESSENGER, M.A. (1988) Seismic stratigraphy. *Annu. Rev. Earth Planet. Sci.*, **16**, 19–54.

DAN, J. & SINGER, A. (1973) Soil evolution on basalt and basic pyroclastic materials in the Golan heights. *Geoderma*, **9**, 165–192.

DAVIES, R.J., BELL, B.R., CARTWRIGHT, J.A. & SHOULDERS, S. (2002) Three-dimensional seismic imaging of Paleogene dike-fed submarine volcanoes from the northeast Atlantic margin. *Geology*, **30**, 223–226.

DAVIES, R.J., CLOKE, I., CARTWRIGHT, J., ROBINSON, A. & FERRERO, C. (2004) Post-breakup compression of a passive margin and its impact on hydrocarbon prospectivity: an example from the tertiary of the Faeroe–Shetland Basin, United Kingdom. *AAPG Bull.*, **88**, 1–20.

DEAN, K., MCLACHLAN, K. & CHAMBERS, A. (1999) Rifting and the development of the Faeroe-Shetland basin. In *Petroleum Geology of Northwest Europe: Proceedings of the 5th Conference* (Ed. by A.J. Fleet & S.A.R. Boldy), *Geol. Soc. London*, 533–544.

DESSERT, C., DUPRE, B., GAILLARDET, J., FRANCOIS, L.M. & ALLEGRE, C.J. (2003) Basalt weathering laws and the impact of basalt weathering on the global carbon cycle. *Chem. Geol.*, **202**, 257–273.

ELDHOLM, O. & GRUE, K. (1994) North Atlantic volcanic margins: dimensions and production rates. *J. Geophys. Res.*, **99**, 2955–2968.

ELLEFSEN, M., BOLDREEL, L.O. & LARSEN, M. (2010) Intra-basalt units and base of the volcanic succession east of the Faeroe-Islands exemplified by interpretation of offshore 3D seismic data. In: *Petroleum Geology: From Mature Basins to New Frontiers – Proceedings of the 7th Conference* (Ed. by B.A. Vining & S.C. Pickering), *Geol. Soc. London*, 1033–1042.

ELLIS, D., BELL, B.R., JOLLEY, D.W. & O'CALLAGHAN, M. (2002) The stratigraphy, environment of eruption and age of the Faroes Lava Group, NE Atlantic Ocean. In: *The North Atlantic Igneous Province: Stratigraphy, Tectonic, Volcanic and Magmatic Processes* (Ed. by DW. Jolley & B.R. Bell), *Geol. Soc. London Spec. Publ.*, **197**, 253–269.

ENGLAND, R.W., MCBRIDE, J.H. & HOBBS, R.W. (2005) The role of Mesozoic rifting in the opening of the NE Atlantic; evidence from deep seismic profiling across the Faroe-Shetland Trough. *J. Geol. Soc. London*, **162**, 661–673.

FISHER, R.V. & SCHMINCKE, H.-U. (1994) Volcaniclastic sediment transport and deposition. In: *Sediment Transport and Depositional Processes* (Ed. by K. Pye) Blackwell Scientific Publications, Oxford, pp. 351–388.

FULLER, R.E. (1931) The aqueous chilling of basaltic lava on the Columbia River Plateau. *Am. J. Sci.*, **5**, 281–320.

FURNES, H. & FRIDLEIFSSON, I.B. (1974) Tidal effects on the formation of pillow lava/hyaloclastic deltas. *Geology*, **2**, 381–384.

GATLIFF, R.W., HITCHEN, K., RITCHIE, J.D. & SMYTHE, D.K. (1984) Internal structure of the Erlend Tertiary volcanic complex, north of Shetland, revealed by seismic reflection. *J. Geol. Soc. London*, **141**, 555–562.

GRIGG, R.W. & MARAGOS, J.E. (1974) Recolonization of hermatypic corals on submerged lava flows in Hawaii. *Ecology*, **55**, 387–395.

HANSEN, J., JERRAM, D.A., MCCAFFERY, K. & PASSEY, S.R. (2009) The onset of the North Atlantic Igneous Province in a rifting perspective. *Geol. Mag.*, **146**, 309–325.

HANSEN, J., JERRAM, D.A., MCCAFFERY, K. & PASSEY, S.R. (2011) Early Cenozoic saucer-shaped sills of the Faroe Islands: an example of intrusive styles in basaltic lava piles. *J. Geol. Soc.*, **168**, 159–178.

HELIKER, C.C., MANGAN, M.T., MATTOX, T.N., KAUAHIKAUA, J.P. & HELZ, R.T. (1998) The character of long-term eruptions: inferences from episodes 50–53 of the Pu'u 'Ō 'Ō-Kūpaianaha eruption of Kilauea Volcano. *Bull. Volcanol.*, **59**, 381–393.

HELIKER, C.C. & MATTOX, T.N. (2003) The first two decades of the Pu'u 'Ō'Ō-Kūpaianaha Eruption: chronology and selected bibliography. *U.S. Geol. Surv. Profess. Paper*, **1676**, 1–28.

HELLAND-HANSEN, W. & HAMPSON, G.J. (2009) Trajectory analysis: concepts and applications. In: *Trajectory Analysis in Stratigraphy* (Ed. by S. Henriksen, G.J. Hampson, W. Helland-Hansen, E.P. Johannessen & R.J. Steel), *Basin Res.*, **21**, 454–483.

HELLAND-HANSEN, W. & MARTINSEN, O.J. (1996) Shoreline trajectories and sequences: description of variable depositional-dip scenarios. *J. Sediment. Res.*, **66**(4), 670–688.

HON, K., KAUAHIKAUA, J.P., DENLINGER, R. & MACKAY, K. (1994) Emplacement and inflation of pāhoehoe sheet flows: observations and measurements of active lava flows on Kilauea Volcano, Hawaii. *Geol. Soc. Am. Bull.*, **106**, 351–370.

JAPSEN, P., ANDERSEN, M.S., BOLDREEL, L.O., WAAGSTEIN, R., WHITE, R.S. & WORTHINGTON, M. (2004) Seismic and petrophysical properties of Faroe Islands basalts: the SeiFaBa project. *Geol. Surv. Denmark Greenland Bull.*, **4**, 53–65.

JERRAM, D.A., SINGLE, R.T., HOBBS, R.W. & NELSON, C.E. (2009) Understanding the offshore flood basalt sequence using onshore volcanic facies analogues: an example from the Faroe–Shetland basin. *Geol. Mag.*, **146**, 353–367.

JERRAM, D.A. & STOLLHOFEN, H. (2002) Lava/sediment interaction in desert settings; are all peperite-like textures the result of magma-water interaction? *J. Volcanol. Geotherm. Res.*, **114**, 231–249.

JERRAM, D.A. & WIDDOWSON, M. (2005) The anatomy of continental flood basalt provinces: geological constraints on the processes and products of flood volcanism. *Lithos*, **79**, 385–405.

JOLLEY, D.W. (2009). Palynofloral evidence for the onset and cessation of eruption of the Faroe Islands lava field. *Faroe Islands Exploration Conference: Proceedings of the 2nd Conference. Annales Societatis Scientiarum Faroensis*, Supplementum 48, pp. 149–166.

JOLLEY, D.W. & BELL, B.R. (2002) Genesis and age of the Erland Volcano, NE Atlantic margin. In: *The North Atlantic Igneous Province: Stratigraphy, Tectonic, Volcanic and Magmatic Processes*

(Ed. by D.W. Jolley & B.R. Bell), *Geol. Soc. London Spec. Publ.*, **197**, 95–110.

JOLLEY, D.W., BELL, B.R., WILLIAMSON, I.T. & PRINCE, I. (2009) Sun-eruption vegetation dynamics, paleosurfaceas and structural controls on lava field vegetation: an example from the Palaeogene Staffa Formation, Mull Lava Field, Scotland. *Rev. Palaeobotany Palynol.*, **153**, 19–33.

JOLLEY, D.W. & MORTON, A.C. (2007) Understanding basin sedimentary provenance: evidence from allied phytogeographic and heavy mineral analysis of the Palaeocene of the NW Atlantic. *J. Geol. Soc. London*, **164**, 553–563.

JONES, J.G. & NELSON, P.H.H. (1970) The flow of basalt lava from air into water – its structural expression and stratigraphic significance. *Geol. Mag.*, **107**, 13–19.

KAUAHIKAUA, J.P., CASHMAN, K.V., MATTOX, T.N., HELIKER, C.C., HON, K.A., MANGAN, M.T. & THORNBER, C.R. (1998) Observations on basaltic lava streams in tubes from Kilauea Volcano, island of Hawai'i. *J. Geophys. Res.*, **103**, 27303–27323.

KAUAHIKAUA, J.P., SHERROD, D.R., CASHMAN, K.V., HELIKER, C.C., HON, K., MATTOX, T.N. & JOHNSON, J.A. (2003) Hawaiian lava-flow dynamics during the Pu'u 'Ō 'Ō-Kūpaianaha eruption: a tale of two decades. *U.S. Geol. Surv. Profess. Paper*, **1676**, 63–88.

KIØRBOE, L. (1999) Stratigraphic relationships of the lower tertiary of the Faroe Basalt Plateau and the Faeroe-Shetland Basin. In: *Petroleum Geology of Northwest Europe: Proceedings of the 5th Conference* (Ed. by A.J. Fleet & S.A.R. Boldy), *Geol. Soc. London*, 559–572.

KNIGHT, K.B., NOMADE, S., RENNE, P.R., MARZOLIC, A., BERTRAND, H. & YOUBI, N. (2004) The Central Atlantic magmatic province at the Triassic–Jurassic boundary: paleomagnetic and ^{40}Ar/^{39}Ar evidence from Morocco for brief, episodic volcanism. *Earth Planet. Sci. Lett.*, **228**, 143–160.

KOKELARR, P. (1986) Magma-water interactions in subaqueous and emergent basaltic volcanism. *Bull. Volcanol.*, **48**, 275–289.

LAMERS, E. & CARMICHAEL, S.M.M. (1999) The Paleocene deepwater sandstone play West of Shetland. In: *Petroleum Geology of Northwest Europe: Proceedings of the 5th Conference* (Ed. by A.J. Fleet & S.A.R. Boldy), *Geol. Soc. London*, 645–659.

LARSEN, M.L., WAAGSTEIN, R., PEDERSEN, A.K.M. & STOREY, M. (1999) Trans-Atlantic correlation of the Palaeogene volcanic successions in the Faeroe Islands and East Greenland. *J. Geol. Soc. London*, **156**, 1081–1095.

MATTOX, T.N., HELIKER, C.C., KAUAHIKAUA, J.P. & HON, K.A. (1993) Development of the 1990 Kalapana flow field, Kilauea Volcano, Hawaii. *Bull. Volcanol.*, **55**, 407–413.

MATTOX, T.N. & MANGAN, M.T. (1997) Littoral hydrovolcanic explosions: a case study of lava-seawater interaction at Kilauea Volcano. *J. Volcanol. Geotherm. Res.*, **75**, 1–17.

MITCHUM, R.M., VAIL, P.R. & SANGREE, J.B. (1977a) Seismic stratigraphy and global changes of sea level, part 6: stratigraphical interpretation of seismic reflection patterns in depositional sequence. In: *Seismic Stratigraphy – Applications to Hydrocarbon Exploration* (Ed. by C.E. Payton), *AAPG Mem.*, **26**, 117–133.

MITCHUM, R.M., VAIL, P.R. & THOMPSON, S. (1977b) Seismic stratigraphy and global changes of sea level, part 2: the depositional sequence as a basic unit for stratigraphic analysis. In: *Seismic Stratigraphy – Applications to Hydrocarbon Exploration* (Ed. by C.E. Payton), *AAPG Mem.*, **26**, 53–62.

MOORE, J.G., PHILLIPS, R.L., GRIGG, R.W., PETERSON, D.W. & SWANSON, D.A. (1973) Flow of lava into the Sea, 1969–1971, Kilauea Volcano, Hawaii. *Geol. Soc. Am. Bull.*, **84**, 537–546.

NAYLOR, P.H., BELL, B.R., JOLLEY, D.W., DURNALL, P. & FREDSTED, P. (1999) Palaeogene magmatism in the Faeroe-Shetland Basin: influences on uplift history and sedimentation. In: *Petroleum Geology of Northwest Europe: Proceedings of the 5th Conference* (Ed. by A.J. Fleet & S.A.R. Boldy), *Geol. Soc. London*, 545–558.

NAVARRE-SITCHLER, A. & BRANTLEY, S. (2007) Basalt weathering across scales. *Earth Planet. Sci. Lett.*, **261**, 321–334.

NELSON, C.E., JERRAM, D.A. & HOBBS, R.W. (2009) Flood basalt facies from borehole data: implications for prospectivity and volcanology in volcanic rifted margins. *Petrol. Geosci.*, **15**, 313–324.

PARKIN, C.J., LUNNON, Z.C., WHITE, R.S. & CHRISTIE, P.A.F. & iSIMM TEAM. (2007) Imaging the pulsing iceland mantle plume through the Eocene. *Geology*, **35**, 93–96.

PASSEY, S. & BELL, B.R. (2007) Morphologies and emplacement mechanisms of the lava flows of the Faroe Islands Basalt Group, Faroe Islands, NE Atlantic Ocean. *Bull. Volcanol.*, **70**, 139–156.

PASSEY, S. & JOLLEY, D.W. (2009) A revised lithostratigraphic nomenclature for the Palaeogene Faroe Islands Basalt Group, NE Atlantic Ocean. *Earth Environ. Sci. Trans. Roy. Soc. Edinburgh*, **99**, 127–158.

PATERNE, M. & GUICHARD, F. (1993) Triggering of volcanic pulses in the Campanian area, South Italy, by periodic deep magma influx. *J. Geophys. Res.*, **98**, 1861–1873.

PAYTON, C.E. (1977) Seismic stratigraphy – applications to hydrocarbon exploration. *AAPG Mem.*, **26**.

PEDERSEN, A.K., WATT, M., WATT, W.S. & LARSEN, L.M. (1997) Structure and stratigraphy of the Early Tertiary basalts of the Blosseville Kyst, East Greenland. *J. Geol. Soc.*, **154**, 565–570.

PILLANS, B. (1997) Soil development at a snail's pace: evidence from a 6 Ma soil chronosequence on basalt in north Queensland, Australia. *Geoderma*, **80**, 117–128.

PLANKE, S. (1994) Geophysical response of flood basalts from analysis of wire line logs: ocean drilling program Site 642, Vøring volcanic margin. *J. Geophys. Res.*, **99**, 9279–9296.

PLANKE, S., ALVESTAD, E. & ELDHOLM, O. (1999) Seismic characteristics of basaltic extrusive and intrusive rocks. *Leading Edge*, **18**, 342–348.

PLANKE, S., SYMONDS, P.A., ALVESTAD, E. & SKOGSEID, J. (2000) Seismic volcanostratigraphy of large-volume basaltic extrusive complexes on rifted margins. *J. Geophys. Res.*, **105**, 19335–19351.

POREBSKI, S.J. & GRADZINSKI, R. (1990) Lava Gilbert-type delta in the Polonez cove formation (Lower Oligocene), King George Island, West Antarctica. In: *Coarse Grained Deltas* (Ed. by A. Colella & D.B. Prior), *Spec. Publ. Int. Assoc. Sedimentol.*, **10**, 335–351.

POSAMENTIER, H.W. & VAIL, P.R. (1988) Eustatic controls on clastic deposition II – sequences and system tract models. In: *Sea Level Changes – An Integrated Approach* (Ed. by C.K. Wilgus, B.S. Hastings, C.G. Kendal, H.W. Posamentier, C.A. Ross & J.C. Van Wagoner), *SEPM Spec. Publ.*, **42**, 125–154.

PRAEG, M., STOKER, M.S., SHANNON, P.M., CERAMICOLA, S., HJELSTUEN, B., LABERG, J.S. & MATHIESEN, A. (2005) Episodic Cenozoic tectonism and the development of the NW European 'passive' continental margin. *Mar. Petrol. Geol.*, **22**, 1007–1030.

RITCHIE, J.D., GATLIFF, R.W., RICHARDS, P.C., FLEET, A.J. & BOLDY, S.A.R. (1999) Early Tertiary magmatism in the offshore NW UK margin and surrounds. In: *Petroleum Geology of Northwest Europe: Proceedings of the 5th Conference* (Ed. by A.J. Fleet & S.A.R. Boldy), *Geol. Soc. London*, 573–584.

RITCHIE, J.D. & HITCHEN, K. (1996) Early Palaeogene offshore igneous activity to the northwest of the UK and its relationship to the North Atlantic Igneous Province. In: *Correlation of the Early Palaeogene in Northwest Europe* (Ed. by R.W.O'B. Knox, R.M. Corfield & R.E. Dunay), *Geol. Soc. Spec. Publ.*, **101**, 63–78.

RITCHIE, J.D., JOHNSON, H. & KIMBELL, G.S. (2003) The nature and age of Cenozoic contractional deformation within the NE Faroe-Shetland Basin. *Mar. Petrol. Geol.*, **20**, 399–409.

ROBERTS, A.W., WHITE, R.S., LUNNON, Z.C., CHRISTIE, P.A.F. & SPITZER, R. & iSIMM Team. (2005) Imaging magmatic rocks on the Faroes Margin. In: *Petroleum Geology of Northwest Europe: Proceedings of the 6th Conference* (Ed. by A.G. Dore & B.A. Vining), *Geol. Soc. London*, 755–766.

ROSS, P.-S., UKSTINS PEATE, I., McCLINTOCK, M.K., XU, Y.G., SKILLING, I.P., WHITE, J.D.L. & HOUGHTON, B.F. (2005) Mafic volcaniclastic deposits in flood basalt provinces: a review. *J. Volcanol. Geotherm. Res.*, **145**, 281–314.

SANGREE, J.B. & WIDMIER, J. (1977) Seismic stratigraphy and global changes in sea-level, part 9: seismic stratigraphic interpretation of clastic depositional facies. In: *Seismic Stratigraphy – Applications to Hydrocarbon Exploration* (Ed. by C.E. Payton), *AAPG Mem.*, **26**, 1165–1184.

SANSONE, F.J. & SMITH, J.R. (2006) Rapid mass wasting following nearshore submarine volcanism on Kilauea volcano, Hawaii. *J. Volcanol. Geotherm. Res.*, **151**, 133–139.

SARG, J.F. (1988) Carbonate sequence stratigraphy. In: *Sea Level Changes – An Integrated Approach* (Ed. by C.K. Wilgus, B.S. Hastings, C.G. Kendal, H.W. Posamentier, C.A. Ross & J.C. Van Wagoner), *SEPM Spec. Publ.*, **42**, 155–182.

SCHMINCKE, H.-U., BEHNCKE, B., GRASSO, M. & RAFFI, S. (1997) Evolution of the northwestern Iblean Mountains, Sicily: uplift, Pliocene/Pleistocene sea-level change, palaeoenvironment, and volcanism. *Geol. Rundsch.*, **86**, 637–669.

SELF, S., THORDARSON, T. & KESZTHELYI, L. (1997) Emplacement of continental flood basalt lava flows. In: *Large Igneous Provinces: Continental, Oceanic, and Planetary Flood Volcanism Geophys. Monogr.* (Ed. by J.J. Mahoney & M.E. Coffin), **100**, 381–410.

SINGLE, R.T. & JERRAM, D.A. (2004) The 3D facies architecture of flood basalt provinces and their internal heterogeneity: examples from the Palaeogene Skye lava field. *J. Geol. Soc.*, **161**, 911–926.

SKILLING, I.P. (2002) Basaltic pāhoehoe lava deltas: large-scale characteristics, clast generation, emplacement processes and environmental discrimination. In: *Volcano–Ice Interaction on Earth and Mars* (Ed. by J.L. Smellie & M.G. Chapman), *Geol. Soc. Spec. Publ.*, **202**, 91–113.

SMELLIE, J.L., JOHNSON, J.S., MCINTOSH, W.C., ESSERM, R., GUDMUNDSSON, M.T., HAMBREY, M.J. & VAN WYK DE VRIES, B. (2008) Six million years of glacial history recorded in volcanic lithofacies of the James Ross Island Volcanic Group, Antarctic Peninsula. *Palaeogeogr., Palaeoclimatol., Palaeoecol.*, **260**, 122–148.

SMITH, J.R., MALAHOFF, A. & SHOR, A.N. (1999) Submarine geology of the Hilina slump and morpho-structural evolution of Kilauea volcano, Hawaii. *J. Volcanol. Geothermal Res.*, **94**, 59–88.

SMYTHE, D.K., CHALMERS, J.A., SKUCE, A.G., BOBINSON, A. & MOULD, A.S. (1983) Early opening history of the North Atlantic – I. Structure and origin of the Faroe-Shetland escarpment. *Geophys. J. Roy. Astron. Soc.*, **72**, 373–398.

SØAGER, N. & HOLM, P.M. (2009) Extended correlation of the Paleogene Faroe Islands and East Greenland plateau basalts. *Lithos*, **107**, 205–215.

SØRENSEN, A.B. (2003) Cenozoic basin development and stratigraphy of the Faroes area. *Petrol. Geosci.*, **9**, 189–207.

SPITZER, R., WHITE, R.S. & CHRISTIE, P.A.F. (2008) Seismic characterization of basalt flows from the Faroes margin and the Faroe-Shetland basin. *Geophys. Prospect.*, **56**, 21–31.

STOREY, M., DUNCAN, R.A. & TEGNER, C. (2007) Timing and duration of volcanism in the North Atlantic igneous province: implications for geodynamics and links to the iceland hotspot. *Chem. Geol.*, **241**, 264–281.

THOMSON, K. & SCHOFIELD, N. (2008) Lithological and structural controls on the emplacement and morphology or sills in sedimentary basins. In: *Structure and Emplacement of High-Level Magmatic Systems* (Ed. by K. Thomson & N. Petford), *Geol. Soc. London Spec. Publ.*, **302**, 31–44.

TRODESON, A.L. & SMELLIE, J.L. (2002) The Polonez Cove formation of King George Island, Antarctica: stratigraphy, facies and implications for mid-Cenozoic cryosphere development. *Sedimentology*, **49**, 277–301.

UKSTINS PEATE, I., LARSEN, M. & LESHER, C.E. (2003) The transition from sedimentation to flood volcanism in the Kangerlussuaq basin, East Greenland: basaltic pyroclastic volcanism during initial Palaeogene continental break-up. *J. Geol. Soc.*, **160**, 759–722.

VAIL, P.R., TODD, R.G. & SANGREE, J.B. (1977) Seismic stratigraphy and global changes of sea level, part 5: chronostratigraphic significance of seismic reflections. In: *Seismic Stratigraphy – Applications to Hydrocarbon Exploration* (Ed. by C.E. Payton), *AAPG Mem.*, **26**, 99–116.

VAN WAGONER, J.C., POSAMENTIER, H.W., MITCHUM, R.M., VAIL, P.R., SARG, J.F., LOUTIT, T.S. & HARDENBOL, J. (1988) An overview of the fundamentals of sequence stratigraphy and key definitions. In: *Sea Level Changes – An Integrated Approach* (Ed. by C.K. Wilgus, B.S. Hastings, C.G. Kendal, H.W. Posamentier, C.A. Ross & J.C. Van Wagoner), *SEPM Spec. Publ.*, **42**, 39–46.

WAAGSTEIN, R., GUISE, P. & REX, D. (2002) K/Ar and ^{39}Ar/4 ~whole-rock dating of zeolite facies metamorphosed flood basalts: the upper Paleocene basalts of the Faroe Islands, NE Atlantic. In: *The North Atlantic Igneous Province: Stratigraphy, Tectonic, Volcanic and Magmatic Processes* (Ed. by D.W. Jolley & B.R. Bell), *Geol. Soc. London Spec. Publ.*, **197**, 219–252.

WEST, B.P., MAY, S.R., EASTWOOD, J.E. & ROSSEN, C. (2002) Interactive seismic facies classification using textural attributes and neural networks. *Leading Edge*, **21**, 1042–1049.

WILGUS, C.K., HASTINGS, B.S., KENDAL, C.G., POSAMENTIER, H.W., ROSS, C.A. & VAN WAGONER, J.C. (1988) Sea level changes – an integrated approach. *SEPM Spec. Publ.*, **42**.

WHITE, R.S., SMALLWOOD, J.R., FLIEDNER, M.M., BOSLAUGH, B., MARESH, J. & FRUEHN, J. (2003) Imaging and regional distribution of basalt flows in Faeroe-Shetland Basin: sub-basalt imaging. *Geophys. Prospect.*, **51**, 215–231.

YAMAGISHI, H. (1991) Morphological and sedimentological characteristic of the Neogene submarine coherent lavas and hyaloclastites in Southwest Hokkaido, Japan. *Sediment. Geol.*, **74**, 5–23.